MODEL AIRCRAFT AERODYNAMICS

NEW EDITION

MARTIN SIMONS

Model Aircraft Aerodynamics

Martin Simons

Argus Books

Argus Books
Argus House
Boundary Way
Hemel Hempstead
Herts HP2 7ST
England

First published 1978
Second edition 1987
Reprinted 1989, 1991, 1993
Third edition, 1994

ISBN 1-85486-121-2

Printed and bound in Great Britain by
Biddles Ltd., Guildford & King's Lynn

Contents

Acknowledgements

The author wishes to thank the many people who helped, sometimes without their knowing it, in the preparation of this book and the new edition. Some of them are aeromodellers whose questions and comments suggested the need for such a work in the first place. Since the publication of the first edition there has been much correspondence and many discussions with model fliers. The author has spoken and answered questions at a good many meetings, formal and informal, at places as far apart as rainswept hilltops in England and dry paddocks in Australia. It is hoped the revised text will stimulate as much thought and interest as the original did. Special thanks are owed to those who challenged some of the statements made or pointed to obscure passages requiring better wording.

Among the constructive critics who have helped with preparation of the revised edition are Noel Falconer, who supplied several pages of most valuable written commentary, Stan Hinds, Freddy Jones and Hans-Julius Schmidt. The new text should accommodate their points. Frank Irving's kind assistance with the first edition has not been forgotten.

Thanks are owed again to Professor Eppler and Professor Wortmann (who died, most sadly, in 1985), and to Dr. Althaus, for permission to use some of their most recent research material. Rolf Girsberger supplied ordinates of his latest aerofoils for inclusion in Appendix 3. Thanks are also due to Michael Selig and Martin Hepperle.

Ron Moulton encouraged the author at all stages in preparation of the first two editions. Thanks are due now also to Beverly Laughlin and Lyn Corson of Argus Books for their help with the third edition.

Preface to the Second Edition

The publication of *Model Aircraft Aerodynamics* in 1978 filled a gap not only in the literature for model fliers but on the shelves of many school and college libraries. The book has proved useful to designers of man-powered aircraft, ultra-light aeroplanes and gliders. Professional aeronautical engineers, researchers and academics, especially those involved with the development of (subsonic) remotely piloted vehicles, found the survey of boundary layer problems contained in the chapters on scale effects and low speed aerofoils particularly valuable as an introduction to this aspect of the subject.

Demand for the book justified several reprints. In the English language at least, it remains the only work of its kind in the field.

The general model aircraft scene has changed remarkably since 1978. Very large models have become almost commonplace. Many of them exceed the old legal limitations and have to be specially licensed for flight. Radio controlled helicopters have become reliable and sophisticated. The emphasis on multi-task and cross country flying for model sailplanes has transformed these aircraft beyond recognition, in ways that were only hinted at in the first edition. Every aspect of model design and construction has been profoundly affected by the increasing use of materials such as carbon fibre, Kevlar, and new kinds of adhesives. Radio control equipment now commonly available is extraordinarily precise and highly reliable. Electric and solar powered models flourish everywhere and begin to rival 'glow plug' engined craft. Further developments in gyroscopic stabilising devices and automatic pilots will make these more accessible in future and there is increasing interest in the development of advanced electronic instruments which will inform the pilot, on the ground, of exactly what his model is doing aloft. Microcomputers, now so commonplace, enable modellers, even without scientific or mathematical training, to design new aerofoil sections and optimise the performance of their aircraft by using commercially available software. Models already fly with small computers on board, not to mention surveillance instruments and cameras.

The need for a new edition of this book became increasingly apparent as the years passed. The basic theory has not changed, but the author has corresponded with many model fliers in many countries. These discussions have indicated to him some passages which were ambiguous or over-simplified in the original. There have been numerous small improvements of wording in the interests of greater clarity and emphasis. Some chapters have been re-grouped or re-arranged to improve the logical sequence. Many more sub-headings have been added to break up and make more legible what is, inevitably, a fairly solid text.

Substantial re-writing has been done in the chapter on trim and stability, not because the first edition was wrong but because a more emphatic statement seems necessary in an area where much confusion remains even among very experienced modellers.

A new section on winglets and tip sails has been included. The very brief notes about wind tunnel testing (in the first edition only part of an Appendix) have now been expanded to a full chapter with some advice on the use of the data coming from various small wind tunnels now operating in several countries.

A new chapter on propellers has been added, since their omission from the first edition drew some criticism. It must still be admitted that a full treatment of this subject would require a different book, but, since the adoption of the turbo-jet engine for full-sized aircraft, there is a notable dearth of modern textbooks on the basic principles of propeller design. Some of the most prestigious libraries consulted were unable even to find the basic works on propellers which, once, were required reading for every student of aeronautics. The need for a very simple explanation seems quite pressing, and in a very limited space, it has been attempted here.

Helicopters too, require books to themselves, yet very little about the aerodynamics of rotors has appeared in a form suitable for the model flier. The final chapter of this edition can pretend to be nothing more than an outline sketch of some theoretical aspects of these extremely complicated devices. It may at least point the interested reader in the right general direction for further studies.

Apart from these changes, wherever possible the results of recent research have been incorporated in amplification and confirmation of the text. Much still remains to be investigated.

London 1986 Martin Simons

Preface to the Third Edition

In the third edition the main text remains but the opportunity has been taken to include brief discussion of the important wind tunnel research undertaken at Princeton University by Selig, Donovan and Fraser during the years 1986–89. Also an explanation of the effects of wind on model flying has been included since so much misunderstanding surrounds this topic. There is an expanded section on tip winglets and crescent wing planforms. The discussion of the centre of lateral area theory has been expanded and the practice of trimming sailplanes using the so-called dive test is examined in relation to the dangerous phenomenon of 'tucking under'. The section on air brakes has been expanded to include the 'crow' or 'butterfly' mix system. A few other minor corrections and additions have been made in the Appendices.

Adelaide, 1994 Martin Simons

Introduction

The purpose of this book is to present in a practically useful form some standard aerodynamic theory as it applies to model aeroplanes, helicopters and gliders.

Anyone whose interest in aeromodelling is more than casual will benefit from understanding the behaviour of his models better. He is less likely to make serious mistakes in trimming or control, will build better, and may be able to improve the design of models. Apart from these considerations, aerodynamics is an interesting study in its own right and adds a further fascination to the sport.

Successful models may be designed and flown by rule of thumb. A sort of evolutionary survival of the fittest has produced a great many extremely efficient aircraft and it is not claimed that this book will bring about any revolution. It is, however, likely that some new ideas for future development will be extracted by those who read with an open mind. Some of the material contained will be familiar to experienced modellers, but in other cases they will find their old notions under criticism. This is particularly likely in discussions of the basic description and selection of aerofoil sections. Model fliers and many books and articles written for them frequently adopt a very misleading aerofoil nomenclature: undercambered, flat bottomed, semi-symmetrical and symmetrical. These terms can lead the beginner into serious trouble. At least the camber of the centre line of the profile should be known and taken together with the profile thickness.

The basic layout and trim of nearly all 'free flight' models also seems to be dominated by fashion to the exclusion of elementary principles. This is not to say that these models do not fly well; clearly they do. But trimming them for consistent performance and safety is made unnecessarily difficult when the centre of gravity is in the wrong position relative to the mainplane, as it almost invariably is. No gain in performance results, indeed, there is some small performance penalty for slow-flying models if the centre of gravity is located where, on current contest-winning models, it usually is. The fact that such models do win is because they are flown very skilfully despite their inherent faults. Arguments in favour of this kind of trim, sometimes loaded with mathematical equations, prove on examination to be mistaken.

Other common misunderstandings arise through the confusion between trimming and stability. This is examined in some detail in Chapter 12.

It is assumed throughout that the reader is a practising model flier and knows at least the essentials of how model aircraft are constructed, trimmed and flown. The mathematics have been kept to a bare minimum. Where numerical examples have been thought important or interesting enough to merit inclusion, they have been placed in an appendix and may be ignored by those who do not wish to become involved in figuring. It is rarely necessary or worthwhile in aeromodelling to carry out elaborate calculations; when a little arithmetic is essential it is usually confined to the four basic rules. The underlying principles are emphasised throughout. Where a reader is prepared to do a little more work, many of the problems arising can be solved to a sufficient degree of precision by the use of simple graphical methods or at most with an ordinary pocket calculator. It helps to have a few additional functions such as square roots and trigonometrical ratios (Cosines, Sines, Tangents etc.), but these are not essential.

On the commercial market now there are various kinds of computer software packages with model aircraft applications. These range from glider performance programs to flight simulators and elementary aerofoil section design. (These last should be distinguished from the highly sophisticated programs used for aerofoil design by professional aerodynamicists such as Eppler, Somers, Williams etc. in university and other research institutions.) Modellers using any such packages should remember that they are all based on fundamental assumptions which may be wrong. If garbage goes into the computer, it emerges in the output. Even with a sophisticated machine it is most necessary to comprehend the underlying theory if the computer is to produce meaningful results. This book should provide the necessary background enabling the model flier to discriminate between sense and nonsense.

The theories discussed are in general use by aerodynamicists but are not to be regarded as final truths. There is always room, and in some cases great need, for new discoveries. On the other hand, model aerodynamics, like any other branch of engineering science, must be firmly based on fundamental natural principles as these have been found by test and experiment. Some of the most basic principles are examined in the first chapter. Readers already familiar with the laws of motion may wish to skip this early section, though it is important that these passages be understood before the later ones are tackled.

Problems associated with flight and airflow speeds approaching the speed of sound are not considered in this book.

1
Fundamentals

1.1 LAWS OF MOTION

All aerodynamic theory depends on the laws of motion. These, originally worked out by Isaac Newton, remain entirely valid in engineering providing the matters under discussion are confined to velocities substantially less than the speed of light, and to objects and fluids of ordinary sizes and densities. Quantum mechanics and the theory of relativity, although fundamentally preferable to the Newtonian laws in advanced physics and astronomy, are not necessary for the understanding of model aircraft aerodynamics.

1.2 EQUILIBRIUM

If a body is in equilibrium, it tends to remain so. All the forces acting on an object in equilibrium are in balance, there is no tendency for it to change its state or accelerate in any direction, or decelerate. This is familiar with respect to things standing on the ground like items of furniture, or a model aeroplane lying on a shelf or workbench, not moving. Such bodies stay put unless something disturbs them, i.e. accelerates them in some way. Moving objects may also be in equilibrium. A model flying straight and level in calm air, neither speeding up nor slowing down, nor turning, is in a balanced state, and will tend to continue moving steadily. The same is true if the model is climbing at a constant speed in straight flight. It is in equilibrium even though gaining height, and will continue steadily along its inclined path unless some change of the forces acting on it occurs. Even if the climb is truly vertical, so long as the speed remains steady and there are no changes of direction, equilibrium prevails. In a steady speed dive the same applies (Figure 1.1). Equilibrium, then, is a very common state of affairs. It is a condition of steady motion or rest, in contrast to states of unsteady motion involving acceleration and negative acceleration or deceleration.

1.3 ACCELERATION, MASS AND FORCE

To disturb equilibrium, changing the speed or direction of flight in any way, requires a force variation to bring about an acceleration in the appropriate sense. The second law of

Fig. 1.1 Static and dynamic equilibrium

a Body standing on ground; no relative motion: static equilibrium.

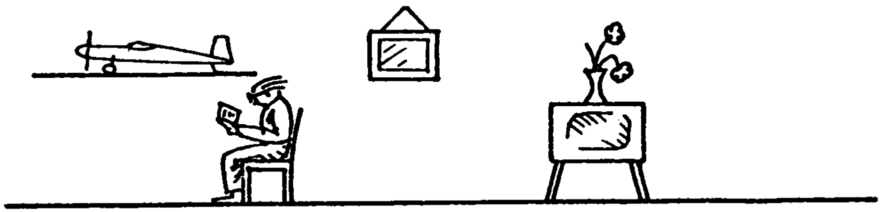

b Vehicle moving at steady rate; no acceleration or deceleration: dynamic equilibrium.

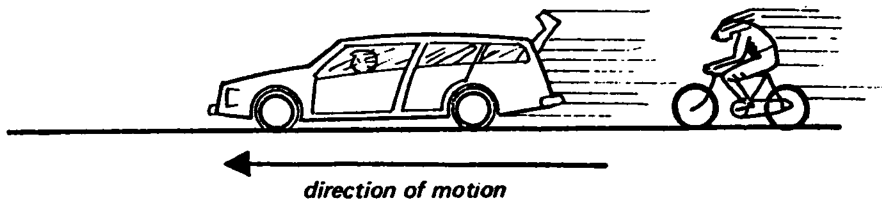

c Model aircraft in straight and level flight, no accelerations, decelerations or turns: dynamic equilibrium.

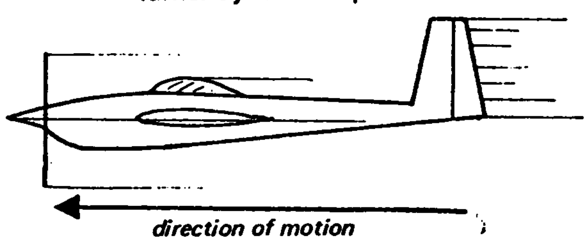

d Model climbing, diving or gliding at steady rate and constant speed: dynamic equilibrium.

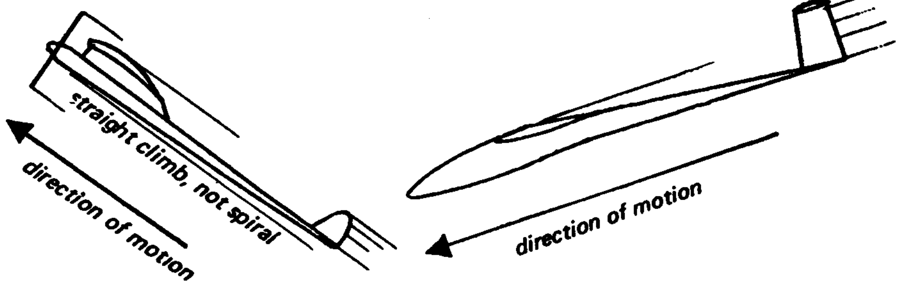

Fig. 1.2 Inertia

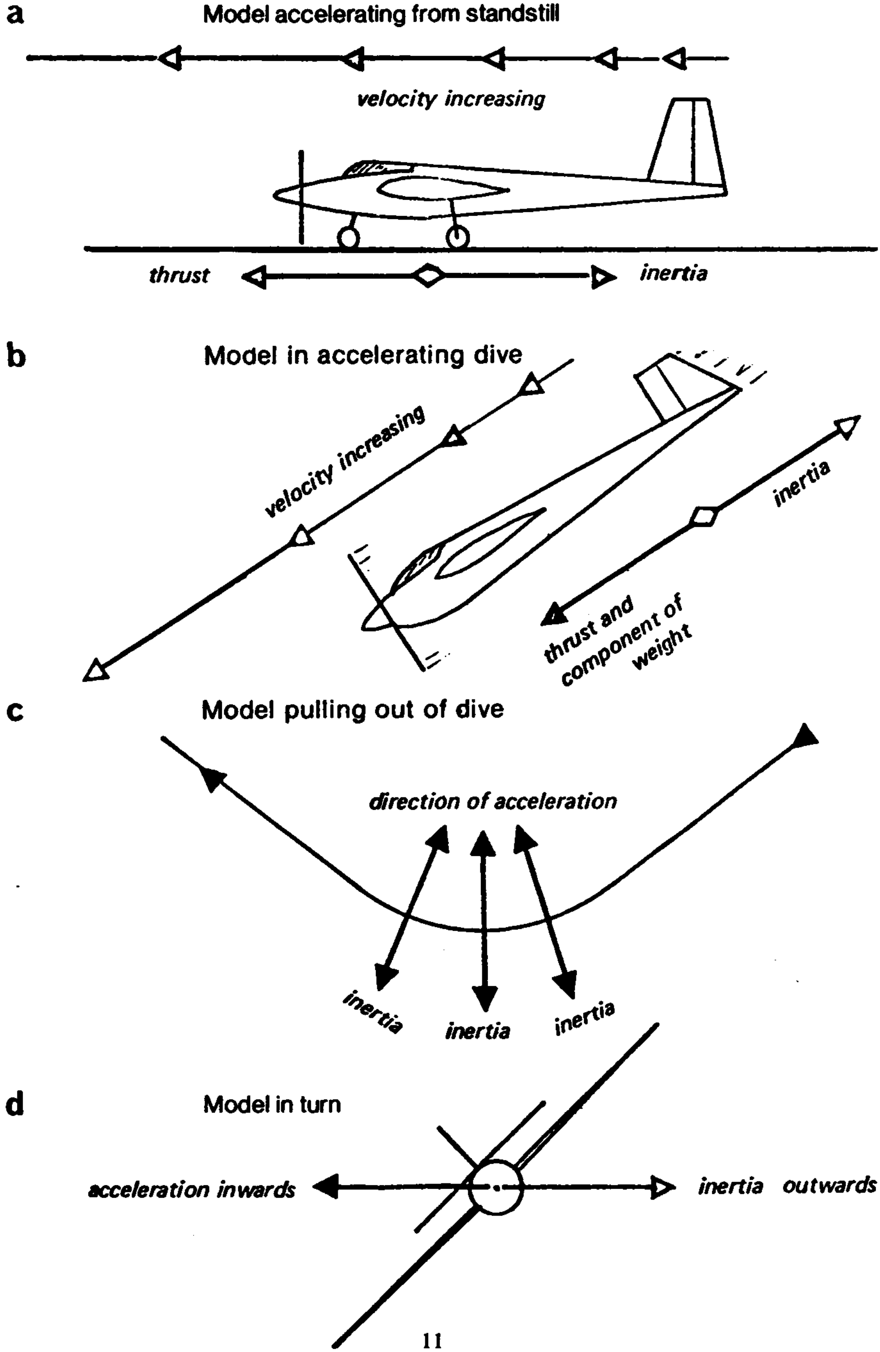

motion states that the strength of force required for any given acceleration depends on the *mass* of the model. Mass is not the same as weight, although in ordinary language, and on the kitchen scales, the two are often equated. Weight is force exerted by a mass. If a model were taken by rocket to Mars for trials in the atmosphere there, it would, during most of the trip, exert no weight, and on arrival would weigh less than on Earth, because of the lower gravity. The mass would be unchanged throughout, because the quantity of material, balsawood, metal, plastic, glue etc., in the model would be the same. An object of large mass requires greater forces to disturb its equilibrium to any given extent than a small mass. This is sometimes advantageous, as when a model is affected by air gusts. A model of small mass might be overturned by a force that would cause only a minor change of direction with a large mass. But the larger mass also requires a larger force to accelerate it to flying speed from standstill, more force to change level flight to climb, more force to initiate and maintain a turn, and more force to bring the model to a standstill again after flight. Whenever there is a disturbance of equilibrium, i.e. an acceleration or deceleration, or a change of direction, this quality of mass, termed *inertia*, opposes the change. In a turn, inertia tends to make the model revert to straight flight. Turning flight is a form of lateral acceleration. Pulling out of a dive involves a change of direction in the vertical plane, mass resists and tends to make the dive continue (Fig. 1.2).

1.4 ACTION AND REACTION

The third law of motion establishes that action and reaction are equal and opposite. When a model is resting on the ground, its weight, a force acting downwards, is opposed and exactly balanced by the equal and opposite reaction from the ground. A car running at constant speed is under the influence of a similar vertical pair, weight against ground reaction, but there is also a traction force moving the vehicle along. This is opposed by reaction forces in the other direction: frictional resistance from the ground, and air resistance or drag.

Any imbalance of forces produces acceleration (Fig. 1.2). A model beginning a take off run along the ground accelerates from standstill because the operator suddenly releases it. The thrust before release is opposed by the holding force; action and reaction are equal so equilibrium prevails. When the reaction force (holding) stops, the model accelerates. As soon as it begins to move, however, air and ground resistance begin and the faster the model goes the larger these resisting forces become. The model will continue to accelerate only so long as the total resistance remains less than the thrust. When the two are equal, with the model flying at some speed, equilibrium is restored (Fig. 1.1c).

In level flight, the weight force acting vertically downwards is opposed by a vertically upwards reaction. This reaction comes, in normal models, from the *lift* of wings and possibly other surfaces, but it may be supplied by other types of force. A helicopter is supported by its rotors, and a jet-lift aircraft is held up by the thrust of its motor. If the upward reaction against weight fails, or is reduced, the model accelerates downwards. To stop this *acceleration* it is necessary to restore an upward reaction to equal weight. This brings equilibrium but will not stop the descent. To do this an additional force must bring about deceleration. All such acceleration and deceleration will be resisted by the mass of the model, i.e. by inertia.

1.5 RESOLUTION OF FORCES

A power model in level flight is under the influence of many forces acting on every part of it, but these may all be added and sorted out into four general forces arranged in action-reaction pairs. The main upward support comes from the wings, but the tailplane also may provide some lift, so its contribution must be added to the total vertical reaction. The propeller shaft may not be aligned exactly along the flight path. This is not only because the model operator may deliberately mount the motor at an angle to the datum line of the fuselage (so-called downthrust or upthrust), but because the fuselage itself may not be aligned to the airflow at the particular speed of flight concerned. How much upward or downward force results from this may be gauged by the trick of resolving forces. As Figure 1.3 shows, any force may be represented, diagrammatically, by an arrow which points in the same direction as the force acts, drawn to a definite scale. A force of three Newtons, for example may be represented by an arrow or 'vector' three centimetres long

Fig. 1.3 Resolution of forces

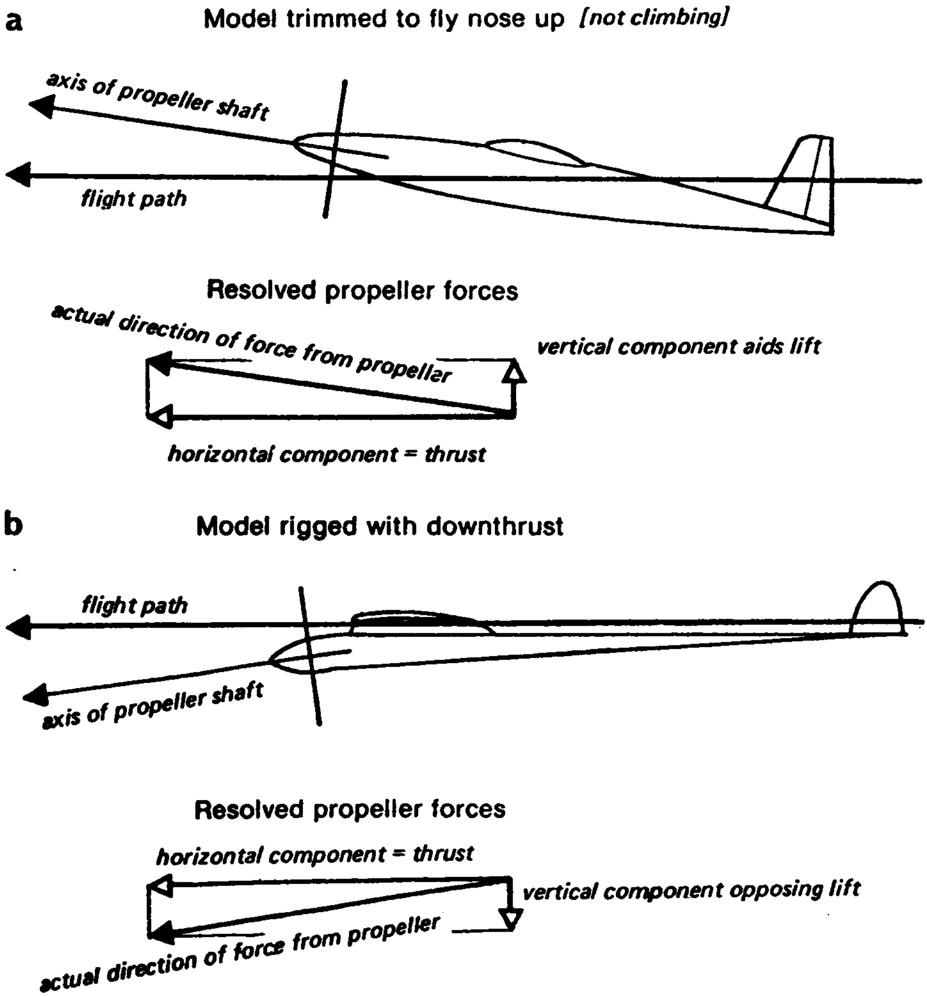

Fig. 1.4 Forces acting on a model in equilibrium

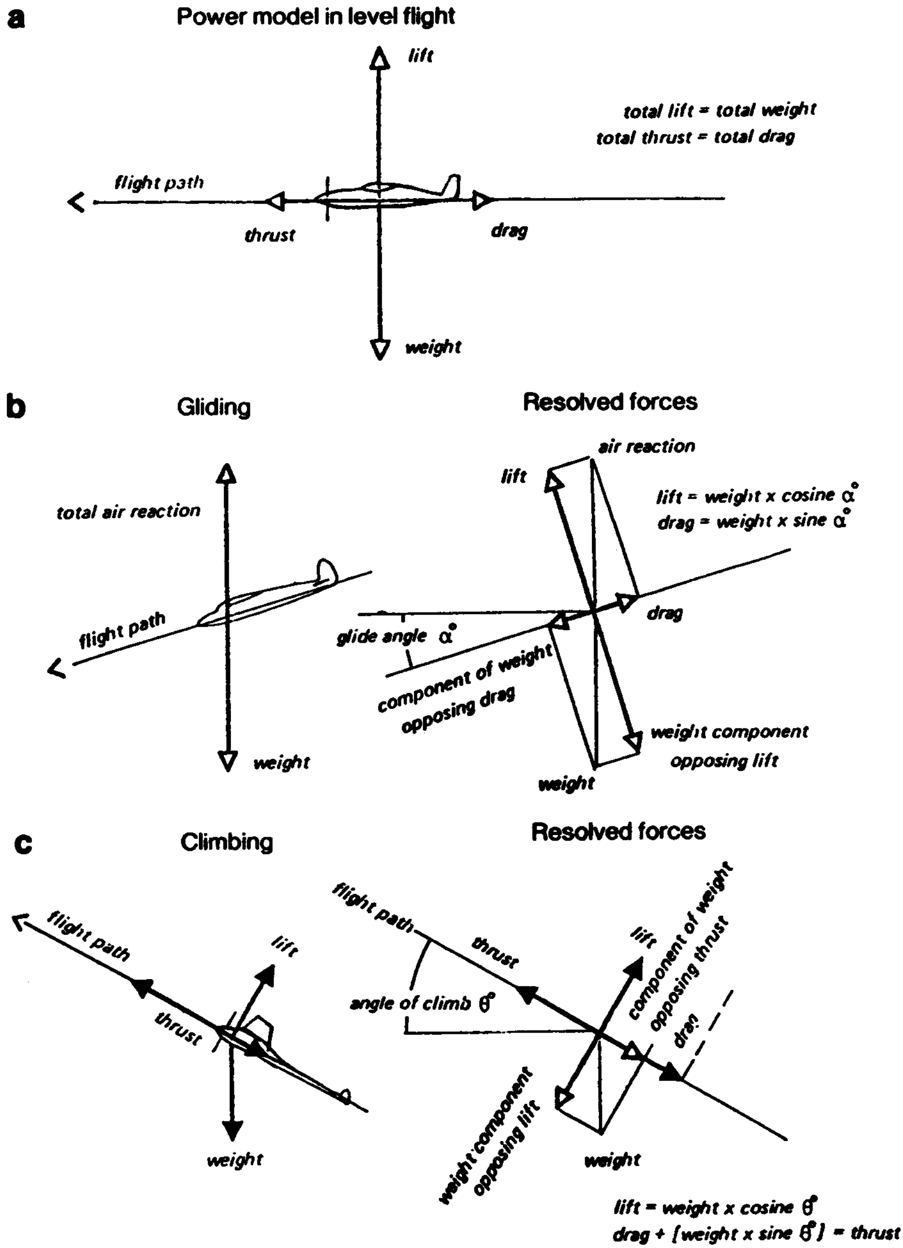

Fig. 1.4 contd.

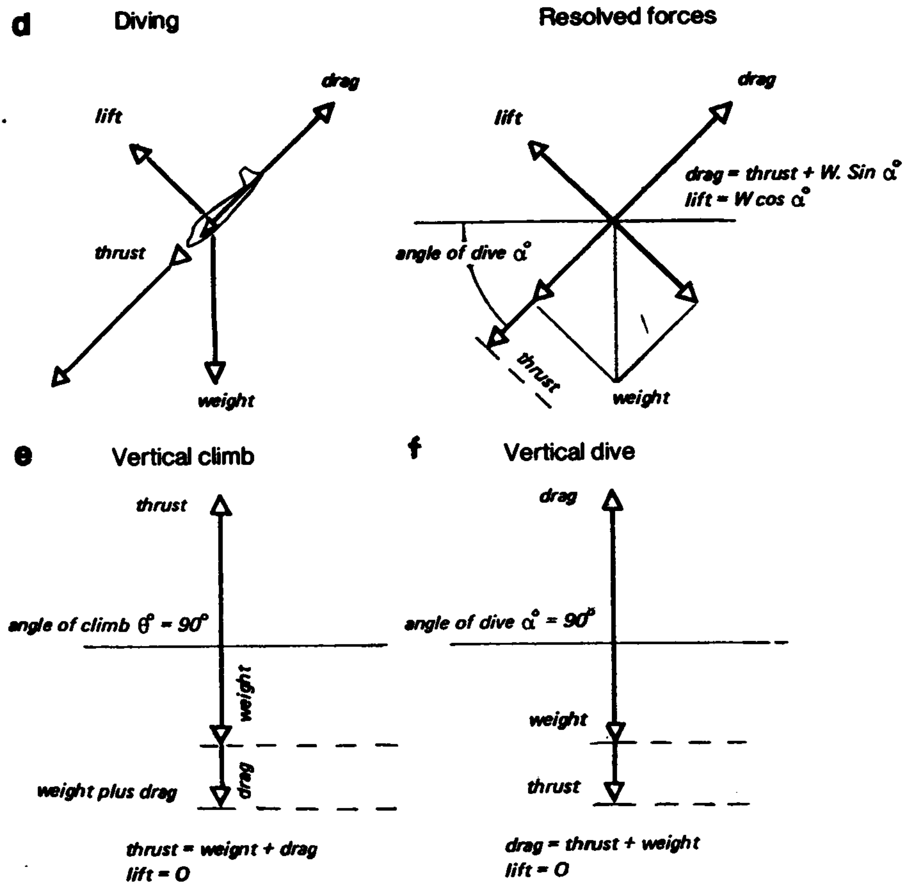

pointing in the required direction. Other forces and directions would then have arrows of proportionate length. To resolve the force from the propeller, into one component along the flight path and one directed vertically, the original arrow is drawn as the diagonal of a rectangle. The length and directions of the two sides of the rectangle then show, to the chosen scale, both the direction and strength of the contribution made by the propeller to thrust and vertical forces. In most cases the propeller shaft will not be very far from alignment with the flight path, so the bulk of the propeller force goes to thrust.

These principles of force resolution are very widely applicable. In Figure 1.4a, a power model is shown in level flight. It is acted on by four forces at right angles: thrust opposed by drag, weight opposed by lift. This is the simplified diagram resulting from numerous additions and resolutions of small forces each making its individual contribution. If the tailplane is exerting a slight downward force to maintain the trim of the model, this has ben subtracted from the total lift. In the same way the drag of the wing, tail, fuselage and undercarriage has been totalled. For level flight, in equilibrium, the final result must be as shown.

1.6 GLIDING

Gliding, either with engine throttled back or with no engine at all, is best understood if the forces are resolved as shown in Figure 1.4b. The weight alone acts vertically downwards, but may be resolved into one force acting along the flight path and another at right angles to it. The glider, or gliding power model, moves forward and slightly downwards under the action of the weight component along the flight direction. The total air reaction force is similarly resolved into lift at right angles to the flight and drag opposing the forward-acting force. The result is a diagram very similar to that for powered flight but it has been rotated through a small angle, known as the glide angle. A steeper glide would cause a larger weight component to pull the model along its flight path. It would accelerate until the drag component of the air reaction once again grew large enough to restore equilibrium.

1.7 DIVING

In a dive, the four force diagram has rotated further, as shown in Figure 1.4d, and in the limiting case the flight path is vertically downwards, weight and thrust (if any) both pull the model down, the only opposing force is drag. The speed at which drag becomes large enough to equal weight-plus-thrust is usually very high and probably before this 'terminal velocity' is reached, the model would hit the ground (Fig. 1.4.f).

1.8 CLIMBING

In a climb, the total support comes from a combination of wings and propeller. The weight may be resolved into two components, one opposing lift and the other directly opposing thrust, assisting the drag. Again, the result is a four force arrangement in balance, but rotated through the angle of climb (Fig. 1.4.c). The limiting case is the vertical climb, when the weight plus drag is opposed only by the propeller. Such flight is commonplace to the helicopter, but a model of orthodox type, if sufficiently powered, is capable of vertical climbing in this fashion also. As the diagram shows, in such a climb the wing lift force must be zero, and its angle of the attack to the air flowing over it must be such as to give no lift. It is therefore obvious that to obtain a steep climb there must be sufficient thrust from the motor since this, rather than the wing, provides the necessary reaction to equal the weight and drag resistance.

1.9 HOVERING

For a helicopter to hover, the thrust from the rotor must equal the weight plus a relatively small addition to compensate for the drag of the rotor's slipstream over the body of the aircraft. In a helicopter ascent some additional rotor thrust is needed because the air drag of the hull in the rotor wake increases. Ordinary model aeroplanes are, given sufficient power, capable of climbing vertically but although they can be made to hover briefly, it is usually not possible to hold them in this position because the airflow over their control surfaces is too slow. Control is quickly lost and the model falls out of the vertical attitude.

2
Factors affecting lift and drag

2.1 ACTION AND REACTION FROM AIR

The air forces which act upon a model, both those which support it and those which resist its movement, arise from the properties of the air, which has mass. To generate supporting force a mass of air must be accelerated or deflected to yield an upward reaction which, for equilibrium, equals the weight. To work on the air the wing or wings of the model must move through it, disturbing it. In addition to the wing, all other components of a model, such as fuselage, tailplane, undercarriage, etc., also disturb the air and add to the total of energy needed, without, in general, adding any lift. The greater the expenditure of energy required to generate a given lift force, the less the efficiency of the model.

The mass of air available for a model to work on depends on three factors: 1) the amount of air in a given space, i.e. the mass density of air where the model operates; 2) the size of the model; and 3) the speed or velocity of its flight (Fig. 2.1 a, b and c).

2.2 DENSITY

Air is a mixture of gases, mostly nitrogen and oxygen. At the fundamental level, gases are regarded as consisting of enormous numbers of separate particles, called molecules, which are in violently agitated motion. The temperature of a gas is the measure of this molecular motion; low temperatures are states of less molecular motion than high temperatures. It is the impact of the moving particles which creates gas pressure on objects immersed in gas. Density is the measure of the number of molecules in a given space.

In low speed aerodynamics it is not necessary to consider the molecular structure of the air. The medium in which models fly is a fluid. This is not to say that air is a liquid. Liquids are fluids which are almost totally incompressible, gases are compressible fluids. Model aircraft do not (as yet) fly at such speeds that the compressibility of the air needs to be allowed for. This is true also for full-sized sailplanes and hang gliders, ultra light, light and commercial aircraft up to medium sized piston-engined transport aeroplanes.

Compressibility problems do arise for jet-driven aeroplanes and for the tips of propellers and helicopter rotors. For modelling purposes, fortunately, the air may always be regarded as an incompressible fluid. Even so, significant variations of density occur. They are related to altitude and weather. In Appendix 1, charts (prepared by Jaroslav Lnenicka) indicate the magnitude of these effects. At high altitudes and in hot weather, the air is less dense than near sea level when cold. Modellers operating on the high plateaux of East Africa or the Americas find air density does make a difference since to

Fig. 2.1 Factors affecting lift

a Air density ρ

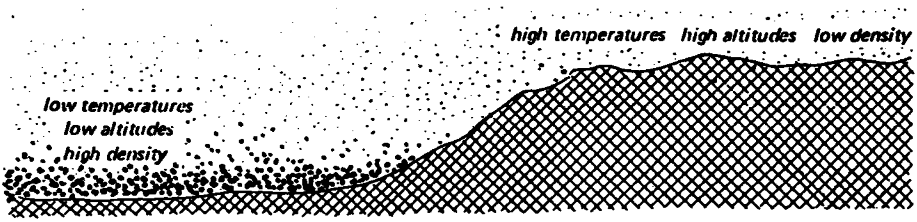

b Model size, usually wing area, S.

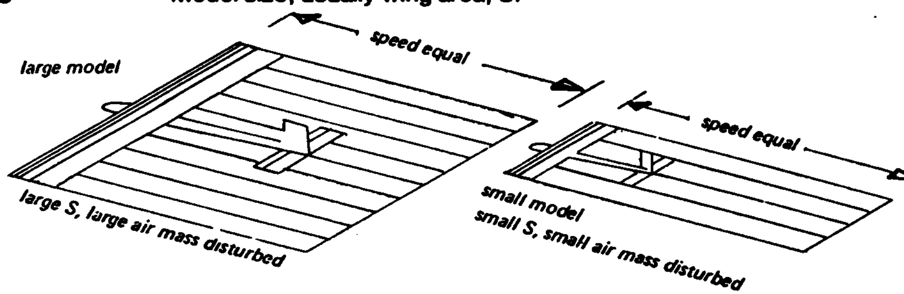

c Velocity, V.

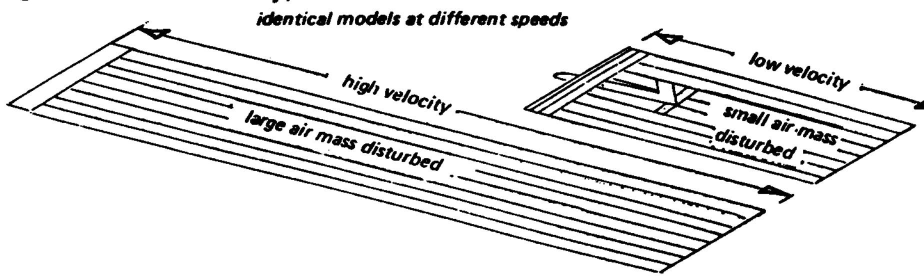

d Aerofoils section geometry and angle of attack

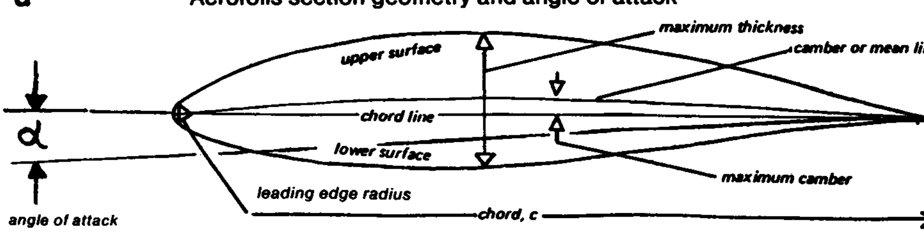

achieve the same air mass reactions to gain lift, their models have to fly faster. Engines and propellers are also adversely affected.

Density is usually expressed in kilogrammes per cubic metre (i.e. mass per unit volume), or in Imperial measure, slugs per cubic foot. In aerodynamics a standard value for density of 1.225 kg/m^3 (.002378 slugs/ft^3) is assumed, corresponding to a sea level value at normal temperature and pressure. For most purposes in design this figure is adequate. In formulae, the Greek letter ρ (rho) is used to stand for density (Fig. 2.1a).

2.3 MODEL SIZE

A large model, flying through air of standard density, must create more disturbance and hence generates more air reaction, both lift and drag, than a small model, at similar speed. The wing span in relation to the model weight, or span loading, is of some importance. A large span wing at a given speed sweeps through a larger mass of air than a short wing. To gain the same reactive forces, with a larger total mass to work on, smaller accelerations are needed. Span loading is expressed as a ratio, weight-per-unit-length (Newtons per metre, or pounds per foot). The capital letter W stands for weight, and the small letter b for span (breadth). Span loading = W/b.

Model size is more conveniently expressed in terms of wing area. Units such as square metres or square feet are employed, though these are rather large for modelling purposes and the F.A.I. Sporting Code quotes areas in square decimetres. (One square decimetre equals 1/100th. sq. metre.) In this book areas will be given in square metres to conform to standard aerodynamic conventions. The capital letter S is used to stand for square measure, i.e., area.

2.4 VELOCITY

With a model of given span and area, a larger mass of air will be disturbed if speed is high than if low. Velocity, V, is expressed in metres or feet per second, rather than kilometres or miles per hour, in standard formulae (Fig. 2.1c).

2.5 ANGLE OF ATTACK AND TRIM

However large and fast a model may be, its ability to gain lift will depend almost entirely on the form of the wing and its *angle of attack* relative to the airflow. The angle of attack is measured in degrees from some more or less arbitrary reference line, usually the straight line through the extreme leading and trailing edges of the wing aerofoil section or profile. In some cases, especially for an aerofoil with a flat underside, such as the Clark Y, a line tangential to the undersurface may be used. The angle between the reference line and the airflow at a distance from the wing is the *geometric* angle of attack. The *aerodynamic* angle of attack, i.e., the angle at which the air actually meets the wing, is almost always different from this, as will be explained in later pages.

The angle of attack (both geometric and aerodynamic) of the main wing is governed in orthodox models by the relative setting of wing and tailplane. The tailplane is a small wing which may or may not contribute lift to the total, but whose main function is to trim the mainplane to the desired angle of attack and hold it there. The angle of incidence of tail and wing to the fuselage must be distinguished from the angle of attack to the air. The fuselage itself may not be aligned with the airflow. (In this book, the term *angle of attack* is reserved for the angle of wing or tail airflow, and *angle of incidence* refers only to the rigging angle of such surfaces relative to some datum line on the drawing board. This convention is not always observed in other works on aerodynamics.)

Tails are sometimes arranged in V form, or even inverted V, when the longitudinal pitching and lateral stabilising and trimming functions are combined in the two surfaces of the V. Many other layouts than the orthodox wing-tailplane-fin style are possible, including tailless, tandem, delta and tail-first or canard aircraft. All these and more can be made to fly and sometimes for special purposes may be superior to the standard arrangement.

Strictly, almost all ordinary aeroplanes and gliders are 'tandems' in that they have two wing-like surfaces disposed one behind the other and set at different rigging angles relative to one another. The relative areas and spans of these surfaces are matters of the designer's choice. Whether one wing or the other carries most of the load or all of it is a matter of trim and centre of gravity position. If one of the pair of wings carries no load or very little, it functions only as a stabiliser and control surface and may then be very small relative to the main load-carrying wing.

In certain circumstances, the so-called 'canard' layout with a small, load-carrying wing ahead of a larger mainplane has certain advantages over the more usual mainplane/tailplane arrangement. The first successful aeroplane, the Wright Brothers' *Flier* of 1903, was a canard.

The reason why most aircraft have tailplanes rather than foreplanes will appear in more detail in Chapters 12 and 13. Although unorthodox aircraft sometimes appear to offer great advantages, the tailless type because it saves the drag and weight of fuselage and stabiliser, for instance, there are always certain disadvantages too, either in terms of excess drag from other causes, structural complexity, or, more often, problems of control and stability.

2.6 AEROFOIL SECTIONS AND LIFT COEFFICIENTS

The efficiency of a wing is influenced greatly by its aerofoil section or profile, which has some degree and type of *camber* and some *thickness form* (Fig. 2.1d). Fuselages and other similar-shaped components of a model also produce some lift force, depending again on their shape and angle of attack. Re-entry vehicles for space flight have been designed as 'lifting bodies' without wings, but for almost all practical purposes in aeromodelling, the lift contribution of fuselages may be ignored. However, a fuselage does produce forces analogous to lift which affect the stability of the model, almost invariably in ways that oppose the efforts of the stabiliser to hold the mainplane at a fixed angle of attack. Similar lateral unstabilising forces are resisted by fins, which are small wings set at right angles to the mainplane, producing sideways 'lift' to correct yaw and sideslipping.

For convenience, aerodynamicists adopt a convention which allows all the very complex factors of wing trim and shape to be summed up in one figure, the *coefficient of lift*. This tells how the model as a whole, or any part of it taken separately, is working as a lift producer. A lift coefficient or C_L of 1.3 indicates more lifting effect than $C_L = 1.0$ or 0.6, while $C_L = 0.0$ indicates no lifting effect at all. C_L has no dimensions since it is an abstract figure for comparison purposes and calculations.

For level flight, the total lift force generated by a model must equal the total weight, so it is possible to write:

Total Lift = Total Weight, or $L = W$ (Action = Reaction).

This will not apply exactly if the model is descending or climbing. The exact relationships between lift and weight for these conditions are given in Fig. 1.4. As Figure 2.1. shows, the factors affecting lift force are model size or area, speed of flight, air mass density and the aerofoil-plus-trim factor, C_L. In every case, an increase in one of these factors, greater

Fig 2.1 Contd.

e Lifting effect or lift coefficient CL

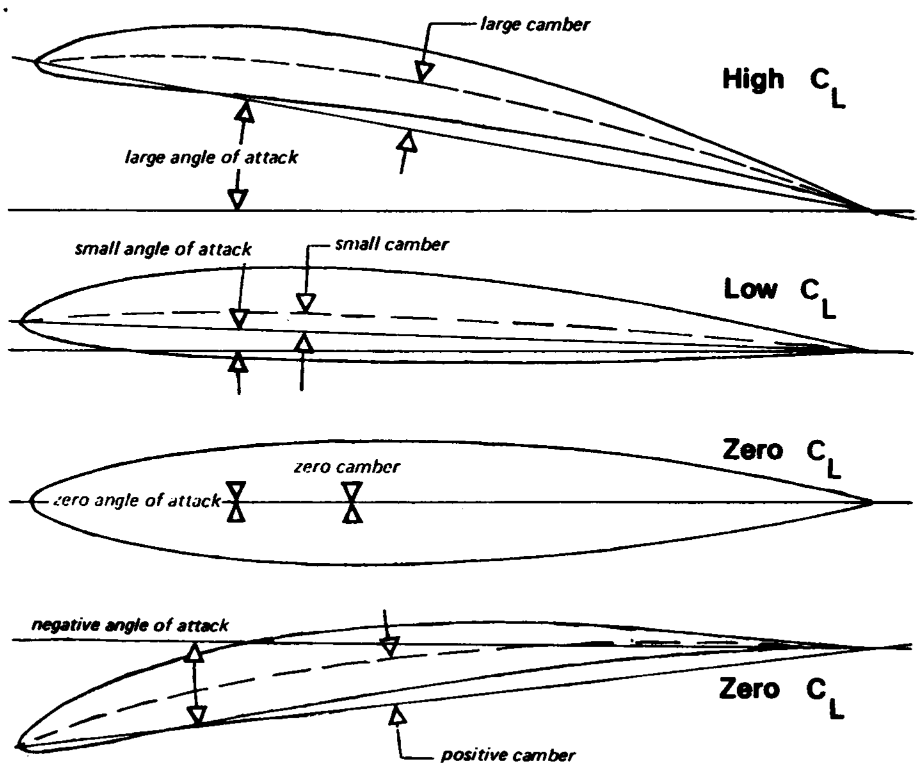

area, more speed, increased density or higher lift coefficient, will produce a larger lift force. It is to be expected that when a formula for lift is worked out, it will include all these factors. In mathematical language,

Lift = some function of ρ, V, S, and C_L

The standard formula, which arises out of the basic principles of mechanics and the pioneer work of Daniel Bernoulli in the eighteenth century, is

$$L = \frac{1}{2} \times \rho \times V^2 \times S \times C_L$$

It is not particulary important for modellers to know this formula but it is necessary to see how the various factors in the lift equation are interdependent. For a model to be capable of level flight, the lift must equal the weight. If the model's weight increases (as when it turns out heavier than expected), a larger lift force will be needed to support it. Some item on the right hand side of the equation, or more than one of them, must be increased. The modeller has no control of air density, ρ. The model could be re-trimmed, increasing the wing's angle of attack to get a higher C_L. More wing area might be added, although this would add mass and increase the speed of flight. Since V is squared in the formula (multiplied by itself), a relatively small increase in V yields a large increase in lift force, other things being equal. It follows from this that a heavy model (of given area, trim, etc.) has to fly faster than a light one. However, to increase V takes energy and in an extreme case the engine of the model may be incapable of giving sufficient power to sustain flight. In such a case, if launched from a height the model would descend at some angle like a glider, even with engine at full power.

2.7 WING LOADING

The importance of weight relative to wing area is apparent from the above. The wing loading, often written W/S and expressed in kilogrammes per square metre (pounds or ounces per sq. ft.), is the easiest way of portraying this relationship. The weight of a model, neglecting small changes caused by fuel consumption, is constant during one flight. The speed at a given trim (angle of attack) will depend entirely on the wing loading. This may be shown by re-arranging the lift formula to bring L/S onto one side. (L = W in level flight.) Dividing both sides of the equation by S gives:

$$W/S = L/S = \tfrac{1}{2}\rho V^2 C_L$$

For gliders, and descending power models, lift and weight are not quite equal (Lift = WCos α, see Fig. 1.4) but for normal angles of dive or climb less than ten degrees there is very little difference and the wing loading formula holds good. Adding weight increases forward speed, but requires more power to sustain flight. (In a glider a more powerful upcurrent is then needed for soaring.)

2.8 WING C_L AND SECTION c_l

The C_L of a *whole model* or *whole wing* should not be confused with the lift coefficient determined in a wind tunnel for an aerofoil section. The *section* lift coefficient is sometimes written c_l, in lower case letters, or C_l, to distinguish it, but this is not always done and confusion results. The C_L of a real wing or tailplane cannot as a rule be arrived at by a simple transfer of values from a tunnel test of c_l. The various effects of cross flow and downwash on a real wing cause the section lift coefficient to vary from place to place across the span, even if the wing is nominally at the same geometric angle of attack to the line of flight. The C_L finally arrived at is approximately the average of all the local values.

2.9 WING C_L AND TOTAL C_L

Further difficulty is caused by the tailplane's contribution to the aircraft C_L. In modelling for competition purposes, the tail area and wing area are both taken into account to prevent competitors from trying to gain unfair advantage in wing loading by fitting oversized tailplanes. (That there is any advantage is an illusion, but the rule was introduced long ago and is unlikely to be changed in the F.A.I. Sporting Code. Any area added to the stabiliser has to be taken away from the mainplane.) If the tail or canard forewing does contribute some lift to the total, the C_L of the whole model may be determined using the combined areas in the lift formula. In full-sized aeronautics the aircraft C_L is usually determined in terms of the wing area alone. This is a convention, no more. Various other conventions are adopted about the parts of wings and tails that are (geometrically) inside fuselages, or enclosed by engine nacelles, etc. What area is actually used in calculations is to some degree a matter of choice and convenience. Problems arise only if inconsistent conventions are adopted.

2.10 STREAMLINED FLOW

When the air meets any body, such as a wing, it is deflected over the surfaces. In accordance with Bernoulli's theorem (see 2.12 below) above and below a wing there is a complex variation of velocity and pressure. For positive reaction, which is the basis of lift, there must be a positive difference in total pressures on top and bottom surfaces. The air over the upper surface is therefore made to flow over a longer route, so that it moves faster than that taking a shorter route below. These effects are felt both ahead of and behind the wing. The flow ahead tends to be drawn upwards towards the low pressure region, which creates an upwash, and beyond the trailing edge it tends to return to its former position, so there is a corresponding downwash (Fig. 2.2). The pressure difference between the two surfaces may be increased up to a point by increasing the angle of attack, or increasing the camber or both. There is a very definite limit to this. If either the angle of attack or the camber is increased too much, the streamlining breaks down and the flow separates from the wing. This is explained in greater detail in Chapter 3. Flow separation not only creates a great deal of drag, but also changes markedly the pressure difference between upper and lower surfaces. The lift force is drastically reduced, the wing is stalled (Fig. 2.3).

Flow separation on a smaller scale is common. On the upper surface, flow may separate somewhere before the trailing edge, as sketched in Figure 2.4, or, as suggested in

Fig. 2.2 The origin of lift

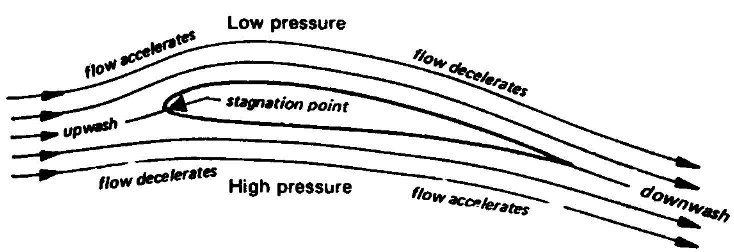

Fig. 2.3 Stalling

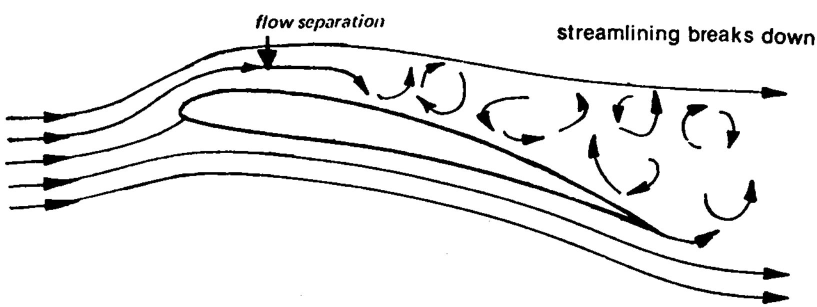

Fig. 2.4 Local flow separation

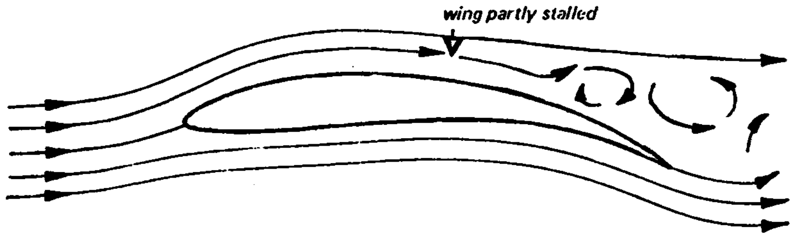

Fig. 2.5 Local separation with re-attachment

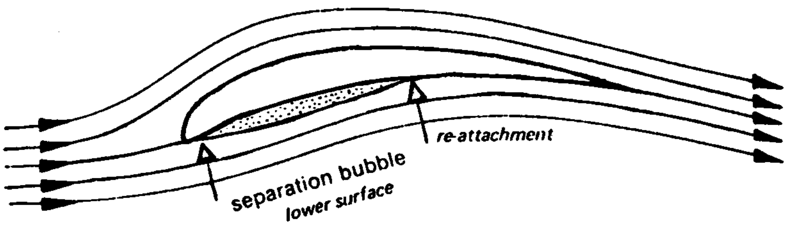

Figure 2.5, there may *on either surface or both* be separation with subsequent re-attachment. This is called 'bubble separation'. Typical results of test on model wings are given in Chapter 8.

2.11 CIRCULATION AND THE BOUND VORTEX

The upwash ahead and downwash behind a wing, with the accelerations and decelerations above and below, suggest that a diagram like that in Figure 2.6 may be drawn. The streamlines behave as if, instead of a wing, there was a rotating and moving cylinder of air, a vortex, with its axis aligned with the wing. Such a cylinder would cause upwash and downwash, acceleration and deceleration of flow, in very much the same way as a real wing, and it would cause identical reaction forces. The strength or speed of the vortex circulation would determine how much reactive force was produced. Many experiments have shown that rotating cylinders do produce lift, but the main value of this idea is that it enables the lifting ability of any wing to be explained or calculated in terms of the strength of circulation of the imaginary vortex. The rotating cylinder is termed the *bound vortex* because it is supposed to be tied to the wing and moves along with it. The idea of the bound vortex is particularly useful in calculations of the lift distribution spanwise across real wings. The strength of the bound vortex at each point is a measure of the lift at that location. The concept is a mathematical model rather than a physical reality.

2.12 BERNOULLI'S THEOREM

Bernoulli's theorem connects the pressure measured at any point in a fluid such as air to the mass density and velocity of flow. This theorem is a special application of the laws of motion and energy which is of fundamental importance to aerodynamics and flight, as well as to liquid flows in pipes, channels and around the hulls of ships, etc.

Fig. 2.6 The bound vortex

Theoretical image: the wing replaced by a vortex

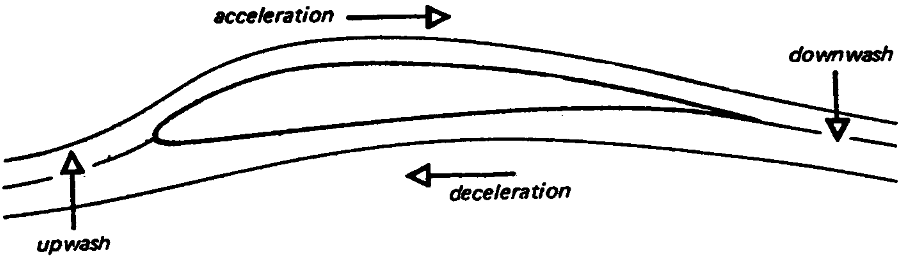

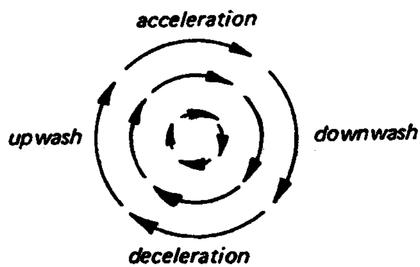

Effect of vortex on flow

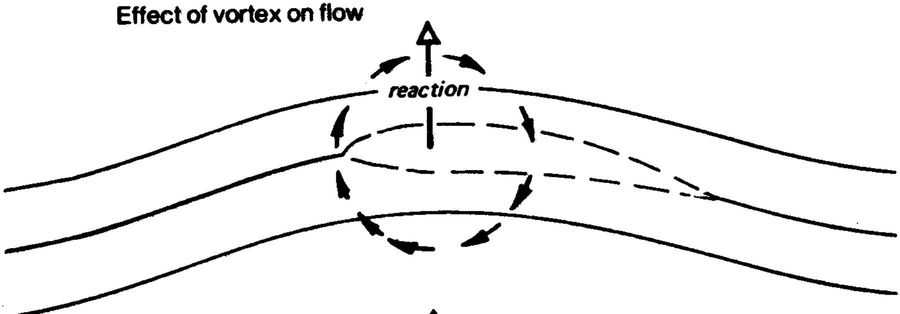

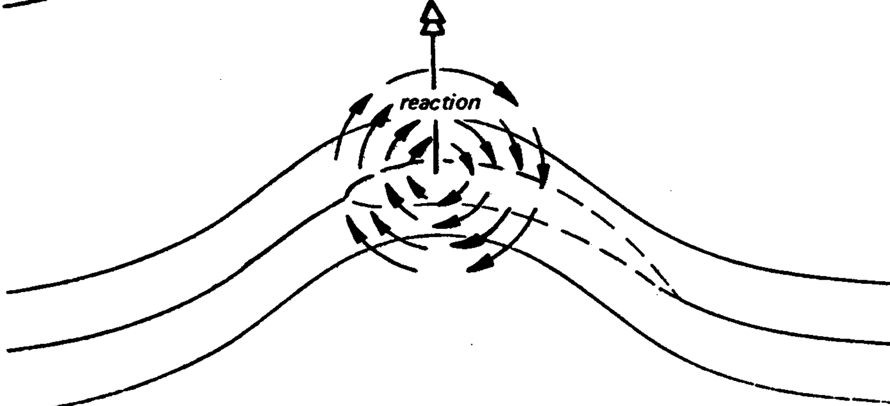

Strong circulation equivalent to higher CL

If a small particle or cylinder of air is imagined as part of a general flow moving smoothly, or in 'streamlined' fashion, the particle will be in equilibrium if the pressures acting on it from all directions are equal. If there is a pressure difference in any sense, the particle will accelerate or decelerate in accordance with the second law of motion. V, velocity, will increase if the pressure on the front face of the cylinder is less than that behind, V will decrease if the pressure behind is less than in front. Hence the particle will speed up as it approaches a region of low pressure, and slow down on approaching a high pressure zone. Since it is not isolated, but part of a general streamlined flow, the same laws apply to every particle in the flow, which therefore speeds up and slows down on approaching low and high pressure regions respectively. The simple mathematical expression of this principle is, where P stands for pressure:

$$P + \tfrac{1}{2}\rho V^2 = \text{Constant} \quad \text{(Bernoulli's theorem)}$$

Air flowing at speeds of interest to modellers is constant in density. Pressure and velocity are the only variables; if one increases the other decreases under all circumstances. A well known application of the principle is the 'venturi' tube which is used in aviation to measure airspeeds or drive instruments, and in every day life to produce high speed jets from garden hoses, taps, etc.

A fluid passing through a constricted tube such as the venturi sketched in Fig. 2.7 contains no vacant cavities. The same mass of fluid must leave the exit, in each time unit, as the mass entering. In the constricted part of the tube, since the cross sectional area is small, the velocity of flow must increase to get the same mass through in the time available. This increase of velocity, in accordance with Bernoulli's theorem, produces a reduction in pressure in the throat. The small cylinder of air imagined above becomes elongated and narrower in cross section in the throat, then returns to its original form after reaching the wider part of the tube. The 'streamlines' thus appear as shown.

A fluid passing over any body, so long as streamlined flow persists, will experience similar deformations of flow, with accordant velocity and pressure changes. This is particularly relevant to the flow over a wing.

The Figure 2.2 showed, in accordance with Bernoulli's theorem that when air passes over a wing it accelerates into the low pressure region on the upper surface. Somewhere it reaches the point of least pressure. From there onwards it flows towards the trailing edge against a pressure gradient tending to slow it down. The pressure above the wing behind the minimum pressure point, although it is increasing, is still lower than the normal or 'static' pressure of the main flow far away from the wing. On the underside, although the pressure is high on average, there is deceleration up to the maximum pressure point (which is often very close to the leading edge) and acceleration thereafter.

2.13 DRAG, THE LIFT: DRAG RATIO

All parts of a model, including wings, tail fuselage and every component exposed to the air flow, contribute drag. Even the insides of cowlings, wheel fairings, etc., will add some drag if air passes through them. As with lift, the actual drag force generated depends on flight velocity, air density, size and shape of the model. The drag coefficient, like the lift coefficient, sums up all the features of the model and is a measure of its aerodynamic 'cleanliness'. The formula is of the same type as that for lift:

$$\text{DRAG} = D = \tfrac{1}{2} \times \rho \times V^2 \times S \times C_D$$

The S, or area in this formula is normally the wing area of the whole aircraft. If the total surface area is used (including tail) for the C_L, the same total area must be used for the drag equation. This enables the drag and lift forces to be compared, usually in the form of

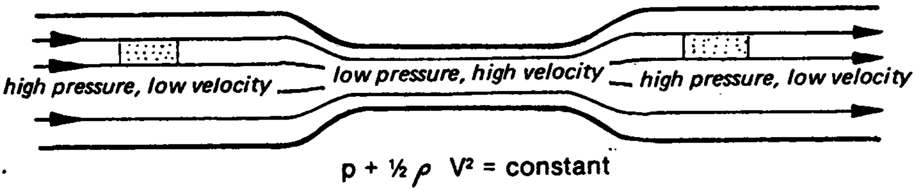

Fig. 2.7 The venturi

a ratio, the lift to drag ratio or L/D. For level flight, lift will equal weight, which is constant (ignoring fuel consumption). Thrust can be increased or decreased by variations of throttle setting. This will change the drag force, since for *level* flight in equilibrium, *thrust and drag are equal*. At high speed, thrust is large and drag is large, but the total lift force remains the same, equal to the weight. The *ratio* of lift to drag is low; drag has increased because of the high speed. At low speeds, still maintaining level flight, drag

Fig. 2.8 Vortex-induced drag

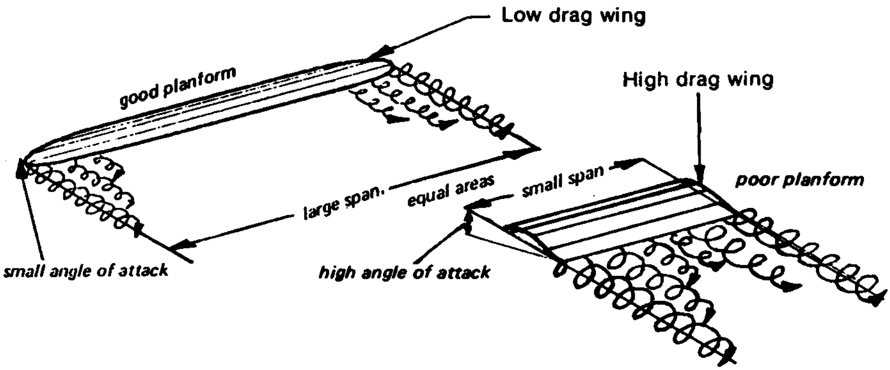

Fig. 2.9 Form or pressure drag

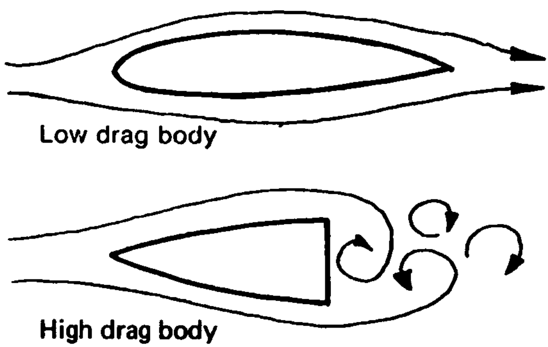

reduces up to a point while lift still equals weight. Hence the L/D ratio increases. This improvement in drag force does not continue down to the slowest speed for any given model, since, as will appear, the total drag *coefficient* itself begins to increase rapidly at low speeds, and this is enough to outweigh the reduction in V. Hence at some speed the model achieves its ***maximum L/D ratio***. The value of this ratio gives a rough measure of the all-round efficiency of the model.

As with lift, confusion arises if wind tunnel tests are wrongly interpreted. In tests of isolated bodies such as fuselages, wheels, etc., the measure of size, S, used in the drag formula is the cross sectional area of the object tested. This gives a wholly different result from the drag coefficient of such items when they are related to the wing area of a whole aircraft. With wing drag figures from tunnel tests, the same applies as to section lift coefficients. The real wing in flight does not reproduce the test figures across the whole span. It is hardly ever necessary to calculate the actual drag of model components. The main thing is to know how drag is caused and how to reduce it. Modellers quite often speak of increasing lift by changing the trim or using a different wing section. In level flight the lift force equals the weight and this remains true after the trim or aerofoil change just as before. Hence although the lift coefficient, C_L, may have been increased, the lift *force* remains equal to the weight in level flight. Every change of this kind however, does change the drag of the aircraft. If the drag is regarded as the inevitable price paid for keeping a given model in the air, reducing the drag price always makes for a more efficient flight.

2.14 VORTEX DRAG

In Figures 2.8–10 the types of drag are illustrated. ***Induced drag*** is now called *vortex* drag because it is associated with the rotating vortices which trail behind any wing, or any surface, which is yielding aerodynamic lift. The appearance of the vortices is directly associated with the lift: the higher the lift coefficient of a given wing, the more significant is the effect of the vortices. Since when flight speed, V, is low, a given model must work at a higher lift coefficient than when V is high, the induced drag increases as the velocity decreases. (Mathematically, vortex-induced drag is proportional to L/V^2.) This is the major, though not the only cause of the reduction of L/D at low speeds mentioned above.

Fig. 2.10 Skin friction or viscous drag

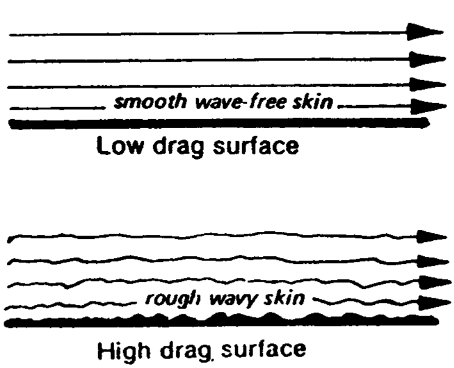

2.15 PROFILE DRAG

Form or pressure drag is caused by the total of all the pressure variations over a body as the air flows round it, and skin friction or viscous drag is caused by the contact of the air with the model's surfaces. Although it is useful to separate these different types of drag for purposes of study, it is clear that they almost always occur together. For instance, the wings shown in Figure 2.8 will produce both form drag and skin friction in addition to vortex drag. The body whose skin is sketched in Fig. 2.10 will probably be part of wing or fuselage which has form drag also. The relationship between skin drag and form drag is particularly close: the two affect one another. For example, skin friction is very much governed by the speed of the air flow, and the speed of the local flow next to the skin is

Fig. 2.11 The composition of the total drag of an aircraft

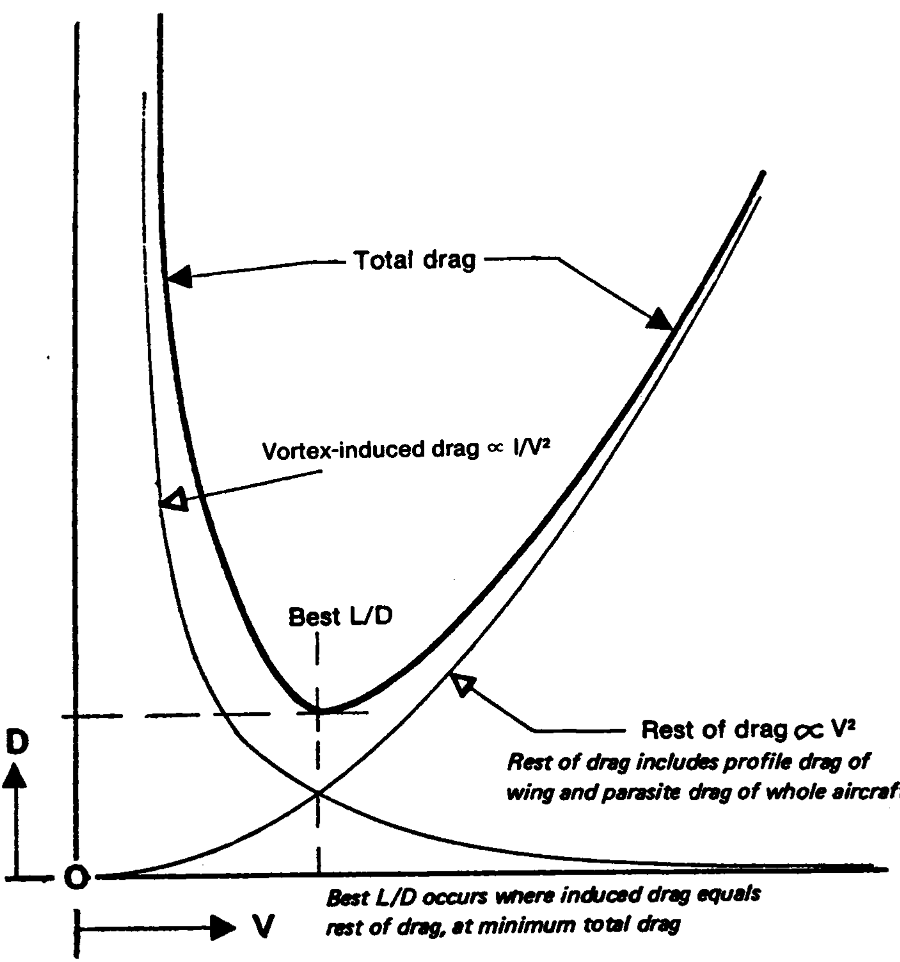

mainly determined by the shape of the body as a whole. (See Bernoulli's theorem, Chapter 3.) For this reason, particularly when wings are concerned, skin friction and form drag are commonly taken together and termed *profile drag*. In contrast to induced drag, skin friction and form drag are both directly proportional to V^2. Thus, as the induced drag falls with rising speed, the form drag and skin drag rise, and vice versa. The result, in graphical form, is shown in Figure 2.11.

2.16 TOTAL DRAG

The total drag of the aircraft is composed of the total vortex and all other drags at each speed. Where the vortex drag equals all the rest, i.e., where the two lower curves in Figure 2.11 intersect, drag is a minimum for the whole aircraft. Since lift is constant, for a given mass of aircraft in level flight, it is at the minimum drag point on the curve that the best L/D ratio of the aircraft occurs. Another, slightly more elaborate, presentation of this information appears in Figure 4.10, and in Figure 4.4 the shape of the polar curve of a sailplane is directly related to this same curve, although presented in different form in that figure, as *sinking speed* plotted against velocity rather than total drag against C_L.

3

Scale effect and the boundary layer

3.1 THE BOUNDARY LAYER

The most important differences between model and full-sized aircraft aerodynamics can be attributed to the *boundary layer*, the thin layer of air close to the surface of a wing or any solid body over which the air flows. Two properties of air, its *mass* and its *viscosity*, determine the behaviour of the boundary layer. Viscosity may be roughly described as the stickiness of any fluid. Treacle and glycerine are highly viscous at normal temperatures. Cream and water are less viscous, air and other gases are less viscous still. The viscosity, like the density of air, is beyond control for practical purposes in model aerodynamics. Like air density, it does vary with temperature and air pressure, as Lnenicka's chart in Appendix 1 shows. Inertia opposes change of direction or velocity. Viscosity resists shearing flows and tends to keep the fluid in contact with surfaces. In situations where fluid in the boundary layer over a surface is accelerating or decelerating, forces arising from mass and from viscosity interact, sometimes reinforcing one another, sometimes in mutual opposition. Where velocities of flow are high and the curvature of surfaces relatively large in radius, as with full-sized wings at high speeds, mass inertia is dominant, the effects of viscosity, though not negligible, are smaller. With model wings, at low speeds, viscous forces become relatively much more important. A very small wing, such as that of an insect, operates in a fluid which seems relatively much more viscous than the air does to the wing of an airliner. Model aircraft, and full-sized sailplanes, man-powered aircraft, hang-gliders, etc., come somewhere between. It cannot be expected that a model wing, even one made to exact scale from a full-sized prototype, will behave in exactly the same way as its larger counterpart. Unfortunately such *scale effects* almost invariably work to the disadvantage of the smaller aircraft.

3.2 THE REYNOLDS NUMBER

Experimental work published by Osborne Reynolds in 1883 showed that there are two distinct types of flow, *laminar* and *turbulent*. These may change from one to the other according to particular conditions. Which type of flow prevails in the boundary layer at any point depends on the form, waviness and roughness of the surface, the speed of the mainstream measured at a distance from the surface itself, the distance over which the flow has passed on the surface, and the ratio of density to viscosity of the fluid. A variation in any of these factors can bring about a change in the boundary layer. Reynolds combined them all except surface condition, into one figure, the Reynolds number. The formula for Reynolds number is:

$$\text{Reynolds Number, Re} = \frac{\text{Density}}{\text{Viscosity}} \times \text{Velocity} \times \text{Length}$$

In the standard symbols: $Re = \frac{\rho}{\mu} \times V \times L$ or $\frac{\rho VL}{\mu}$ or $\frac{V \times L}{\nu}$

(The Greek letter ν 'nu' stands here for the kinematic viscosity of the fluid)

Viscosity is measured in kilogrammes per metre per second, the standard value for air is 17.894×10^{-6} or .0000179 kg/m/sec ($.373 \times 10^{-6}$ slugs/ft/sec). As the equation shows, as viscosity increases, Reynolds number decreases. The average Re of a model wing or tail surface may be found using the normal flying speed as the velocity and the average chord as the length, so, for example, a wing of chord 0.1 metres flying at 10 metres per second with standard density and viscosity has Re $(1.225/.000017894) \times 0.1 \times 10 = (68459) \times 1 = 68459$. A useful abbreviation for most modelling needs is thus provided by the simplified equation:

$$Re = 68459 \times VL$$

where V and L are in m/sec and metres. If V and L are in ft/sec and feet, $Re = 6363 \times VL$. As density, velocity and length increase, Reynolds number increases. It is often suggested that since density and viscosity are not under control, for modelling purposes the VL figure alone is important and in most ways this is true providing it is remembered that the VL is expressed in units (metres × metres/sec., or ft. × ft/sec.) whereas the Re is non-dimensional. For a fuller understanding of Re effects, however, the *ratio* of inertia forces to viscosity forces in the boundary layer is what counts, relative to the speed of flow at each point. This ratio does vary appreciably according to seasonal conditions and altitude. Reynolds numbers rise in winter. (See Appendix 1).

3.3 TYPICAL AVERAGE REYNOLDS NUMBERS

Aircraft type	Reynolds Number
Commercial aircraft	10,000,000 upwards
Light aeroplane	1,000,000 upwards
Sailplane at max. speed, wing root	5,000,000
Sailplane at min. speed, wing tip	500,000
Pylon racing model aeroplane at max. speed	1,000,000 (roots)
	500,000 (tips)
Hang gliders, man-powered aircraft, ultra light aeroplanes	200,000 (tips)
	600,000 (roots)
Multi-task R.C. sailplanes	
in speed task:	400,000
when soaring:	100,000
Large model sailplanes	
Thermal soaring:	100,000
penetrating:	250,000
A-1, A-2 sailplanes, Wakefields, Coupe d'Hiver etc. max.	80,000
min.	30,000
Indoor models, 'peanut' scale etc.	10,000

Large soaring bird, (e.g. albatross or eagle)	200,000
Seagull	100,000
Butterfly (gliding)	7,000

(The above figures are all approximate and depend on the actual speeds of flight, wing chords, etc.)

Typical values of Re for various types of model are shown in the table. It is important to remember that the chord of a wing tip is usually smaller than the root, so the Re is less. For the example model with Re average about 68000, the tip chord might be 0.08 metres and the root 0.12, so the Re at each would be about 48000 and 81000. This is of special importance for the phenomenon of wing tip stalling in models.

No model flies at constant speed for long. Each change of speed alters the Re, in simple proportion. The faster the flight, the higher the Reynolds number. If the tailplane has smaller chord than the wing, the operating Re will be less for the tail.

3.4 THE BOUNDARY LAYER Re NUMBER

Reynolds number applied to a wing chord is not the same as the Re inside the boundary layer itself. As the airflow meets the wing near the leading edge, there is a point, called the stagnation point (Fig. 2.2) where the flow divides, some to pass above and some below the wing. The Re in the boundary layer at this point is zero, since the distance covered over the surface is nil. The boundary layer flow moves from the stagnation point along the skin of the wing and the Reynolds number at each point is based on the distance of that point measured round the aerofoil profile, from the stagnation point. Hence the Re in the boundary layer increases as the distance from the stagnation point increases.

By the time the boundary layer reaches the trailing edge its Re will be higher, because of the greater distance covered, than the average worked out crudely using the wing chord, which is the straight line distance from leading edge to trailing edge. Since most aerofoils have different contours on upper and lower surfaces, and the wing is normally operating at some angle of attack, the boundary layer Re at opposite stations on top and bottom will differ a little. In what follows it is important to distinguish the so-called 'critical Re' of an aerofoil profile from the 'critical Re' in the boundary layer itself.

3.5 LAMINAR BOUNDARY LAYERS

Laminar flow causes considerably less skin friction than turbulent. In a laminar boundary layer the air moves in very smooth fashion, as if each tiny layer of the fluid was a separate sheet, or lamina, sliding past the others with only slight stickiness or viscous stress between. There is no movement of particles of air up or down from layer to layer. The lowest lamina is stuck to the surface. The layer above it slides smoothly over this immobile layer, and the next above smoothly over that and so on until at the outermost limit of the boundary layer, the last lamina of all is moving almost at the speed of the main stream. The total thickness of the whole boundary layer may be a few hundredths of a centimetre. If measurements are made of the speed of flow at each level within this layer, diagrams such as Figure 3.1 may be drawn. Each arrow represents the flow speed at a point above the surface. It is found that the velocity increases fairly steadily from bottom to top. The laminae near the surface are creeping along, those next above move only slightly faster. It is this slow, smooth movement of the layers near the surface that reduces the skin friction. But because these layers are so slow, and receive little traction from the main stream, they are all too easily brought to a standstill.

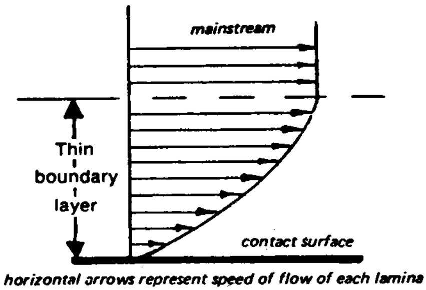

Fig. 3.1
Laminar boundary layer profile

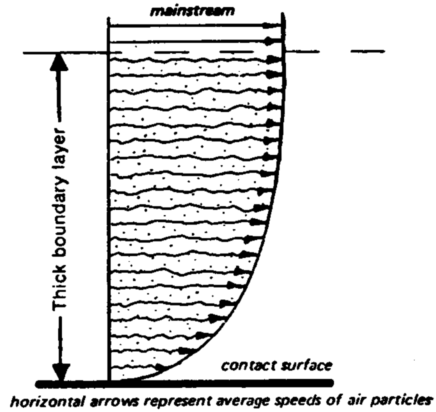

Fig. 3.2
Turbulent boundary layer profile

3.6 TRANSITION

Small surface imperfections such as rough spots, blobs of paint, fly specks, or, on a model, flaws in covering, bumps caused by protruding spars, etc., tend to disturb the laminar boundary layer, but at low *boundary layer* Reynolds numbers (i.e., near the leading edge of the wing), viscosity tends to damp down the disturbances and the laminar flow successfully over-rides them. Low flying speeds and small dimensions encourage the formation of laminar boundary layers on the leading edges of model wings. Even when the surface is not perfect, and no surface ever is, the boundary layer will initially be laminar. As the flow continues to move over the surface, the boundary layer Re rises with distance covered, and the damping effect of the viscosity becomes progressively less. Somewhere a critical point will be reached at which the small air ripples caused by surface irregularities just manage to maintain themselves without being damped out, and a small distance behind this point any minute disturbance will overcome the damping effect altogether. A distinctly wavy or rough surface will cause this sooner, i.e., at a lower Re. The laminae break up rather sharply and the flow makes a transition to turbulence (Figure 3.3). The

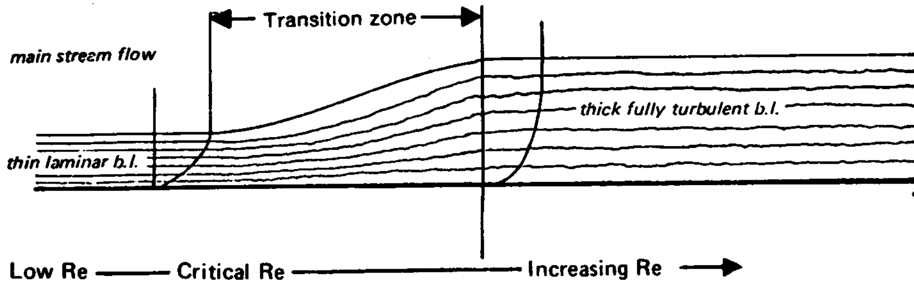

Fig. 3.3 Boundary layer transition

point or narrow zone on the surface where this occurs is the transition zone, and it is associated with a critical boundary layer Reynolds Number. At higher b.l. Re (that is, behind this zone on the wing) the boundary layer will be turbulent.

3.7 TURBULENT BOUNDARY LAYERS

In a turbulent boundary layer there is no tidy system of sliding layers. Instead air particles move with a good deal of freedom, up and down as well as in the general direction of the main flow. Although any one particle moves along at unsteady speed, the average rate of flow *near the wing skin* in the lowest parts of the turbulent boundary layer is considerably faster than it was before transition. This increases the skin friction, but because the particles are moving faster, they have greater momentum and are less easily halted. A typical velocity diagram for such a boundary layer after transition is considerably thicker as a whole than before, and as the Re rises further (i.e., as the flow moves further towards the trailing edge), the turbulent boundary layer continues to thicken. The main airstream above the boundary layer has to accommodate to this sharp thickening of the b.l. in the transition zone, and to the further thickening thereafter. In

Fig. 3.4 Effect of transition on main stream flow

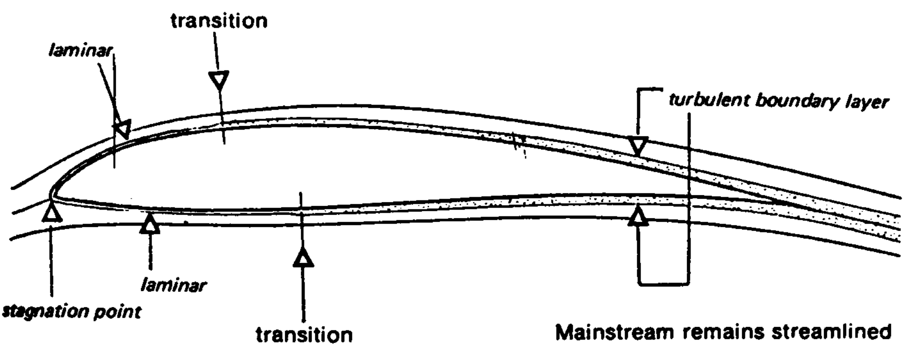

addition to the increased skin friction, the turbulent boundary layer, by compelling the main flow to accommodate in this way, increases the form drag of the wing profile (Fig. 3.4). It is as if the profile were thicker, causing a larger disturbance to the mainstream.

A very smooth surface, free from dirt, waves and other flaws, may delay transition. Transition on such surfaces moves aft, the critical Re in the boundary layer is high. A rough surface, or one with relatively large waves or bumps, brings transition forward, reducing the critical Re. For each type of surface there is a critical boundary layer Reynolds Number which for a given speed of mainstream flow is reached at some particular point. If the mainstream flow speeds up, the critical Re remains the same but it is reached earlier; i.e. the transition point or zone moves *forward* as speed rises, and *back* as speed is reduced. With full-sized aircraft transition usually takes place quite near the leading edge of wings, unless special aerofoils and very smooth surfaces, or other devices such as boundary layer suction, to remove the turbulent layers as it forms, are used. With models laminar flow tends to persist, which at first seems to give such small wings an advantage in terms of drag. Unfortunately other factors arise because of changes of pressure associated with the generation of lift by the wing.

3.8 LAMINAR SEPARATION

In Figure 3.5 it is supposed that a model wing has a laminar boundary layer at the leading edge, with fairly high angle of attack. Over the front portion of the wing the pressure decreases as the airflow accelerates. The upper laminae thus feel slightly more viscous traction from above. They speed up, and pass this acceleration down from layer to layer so that the whole boundary layer gains momentum. The increasing velocity helps to

Fig. 3.5 Laminar separation over a model wing

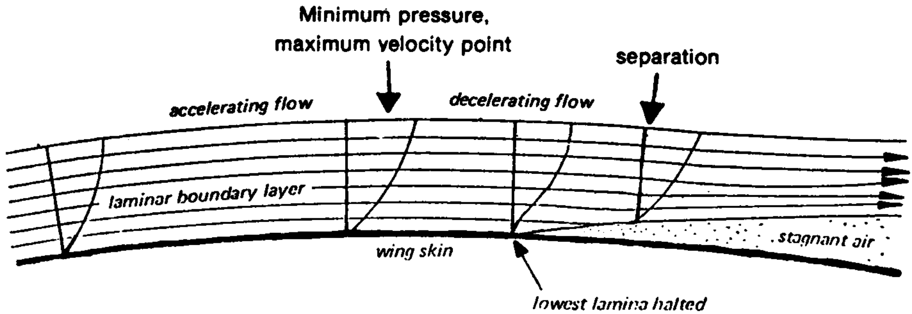

Fig. 3.6 Laminar separation with turbulent re-attachment

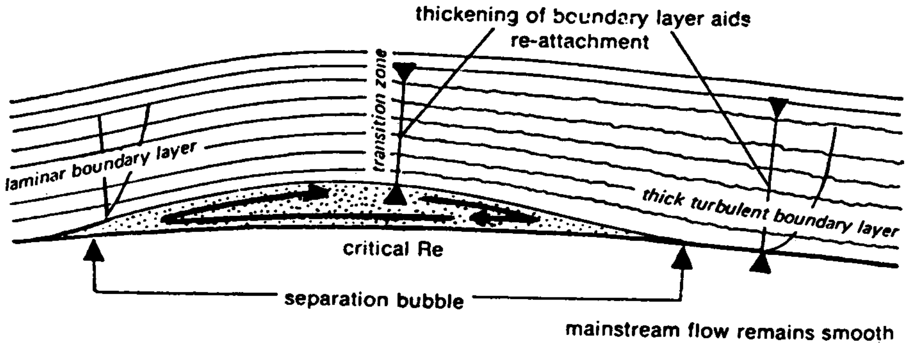

Fig. 3.7 Laminar separation with no re-attachment

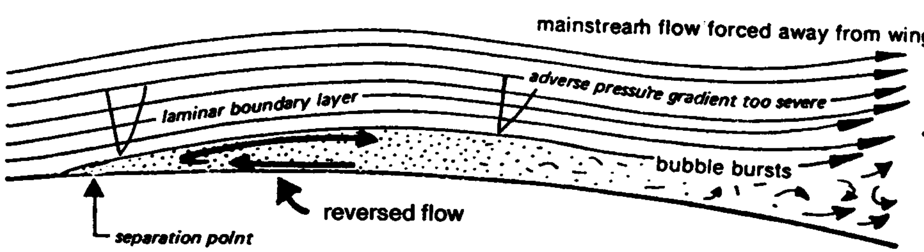

Fig. 3.8 Typical small model wing at low angle of attack

Laminar separation with long bubble and turbulent re-attachment

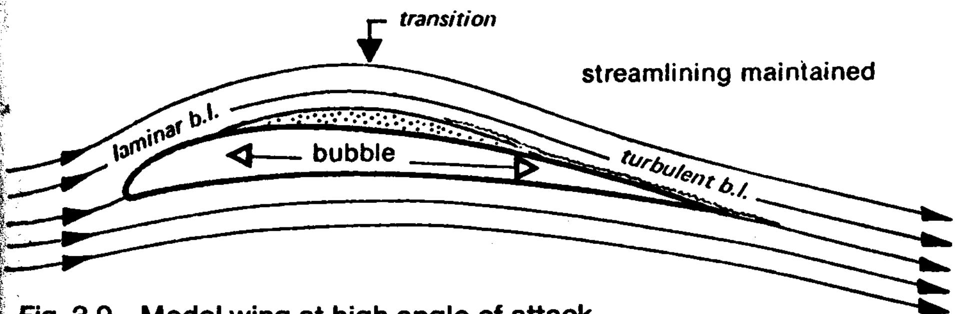

Fig. 3.9 Model wing at high angle of attack

Short bubble with turbulent re-attachment

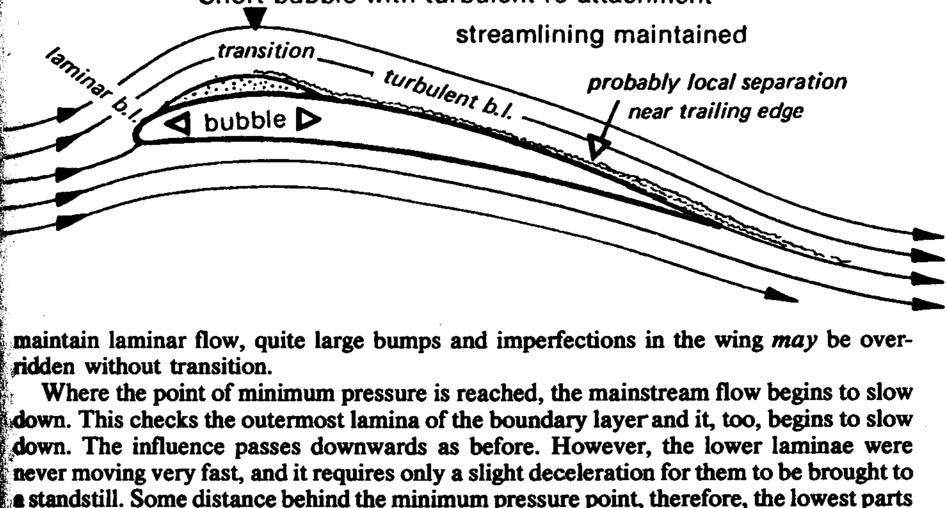

maintain laminar flow, quite large bumps and imperfections in the wing *may* be over-ridden without transition.

Where the point of minimum pressure is reached, the mainstream flow begins to slow down. This checks the outermost lamina of the boundary layer and it, too, begins to slow down. The influence passes downwards as before. However, the lower laminae were never moving very fast, and it requires only a slight deceleration for them to be brought to a standstill. Some distance behind the minimum pressure point, therefore, the lowest parts of the laminar boundary layer halt. The air at this point is stagnant, and it forms a barrier to the air moving in from upstream. The longer the deceleration continues, the more the boundary layer slows down. The stagnant barrier grows in size, forcing the flow off the wing surface altogether. This is *laminar separation.*

3.9 SEPARATION BUBBLES

With favourable circumstance, if, for example, the deceleration of flow behind the minimum pressure point is gradual, laminar separation may be followed by turbulent re-attachment (Fig. 3.6). The barrier of stagnant air disturbs the boundary layer in much the same way as a ridge or hump on the wing and if the Re at this point is large enough, this may bring about transition to turbulent flow. The increased thickness of the turbulent layer brings it back to the wing surface, leaving the zone of stagnation as a *separation bubble* underneath. After this, the turbulent boundary layer continues against the pressure gradient and may reach the trailing edge without further separation. The greater average momentum of the air particles in the lowest layers enables them to keep moving against the pressure forces tending to check them.

Within the separation bubble there is a local, detached circulation of flow with the layers of air nearest the skin flowing forwards. A very flattened vortex forms, extending spanwise. It has also been found that cross-vortices develop in the boundary layer behind the bubble, aligning themselves more or less chordwise.

Laminar separation bubbles are almost always present on model aircraft wings, often despite efforts to prevent their appearance by use of turbulators. They occur also on full-sized sailplanes and other small, slow-flying aircraft, though with less serious effects. The lower the Reynolds number, the larger the effect of the separation bubble on the total drag of the wing. Sometimes the separation bubble may be 40% of the wing chord in extent, the flow separates over the whole middle part of the upper surface, but re-attaches before the trailing edge (Fig. 3.8). At high angles of attack the minimum pressure point on many aerofoils moves forward and the bubble follows close behind, sometimes becoming shorter. The turbulent boundary layer after the bubble may then not have sufficient energy to enable it to remain attached completely, and it may separate somewhere before the trailing edge. As the angle of attack increases further, the separation point moves almost to the leading edge, and eventually the 'bubble' bursts. This is how most model wings stall (Fig. 3.7 and 3.10). *The direct result of the low Reynolds number is an early stall.* In subsequent chapters these effects are examined in respect of their influence on the design of aerofoil sections for models.

On large wings at high speeds, laminar flow rarely persists far behind the leading edge because Re is high and small imperfections of the surface force early transition without a separation bubble. Full-sized powered aircraft are thus usually free from laminar separation problems (Fig. 3.11).

Fig. 3.10 Model wing at stall

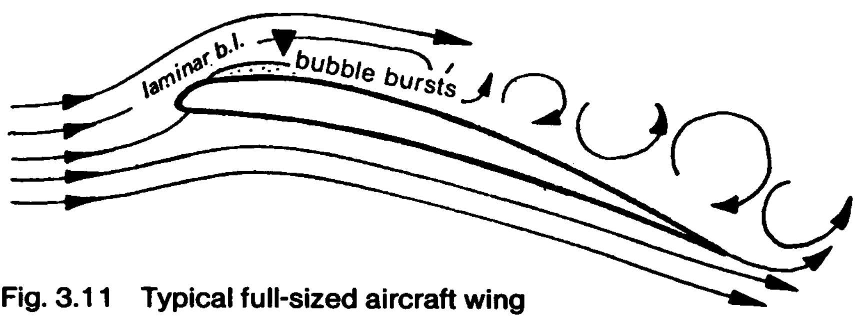

Fig. 3.11 Typical full-sized aircraft wing

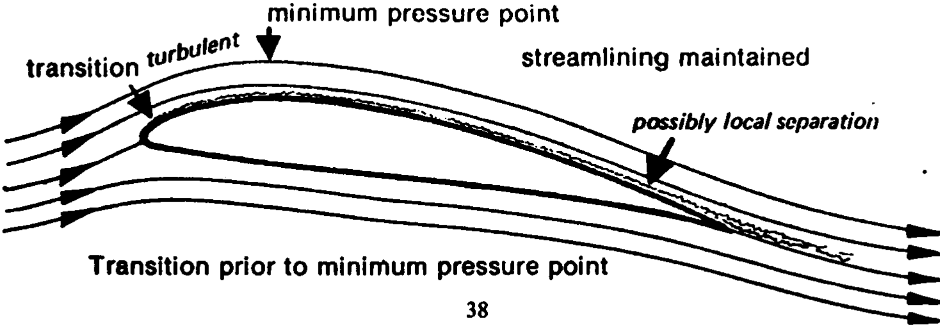

Transition prior to minimum pressure point

4

Basic model performance problems

4.1 GENERAL POINTS

The diagrams of Chapter 1 and the main relationships of lift and drag to flight velocity, wing area, etc., help in the analysis of all model performance problems. For engine driven models the need is usually either to achieve maximum speed with full control, for a pylon racer, or maximum rate of climb with a few seconds' engine run, followed by a safe transition to gliding with a slow rate of sink, for duration types. For rubber driven models the climb problem is to make the most effective use of the energy stored in a given weight of rubber, with, again, a smooth transition to gliding at the minimum possible rate of descent. For motor-assisted gliders, and electric-powered models, the primary concern may be with the margin of power available for climbing above the bare minimum required for level flight. For sailplanes the achievement of minimum sinking speed is always important, with safe characteristics on the towline for thermal soarers. For radio-controlled sailplanes, the quality of 'penetration' is equally necessary. A model with good penetration is one which still retains a low rate of descent when flying fast. This will enable it not only to make headway against a wind without too much loss of height, but in cross-country and slope soaring it will be able to pass through areas of sinking air more easily and reach the next upcurrent zone both sooner and higher than a sailplane with poor glide at high speeds.

For speed tasks, a sailplane has to fly very fast down a steep glide slope, with high speed reversals of direction at each end of the course. The requirements are very similar to those of the powered pylon racer, with the difference that the same model must also soar.

4.2 SPEED MODELS AND RACERS

To increase the maximum speed of a racer in level flight, it is easily found from Figure 1.4 that either an increase in thrust or a decrease in drag will cause acceleration. Thrust is a matter of engine tuning and correct choice of propeller. To cut drag, the model must be 'cleaned up', i.e., the total coefficient of drag, C_D, must be reduced. After the acceleration, when equilibrium is restored, drag *force* will be once again equal to thrust, but since this has been achieved by reducing C_D, the drag equation balances at a higher speed, as required. The lift force also depends on speed of flight (Fig. 2.1). To balance the lift equation at the new, higher speed, assuming the 'cleaning up' process has not involved any change of wing area or weight, the lift coefficient, C_L, must be reduced. The wing must be trimmed at a lower angle of attack. This re-trimming alone will reduce the vortex

Fig. 4.1 The lift to drag ratio of a gliding model

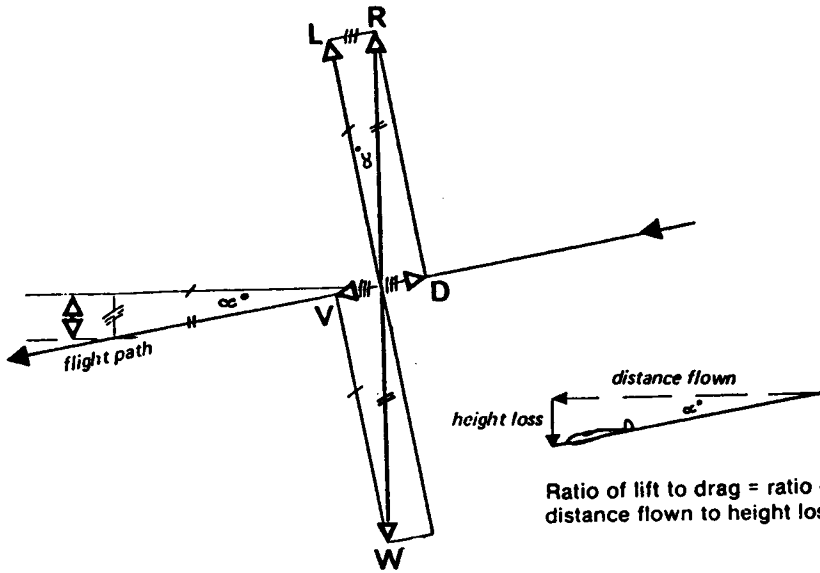

Ratio of lift to drag = ratio of distance flown to height lost

induced drag. A reduction of parasite drag of a speed model carries a bonus in the form of this reduction in induced drag after re-trimming. Also, re-trimming to another angle of attack changes the profile drag of the wing. It may or may not decrease it; this depends almost entirely on the choice of aerofoil section, especially on its camber and its thickness form.

If the minimum weight of the model is not controlled by contest rules, a lighter model requires less total lift force for level flight at any speed. This means that a lighter racing model will fly at a lower angle of attack than a heavy one of identical size and shape. This will cut induced drag, and, as before, may cut profile drag, depending on the aerofoil. A light, clean, model, with appropriate aerofoil, will fly faster.

4.3 GLIDERS: SOARING

In Figure 4.1 the forces (resolved again as in Figure 1.4) on a gliding model are shown. From the geometry of this diagram it is found that the angle of glide, α, is the same as the angle between the total air reaction force, R, and the resolved lift component, L. From this it follows that the ratio of height lost to distance covered in the glide is exactly the same as the ratio of lift to drag. (The various equalities of triangles are marked in the diagram.) For this reason the glide ratio is often quoted as the Lift to Drag or L/D ratio.

Flight at minimum sinking speed is slow at a high C_L. The minimum rate of descent occurs when the ratio of $C_L^{1.5}$ to C_D is highest. (The derivation of this is given in Appendix 1.) This ratio is often termed the power factor for a model, since it also indicates the trim condition for level flight with minimum motor power. The ratio is written in a number of ways which are all equivalent:

$C_L^{1.5} / C_D$, $C_L^{3/2} / C_D$, $\dfrac{\sqrt{C_L^3}}{C_D}$

Also, to simplify calculations advantage may be taken of the fact that:

$$\frac{\sqrt{C_L^3}}{C_D} \times \frac{\sqrt{C_L^3}}{C_D} = \frac{C_L^3}{C_D^2} = \frac{L^3}{D^2}$$

(The last gives a value which is equal to the power factor squared.) The power factor should not be confused with the maximum L/D ratio. The flattest glide, covering greatest distance over the ground in still air, is *not* the best trim for minimum sinking speed, which requires slower flight at higher C_L. Depending on the wing profile, the minimum sinking speed may occur at angles of attack fairly close to the stall, or, in many cases, at a flight speed about 75% of that for the best L/D. This is the trim to be sought when a glider is soaring.

4.4 GLIDERS: PENETRATING

Gliders hardly ever need to fly at the speed which yields the best L/D ratio or flattest glide in still air. As a rule, they are either soaring or penetrating. When penetrating, a speed faster than that for L/D max is needed. For example, in making headway against a wind, if the model's best L/D airspeed is 10 metres/sec., and it faces a wind of slightly more than that speed, flight at best L/D will cause it to move backwards relative to the ground. A higher speed would enable some forward progress to be achieved, albeit at a high rate of descent. In addition, between upcurrent zones, thermal or hill lift, there is almost always sinking air. A detailed analysis of the behaviour of sailplanes in such conditions is to be found in most books about full-sized gliding, but the modeller does not have the benefit of instruments and computers in the cockpit to tell him what his best speed to fly should be. As a very rough approximation, the model might achieve best results on many occasions

Fig. 4.2 Crossing the gaps

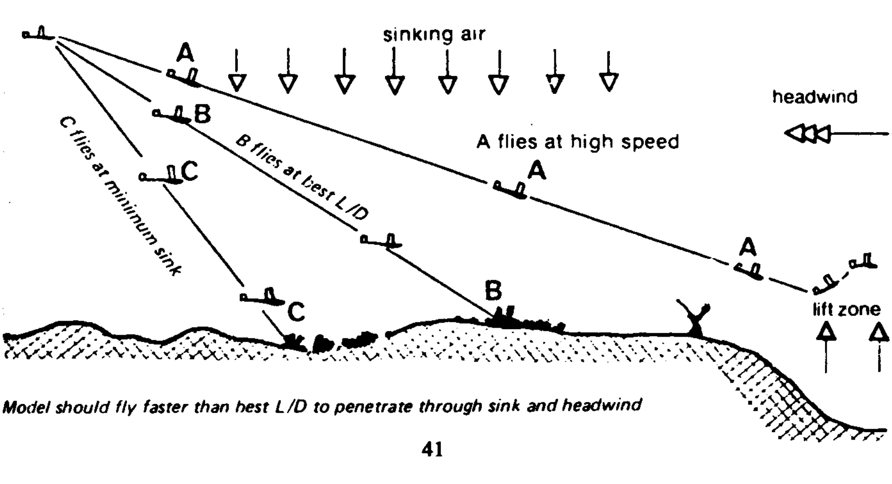

Model should fly faster than best L/D to penetrate through sink and headwind by flying between lift areas at about twice its stalling speed, and faster still if it needs to make ground against the wind (Fig. 4.2). This requires efficient, low drag aerodynamic design over a wide range of lift coefficients, from, perhaps, C_L 1.0 down to C_L 0.2 or 0.3. While the best L/D ratio remains a useful indication of a model's all-round efficiency, it is rarely important in practice.

4.5 GLIDERS: BALLAST

The addition of extra weight to a glider, assuming no other changes are made, will not affect the angle of glide or glide ratio, as Figure 4.3 shows. However, to support the additional load, the extra reaction force must be found, as indicated at R. This compels the model to fly faster down the glide path.* Ballasting a model glider does not affect the

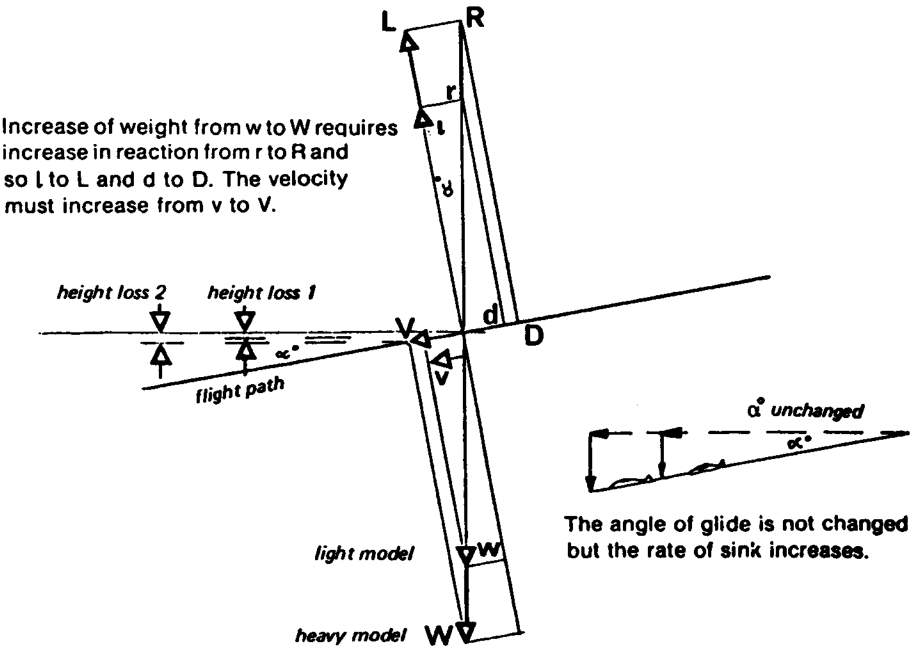

Fig. 4.3 Effect of increased weight on a glider

glide ratio but does increase the sinking speed at any particular trim. Full-sized gliders frequently carry water ballast, sometimes totalling more than the pilot's weight, to obtain good penetration, that is, good glide ratios at high speeds (Fig. 4.4). If thermals become weak, the ballast is jettisoned to reduce wing loading, W/S, and span loading, W/b, both of which reduce minimum sinking speed. There is no reason why model gliders should not adopt this technique. The advantage of jettisonable ballast for a R.C. glider is that the water may be dumped prior to landing, with much less danger to structure than the usual lead weight box. The ballast in full sized gliders is usually carried in plastic bags inside the leading edges of the wings ahead of the main spar, so their effect on trim is slight. The

*The increase in V will increase Re slightly and so change the character of the boundary layer. In practice any change in glide ratio resulting from this is small.

Fig. 4.4 Effect of weight on penetration of sailplane

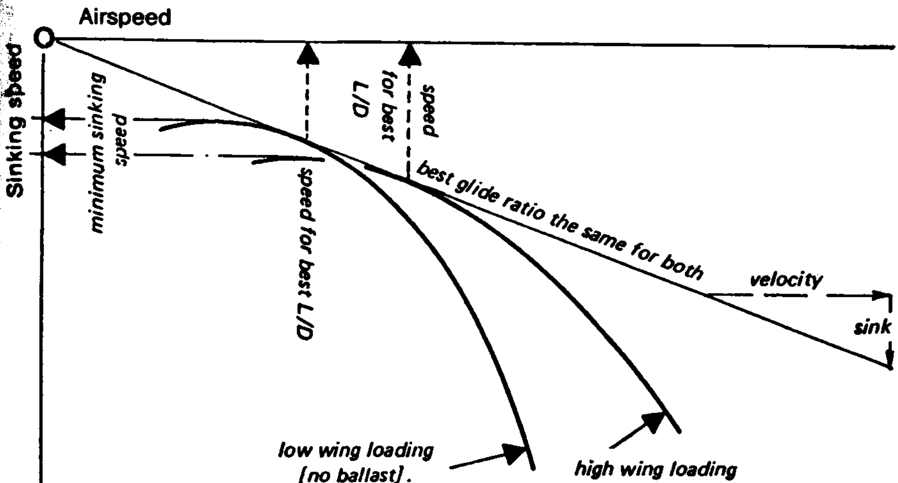

Sink of 1 metre per second at airspeed of 15 m/sec. gives glide ratio 1:15, sink of 2m/sec at 20 m/sec gives L/D 1:10 and so on. For full analysis see 'New Soaring Pilot' by Welch & Irving.

Fig. 4.5 Effect of good aerodynamic design on performance of sailplane

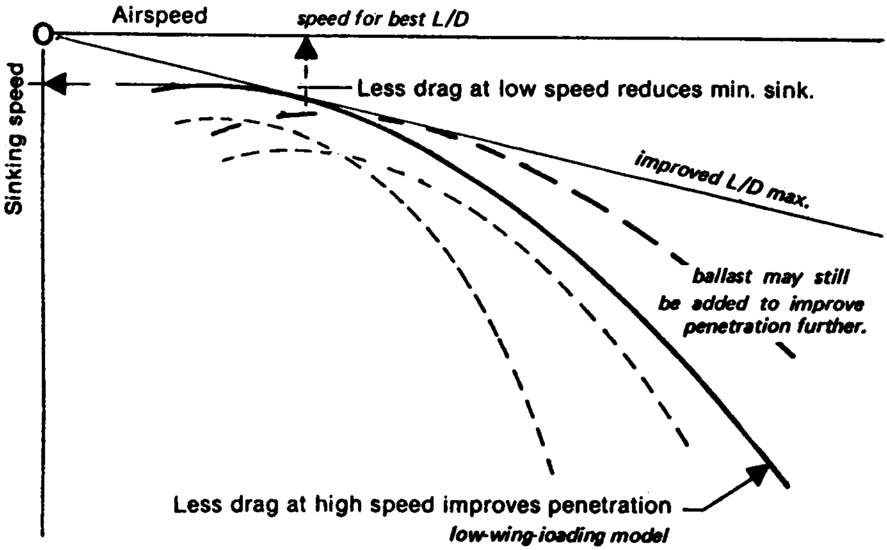

inertia in steep turns or in up-gusts actually relieves the spars of some up load. In landing the reverse occurs, so the water must go before touch down.

Adding ballast does nothing to improve the basic aerodynamic design. If the design is bad, increasing W/S will improve penetration slightly at some cost in sinking speed for soaring. By the same token, reducing wing loading will help the sinking speed but at a high cost in speed performance. A well-designed sailplane with low drag will sink slower *and* penetrate better than a clumsy design. If it is light to start with there is still the option of adding or subtracting ballast as required by conditions (Fig. 4.5).

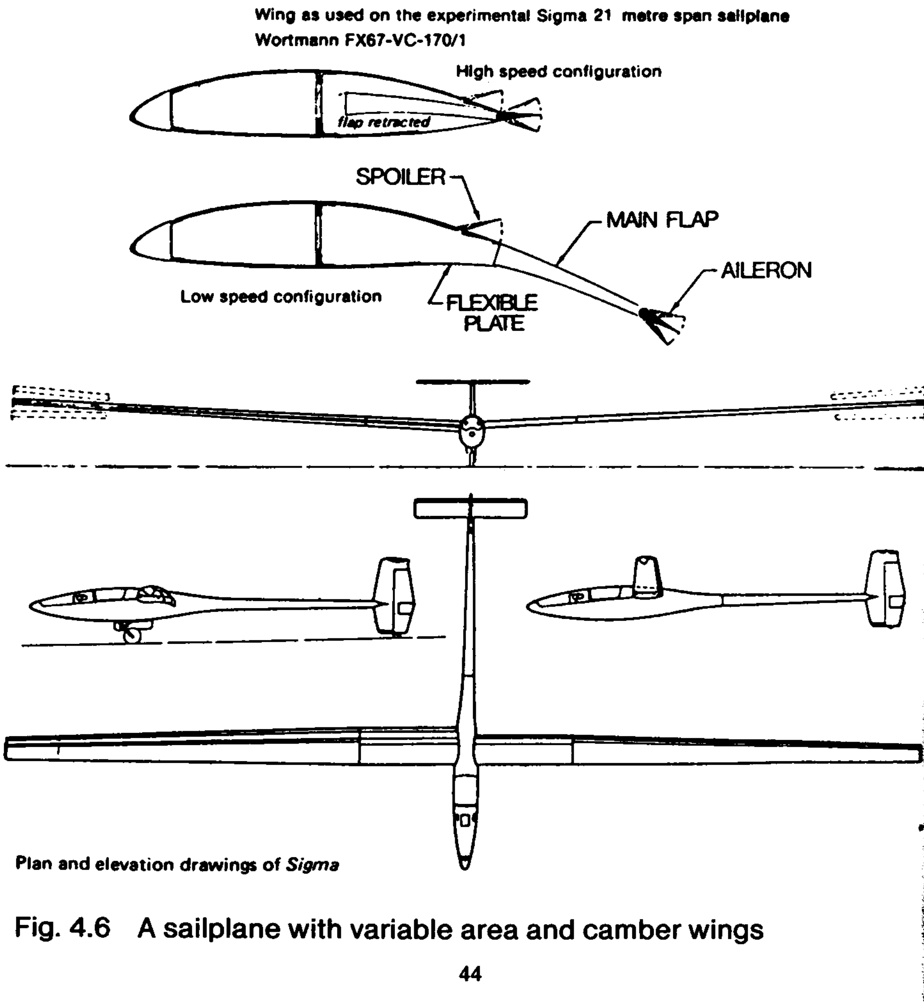

Fig. 4.6 A sailplane with variable area and camber wings

Fig. 4.7

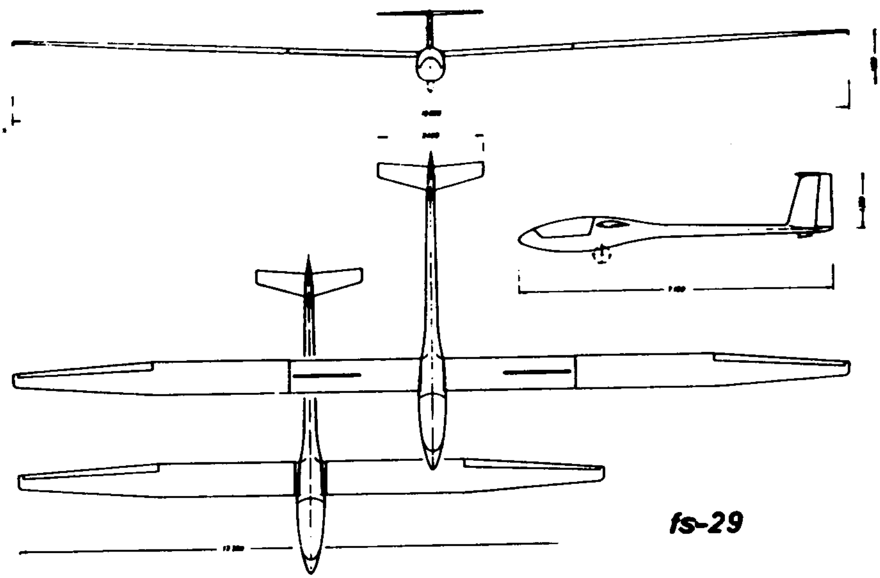

The FS-29, an experimental 13 to 19 metre sailplane with telescopic wings, enabling wing area and aspect ratio to be varied in flight: large span, high a.r., low span loading and low w/s for soaring, small span, low a.r. and high w/s for penetration. Compare with Figure 4.6 on p.44.

4.6 GLIDERS: THE SPEED TASK

At high speeds, the R.C. glider, like the racing power model, must fly at low C_L. The wing profile, for both good penetration and soaring, is expected to produce low drag at both high and low speeds. It should be specially designed to do this, as described in Chapter 9. In addition, the wing profile may be varied in flight by means of flaps or camber changing devices. In full-sized sailplanes both techniques are employed. The importance of wing loading is also brought out by mathematical analysis. The glider with light wing loading sinks slowly at low speed, at high speed a high wing loading improves penetration. The two conditions are incompatible unless wings of variable area can be used. Such complex devices have been employed on models and full-sized gliders. Large flaps, or even flexible, sail-like surfaces, may be extended on outriggers behind the wing (see Fig. 4.6). Apart from mechanical complications which tend to increase the weight and so to some extent defeat the purpose, the vortex-induced drag at low speeds of a broad chord is high. In terms of sinking speed, results tend to be disappointing, but when the flaps are retracted the penetration is improved greatly. Another solution, but involving much greater mechanical difficulties, is the variable span sailplane with wing extensions, either telescoping or folding. Perhaps inspired by the full-sized experimental FS-29 (Figure 4.7), Rolf Decker developed and flew a telescopic winged model sailplane in 1985. This may well prove to be successful in contests. Reliability of operation is very difficult to achieve. Models with interchangeable wings of various areas are fairly common, but while they enable adjustment to be made to conditions before each flight, there is no means of making changes during a flight, which is the real aim. For soaring, light wing loading and low span loading are required, for penetration wing loading should be high and span loading is less significant in terms of glide ratio at speed. Such models are not permitted in the main championship classes, unless the change of geometry can be controlled remotely by radio. It is allowed to add or remove solid ballast between flights, but not to change wings. Folding wings are another possibility.

4.7 POWER DURATION MODELS: GLIDING

Models which have only a small excess of power available for climbing, beyond that needed to sustain level flight, are necessarily trimmed to fly both under power and in the glide, at the maximum possible $C_L^{1.5}/C_D$ condition, and must be as light as possible if they are to climb at all. This also applies to many types of rubber powered model towards the end of their power run, since it is important that the climb should continue rather than the model, still under power, losing height. After the power is exhausted, these models become soaring gliders, and the same design and trim requirements govern both flight modes. They may be trimmed for minimum sinking speed in the glide and this trim should be retained as far as possible for the later stages of the powered flight. With a power assisted glider or an electric powered model the same rules apply.

Fig. 4.8 The spiral climb at high CL

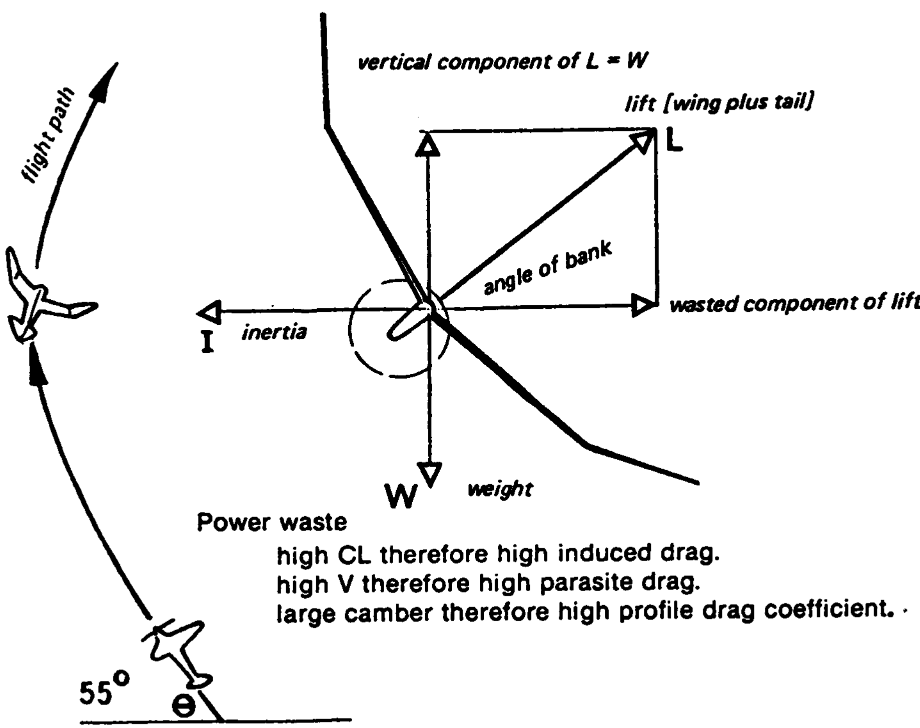

Fig. 4.9 The straight climb at low CL

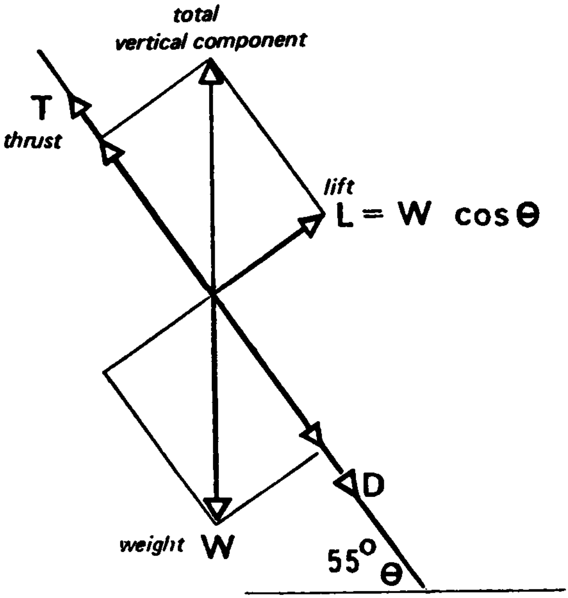

No power waste
low CL therefore low induced drag.
Small camber therefore low profile drag coefficient.
High velocity therefore high parasite drag.

4.8 POWER DURATION MODELS: CLIMBING

Many models, including modern electric-powered aircraft, have much greater power available than is necessary merely for sustained flight or a slow climb. This applies to rubber driven models immediately after launching and to all successful engine driven duration models. With these, the best trim for the glide is incompatible with that for the fastest climb at maximum power.

Consider a model with a fixed trim flying straight and level under power. The tailplane holds the wing at a constant angle of attack and so at constant C_L. If the power is increased, slightly, the first result is a forward acceleration. The C_L remains the same so this increase in V causes an increase of the lift force, and this accelerates the model upwards. It begins to climb at some angle. When it settles down again to equilibrium, as was shown in Figure 1.4, the lift *force* is *reduced* because some of the weight is supported by a component of propeller thrust. To get a reduced lift with fixed C_L velocity *along the inclined flight* path must be reduced. This is essential to balance the lift equation.

Suppose that after a flight in this condition, a little more power is added. The result will be, again after a short period of non-equilibrium, a climb at a steeper angle, but again, velocity must be reduced. The wing is still held firmly by the tailplane at its original angle of attack to the *airflow*, and as more and more power is applied, the wing lift force required is progressively reduced. For each power setting of the motor, there is one angle of climb, and only one, at which equilibrium can be established, and the steeper the angle, the slower the flight speed. Going to the extreme position, represented in Figure 1.4d, it is possible to increase power until the angle of 'climb' is 90 degrees. ***The wing then must yield no lift.*** Since the tail is still holding the wing at its constant angle of attack, the only way the wing can give no lift is if its forward velocity is zero. For equilibrium in such an attitude, a ***fixed trim*** power model must hover with no rate of climb at all. Any forward speed would generate lift on the wing and the model would begin to loop the loop. To achieve the vertical attitude and hold it, the model requires more power than it did at some less-steep attitude. (It actually climbed quite well under reduced power, whereas now at a higher power it gains no height at all.)

4.9 POWER DURATION: THE SPIRAL CLIMB

For the most efficient results in terms of rate of ascent, ways of using excess power without producing perpetual looping must be found. A model with fixed trim for minimum sink on the glide allows only one solution. Since equilibrium is impossible at full power, there must be acceleration. Looping flight is a form of acceleration, the inertia being directed outwards while the excess lift, generated by excess speed and power, is used to oppose the inertia. Instead of looping the loop, such a model must be made to turn in a spiral as it climbs. An inertia force will appear, directed outwards against the turn. The excess lift generated by the high speed will be opposed to the turning inertia by banking the wing and directing some lift force sideways. If the rate of turn is not rapid enough, excess lift will raise the model to a steeper climb angle, and rate of ascent will slow down. If the turn rate is too fast, too much lift will be directed laterally and again, the climb rate will suffer (fig. 4.8).

Although very effective, the spiral climb is wasteful of power, some of that thrust being used only to generate the sideways component of wing lift. This creates high vortex drag. Stability problems also arise.

4.10 POWER DURATION: VARIABLE TRIM

The spiral climb is effective in that it allows motors to be operated at maximum power. High rates of climb are achieved, but even better rates of climb would result if the model did not have to spiral. The speed of flight up the climb path would be greater if the excess lift force could be prevented from appearing. This can be done by reducing the angle of attack and camber of the wing, but this unfortunately spoils the gliding trim (Fig. 4.9). The best aerodynamic solution to the problem is variable trim and/or variable wing camber. By trimming the model under power to climb ***with a low C_L***, and therefore no excess lift, energy wastage is reduced and there is no need to spiral. The wing camber should be reduced to that which gives least drag at the low lift coefficient, and the tailplane trim adjusted accordingly. When the motor run ends, both camber and trim should change mechanically to give the best possible glide. During the climb, torque and slipstream effects tending to make the model turn should be trimmed out as far as possible, to keep the flight straight.

Since the climb is at low C_L and high velocity, as Figure 2.11 indicates, vortex-induced drag will be low, much lower than with the high C_L spiral climb. The parasite drag will be high, but if the correct camber is chosen, profile drag can be reduced as discussed in Chapter 7. A considerable improvement in climb results.

The rubber powered model also tends to loop under the surge of power from the motor just after release, and there is a good case for variable trim in this situation too. The tailplane setting should change progressively from that for low C_L when the motor is at full power to high C_L as the power fades. (Practical mechanisms were published in the *Aeromodeller Annual* for 1972, page 78, and in *A.M. Annual* 1974–5, pp. 122–127).

4.11 THE DRAG BUDGET

In Figure 4.10 an attempt has been made to summarise in one diagram the relative importance to different types of model of the various main types of drag. At high speeds and low lift coefficients, parasite and profile drag are dominant, vortex-induced drag is small. It follows for all models such as racers, gliders when penetrating and high powered duration models in the climb, that design efforts should be concentrated on reducing profile and parasite drag. For slow flying models, such as soaring gliders and gliding

Fig. 4.10 The drag budget

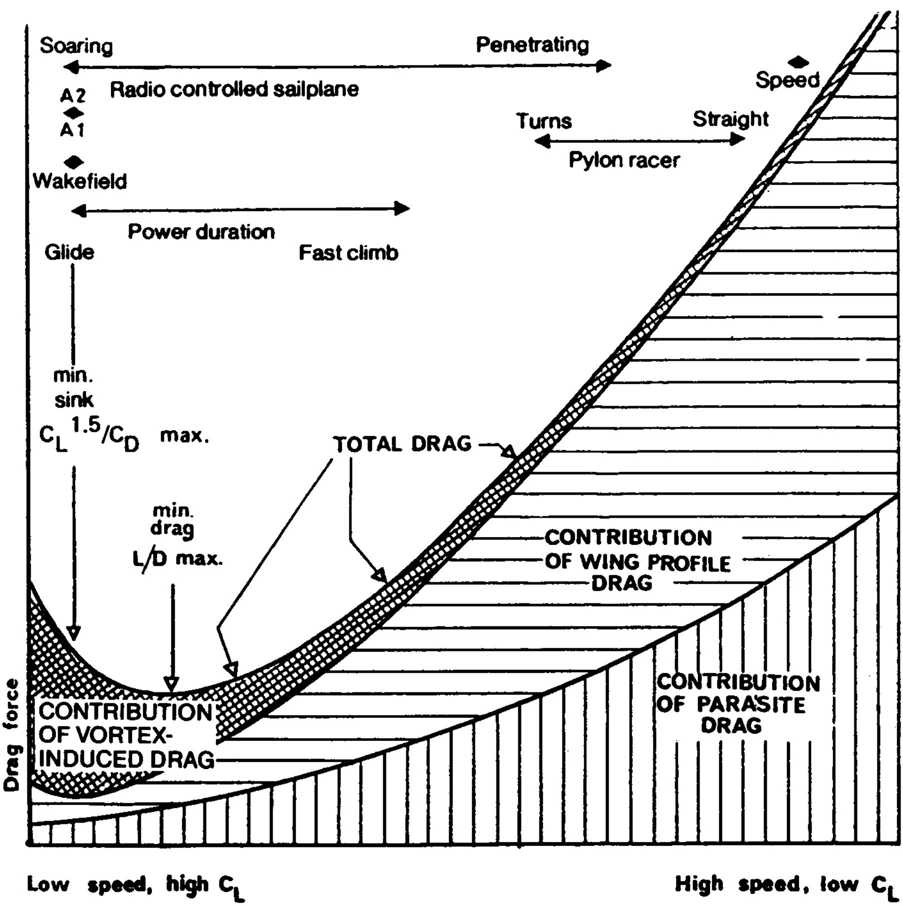

duration types, induced drag is dominant, profile drag comes a very poor second (unless by very bad choice of aerofoil, laminar separation occurs), and parasite drag is relatively unimportant. The diagram has general value, and is in many respects the key to the rest of this book. Obviously, if a racing model has been refined as far as possible with respect to profile and parasite drag, a *very little* further improvement will result if some attention is finally given to vortex drag reduction. Similarly, if a 'duration' model on the glide has vortex and profile drags cut to the minimum possible, a general 'clean up' of parasite drag items will bring further, but *minor*, improvement. The diagram gives indications as to where the main emphasis must lie. (The methods used in calculating such a drag budget for a particular model are outlined in Appendix 1.)

In all cases it should be noted that the wing alone is the main source of drag, either because of the vortex-induced drag at low speeds or because of aerofoil profile drag at high velocities. Parasitic drag – of tail or forewing, fuselage, interference between the various components, gaps and small protrusions – becomes important for all fast flying models but the wing is still dominant.

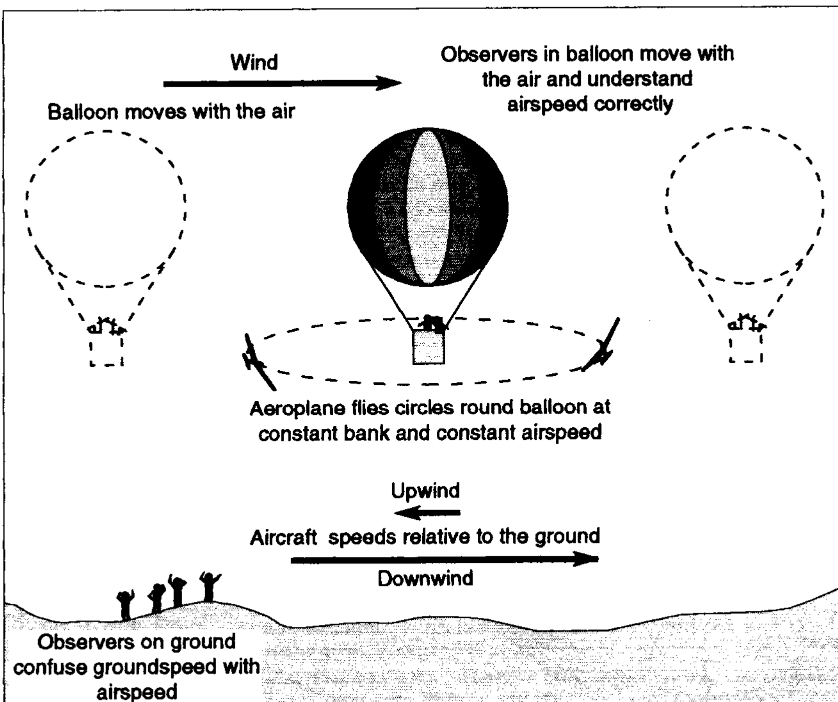

Fig. 4.11

A balloon moves with the air in which it flies. The people on board feel no breeze. A model aeroplane flying perfect circles in the air with the balloon basket as the centre, will maintain a steady airspeed and constant bank angle. From below, observers on the ground see the aircraft changing its apparent speed and become confused. To fly a model correctly the pilot should imagine only the airflow passing over the model.

4.12 THE EFFECT OF WIND

Days with no wind at all are rare. Strictly, the effect of wind on flight is not a problem in aerodynamics but one of human perception, psychology and understanding. It nevertheless seems necessary to make a brief statement since despite innumerable attempts to correct falsehoods, the errors come up repeatedly in conversations at club level and in otherwise reputable model magazines. Even some of those very experienced persons who set out to teach beginners how to fly are seriously confused about this topic and perpetuate the misunderstandings. The true facts have been known for more than a century and have been amply demonstrated in practice.

It is wise to take off and land into the wind because this reduces the speed over the ground at the moment of leaving it or arriving on it. Landing or taking off downwind or across the wind produces a much longer ground run, with more chance of the aircraft swerving to one side, running out of room or striking a bump and tipping over. Once airborne this effect disappears and *airspeed*, not groundspeed, is what matters.

The air low down is slowed by contact and friction with the ground, producing the so-called wind gradient. Coming down through the wind gradient to land has the model passing from a fast moving airstream into one that is nearly stagnant. This can precipitate a premature stall and heavy arrival, so a little extra *airspeed* is advisable during the final approach, to allow for this. Climbing out after take off, the model passes from the slow moving air at ground level into the brisker flow a few metres above. This causes a surge in *airspeed* which may require some slight trimming action from the pilot. Above a certain level, and maintaining a more or less constant height, the wind gradient does not affect the model.

On a windy day, the air low down tends to be more turbulent so it is necessary to maintain slightly higher *airspeed* when near the ground, to ensure that control is retained. This is true whether the model is flying into the wind direction, across it, or downwind when the gust strikes. At higher levels, the air is usually relatively smooth. An occasional gust can still occur but there is enough height to recover without danger.

The effect of wind on a glider attempting to make headway against it, is dealt with in Fig. 4.2 and associated text.

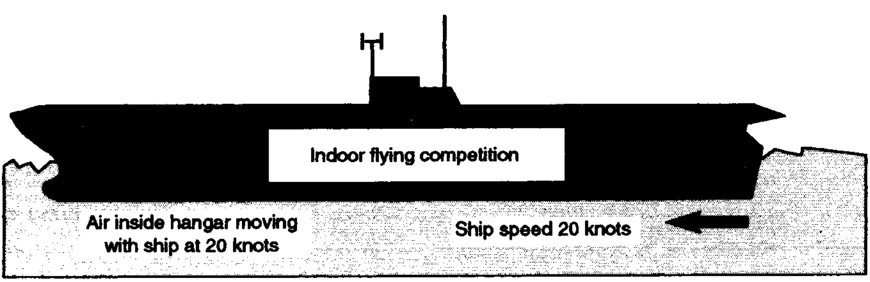

Fig. 4.12 This aircraft carrier is steaming at 20 knots.

Inside the hangar the air is moving with the ship. An indoor flying competition is being held. The models are flying in a mass of air which is moving at 20 knots. The models behave just as they would in a steady wind of this speed. There are no strange inertia or momentum effects caused by turning this way or that. The model fliers are moving with the air so they feel no wind.

The more serious muddle concerns flight when the model is well above ground.

Despite innumerable authoritative published corrections and clarifications, there are many modellers who still believe that they should trim and control their aircraft differently when flying upwind or downwind and making turns. They do not understand that airspeed and groundspeed are two quite different things, but judge the speed of the model by its apparent motion relative to their own position. Certain types of model, and certain wing profiles, are said to be sensitive to wind direction, models are said to surge upwards when faced into wind and sag when flying downwind, and so on. It is even claimed sometimes that model engines run faster when the model is going against the wind and lose revolutions or overheat when they are facing the other way. This is all nonsense. The corrective actions which are sometimes recommended actually cause accidents rather than preventing them.

A wind is the movement of a huge body of air as a whole. When a model is in flight it is totally in the air and all forces and reactions on it, including inertia, kinetic energy and momentum, result from its passage through the air with no influence at all from the ground below other than gravity. The aircraft does not feel the wind passing over the ground – it is in the air and the flow over it is generated by its own *airspeed*. This has nothing whatever to do with the motion of the air mass itself as a whole over the ground.

Two analogies may be helpful: A balloon floats in the air and if there is any wind, moves with it. Passengers in the basket feel no wind blowing them along. If they put out a flag it hangs straight down even if flags on masts below are fluttering briskly. The balloonists see the ground moving by at the speed of the wind. If one of them could launch a model aeroplane from the basket and control it from this position, it could be made to fly round and round the balloon in circles with no reference whatever to the ground. There would be none of the supposed surges and trim alterations because the pilot would be moving with the air in which the model would be flying. Flying upwind, downwind or turning in any direction, would be all the same.

Imagine flying a model aeroplane inside a large enclosed cabin, such as an empty furniture van moving on the road, or inside the enclosed hangar on an aircraft carrier at sea, or in the cabin of a huge airliner flying at 600 knots. The package of air inside the enclosed space is moving rapidly relative to the ground. The model may fly in any direction at all inside the moving air package, with no effects whatever coming from the motion of the air itself relative to the ground or sea.

The model pilot, however, is on the ground and feels the wind as a flow of air in a certain direction. From this fixed position it is easy to forget that the model is not influenced by the sensations felt on the ground. To control a model safely the pilot needs to think of the model as a thing in the air, and fly it accordingly. Pilots of full sized aircraft do this automatically for the most part and there is no reputable text book or flight instructor in full scale aviation, which confuses airspeed with groundspeed in the way modellers commonly do.

5

Reducing vortex-induced drag i. Aspect ratio

5.1 THE TRAILING VORTICES

The association between induced drag and the trailing vortices behind a wing was mentioned in the closing paragraphs of Chapter 2. This will now be examined in more detail.

The cause of the vortices is the difference in pressure between the lower and upper surfaces of the wing when it is generating lift. Near the ends of the wing the high pressure air below tends to flow outwards and round the tips towards the low pressure side. The main fore-to-aft flow stream is deflected slightly outwards on the under surface and slightly inwards above. There is also an upward component of flow outside the ends of the wing. A vortex forms behind the wing tip and trails off downstream as shown in Figure 5.1. In a simple theoretical representation, the tip vortices may be envisaged as continuations of the bound vortex of Figure 2.6. The bound vortex cannot end abruptly at the end of the wing, so it may be supposed to turn back through a right angle to form a U or horseshoe shaped vortex system as sketched in Figure 5.2.

The real picture is more complex. The cross flow at the tips influences the inner portions of the wing causing similar, though less pronounced, cross flows under and over the wing all along the span. This effect progressively weakens as distance from the tip increases, but the result is that behind the wing not a single pair, but a whole sheet of vortices forms as suggested in Fig. 5.3. Some distance behind the wing the vortex sheet rolls together into two simple vortices, the horizontal distance between them being somewhat less than the geometric wing span. The simple horseshoe vortex gives a comparable result well aft of the wing, but near the lifting surface itself a better image is of a large number of horseshoe vortices fitting one inside the other. The tip vortex at the extreme end of the wing remains the strongest, unless a very poor wing planform is chosen.

5.2 DOWNWASH

If the wing and its 'rolled up' vortex system is viewed from the rear, as indicated in Figure 5.4, the effect of the rotation of the vortices is to create downwash behind the wing and upwash on the outer sides. This downwash is not the same as the downwash, associated with the upwash and pressure distribution, of Fig. 2.2. That was part of the lift or bound vortex mechanism. The *tip vortex* downwash produces no useful lift, but it does change the general direction of flow over the wing as a whole. The streamlined flow pattern of Figure 2.2 must be considered as superimposed upon the vortex-induced downwash. The wing is at some geometric angle of attack to the undisturbed airflow remote from the wing, but near the wing the downwash effect of the trailing vortices distorts the whole flow

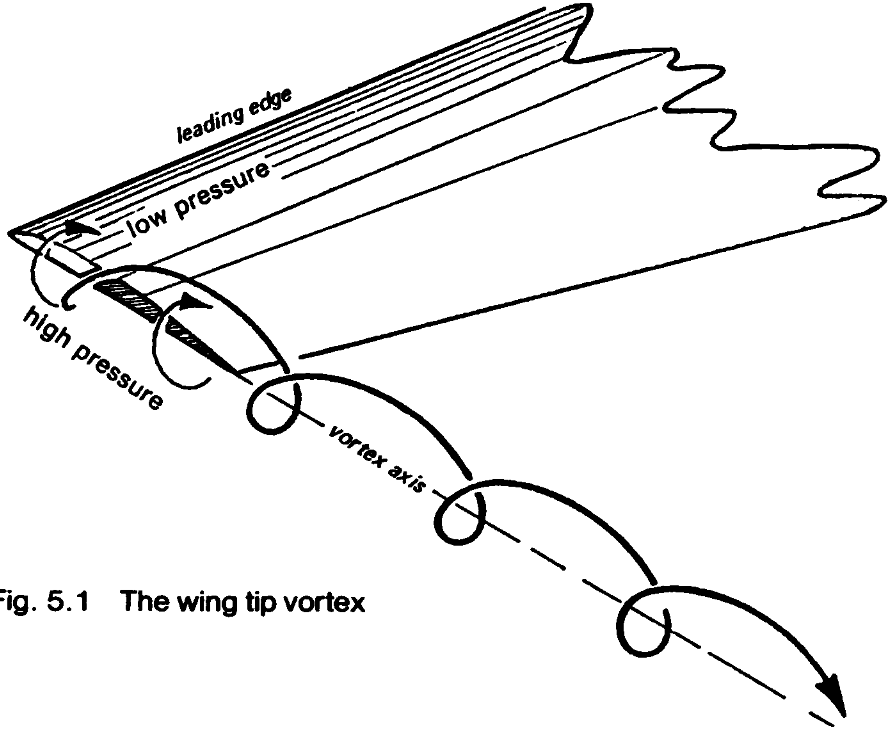

Fig. 5.1 The wing tip vortex

Fig. 5.2 The tip vortices as extensions of the bound vortex

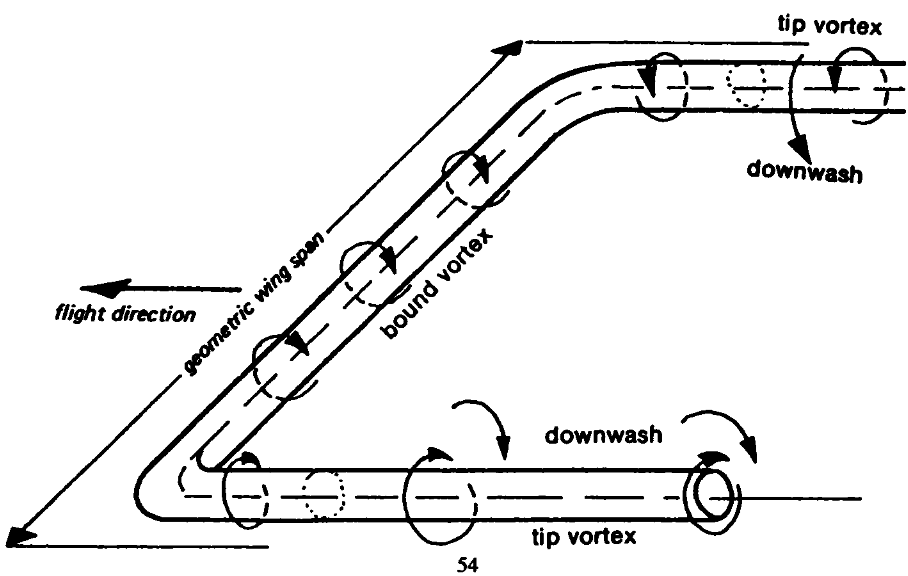

Fig. 5.3 The vortex sheet behind a real wing

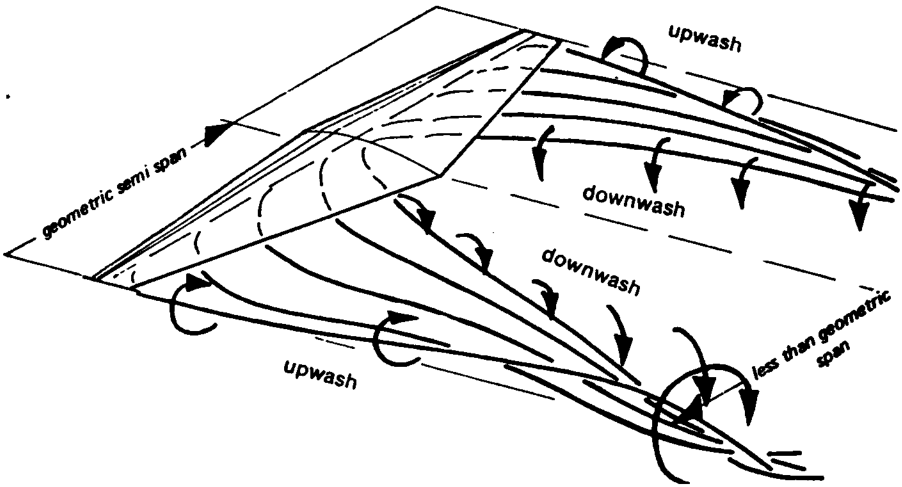

system in proportion to the strength of the vortices (Fig. 5.5). The aerodynamic angle of attack is *reduced* by the vortex downwash.

The lift force required for flight must be directed at right angles to the flight path, but the wing reaction force (neglecting profile and skin drag) is at right angles to the local airflow as changed by the downwash. The resolution of forces in Figure 5.6 shows the origin of vortex-induced drag as a component of the total reaction, directed aft. The greater the geometric angle of attack, the higher the C_L at angles below stall. The higher the C_L for a given wing, the stronger the tip and other trailing vortices, and so the more downwash influence on the angle of attack and the more induced drag. The importance of vortex-induced drag for models flying at high C_L is established.

Since the cause of the downwash is the flow round the wing tips, and since this influences the rest of the wing, if there were no tips there would be no vortex drag. A wing of infinite span is impossible but a constant chord, wing-like surface, mounted across a duct in a ventilation system or in a wind tunnel, from wall to wall, generates no trailing vortices and hence no vortex drag. Practical aircraft wings must have tips, but a wing with a very large span in relation to its area, i.e., a wing of high aspect ratio, comes closer to the ideal 'infinite' span wing than a short, relatively broad lifting surface.

Fig. 5.4 The downwash behind a wing between the tip vortices

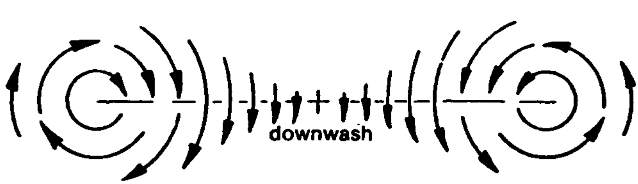

Fig. 5.5 Streamlined flow over a wing with tip vortices

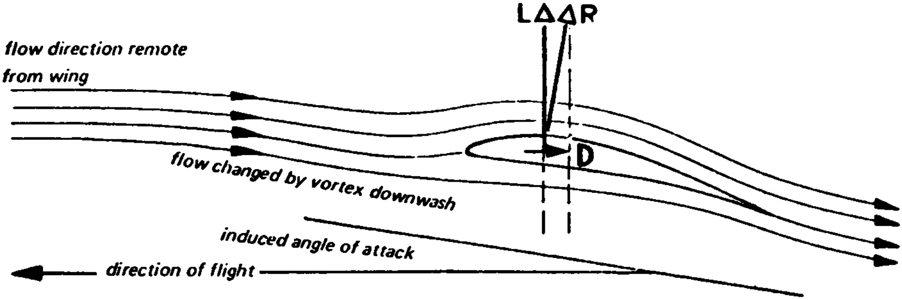

5.3 ASPECT RATIO

The aspect ratio of a wing or any other surface is found by dividing the span by the mean chord, or in cases where the mean chord is hard to determine, by dividing the square of the span by the total area, thus: $A = b^2/S$, in the standard symbols. Among models, 'A-2' sailplanes tend to the high aspect ratio side, aerobatic power models to the low. Full-sized

Fig. 5.6 Induced angle of attack

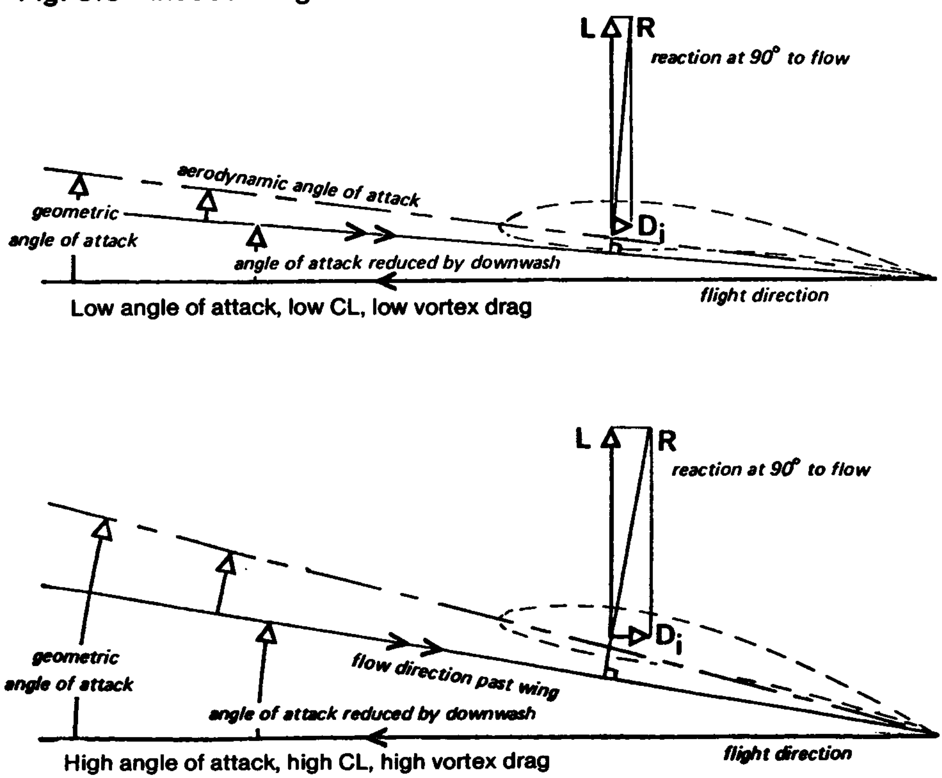

delta winged aircraft like the *Concorde* have very low aspect ratio, at the other extreme 'Open Class' sailplanes currently average about 30 to 1, while some experimental types such as the British 'Sigma' and the Brunswick S.B. 10 exceed 36:1. With a span of 29 metres the S.B. 10 has an average wing chord of just under 80 cm (95 ft 2 ins, 26¼ ins). Such long, narrow and thin wings present great problems to the engineer and to the pilot, or operator of a model. In spite of the difficulties, high aspect ratio wings are *essential* for good performances at the low speed end of the C_L scale to reduce the vortex-induced drag.

Fig. 5.7 Aspect ratio

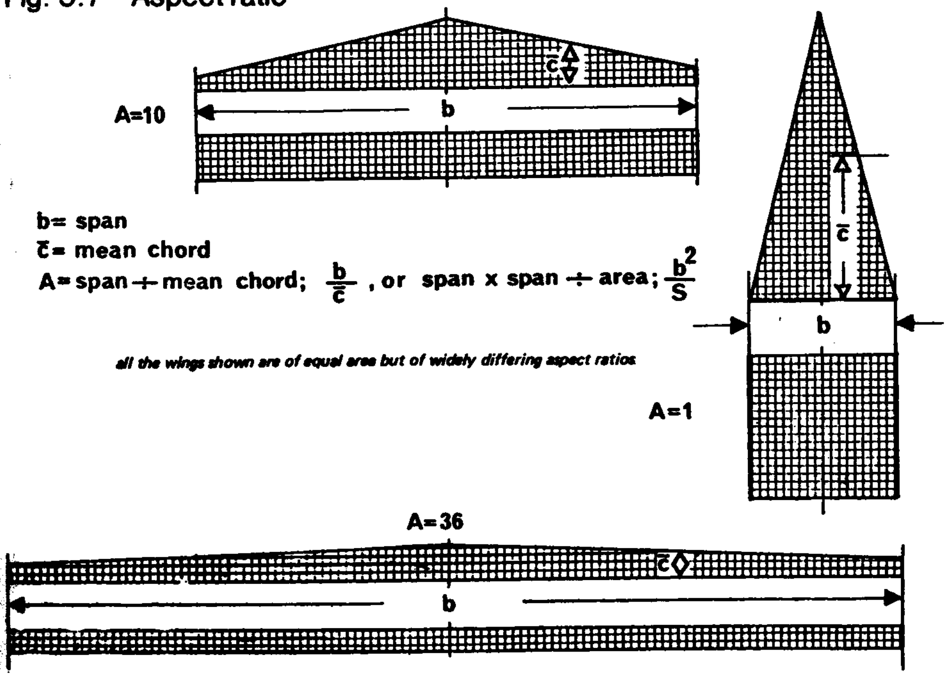

5.4 VORTEX-INDUCED DRAG COEFFICIENT

How powerful the effects of A.R. may be can be judged from the standard formula for estimation of induced drag of wing. Where C_{Di} is the vortex-induced drag coefficient, and A is the aspect ratio,

$$C_{Di} = k \times \frac{C_L{}^2}{3.1416 \times A}$$

The factor k in this equation is a correcting figure to allow for wing planform. For a well-designed wing it is only a little over 1.0. It will be given more attention in the next chapter. Otherwise, the formula shows that *doubling the aspect ratio halves the vortex drag coefficient*. The effect on the sinking speed of a contest glider or any gliding duration model is very large. As shown in Chapter 4, the sinking speed depends on the maximum value of the ratio $C_L{}^{1.5}/C_D$. Most of the C_D in slow flight is the vortex-induced drag coefficient. An example is worked in more detail in the appendix, where it is shown that increasing the aspect ratio of a model from 7.5 to 15 increases the power factor from about 16:1 to nearly 26:1. It is for this reason that full-sized sailplanes have such high aspect ratios. The reduction in sinking speed is vitally important for staying aloft in weak lift and also for climbing as rapidly as possible in stronger upcurrents. ***With a high aspect ratio sinking speeds can be very low even if the wing loading is high.*** High aspect ratio with high wing loading is one way of achieving a good soaring performance ***combined*** with good penetration. For absolute minimum sink, both high a.r. and low wing loading are needed, i.e., low ***span loading***, W/b.

5.5 THE REYNOLDS NUMBER LIMIT

There is an aerodynamic limit to the benefits of high aspect ratio, connected with scale effects as mentioned in Chapter 3, and further discussed in Chapter 7. It may be expected that if the increase of a.r. with a wing of given area results in too small a wing chord, the Reynolds number of the wing will be too low for efficient flight. This can usually be prevented by careful attention to choice of aerofoil sections of such a wing. To anticipate Chapter 7, thin aerofoils are required for low Re wings, and at tips on tapered wings.

5.6 ASPECT RATIO AND TRIM SENSITIVITY

It follows directly from the effects of downwash on the angle of attack that high aspect ratio wings are inherently sensitive to changes of trim and to up and down gusts in flight. The effect is compounded by what has just been said about the choice of aerofoils for operations at low Re. The thin type of profile needed for low Re turns out to be especially sensitive to slight changes of angle of attack because of the behaviour of the separation bubbles which form on the upper surfaces of such aerofoils. Quite apart from this if the variation of C_L with angle of attack is plotted on a graph for wings of various aspect ratios, as shown in Figure 5.8, it is found that the slope of the lift curve for the high aspect ratio wing is greater than that of the low a.r. surface. This follows from what has been said before; to achieve the same C_L with a low a.r. and large downwash, the geometric angle of attack must be higher. The aspect ratio has no effect on the angle at which the wing reaches C_L zero; this depends almost entirely on the wing camber. On the other hand, the maximum C_L of the high and moderate a.r. wings is the same since the occurrence of the stall depends on details of the boundary layer flow as described in Chapter 3. The high a.r. wing reaches this maximum C_L at a lower stalling angle, and as the diagram shows, the usable range of angles of attack is smaller.

A wing of infinite aspect ratio would have the greatest possible lift curve slope, as suggested by the broken line in Figure 5.8. The actual slope would depend on the aerofoil, but it can be shown that many aerofoils at high Re values, increase c_l by about .11 for each degree increase of angle or attack, at angles below stalling. Thin aerofoils at low Re, however, have unusually steep lift curve slopes, more than 0.11 per degree, which makes the high aspect ratio models using them even more sensitive in pitch. A gust in flight may easily change the angle of attack of a slow flying model by several degrees, and if the lift curve slope is steep such a change may take the wing up to the stall or down close to zero lift.

Apart from gust effects, radio controlled models with high aspect ratio, like full-sized sailplanes, are highly sensitive to elevator control. A small elevator movement can change the angle of attack of the main wing enough to cause a dramatic and sudden change of the lift forces: the lift momentarily exceeds the weight by a large margin. Violent acceleration

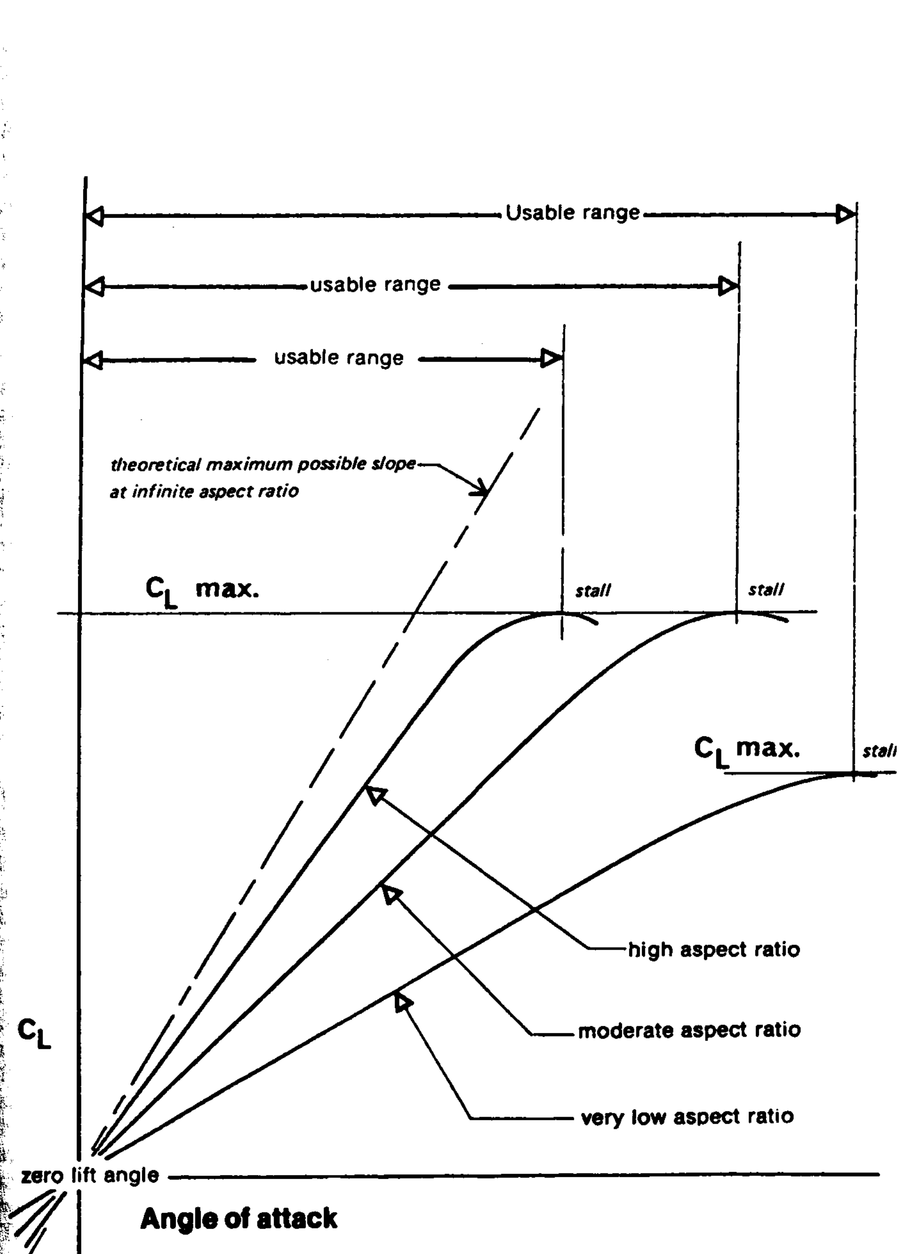

Fig. 5.8 The slope of the lift curve at different aspect ratios

results, and the inertia, or 'g', of the fuselage and all the concentrated items of mass in the model, oppose this. The wings deflect like archery bows and if insufficiently strong, may break. Such large deflections may also have unpredictable side effects, changing the stability and balance of the model, causing control rods in wings to bind or jam, wrinkling the covering or initiating wing flutter.

In trimming high a.r. models, small slivers of packing under the tailplane or wing have relatively large effects on the rigging angles of the narrow chord surfaces. On radio controlled models, for the same reason, sloppy control hinges, badly fitting push-rod ends, inaccurately centring servos, control rods that bend under load or expand in hot weather, all cause more trouble than they do on low a.r. models.

5.7 ASPECT RATIO AND ROLL RATES

In addition high a.r. models are inherently slow in roll. This is partly because of the mass of the long wing, which opposes any force tending to inititate a roll, and, once the roll has begun, resists any force tending to stop it. More important, however, is the effect of aerodynamic damping. In a roll, the down-going wing experiences an increase in angle of attack, and the up-going wing a decrease. This applies only during the rolling movement (Figure 5.9). When the roll has settled to a steady rate, inertial resistance disappears, but the downgoing wing has a higher angle of attack and the up-going surface has a lower angle of attack. This generates lift forces opposed to the roll. To keep the roll going, a

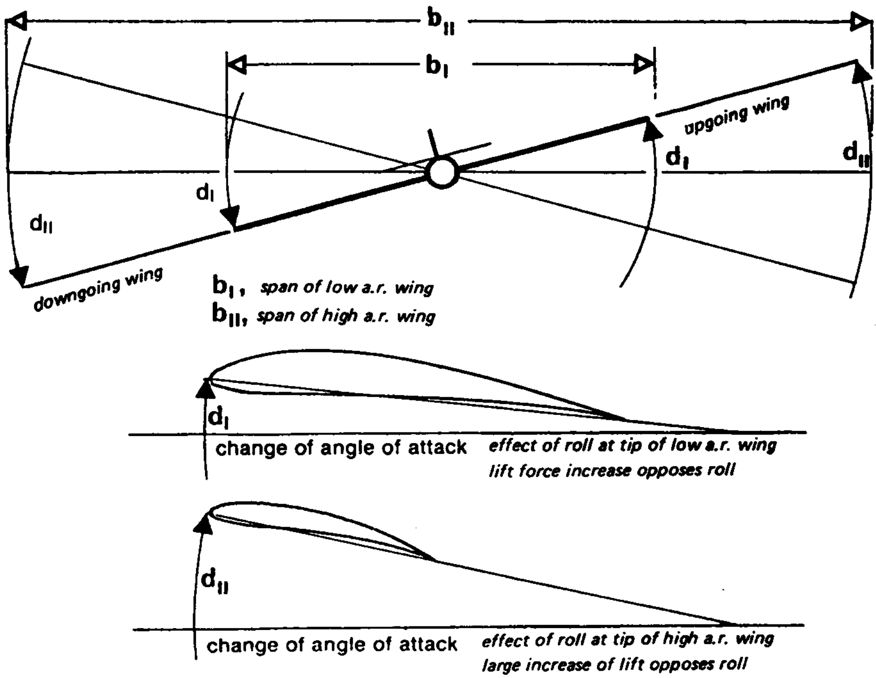

Fig. 5.9 Aerodynamic damping of roll

A large span wing tends to damp any rolling movement more than a short span, hence to achieve satisfactory rate of roll a high aspect ratio wing requires more effective controls powerful force against the aerodynamic damping must be provided, usually by ailerons. The long span of a high aspect ratio wing compels the outer panels of the wing to move through larger arcs for a given rate of roll. This creates larger damping forces. Accordingly the force to keep the roll going must be greater. Either larger ailerons are required, or they must be moved to larger angles, or other controls such as spoilers, etc., may be used to reinforce aileron effects. Many model sailplanes are controlled in roll entirely by the secondary effect of the rudder. As the aspect ratio rises this method becomes less satisfactory because the rudder is relatively ineffective in overcoming the rolling inertia and less efficient in countering wing aerodynamic damping. On the other hand, once a high a.r. wing has achieved a desired angle of bank it resists all forces tending to roll it out of the resulting turn, so such models may be steady in circling flight. A further difficulty results from the increase of speed of the outer wing tip during a turn, with a corresponding slow speed on the inner wing. This causes the lift force on the tips to change in a manner tending to steepen the angle of bank. Control of man-powered aircraft with spans over 100 ft. has proved very difficult partly because of this effect. In full-sized sailplanes it is normally necessary to 'hold off' bank in turns, by applying aileron against the turn direction. Model sailplanes require the same type of control. To maintain a steady rate of turn in a thermal a little aileron trim against the turn may be needed.

5.8 LOW ASPECT RATIO

A very low a.r. wing can fly safely at a wide range of angles, is easier to trim and less critical all round. The usable range of angles of attack is wider and gusts have less influence. A very low a.r. wing tends not to reach such high values of C_L, since such a wing is, in a sense, all tips and there are very strong cross flows. But the stall is postponed, possibly even to 45 degrees. This explains why low a.r. aircraft and deltas adopt nose-up attitudes on the approach to land.

5.9 TAIL UNITS AND ASPECT RATIO

The steeper slope of the lift curve of high aspect ratio wings is significant also for tail units. Fins in particular are often very insensitive and on radio controlled models the rudder attached to a low a.r. fin also may be ineffective. Because of the low aspect ratio a large change of angle of attack is needed to bring about a moderate change of C_L, so the stabilising or control force is weak unless the fin area is considerably enlarged to compensate. The habit of designing fins for their fashionable appearance rather than for efficiency is partly to blame. A fin is a small wing and should be treated as such. Sweepback adds nothing aerodynamically other than extra drag. The higher the aspect ratio, the more sensitive the surface will be to small disturbances or control movements. Perhaps the only modellers who have always had to recognise this are the magnet-steered-sailplane enthusiasts who obtain satisfactory control with very tall and light rudders. The low aspect ratio fin may have advantages on an aerobatic model for spin recovery. In a spin, the fin may be required to provide a correcting force in conditions of very marked cross flow. The high a.r. surface might be stalled at such an angle, with disastrous results, while the comparatively insensitive low a.r. fin will be capable of stopping the rotation. The dorsal fin extension sometimes added to full-sized aircraft has a similar effect, adding some area, reducing the fin a.r., without requiring major structural alterations.

Tailplanes and foreplanes on canards too are more sensitive if they have high a.r. It is vital that the stabiliser should not stall before the main surface on an orthodox layout. The tail aspect ratio must, for safety's sake, be somewhat lower than the wing, but within that limit should still be as high as possible. If the tail is called on to carry a proportion of the total lift in normal flight (although this is not the most efficient way to design a model), it generates vortex drag which can be reduced somewhat if its a.r. is high. With high a.r., even a 'non-lifting' tail is more responsive to small departures from the desired trim angle than a low a.r. surface, and can be reduced in area. The drag of a small, symmetrical-sectioned tail-plane at zero lift angle of attack is very low. The high a.r. tail also has a smaller proportion of its area in danger of being blanketed by the fuselage wake or cross flow from the fin. With canards, stalling of the rear plane before the foreplane is disastrous and leads to uncontrollable nose-up pitch. The foreplane must stall first and may therefore have a high aspect ratio.

5.10 DOWNWASH AT THE TAIL

All considerations of tailplane design and rigging must allow for the downwash effect of the wing on the airflow at the tail. The lower the a.r. of the wing, and the shorter the fuselage, the more downwash effect there will be. As a result, the tailplane's true angle of attack is often significantly less than the geometry of the design suggests. At the trailing edge of the wing, if the planform is roughly elliptical (see Chapter 6), the downwash angle is approximately given by the formula:

$$\text{Downwash} = \varepsilon^\circ = \frac{18.25 \times C_L}{A}$$

where A is the aspect ratio and C_L the wing lift coefficient (i.e. not including tail areas in the calculation).

At the tail for an orthodox model layout, the tip vortices will have almost completed their 'roll up', so the downwash angle there will be almost doubled. For most design purposes, it is found from the approximate equation:

$$\text{Downwash} = \varepsilon^\circ_{(t)} \frac{35 \times C_L}{A}$$

With a canard, the forewing is in the influence of the vortices of the mainplane, since, as has been said, the upwash effect is felt ahead of the lifting surface as well as behind. The effect is roughly half as great, i.e. the upwash at a foreplane would be about half the downwash if a tailplane were at the same distance aft of the wing aerodynamic centre as the foreplane is ahead of it.

It may be seen from these rough equations that a model trimmed for a high angle of attack, such as a free-flight gliding model, may easily experience a downwash angle of 3 or 4 degrees at the tail. In setting up rigging angle on the drawing board, account must be taken of this. A tailplane set at zero degrees geometrically would, in the downwash, be operating at a distinctly negative angle of attack. In a dive, of course, C_L is much reduced and the downwash approaches zero, so a tailplane set at zero geometrically would be closer to its aerodynamic zero. Many models built with 'lifting' tailplanes in fact when trimmed have their tails set, relative to the true local airflow, at a negative angle of attack. The camber then being the wrong way, they create more drag than they should.

5.11 STRUCTURAL PROBLEMS

From the engineering point of view, high a.r. wings are thinner and narrower at the roots, where stresses are high. There is less space in the wing for spars, fittings, servo mounts, etc., while the long span, relative to wing area, increases the bending moments. Wing tips are more vulnerable, because more likely to hit the ground in a low turn, yet they need to be lightly built to reduce inertia in roll and yaw. During building, the long, narrow wing requires greater care, since not only are warps more likely to develop, because of the greater length, but their effect in flight is greater because of the steep lift curve slope and added sensitivity to smaller angular changes.

In spite of such problems, for all models which are expected to soar in weak upcurrents or to climb on low power, the high aspect ratio wing is essential. The inevitable penalty in terms of extra structural weight and higher wing loading is repaid, for the radio controlled sailplane, since high wing loading aids the glide at speed for penetration. For 'duration' models too great a weight penalty is not acceptable because of the large influence of weight on the rate of climb. Even so, if the high a.r. wing can be built down to the minimum weight required for a contest model, the performance improvement on the glide will be large providing that the Reynolds number is not too low for the aerofoil section.

Aerobatic models must not be over-sensitive in pitch, and must be quick in the roll. A high aspect ratio is most undesirable for such models, although as will be mentioned again in Chapter 13, long, narrow ailerons are superior to short, broad ones of the same area. For pylon racers and speed models, aspect ratio is relatively unimportant from the drag point of view, and as with the aerobatic type, sensitivity in pitch, especially at the turns, is undesirable since it may lead to high speed stalling and an inefficient, wavering flight caused by small over-corrections by the operator.

6

Reducing vortex-induced drag: ii. Planform, twist, wingtips and winglets

6.1 PLANFORM OF WINGS

Aspect ratio is by far the most important factor in reducing vortex drag, but some model aircraft designers throw away part of the advantage gained from high a.r. by carelessness in detail. As suggested in Figure 5.2., the aerodynamic or effective span of any wing is always slightly less than the physical length of the surface, because the tip vortex leaves the wing slightly in-board of the tip. A bad choice of tip shape, or a bad planform, or a wing with too much or too little twist (variation of rigging angle from place to place), reduces the effective wing span: the wing will behave as if it were smaller in both area and aspect ratio. The factor 'k' in the induced drag equation will enlarge.

6.2 THE RECTANGULAR WING

The easiest type of wing to build is one with rectangular plan. All the ribs are identical and there are no awkward joints in leading or trailing edge members. Such a planform is not the best aerodynamically, the basic reason being that some parts of such a wing are underemployed, not carrying their fair share of the model's weight.

The circulation of air and vortex strength over one part of a wing influences the direction of flow over the adjacent parts and changes the local angle of attack. With a rectangular wing the tip vortex is strong and hence the downwash near the tip large. The closer a segment lies to the tip, the more it is influenced by the vortex. The section angle of attack near the tip, and hence the section c_l, is reduced and almost zero. Thus, although the wing chord is constant, the load carried by each chordwise section falls off sharply towards the tips. The wing, even with no geometric twist, works at reducing aerodynamic angles of attack over the whole outer span, with the result that the load distribution resembles that sketched in Figure 6.1a.

Assuming the wing is of constant aerofoil section throughout, the maximum possible section c_l, at each point is the same. Since, however, the tips are at a lower angle of attack, they are still well below the stalling angle when the roots reach it. The rectangular wing thus has an inherently safe stalling character, the wing in the centre stalls while the tips are still lifting. There is no tendency for a tip to drop first. If the model is radio controlled, the ailerons remain effective over the outer sections even when the centre is on the verge of stalling. Such wings need no geometric washout, but this is at a cost in terms of *effective* wing loading. If some of the area were taken from the tips and distributed over the central portions of the wing, the wing ***as a whole*** would stall later, at a higher total C_L, since the total C_L is made up of the average of all the section c_l's across the span.

Fig. 6.1 Planforms and load distributions

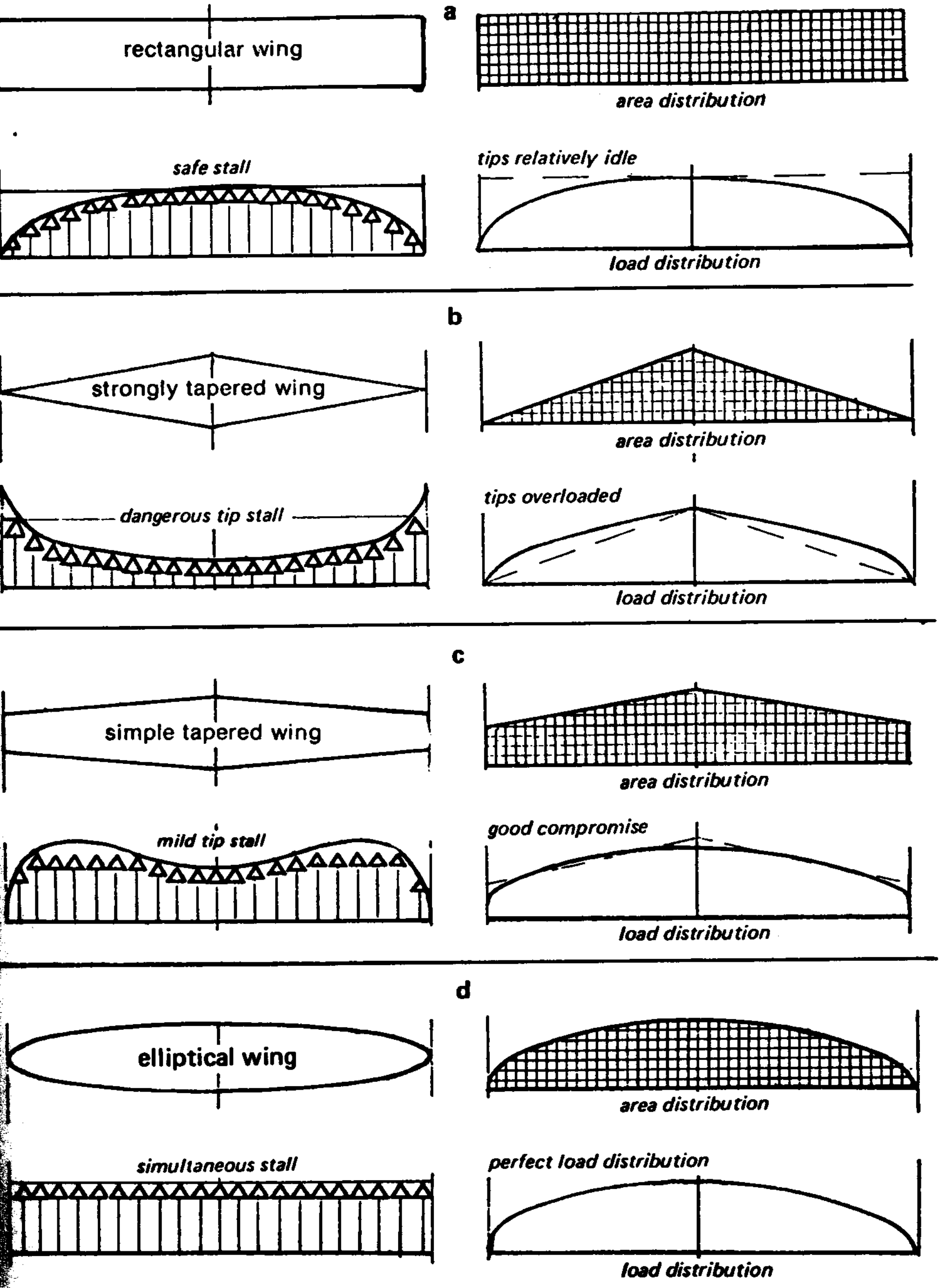

Fig. 6.2 Alternative forms of elliptic chord distribution

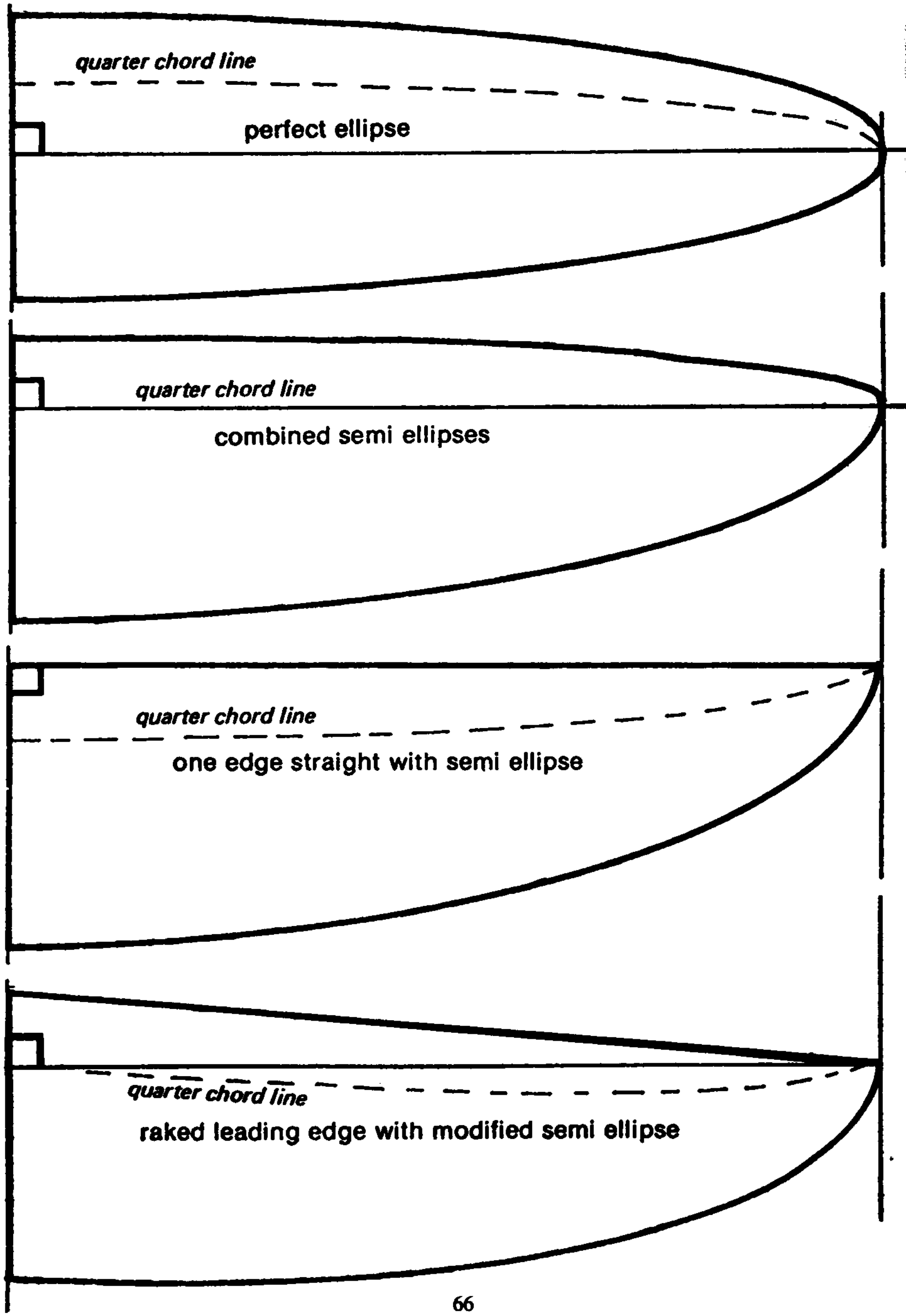

When a model wing is drawn out with a certain total area, it is too easily assumed that each part of it will carry a share of load which is in proportion to the area at each point. This is encouraged by the simple expression (see Chapter 2) for wing loading, W/S, which implies that weight divided by total area gives a true standard of comparison between models of various types. If, however, because of bad planform, some parts of a wing are relatively idle, the rest has to take on an extra burden. This implies that while one portion of the wing is lifting very little, working at a low C_L, the other parts are at higher C_L to compensate. As the equation for induced drag shows, ($C_{Di} = (C_L^2/3.142 \times A) \times k$) increasing C_L (or c_l, the section lift coefficient at a point along the span in this case) causes vortex drag to rise proportionally to the square of C_L, so the drag of the whole wing is higher. At the same time, the idle part of the wing still contributes some skin drag and profile drag. Such a bad distribution of lift is reflected in the planform correction factor, k. Noticeable losses of performance can result.

6.3 THE STRONGLY TAPERED WING

The converse of a rectangular wing is one such as that shown in Figure 6.1b, strongly tapered with tips almost pointed. This is not only very inefficient but dangerous. The strength of downwash over the various parts of such a wing is such that the local angle of attack increases towards the tips, where the *area* is smaller. There is an aerodynamic 'wash-in', the tips are over-loaded and stall first, indeed, with a wing like that sketched, they would be almost permanently stalled. The narrow outer panels are called upon to provide far more lift than their section c_l max. permits, while the roots contribute little. The model would fly better if its ends were cut off altogether, squaring the tips.

6.4 WASHOUT

The strongly tapered wing does possess one advantage. Because it has a very broad and thick root, it may be very lightly built without loss of strength. For this reason some early full-sized sailplanes such as the Rhonadler of 1932 adopted this type of wing. The tip stalling problems were avoided by giving the whole wing a marked twist or wash-out to reduce the geometric angle of attack over the outer panels by approximately the amount needed to equalise the downwash across the span. This tended to distribute the load more in proportion to the area and so reduced the vortex drag. The result was an efficient wing, but at only one airspeed. At the designed speed, the whole wing was working at roughly constant aerodynamic angle of attack, but at any other speed the distribution changed. In particular, as the speed increased, the wing tips reached their local zero angle of attack quite soon as the average angle of attack of the whole wing decreased. At any higher speed than this, the outer wing panels actually operated at negative angles of attack to the local airflow, and began to 'lift' downwards. Although this lift force was directed down, the resolved drag component was still directed aft. Thus, not only did the tips of these highly twisted wings throw extra down loads onto the rest of the wing, but they added vortex drag. More importantly, as the speed increased, the profile drag at the tips, operating at negative angles of attack, rose rapidly. From the cockpit the wing tips could be seen to bend *downwards* at some quite moderate airspeed, and the penetration suffered accordingly. The same effect may be observed on many model sailplanes with too much washout. Too much wing twist, introduced to cure a bad choice of planform, results in a 'one speed' wing. This may be exactly what is desired for an F1A ('A2') sailplane, but not for any type that needs to fly at varying speeds. Even for an 'A2', wing twist renders the model more sensitive to slight trimming errors. A small departure from the ideal airspeed causes a disproportionate rise of drag.

For reasons to do with high profile drag and premature stalling at low Reynolds numbers, calculations show that almost all the aerodynamic advantages of the tapered wing are lost on small free flight models. For this reason rectangular wings are preferred for all these. By careful use of washout, the tip vortices may be reduced in power even on such a wing, at the single trim for minimum rate of sink.

Washout often proves very useful in preventing dangerous tip stalling on all models, particularly for scale types where the wing of the prototype is strongly tapered. Washout also aids aileron control at low speeds (see Chapter 7).

6.5 WASH IN

'Wash in', the twisting of a wing to a higher angle of incidence at the tip, promotes tip stalling, increases the strength of the tip vortex and should be avoided. If, in order to trim a model for turning flight or to balance out torque reactions from the propeller, it is necessary to rig one wing at a different angle from the other, this should normally be done by warping one tip to a smaller angle, 'wash out', rather than 'washing in' the opposite tip.

'Wash in' has the same effects as drooping an aileron. Differential ailerons (see Chapter 13) are geared so as to mitigate the ill effects of this by raising ('washing out') the aileron on one side much more than drooping the other. Adverse aileron drag, causing an undesired yaw, is caused by the difference in vortex drag between the downgoing and the upgoing sides.

6.6 THE ELLIPTICAL WING

Mathematical analysis and experiment show that the only type of wing that will produce, at all speeds, constant down wash and a load distribution exactly matching the area is one with elliptical planform distribution (Figure 6.1d). This is not quite the same thing as saying the wing should be a perfect ellipse. It may be so, but any other form which gives a chord at each point the same as the pure ellipse will have the same effect. In Figure 6.2 some of the possible variations are illustrated. The effective angle of attack everywhere is the same and the C_L max. is reached simultaneously along the entire span. This follows from the equal distribution of load, area for area, of the wing. In practice, such a simultaneous stall is rarely achieved, since the wing is usually slightly yawed or 'one wing low' prior to the stall, and the elliptical planform will then appear to cause tip stalling of a mild kind. Tip stalling is also encouraged by the lower Re of the outer wing. To prevent this an increase of outer chord above that of the pure ellipse is needed. The perfect load distribution is also upset to some extent by the presence of the fuselage which disturbs the flow and, with some wing positions, may reduce the load-carrying capacity of the centre section of the wing to nothing. For these reasons the ellipse is best regarded as an ideal to be approached as closely as possible, rather than the best practical wing planform. For small models the bad effects of low Re at the tip may dictate a rectangular plan, as mentioned above.

6.7 COMPROMISES WITH THE ELLIPSE

Perfectly elliptical wings are not easy either to lay out on the drawing board, or to build accurately. Many good compromise shapes are available and these can be made lighter, because of their simplicity, so the small aerodynamic losses may safely be ignored. Several popular examples are shown in Figure 6.3. Of these, (a) was commonly found on full-sized sailplanes during the 1920s and 1930s, and still appears on many models. If used, it might be slightly modified by employing a squared tip, as shown. The curved

Fig. 6.3 Compromise with the ellipse

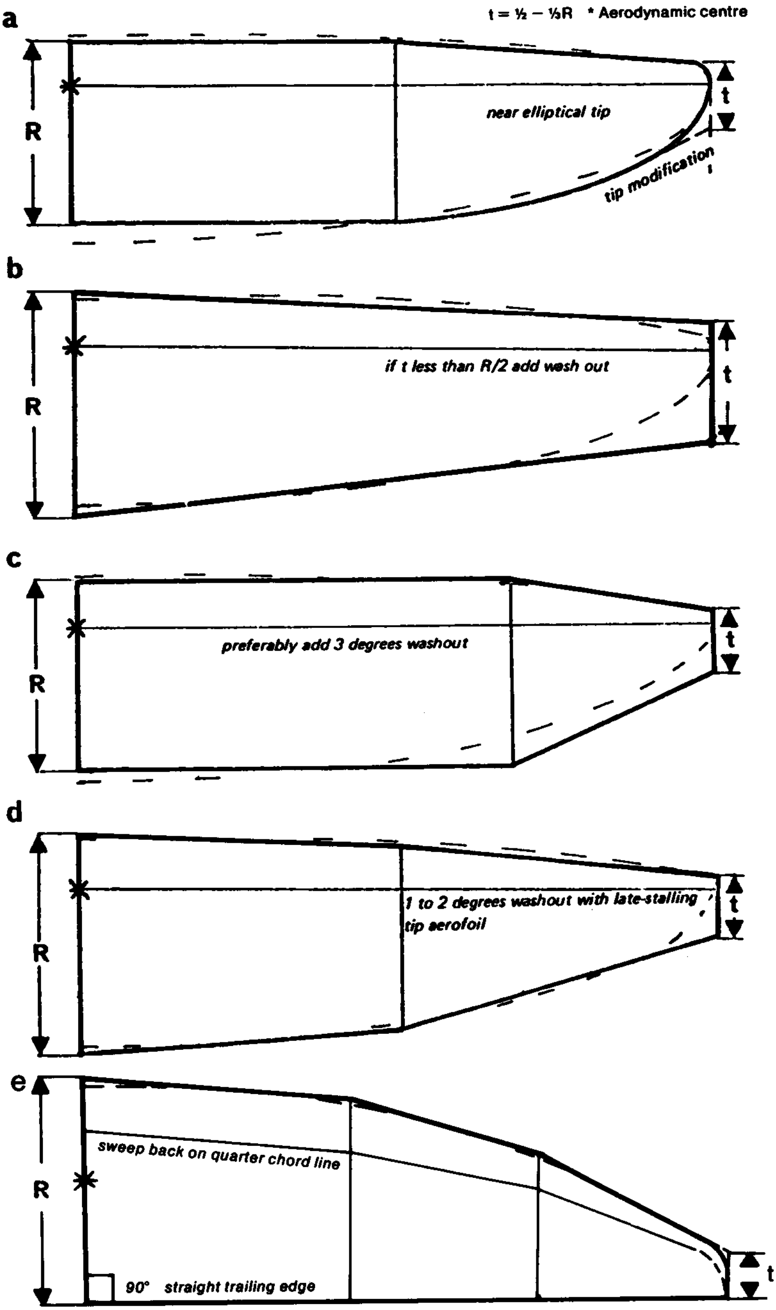

trailing edge is not altogether easy to build. Ribs over this section of the wing cannot be made by the 'sandwich' method of construction. Each rib has to be plotted and cut individually. The form in Fig. 6.3b is very good from a structural point of view, giving ample root depth for spars, and can be safe if the tip chord is not reduced too far. The stall will occur first somewhere about half way out along the wing (Fig. 6.1c). This will usually cause a mild wing drop and for aerobatic models this may help to enter spins and flick rolls. The uncontrollable tip stall of the too-strongly tapered wing, however, is never desirable. Tip stalling can be avoided altogether by careful choice of aerofoil section, as will be discussed in Chapter 7.

The planform (c) in Fig. 6.3 is good in all respects except that the root tends to be somewhat thin. It is easy to build and the departure from the ellipse is quite small. A convenient place for a dihedral joint is provided by the start of the tapered panel. Calculations by F.X. Wortmann suggest that if such a wing is built with three degrees of washout (i.e. reduction of incidence towards the tip), its performance is improved over a wide range of speeds. The washout should be progressive along the entire semi-span, rather than confined to the tapered panels only, as modellers usually do it.

The planform in Fig. 6.3d is that currently preferred by most designers of full-sized sailplanes. The approximation to the ellipse is very close and the wing root is deeper than for the previous type. To build such a wing requires a little more work, but if ribs are cut by the sandwich method only one extra template is needed, for the semispan position, and it is possible to space the ribs more widely with lighter spars and covering over the outer panels, if desired, to save mass. Again, a convenient dihedral joint is provided, and on larger models the wing may be designed to part at the mid-span position for transport.

It is argued by some aerodynamicists that a wing will produce a trailing vortex at every point where the trailing edge departs from a straight line. This is probably true where there is a marked change of dihedral, as on many model aircraft, or if there is a sharp break of taper. Following this argument some designers have adopted the planform shown in Figure 6.3e. The trailing edge of the wing is straight and is drawn at 90 degrees to the aircraft centre line. All the taper, still approximating the elliptical chord distribution, is on the leading edge. The result is a slightly swept back wing with respect to the quarter chord line so the aerodynamic centre of the whole wing is aft of the root quarter chord, which must be taken into account when positioning the centre of gravity.

Whether such a planform produces any detectable gain in vortex drag is hard to discover in practice.

Fig. 6.4 Planform to be avoided

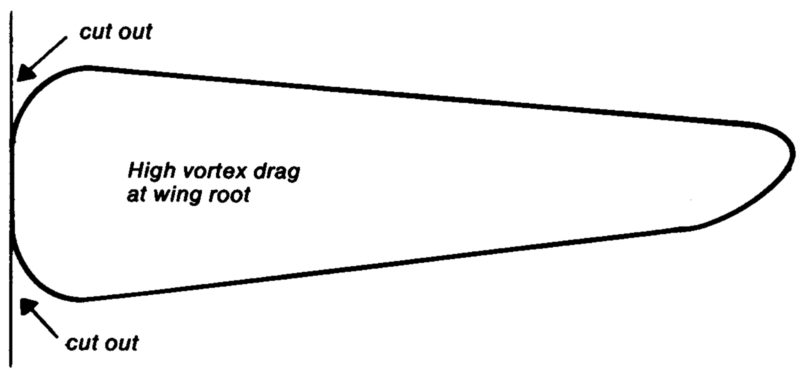

6.8 BAD PLANFORMS

Some models have appeared with the planform shown in Figure 6.4. This is no doubt intended to reduce the interference drag where the wing root meets the fuselage, but the effect is wholly bad. Vortices are created which reduce the effective span and aspect ratio of the wing. The result is somewhat similar to opening a gap between wing and fuselage at the root, in effect making the monoplane wing into two separate surfaces. On some scale models of very early aeroplanes and gliders, this may be inescapable but it has drastic influence on performance.

6.9 SWEPT WINGS

Swept wings, back or forward, are used on full-sized military and commercial aeroplanes because they are beneficial for flight approaching the speed of sound. Low speed aircraft,

Fig. 6.5 Swept wings

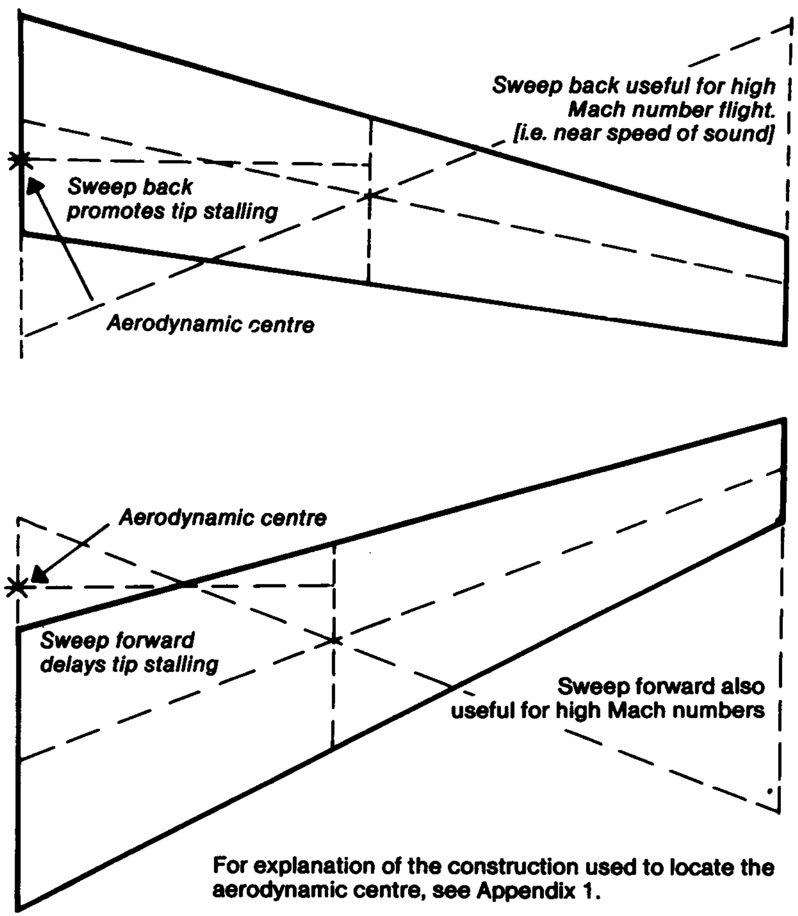

particularly two seat sailplanes, often use swept wings to assist with balance and cockpit layout. The rear pilot of a sailplane like the Blanik or Ka 13 needs a view to the sides and upwards. If the wing is straight, balance requires the rear seat to be close to the main spar of the wing and the view is then seriously restricted. Sweeping the wing forward improves the outlook (Figure 6.5). Tailless aircraft commonly have swept back wings for reasons of stability. (See Chapter 12).

Small amounts of sweep have very little effect on vortex drag. Sweep forward actually aids control at low speeds, delaying wing tip stall, but back sweep has the reverse effect and control at low speeds may require the use of special devices such as slots, boundary layer fences, etc.

Modellers using pronounced sweep-back as, perhaps, on a scale model of a jet aircraft, may find similar devices essential. Sweep-back also has a slight positive dihedral effect and may be justified on aerobatic models which, in the absence of normal dihedral, may find this effect useful for steadier flight both inverted and right side up.

Sweep forward works in the opposite sense, slightly de-stabilising the model in the lateral direction.

6.10 POINTS OF DETAIL

With all tapered wings on models, the tip chord should err on the generous side to avoid tip stalling caused by scale effects and laminar separation. The aerofoil section at the tip should normally be thinner than at the root, for the same reason.

Whatever the planform of the model, serious losses occur if there are gaps through the wing at any point. These often do appear in flight, particularly on large sailplanes, where the wings flex and work slightly apart at rigging joints. Through such gaps the air flows from the high to the low pressure side of the wing, creating turbulence and reducing lift. Control gaps have similar effects. All such leakages should be carefully sealed.

6.11 WING TIPS

Compared with aspect ratio and the general planform and twist of the wing, wing tips are of small importance in terms of drag saving although, if a wing has a very bad tip, the resulting disturbance of airflow may cause tip stalling. In the case of a radio controlled aircraft, aileron control may be affected. In general, however, the difference in performance between a model with a good tip shape and a poorish one will be barely detectable in flight. There may be something to be gained by trial and experiment, but probably not very much. Practical aircraft wings must end in tips of some kind, and wherever there is a difference of air pressure above and below a wing (or tailplane, fin, forewing etc.) a vortex will form at or near the tip. There will be a drag penalty. The greater the relative difference of pressure (i.e. the higher the C_L) the more severe the penalty will be. One of the reasons why biplanes and triplanes, and other types of multiplane, are relatively inefficient in terms of drag relative to lift is that instead of the two tip vortices of a monoplane wing, there are four, six or more.

6.12 TANDEMS AND CANARDS

If the total lift load required to support the weight of the aircraft is shared between two main lifting surfaces disposed fore and aft, as in a true tandem layout, then as with the biplane there will be four instead of two tips and four tip vortices. As mentioned before (2.5) an aircraft which has a load-carrying tail, or forewing in the case of a canard, is in a strict sense a tandem and there will be some excess vortex drag. Only if the stabiliser is

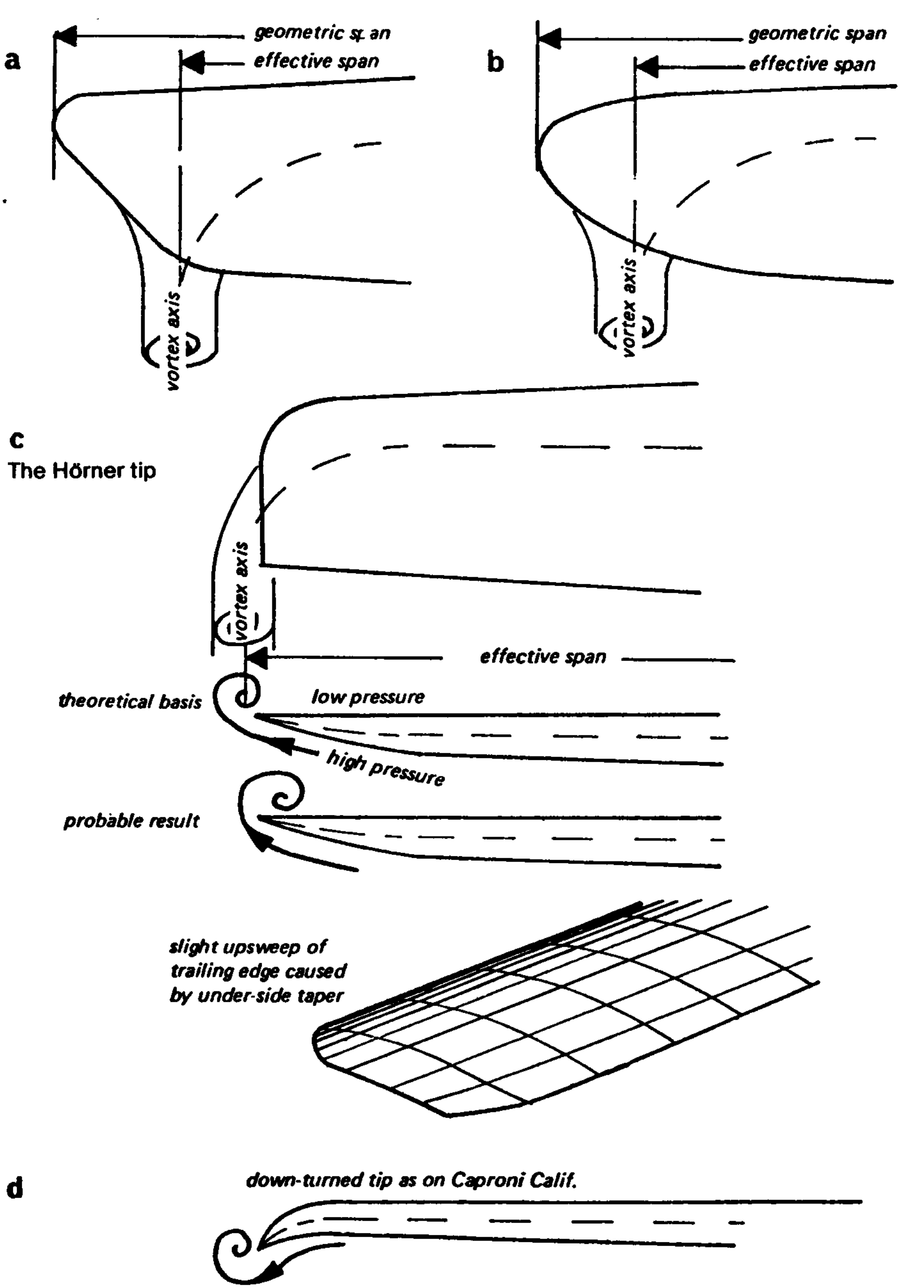

Fig. 6.6 Wing tip shapes

rigged to carry zero load in normal flight does the difference in pressure above and below the surface disappear. With it goes the tip vortices and the associated drag. Neither the tandem nor the canard permits this arrangement, which is achieved by appropriate positioning of the centre of gravity. (See further explanation in Chapter 12.)

6.13 TIPS ON FAST FLYING MODELS

It has already been emphasised that the vortex drag is most important for aircraft flying at high lift coefficients, i.e. at high angles of attack, slowly. It follows that little vortex drag is to be saved on high speed aircraft by modification to the wing tips. Parasite and profile

Fig. 6.7 Tail unit end plates

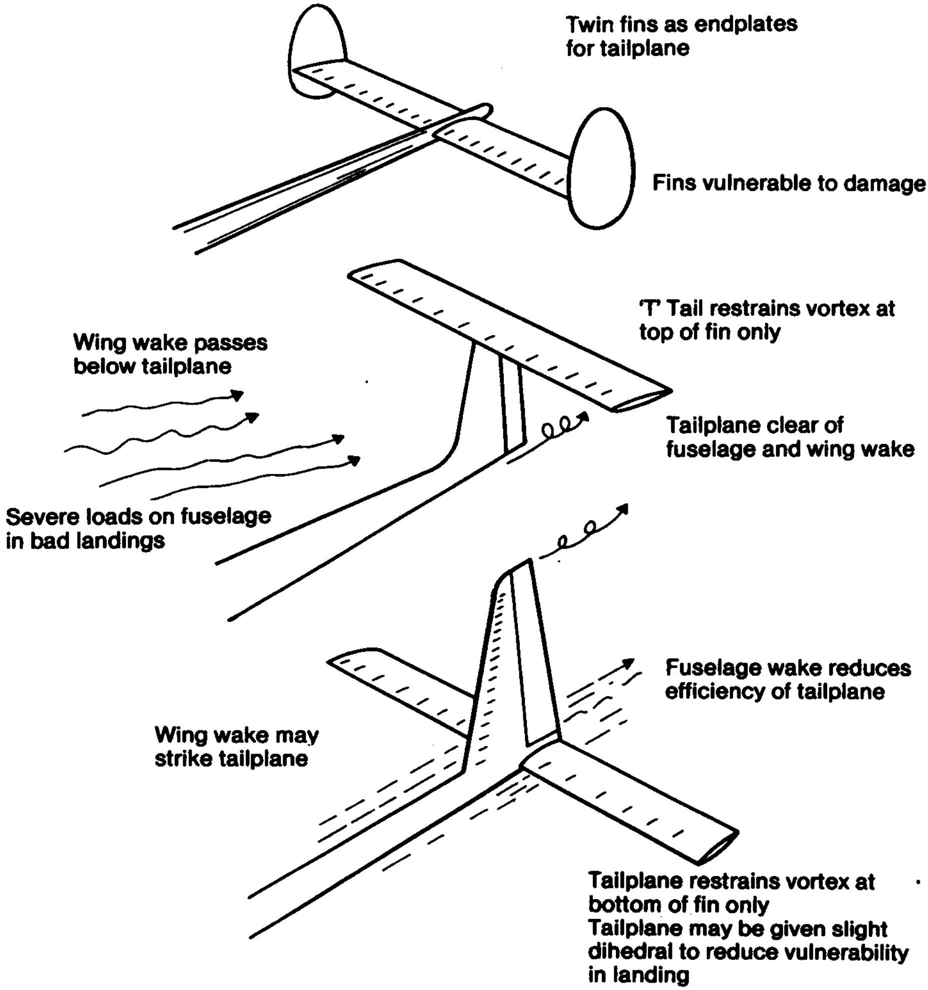

drag are much more important for such models and the wing tip should be designed for savings here. The plain squared off tip probably does lose something and should be rounded off in both front and plan views. There is not much else to be done.

What is more important is that the wing tips should be as simple as possible. Fancy appendages undoubtedly add parasitic drag and should be avoided. So should excrescences such as tip wheels, skids, etc.

6.14 TIPS FOR SLOW FLIGHT

Sailplanes and other models trimmed for flight at high angles of attack should gain something from a tip design which reduces the strength of the tip vortex or, if this can be done, compels it to form further out in the spanwise sense. Aerodynamically, the effective span of a wing is not determined merely by the geometric span. If the vortex forms somewhere inboard of the tip, which it nearly always, if not always, does, the wing loses efficiency in proportion to the inboard migration of the vortex. This is often represented by a 'span efficiency' figure and very few real wings are better than 95% efficient in this sense. Attempts to improve the wings of sailplanes and gliding models have tended to concentrate on devices to prevent the vortex forming inboard, thus seeking to increase the span efficiency as much as possible. It has not, however, been established that these methods succeed. Early full sized aircraft and many models have wing tip shapes which encourage premature formation of the wing tip vortex. If, for example, the tip is raked forward (Fig. 6.6a) or generously curved at the trailing edge (Fig. 6.6b), the vortex may be expected to form close to the point where the trailing edge curvature begins.

6.15 IMPROVING THE WING TIPS

Evidence from wind tunnel tests and flight tests on full sized sailplanes and some powered aircraft has been gathered over recent years to show that the airflow near the tip of a wing can be improved by adopting a generally upturned form.

The first support for this came from the German aerodynamicist S. Hörner, whose book *Aerodynamic Drag* was published in 1951. A development of the Hörner tip was widely adopted for full sized sailplanes, as illustrated in Fig. 6.6c. The tip is essentially square but the leading edge is curved back to meet the trailing edge approximately at right angles. On the underside the wing tapers in thickness upwards to a crisp edge, rather than a rounded form. The purpose of this is to allow the high pressure air below the wing to sweep easily to the tip where its energy may serve to carry the vortex to the extreme limit of the span. In practice the full effect does not seem to occur but the extension of the trailing edge to the extremity probably does carry the vortex slightly further out than with a rounded tip.

The Hörner tip is easy to make, quite elegant in appearance, and practical in service.

More recently, sailplanes with distinctly up curved and back swept tips have appeared, as illustrated in Fig. 6.12. These are combined with the type of wing plan shown in Fig. 6.3e. The outermost panel of the wing, usually made detachable, has a slightly increased dihedral angle which blends to a Hörner tip, and at the trailing edge of this tip a small winglet is added (see section 6.19). Because the winglets have the effect of changing the general lift distribution, the main wing is slightly less tapered than usual. For the Schempp Hirth *Ventus* 2 sailplane a reduction in the minimum rate of sink of 6% has been claimed. (This amounts to a matter of 3 cm per second or 7 inches per minute.) What is probably of more importance to the model flier is that the slight additional dihedral and the smoother flow over the tips, improves the handling of the aircraft at low speeds and gives better aileron control. Tip stalling is less likely.

Not all aerodynamicists are fully convinced of the benefits and it is always difficult to distinguish gains in performance made by improved wing section design, turbulators and the introduction of new structural materials, allowing wings to be thinner and stiffer, from the wing tip effects.

6.16 DOWNTURNED WING TIPS

Tips that turn downwards, as shown in Fig. 6.6d, have frequently been used on sailplanes. These should not be confused with the upswept Hörner tip described above. Their purpose is mainly to protect the wing tip and ailerons from damaging contact with the ground.

Aerodynamically, the downturned tip may have some good effect, tending to confine the high pressure air and restrict its movement round to the upper side, the opposite of the Hörner tip. In an exaggerated form, if the camber of the wing is carried round all the way, the result resembles the lower part of a Whitcomb winglet (Fig. 6.8). As before, there may be some benefits for aileron control and tip stalling, although little is known of this.

In the highly competitive sailplane market, fashion sometimes seems to be quite influential. There is a tendency for manufacturers and designers to introduce changes if there is even a small amount of experimental evidence to support them. The changes draw attention to their products. They stress the latest research findings, hoping thereby to make more sales to leading pilots. (These outstanding pilots usually win the competitions anyway, even when flying aircraft of slightly inferior performance.) Research goes on. Further changes, again with some scientific support, may follow after a few years. In terms of practical experience in flight, it is very difficult to show that any particular type of wing tip has a large advantage. This is the case with full sized aircraft. It is even more so with models.

6.17 TIP PLATES AND TIP BODIES

When a wing is mounted so that it completely bridges the walls of a wind tunnel, no wing tip vortices form. The bound vortex extends from wall to wall and is cut off cleanly. The wing then behaves as if it had infinite aspect ratio and vortex-induced drag is nil. Attempts have been made many times in the past to get the benefits of an infinite aspect ratio by fitting end plates or large, streamlined tip bodies which, on some full-sized aircraft, have been used as fuel tanks. The plates or bodies are intended to act like the tunnel walls and prevent the formation of tip vortices. They do succeed in this to some extent, but to be completely successful they have to be very large. (They also steepen the slope of the lift curve.) This is not achieved without penalty. The tip plates themselves cause form and skin friction drag, and this parasitic drag in total may easily be larger than the saving. This depends very much on the C_L at which the model flies. Since at high speeds vortex drag is small in any case, while form and parasite drag are large, tip plates and bodies have a very bad effect and their use cannot be justified at all for aircraft that commonly fly faster than their speed for best L/D. (See Fig. 4.10). At lower speeds, a model with a *low* aspect ratio wing may be improved by fitting end plates. The best size is about *twice* the wing *root* chord in length, according to tests carried out by A. Raspet of Mississippi State College. Such plates would be a considerable nuisance on any practical model aircraft. If the wing is already of high aspect ratio, large end plates of this type will have little effect. Since the a.r. is already high, the gain in drag from the end plate is proportionately smaller, and parasite drag no less. Tip vulnerability is greater. Plates, or tip bodies, smaller than the recommended size do not inhibit the tip vortices enough to make much difference, and still add their quota of parasite drag. They should be avoided. The few full-sized aircraft and sailplanes which do have tip bodies usually do so for non-aerodynamic reasons: for example, a sailplane wing and aileron end may be protected by a small tip body such as that of the Blanik two-seater, or the powered aircraft may lack internal space for large-capacity fuel tanks, and the wing tips may be the best place for mounting external ones.

6.18 TAILPLANES AND FINS AS ENDPLATES (see Fig. 6.7, p.74)

Tip endplates can be useful to increase the effective aspect ratio of a tailplane or fin, with possibly good effects on stability and control response. A tailplane or canard forewing fitted with end fins will have a steeper lift curve slope and become more powerful. The end fins can serve as fins for the whole model so their drag will be hardly any greater than that of a simple central fin of equal, or slightly less, area. However, the twin fins will have four tips and their aspect ratio will be very low reducing their effectiveness, and this, with their structural vulnerability, makes their use of doubtful value. They may cause more trouble than they are worth in practice. However, the tailplane itself may act as an end plate to a fin, if it is mounted on top of the fin, in 'T' configuration, or if the fin is mounted entirely above it. This restrains the vortex *at one end* of the fin and increases its effective aspect ratio. The T tail arrangement also carries the tailplane out of any possible airflow disturbance caused by the wing-root-to-fuselage junction. Both fin and tailplane may then be slightly reduced in area, which helps to compensate for the increase in structural weight caused by the necessity to stiffen the fin to carry extra loads. A high mounted tailplane is also less likely to blanket the fin during the towline launches or spinning. It is more vulnerable in ground loops and heavy landings but less easily damaged in normal landings because higher off the ground than a low tailplane.

Fins mounted ahead of or behind the tailplane are often preferred for their structural simplicity.

6.19 WINGLETS

Wing tip plates of the kind just described should be distinguished from winglets and tip sails, which are different in principle. A tip plate or body is intended to restrict or prevent the tip vortex. Winglets and tip sails are designed to use the vortex by extracting some of its energy. This not only weakens the vortex but, if the energy can be turned into a force in the right direction, there is a further small gain. Winglets of the type sketched in Figure 6.8 were first developed by R.T. Whitcomb. As shown in Figure 5.1, the airflow round a wingtip is inclined outwards on the underside, upwards just beyond the tip, and inwards above. The precise angle of the flow to the direction of flight changes as the strength of the vortex varies at different angles of attack and flight speed. If an aircraft such as a commercial jet transport operates most of its time at one steady speed, it is possible to design a set of winglets which project into the vortex flow at such angles that they can, like small wings, extract some 'lift' force. If the winglets are set correctly this force will have a forward-acting component which can appear in the general force diagram for the whole aeroplane, as an addition to the thrust. The bulk of the winglet's lift will, however, be directed laterally and this will not only tend to bend the winglets themselves but will increase the bending loads on the wing main structure. Since the winglets generate lift, each winglet will have a vortex at its end but this will be less intense than the main wing vortex without winglets. Some saving in drag results.

Winglets, as shown in the diagram (Figure 6.8) are cambered and twisted to meet the flow at each point at the most effective angle of attack. They are quite complicated to design and construct and are most efficient over a rather narrow range of flight speeds.

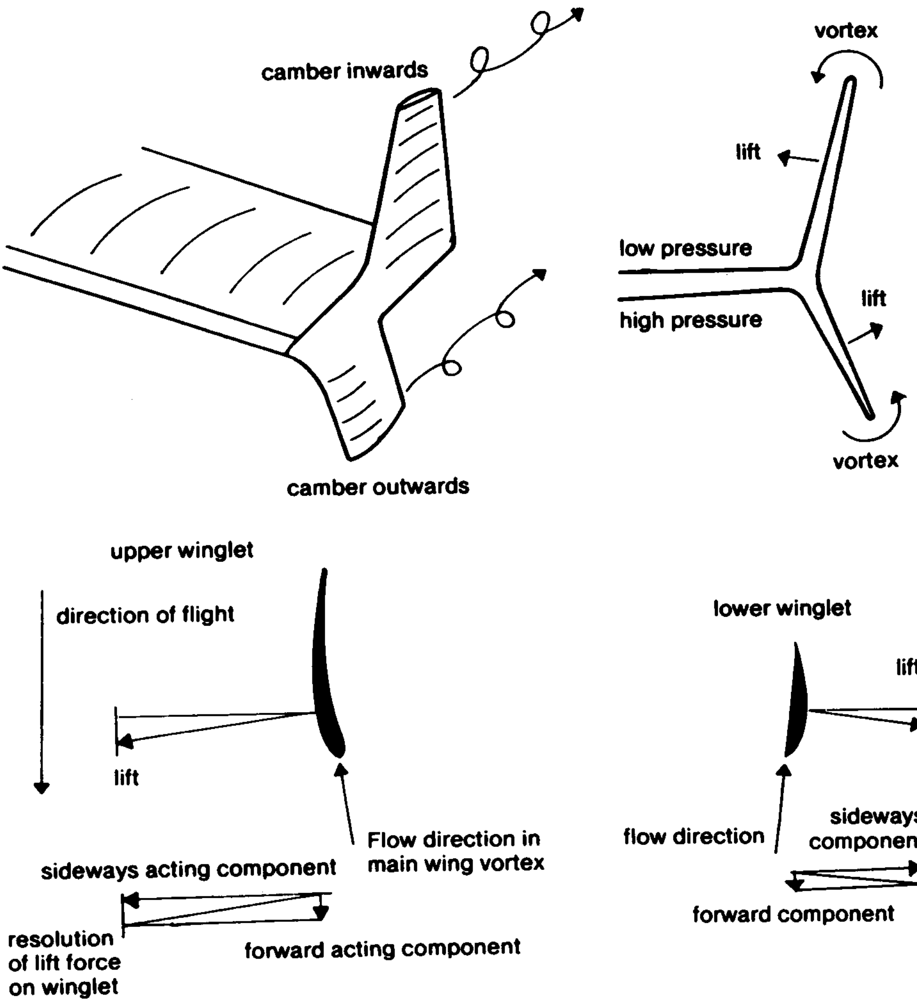

Fig. 6.8 The Whitcomb winglet

6.20 THE COMMERCIAL EQUATION

If an existing aeroplane is fitted with winglets, the increased bending loads compel some strengthening of the mainplane, adding weight, and there is a reduction in load carrying capacity. This may be compensated by the increased efficiency so that some fuel is saved. Clearly, whether the aircraft should or should not have winglets is finally determined not by aerodynamic considerations alone but by commercial factors such as the cost of the materials and the investment in design and the wind tunnel testing time, and the price of fuel. That the winglets do work as their inventors claim is not doubted, but this does not imply they should necessarily be fitted to every commercial aeroplane.

Fig. 6.9 Spillman (Cranfield) tip sails

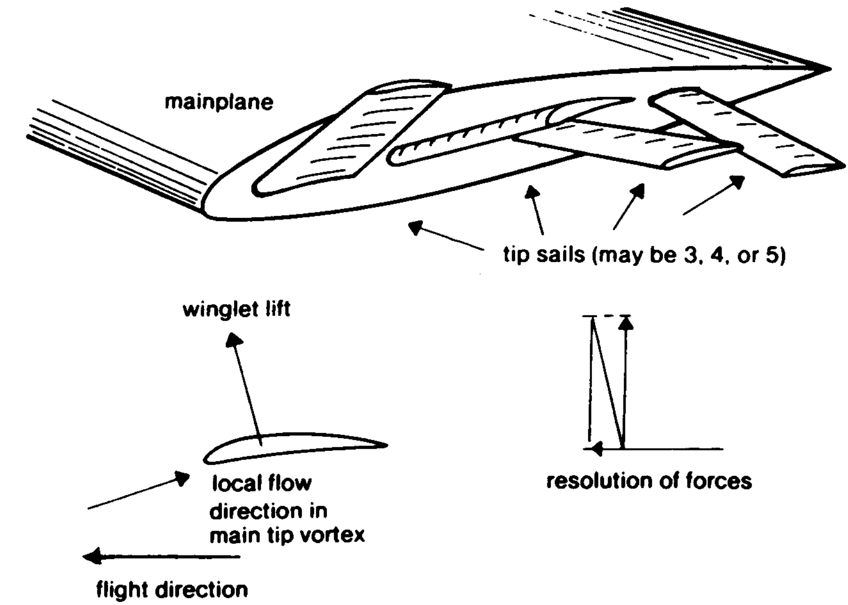

6.21 DISADVANTAGES OF WINGLETS

It has been shown in Chapter 5 that the most effective method of reducing vortex drag is by increasing the aspect ratio, i.e. increasing the wing span for a given total area. It follows that whatever the gain from using winglets, a similar improvement could be achieved by an increase in aspect ratio. This could be done by fitting a simple wing extension. Such a span extension would, of course, increase the bending loads on the mainplane and would add weight, so the best solution is again decided by economics rather than aerodynamics. Nonetheless, whereas winglets require considerable research and, usually, wind tunnel testing to ensure they are of the most favourable shape and set at the best angle, to lengthen the wing is comparatively simple. Moreover, stretching a wing in this way is guaranteed to reduce vortex drag at all airspeeds. A longer wing is more prone to flutter problems and slower in roll than a short wing, but adding winglets to a short wing also increases the danger of flutter and the additional mass at the tip creates more rolling inertia.

6.22 TIP SAILS

At about the same time as the Whitcomb winglets were being developed, J.J. Spillman was working on tip sails of the kind shown in Figure 6.9. These were inspired by the wing tip feathers of some large soaring birds, which are spread, finger-like, to form a series of separate wing extensions with slots between. Essentially, these are intended to work in the same way as the Whitcomb winglets, but there may be three, four or five tipsails, arranged radially and 'en echelon' round the tip. Each sail is adjusted to extract lift from the flow in its neighbourhood and, as with the winglet, some of this force is directed forwards, the rest

Fig. 6.10 N.A.S.A. wing sails

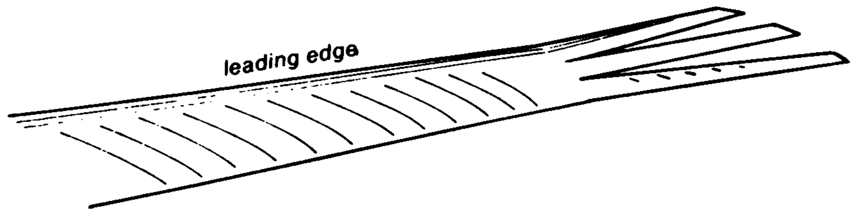

adds bending load to the wing. The results are comparable and the same economic considerations apply. As before, an increase in aspect ratio has the same effect.

6.23 NASA TIP SAILS

Even more reminiscent of the bird wing, the NASA tip modification suggested in Figure 6.10 is intended to spread the tip vortex and reduce its strength, and this, too, reduces the vortex drag. Additional loads, as usual, must be borne by the mainplane structure and the slender tip 'feathers' are prone to flutter.

6.24 WINGLETS AND TIP SAILS FOR MODELS

As far as model aircraft are concerned, very few tests have been performed with winglets or tip sails. They are unlikely to produce benefits unless they are properly adjusted and very few modellers have access to wind tunnels for testing purposes. If there is no restriction on the wingspan of the model, it is safer to increase aspect ratio than to use winglets unless these have been correctly designed. There are, even so, occasions when the wingspan is restricted by contest rules, or where an increase of aspect ratio (with a reduction in mean wing chord) might take the wing down to a low Reynolds number and so lose efficiency. In such cases winglets, especially of the Whitcomb type, offer some prospect of worthwhile gains.

The two metre sailplane class is a case in point. In 1980 tests of a model in this category were reported by Chuck Anderson (in *Model Aviation*, May 1980, pp. 52-5). On a wing with 25.4 cm chord, of rectangular planform, aspect ratio 7.87, winglets as shown in Figure 6.11 were fitted. These seemed to improve the performance while remaining within the two metre restriction. They also had some less desirable effects on lateral stability and control. It must also be pointed out that such additions to the tips are rather vulnerable to damage, especially in ground loops or landings which end with the model upside down.

For small free-flight models and even for F1A (A2) sailplanes, as mentioned above (6.4), wing taper is not generally desirable but the addition of winglets or sails to a rectangular wing may prove worthwhile. The Reynolds number of the mainplane would be unaffected and the tip vortex, providing the winglets were well designed, would be reduced. Anderson's two metre sailplane, very wisely, was made with the angle of the winglets adjustable so that by repeated test flying, the best setting could be discovered.

Noel Falconer has used a refined winglet design on tailless sailplanes and electric powered models. Apart from saving drag, which is rather more severe on a swept-back wing, the winglets also serve as fins, providing very necessary lateral stability on the tailless aircraft.

Fig. 6.11 Winglets on a two metre sailplane (Chuck Anderson)

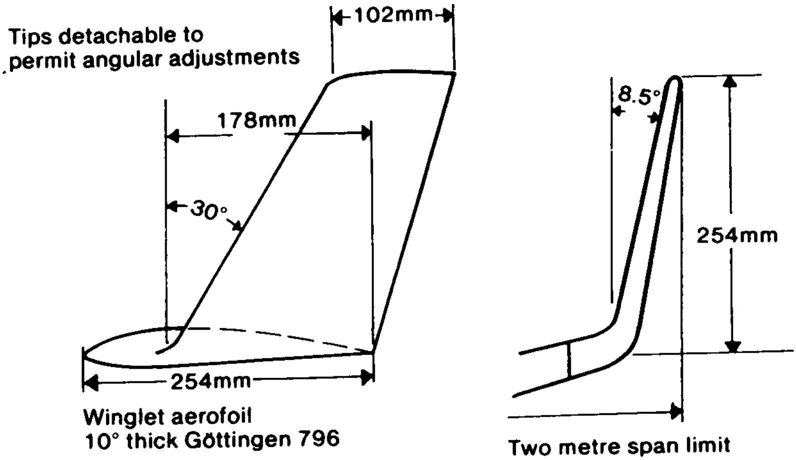

For comparison: NASA/Whitcomb winglet dimensions given as fractions of the mainplane tip chord.

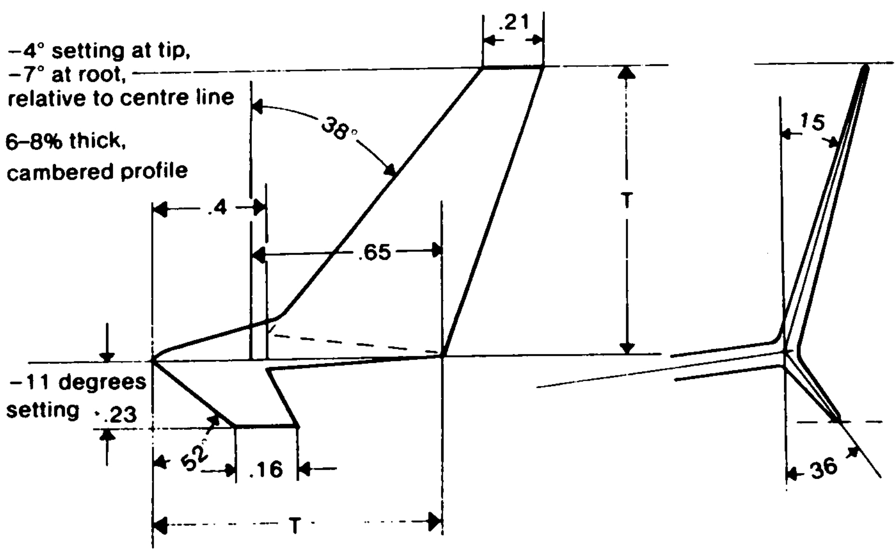

Fig. 6.12

The wing of a modern full sized sailplane, using all the information gathered in recent decades about the best planform, wing tip shape and winglets (based on the *Ventus 2*).

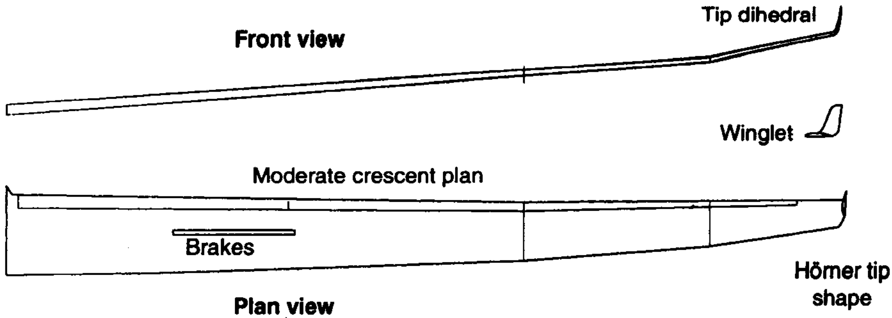

6.25 CRESCENT SHAPED WINGS

Research into wing planforms in recent years suggests that some saving of vortex drag may be made by adopting a distinctly crescent shaped wing plan, resembling that of the swallow bird wing, or the curved fin of a shark. The planform shown in Fig 6.3e, to be seen on some modern full-scale sailplanes, represents a move part way in this direction but the full crescent wing is more extreme, with the trailing edge curving progressively more backwards towards the tip and a relatively sharp extremity. The basic distribution of chord across the span remains nearly elliptical but the ellipse is progressively sheared backwards to produce the shark fin form.

Advanced calculation methods were used in the first place, to establish a theoretical basis for this study. Wind tunnel and flight tests lend some further support to the idea. More work is being done.

A point that needs to be taken into account is that sweptback wings are more prone to tip stalling and to wing flutter (see Sections 6.9 and 13.9 here). There may well be some improvement in theoretical performance with such wings, but they are more difficult to construct and if handling difficulties appear in flight, the gain will not be realised. The author has built and flown two sailplanes with wings approximating this plan. One of them exhibited tip stalling problems and the other developed severe wing flutter at moderate airspeeds, despite corrective surgery. Whether any real saving in drag resulted remains uncertain.

7
Aerofoil sections: i. Camber

7.1 THE SIGNIFICANCE OF THE AEROFOIL SECTION

Quite often modellers draw out their own aerofoils freehand or with the aid of the simplest drawing instruments. It has even been said that a successful model wing has been designed by drawing round the edge of a favourite bootsole to produce nicely curved lines for the upper and lower surfaces of the profile. Such apparently casual methods can yield good results if informed by a good deal of experienced judgement. The aerofoils produced in these ways are very orthodox. They resemble forms that have been in widespread use for many years, and these prototypes were originally designed under sound theoretical principles by aerodynamicists. The modeller who is content always to do what was done before will usually produce a model which flies very much like the one before but it will not represent any advance in development. An even safer procedure is to copy slavishly the wing of a well-known successful model of identical type, and again, good results may be expected. Unfortunately this procedure leads to stagnation as modellers follow current fashions without much fundamental re-thinking.

The effects of a moderately bad aerofoil on a *slow*-flying high C_L model, as Figure 4.10 suggests, may not be very serious because profile drag is a comparatively small proportion of the total. By skilful tactics and experienced judgement about when to launch, contests may be won with models which are reliable, structurally sound and carefully trimmed, even if the wing profile is not ideal. Just as easily, a good wing design can be ruined by faulty construction, clumsy trimming or inexperienced operation. Nonetheless, contests are often decided by a few seconds here and there, and profile drag may be responsible for more than a few seconds at the end of a day's flying. This is especially likely if the aerofoil is such that it is itself a cause of unreliability or instability. A serious contestant cannot afford a casual attitude to anything that can give his models a small advantage over the opposition.

For high speed models piloting skill and experience are even more important, particularly for aerobatics and pylon racing, where judgement of the model's position plays such a large part. Nevertheless with equal or nearly equal pilots, the faster model obviously has the better chance. Here profile drag is of major significance.

Modellers frequently modify aerofoils in rather arbitrary ways. Sometimes the upper surface of some well-known profile is used, but with a flat undersurface to make the wing easy to build. This has unpredictable effects on the profile; it is changed in both camber and thickness form. Less-intentional changes occur on the drawing board or in the workshop. Profiles may be inaccurately enlarged from drawings in magazines; a commercially produced leading edge member may be used, although it does not quite fit

Fig. 7.1 Aerofoil families

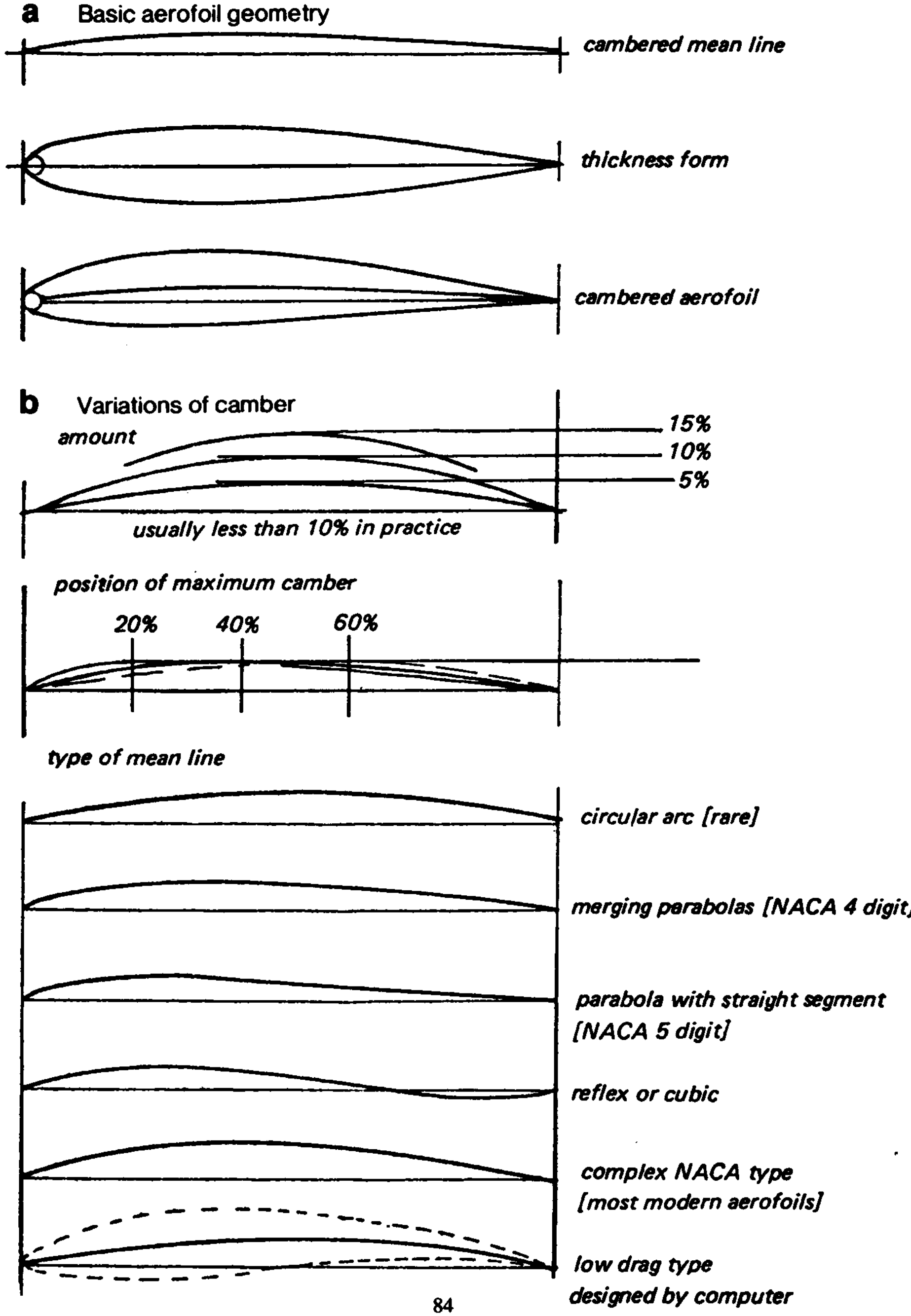

the profile as designed, a moment's too much rubbing with a sanding block can alter the shape of wing ribs quite a lot, and so on. For these reasons modellers are rightly doubtful of theories which seem to demand a wholly unrealistic standard of craftsmanship. However, while for the smallest and slowest-flying models, traditional structures with flimsy covering sagging between ribs and stretched over protruding spars seem likely to be best both aerodynamically and structurally, theory does suggest the possibility of considerable improvements for larger and faster models, if attention is given to greater accuracy of wing surfaces. In the full-sized sailplane world, the introduction of new materials and methods of manufacture brought about a revolution which transformed the sport; performances once deemed impossible are now commonplace. In modelling, the equivalent may be found in veneer-covered, foam-plastic-cored wings, skinned with glassfibre reinforced plastic which enable wing profiles to be produced which do come close to the contours of wind tunnel models. New kinds of sandwich wing skins are also capable of reproducing aerofoils accurately.

7.2 AEROFOIL GEOMETRY AND FAMILIES

In designing aerofoils it is usual to consider the effects of camber and thickness form separately. This is justifiable only up to a point. The detailed airflow over the wing is affected equally by both camber and thickness, so both need to be considered simultaneously. It is useful, however, to begin with camber as an introduction to aerofoil theory and practice. In later chapters the complicating effects of the thickness form of the profile will be considered.

Any aerofoil may be considered as a basic 'thickness form' which has been bent round or fitted to a curved camber or mean line (Fig. 7.1). Profiles may be classed in families. A given basic thickness form may be fitted to a whole series of different camber lines, some curved more than others, some with the curvature concentrated towards the leading edge, some with it mostly towards the trailing edge, and so on. For example, a simple flat plate has a small thickness, has a leading edge shape – perhaps square, pointed or rounded, and a trailing edge form. It may be cambered in any way to create a family of aerofoils. The mean line might be a simple arc of a circle, or it might be a more complex form derived mathematically. When aerofoil ordinates are published the camber is sometimes stated in terms of percentage of the wing chord, and possibly the position of the maximum camber point is also given. Thus, aerofoils of the N.A.C.A.* series contain this information in their designations. When four digits appear after the letters NACA, the first digit refers to the camber amount, the second gives the chordwise location of the point of maximum camber. The last two figures give the thickness of the profile. All these are expressed in percentages of the chord. Thus, the NACA 6409 profile has 6% camber with the highest point of the mean line at 40% of the chord, measured from the leading edge, and the thickness is 09%. The 4412 profile has 4% camber at 40%, and is 12% thick. In the more modern NACA aerofoils of the 'six digit' series, the information about camber is given in a different form. The fourth figure in this series gives the lift coefficient, c_l, for which the profile has been designed. The larger this figure, in general, the more cambered the profile, so for example the NACA 63_3615 and 63_3215 have 'design lift coefficients' of .6 and .2 respectively.** The last two figures give the thickness percentage as before. In some cases, following the six digits, a further statement appears, such as a = 0.5. This means that a certain type of cambered mean line (see Figure 7.2) has been used. Where

* N.A.C.A., National Advisory Committee for Aeronautics, U.S.A., now replaced by N.A.S.A.

** For explanation of the first, second and third digits of these aerofoils, see Chapter 9.

this statement does not appear, the NACA a = 1 mean line has been used. Other aerofoil systems adopt other methods of nomenclature which may include details of camber (see Appendix 3). The precise form of the mean line may differ from profile family to profile family. It is very rare to find a simple circular arc. Usually the curve is designed to serve a particular purpose. For example the NACA four digit profiles have mean lines which are made up of two parabolic curve segments joining tangentially at the point of maximum camber. The 'five digit' series (e.g. NACA 23012) have mean lines with the high point unusually far forward, designed to yield high maximum lift coefficients (Fig. 7.3a). It is more usual now to design mean lines to give a desired chordwise load distribution. The most commonly employed of these is the NACA a = 1 mean line (see Fig. 7.2a), which gives an even chord load distribution. The advantage of this is that each part of the profile is contributing its appropriate share of the lift, and hence, for any given value of c_l, the least possible camber is required. This means less profile drag, other things being equal. However, there may be good reasons sometimes for using other forms of mean line, to reduce wing-twisting and pitching loads, for example, or, when aerofoils are designed for laminar flow, to help control the detailed pressure distribution.

7.3 DESIGNING A NEW PROFILE

Knowing the mean line of any aerofoil, it is possible to experiment with a family of profiles based on it. Different thickness forms may be fitted to it, and new aerofoils created in this way. Alternatively, a preferred thickness form may be fitted to various differing mean lines to try the effects of increasing or decreasing camber, moving the point of maximum camber forward or aft, and so on. Methods of doing these things are outlined in Appendix 3.

7.4 ERRORS AMONG MODELLERS

Modellers sometimes have mistaken ideas about camber. For example, aerofoils such as the well-known Clark Y, with flat undersides may be more cambered than some thinner sections which have concave undersides. In the same way, changing the thickness form of a profile does not change its camber – the NACA 4415 and 4409 are cambered both by 4%, but while one appears 'undercambered' the other is convex on both surfaces. For these reasons, the widespread habit of classifying aerofoil sections as 'undercambered', 'flat bottomed' and even 'semi-symmetrical', is very misleading and should be abandoned. The so-called semi-symmetrical profile is a cambered section and the camber may vary greatly from one such aerofoil to another, depending on the shape of the camber line itself in combination with the thickness form. Even perfectly symmmetrical sections differ considerably in flight because of their various kinds of thickness distribution. From the table of ordinates used to plot an aerofoil, the camber can be found by arithmetic, or from an accurate drawing it may be found graphically. (See Appendix 1). It is seldom possible to judge it by eye. It is also undesirable to modify camber arbitrarily. Some modellers, in the hope of obtaining more lift without increasing drag, 'droop' the trailing edge of their aerofoils. This introduces a kink in the mean line with effects usually bad. It would be better to choose a new properly designed mean line with an increased camber. In a similar fashion, either by design or by various tricks and dodges on the building board, modellers sometimes 'reflex' the trailing edge of a wing near the tips, intending to give a desirable 'washout'. The effect in many cases is the opposite: a reflexed profile tends to stall sooner, rather than later, than an ordinary one of similar leading edge shape. The purpose of the reflex camber line is to reduce the pitching moment of the aerofoil, not to delay stalling (Fig. 7.3b). Another common term, referring to the leading edge of the

Fig. 7.2 NACA camber lines. Scale up or down to required maximum camber

a NACA A=1.0 MEAN LINE

b NACA A=0.9 MEAN LINE

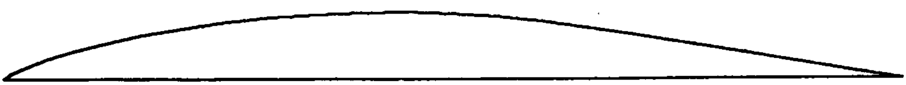

c NACA A=0.5 MEAN LINE

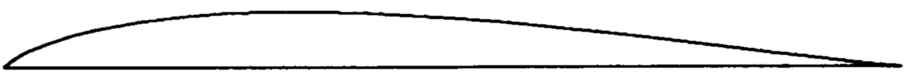

d NACA A=0.0 MEAN LINE

Fig. 7.3

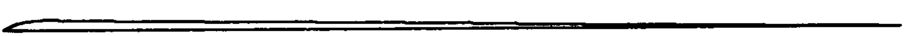

a NACA 210 MEAN LINE CL IDEAL 0.3

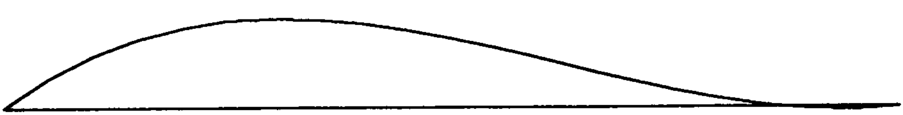

b REFLEX MEAN LINE FOR ZERO PITCHING MOMENT. SCALE TO REQUIRED CAMBER

Fig. 7.2 Mean line ordinates.

To obtain a mean line of a desired maximum camber, muliply each YU figure in the table by an appropriate factor.

a NACA A = 1.0 MEAN LINE		b NACA A = 0.9 MEAN LINE		c NACA A = 0.5 MEAN LINE		d NACA A = 0.0 MEAN LINE		NACA 210 MEAN LINE		REFLEX MEAN LINE	
CHORD STATION	ORDINATE	CHORD STATION	ORDINATE	CHORD STATION	ORDINATE	CHORD STATION	UPPER SURFACE	CHORD STATION	ORDINATE	CHORD STATION	ORDINATE
XU	YU	XU	YU	XU	YU	XU	YU	XU	YU	XU	YU
0.000	0.000	0.000	0.000	0.000	0.000	0.000	0.000	0.000	0.000	0.000	0.000
.500	.250	.500	.269	.500	.345	.500	.460	1.250	.596	5.000	3.240
.750	.350	.750	.379	.750	.485	.750	.641	2.500	.928	10.000	5.770
1.250	.535	1.250	.577	1.250	.735	1.250	.964	5.000	1.114	15.000	7.650
2.500	.930	2.500	1.008	2.500	1.295	2.500	1.641	7.500	1.087	20.000	8.940
5.000	1.580	5.000	1.720	5.000	2.205	5.000	2.693	10.000	1.058	25.000	9.700
7.500	2.120	7.500	2.316	7.500	2.970	7.500	3.507	15.000	.999	30.000	9.990
10.000	2.585	10.000	2.835	10.000	3.630	10.000	4.161	20.000	.940	35.000	9.880
15.000	3.365	15.000	3.707	15.000	4.740	15.000	5.124	25.000	.881	40.000	9.430
20.000	3.980	20.000	4.410	20.000	5.620	20.000	5.747	30.000	.823	45.000	8.700
25.000	4.475	25.000	4.980	25.000	6.310	25.000	6.114	40.000	.705	50.000	7.760
30.000	4.860	30.000	5.435	30.000	6.840	30.000	6.277	50.000	.588	55.000	6.660
35.000	5.150	35.000	5.787	35.000	7.215	35.000	6.273	60.000	.470	60.000	5.460
40.000	5.355	40.000	6.045	40.000	7.430	40.000	6.130	70.000	.353	65.000	4.240
45.000	5.475	45.000	6.212	45.000	7.490	45.000	5.871	80.000	.235	70.000	3.040
50.000	5.515	50.000	6.290	50.000	7.350	50.000	5.516	90.000	.118	75.000	1.940
55.000	5.475	55.000	6.279	55.000	6.965	55.000	5.081	95.000	.059	80.000	0.990
60.000	5.355	60.000	6.178	60.000	6.405	60.000	4.581	100.000	0.000	85.000	0.260
65.000	5.150	65.000	5.981	65.000	5.725	65.000	4.032			90.000	−0.190
70.000	4.860	70.000	5.681	70.000	4.955	70.000	3.455			95.000	−0.300
75.000	4.475	75.000	5.265	75.000	4.130	75.000	2.836			100.000	0.000
80.000	3.980	80.000	4.714	80.000	3.265	80.000	2.217				
85.000	3.365	85.000	3.987	85.000	2.395	85.000	1.604				
90.000	2.585	90.000	2.984	90.000	1.535	90.000	1.013				
95.000	1.580	95.000	1.503	95.000	.720	95.000	.467				
100.000	0.000	100.000	0.000	100.000	0.000	100.000	0.000				

EXAMPLE The A = 1.0 camber line reaches its maximum 50% chord, where the YU ordinate is 5.515 (5.515%) To reduce this to a 2% camber line, multiply all the YU figures by $\frac{2}{5.515} = 0.3626$.

(Use an electronic calculator). Thus the new ordinates will read 0.0, 0.0907, 0.1269, 0.1940 etc.

aerofoil, is 'Phillips entry'. A profile with Phillips entry is one which has a modified camber line over the front 20–30% of the section, reducing the camber in this region. The camber of the profile should be considered as a whole and it is not good practice to modify a part of the aerofoil without considering the shape of the mean line from leading edge to trailing edge.

As will become apparent in what follows, to vary the camber of a wing towards the tips is an extremely useful design technique, enabling tip stalling to be prevented without any bad effects on performance. The technique, however, requires care.

7.5 THE AERODYNAMIC ZERO

If a symmetrical aerofoil is at zero angle of attack, it yields no lift, whereas a cambered one will lift when its *chord line*, i.e. the straight line from extreme leading edge to trailing edge, is parallel to the general airflow. But a cambered profile can be moved to some negative angle at which it, too, will produce no lift. This angle is most important and is known as the *aerodynamic* or *absolute zero angle of attack* for a particular aerofoil. The more cambered the mean line, the more negative, relative to the chord line, will the absolute zero angle be. On graphs of lift against drag for aerofoils in one family the more cambered profiles' lift curves are always to the left, i.e. towards the negative side, as shown in Figure 7.4. However, the slope of the lift curve on such graphs, for one aerofoil family, is the same in each case. This remains true so long as the camber is not so great that streamlining breaks down. As shown, the more cambered aerofoil of a family tends to reach a higher value of C_L before stalling than the less cambered, but the *geometric* angle of attack at which the stall occurs is *earlier*. Only if the angle of attack is measured from the absolute zero in each case does the more cambered profile stall later. This suggests some important practical points for the design and construction of model wings.

7.6 STALL CONTROL BY CAMBER CHANGES

By varying the camber along the span, the stalling characteristics may be controlled. If the camber is reduced towards the tips, with no geometric twist (i.e. the true chord line of each rib is at the same angle to the building board or datum line), the wing will have an *aerodynamic* washout because the *aerodynamic* zero angle of attack at each point will differ. Assuming a nearly elliptical planform, the wing roots, because of the greater camber there, will reach their stalling angle *before* the tips. This is good in the sense that it prevents tip stalling. At high speeds, however, when the roots are still lifting, the tips will already be close to their aerodynamic zero. The lift distribution will not be elliptical, and at some speed the tips will begin to bend downwards like a wing with marked geometrical washout (Fig. 7.5). To restore elliptical lift distribution, the tips should really be twisted the other way (wash-in), which will unfortunately cause tip stalling because the less-cambered profile has a lower c_l maximum. Many models have been built with reduced camber at the tips *plus* a few degrees of washout. This combines both aerodynamic and geometric washout; the total effect may be as much as six or seven degrees of aerodynamic twist. The tip stall is controlled, but the efficiency suffers.

If, instead of camber decreasing at the tips, it is increased, or decreased at the roots, the tips will tend to stall first, which is highly undesirable. However, if the aerodynamic twist or 'wash-in' caused by the increased tip camber is counteracted by an equal geometric twist or washout in the opposite direction, the result is excellent. If, for example, the difference in absolute zero of the aerofoil at the wing root and that at the tip is two degrees, with the more cambered form at the tip the geometric twist should be two degrees washout or, to be on the safe side, a little more. The whole wing then reaches its aerodynamic zero at the

Fig 7.4 The effect of camber on the lift curve

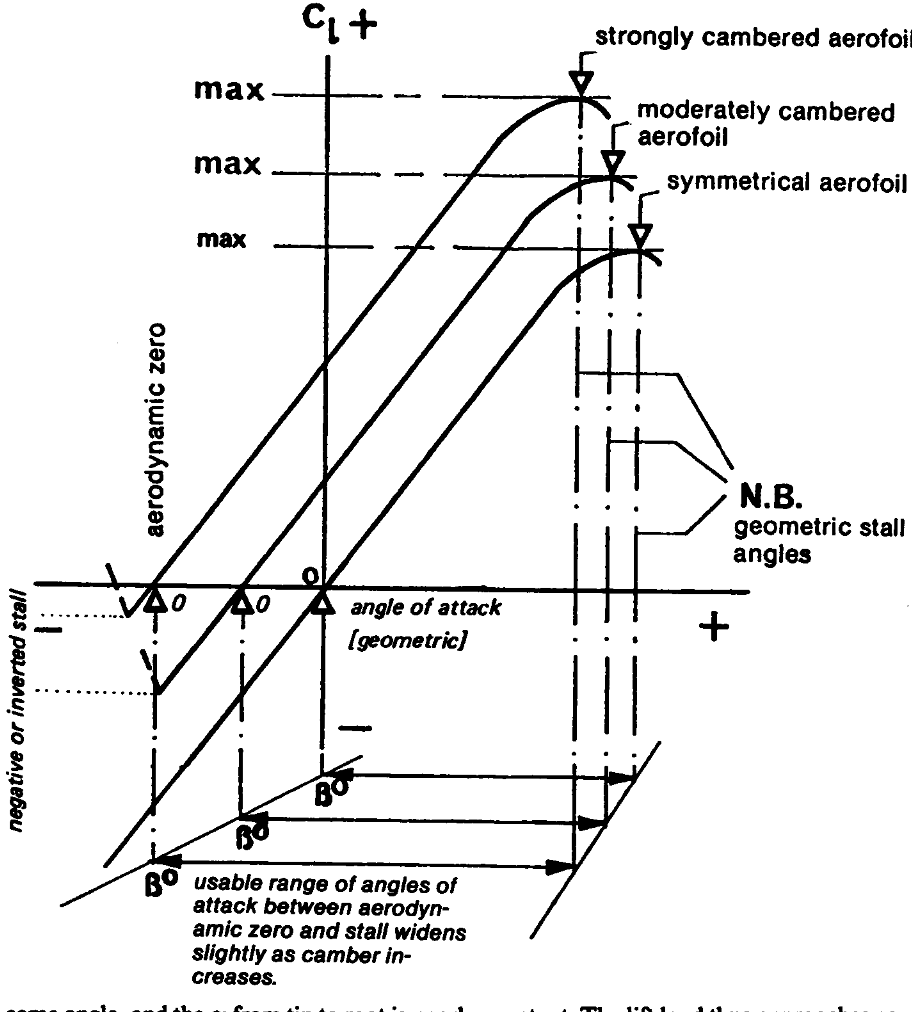

same angle, and the c_l from tip to root is nearly constant. The lift load thus approaches as closely as possible to the ideal (assuming the planform of the wing is a good approximation to an ellipse). There is no tip stall, because the more cambered profile has a higher c_l max., and, measured from the *aerodynamic zero*, stalls later. Hence the root reaches the stalling angle first. The wing is efficient over a wide range of speeds. This technique is widely used by designers of full-sized sailplanes and may be applied to models in exactly the same way. In design it is essential to know the zero-lift angle for the profiles used. This may be obtained from wind tunnel results if available. In some cases the figures are given with the aerofoil ordinates (as with the Eppler profiles whose ordinates are given in Appendix 3). Wind tunnel results do not always confirm the computed figures. On the building board it is of course very important to lay out such a

Fig. 7.5 Camber, aerodynamic and geometric twist

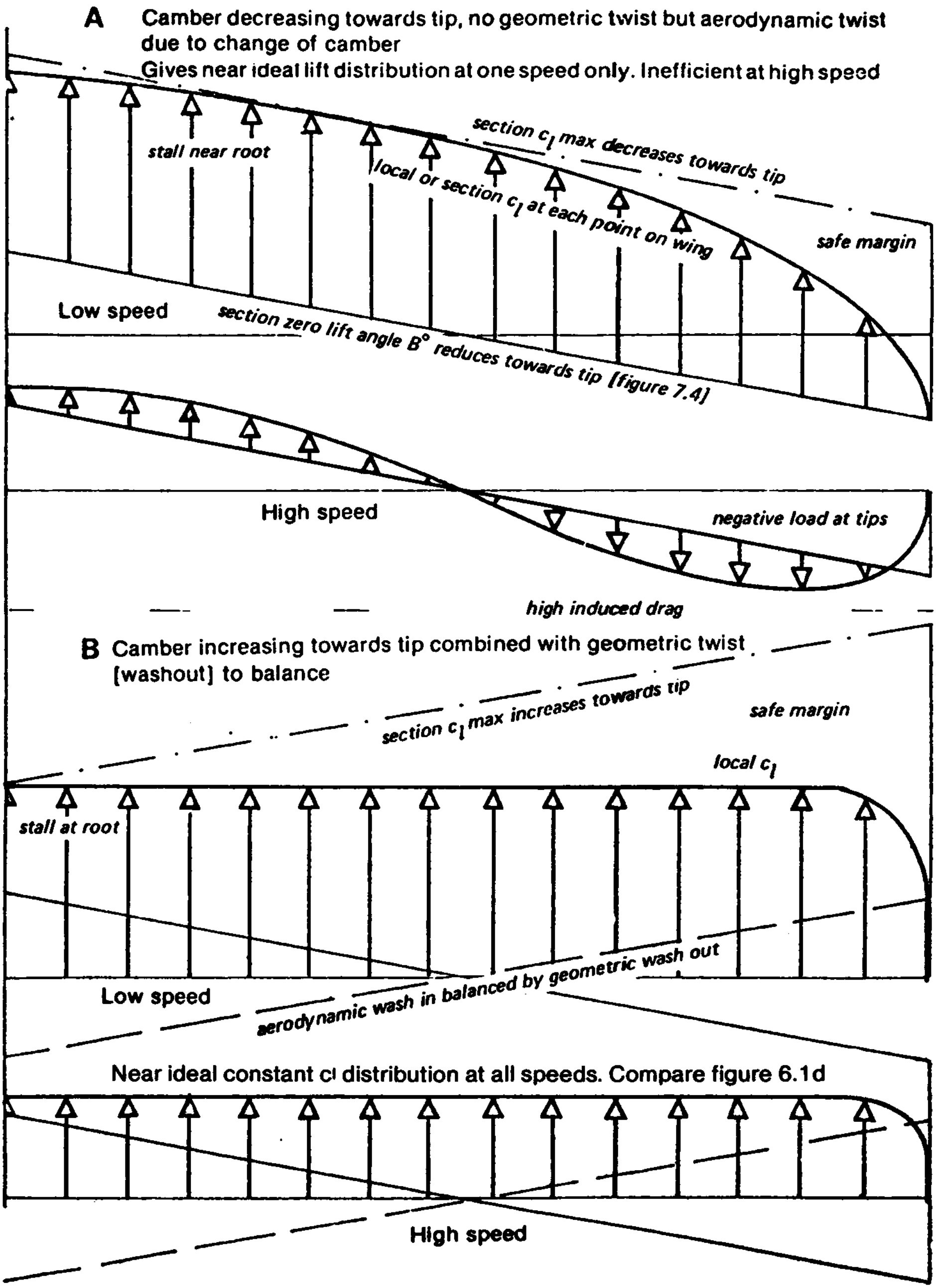

wing accurately. The ribs may be cut by the sandwich method between templates of the appropriate aerofoils at tip and root, or the section may be constant to the semi- or two-thirds span position and changed progressively from there to the tip. Cutting foam plastic wings is equally straightforward. On assembly, careful work should ensure that the angle of each rib is correct relative to its designed chord line. A casual chocking up of the trailing edge to some angle or other is not good enough.

7.7 FLAPS AND CONTROLS

Highly cambered aerofoils are often referred to as 'high lift' sections. It is true, as Figure 7.4 shows, that the highly cambered section has a higher c_l max. This is familiar enough and is the reason why full-sized aircraft and some models have landing flaps. The point is not that such surfaces, or their equivalent, highly cambered wings, develop more lift *force*. In equilibrium, lift equals weight. The wing with flap down has to support only the same aircraft weight, but, operating at a high C_L, it can do this work at a lower airspeed. Hence the value of flaps for landing and take off. Figure 7.6 shows the effect of moving any hinged surface such as an aileron, rudder or elevator, or a wing flap of the plain variety, to different angles. As the flap goes down, the whole c_l curve moves to the left on the graph, and upwards. At the same time, if the attitude of the aircraft to the flight path is not altered, the effective angle of attack increases because the chord line of the wing is in a new position. On raising the flap, the converse happens. The effect of such hinged surface movements is a combination of increased camber and increased angle of attack, or vice versa. Split flaps have similar camber-changing effects, but have the advantage for landing of also creating high profile drag. This decreases the L/D ratio and steepens the glide path on the approach, helping the pilot to judge his touch down position accurately. Such flaps have value on models required to carry out precision landings. Under-surface airbrakes, mounted at about 50% of the chord, also change the wing camber and increase c_l max. slightly, with high drag. This type of brake has been used in some full-sized sailplanes but is vulnerable to ground damage. All camber-changing devices change the *pitching moment* of the aerofoil, as discussed more fully in the last section of this chapter.

7.8 CAMBER AND DRAG

For most of the time the landing condition is not particularly significant for models. The reason that slow flying models should have well cambered profiles, and fast models less cambered ones, is entirely a matter of drag reduction. The influence of camber on drag of an aerofoil is shown in Figure 7.7. Compared with symmetrical wings, the cambered surface has a slightly higher minimum profile drag, but far more significant is the movement of the drag curve as the camber increases. The angle of attack in Figure 7.7a is the *aerodynamic* angle, measured from the absolute zero. In some earlier wind tunnel testing, the drag graph was plotted against angle of attack measured geometrically. The rightward shift of the curve was to some extent concealed, since it was easy to overlook the *left*-ward shift of the lift curve with camber. In modern practice, the drag curve is always plotted against c_l directly (Fig. 7.7b) and the true relationship is then clear. (The angle of attack has to be found by cross plotting to the c_l curve.) In practice the modeller seldom knows at what angle of attack the wing operates, since the model's attitude changes frequently. Downwash in any case induces a different angle from the simple geometric expectation, but the wing C_L is controlled by trimming. It is of utmost importance that the camber should be correctly chosen to give minimum drag at the particular C_L at which the model is flying. This is particularly vital for high speed models

Fig. 7.6 Hinged control surfaces

Geometrically the angle of attack is always measured from the chord or other reference line with zero control deflection. The aerodynamic effects are as shown when controls are deflected.

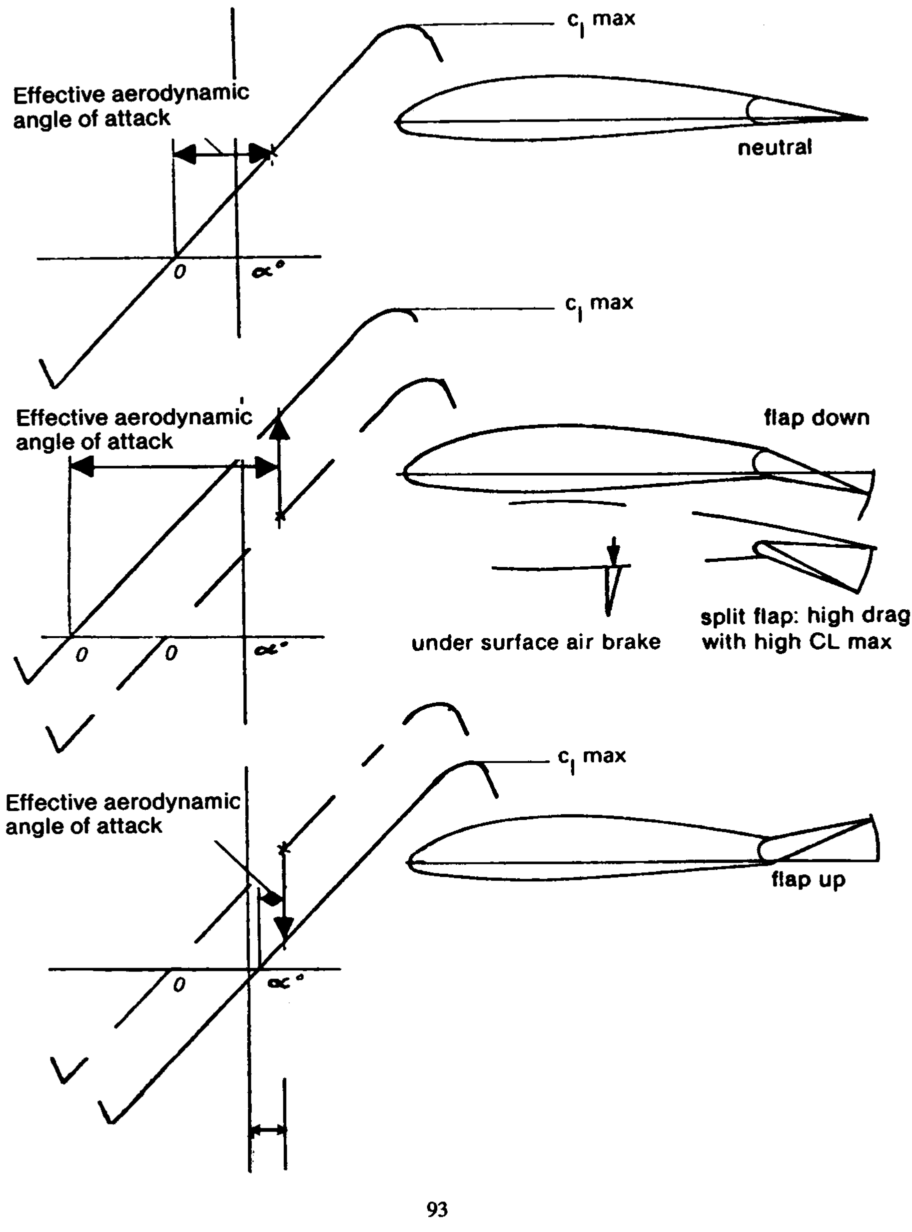

Fig. 7.7 The influence of camber on profile drag

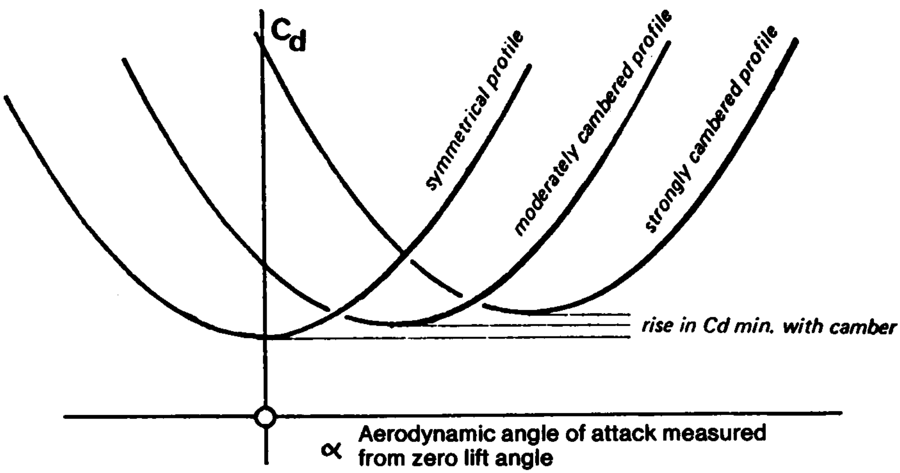

a Profile drag plotted against angle of attack

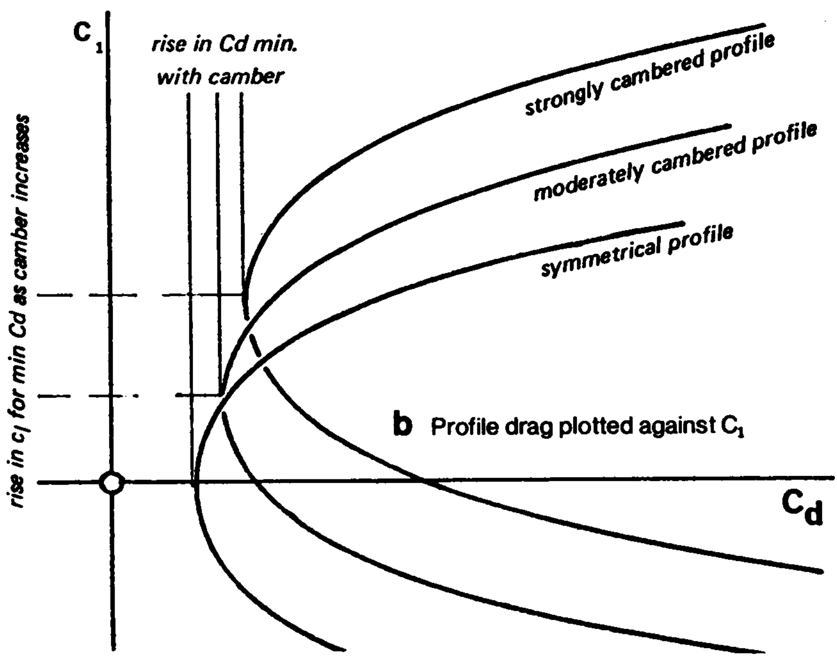

b Profile drag plotted against C_1

where profile drag is such a large item in the drag budget; it is less important, though still significant, for slow flying models.

Some pylon racers have been built with the wrong camber As Figure 7.7 shows, there is one value of c_l at which profile drag is a minimum for each value of camber. If a symmetrical wing is trimmed to fly at a positive angle of attack, as it must be for flight in equilibrium, it will operate at some point on the drag curve above the minimum. On the other hand, if a cambered profile is trimmed at too low a c_l, it too will produce too much drag.

Fig. 7.8 Forces in a turn

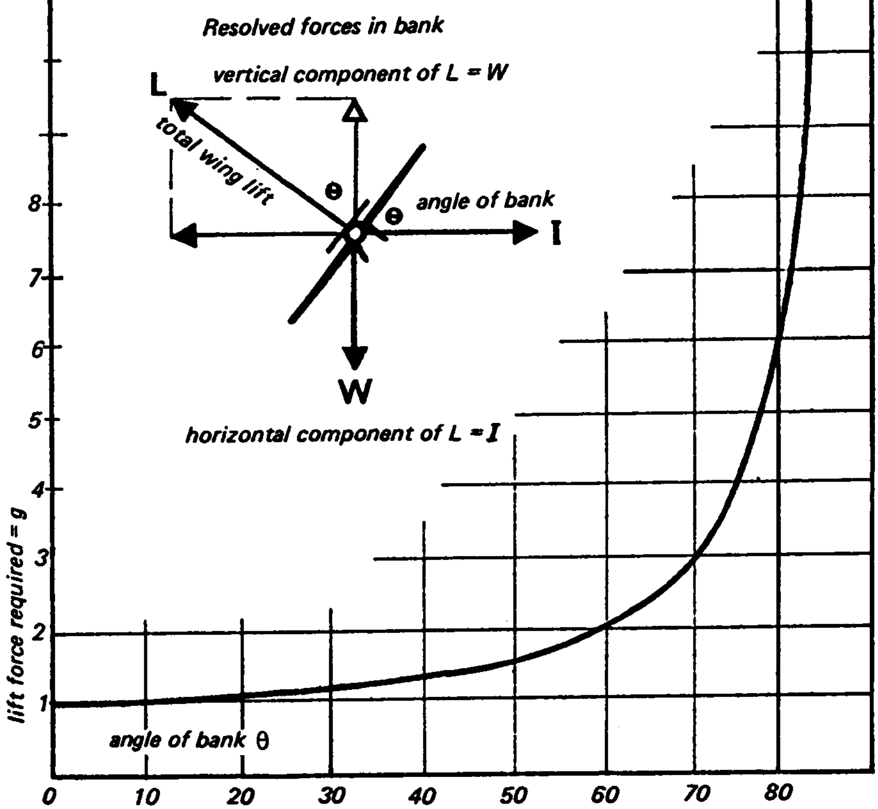

Graph of lift force required at various angles of bank

With the help of a little arithmetic it is possible to determine the best camber for any speed model, if its actual speed, or the speed hoped for in the design stages, is known. This is explained in Appendix 1. At maximum speed in level flight very little camber is required, with a light model, but racing models spend comparatively little of their flying time in equilibrium, they not only fly straight and level, but have to bank round the pylons. This, as shown in Figure 7.8, increases the c_l at which the profile operates, to generate the extra lift force to counteract inertia in the turn. How much extra force is needed depends entirely on the angle of bank; a bank angle of 60 degrees doubles the effective lift required, a further eleven or twelve degrees triples the load, and banking angles of 80 degrees or more send the 'g' forces rocketing. In such steep turns the wing is forced to a higher angle of attack, and with the thin slightly cambered profiles commonly used, this may cause a considerable increase in drag or even a stall. The extra drag slows the model down, reducing the average speed for the lap in any case. It may be much more significant than that. The reduction of V in the lift formula means that the C_L must go still higher. With a thin, slightly cambered wing, this too can produce a stall and the race ends immediately for that model. The model needs either a wing which produces low drag over a range of c_l values, such as one of the laminar flow aerofoils discussed in Chapter 9, or it needs a variable camber wing, i.e. flaps which can be lowered slightly at the turns; not so much to increase C_L, but to shift the drag curve to give minimum profile drag at the higher angle of attack in the turn.

For duration models and gliders which are trimmed to fly at $C_L^{1.5}/C_D$ maximum, it is necessary to reduce profile drag as far as possible by moving the drag curve to a high c_l position, accomplished by cambering more. This also raises the c_l maximum, enabling the model to be trimmed for slow flight. The ideal camber is harder to determine than for a speed model, since the calculation method requires detailed wind tunnel test results for the profile used, and these are rarely available. Given such figures, like those presented in Appendix 2, the value of $C_L^{1.5}/C_D$, duly corrected for the aspect ratio and with allowance for parasite drag, may be calculated by arithmetical methods and plotted on a graph to find the best operating C_L and check the camber again. The model may then be trimmed to fly at the airspeed appropriate to the C_L. Some examples of the type of calculation required are given in Appendix 2.

7.9 VARIABLE CAMBER

Models which are required to perform efficiently over a wide range of airspeeds present great difficulties. This applies particularly to cross-country and multi-task radio controlled sailplanes. When soaring, they must be trimmed for a high C_L and for low drag should have a strongly cambered wing. At speed, a low-camber or even a symmetrical profile is required. As noted previously, a high aspect ratio is the chief means of achieving a low sinking speed, but profile drag is not negligible. At speed, profile drag is most important. No one value of camber can be ideal for all flight conditions. If a simple wing is used, the camber should be on the low side, for high speed, relying on high a.r. for the soaring flight. The aerofoils used should be chosen to give low drag coefficients over wide range of angles of attack. Preferably a laminar flow aerofoil with a wide low-drag-range or 'bucket' should be used (Chapter 9). Even better, such a profile combined with a variable camber wing allows the drag to be reduced in all conditions. Plain flaps widen the speed range as shown in Fig. 7.9. Most modern full-sized sailplanes combine flaps with wide-drag-range aerofoils. In thermals or hill lift, the flaps are depressed, shifting the drag curve to the right and the lift curve left. Between upcurrents, to achieve good penetration, the flaps are raised, usually beyond the neutral position, to shift the drag and lift curves in the opposite directions. The pilot constantly adjusts the flaps as the airspeed is changed. With a well-balanced design, the *attitude* of the fuselage to the airflow hardly changes, in fact one well-known high performance sailplane could be trimmed by means of a spirit level – at any speed with appropriate flap setting, the attitude remained exactly the same. The advantage of this was that the fuselage presented the same aspect to the airflow at all speeds, and thus parasite drag was a minimum for the particular shape used. (See also 11.4). With less refined design, the fuselage changes its angle of attack somewhat, and produces more drag, with different flap settings.

For powered duration models the advantage of variable camber is also clear. The low

C_L required for the high speed climb is achievable by trimming the tailplane, to hold the wing at a low angle of attack, but with a high camber, this produces much too much profile drag. It is better to reduce the wing camber for the climb, cutting profile drag at speed. Then for the glide, the low drag and high C_L required may be achieved by increasing camber, lowering wing flaps after the motor cuts. Re-trimming the tail will also probably be necessary.

7.10 DESIGN OF CAMBER FLAPS

The design of variable camber wings is not easy. The air must not be forced to flow round sharp corners or meet severe adverse pressure gradients, since the boundary layer can easily separate and cause very high drag. Flap hinge lines must be carefully sealed to prevent leakages from high to low pressure sides of the wing, or from inside the wing to the outside. Ideally, the whole aerofoil should be designed for use with flaps. The flap should

Fig. 7.9 Plain flaps used to widen the speed range of a sailplane

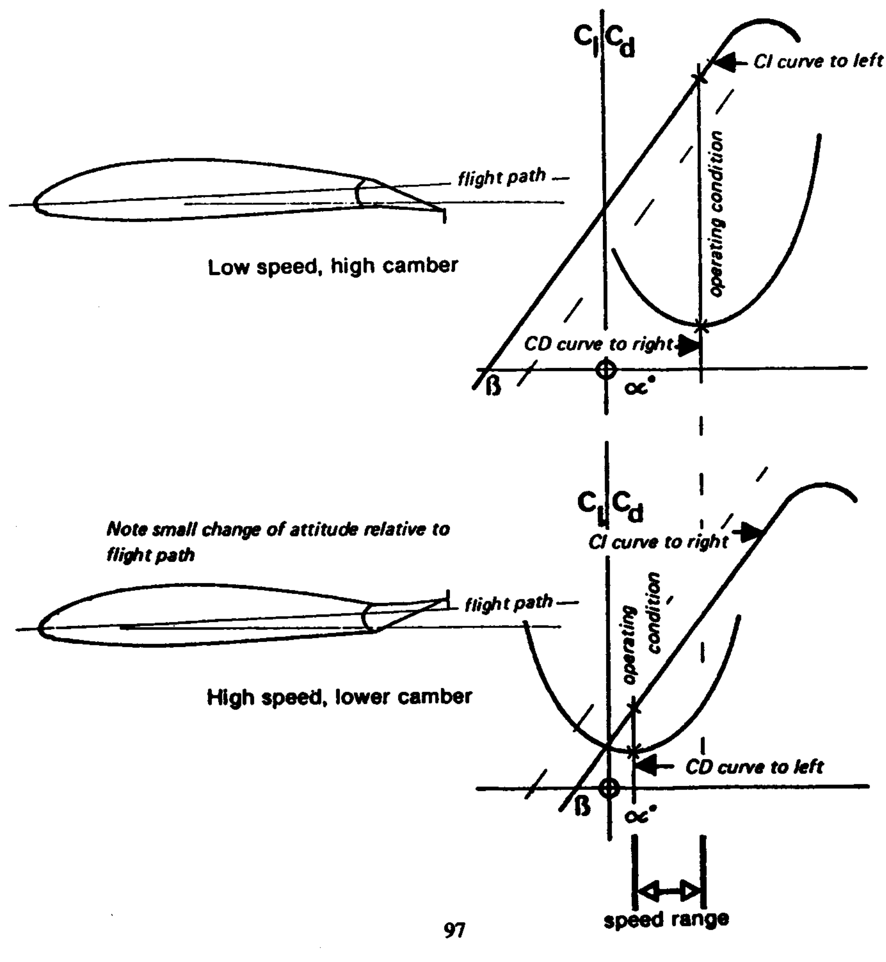

extend across the whole span, not terminating at the ends of the ailerons. The ailerons should droop or rise together with the flaps. This is particularly important at low speeds, since the sharp change in angle of attack caused where the flap ends amounts to giving the wing a very pronounced and abrupt washout, with bad effects on the carefully designed elliptic lift distribution, and hence high induced drag. The flaps may also be used by themselves as landing aids. Some successful multi task sailplanes use ailerons and flaps opposed for landing, both the ailerons being deflected up as the flaps go down. This creates both high profile drag and vortex drag where the flap and aileron meet at very different angles. Advances in electronic coupling of controls has greatly eased the problem of engineering involved in such a system. It is commonly found that, with this arrangement, some aileron control is lost at low speed.

A true variable camber wing, with a flexible skin on one or both surfaces and internal levers to increase or decrease curvature, is aerodynamically superior to a wing with flaps. Some full-sized sailplanes have adopted such devices (e.g. the HKS series, and the Polish Jantar). With modern plastic materials it is quite feasible for a model to have a flexible surface on one side, so that the simple flap joint is fully sealed and smoothly curved, rather than sharply kinked (Fig. 7.11).

7.11 AEROBATIC MODELS

It is undesirable to camber the wing, or tailplane, of any 'pure' aerobatic model. For inverted flight, it is important that control response and model behaviour in all respects are the same as when flying normally. A symmetrical profile is necessary. Such models may, indeed, be fully symmetrical about the thrust line, except for the undercarriage. (Indeed, with an undercarriage on both sides, inverted 'touch and go' landings would be possible.) Aerobatic sailplanes usually require some camber to permit soaring when conditions are weak. Camber flaps, carefully designed and acting also as ailerons, should be employed, to allow camber to be adjusted to suit conditions, and or inverted soaring.

7.12 CAMBER AND CENTRE OF PRESSURE

There are two equally valid ways of describing the forces which are generated by a wing in flight. The older and more traditional method dates back to the time of sailing ships and was employed by the first scientific research workers who used wind tunnels to investigate the behaviour of wing profiles. When a test wing was mounted in the wind tunnel, the lift was measured as a force at right angles to the airflow and the drag as a component of force directly downstream. There was also an additional force tending to twist the wing round to a different angle of attack from that chosen by the technician. This force, tending either to pitch the wing to a higher angle or to a lower angle of attack, was measured as a pitching moment but its direction and strength seemed to vary from one wind tunnel to another. It was soon realised that the point at which the test wing was suspended, whether at the leading edge, or at the mid chord point, or somewhere else, was responsible for these apparent variations. It was as if the point of action of the lift force moved back and forth relative to the wing chord and when looked at in this way, it became possible to plot the position of this apparent point, in terms of percentages of the chord from the leading edge.

Now termed the *centre of pressure*, as the sailing masters had termed it, all wind tunnel engineers reported similar results in terms of centre of pressure movements. As the angle of attack was reduced, the c.p. seemed to move aft, and as the angle was increased, it moved forward. It never came further forward, however, than about 25% of the chord. At the stall, as the flow separated, the centre of pressure moved rapidly towards the 50%

chord position. Symmetrical wing profiles did not fit into this pattern very well, since they seemed to have centres of pressure practically fixed at one point at all angles below the stall. There was also a difficulty when the wing section was turned to its angle of zero lift. If movement of the lift action point was causing the pitching moment, when zero lift was produced, the pitching moment ought also to be zero. This was not so. At zero lift, all cambered wing profiles have a marked nose down pitching moment.

It is important to remember that the centre of pressure movement was always a result of calculation, using the basic information from the tunnel apparatus, which gave three distinct forces: lift, drag and pitching moment measured at one point on the wing. The centre of pressure was an abstract, theoretical point, for there was no way the measuring apparatus could be moved back and forward in the tunnel to track its supposed movement. Arithmetically dividing the measured lift force by the pitching force produced a length for the supposed moment.

At moderately low angles of attack, corresponding to a fast aeroplane flying at maximum airspeed, calculation and plotting of the centre of pressure showed it had moved far to the rear, so far that it was no longer within the wing chord at all but must be considered as lying somewhere beyond the trailing edge. The idea that the lift generated by the wing was taking effect somewhere behind the surface causing it created difficulties for the imagination (See Figure 10.5). The lift, after all, supports the aircraft and to suppose it to have its effect somewhere behind the main supporting component was strange. The calculations produced the extraordinary conclusion that the centre of pressure at zero lift (i.e. corresponding to an aeroplane in a vertical dive), must lie an *infinite* distance behind the wing.

Providing it is remembered that the centre of pressure is an abstraction, this rather old method of describing the wing forces remains quite valid and some modellers still use it. Nonetheless, it can cause confusion because it is often quite wrongly assumed that the centre of pressure cannot move beyond the trailing edge, or that it stops somewhere before reaching the trailing edge. This impression is reinforced by the older textbooks of aircraft engineering, which describe methods of calculating the loads on a wing for two conditions: 'centre of pressure forward' and 'centre of pressure back'. In these respectable ancient texts, 'centre of pressure back' corresponded to the loads expected when the aircraft was flying at its normal maximum permitted airspeed and the aerodynamic fact that the c.p. would move further aft if, for instance the aircraft was in a steep dive, was not always mentioned.

7.13 THE AERODYNAMIC CENTRE

That symmetrical wing sections would have a fixed centre of pressure at the quarter chord point, so long as the airflow did not separate, was predicted by theory long before wind tunnel engineers discovered it to be so in practice. The same theory also gave special significance to the 25% chord point for cambered profiles. It was calculated that in the wind tunnel (with a constant speed of flow regardless of the angle of attack), even though the lift and drag forces varied as the angle of attack changed, if the pitching moment was always measured at the 25% point, it would remain *constant*. This was very easily tested in the wind tunnel and it was soon proved to be correct, or so nearly so that it could be assumed true for all practical engineering purposes. Wind tunnel results at the present time are obtained by measuring all the forces on the wing at the 25% point. Lift and drag forces are reduced to coefficient form, using the equations given in Chapter 2 (2.6 & 2.13). The pitching force is treated in exactly the same way. The result is that although the lift and drag curves, on the results charts, show great variations with angles of attack, the pitching moment coefficient normally appears as a straight line at some constant or nearly

Fig. 7.10 Flap detail design

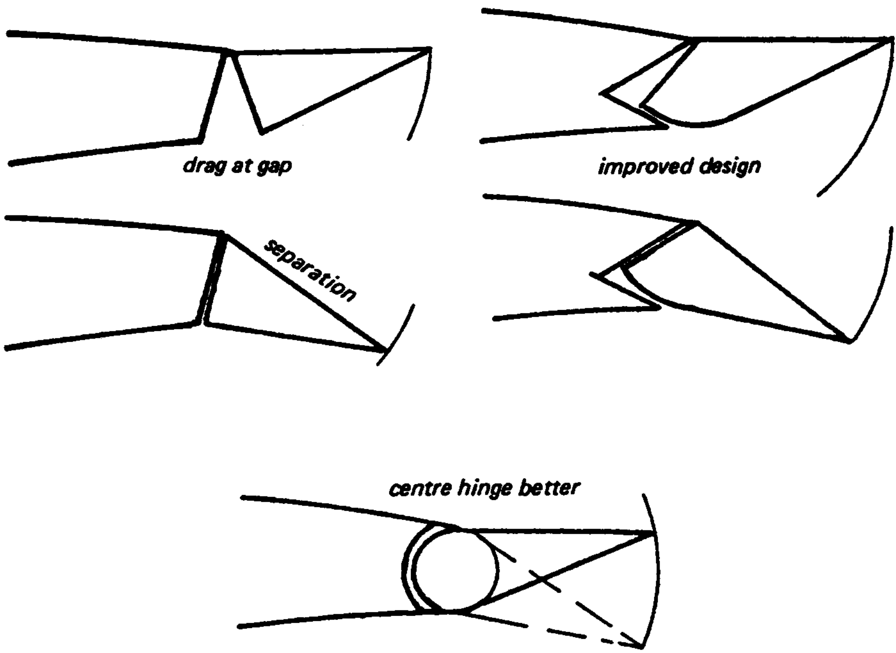

Fig. 7.11 Improved flap design

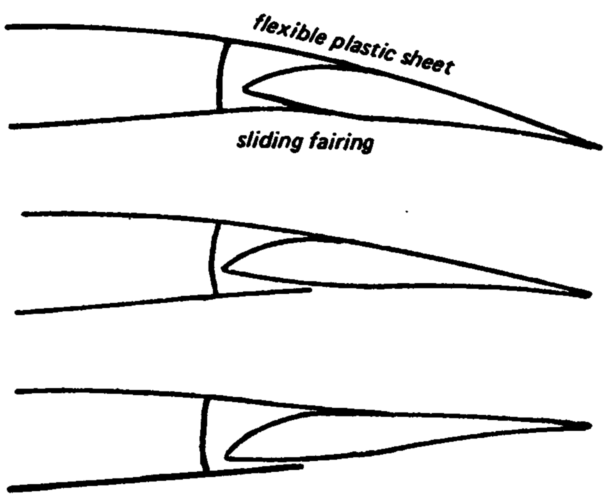

constant figure. The point on a wing at which the pitching moment coefficient is constant is defined as the *aerodynamic centre* of the wing.

The lift and drag both act at the aerodynamic centre; the lift force does not in fact migrate to and fro. At the a.c. there will also be a pitching moment. In the case of symmetrical wings this is zero unless the flow separates, in which case it changes sharply to a nose down or negative force. With cambered wings of the usual kind there will always be a negative, nose down pitching moment, its strength depending almost entirely on the camber. The more nearly symmetrical the wing section is, the weaker the negative pitching moment. As before, if the flow separates, the pitching moment changes as for symmetrical sections, becoming more negative.

Some specially designed wing profiles, particularly those with reflexed camber, may have zero pitching moment like symmetrical sections, or, if the reflexing is exaggerated, a positive, nose up pitching moment may be made to appear. In fact, an orthodox cambered profile, when inverted, behaves like a strongly reflexed aerofoil and tends to pitch nose up. (An example of a reflexed camber line is given in Figure 7.2).

When the airflow over the wing separates locally, as nearly always happens on model wings at low Reynolds numbers, the aerodynamic centre may sometimes move slightly from its expected location. Wind tunnel work in this area is still needed to be sure, but it seems that the lift point of action may vary either way perhaps by one or two percent, to 24 or 26%. For practical purposes, however, until research proves the contrary, modellers may take it that the *25% mean chord* point is the place where the lift force acts. The mean chord is mentioned here because allowance must be made for any wing sweep, back or forward, when working out where the aerodynamic centre of the wing as a whole lies, as distinct from the a.c. of the aerofoil in the wing tunnel (See Figure 6.5 and Appendix 1)

7.14 LOADS IN FLIGHT

A constant pitching *coefficient* in the steady speed flow of a wind tunnel does not imply a constant pitching *force* when a cambered wing is in real flight. The standard equations of Chapter 2 point to the powerful influence of flight velocity: all aerodynamic forces increase in strength with the *square* of the airspeed. Thus, a constant pitching coefficient means a nose down force which increases enormously as the airspeed rises. This force tends to distort the wing, raising the trailing edge and, since the tips are less rigid than the root, the wing acquires a 'washout' that was not intended by the designer. If the wing is suitably stiff in torsion, the twisting will be slight, although there is always some. If the model is comparatively flimsy, with wings covered with plastic film, the distortion may be very severe and has highly undesirable effects. In extremis, the wing itself may twist so far that the tips are 'lifting' downwards and they may break off in the downward direction. At best, the carefully designed elliptical lift distribution will be lost at high speed. The twist may also initiate flutter or jam aileron control rods.

The pitching force, nose down, must be balanced in some way, or the model as a whole will be incapable of flight in equilibrium. The tailplane, in an orthodox model, provides the balancing force. At high speed with a cambered wing the direction of this tail force is invariably downwards – the pitching moment tries to pitch the model nose down, the tailplane must restrain this. The more cambered the wing, the larger this load on the tail will be, at a given speed. Some radio controlled model sailplanes, designed primarily for thermal soaring and based on 'free flight' model principles, have been known to break up in the air when 'penetrating'. The tailplanes may break, or the wings, or both. For high speed flight, wings must be stiff in torsion and tails strong in downward bending. A sailplane may 'tuck under' into a dive beyond the vertical, if the tailplane is incapable of resisting the pitching force of the cambered wing at speed. (See also 12.22) Another reason for reducing camber on all fast flying models, including pylon racers and multi-task sailplanes is to reduce the download on the tailplane.

7.15 AILERON REVERSAL

The effect of ailerons is not only to change the section c_l of the parts of the wings where they operate, but also the pitching moment. A down-going aileron tends to twist the wing to smaller angle of attack and an upgoing aileron vice-versa. As before, such twisting forces increase when the model is at high speed. If the wing is flexible, the effect of the camber change may be equalled and cancelled out completely by the effect of the wing distortion on the angle of attack. A model which suffered from this, as some do, might be deemed to have suffered a radio failure or the servos might be thought overloaded. While such faults as these do sometimes develop, torsionally stiff wings are essential for aileron control at high speeds, particularly on high aspect ratio sailplanes which tend to be flexible and which also require large ailerons.

8
Aerofoil sections: ii. Turbulent flow aerofoils

8.1 PRESSURE DISTRIBUTIONS AT LOW Re

The appearance of a separation bubble on a wing as described in Chapter 3 causes a change in the air pressure and thus affects the lift. It also changes the effective shape of the wing, since the main flow has to accommodate. This changes form drag. There are various techniques for observing, in the wind tunnel, such effects. Tests by K. Kraemer published in 1961 are summarised in Figures 8.1 – 8.3 for the popular model aerofoil, Göttingen 801 (similar to MVA 301). Later research has amply confirmed and extended these results. In these diagrams, the pressure at each point on the upper and lower wing surface is plotted against the chord for several different angles of attack. For positive lift to be developed there must be a substantial difference between the two surfaces. Consider Figure 8.1 first. The pressure is plotted as a ratio of the local value to the static value in the mainstream (reduced to coefficient form in this case in the usual way by dividing by $\frac{1}{2}\rho V^2$). The reduced pressure on the upper surface is plotted as series of curves generally on the negative side of the graph, while the pressure increase beneath the wing is plotted on the other side of the zero line. At an angle of attack of 6 degrees, pressure on the *upper* surface *falls* to a minimum at about 15 percent of the wing chord, and then gradually rises to near the static value at the trailing edge. At 12 degrees the minimum pressure point is further forward and lower, while at 18 degrees the curve reaches its negative 'peak' very close to the leading edge and lower still, as could be expected from an aerofoil generating high lift. In accordance with Bernoulli's theorem, flow velocity varies in step with the pressure. The curves give no sign of separation, the aerofoil is working efficiently. At the Reynolds number of 400,000 (*wing* Re based on chord) the boundary layer makes a natural, unforced transition to turbulent flow somewhere ahead of the minimum pressure point as in Fig. 3.11. At the lower Re of 75,000, well within the model range, a very different pressure pattern is found (Fig. 8.2). At angle of attack 6 degrees, while the pressure minimum is about the same, a section of the curve is flat between about 40 and 76% of the chord. This indicates almost constant pressure over this zone, characteristic of a long separation bubble. However, the boundary layer leaps over the bubble safely and re-attaches. At 12 degrees the peak is further forward as before, the separation bubble is shorter. At 18 degrees the bubble extends over about 30% of the chord, beginning at about 38%. The aerofoil at Re 75,000 is in a near critical condition. It works efficiently though rather less so than at the higher Re. Further reduction of Re has serious effects. These are shown in Figure 8.3. At all angles of attack, complete flow separation occurs a little way behind the minimum pressure point, and there is no re-attachment. Some lift is generated, but above an angle of attack of 6 degrees the wing is completely stalled, drag is

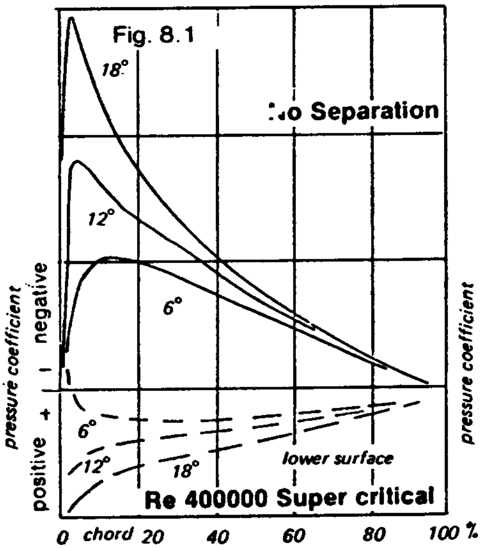

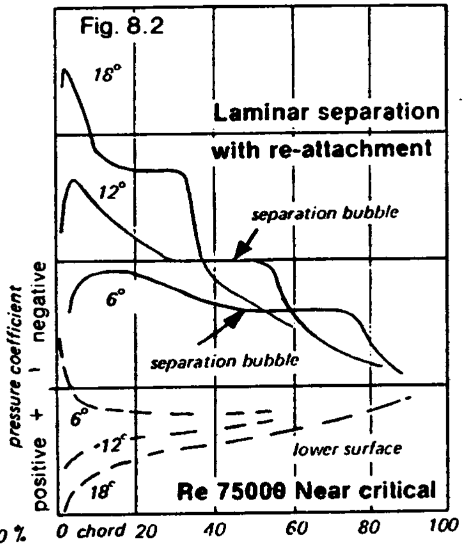

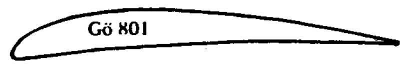

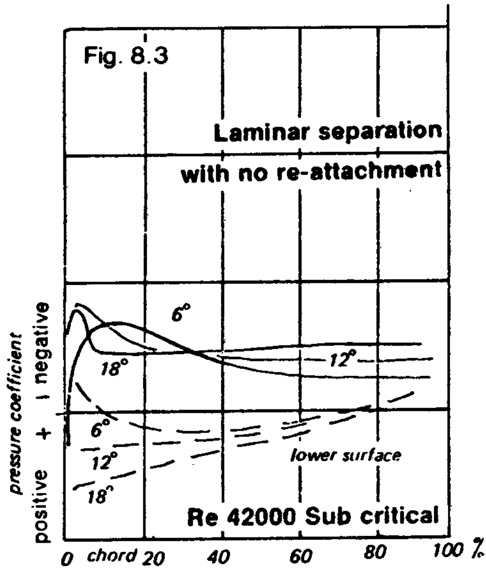

Figs. 8.1, 2 and 3
Tests on Göttingen 801 aerofoil by K. Kraemer

extremely high. The aerofoil is clearly unsuitable for use on any model operating in this Re range.

8.2 THE CRITICAL REYNOLDS NUMBER OF AEROFOILS

Detailed wind tunnel results for the Göttingen 801 profile are given in Appendix 2. For any aerofoil of this type, there is a *critical wing Reynolds number* at which separation is followed by re-attachment. Above this Re, the wing will work well, below it, it will be very inefficient. A model with such a profile below critical Re will hardly be capable of flight.

The first important investigation of wing profiles at model aircraft values of the wing Re were made at Cologne during the late nineteen thirties by F.W. Schmitz. His book, *Aerodynamik des Flugmodells* (*Aerodynamics of Flying Models*) published in 1942 remains a classic.* Because of the war Schmitz's work did not become generally known until after 1946, but since then his recommendations have been widely accepted and further work by K. Kraemer and G. Muessman and many others more recently, has tended to confirm and amplify most of Schmitz's original findings. This has led to the concentration of effort by modellers on aerofoil profiles with low critical Reynolds numbers. Techniques and devices have been adopted which ensure that the boundary layer over small model wings is made turbulent as early as possible. This causes an increase in skin drag, but this loss is far less significant than the prevention of early flow separation on the grand scale indicated by Figure 8.3.

8.3 HYSTERESIS

One of Schmitz's original diagrams is reproduced in Figure 8.4. An accurately made model of the N-60 was suspended in a wind tunnel and the speed of the tunnel fan was gradually increased to give a rising Reynolds number. Coefficients of lift, drag and pitching moment were measured stage by stage. Consider first the lift curve (C_L). The flow is sub-critical, completely separated, at the lower Re values, and although the lift improves slightly as the Re rises, the super-critical condition does not arrive until Re 147,000 when the curve leaps to a higher value. In the drag diagram (C_d), there is a corresponding sudden fall. This marked change of efficiency is indicative of re-attachment of the flow, and is accompanied by a change of the pitching moment. In the next test, the flow speed was gradually reduced, and, as before, the coefficients were measured at each stage. This time, super-critical flow continued down to Re 82,400, as shown by Schmitz's curve C′ to E′. Then, with little warning, the flow separated and the lift collapsed, with large rise in drag. Between Re 82,400 and 147,000 there is what is known as hysteresis loop. Schmitz found that, starting with separated, sub-critical flow between Re 82,400 and 147,000 he could cause a great improvement in aerofoil performance if he could make the flow turbulent. This he did by briefly inserting a stick into the tunnel airflow stream ahead of the wing model. The flow immediately re-attached, and the lift leapt up to the higher curve. On removing this crude 'turbulator', the flow remained attached. Below 82,400, i.e. outside the loop, on the low Re side, the turbulator had a similar effect when inserted, but as soon as it was removed, the flow returned to sub-critical and separated from the wing. *At other angles of attack, the critical Re was different.* Schmitz found that flow separation on the N-60, without turbulator, was inevitable below Re 63,000 at any angle of attack. This figure is usually quoted as the 'critical Re' for this aerofoil, but at various angles of attack the separation occurs at different Re. Even at Re 168,000, a hysteresis loop was still present at high angles of attack, hence the N-60, for reliable use on models flying at high C_L, would be best fitted with some device to introduce artificial turbulence into the airflow.

Schmitz also tested the much thicker, highly cambered profile, Göttingen 625, which was found to have a higher critical Re than the N-60, the loop beginning at 105,000. But

*Apart from copies at the library of R.A.E., Farnborough, and at the Science Museum Library in South Kensington, an English translation is available from the British Library, catalogued as *R.T.P. Translations Numbers 2460, 2204, 2457 and 2442*. A N.A.C.A. translation is also obtainable through the U.S. Information Service. A new German edition was published in 1976.

again, the introduction of a turbulator, in the form of a wire mounted just ahead of the leading edge (see Fig. 8.5), brought the critical value down to about 50,000. Neither the N-16 nor the Gö 625 is popular among modellers, but they are representative of a type of profile which remains in widespread use. In 1958–59, G. Muessmann, investigating profiles for gas and steam turbine blades, published test results on four flat-bottomed aerofoils of varying thicknesses and cambers. These closely resemble the profiles favoured for beginners' and sport models, and tailplanes, the so-called 'Clark Y' type aerofoils. From these tests it was found that the Gö 796, generally similar to the Clark Y, had a critical Re (lowest value) very similar to that of the N-60. The well-known NACA 4412 is about the same. On the other hand, Muessman's 20% thick profile, the Gö 798, had a critical Re similar to the equally thick Gö 625, while the thin Muessman Gö 795 began to show signs of general flow separation only at the lowest Re of the tests, 38,000.

Fig. 8.4 F. W. Schmitz's test results on the N.60 aerofoil at 10° angle of attack at Re from 20,000 to 165,000 showing the hysteresis loop

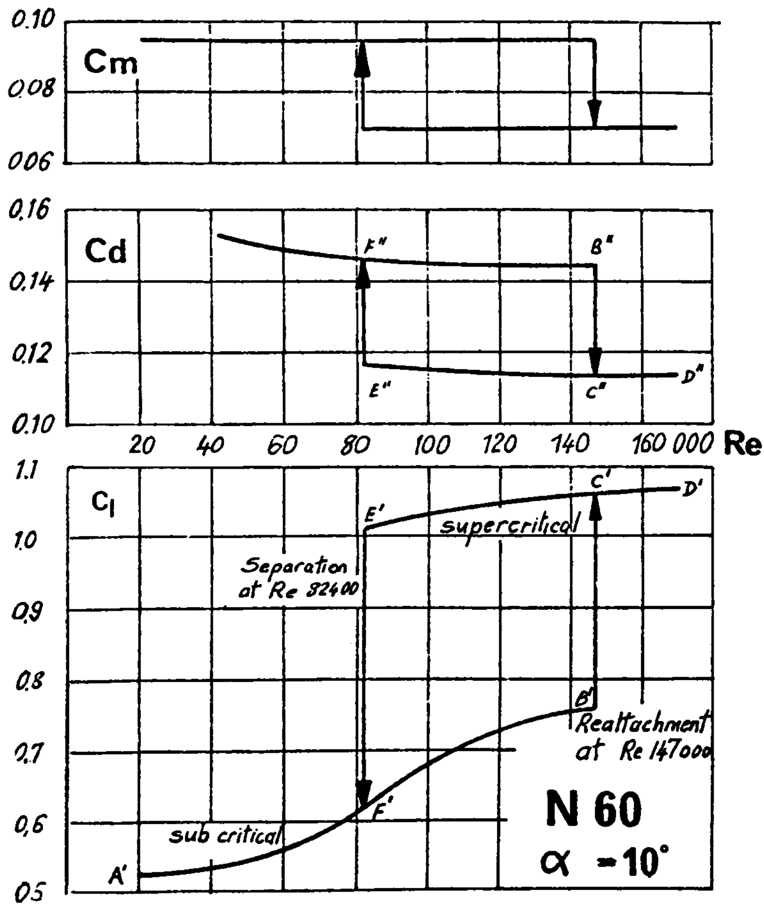

Fig. 8.5 Flow near a wing leading edge

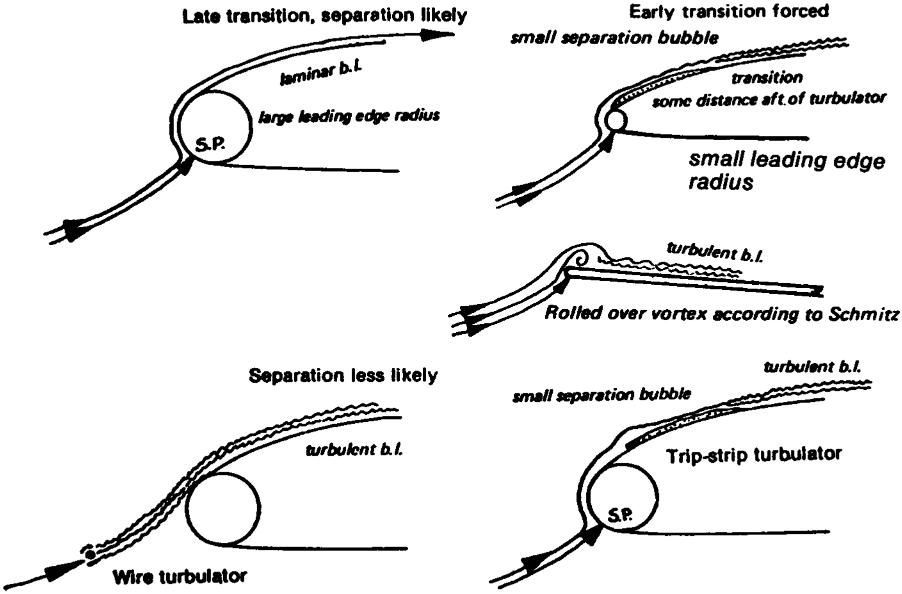

These results confirmed Schmitz's own tests. By far the most efficient profiles tested by Schmitz were the thinnest, the curved plate, Göttingen 417a, and the slightly thicker more cambered plate 417b. (His work on the latter was not published till 1953.) Within the range of his tests, these profiles showed little signs of flow detachment. Their critical Re was too low to be measured on his equipment. This, Schmitz pointed out, explained their obvious success on indoor flying models.

8.4 THE LEADING EDGE RADIUS

The reason for the low critical Re of thin profiles was, Schmitz argued, their combination of very small nose or leading edge radius and relatively small upper surface curvature. The stagnation point of the airflow near the leading edge of a wing at a positive angle of attack is, as Figure 2.2 shows, always slightly below the geometric leading edge. The boundary layer thus begins its journey over the upper surface by flowing around the leading edge itself. At high angles of attack, the flow in this neighbourhood is even slightly upstream (Fig. 8.5). From near stagnation, the boundary layer thus moves towards a low pressure region on the upper surface, and accelerates. If the profile has a smoothly rounded leading edge of large radius, as thick aerofoils usually do, the boundary layer can follow this curve easily and remains laminar. If the leading edge radius is small, as on thin profiles, the boundary layer is compelled to flow round a very sharp curve or even a knife-like edge, changing direction very sharply while accelerating rapidly towards the low pressure point which, on profiles of this early kind, lies only a small distance behind the leading edge. The boundary layer inertia may be expected to overcome the viscous forces at the sudden change of direction, and separate from the wing surface. It re-attaches immediately the corner is passed, but a very small separation bubble, or what

Schmitz called a 'rolled over vortex' forms in the boundary layer. The small leading edge radius thus introduces some artificial turbulence into the airflow, and this encourages early transition. The transition and re-attachment is not instantaneous. A separation bubble forms, and the boundary layer re-attaches some distance aft of the leading edge.

8.5 TURBULATORS

The effect of the sharp leading edge is very similar to that of a turbulator wire in the main stream ahead of the leading edge. A similar effect is obtained by mounting, on or just behind the leading edge, a raised 'trip strip' or leading edge turbulator, which may be of various forms and sizes. In each case, what is required is a brief separation bubble followed by turbulent re-attachment downstream. A 'turbulator' which is too small will not achieve the early transition, but one which is too large may itself cause flow separation.

Once the boundary layer has been forced into turbulence, it remains important that it should not separate from the upper surface. A profile with a turbulator or sharp leading edge still requires the air to flow against an adverse pressure gradient once it has passed the minimum pressure point. A thin profile presents a less formidable task to the boundary layer, so separation may be avoided, on the upper surface. On the underside, at high angles of attack flow separation is unlikely since once the point of maximum pressure is passed, the flow speeds up and tends to follow the surface of a thin profile closely. At low angles of attack under-side separation is very likely behind the leading edge, but re-attachment is still probable before the trailing edge (compare Fig. 2.3).

8.6 SEPARATION BUBBLES

Schmitz did not investigate in detail the size of separation bubbles over his aerofoils, and as shown in Fig. 8.2., these may be very extensive. The Gö 801 profile tested by Kraemer is of smaller thickness than the N-60 (10% as against 12.6%). It has a slightly smaller nose radius, but greater camber (7% at 35% compared with 4% at 40%). It thus comes somewhat closer to the thin curved plate profile, and its critical Re is slightly lower than that of N-60. Some detailed measurements made by Charwat at the University of California in 1956 –57 showed that a profile of the shape shown in Figure 8.6, with the small nose radius of 0.7%, also exhibited separation bubbles very similar to those of the 801 profile. The aerofoil in this case, designed by Seredinsky, following one of Schmitz's suggestions, was based on a profile of orthodox type, but the underside of the leading edge was cut away to try to produce a profile with room for wing spars, yet with the advantages of a small leading edge radius. In these tests, a separation bubble formed over about 35 to 40% of the chord. Above 7° angle of attack the bubble moved forward. Turbulent flow separation occurred over the rear of the profile prior to the stall, but the profile worked well. The effect of the separation bubble's formation and movement is of considerable significance. The bubble is sufficiently large to divert the main airstream over the upper surface round a longer path, just as if the profile was more cambered. It has been established that a profile with the maximum camber point well forward develops a high maximum lift coefficient. (This was the reason for the NACA 210 camber form.) The result of this effective camber increase *together with bubble movement forward* at high angles of attack, is to increase the slope of the lift curve (compare Chapter 5) above that which is predicted by theory. Such evidence as there is from model operations tends to confirm that some aerofoils on A 2 sailplanes behave erratically. This may be attributable to shifting of the separation bubble, and its flattening effect on the chordwise pressure curve, to and fro on the wing as the angle of attack varies slightly. The fluctuating pressures over the profile cause sharp changes of the pitching moment which, as shown in Chapter 7, is already large because of the high camber of such wings. The hysteresis loop is caused by the bursting and re-forming of the separation bubble. A model in this critical Re region, capable of stable flight in smooth air, may become uncontrollable in rough conditions. These factors come together with the inherently pitch-sensitive qualities of the high aspect ratio wing to make the model sailplane operator's difficulties more severe. Providing these problems can be overcome, there is no doubt that, for high performance at low wing Re, thin, small leading-edge-radius profiles, appropriately cambered, are excellent.

By adding turbulators to thicker profiles, the low speed performance may be greatly improved, and even with the specialised 'low critical' profiles turbulators may be very useful. The turbulators used by Schmitz and others were usually wires mounted ahead of the leading edge on light outriggers; suitable positions for these are indicated in some of the diagrams in Appendix 2. For practical models, wires may be replaced by thin elastic or plastic strings. These are, however, rather a nuisance in operation, and the leading edge 'trip strip' may be easier to manage. Such strips have the advantage that they may be lightly pinned or 'tack glued' in various positions for trial, and moved or changed in size to give best results. If the critical Re of the profile chosen is already low turbulators cannot have much influence on still air performance. However, by triggering separation at a fixed point on the wing, they probably stabilise the position of the separation bubble, reducing the fluctuations of moment coefficient. The result should be an improvement in

Fig. 8.6 Separation and re-attachment on the Seredinsky aerofoil

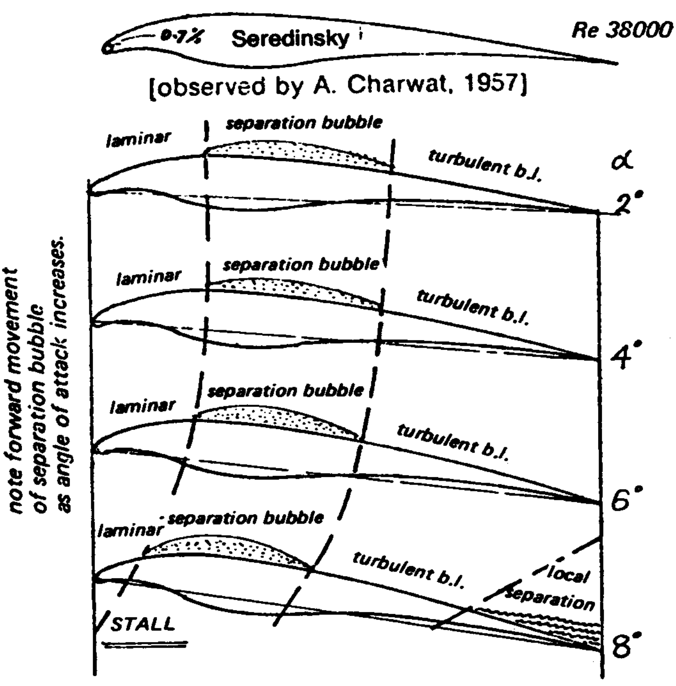

Fig. 8.7 Jedelsky wing

controllability of the model. A great deal of work has been done in 'full-sized' wind tunnels to determine the minimum size of such trip strips so that they are just big enough to cause transition to turbulent flow without causing wholesale flow separation. (This is because wind tunnel tests at low Re are not applicable to full-sized aircraft without such control of the boundary layer transition point.) For models, the best approach is that of systematic practical trials with turbulators of varying type and size in various positions.

8.7 THE EFFECTS OF STRUCTURE AND SURFACE

Models constructed on traditional lines may in effect have turbulators built in. The sag of tissue or other thin covering behind the leading edge spar between the ribs creates a bump in the profile. This may have an entirely beneficial effect on transition, and the good performance of some models can be explained only in this way. Among his tests on the Gö 801, Kraemer included tests of a paper-covered model which showed that sub-critical flow prevailed down to Re 42,000, comparable with the same aerofoil with a turbulator wire. Wind tunnel results on a number of balsawood and tissue covered wings, carried out at Stuttgart University and reported by Dr. D. Althaus (***Profilpolaren für den Modellflug***, Vol. 2) have shown the same effect at free flight model wing sizes and speeds. This suggests that attempts by modellers to preserve very accurate profiles over the front part of *low speed* model wings are sometimes misguided. The simple tissue-covered leading edge may prove more efficient than one with smooth sheet balsa covering, especially if the wing profile used is on the thick side with a large leading edge radius. It should be emphasised, nevertheless, that when the model is large enough or fast enough to avoid sub-critical Re problems, turbulators and surface irregularities at the leading edge cause drag to rise and c_l max. to fall. This may be confirmed by study of Appendix 2.

8.8 TURBULENT FLOW AEROFOILS

Arising directly out of Schmitz's researches, Sigurd Isaacson and Georges Benedek designed a whole series of aerofoil sections for use on models. The Wortmann M2 is also of this type. These are all intended to fly with turbulent boundary layers, at low speeds. All are thin. They have enjoyed wide popularity, many modellers use them without knowing their principles and may defeat the designer's purpose by rounding the leading edge too much during the final stages of sanding before covering the wing. As suggested above, this may not matter much if there is covering sag behind the leading edge, but in some cases the inaccuracy may cause a deterioration of performance.

The Seredinsky type of wing (Fig. 8.6) resembles the wing profile of some larger soaring birds. Although difficult to construct, it may prove very effective on smaller models, or models with very high aspect ratio, and hence small wing chords. The leading edge is similar to that of a simple curved plate, but the thickening of the profile on the underside provides room for a strong main spar without much effect on the upper surface flow.

Some of the Benedek aerofoils are intended for the Jedelsky type of structure, in which the necessary strength and stiffness is obtained by building the whole wing of solid balsa sheet, thick at the front with a thin sheet over the trailing portion, stiffened by ribs but without tissue covering. There is no doubt some penalty in higher drag on the underside of such profiles, but this may be acceptable if the aerofoil is more efficient at low Re. Unfortunately no wind tunnel tests have been published on such profiles (Fig. 8.7).

8.9 BOUNDARY LAYER INVIGORATORS

Research by Martyn Presnell in a wind tunnel at Hatfield has shown that considerable improvements in the performance of free-flight model sailplanes and rubber driven aeroplanes can be achieved by the use of multiple 'trip strips' or, in Presnell's terminology, 'invigorators'.

Test wings using the Benedek 6356b aerofoil (see Appendix 3) were constructed from materials exactly like those used in a typical F1A (A2) sailplane model. Balsa wood wing ribs and spars were used, the framework being covered with tissue paper, doped, and in one case, the forward third of the wing was skinned with thin sheet balsa. Not only were lift and drag forces measured, but some flow-visualisation tests were done. These involved coating the test wing with pigmented kerosene to reveal the nature of the boundary layer. Where the b.l. was turbulent the kerosene evaporated rapidly, leaving a film of pigment. Within the laminar separation bubble, the evaporation was less rapid so the flow of the air nearest the wing skin could be seen as the liquid moved upstream (See Figure 3.6). In the fully laminar flow regions the kerosene remained liquid longer still and flowed in the normal downstream direction. The flow separation point and re-attachment downstream of the bubble could then be discovered for each angle of attack. (Modellers have sometimes noticed that, when flying in the late afternoon or early evening at dewfall, dew deposited on a wing before flight will still sometimes be present after the flight on the leading edges where the flow is laminar, but evaporates from the rear parts of the wing where turbulent boundary layers are expected.)

The addition of a single turbulator at 5% of the wing chord improved the measured lift and drag figures, as expected, at Reynolds numbers below 40,000, although the separation bubble was still present. The turbulator consisted of a thin strip of adhesive plastic tape 0.15mm thick and 0.75mm wide, running spanwise.

It was then found that the addition of further strips of the same thin tape at various positions on the chord aft of the turbulator resulted in further improvements of lift and drag figures. The best results at Re below 70,000 were found with five of these invigorators in the positions shown in Figure 8.8. The original 5% turbulator remained in place throughout.

Presnell noted that placing an invigorator within the separation bubble, as revealed by the kerosene, made no detectable difference. The first invigorator must be placed just aft of the re-attachment point and the others spaced over the rear part of the wing in the turbulent boundary layer. The exact mechanism of the invigorators is not fully understood at present. It may be that they aid the already turbulent boundary layer to remain attached to the wing after the bubble has been passed. Presnell points out that several leading contest model fliers have used invigorators with success.

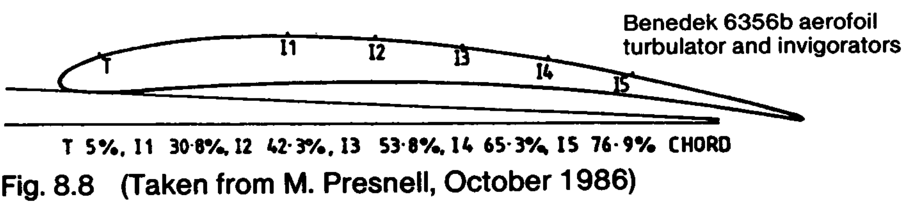

Fig. 8.8 (Taken from M. Presnell, October 1986)

8.10 OTHER FORMS OF TURBULATOR

The fineness of the tape used for turbulators in all wind tunnel testing is worthy of note. Modellers have sometimes employed much thicker ones, sometimes using strips of 1mm or 1.5mm balsa where thicknesses one tenth of this should be sufficient. Turbulators, or invigorators, which are too thick can cause flow separation rather than improving the boundary layer conditions.

8.11 ZIG ZAG TURBULATORS

There is much to be said for laying the turbulator tape in zig-zag fashion. Tests at Delft University have shown that a zig zag tape turbulator just ahead of the separation point on the wing has a better effect than a straight strip. The best spacing of the zig zags is a matter for experiment on a given wing. The best results are obtained when there is a definite relationship between the natural tendency of the flow within the separation bubble to develop waves and small, chordwise vortices (see paragraph 3.9). The modeller is unlikely to know what this is without very costly tunnel tests and some calculation, so trial and error is the likely way of discovering the optimum arrangement. Possibly pinking shears of different sizes could be used to produce tapes for trial.

8.12 PNEUMATIC TURBULATORS

Perforations, such as a row of pin holes through the wing skin instead of a tape strip, can act as a turbulator.

The air pressure inside a wing is usually somewhat greater than that on the upper surface, so air is drawn through the perforations and injected into the boundary layer. This in effect trips the flow and may be sufficient to make it turbulent. (The effect was first noticed by M.M. Gates in wind tunnel tests carried out in the 1950s.) Many full-sized sailplanes also use pneumatic boundary layer control, especially on the underside of the wing near the trailing edge, where a separation bubble commonly forms. High pressure air is taken in by a small intake, positioned under the wing, and this raises the pressure in the hollow chamber inside the wing. Very fine holes are drilled, at small spacing, through the skin just ahead of the separation point of the bubble. The injected air blows the boundary layer off the wing altogether and reduces the profile drag. Keeping the many small holes open is a problem of maintenance.

8.13 THE EFFECT OF NOISE

In measurements of boundary layers in low turbulence wind tunnels, it has been recognised for some time that noise alone can cause a delicate boundary layer flow to change sharply. Noise generated by the fan or motor of a wind tunnel can provoke early transition of a laminar boundary layer, and even the sound of someone walking past the test section may cause a change. Elaborate tests have been made with artificially generated sounds of varying pitch and volume, which show that separation and stalling can to some degree be controlled by this means. Sound is, basically, a series of small compression waves in the air and this may be enough to change the microscopic turbulence. Alternatively, the air noise may cause sympathetic vibrations in the solid wing skin, which could cause the boundary layer flow to change.

In practical model flying it is quite likely that the noise and vibrations caused by the engine and propeller cause the boundary layer to make transition to turbulence sooner than would occur on a sailplane, for instance. (It is highly unlikely that shouting, screaming or even singing at a model sailplane will have any effect!)

9
Aerofoil sections: iii. Laminar flow aerofoils

9.1 VELOCITY AND PRESSURE DISTRIBUTIONS

Aeromodelling has undergone a revolution since the time of F.W. Schmitz. Free flight models still operate close to critical Reynolds number conditions but radio controlled models, especially the larger sailplanes, high speed racers and aerobatic models are usually outside the danger area. Many such models fly quite successfully with profiles similar to the Clark Y or Göttingen 796 and it is obvious that problems of sub-critical flow separation have been left behind. Part of the reason for this is that such models do not usually fly at very high angles of attack. As Schmitz's results showed, a profile like the N-60 operated efficiently at a low angle of attack but stalled early even when operating, nominally, above its critical Re. The same thing was found on the Gö 801, separation problems at high angles of attack did not entirely disappear until about Re 170,000. Modellers have put up with the premature stall of such profiles. Performance at higher speeds is quite good. The pylon racing model is in any case operating most of the time at Re's quite comparable with those of full-sized sailplanes and even some light aeroplanes. Very great improvements in performance have been achieved in full-sized sailplanes, and some powered aircraft, by the use of so-called laminar flow profiles. The advantage in terms of saving skin friction are very large, especially at high speeds where profile drag becomes of major importance (Fig. 4.10). Early work in this area by the Low Speed Aerodynamics Research Association has been largely overlooked by modellers, but the aerofoils LDC2 and LDC3M produced were used on some models at the time, about 1948, when they first appeared.

As described in Chapter 3, on any wing, the boundary layer will be laminar at first near the leading edge, but will make a transition to turbulent flow when it reaches the critical boundary layer Re. The value of this critical Re will depend on the quality of the wing surface. Many full-sized aircraft have poor surfaces. Even if highly polished, there are waves and ripples in the skin caused by rivet tension and humps created by stiffeners and spars. It is very difficult to preserve laminar flow over such a wing for more than a few centimetres near the extreme leading edge, and even when great efforts are made to achieve an accurate profile, the large Reynolds number associated with the high flight speed and large wing chord, promotes early transition. The smallest defect in the surface, even a fly speck or the crushed body of an insect, can cause transition. For these and similar reasons designers of full-sized light aeroplanes have not been able to achieve all the benefits of low drag, laminar flow, and many still prefer to use relatively old-fashioned profiles. However, as the Reynolds number falls, the chances of preserving laminar flow over more of the wing increase. Small defects that, at higher velocities, cause transition, may be over-ridden by the relatively more viscous boundary layer, and if wings can be made accurately, as they are in modern full-sized sailplanes, the aerodynamicists' predictions, based on theoretical studies and wind tunnel tests, come true. The problem for modellers is the reverse of that for the turbulent flow aerofoils. At sub-critical Re, turbulators and protrusions caused by spars may improve performance by forcing transition in the boundary layer. Laminar flow models should seek to maintain profile accuracy at least as far back as the point where the boundary layer will make its transition naturally. The standard of precision required is, because of the low Re, less than that needed for the full-sized aircraft.

Providing the wing surface is smooth, a laminar boundary layer will tend to prevail as long as the speed of flow is rising under the influence of the low pressure area above the wing (Fig. 3.5). Behind the minimum pressure point the laminar flow persists for some distance but then a separation bubble forms and (providing super-critical Re prevails), the flow re-attaches as a turbulent boundary layer. In Figure 9.1 velocity measurements made on two wing profiles are shown. These show how the speed of flow over the upper and lower surfaces vary at different angles of attack. On the Göttingen 389, for example, at 2.8 degrees angle, the flow on the upper surface increases rapidly to a maximum within the first ten percent of the wing chord. Laminar flow will persist up to this point and a little way beyond it, but then transition will occur and turbulent, high drag flow covers most of the wing. At a lower angle of attack, −3.1 degrees, the maximum velocity point on the upper side is somewhat further back, but at higher angles it moves forward so that near the stall, at 14.6 degrees, the whole upper surface is in turbulent flow. Meanwhile, on the underside the velocity peak of the upper surface is opposed by a velocity decrease close to the leading edge, and thereafter the air accelerates towards the trailing edge. Transition

Fig. 9.1 Velocity profiles of two Göttingen aerofoils

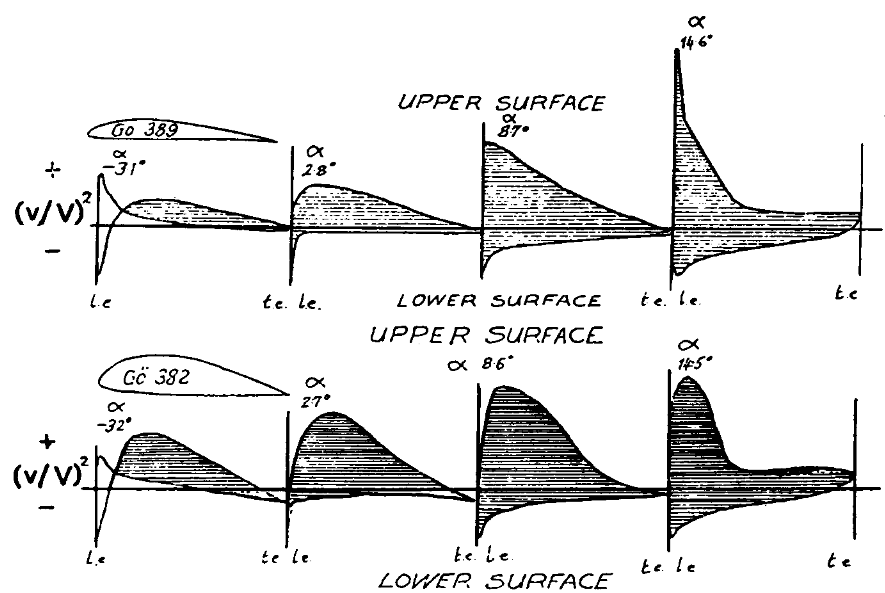

Fig. 9.2 Basic NACA 4 digit thickness forms, velocity, profiles.

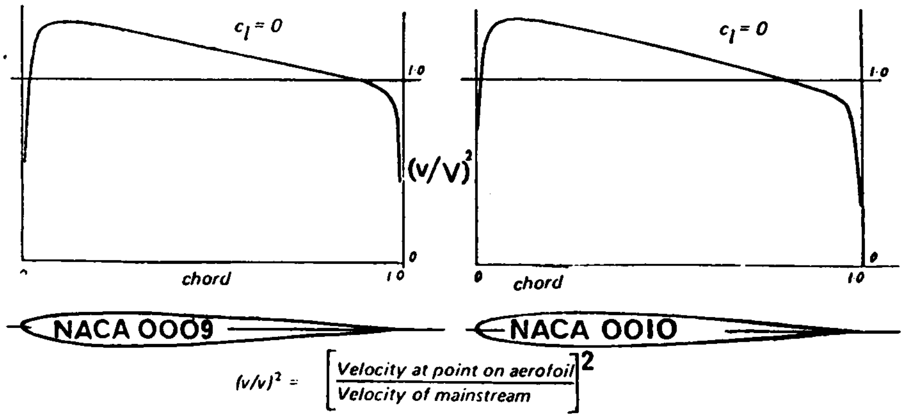

will already have taken place and the boundary layer will be turbulent. At the more negative angles of attack, the roles of upper and lower surfaces are reversed as the wing begins to 'lift' downwards.

The Göttingen 382 profile is a thicker version of the 389, but the velocity measurements show important differences. At 2.7 degrees angle, the velocity maximum on the upper side is about ten percent further aft than on the thinner profile, and even near the stall there is a likelihood for laminar flow back to about ten percent before the velocity decrease causes transition.

The details of the velocity of airflow over a wing depend on both its thickness form and its camber. The typical, pre-1940 aerofoils of Figure 9.1 and others of the same vintage, such as the Clark Y, N-60, etc. were designed around what was then thought to be the ideal form for any streamlined body. The same basic shape, thickened or thinned appropriately, was used for strut fairings, streamlined wires, tailplane and fin profiles, wheel spats and whole airship hulls. Typical ordinates are given in Figure 9.2 which refer to the NACA 'four digit' aerofoils. The velocity distribution graphs given with the profiles show that at zero angle of attack, the velocity peak (and hence minimum pressure point) on both surfaces is reached at about ten percent of the chord. A short distance aft of this, transition to turbulent flow occurs. Cambering changes this basic feature only slightly; such profiles are fundamentally incapable of preserving laminar airflow over much of the wing.

9.2 THE NACA '6' AEROFOILS

Aerofoils are no longer designed by 'cut and try' methods, but are worked out to fit their special purposes. The first substantial gains achieved were the NACA '6' series aerofoils developed before and during the Second World War. They were used, in slightly modified form, first on the P-51 'Mustang' fighter. These aerofoils were designed to achieve very low profile drag by preserving laminar flow over as much of the wing as possible. The improvements in practice were less than hoped for, because of the inaccuracies of the wings in service, but there were genuine overall benefits. The main method of achieving

Fig. 9.2 cont.

NACA 0009 LE RADIUS 0.89 PERCENT

CHORD STATION	UPPER SURFACE	CHORD STATION	LOWER SURFACE
XU	YU	XL	YL
0.000	0.000	0.000	0.000
.600	1.010	.600	- 1.010
.800	1.170	.800	- 1.170
1.250	1.420	1.250	- 1.420
2.500	1.961	2.500	- 1.961
5.000	2.666	5.000	- 2.666
7.500	3.150	7.500	- 3.150
10.000	3.512	10.000	- 3.512
15.000	4.009	15.000	- 4.009
20.000	4.303	20.000	- 4.303
25.000	4.456	25.000	- 4.456
30.000	4.501	30.000	- 4.501
40.000	4.352	40.000	- 4.352
50.000	3.971	50.000	- 3.971
60.000	3.423	60.000	- 3.423
70.000	2.748	70.000	- 2.748
80.000	1.967	80.000	- 1.967
90.000	1.086	90.000	- 1.086
95.000	.605	95.000	- .605
100.000	.095	100.000	- .095

NACA 0010 LE RADIUS 1.10 PERCENT

CHORD STATION	UPPER SURFACE	CHORD STATION	LOWER SURFACE
XU	YU	XL	YL
0.000	0.000	0.000	0.000
.600	1.120	.600	- 1.120
.800	1.250	.800	- 1.250
1.250	1.578	1.250	- 1.578
2.500	2.178	2.500	- 2.178
5.000	2.962	5.000	- 2.962
7.500	3.500	7.500	- 3.500
10.000	3.902	10.000	- 3.902
15.000	4.455	15.000	- 4.455
20.000	4.782	20.000	- 4.782
25.000	4.952	25.000	- 4.952
30.000	5.002	30.000	- 5.002
40.000	4.837	40.000	- 4.837
50.000	4.412	50.000	- 4.412
60.000	3.803	60.000	- 3.803
70.000	3.053	70.000	- 3.053
80.000	2.187	80.000	- 2.187
90.000	1.207	90.000	- 1.207
95.000	.672	95.000	- .672
100.000	.105	100.000	- .105

Note that the ordinates of the 9% thick profile are exactly 90% of the 10% profile. NACA four-digit symmetrical sections may always be scaled up or down to different thicknesses by simple arithmetic.

Fig. 9.3 Basic NACA '6' series thickness forms, velocity profiles

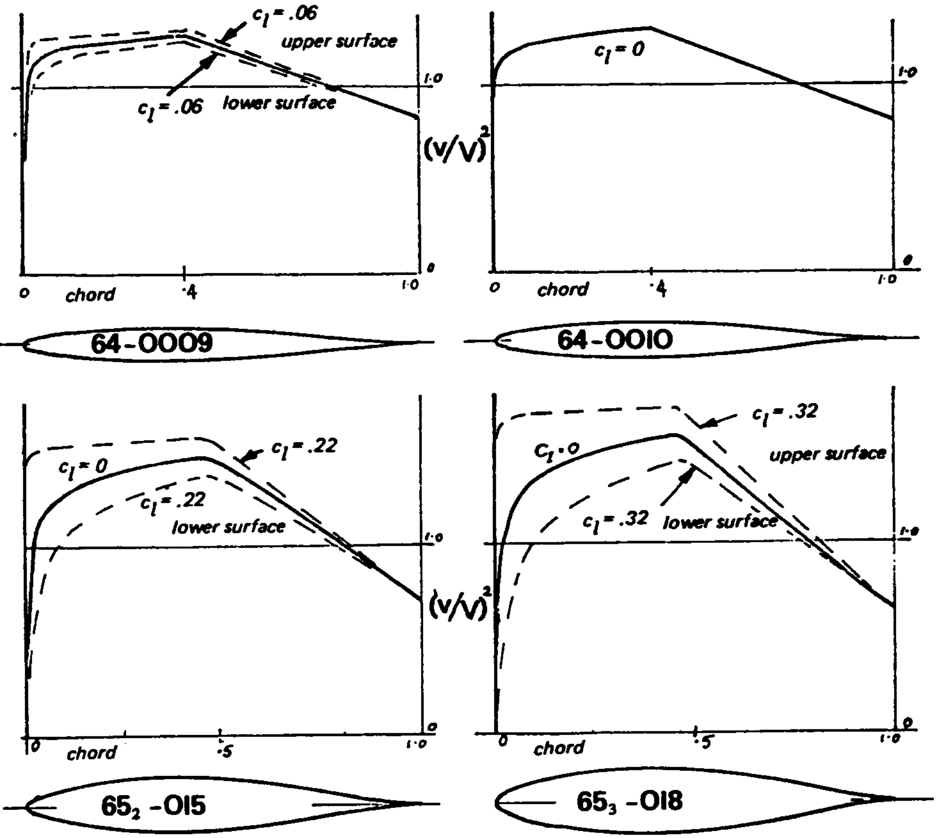

Fig. 9.4 Velocity gradients over a cambered NACA 6 profile

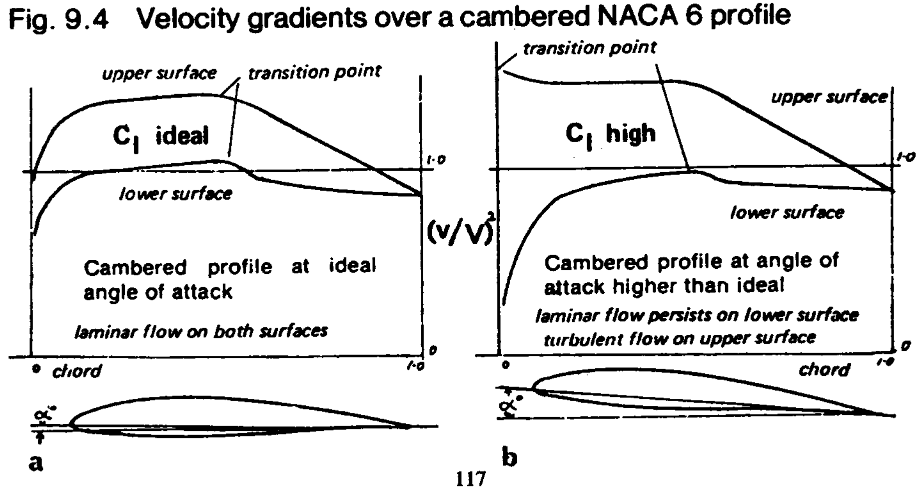

the lower drag was to employ aerofoil thickness forms similar to those shown in Figure 9.3. As the velocity diagrams show, at zero angle of attack the maximum velocity/minimum pressure point on these profiles is at 40% or 50% of the chord. Other thickness forms were designed with this point further back or further forward. The second digit of an NACA profile designation, such as the 4 in 64_3618, indicates the position of the maximum velocity point. The boundary layer, on a suitably smooth wing, will remain laminar to a point somewhere aft of the 40% chord position on such an aerofoil. (By suitably smooth is meant a wing free from ripples, humps or hollows rather than one which is highly polished.) As shown in Figure 9.3, at small angles of attack the velocity distribution *on both surfaces* is favourable for laminar flow back to the 40% point, the 9% thick profile at c_l of .06. The thicker profile, 65_2015 shows that laminar flow is preserved on both sides up to a c_l of 0.22. This is of great importance. A thicker wing at a high angle of attack may have greater percentage of laminar flow and hence lower drag than a thin profile. (Compare also the 65_3018 profile.) This applies equally to cambered profiles. If one of the symmetrical sections of Figure 9.3 is cambered round the NACA a = 1 mean line, the basic character of the velocity distribution, and hence laminar flow, is not changed. Figure 9.4 shows the results in graphical form. The amount of camber given to the profile is determined by the desired operational C_L, as described in Chapter 7. At this value, laminar flow prevails over both upper and lower surfaces, up to the peak velocity position and slightly beyond it. At a higher angle of attack, the velocity graph resembles that of Figure 9.4(b). Transition on the upper surface occurs futher forward. There may even be flow separation further aft, but this is not important since the aircraft is not intended to operate far from its designed C_L. The result in terms of drag at the design c_l of the profile is very substantial improvement.

9.3 THE LOW DRAG BUCKET

In Figure 9.5 is shown a typical curve of profile drag plotted against c_l for any of the NACA 6 series aerofoils. At the design c_l, drag is much lower than for an orthodox or old-fashioned section. On either side of this value there is a low drag range or 'bucket' in the graph, so that small departures from the ideal operating conditions cause no change in profile drag coefficient. At either side of the low drag bucket, on one surface or another, the velocity distribution changes and the boundary layer becomes turbulent, with an associated sharp rise in drag. In the NACA designations of these aerofoils, the third digit,

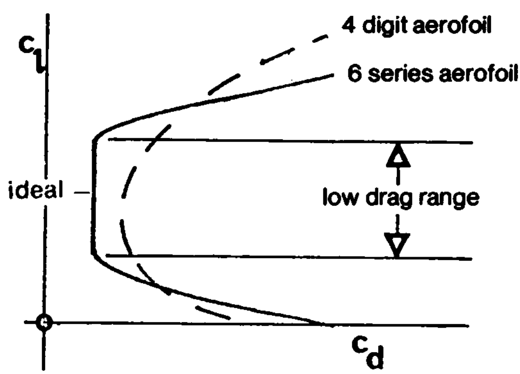

Fig. 9.5 The low drag range (drag bucket) of '6' series aerofoils

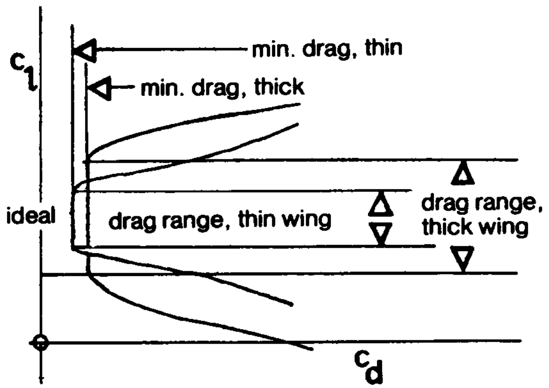

Fig. 9.6 The low drag range of thick and thin profiles

usually written as subscript thus: NACA 64_3418, indicates the width of the low drag bucket, in this case 0.3 c_l on either side of the ideal designed value for the profile. A profile with the subscript $_3$ as above, designed for a c_l of 0.4, will work efficiently at c_l down to 0.1 and up to 0.7. (Note, however, that constant drag coefficient does not mean constant drag *force* – the higher speed associated with lower C_L of the wing increase drag *force* at a constant C_D – see Chapter 2.) The fourth digit of the aerofoil number gives the design ideal lift coefficient, in tenths, and the final two figures give the profile thickness as a percentage of the chord.

As already noted from the velocity profiles of the thick profiles of Figure 9.3, favourable flow conditions are preserved on thicker aerofoils over a greater range of c_l than on thin ones. The absolute minimum drag of a thick profile is slightly more than for a thin section of similar camber, but the drag bucket of the thick profile is wider. This is indicated in Figure 9.5. Such a thick wing has a wider speed range, and, in the case, for example, of a racing model, will be less affected by slight inaccuracies of flying, and less slowed down in steep turns, than a model with thin wing and higher maximum speed straight and level.

As the Reynolds number is reduced, so long as flow remains super-critical (i.e. re-attachment after the separation bubble), the natural tendency for laminar flow to persist shows up. The minimum drag of the laminar flow profile is slightly higher (because the relative viscosity of the air at low speeds is greater compared with the density-speed-chord factors), but the boundary layer, after passing the maximum velocity point on the wing, remains laminar for a greater distance and this has the effect of widening the drag bucket slightly. The result is shown diagrammatically in Figure 9.6.

9.4 SAILPLANE AEROFOILS, SCALE AND FULL SIZE

All these features of the NACA '6' profiles were recognised in the 1950s by designers of full-sized sailplanes. The great width of the low drag range of the thicker profiles at sailplane Re led to the adoption of profiles such as the NACA 63_3618 and 63_3621 for such successful types as the Ka 6 and Skylark series respectively. The performance, particularly at high speeds, was a vast improvement on earlier types such as the Olympia and Weihe which had *thinner* wings (Göttingen 549) but with turbulent flow. However, although the new profiles were cambered for c_l 0.6, and worked efficiently up to c_l 0.9 and

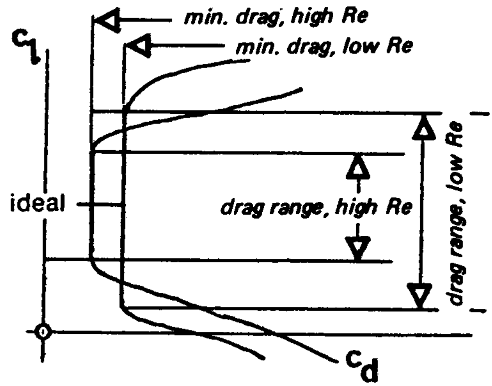

Fig. 9.7 The low drag range at high and low Re

a little beyond (because of the wider low drag bucket at low Re), there were still problems at higher c_l. Cambering the wings more led to flow separation at the low speed end of the range, and tended to spoil the high speed performance below c_l 0.3. How the '6' series profiles perform at Re lower than 700,000 is hardly known, since few wind tunnel tests have been carried out below this figure. They have been successfully used on man-powered aircraft and a few of the better hang gliders. They should perform very well on fast models, providing the correct camber value is chosen. The temptation to thin the profile on a speed model too much should be resisted. For practical racing, a thicker profile is less sensitive to errors and enables turns to be flown economically without danger of sudden increases of drag.

For scale model sailplanes, the great thickness of the typical '6' series aerofoils used on the prototypes may cause difficulties. Such aerofoils still have a critical Re below which flow will separate and not re-attach. Unless the model is very large in chord, the profile, while it should retain a laminar flow thickness form, will require thinning down. Of course, full-size sailplanes have very narrow, high aspect ratio wings. The very thick aerofoils on such types as the Skylark 2, 3 and 4 are not suitable for small models of these aircraft. Their wide low drag range cannot, therefore, be employed on small models. The same applies to more recent sailplane designs which still may have aerofoils of 17% thickness, with even higher a.r. Earlier, pre-laminar flow sailplanes make more suitable prototypes for scale modelling since they usually had lower aspect ratios (broader chord), and thinner aerofoils. However, some of these aerofoils had unduly large leading edge radii and hence high critical Re. Scale model sailplanes should, in general, be as large as possible if the same aerofoil is to be used on the prototype. Otherwise the flying performance will be very disappointing. The same argument applies, of course, to all scale models, but with full-sized powered aircraft speed *range* is less important so the aerofoils used are usually as thin as possible for the sake of efficiency at one speed. Hence the scale aerofoil tends to have a lower critical Re and there is more prospect of success for the small model. Also, with most prototypes, there are irregularities in the neighbourhood of the leading edge which allow the modeller to 'turbulate' the airflow. This applies with special force to so-called 'peanut' scale models. Some of the best full-sized prototypes for such models are the very early aeroplanes which had thin wings resembling the curved plate profiles of the previous chapter.

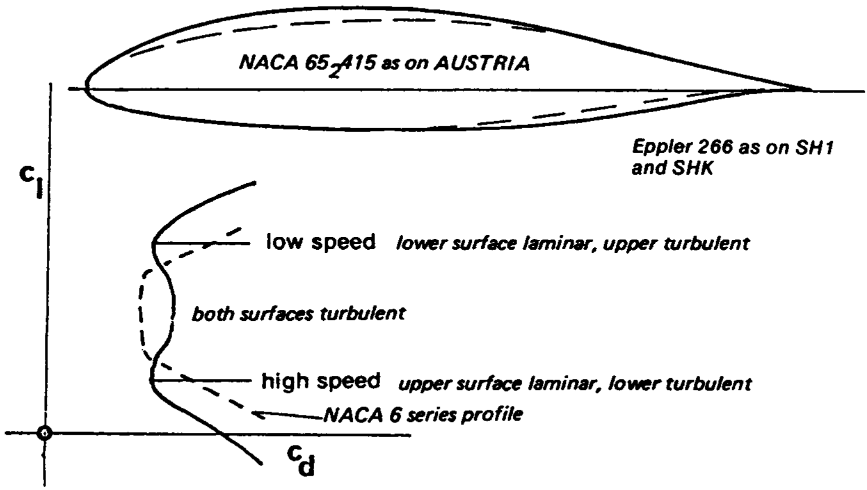

Fig. 9.8 The double drag bucket of early Eppler aerofoils

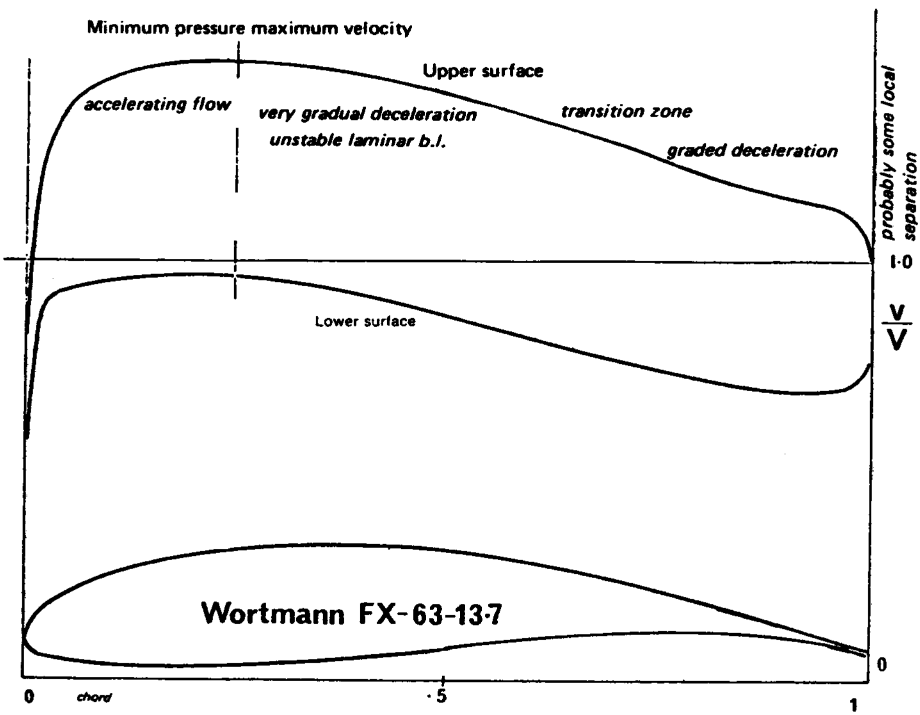

Fig. 9.9 Velocity gradients over a Wortmann low speed aerofoil for man-powered aircraft. 13.7% thick.

9.5 EPPLER AND WORTMANN PROFILES

In designing aerofoils the next important steps forward were taken by R. Eppler and F.X. Wortmann, working independently in Germany during the 1950s and 60s. Eppler's early full-sized sailplane profiles should not be confused with those he has more recently produced for models. They are designed on different principles, and may be distinguished by their more complex-seeming designations, such as EA 8 (−1) 1206. (One such experimental section was, unlike the others, intended for models, and has been tested by Kraemer in the wind tunnel. The results are given in Appendix 2, the Göttingen number being 804.) On full-sized sailplanes, the earlier Eppler profiles are now rarely employed, although in their day they were a distinct improvement, as far as *speed range* was concerned, over the NACA '6' profiles. Eppler argued that sailplanes never operated at one design value or ideal C_L, but were always either climbing in thermals at minimum sink corresponding to high c_l, or 'penetrating' at low C_L (see Fig. 4.3). Rather than trying to widen the low drag range of NACA profiles, he designed profiles which in effect split the bucket into two, as indicated in Figure 9.8. The first glassfibre sailplane, the record breaking Phönix, had a profile of this type, and so did the subsequent Phoebus series. The original (wooden) Standard Austria design with the NACA 65_2415 profile was much improved when it was re-winged with an Eppler profile to create the SH 1, even though this profile was slightly thicker. Eppler achieved his results by designing for laminar flow on one surface of the wing at high angle of attack, and the other surface at low angles of attack. In between, both surfaces were turbulent, but he argued that this hardly mattered. Flight measurements on the Phönix confirmed his theoretical expectations. It is, however, doubtful if these profiles are of value in modelling, and they will not be discussed further here.

F.X. Wortmann's work followed a different line.* On full-sized sailplanes, at the 1974 World Championships every sailplane competing had Wortmann aerofoils. The thinner examples work well on larger model sailplanes. Some of the less cambered Wortmann profiles might also be superior to the NACA '6' series for racing powered models. Wind tunnel results are promising. For gliders Wortmann concentrated on widening the low drag bucket of laminar flow profiles, using electronic computer techniques to achieve the desired grading of the velocity distribution curves.

The velocity distributions of the NACA profiles, as shown in Figure 9.3, exhibit a sharp kink in the curve at the maximum velocity/minimum pressure point. A straight line was drawn from here and the profile thickness designed to produce this sharp change. The airstream velocity after the sudden onset of deceleration slows down at a steady rate all the way. At low Re the separation bubble forms, on such a profile, almost immediately behind the minimum pressure point. After re-attachment, the turbulent boundary layer steadily loses momentum, and although it does not separate immediately, as it becomes slower and slower it loses its ability to maintain contact with the wing, and some separation is very likely before the trailing edge is reached. This separation marks the limit of the low drag bucket. At lower Re, to take advantage of the natural tendency to greater laminar flow, the sharp kink in the curve, Wortmann argued, should be smoothed out. The laminar boundary layer would then be able to persist further behind the minimum pressure point, and if the flow deceleration over this portion of the wing was gradual, it might be capable of continuing even as far as 70% of the way to the trailing edge. Transition, with separation bubble, would eventually come, however, and here again a different principle was needed. After transition, the boundary layer has plenty of momentum (providing it has not completely separated), and can remain attached to the wing even against a sharp pressure gradient. As it nears the trailing edge, the energy

* Professor Wortmann died in 1985.

available is less, so it should be required to fight a less severe gradient. The result of this reasoning in terms of graded velocity profile for a man-powered aircraft aerofoil is shown in Figure 9.9 and for a high speed aerofoil in Fig. 9.10.

Profiles designed around these principles have been extensively tested in wind tunnels and in flight, and the expected results are achieved. The low drag bucket is no longer so flat-bottomed, i.e. there is some increase of c_d as the c_l rises above the designed value, but the total width of the 'bucket' is considerably more than that of equivalent NACA profiles. Performance at high c_l is better. Ordinates for the thinner types of Wortmann profile are given in Appendix 3. The thicker profiles are probably not good for models. The FX 63-13.7 has been tested extensively by a number of different research organisations over a considerable range of Re numbers. It is too strongly cambered for most model applications, since it was designed for a man-powered aircraft. A number of flapped sections is also given. The flapped profiles give good results only if the flap is of the correct size, as specified, and the flap should be set correctly for each flying speed. If this is not done, the profile is actually less efficient than the un-flapped versions. However, with flaps correctly used and gaps sealed, the width of the low drag range is even further increased.

The Wortmann aerofoils are mutually compatible with one another for use in tapered wings. In particular the FX 60-126 was intended for use at wing tips. It has a late stall and so may be employed without washout, or only a very small amount. Large model sailplanes have been successful with these profiles. The FX 60-100, a thinner version, has been very popular with model fliers. At Re lower than 100 to 200 thousand the behaviour of most Wortmann sections remains to be investigated.

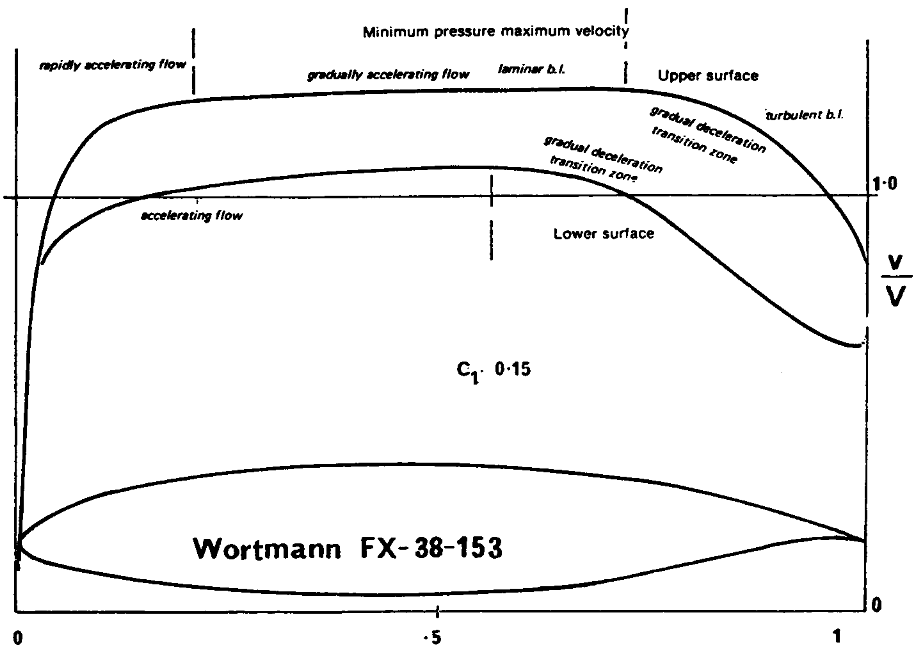

Fig. 9.10 Calculated velocity gradients over a Wortmann high speed aerofoil. 15.9% thick

9.6 EPPLER MODEL PROFILES

The aerofoils designed specifically for models by R. Eppler have achieved great popularity. They range from thin, highly cambered profiles intended for free-flight duration models, to much thicker sections for large sailplanes. By an extension of his earlier thinking, Eppler designed these profiles so that a pressure gradient favourable for laminar flow is preserved as far as possible on at least one surface of the wing – the upper surface at low angles of attack, the lower surface at high angles. However, at some intermediate angle, instead of both surfaces being turbulent (as with his full-sized profiles, Fig. 9.7), there is a range of angles over which laminar flow should exist on both surfaces for some distance. Examples, in terms of computed velocity distributions, are shown in Figures 9.11 – 9.13. At 9 degrees angle of attack the E 203 profile has an accelerating boundary layer on the underside up to about 35% of the chord. (The speed of flow remains less than that of the mainstream, to produce positive pressure.) After the maximum velocity point, the decrease is very gradual, so there is every chance for the laminar boundary layer to persist for some distance, and then become turbulent. On the upper surface, the velocity maximum is very close to the leading edge and the boundary layer is expected to become turbulent somewhere behind this minimum pressure point.

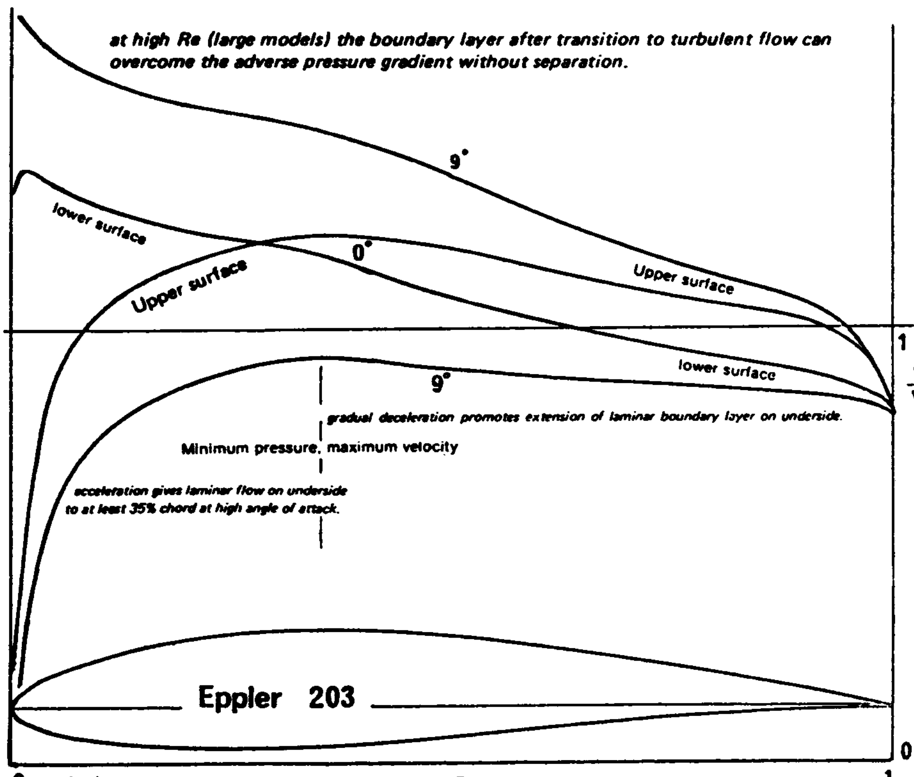

Fig. 9.11 Calculated velocity gradients over Eppler 203 aerofoil at 0° and 9° angle of attack

This profile is designed for large models, and there should be no danger of premature stall. After the separation bubble the boundary layer re-attaches, overcomes the adverse pressure gradient and remains attached. At zero angle of attack, close to the zero lift angle for this profile, the upper surface has laminar flow while the underside now has the early pressure peak and gradual deceleration thereafter. At angles between these two, the profile should have extensive laminar flow on both surfaces, and the minimum profile drag will be achieved. This is a relatively high speed profile. A similar set of curves for a lower speed profile, the E 385, is shown in Figure 9.12.

For very low Re, the thin profiles E 58 and 59 have been designed. The likelihood of flow separation at low Re is much greater, as stressed in Chapter 7, and Eppler admits that some separation does occur even on these very thin profiles due to the very sharp decrease of flow speeds near the trailing edge on the upper surfaces (see Fig. 9.13). However, at the designed angle of attack, the computed velocity and pressure gradient on the upper side is almost constant over a large proportion of the chord. This allows the laminar boundary layer to continue as far as possible and make a safe transition to

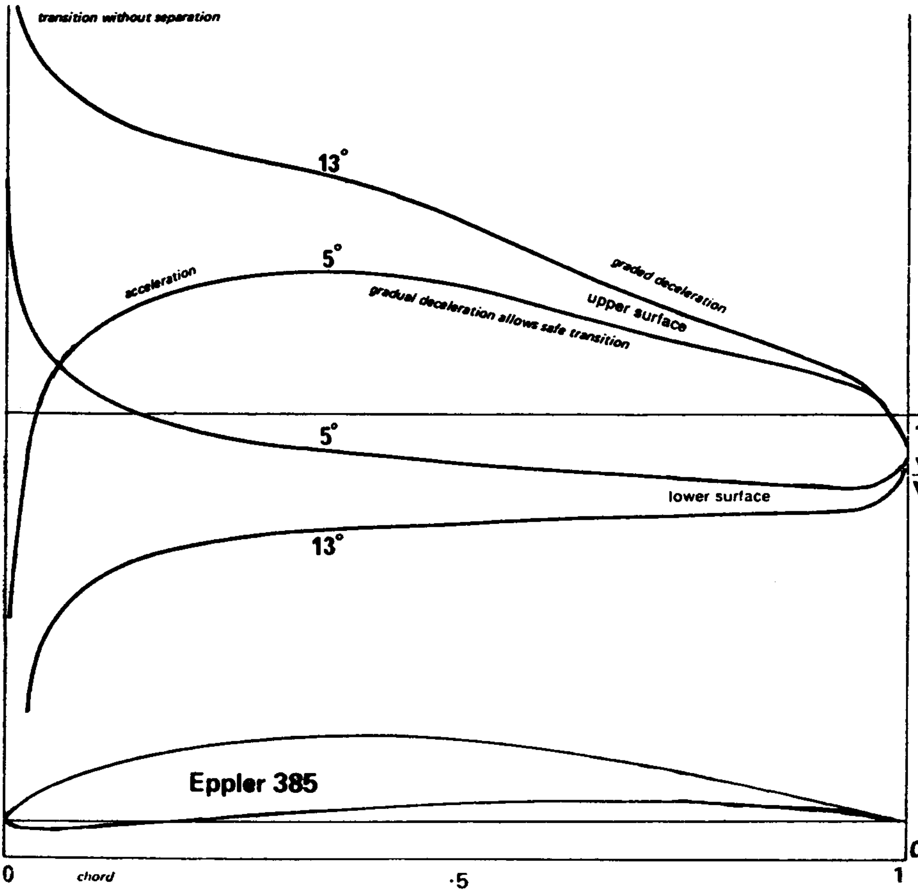

Fig. 9.12 Calculated velocity gradients over Eppler 385 aerofoil at 5° and 13° angle of attack

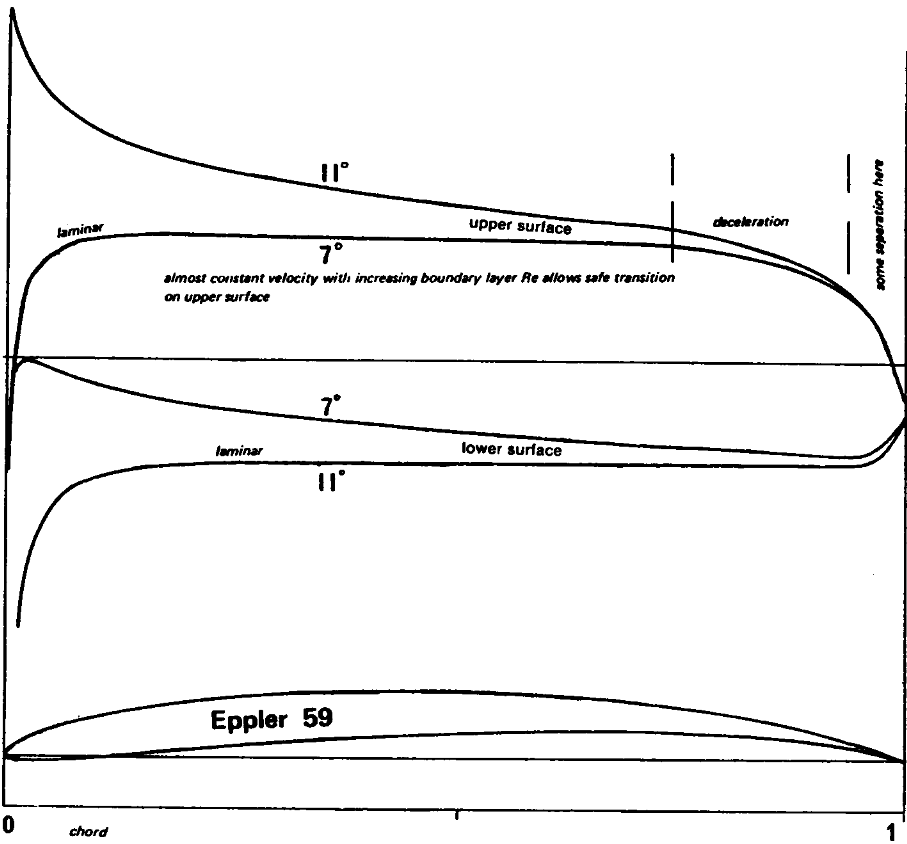

Fig. 9.13 Calculated velocity gradients over Eppler 59 aerofoil at 7° and 11° angle of attack

turbulent flow either as or before the deceleration begins. Although, as with all thin, highly cambered profiles, such wings will be critical in trimming and will require large stabilisers, the performance gain should be worthwhile. This is, of course, still subject to the limitation that profile drag on a model at low speed is relatively much less significant than aspect ratio. Unlike the 'turbulent flow' aerofoils of the previous chapter, these profiles should be built without leading edge waviness. Sheet balsa covering or even solid balsa construction at least over the front half of the wing should be regarded as essential. Theoretical drag polars of several Eppler aerofoils are given in Figure 9.14 and 9.15.

9.7 A CAUTIONARY NOTE

It must be emphasised that at Re below 500,000 boundary layer flows and separation bubbles are very complicated and up to the time of writing, mathematical and theoretical analysis has not been able to deal adequately with them.

Since the first edition of this book was published in 1978, a great deal of research of both theoretical and practical kind has been done. Leading roles in this have been taken

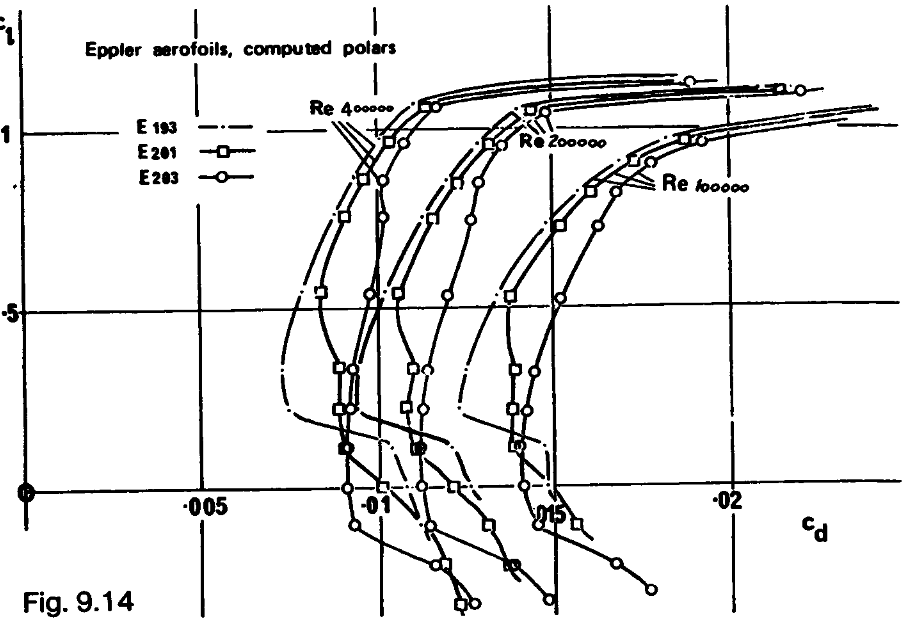

Fig. 9.14

Fig. 9.15

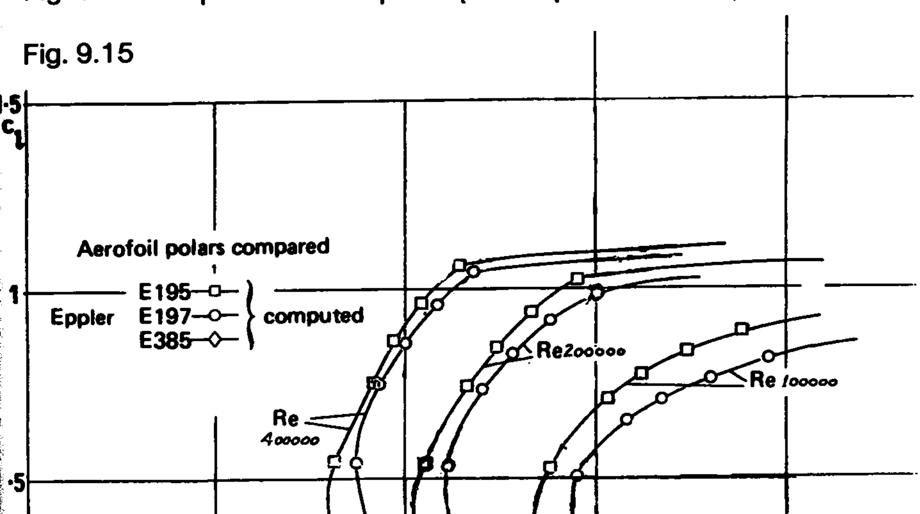

by universities at Stuttgart and Brunswick (Germany), Delft (Netherlands), Southampton and Cranfield (U.K.) and Notre Dame (U.S.A.), with other important contributions by S.J. Miley and R.H. Liebeck, and D. Somers and S.M. Mangalam at NASA, where Walter Pfenninger also has worked for many years. Many of the most significant results were presented in the form of papers and summaries in academic journals, and at conferences, especially one at Notre Dame in 1985 and a larger international meeting at the Royal Aeronautical Society in London in October 1986. Although often of a highly technical and mathematical kind, many of these reports contain information of great significance for model fliers and should be consulted for detailed information on specific points. (See the list of references following Chapter 10). Some of the work remains unpublished or is available only from technical libraries or direct from the university departments concerned.

9.8 EPPLER'S RESEARCH

Of particular importance has been the publication of Professor Richard Eppler's computer programme, in co-operation with Dan Somers. This programme was developed in order to enable a wing profile to be designed exactly to fit any required specification and it has been used with excellent results for full-sized as well as model aeroplane and sailplane aerofoils. It has also been applied to model wing sections, notably by Rolf Girsberger in Switzerland, Helmut Quabeck and Martin Hepperle in Germany, and Michael Selig in the U.S.A. (Note, the HQ profiles designed for models by Quabeck

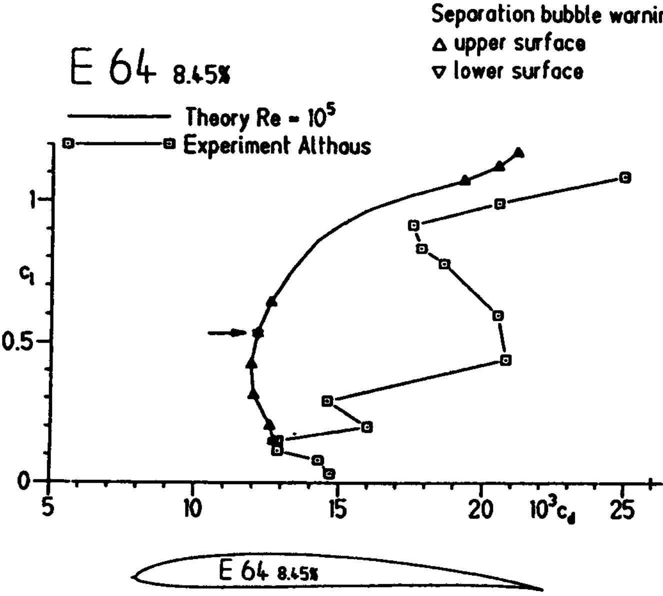

Fig. 9.16 Drag polar of Eppler 64, 8.5% thick aerofoil, as measured in wind tunnel, compared with theoretical prediction at Reynolds number 100 000.

Note where theory predicts separation bubbles on both upper and lower surfaces, measured drag is far greater. Note also that the C_d scale does not start at zero. [Chart published first by R. Eppler in his paper read at the R.Ae.Soc. Conference, October 1986].

Fig. 9.17 Theory and test of the Eppler 65, 8.86% thick profile, at Re 100 000 and 200 000.
Note the different scales of drag, starting at 0.01 and 0.0 respectively.

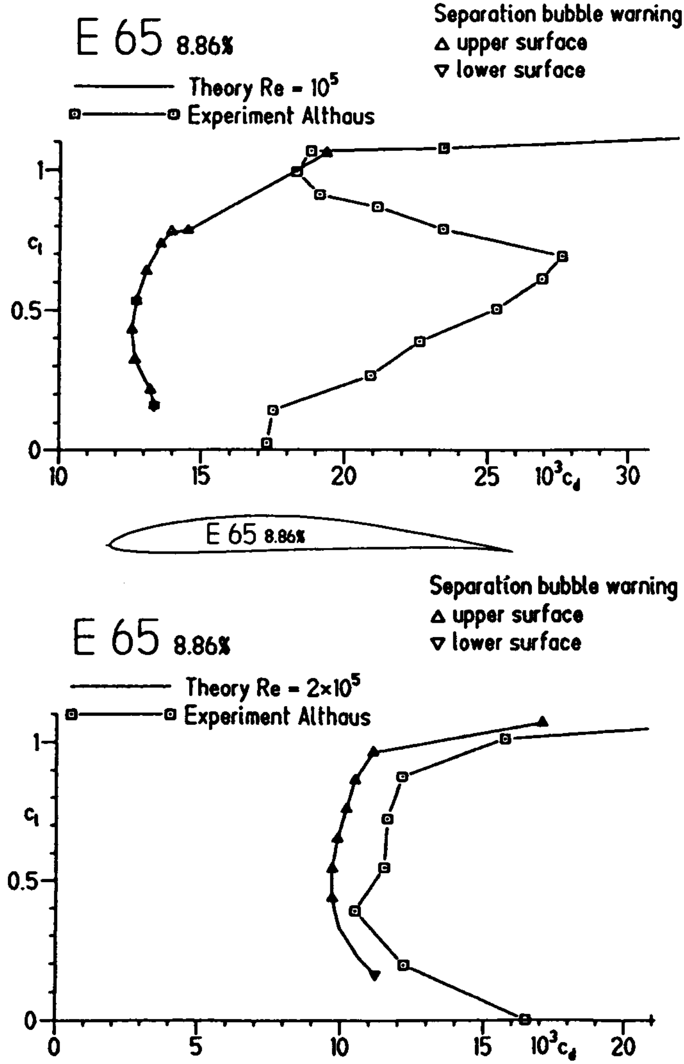

should not be confused with the Horstmann and Quast HQ series for full-sized aircraft.)

The Eppler programme, when applied to very low Re numbers, gives warning when laminar separation bubbles on the wing are likely to cause significant departures of the actual lift and drag figures achieved in flight, from the theoretical predictions. Drag polar curves similar to those of Figures 9.14 and 9.15 now usually appear with 'bubble warning' tags at various points. Practical wind tunnel tests, mostly by Dieter Althaus at Stuttgart, demonstrate that wherever a bubble warning appears on the computed charts, the drag curve will depart quite seriously from the computed figures, almost invariably moving to the high drag side.

Some of the results are illustrated in Figures 9.16–9.18. These have been published by Eppler himself. In Figure 9.16, a drag polar for the Eppler 64 profile is shown for Reynolds number 100,000. The computer predicts bubble separation over most of the operating range of the aerofoil. The two curves diverge markedly, especially where the computer programme predicted the minimum drag coefficient. Near this location on the curve, separation bubble warnings appear on both upper and lower surfaces of the wing (indicated by overlapping triangles making a six pointed star). Agreement of the theoretical curve with the measured one is better at higher Re.

In Figure 9.17 results are shown for the Eppler 65 at two different Re numbers. At the higher Re of 200,000, agreement of theory and measurement is not too bad although far from perfect. The computer predicts separation bubbles over most of the usable range of c_l values. At the lower Re of 100,000, the two curves match nowhere except over a very narrow range at high c_l, very close to the stall. Again this is no surprise in view of the bubble warnings.

Eppler concludes that while the bubble warnings on the computed polars are useful, their true significance is that modellers cannot rely on the computed drag curves of any aerofoil produced by these methods when the warning tags appear. These remarks apply equally to profiles designed by others using the Eppler programme or equivalents to it. Profiles by Helmut Quabeck, Rolf Girsberger and Michael Selig have been well proved in practice, as have those of Eppler himself, but at low Re they do not perform as efficiently as expected. Laminar separation bubbles do occur on all of them and do affect the drag. (Eppler points out that E65 is of theoretical interest only and is not recommended for practical use.)

9.9 RESEARCH BY SELIG, DONOVAN AND FRASER

Important new research on model aerofoil section design was carried out at Princeton University between 1986 and 89 by Michael Selig, John Donovan and David Fraser.

Using the aerofoil design program developed by Eppler and Somers, combined with that of Drela and Giles, which in some respects has been found more accurate for predictive purposes at low Reynolds numbers, a family of entirely new profiles was designed and tested in the Princeton wind tunnel. The theoretical basis of the new series, all carrying the prefix SD followed by a four digit number (e.g., Selig-Donovan SD 7032) is adjustment of the pressure distribution over the upper surface of the profile by introduction of a 'bubble ramp'. (The SD profiles should be distinguished from the earlier series 'S' designed by Selig, mentioned in Section 9.8 above.)

If the transition from falling pressure to rising pressure over the upper surface of the wing is too sudden and the pressure recovery gradient aft too steep, a separation bubble is almost sure to form. If, however, the rising pressure gradient can be smoothed out and made very gradual, transition in the boundary layer from laminar to turbulent flow may be achieved without separation.

The SD profiles for models have the recovery aft of the lowest pressure point carefully

Fig. 9.18 Velocity/pressure distributions, SD 6060 compared with Eppler 374 at a lift coefficient of 0.55

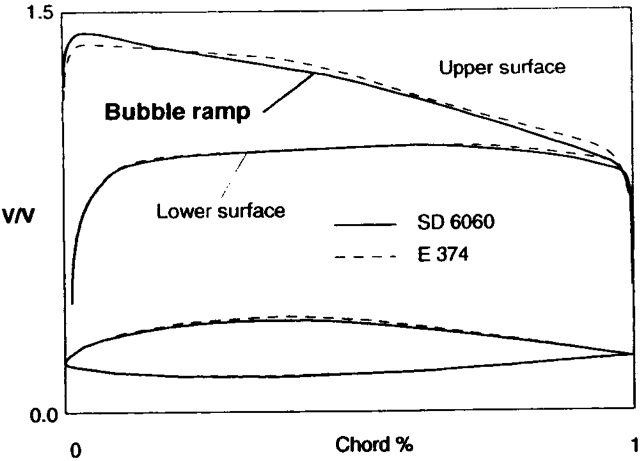

Fig. 9.19 Comparison drag curves for the Eppler 374 and SD 6060 tested at Princeton at two Reynolds numbers

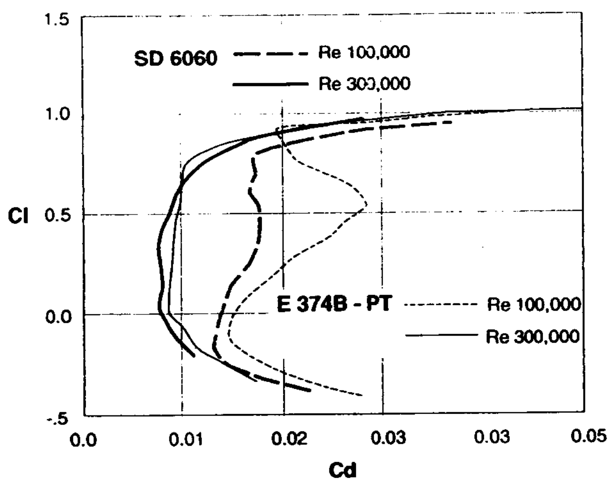

calculated to be as smooth and even as possible with no changes in the rate of change until very close to the trailing edge. The long, gentle pressure recovery zone is termed the bubble ramp. It should be compared with the very abrupt change in the upper surface pressure distribution shown for the NACA 6 Series profiles (Fig. 9.3 above). A comparison of the SD 6060 profile with the well known Eppler 374 is shown in Fig. 9.18. The wind tunnel results show a very worthwhile drag reduction, especially noticeable at the lower Re (Fig. 9.19).

Further brief discussion of the Princeton wind tunnel test work appears in the next chapter.

9.10 TURBULATORS ON LAMINAR AEROFOILS

There is some evidence to suggest that even a 'laminar' flow wing may be improved by careful use of a 'trip strip' turbulator. It has been shown earlier that when a laminar boundary layer meets an adverse pressure gradient, separation may occur. If a laminar flow profile, such as one of those designed by Wortmann or Eppler, suffers from flow separation behind the minimum pressure point, by placing a turbulator strip just ahead of the danger point, the boundary layer may be forced into turbulence a little early. When it arrives at the critical spot it may have enough momentum in its lowest layers to carry it through. In Figure 9.21 the results of an experiment by Sawyer with a turbine cascade blade not unlike a model wing profile in appearance are given. Although these tests were carried out at a Re of 570,000, higher than that of all but the larger and faster models, they do indicate a possible, and encouraging, line for experiment. The angle of attack of these tests was very high – about 14 degrees. Some degree of flow separation might have been thought inevitable so close to the stall. Separation on the plain aerofoil did occur on the upper side shortly after the pressure minimum, which was at 50%. This is indicated on the diagram by the sharp rise of pressure and the flat segment of the curve trailing aft. The whole rear part of the wing profile was stalled. By placing a thin trip strip just ahead of the 50% position, a separation bubble was brought into being. The flow re-attached as a turbulent boundary layer at about 80% chord – i.e. the bubble extended over 30% of the wing. After re-attachment, the pressure returned almost to the desired theoretical value and the profile was very efficient. Compare this also with Pfenninger's results on a very thin profile, given in Appendix 2, at Re's down to 100,000. It seems likely, therefore, that models using laminar flow profiles may also be tried with trip strips near the minimum pressure point on the wing, which for practical purposes may be assumed to lie near the position of maximum thickness.

Misplacing of the turbulator can do more harm than good. Results of a test on the Eppler 65 are shown in Figure 9.20. With a turbulator at 28% of the chord on the upper surface

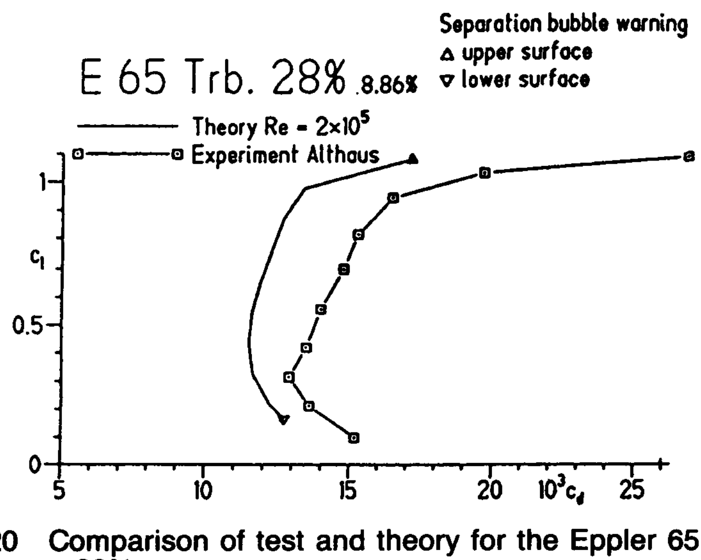

Fig. 9.20 Comparison of test and theory for the Eppler 65 with turbulator at 28%

Note the scale starts at C_d = .005.

the match of theory and measurement is somewhat less good than without the turbulator, and the drag all round is somewhat higher (note the scales are not the same on the diagrams, which tends to obscure this). The theory does not predict bubble separation in the low drag bucket, but clearly it does occur even with the turbulator. A different position for the turbulator would very possibly change this situation.

As usual, the systematic experimental approach with a particular model is the best; no general rules can be laid down in the absence of extensive wind tunnel test results. The object is to retain laminar flow as far as possible but to avoid separation behind the minimum pressure point. If this can be achieved the new profiles should perform very well.

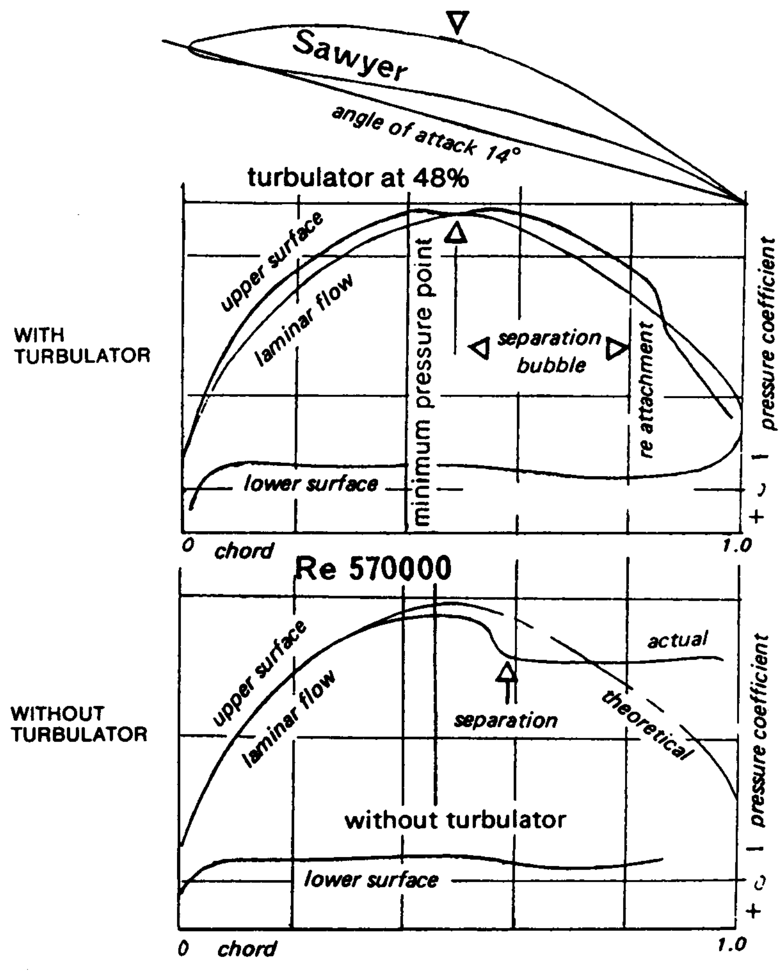

Fig. 9.21 Flow separation on a turbine cascade blade

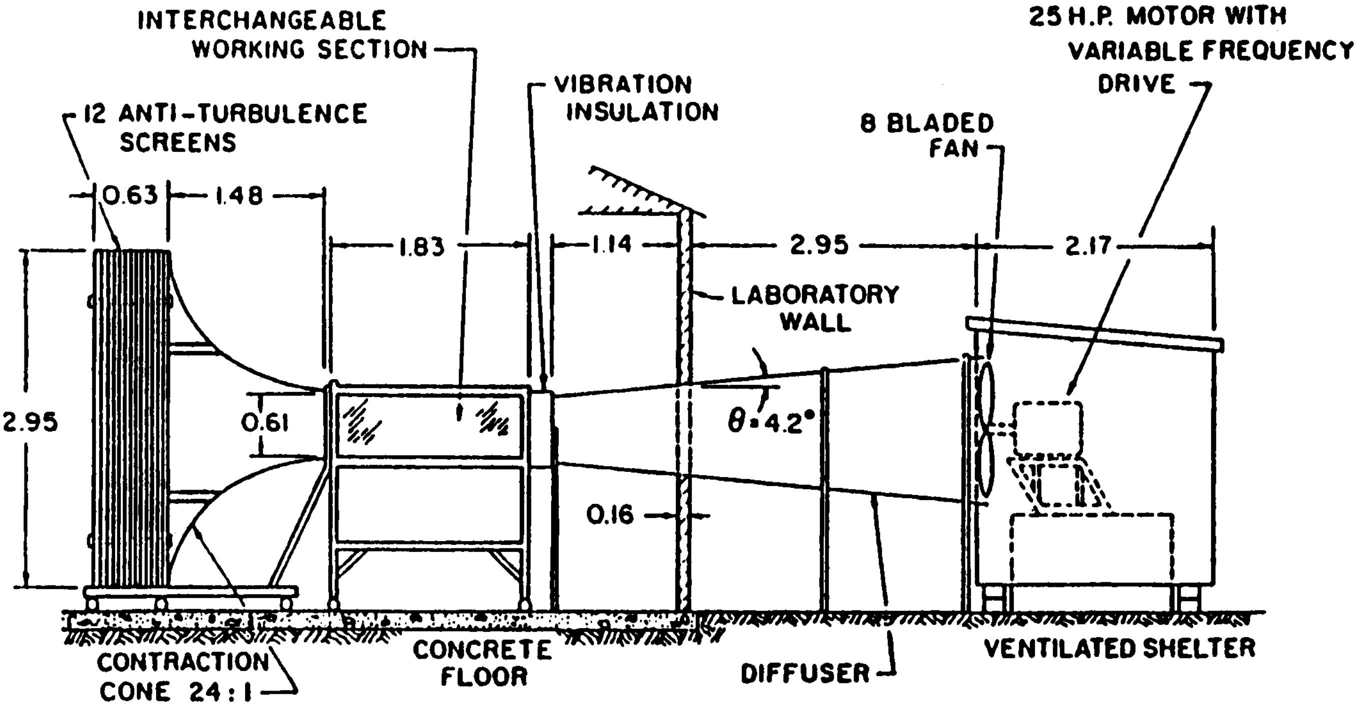

Fig. 10.1 A modern low speed research wind tunnel of the open return or Eiffel type at Notre Dame University, Indiana, USA.
Note both intake and exit are sheltered. ALL DIMENSIONS ARE IN METRES.

10
The wind tunnel

10.1 UNDERSTANDING THE WIND TUNNEL

The basic idea of a wind tunnel is easy to grasp. The forces on a wing in flight may be exactly imitated if the wing is held fixed and an airstream blows over it at an equivalent speed. To make a very simple wind tunnel is easy and has been undertaken as a project in schools. A fan draws the air through a duct. A section of the duct is fitted with removable panels for access to allow models of wings or other components to be mounted safely in the flow. Simple spring balances can be used to measure forces, and probes connected to pressure manometers can be moved by hand to investigate flow speeds, etc. Much can be learned from the simplest such tunnels but to make *accurate* measurements is difficult. For work at model aircraft speeds and sizes, it is particularly vital to keep the flow in the test section of the tunnel as free as possible from turbulence. This requires not only flow straighteners in the tunnel but diffusers and fine mesh grids, or even screens of fabric through which the air is drawn. These reduce turbulence to such fine dimensions that natural damping tends to reduce the small disturbances in the flow very quickly. In addition, the flow after passing through the screens enters a carefully designed contraction in the tunnel before the test section. The contraction has a venturi effect (see Figure 2.7), speeding the flow up while at the same time narrowing the stream. This further reduces turbulence, since any remaining small lateral oscillations in the flow become stretched out longitudinally and restricted laterally.

After the test section has been passed, further flow straighteners are usually fitted and, since the fan rotates, the shape of the tunnel in cross section has to be changed to circular from rectangular or square. This change has to be fairly gradual since it is easy for disturbances in the flow downstream to make themselves felt in the test section.

Because of the effects of sound on the boundary layer (see 8.12), the noise of the fan blades and the fan motor itself must be suppressed and vibrations must be prevented from disturbing the measuring instruments.

Tunnels of the open return type, in which the air after passing the fan is allowed to escape into the laboratory building or even to open atmosphere, with new air constantly drawn in through the screens at the other end, are often affected by external weather, especially wind which can cause fluctuation in the flow speed through the tunnel. Such tunnels may be sited in sheltered places, such as wood or forest lands, to shield them. The closed return type of tunnel is less subject to weather but because the same air is re-circulated to the intakes after passing the fan, additional precautions are needed to prevent vortices from the fan blades persisting all the way through the tunnel. Figure 10.1 shows in schematic fashion the layout of a very good modern wind tunnel.

10.2 CALIBRATION

In all wind tunnels, the drag of the walls, floor and ceiling tends to slow the stream down at the edges and the walls have their own boundary layer characteristics, introducing errors into measurements taken near them. Before a tunnel is used, it has to be established by careful testing that the flow speed is even through and across the whole test section.

A measurement of particular importance for low speed work is the turbulence factor of the tunnel. Since so much depends on the boundary layer and its transition from laminar to turbulent flow, any small, microscopic turbulence in the tunnel will have a disproportionately large influence on the drag of the aerofoils under test. In serious test work, the tunnel turbulence factor is reported and, to allow a very rough correction to be made, the Reynolds number of the test may be multiplied by this factor to yield an equivalent Re. It is also found that tunnels tend to have somewhat different turbulence factors at different flow speeds, so strictly a whole spectrum of turbulence measurements should be made. This is not often done.

Before F.W. Schmitz could carry out his classic tests on wing profiles at Cologne (see Chapter 8 and Appendix 2), he had to work for more than a year to improve the wind tunnel. He reduced the turbulence factor to 1.06. Modern tunnels should be better than this. Schmitz's results are probably reliable to within 6% of the stated Reynolds numbers.

A few years earlier, the NACA in America had carried out an extensive series of tests in the compressed air tunnel, down to Reynolds numbers of 42,000. The results published in NACA Report 586 covered all the most popular NACA four digit profiles, the 6409, 4409, 4412, etc. and are still quite often quoted by writers in modelling magazines and presumably are used in designing some models. Unfortunately, as the NACA authors reported at the time, the turbulence factor was 2.64, which implies that the stated Re of each test should be multiplied by this figure to arrive at a better but still very crude approximation to the truth. In other words, the Re of 42,000 of these tests (apparently well within the free flight modelling range), represents a true Re of 110,880, which takes these test results above the usual critical Re for most aerofoils. NACA Report No. 586 is not in general of much value to modellers. Other tunnel tests have suffered from the same difficulties, though when published, the turbulence factor is not always stated, so that not even the crudest correction can be attempted. *Modellers should not take seriously any wind tunnel results which are quoted or published if the turbulence factor is not known.*

10.3 DELICACY OF INSTRUMENTATION

The forces on model wings at low speeds are so small that very refined instruments are required to measure them accurately. This is particularly the case with drag. For example, if a test wing is developing a lift force equivalent to a weight of a few grammes, the drag may be a hundredth of this. A wind tunnel balance which can read to only one percent accuracy would be useless. In Schmitz's tunnel, the model wing under test was suspended on wires in the open sided test section. The forces were found by careful weighing. Most modern tunnels have fully enclosed test sections, which keeps the models free from extraneous disturbances. Various methods are used to measure the forces, many of which do not depend on weighing. The Stuttgart model tunnel, for example, has a series of small holes drilled through the tunnel walls so that the pressure variation of the airstream as it passes round the wing can be accurately measured. This allows the lift to be computed. The drag is measured by a wake rake. This is an array of capillary tubes with open ends, rather like a comb in appearance, which is positioned vertically in the airstream immediately behind the trailing edge of the wing. By measuring the speed of the

Fig. Fig. 10.2 Drag measurement with a wake rake

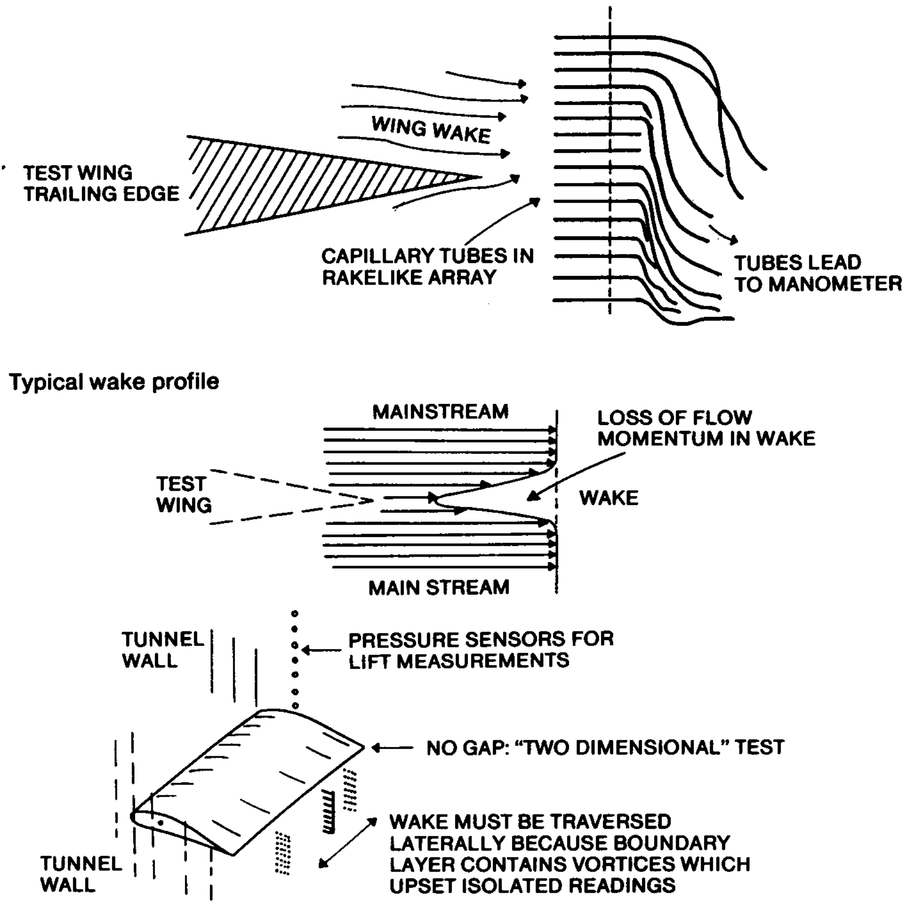

flow at each point the loss of momentum caused by the resistance of the aerofoil can be calculated and, hence, the drag (Figure 10.2). Because of the small vortex flows discovered where separation bubbles occur, the wake rake has to be moved laterally to sample flow across the span of the test model. The final outcome is an average drag coefficient. In other wind tunnel laboratories other methods are used, including strain gauges and very sophisticated electronic balances.

10.4 CORRECTIONS TO RESULTS

In all cases, the raw force measurements coming from the instruments have to be corrected to allow for various defects which cannot be entirely removed from any tunnel. The model, for instance, tends to block the flow through the test section and this blocking effect varies with the angle of attack. Models of different chord and thickness cause more or less blocking. The constraint of the air by the tunnel walls must be allowed for. If there are any supporting struts or wires, an estimate of their effect on the figures has to be made. Where balances, rather than pressure measurements and wake rakes, are used there are often small gaps at the ends of the tunnel model, where they must be free to move and not jam against the walls. These gaps may affect results. When the model is fixed to the wall (giving the effect of infinite aspect ratio as mentioned in 6.17), there are problems caused by interference of the flow in the corner. The corrections applied are carefully worked out but are always somewhat approximate. For all these and other reasons, including inaccuracies in models used for testing, the results reported from one wind tunnel always differ to some extent from those originating elsewhere.

While the general pattern of the results emerging is clear enough, small differences in performance between sections tested in different tunnels may not be taken too seriously. Such variations are due to the variations of experimental technique. It is fair to compare Kraemer's tests of the Gö 801 with his test, in the same tunnel, of the Hacklinger designed section, Gö 803, or the Gö 804, but it is hardly safe to compare the Kraemer results directly with those of Pfenninger or Muessman etc. The importance of Dr Althaus's results from Stuttgart is that all come from the same tunnel, and may be compared with one another. Yet even when, as in this case, a series of reports have been published from one research laboratory, over a period the test apparatus is likely to have been improved or altered so that results from one early test may not be exactly comparable with a later one.

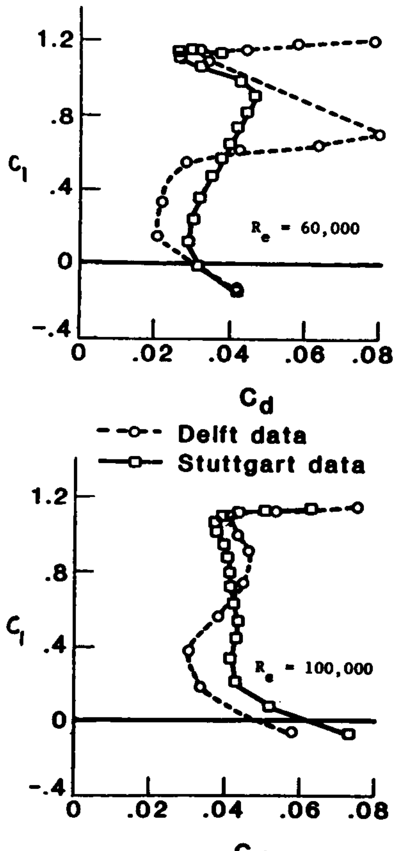

Fig. 10.3 Comparison of drag data from two modern wind tunnels
(Eppler 387 aerofoil)

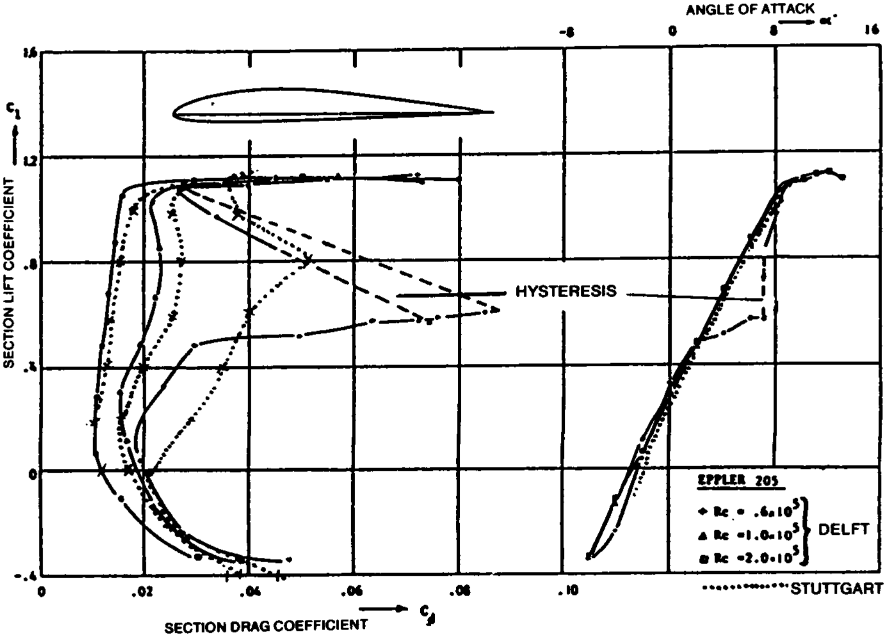

Figure 10.4 Comparison of two different wind tunnel measurements of the Eppler 205 aerofoil.
At the highest Re, 200 000, agreement is very good, but it is less good at Re 100 000 and poor at 60 000. The Delft measurements show a pronounced hysteresis loop at Re 60 000, which does not appear in the Stuttgart tunnel. [See Chapter 8, 8.3] The lift curve as well as the drag is shown, as explained in Paragraph 10.5.

As an example of what may occur when an apparently identical aerofoil is tested in two different laboratories, Figure 10.3 shows the drag polars for the Eppler 387 at Re 60,000 and 100,000, as measured at Stuttgart and Delft. A similar pair of results is shown in Figure 10.4 for the Eppler 205. (See also Appendix 2). The Göttingen 795 aerofoil, which has attracted attention because it seems less affected by low Re numbers than many ofther profiles, has been tested in three separate tunnels, charts from two of which appear in Appendix 2 and the third in Dr. Althaus's book, *Profilpolaren für den modellflug*, Vol. 1. The comparison is left to the reader.

10.5 OTHER WIND TUNNEL EXPERIMENTS

Apart from straightforward measurements of the three basic forces, lift, drag and pitching moment on a wing, wind tunnels allow many other kinds of investigation to be made. If the test model is fitted with suitable internal tubes and perforations, the pressure variation over the surfaces may be discovered. The diagrams of Figures 8.1, 8.2 and 8.3 were constructed in this way. Flow visualisation tests of the kind used by Pressnell (8.9) are widely done, with various types of liquid and, in recent times, liquid crystal material for the coating substance. Powder may be introduced into the flow through small holes in the

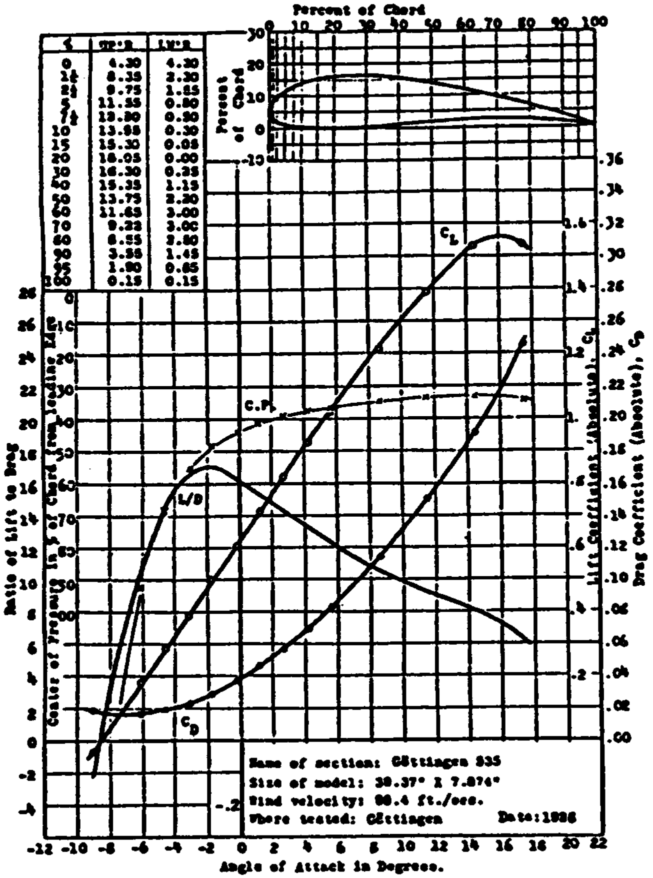

Fig. 10.5 A typical wind tunnel test result of 1925, as published in standard form by the N.A.C.A.
Note that the centre of pressure is shown as lying at 120% (i.e. aft of the trailing edge) at a lift coefficient of 0.2, corresponding to a fairly fast flight speed, at minimum profile drag. The model size of 20cm × 1 metre gave an aspect ratio of 5. The Reynolds number at a flow velocity of 30m/s was approximately 410,000, the wind tunnel being at Göttingen University.

model wing, to trace the boundary layer from any chosen point. A very common and useful technique is to inject fine streamers of smoke into the test section upstream of the model. This reveals not only the general flow of the streamlines but where the smoke becomes trapped in the boundary layer the separation bubbles show up. The smoke is sometimes made by trickling oil down a hot, vertical wire, which has very little effect on general turbulence.

A simple stethoscope connected to a fine capillary probe may allow the experimenter to listen to the boundary layer and this is one of the most sensitive methods of detecting the point of transition from laminar to turbulent flow. Where the flow is laminar, a faint hissing is heard. Turbulent flow emits a distinctive crackling. This device was used many years ago by August Raspet to detect separation on full-sized sailplane wings in flight, but it has proved useful in the wind tunnel many times since. To avoid disturbing the delicate flows being studied, the probe must be inserted always from the downstream side.

10.6 CHARTING THE RESULTS

Early wind tunnel test charts were usually very simple, showing how the lift coefficient and drag coefficient varied with angle of attack. The pitching moment was used as a basis for calculation of the abstract centre of pressure movement, as described in 7.12. The wind tunnels were usually of the open working section type. The models were of low aspect ratio. The size and shape of the test piece were usually stated on the results chart, so corrections for different aspect ratios were left to the aircraft designer. For several decades, every wind tunnel in the world had its own conventions and methods of plotting, so there was great confusion. In an effort to bring order, the NACA during the 1920s published a great series of reports which consisted of collected wind tunnel results from all over the world, reduced to standard form and plotted on a standard type of graph. An example is given in Figure 10.5. Charts from this era still crop up from time to time in the modelling press, because the sizes and flow velocities are sometimes comparable with model Re numbers. Unfortunately, these early results cannot be regarded as reliable now. The test methods used were relatively unrefined, and every tunnel was different. (NACA and the Royal Aircraft Establishment at Farnborough actually exchanged wind tunnel models across the Atlantic, to see whether they would produce similar results when tested in two of the best wind tunnels available. The outcome caused great concern at the time, for there was little agreement. It was after this that the importance of Reynolds number and tunnel turbulence began to be recognised.)

Modern tunnel results are almost always plotted in a standard fashion, similar to that used in this book, although minor differences still appear. (See Figure 10.4 and Appendix 2). Most importantly, the measurements are given for the aspect ratio of infinity. That is, if the wind tunnel model did not actually span the test section completely, the results are still presented after correction for the theoretical infinite state. In this respect, the designer choosing a wing section does not have to worry about variations of tip vortex drag. No vortex drag is supposed to appear in the wind tunnel results. This does of course mean the designer must make suitable corrections once the wing aspect ratio and planform have been decided, but the aerofoil data can be studied without this factor at first. Such wind tunnel data is described as 'two dimensional' because the airflow in the tunnel, or after correction, is without lateral motions. (The occurrence of tiny vortices chordwise in the boundary layer after a separation bubble does invalidate this slightly but these vortices are quite different in origin, and effect, from the large wing tip vortices of a finite wing.)

The section lift coefficient, c_l, is plotted against angle of attack. Where the c_l curve crosses the zero line is the aerodynamic zero and in the case of cambered section this is always at some negative angle, geometrically. The section drag coefficient, c_d, is plotted in its turn against c_l. The same vertical scale of c_l is used for both drag and lift, so it is perfectly straightforward to read from the angle of attack up to the c_l, and horizontally across to the c_d curve, whose scale is horizontal at the bottom of the chart.

The pitching moment coefficient is plotted on the same graph as the c_l curve or sometimes on its own separate part of the chart, but always easily and directly related to the c_l curve. It is particularly important to remember that the c_m of cambered profiles is negative (nose down) at all normal angles of attack. Conventions still vary between different laboratories as to whether the c_m scale reads upwards towards the more negative values or downwards, and when the scale is arranged horizontally, whether the negative values appear on the left or the right. The pitching moment is not usually expressed as centre of pressure movement now.

10.7 THE AERODYNAMIC CENTRE MEASUREMENT

All modern wind tunnel measurements are taken at the 25% chord position on the test model, or are subsequently corrected to this location before the charts are plotted. With full scale aerofoils this almost always produces a c_m of constant value at all usable angles of attack (i.e. below the stalling region). If the true aerodynamic centre of the aerofoil is slightly out of the 25% position, which does happen sometimes, the c_m plot will still, as a rule, be a straight line over the flying range of c_l, but the line will slope down at some small angle instead of showing a constant value. This does not mean that the moment coefficient actually varies, but only that the aerodynamic centre is either slightly ahead of, or behind the expected 25% point. It may also be slightly above or below the centre camber line which has the same effect on the charts. If the c_m line slopes from a high negative value at low c_l to a less negative value at high c_l, the aerodynamic centre lies ahead of the 25% point, and conversely, if the c_m curve slopes from low negative at low c_l to high negative at high c_l, the a.c. is somewhat aft of 25%. Some wind tunnel test results report the exact a.c. position. Departures from 25% of a few decimal points are in practice hardly enough to matter.

With model-sized measurements, as previously noted, the movements, lengthenings and shortenings of the laminar separation bubbles cause the moment coefficient curves to wander a little. Even so, it is nearly always possible to show that, over the usable range of c_l and angles of attack, a part at least of the c_m curve is more or less straight, although it may be sloping. As before, the direction of the slope indicates whether the aerodynamic centre is ahead of or behind the 25% point. So far, when the c_m has been measured at all, the indications are that the a.c. centre of model wing profiles is always, as with full sized aircraft, very close to 25% of the chord.

The profiles most likely to depart from these generalisations are the very thin, highly cambered types used on indoor flying models and on small free-flight aircraft. Very little reliable test work has been done on these and some of the moment coefficient curves published in recent times are now though to have been wrongly plotted. F.W. Schmitz's early measurements of the curved plate sections (see Appendix 2) and those by Kraemer of the Göttingen 803 and 804 indicate quite large departures from the straight line c_m curves, although even here some parts of the plot are nearly straight, indicating a fixed aerodynamic centre over a certain range of trims (e.g. on the Gö 803 between c_l 0.5 and 1.5, at Re 100,000 and 150,000). Where separation bubbles of great length occur, or where flow separation takes place on an even larger scale, standard theory breaks down and there is, as yet, no alternative but to rely on experience with these very thin profiles. To test a microfilm model wing in any normal wind tunnel would in any case be impossible.

It is also worth noting that a profile which behaves badly at very low Re in the smooth and polished condition can often be greatly improved and stabilised by the use of turbulators. The Gö 803 tests with the turbulator show a fixed aerodynamic centre for this profile, at 150,000 Re, between c_l 0.4 and 1.5, at 25% chord, and this apparently applies also to the lower Re of 50,000.

10.8 APPLICATION OF RESULTS

Even in full-sized practice, wind tunnel results are not applied directly. A suitable wing profile may be chosen in the first place on the basis of its comparative success against other profiles in the tunnel, but when final calculations are made, it is assumed, rightly as a rule, that the wing in service will not be accurate enough to give the same performance. Corrections are applied to reduce the tunnel results to those expected in reality. These corrections are arrived at in much the same ways as modellers arrive at their results: wings are built and tested in service and experience is accumulated in this way for future designs. Often so called 'practical construction' wing profiles, produced by normal factory methods, are tested in the wind tunnel.

There has also been extensive work on the effect of roughness and polish on wings. In full-sized work this almost invariably shows the advantage of a smooth, wave-free surface. At model sizes, a difference appears. Some wing profiles tested at Stuttgart were made by aeromodellers using balsawood and traditional methods of construction with frameworks of ribs and spars covered with sheet balsa or tissue and doped. Several of the open framed, tissue-covered examples performed better at very low Re numbers than did smooth and polished solid wood models of the same nominal profile. The exact shape of a tissue covered aerofoil is very hard to find, since the tissue always sags to some extent between the ribs and, if spars protrude, these too change the profile. The precise shape is hardly under control. The two most important features of any aerofoil, camber of the mean line and general thickness form, are probably by far the most important factors for the free flight modeller to worry about.

Radio controlled models, except for the very smallest hand-launched gliders, fly at Re numbers about 100,000 and upwards (see Chapter 3, paragraph 3.3). At about Re 100,000 a tissue or film-covered framework wing often seems to perform just as well as a perfectly smooth and wave-free wing. Some modellers find that a different covering material, such as slightly rough fabric rather than glossy smooth plastic film, can improve the behaviour of the model, suggesting that such a surface may promote transition in the boundary layer and so delay flow separation. Pressnell's invigorator effect may also be working with these slightly roughened surfaces (see 8.9). Turbulator strips too may be of use. However, as the size and flight speed of the aircraft increases, the benefits of a perfectly accurate and smooth wing become increasingly obvious. Wind tunnel test results also show greater reliability and predictability as the Re numbers rises to 200,000 and above, so it is here that such test results will find their greatest use. Faster, larger models are in this Re region.

10.9 AEROFOIL SELECTION

For aerofoil selection purposes it is useful to know that the best lift to drag ratio of a profile may be estimated directly from the drag curves as reproduced here. This is done by drawing a tangent from the origin or zero point of the drag graph to touch the plotted drag curve at a tangent (the curve appropriate to the Re of the model should be used). This is illustrated (Fig. 10.6). Tangential lines to the drag curves or 'polars' of several aerofoils are compared. The steeper the slope of the tangent, the higher the l/d ratio of the profile. The application of the method is limited to tests at identical, or at least similar, Re. In a similar way, values of the profile power factor may be worked out and plotted as shown in Appendix 1 and Figure 10.7. This is the important figure for free flight duration aircraft of all types, and soaring sailplanes.

For very fast models such as racers and multi-task sailplanes, or pure speed models, the minimum drag figure from the wind tunnel charts at the appropriate (high) Reynolds number is most significant. To read this alone without reference to the c_l and angle of attack at which it occurs is a mistake. Depending on the camber of the wing, the minimum drag point will occur at a higher or lower angle of attack (see Chapter 7, Figure 7.7). In Appendix 1 a method is given for calculating the wing C_L at a given speed for a model of known weight. This simple calculation should be done, using an existing successful model as a guide, before choosing the wing profile for a new model. The operating C_L then being known, a profile with minimum drag at the equivalent section c_l should be chosen. The required camber will usually be very small and many 'all out' speed models do very well

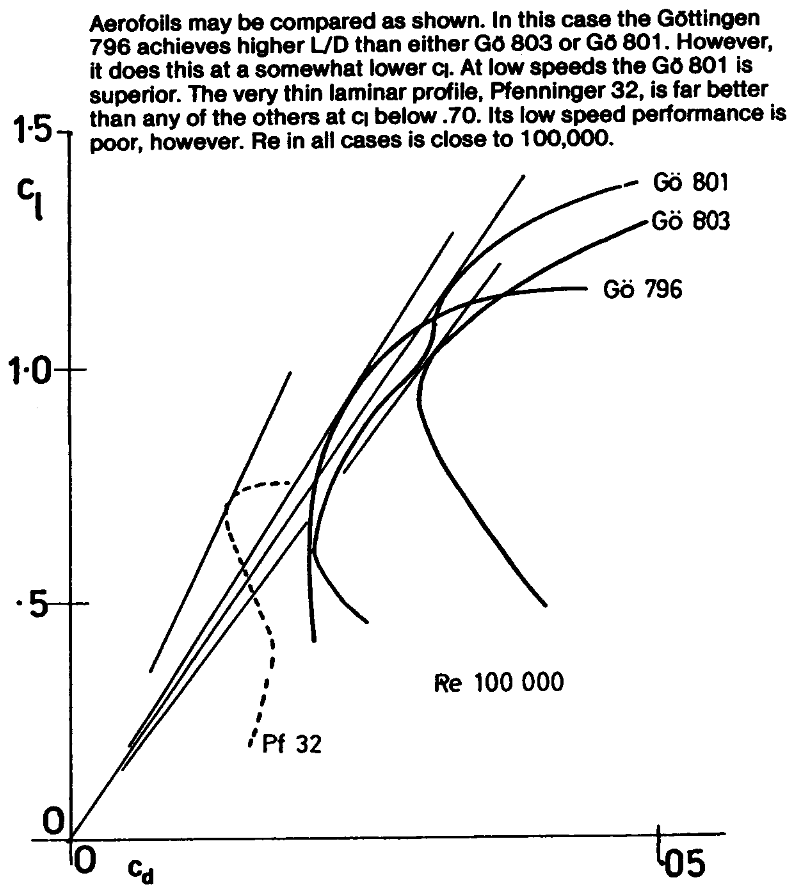

Fig. 10.6 Graphical comparison of drag polars

with symmetrical aerofoils, especially if these are of the wide drag bucket kind (see Figures 9.5 & 9.6). A little positive camber may be necessary for sailplanes since these also must perform well at low speeds. Alternatively, flaps may be raised for the high speed flight, bringing the minimum drag point to the low C_L trim for the speed task.

10.10 THE AIRCRAFT POLAR

To obtain a complete picture of the performance of any model aircraft in straight flight, a polar curve of the lift-to drag ratio may be calculated and plotted against airspeed. Wind tunnel test resuls are essential for this.

An outline of the method is given in Appendix 1. There are, however, several important points to watch. The increasing availability of wind tunnel test results has tempted some modellers to apply these rather crudely, choosing a single test curve for an aerofoil at a Reynolds number approximating that of the model in flight. During flight the Reynolds number of a wing is not constant. At each airspeed, and on a tapered wing, at

Fig. 10.7 Comparison of two aerofoils

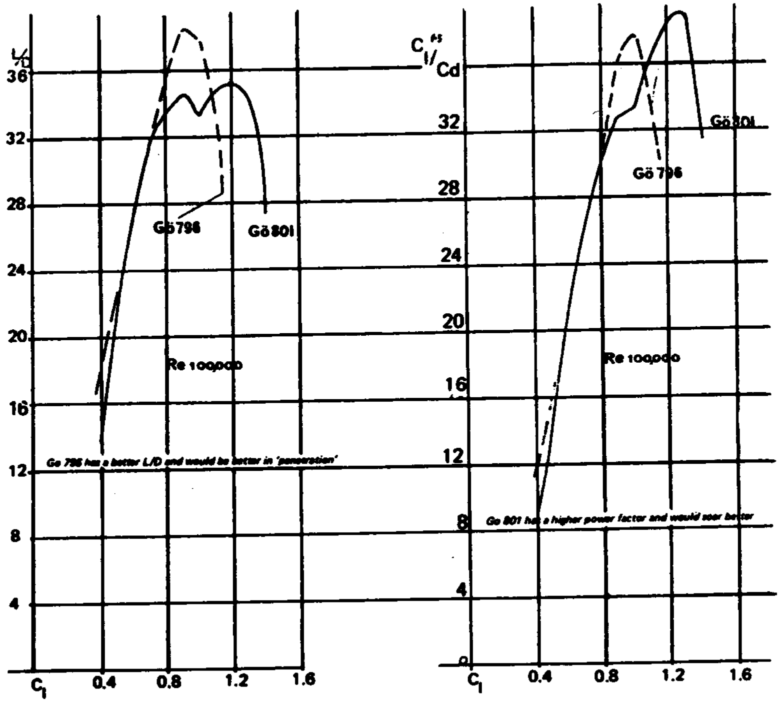

Using the calculation methods of Appendix 1, the Power Factor and L/D ratio of a wing profile may be worked out and plotted as shown here. Note: the figures make no allowance for vortex drag. Aspect ratio correction therefore must be applied to arrive at L/D or power factor for the wing.

each place along the span, the Re will differ. These variations may be dealt with by constructing, from the basic wind tunnel force curves, diagrams such as those for the Gö 796 and 797 (Fig. 10.8). Here, the section lift coefficient at a given angle of attack is read from the tunnel results at each Reynolds number, and plotted as a more or less horizontal line on the charts, with a marked break at the critical Re for that angle and that profile.

Assuming the aircraft is flying at a particular wing C_L its flight speed and hence the average Re number of the wing can be worked out. From this, if the wing is tapered, the chord Re at several spanwise points is found by simple proportion. (Twenty span points are usually taken, but the calculations need to be done only for one side, ten points, since the wing is symmetrical about the aircraft's centre line.) The profile drag of the wing at each point across the span may then be found from charts like those of Figure 10.4, by interpolation, and the wing C_D (Profile) is then obtained by integrating all the local section c_d coefficients. There then has to be a total wing C_D (vortex-induced) drag computation based on the aspect ratio, corrected by the factor k for the planform

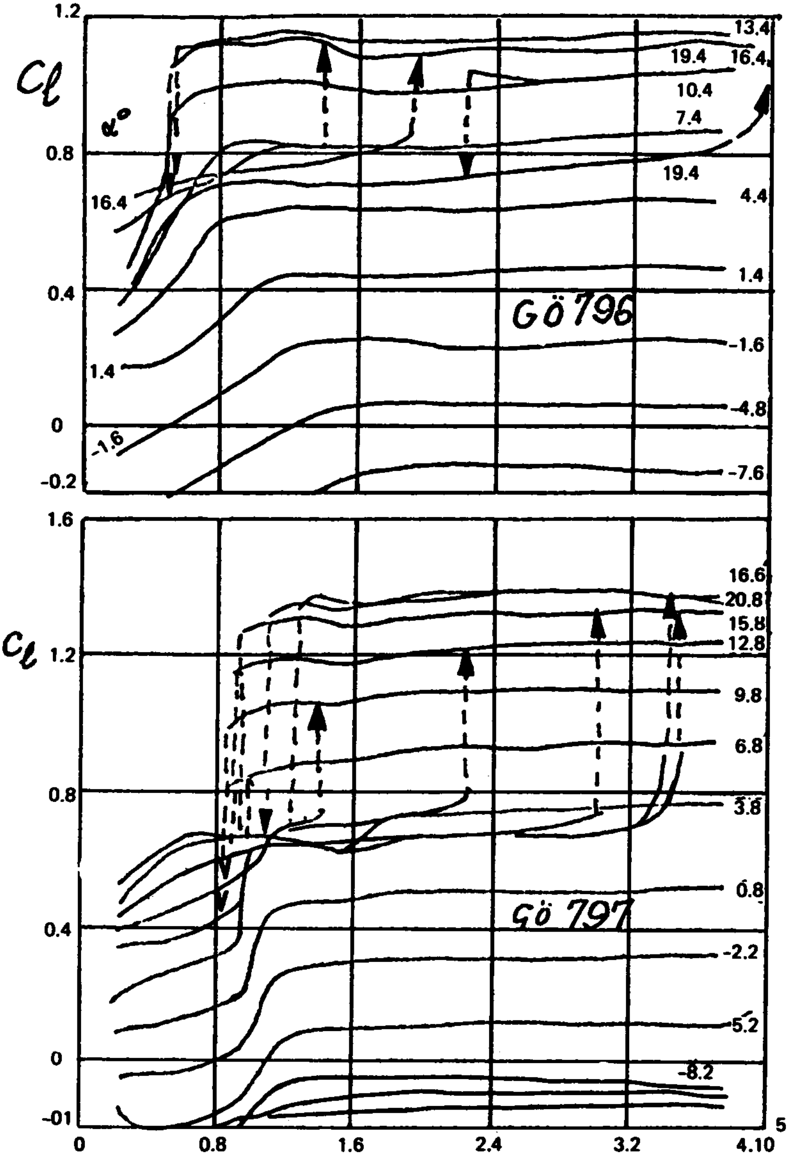

Fig. 10.8 Plots of C_l variations with Reynolds number for two different aerofoils. The numbers at the right are angles of attack.

departures from the ellipse (see 5.4), and the wing C_L. To the total of profile drag and vortex drag for the wing alone must be added the parasitic drag coefficients for the rest of the model. Only after this rather lengthy exercise has been completed is the lift/drag ratio at one flight trim discovered. To find the L/D at any other trim requires a complete repetition of the whole work for a different C_L. To construct a polar curve for the aircraft requires all this to be done at least five or six times, with extra work when the exact trim for best L/D or, with a glider, minimum sinking speed is required. Clearly, very few model enthusiasts will wish to spend the time required to do all this with pencil and paper.

Results of several such exercises by the author, where the work has been done by computer, are listed at the end of this chapter. See also Appendix 1.

10.11 POLAR CALCULATION BY COMPUTER

The widespread availability of micro computers has rendered the working out of aircraft polars very much easier and software is on the market which enables the model flier without much aerodynamic knowledge, or mathematics, to produce a polar curve in a very short time. Before using such software it is wise to investigate the basis of the calculations incorporated in the programming. From the description given above, it is obvious that for a full computation some fairly sophisticated computer programming is necessary, with interpolation from wind tunnel results and allowances for wing taper, planform, and other factors. Much of this information may have to be fed to the machine by hand from the keyboard and the work involved in this is not negligible. If the software package does not call for such input, and if the time taken for the results to appear is very brief, the chances are that the programming is not in fact very thorough and the results will at best be crude in proportion. A program which does the task properly is likely to be quite costly and may take an appreciable time to run on the computer, as well as demanding more attention from the modeller using it.

10.12 LIMITATIONS OF COMPUTED RESULTS

Even when the computer has been correctly programmed, the user should not expect the results to be correct in an absolute sense. That is, if the best L/D ratio is calculated at 1:20 at 35 m/s, it is very unlikely that these figures will be achieved exactly in flight. There are always too many imponderables such as wind tunnel errors, faults in model construction and finish, variations of engine power, etc. which render the results more or less doubtful. What may be safely inferred from the calculations is that comparisons will remain valid. In other words if the computer indicates that this or that aerofoil or wing planform will yield an improvement in performance compared with another, this will probably be true and will show up in flight. The actual achieved L/D ratio or top speed may not be as calculated, but there should be an improvement if the new wing is built, finished and flown to the same standards of accuracy as the old one.

10.13 EXPLANATION OF APPENDIX 2

When the first edition of this book was written an attempt was made to include, in Appendix 2, all the known, reliable wind tunnel test results on aerofoils at model aircraft values of Reynolds number. There were not many such results and they were not easily found in the aeronautical literature. Some other useful material, notably from Lnenicka and Horeni in Czechoslovakia and from Dr Galés' Group in Italy, came to the author's attention too late for inclusion. In this edition, the old measurements, still not easily accessible to the ordinary reader, are retained and still provide useful information. To them have been added, with permission, some of the charts produced by Jaroslav Lnenicka. Although these have been published in Czechoslovakia, they are not widely known elsewhere.

Much more tunnel testing has been done since 1978 and it is no longer possible to assemble all into a single appendix of reasonable length. The Delft, Cranfield and Notre Dame studies have been mentioned briefly in Chapter 9, and those seeking to know more will have to search the literature emanating from these institutions. The list of references at the end of this chapter will be a useful starting point. Most model fliers know already of the Stuttgart wind tunnel and the results from there published by Dr Althaus, in the series *Profilpolaren für den Modellflug*. No serious aeromodeller should be without these volumes. The charts are easily understandable by anyone who has read this book, and the brief text in German, describing the wind tunnel and the methods used in measurement, is not of fundamental importance from the modeller's viewpoint. With Dr Althaus's permission, four test results on two Eppler and two Selig aerofoils carried out in 1986 are included in the Appendix.

During the years 1986–89 the team of Selig, Donovan and Fraser at Princeton University carried out a series of wind tunnel tests at model values of Re. The results were published in 1989 in a single volume, *Soartech 8, Airfoils at Low Speeds*. (See full details in the References listed below.) This represents by far the most extensive and valuable body of work on model wing profiles so far accomplished and for the serious model aircraft designer, like the Althaus volumes, it is indispensable.

The Princeton wind tunnel, described in the volume, was most carefully calibrated. Over sixty distinct profiles were tested but in many cases more than one test piece was used, for comparison. Where it seemed appropriate turbulators were tried in different positions. More than 130 charts and associated tabulated figures were produced.

Of particular importance is the fact that all the test wings were made for the Princeton group by practising model aircraft builders, rather than by specialist wind tunnel craftsmen. Some of the profiles submitted were favourites of the modellers who made them, others, including the new SD series, were made to order. Every model wing tested was submitted to close scrutiny and departures from perfect accuracy were noted and published with the measured figures. Those using the results may therefore be confident that, with ordinary workshop equipment and sufficient attention to detail, it is possible to achieve results in a real wing which are similar to those from the Princeton tests.

Michael Selig, after leaving Princeton, became Professor in the Department of Aeronautical and Astronautical Engineering at the University of Illinois, Urbana. In 1993 a new programme of research and wind tunnel testing was announced, calling as before on ordinary modellers to make the required test wing sections. Results, when published, will be of great interest and importance.

The cautionary remarks made elsewhere in this chapter still apply.

10.14 FLIGHT TESTING

With all its disadvantages, the wind tunnel remains the easiest and most accurate method of testing wings and other aircraft components under standard conditions. Model fliers rightly regard such results as slightly doubtful, since the aerial conditions in which their aircraft fly are never as consistent as those of the laboratory. For instance, with all the effort put into reducing turbulence in wind tunnels, it is still not known what the turbulence of the air of the ordinary atmosphere is when the model is flying at different altitudes, different temperatures and in conditions of varying humidity, etc. The final test is always in real flight and even full-sized aircraft sometimes surprise their designers after years of preliminary studies and tunnel tests.

Fig. 10.9
Test glider used by T.J. Patrick to measure performance of wing profiles in flight. Flights were made in calm air, usually soon after dawn. A minimum flight distance of 50m was required for consistent results. Launches were by means of a simple, adjustable, catapult to prevent false results due to variations of hand launching.

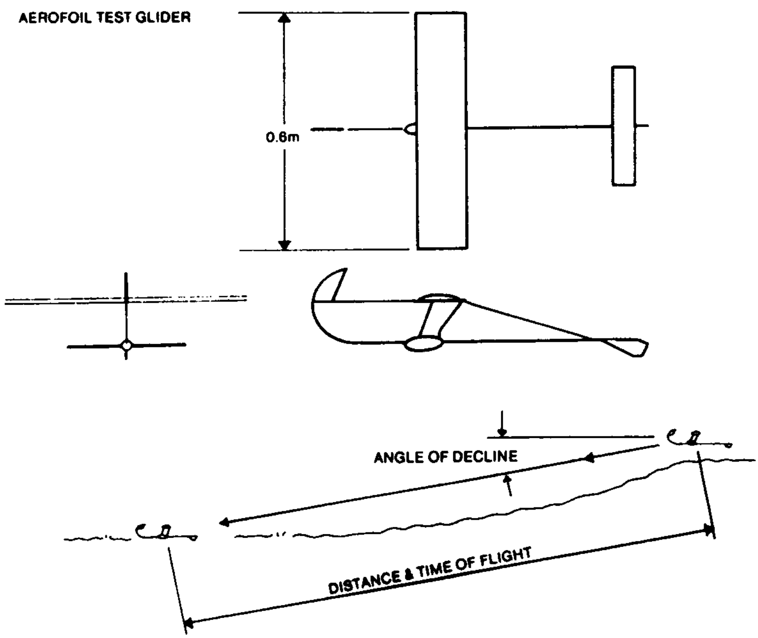

Some model fliers, such as V. Seredinsky and T.J. Patrick, have attempted to test model wing sections by gliding small, specially constructed free flight models in calm conditions from the tops of hills. Useful results can be obtained in this way although there is a good deal of statistical 'scatter' in the figures. Such test methods are at the mercy of the weather. The models tend to wander off course, rendering exact timing and distance measurements very difficult. Indoor tests of the same kind rarely produce usable results because the distance available for the glide is too short to allow the model to settle to a constant airspeed. (See Figure 10.9)

With radio control, much more is possible and some preliminary testing has been done by a group in California, as reported by B.K. Rawdon. On occasions of true calm, gliding models can be timed at various trims over a series of long glides, with altitudes measured by photography and various triangulation techniques. Statistical scatter is still a problem but useful figures have been found in this way.

There is a great deal of scope for refined instrumentation of large model aircraft. A model may be equipped with sensitive electronic devices to measure altitude and flight speed, angle of attack, and even air turbulence. The wing may be fitted with pressure tapping perforations, just as wind tunnel models are, and wake rakes may be used. The data found in these ways may be recorded, either in the model itself or transmitted to the ground for immediate plotting. At the time of writing, no such results have been published, although work along such lines is proceeding in a few places and research into remotely piloted military surveillance aircraft (effectively, large, long range model aeroplanes) is proceeding in many places. The future should produce some extremely important discoveries.

10.15 REFERENCES

Serious model fliers should seek out where possible reports of wind tunnel tests and other research at Reynolds numbers appropriate to their interests. There is a great deal of literature now in this area, although most of it remains in academic journals, reports of conferences and technical memoranda, student theses and university departmental libraries.

The list below is no more than a starting point for the interested reader. To compile a full bibliography would be impossible and new material is constantly being produced. Where difficulty is found in obtaining copies of the reports or papers, enquiry at a local public library, or university department of aeronautics, will nearly always yield access to the works required, though often after a wait of some days or weeks.

The items are arranged alphabetically under author's names, naming only one author where more than one contributed. Proceedings of the R.Ae.Soc. Conference on Low Re Number Aerodynamics, 1986, may be obtained from the Royal Aeronautical Society.

D. ALTHAUS *Profilpolaren für den Modellflug* Volumes 1 & 2 (further volumes in preparation). Neckar Verlag, Villingen Schwenningen, W. Germany 1980 &1985

D. ALTHAUS *Recent Wind Tunnel Experiments* R.Ae.Soc. Conference, 1986

B.H. CARMICHAEL *Low Reynolds Number Airfoil Survey* N.A.S.A. CR-165803 1981

M. DRELA & M.B. GILES *ISES, a two dimensional Viscous Aerodynamic Design and Analysis Code* AIAA Paper 87-0424, January 1987

R. EPPLER *Airfoil Design for Reynolds Numbers Between Re 50,000 and 500,000* Proceedings of the Conference on Low Re Airfoil Aerodynamics, University of Notre Dame, Indiana 1985

R. EPPLER *Recent developments in boundary layer computation* R.Ae.Soc. Conference, 1986

S.S. FISHER *A Smoke Wire Study of Low Reynolds Number Flow Over an LRN(1)1007 Airfoil Section* R.Ae.Soc. Conference 1986

A.F. HUBNER *The Effect of Grit Roughness on the Performance of the Wortmann FX 63-137 Airfoil at a Chord Reynolds Number of 100,000* R.Ae.Soc. Conference 1986

P.B.S. LISSAMAN *Low Reynolds Number Airfoils* Annual Review of Fluid Mechanics, Vol 15, pp 223–239, 1983

S.M. MANGALAM et al, *Transition and Separation Control on a Low Reynolds Number Airfoil* R.Ae.Soc. Conference 1986

S.M. MANGALAM & W. PFENNINGER *Wind Tunnel Tests on a High Performance, Low Re Number Airfoil* AIAA Paper 84-0628, 1984

T.J. MUELLER *Experimental Studies of Separation on a two Dimensional Airfoil at Low Reynolds Numbers* AIAA Journal of Aircraft 20, No 4, pp 457–463, April 1982

T.J. MUELLER *The Influence of Laminar Separation and Transition on Low Reynolds Number Hysteresis* AIAA Journal of Aircraft 22, pp 763–770, September 1985

T.J. MUELLER *Low Reynolds Number Wind Tunnel Measurements* R.Ae. Soc. Conference 1986

P. LeBLANC *Boundary Layer and Performance Characteristics of a Low Reynolds Number Liebeck Airfoil* R.Ae.Soc. Conference 1986

T.J. PATRICK *Wind Tunnel Test Results of Eppler 387 Aerofoils and Their Corroboration By Flight Test* R.Ae.Soc. Conference 1986

W.H. PHILLIPS *Low Speed Wind Tunnel Tests of Two Airfoils Suitable for Models* 9th Symposium of the National Free Flight Society NFFS Symposium, Chenautt Field, Lake Charles, Louisiana

W.H. PHILLIPS *Building a Wind Tunnel – An Educational Experience* 19th NFFS Symposium 1986, (address above).

M. PRESSNELL *The Performance of Model Aircraft Using Flow Invigorators* R.Ae.Soc. Conference 1986

B.K. RAWDON *Radio Controlled Sailplane Glide Polar Measurements* Symposium on Design of RC Gliders, Aero Club Vergiate, 1978 (Italy)

M.S. SELIG, J.F. DONOVAN & D.B. FRASER *Airfoils at Low Speeds* Published as *SOARTECH 8* by H. Stokely, 15904 North Horseshoe Circle, Virginia Beach, Virginia 23451, USA

M. SELIG *The Design of Airfoils at Low Reynolds Numbers* Soartech III c/o H. Stokely, 1504 Horseshoe Circle, VA 23451, USA. See also Soartech IV, Jan 1985, Addendum

M. SIMONS *Using a Hand Held Programmable Calculator in Estimations of Model Sailplane Performance* Soartech 1, (address above)

M. SIMONS *The Two Metre Sailplane* Soartech III (address above)

M. SIMONS *Design Studies of F1A Sailplane Wings* NFFS 19th Symposium, 1986 (address above)

M. SIMONS *The Use of Windtunnel Test Results in the Design of Radio Controlled Contest Sailplanes* R.Ae.Soc. Conference 1986

D.F. VOLKERS *Preliminary Results of Windtunnel Measurements on Some Aerofoil Sections at Re. Between 600,000 and 500,000* Memorandum M-276, Delft University of Technology

11
Parasite drag

11.1 THE IMPORTANCE OF PARASITE DRAG

As shown by Figure 4.10, parasite drag is a major problem for the designer of high speed models, racers and cross country or multi-task sailplanes. It is very much less important for free-flight and other duration models. The old controversy (in the days of '8 ounce' unlimited rubber Wakefield duration models) between advocates of streamlined and 'slabsided' fuselages was partly based on a misunderstanding of this. The streamlined fuselage model gained very little in the glide, and only a little more in the faster part of the climb, from its lower drag coefficient. To build a refined, streamlined fuselage always added some weight. The rubber motor weight was then usually reduced, so sacrificing climb performance. In general, the same still applies, although with rubber quantities limited as they usually are, there may be a little extra weight to spare for structures and nothing is *lost* by refining the shape of the parasitic components (except the time taken in building them). The engine powered duration model, climbing at high speed with flaps up and at low C_L, gains more in the climb by a good fuselage design, and will not suffer for it in the glide.

There is hardly any model aircraft that could not be improved to some extent by greater attention to parasite drag. It is easy to recommend smooth and polished surfaces, sealing all gaps, burying all protuberances, such as control horns, dowel ends, rubber bands, etc. removing struts, and retracting undercarriages. The general principles are clear, but it is often very much less simple to achieve such perfection from the engineering point of view.

Any part of a model which does not contribute directly to the lift or which is not absolutely essential to control and stability should either be removed or buried inside so that the air does not flow over it. Where some component, such as the fuselage, wheel strut, engine, etc. simply must exist it should be of minimal cross section, faired, smoothed and polished. On power models, because of the disturbance caused by the propeller, flow over the fuselage is usually turbulent. Little is to be gained by designing such a fuselage for laminar flow under power, although this does not mean the fuselage shape should be clumsy. Ordinates for the basic form of a streamlined body should be taken from Appendix 3. Depending on the length and cross sectional area (which should always be as small as possible compatible with good shape), the low drag body ordinates may be scaled up or down to give the plan and side view of the fuselage. It is hardly ever possible to retain the perfect form, but it should be regarded as the ideal and departures from it should be as small as possible. Probably the most likely alteration will be to simplify and extend the tail cone as suggested in Figure 11.1b, to make construction easier. This will have slight effects on drag. Protuberances such as cockpit canopies are undesirable from the aerodynamic point of view but if they are required they should be as low as possible and carefully faired. Where such things as silencers must protrude, they should be of streamlined form and carefully aligned with the average airflow, allowing as far as possible for the fact that the flow over the fuselage itself is not straight. On 'duration' models, propellers should fold or feather on the glide.

11.2 UNDERCARRIAGES

Wheels if not retractable should be as thin as possible and enclosed in a well-fitted 'spat', with a streamlined strut. On some racing models the wheels are arranged in tandem, one behind the other, which is aerodynamically good since two wheels in this position cause less drag than two separately, one lying in the wake of the other. If close together, the rear wheel acts as a rough fairing for the front one and drag may then be less than for a single wheel. If too far apart there may be a net loss.

11.3 COOLING DRAG

On racing models, attention should be given to airflow through the engine cowling. Drag inside the cowling is just as effective in slowing the model as drag outside it, and the smooth flow inside a good cowl will help engine cooling. The air intake should be designed to admit enough air and direct it where it is needed for cooling (usually through the fins on the cylinder head) rather than allowing it to disperse generally inside a chamber. Provision for exit of the heated air must also be made, not through a ragged hole somewhere at the rear, but through a smooth passage. Though unlikely to be noticeable in practice, the expansion of the air caused by the engine cooling function can be used to give a small increase of thrust if the air channels are arranged like those of a jet engine. The exit for the hot air should be larger than the intake.

11.4 SAILPLANE FUSELAGES

In designing fuselages for sailplanes, some laminar flow may be expected over the front portion, perhaps as far back as the wing. This suggests that the 60% laminar low drag bodies given in Appendix 3 should always be used for the nose at least. Apart from very low drag, the advantage of these bodies, designed by Young, is that even when the fuselage is at a slight angle to the local airflow, when the model is yawed or when it flies at different angles of attack, the drag is not increased. The Young bodies (as opposed to old bodies) have a low drag range analogous to the low drag bucket of NACA '6' series aerofoils. Cockpit canopies, access hatches etc. should fit closely and be free from steps or humps. Taking a hint from the full-sized sailplane built in 1975–9 by Gary Sutherland in Australia, a complete nose cone of 'Young' form was used on Australian contest model sailplanes in 1982 and since copied widely. Laminar flow is thus almost assured. Aft of the point where the boundary layer becomes turbulent, skin drag will be high. It is the practice on most full-sized sailplanes to contract the cross section of the fuselage, producing a 'pod and boom' or tadpole shape. (See, for example, Figs. 4.6 & 4.7). This reduces the area of skin exposed to the turbulent boundary layer. The gain is not very large and can easily be outweighed if the contraction is too sharp. This can cause flow separation. The effects are particularly bad if the fuselage upsets the airflow over the wing roots. Some well-known full-sized sailplanes suffer from this problem. The pilot can hear, at low speeds, the flow breaking away from the wing and fuselage just aft of the cockpit area, with quite noticeable effects on sinking speed. This is particularly likely when the

Fig. 11.1 Fuselage design. Racers

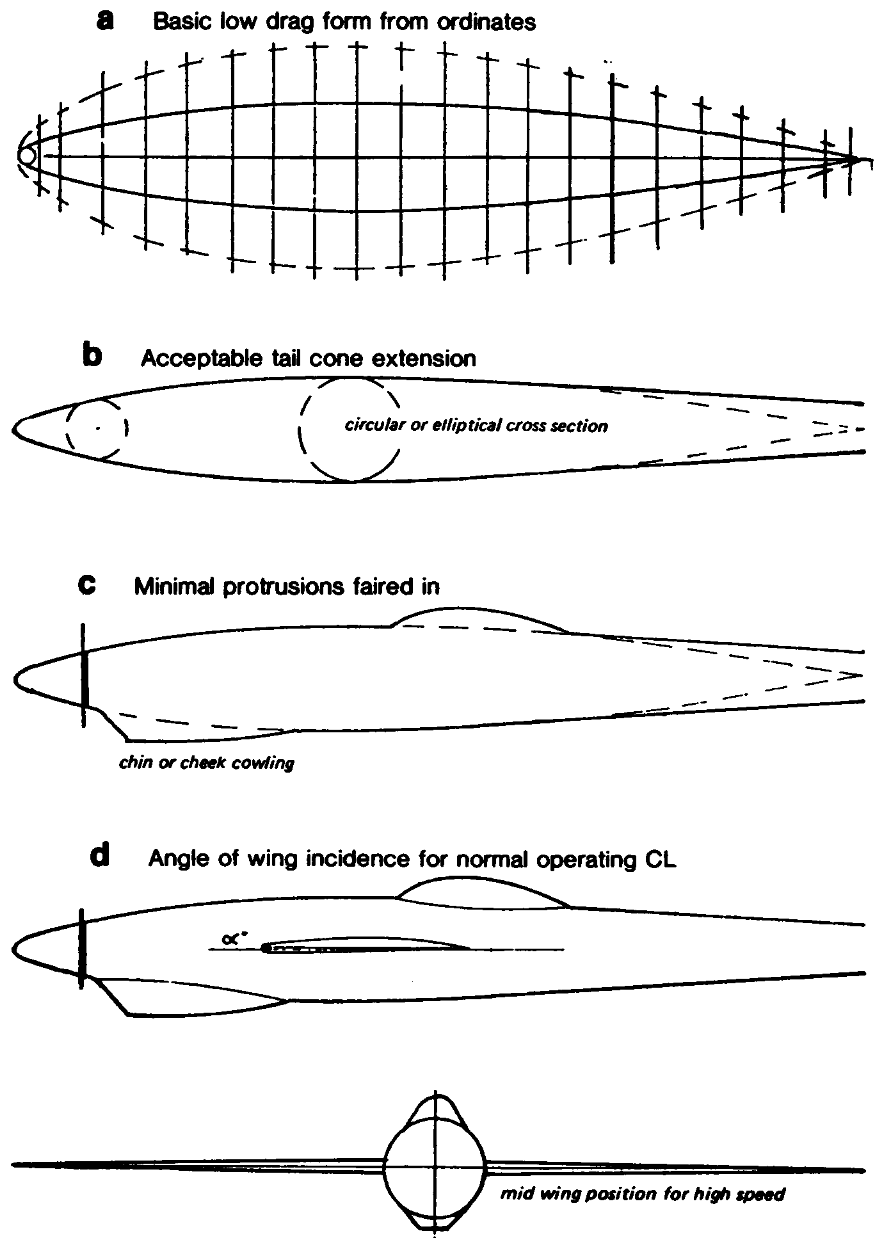

Fig. 11.2 Fuselage design. Sailplane

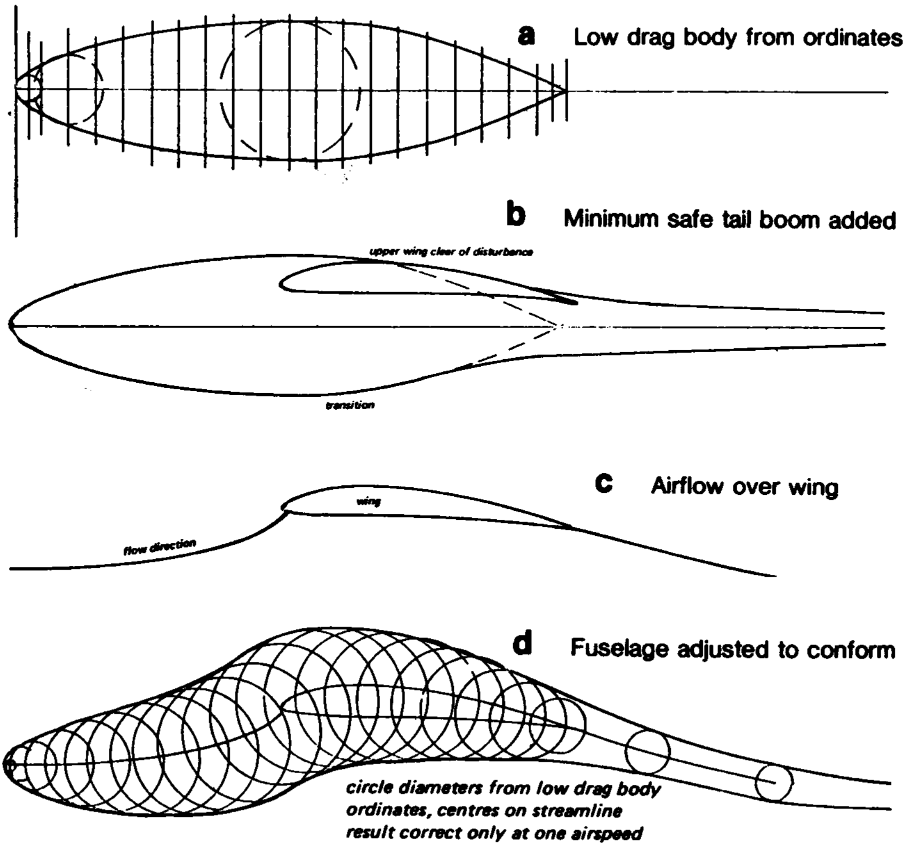

sailplane is in a turn, as when thermalling, since there is nearly always some slight slip or skid, causing cross flows. For this reason the high wing position is probably better all round than the mid-wing mounting, which is ideal for high speed flight. For models, there is only small advantage in the tadpole shape unless the fuselage cross section in front has to be increased to provide internal space for radio gear, etc. For free flight sailplanes the 'stick' type fuselage is best. However, for a radio sailplane, a low drag body should be used for the front 'pod', and after the contraction, a minimum tail boom of round section is all that is required to carry the tail.

11.5 WING-FUSELAGE INTERFERENCE

The flow over the fuselage is affected by the upwash and downwash caused by the wing. The approximate form of the streamlines is sketched in Fig. 11.2c and d. A way of reducing fuselage drag at one selected speed is to lay out the fuselage datum line as shown in Figure 11.2d, along the central streamline. Then the ordinates of a suitable low drag body are used, to construct a curved fuslage which follows the actual airflow. The result

Fig. 11.3 Fafnir 2 wing-fuselage junction

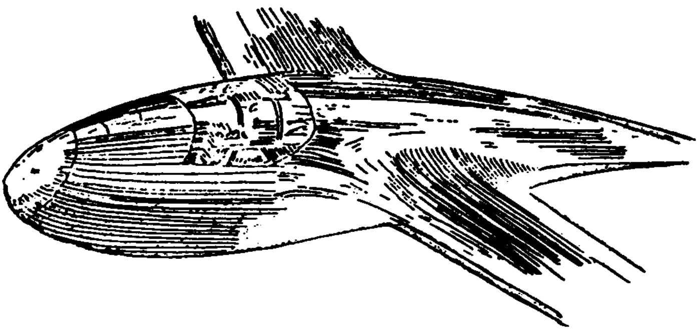

will vary according to the presumed flow pattern. Without wind tunnel tests it is difficult to establish the correct form and even when done, it can apply only to one flight speed. Probably the gain is too slight to justify the effort.

In the early thirties, after considerable research, Alexander Lippisch designed the Fafnir 2 full-sized sailplane, which had a wing-fuselage junction resembling that of Figure 11.3. The fuselage was treated as if it were part of the wing, each longitudinal cross section being adjusted to produce lift, the idea being to carry the lift loading right across the span instead of allowing the fuselage to interfere. The result at one speed of flight was very good, but at other speeds it was less so. A somewhat similar, though less elaborately worked out, system was used on the 'Fillon's Champion' model sailplane popular in the 1950s for free flight and radio control. It is probably better for all round performance to adopt the simplest low drag form, reduce cross sectional area as far as possible and add only the minimum fillets, for example, under the 'armpits' of a high wing sailplane, to fill in any sharp corners. Large fillets at the trailing edge may be necessary on some low-winged aircraft, but in most cases the trailing edge should run straight to the fuselage, with a small fillet of the 'radius' type at the junction. Larger fillets here promote turbulence at all angles of attack except one. On sailplanes, refined fuselage design is aimed primarily at improving penetration at high speed. This should be borne in mind. A streamlined fuselage on an F1A ('A2') sailplane will possess only a very slight advantage since flight speeds are so low.

To reduce interference drag between wing and fuselage, or between any two components where they join, the first rule is that the angle of junction should not be less than 90 degrees. If two surfaces, or a strut and another, larger component, join at a more acute angle, the air is forced to flow through a constricted channel and the drag increases rapidly as the angle becomes more acute. If such narrow channels cannot be avoided, they should be filleted; the fillet itself may be quite simple, but some care is needed to ensure that in itself it does not cause further flow separation problems (Fig. 11.4).

11.6 TAIL UNIT DRAG

As part of the total drag of a model, the contribution of the tail unit is small, but the same rules apply as for wings. The vortex drag of tailplanes depends on the trim of the aircraft, which is discussed in Chapter 12. Otherwise, it becomes important at high speeds for aircraft with strongly cambered wings. The whole unit should be as small as possible commensurate with its necessary function of stabilising and steering. Some reduction of total drag is possible in theory if the three surfaces of fin, port and starboard tailplane, are

Fig. 11.4 Reducing interference drag

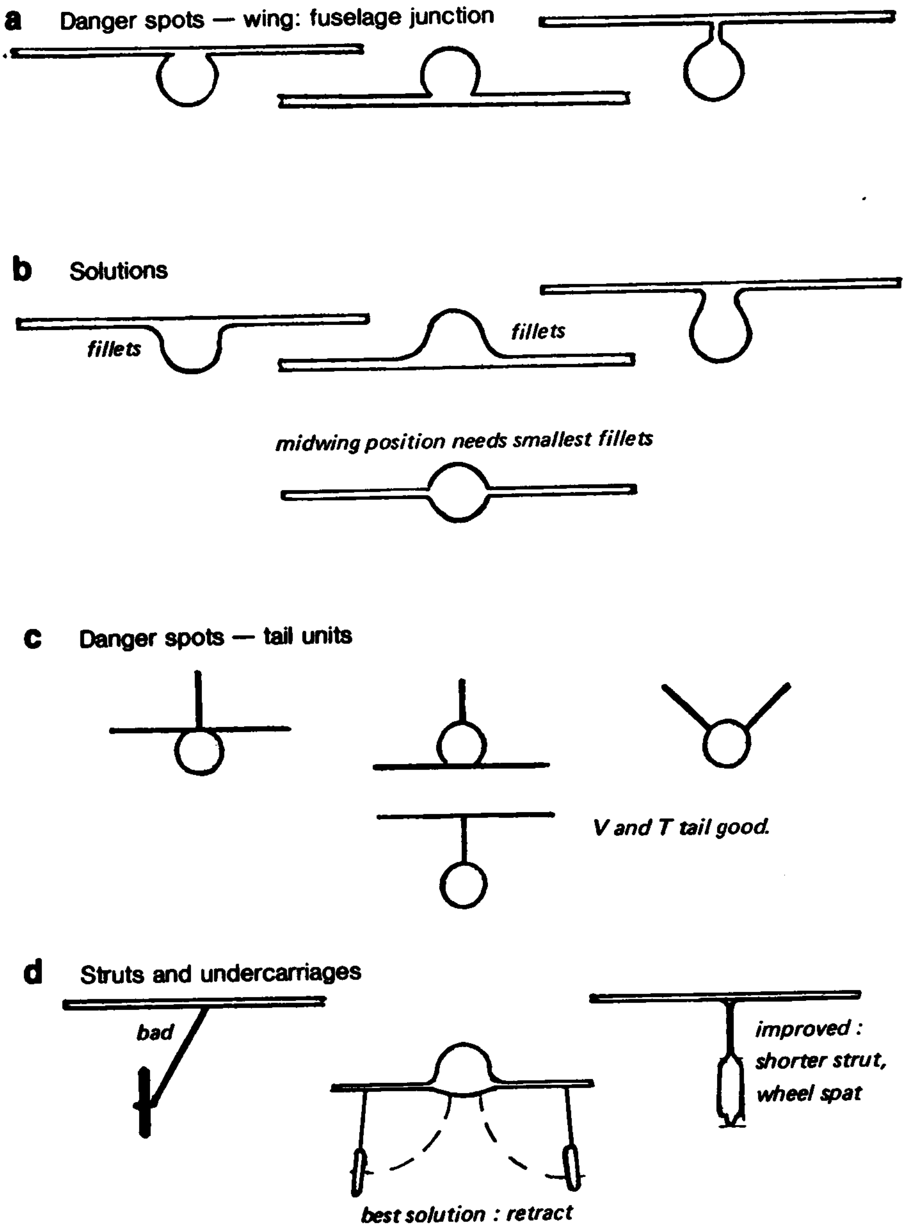

reduced to two by arranging the unit as a V tail, the angle between the two surfaces being then approximately 110 degrees. However, the required *total* area for such an arrangement is no less, and may be slightly more in practice, to achieve the same stability. In some flight positions it is possible for one side of a V tail to be stalled or to be blanketed by the other and this had been known to cause control difficulties. Since the elevator and rudder control effects are obtained by coupling only two hinged surfaces, there are some situations where full control is not available. If, for example, full elevator is applied, and full rudder is required at the same time, the angle to which one of the control surfaces is required to move is very large and it may stall. (Recovery from spins, requiring full rudder against the rotation with elevator down to unstall the wing has been found difficult or even impossible in some full sized 'V' tail aircraft.)

11.7 THE WING ANGLE OF INCIDENCE

For fast models, including cross country and 'F3B' sailplanes, it is important that when the model is at high speed, the fuselage should be aligned as closely as possible to the airflow. At low speeds, since parasite drag is less vital, this is not so important, though of course some reduction in drag will result if the fuselage is accurately aligned. Visual judgement of the model in flight is a rough guide but it must be a judgement of the fuselage's angle relative to the true flight path. With gliders, the flight path is always inclined somewhat downwards, so a glider which, when trimmed, adopts an apparently 'nose up' attitude, will actually sink a little more rapidly due to extra drag than one which has the fuselage pointing directly along the path of glide. At high speeds the same applies – a model which, at maximum speed, appears to fly either nose up or down has its fuselage at an inefficient angle of attack to the airflow. It is best in design stages to think of the wing and tail as being fixed to give flight in one desired position, and then the angle of the fuselage is adjusted to this, rather than thinking of the fuselage as fixed with the wings set at some angle of incidence. Unless carefully designed, the flight line will certainly not be direct extension of the fuselage datum line on the plan (see Fig. 1.3). Trimming the model, by adjusting the centre of gravity and altering the relative angles, one to the other, of wing and tail, will determine the angle of attack of the wing. The flight path will then be at the angle to the wing. The fuselage should be set at this angle to give least drag in that condition. If suitable wind tunnel test results are available calculations can be of assistance. By studying the results given in Appendix 2, the C_L at which the model will operate may be found. From the section test results, corrected for aspect ratio and downwash effects, the geometric angle of attack at which this C_L develops may be estimated. If the wing is twisted and tapered, the *average* value for the wing as a whole should be taken, rather than that at one station, such as the wing root. The method is explained with some examples in Appendix 1.

The validity of this method depends on the model in practice being correctly trimmed at the designed C_L, and the wing profile being accurate and reproducing fairly closely the wind tunnel figures. However, small errors of the wing setting angle will not make a great deal of difference in practice. The calculations should be regarded as a safeguard against gross errors in design, and in the workshop the modeller should maintain as high a standard of precision as is practical.

11.8 CANARD FOREPLANE DRAG

Some discussion of potential savings in vortex drag appears in Chapter 12. Canard foreplanes work in relatively undisturbed air and should be designed for laminar flow, to save parasite drag. The wake from the foreplane may turbulate the flow over some of the mainplane.

12
Trim and stability

12.1 DEFINITIONS

Probably no aspect of aeronautics has caused so much confusion among model fliers as stability, so it is well to begin with some simple basic concepts and definitions.

An aircraft is stable if, after a disturbance, it tends to return to the flight attitude determined by its trim. This is not the same thing as saying it will always seek to return to straight and level flight. If, and only if, the controls are centralised, a stable model will try to keep straight and level. If the controls are set for a steep dive, a stable aircraft will strive to retain this attitude. That is, it will go on diving until the trim is changed. A stable aircraft trimmed for a steady rate of turn at a suitable angle of bank will tend to continue in the steady turn, and so on for every other kind of trim. A model may be trimmed to fly inverted. If it is stable it will tend to remain inverted as long as the controls are set so. (Models with a fair amount of wing dihedral are seldom stable inverted, they tend to roll upright. An aircraft with no dihedral but with some degree of sweepback on the mainplane may be quite stable both upright and inverted.)

Gusts and other upsetting influences, including the actions of the pilot, frequently cause departures from the trimmed attitude but stability will strive to return the aircraft to the position prescribed by the controls wherever they are at a given moment. There will always be some oscillations to and fro on either side of the trimmed attitude, somewhat like a pendulum, but the stable model will generally damp down such variations fairly quickly if left alone. A truly stable aircraft will usually fly more efficiently if it is allowed to settle down to its trim without constant interference from the pilot. Too many small twitches on the controls achieve little but create extra drag and upset the flight.

12.2 CONTROLLABILITY AND STABILITY

It follows from the above that stability and controllability must be considered together. A stable aircraft will obey the controls predictably because whatever their position at any instant, it will strive to obey them. A genuinely unstable aircraft will, in contrast, not settle down in any position. Every small divergence from the desired flight path will be magnified. If the model is in a shallow dive this will tend to become steeper unless the pilot corrects it. A shallow turn will very quickly become a tightening spiral. If flying inverted, an unstable model will roll over or bunt, unless the pilot makes constant corrections at every moment. An unstable radio controlled aeroplane is difficult to fly, although it can be done. A momentary inattention may produce disaster but with extreme concentration the aircraft can be saved. An unstable free-flight model will almost certainly crash.

Even so, too much stability in a radio controlled model can be a liability. Since the forces involved in holding position are relatively powerful, it is evident that changing from one attitude to another requires large forces too. Unless the control surfaces are unusually effective, this makes the over-stable aeroplane sluggish in response to the pilot. If the model is flying towards a tree or some other obstruction, it is very important to have quick response to commands. Hence although a high degree of stability is very desirable for the beginner's radio controlled model, and for all free-flight aircraft, most model fliers prefer to have only moderate stability for the sake of more immediate control reaction.

12.3 NEUTRAL STABILITY

A stable aircraft will always tend to hold its trimmed attitude and an unstable one will always diverge. Between these two conditions is a narrow zone where the model will do neither. This is 'neutral stability'. A neutrally stable aircraft is less difficult to fly than a truly unstable one. Any change of attitude, however caused, will not be corrected and the next gust or other disturbance will also not be countered, so the aircraft, while not positively diverging, will be at the mercy of every small atmospheric change and will wander away from the trimmed position constantly. A good example of neutral stability is seen in a ground training device sometimes used to teach pilots to fly radio controlled helicopters. A flat table which can be tilted by servo motors under radio control, has a steel bearing ball or marble rolling on its surface. The trainee has to position the ball on the table. Every smallest tilt sets it rolling towards the edge and it keeps on rolling until the table is tilted appropriately to stop it. It then has to be tilted the other way to roll the ball to another position, and tilted again to stop it when it gets there!

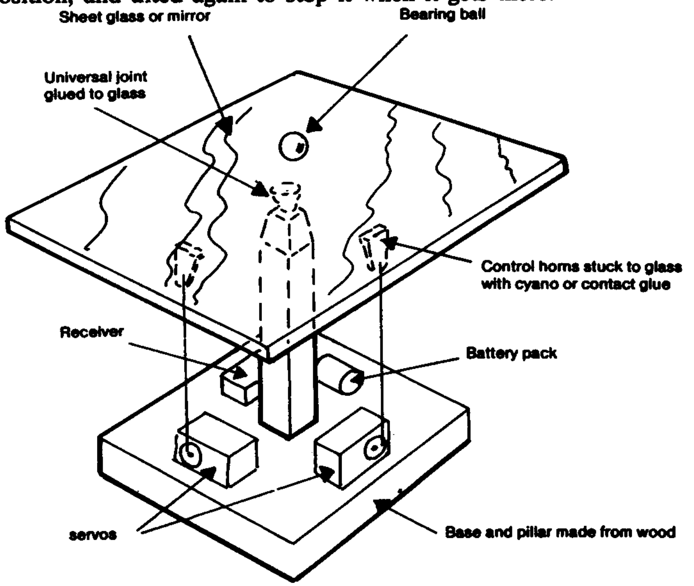

Fig. 12.1 Neutral stability: a helicopter 'simulator' in which the trainee pilot must keep the bearing ball on the flat, but tiltable, table (From Dave Day's book, Flying Model Helicopters). Positive stability corresponds to a shallow dish in place of the table. Instability would replace the table with a domed surface.

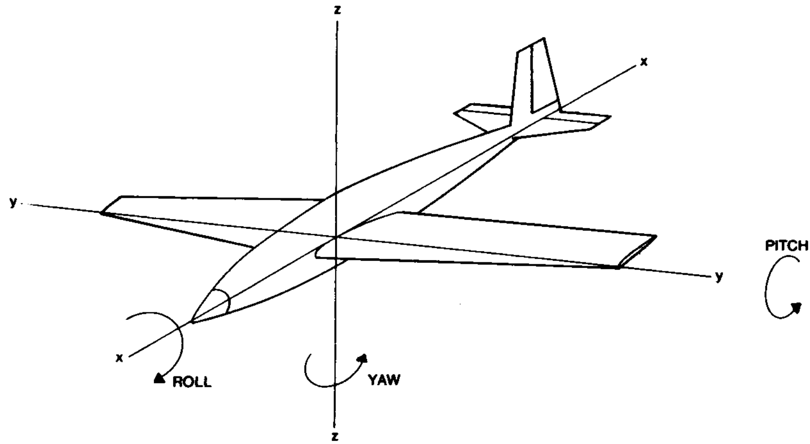

Fig. 12.2 The three conventional axes of an aircraft, used for balance and stability calculations.

In contrast, a stable aircraft could be imitated by a similar device with a shallow dish instead of a flat plane. Centralising the controls would allow the ball to settle down in the middle. Holding the dish steady in some tilted position would find the ball bearing seeking the new position of the lowest point and it would soon settle there. A truly unstable situation would be to replace the table with a domed surface. A brilliant juggler might be able to keep the ball centred but very few model fliers could do it and the same applies to real model aircraft of all types. Aircraft lacking inherent aerodynamic stability are flown but require automatic stabilising devices, usually of gyroscopic and electronic kinds. They are highly manoeuvrable.

12.4 THE THREE AXES

Stability and control problems in aircraft are complicated because a model which is stable in pitch, i.e. in nose up and nose down senses, rotating about the crosswise or Y axis (Figure 12.2), may be unstable about the other axes, in yaw, about the vertical, Z, axis and in roll about the fore and aft or X axis. The three axes are assumed to cross one another at right angles through the centre of gravity of the aircraft. This conventional system of axes does not imply that the aircraft is somehow bound to rotate, when it rotates, round the axes as if they were skewers.

The axes are in fact no more than convenient reference lines for trim, balance and stability calculations.

12.5 LONGITUDINAL BALANCE AND TRIM

Balance, or trim, and stability are closely connected, but they are distinct. Consider balance first. If a model is to fly at all, it must be in a balanced trim although being in balance is not enough to guarantee stability. A juggler keeps things balanced despite their instability. If he cannot achieve balance, everything comes crashing down and model aircraft are very similar. Only when balance, or trim, is achieved do questions of stability arise. Stability then may be regarded as restoring balance; the balance must be possible in the first place, if it is to be restored.

For flight in balance, or equilibrium (climbing, diving, or flying level at constant speeds) there must be no tendency of the aircraft to pitch nose up or down. Mathematically, when a model is trimmed for a particular flight attitude the longitudinal moments taken at any convenient point will total zero. On a practical aircraft this means that a state of balance must be possible in all the flight attitudes the pilot is likely to require. Even if the equilibrium is deliberately upset in order to change position (from steep climb to glide, for instance, or from level flight to inverted) if the model is to hold the new attitude for more than an instant, it must be trimmable at this position. The balanced state must be attainable, by use of the controls, over a wide range of attitudes.

12.6 BALANCE WITH A TAIL DOWNLOAD

In figures 12.3 to 9, a number of different ways of achieving trim balance are illustrated. In the most orthodox case (Fig. 12.3) the centre of gravity of the aircraft is located at the aerodynamic centre of the mainplane. (The allowance for wing sweep and planform, as always, must be made.) Since the wing in this case has some camber, there will be a nose down pitching moment, so even though the weight and lift are exactly opposed and create no pitching tendency, the tailplane must carry a download to balance out the wing's inherent moment. If the wing were truly of symmetrical section there would be no wing pitching moment and the tailplane would not need to carry any load, but the greater the camber, the greater the tail load at a given airspeed.

Since the tailplane lies behind the main wing, it will be working in the region affected by the vortex-induced downwash of the wing. This may be several degrees, depending on the wing's planform and the wing lift coefficient, C_L, at which the model is trimmed to fly. Since C_L is high at low flight speeds, the downwash may be several degrees. (See the approximate formula in para 5.10). If the model is trimmed for fast flight, C_L will be lower and there will be less downwash. But in every case the tail must be set at just the angle required, relative to the airflow in its location, to provide exactly the downforce needed to bring the total of all the pitching moments to zero.

Fig. 12.3

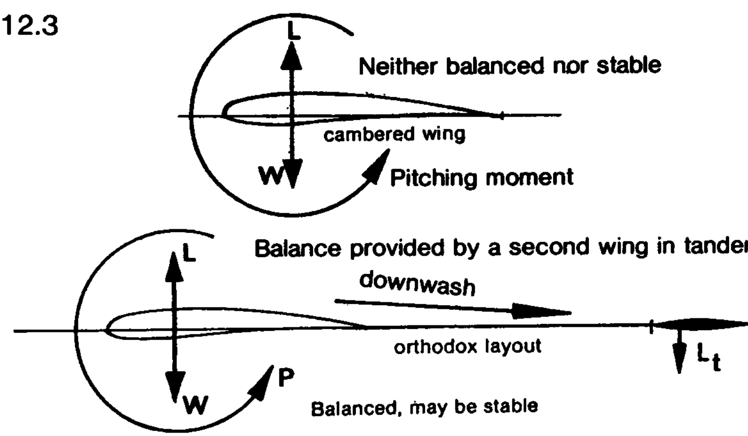

The most usual arrangement of forces for balance with a tailplane. The tailplane is rigged at a slight negative angle of attack relative to the air in its neighbourhood. The tail 'lift' is downwards. The additional load must be carried by the wing, and some additional vortex drag, of both tail and wing results. [$L - L_t = W$] This is also a safe, stable layout.

To achieve a required new trim the whole tailplane may be moved to the new position, or, more often, it may be provided with a hinged portion, the elevator, which changes both the camber and the effective angle of attack of the tail to produce the same effect. A different trim setting is required for every different flight condition. If the control is insufficiently powerful, some attitudes may be impossible to hold.

With the centre of gravity in this position, there will always be a download on the tail. It will be rigged at a more negative aerodynamic angle than the mainplane: this difference is often termed 'decalage' or 'longitudinal dihedral'. In a vertical dive the lift is zero and the weight acts vertically, so there is no pitching moment arising from these two forces. The wing camber is still present, however, and its direction is such that it would turn the model through the vertical into a bunt unless balanced by the tailplane. Thus, although the elevator is moved down to produce the dive, and held down to keep the dive going, the tail load is still down. (This is discussed further below.)

12.7 BALANCE WITH A CANARD LAYOUT

In Figure 12.4 the canard layout is shown. All the same principles apply. The centre of gravity and the lift are arranged to produce no moment, but since the mainplane is cambered, the foreplane must produce a balancing upload. (This is one of the claimed advantages of the canard, but to anticipate a later paragraph the arrangement shown in Figure 12.4 would be dangerously unstable, aerodynamically. It would need 'fly by wire' devices to fly safely.)

Since, here, the forewing is lifting, it produces downwash which affects the angle of attack of mainplane behind it, but if the forewing is relatively small and of high aspect ratio, this is not a large effect. It is worth noting all the same that whenever two or more lifting surfaces are in proximity, they do have mutual downwash effects. The forewing also lies in the vortex-induced upwash of the rear plane, which is a significant point.

As with the orthodox layout, the forewing must produce the required balancing load in all trimmable conditions. In a dive, the load on the foreplane will be up, to prevent the bunt.

12.8 BALANCE WITH ZERO TAIL LOAD

As mentioned above, if the mainplane is of symmetrical section, the tailplane will carry no load. (A stabiliser will still be needed.) This situation can be attained at one flight speed, if the centre of gravity position is aft of the mainplane aerodynamic centre, as suggested in Figure 12.5. Here, there is a nose up moment produced by the lift and weight couple. This can be adjusted, by careful c.g. location, so that it exactly equals and so balances the

Fig. 12.4

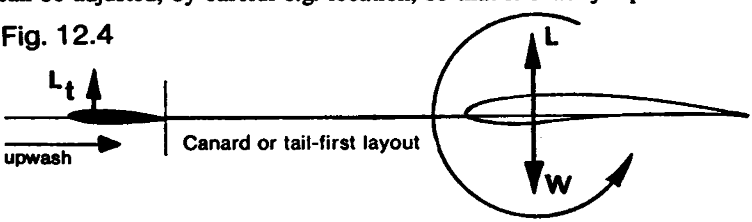

With the canard, balance is achieved with an upload on the forewing.
[$L + L_t = W$]. The forewing creates some vortex drag but relieves the mainplane of some load. Stability problems would arise with this arrangement. The mainplane creates upwash in the neighbourhood of the foreplane. This has an effect on rigging angles.

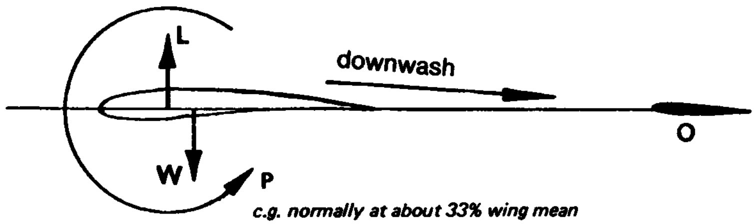

Fig. 12.5
Balance with zero tail load may be achieved with the centre of gravity slightly aft of the wing's aerodynamic centre. [L = W] There is no vortex drag penalty on the tail, at one chosen speed of flight only.

camber-induced nose-down moment. The tail then has no balancing role in this flight attitude and is only a stabiliser.

In the days when designers thought in terms of a moving centre of pressure, it was often recommended that the centre of gravity should be located at about 33% of the mean wing chord, to produce this kind of balance. This was because the models were intended always to fly at low speeds and the wind tunnel charts (see Figure 10.4) available in those times showed that at high lift coefficients the centre of pressure on many well cambered wing sections just below the stalling angle was at about 33%. In modern terms, the effect is still the same. It happens that with well cambered profiles, at high c_l the pitching moment coefficient at the aerodynamic centre is roughly equivalent to a rearward movement of the centre of pressure of about 8%. Hence the old balance remains about right for the one, slow, flight speed. It is clear, all the same, that at any other trimmable speed, faster or slower than the one favoured for the old free-flight models, the tail load can be brought to zero only if the centre of gravity is in some other location. Putting this again in centre of pressure terms, at high speeds, as the old chart shows, the c.p. moves back, so the tail load can be made zero only by moving the centre of gravity back, to increase the strength of the lift-weight couple.

The advantage of trimming for zero tail load is that when the tailplane is not lifting, it creates no tip vortices and hence no vortex drag. With a thin, symmetrical profile its parasitic drag is then at an absolute minimum. Fortunately, at low speeds the parasitic drag contribution to the total drag of a model is quite small (see Figure 4.10) so on the free flight models such a balance was of very slight advantage. Saving a fraction of the tail drag saves only a fraction of a fraction of the parasitic drag of a model. At low speed, this itself is a small fraction of the whole. There are dangers in this trim as far as stability is concerned, but for the moment consider only the case of a dive. In a vertical dive, there is no wing lift. The weight of the model acts straight down. There is now NO pitching moment or couple of the weight with the lift to produce a nose up moment. Yet the wing camber remains and the nose down pitching force from this cause is very powerful, because the airspeed is high. The tailplane, even though originally rigged for zero load, must provide a powerful balancing down force to prevent the model bunting. It is clear again that although the zero load trim operated at slow speed, at high speeds the tail must carry a down load if balance is to be achieved.

On fast models with wings of slight camber, the zero tail load condition can be achieved by locating the centre of gravity aft, as before. This can result in quite substantial drag savings because parasitic drag becomes very important at high flight speeds. It still follows that the tail must produce a download at steep diving speeds, and an upload at low speeds, to maintain balance. In general, then, any model with a cambered wing profile

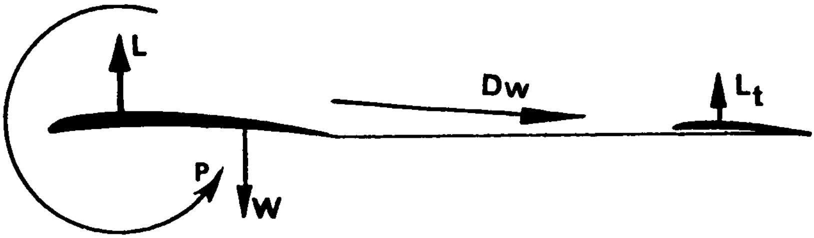

Fig. 12.6
A balanced arrangement with a lifting tailplane. As with the canard, stability problems may arise, but the tailplane relieves the wing of some load. Tailplane vortex drag increases but there is a small saving wing vortex drag [$L + L_t = W$]
The arrangement of Figure 12.5 is superior and more stable. As before, balance in a trim of this kind can be achieved at only one speed.

may be trimmed for zero tail load at one flight speed, but at faster speeds than this it will carry a download and at slower speeds, an upload.

With canards all the same points apply, but the load's direction is the other way, and stability problems arise, more severely as the centre of gravity is moved aft.

12.9 THE LIFTING TAIL

In Figure 12.6 a trim very commonly used for free-flight models is shown. The centre of gravity is located well aft, even beyond the 33% mean chord point, so that at low speeds there is an excess nose-up pitching couple of the weight and lift. To balance this, the tailplane must carry an upload and is usually cambered appropriately for this. Although this trim is almost universal on these models, it has no advantages in terms of drag saving. The tailplane produces tip vortices and the lift force generated by the tail is not enough in proportion to make this penalty worthwhile. Every attempt to prove the opposite has been proved mathematically fallacious. In contest models the fallacy is more than usually apparent because, as will appear, to provide stability with this trim requires a larger tail contribution than other trims, so there is a penalty in terms of profile drag as well as vortex drag. Every increase of tail area robs the mainplane of an equivalent amount. Yet the wing is invariably more efficient than the tail, producing its lift for a smaller relative drag penalty.

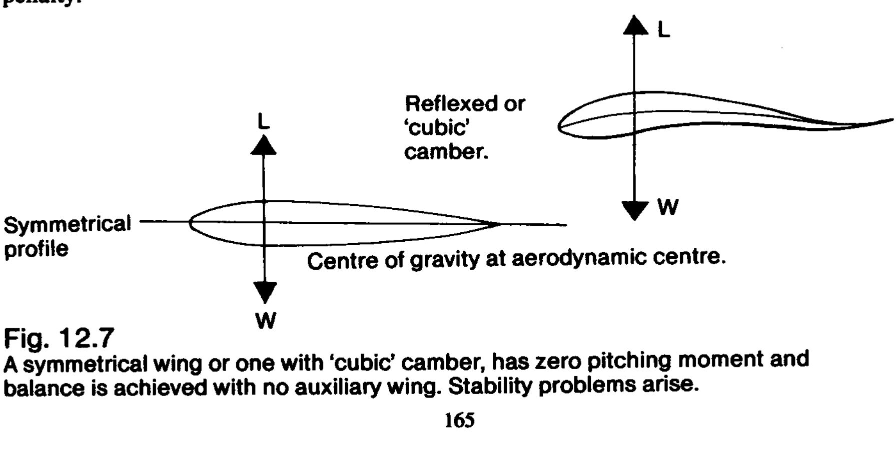

Fig. 12.7
A symmetrical wing or one with 'cubic' camber, has zero pitching moment and balance is achieved with no auxiliary wing. Stability problems arise.

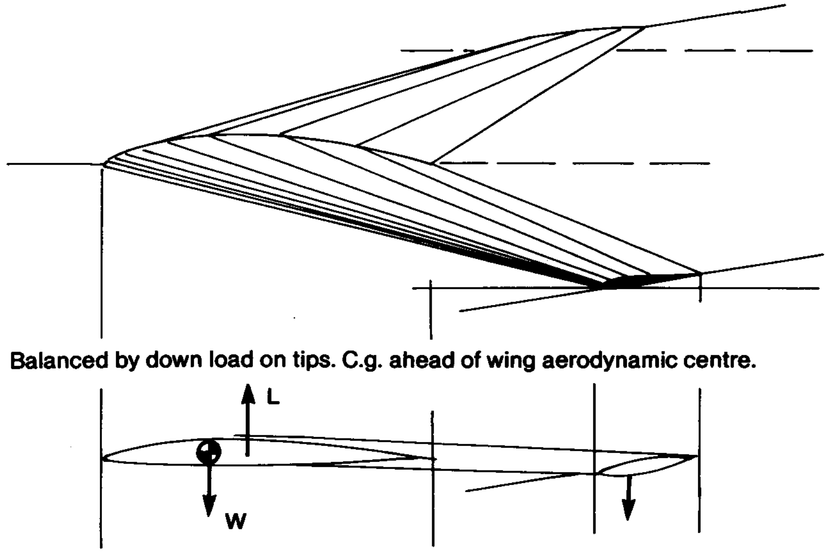

Fig. 12.8 Balance with a tailless swept-back wing
A tailless aircraft may achieve balance (and stability) with sweepback combined with wash out at the tips.

As before, although free flight models are not expected to enter steep dives, they can be upset by gusts and if, after such disturbance, they enter a dive, the wing pitching moment will tend to steepen the dive into a bunt unless the tailplane provides a corrective, downward force. Thus, a 'lifting' tail at one speed must still become a downward acting surface at high speeds. At some point between the steep dive and the slowest possible

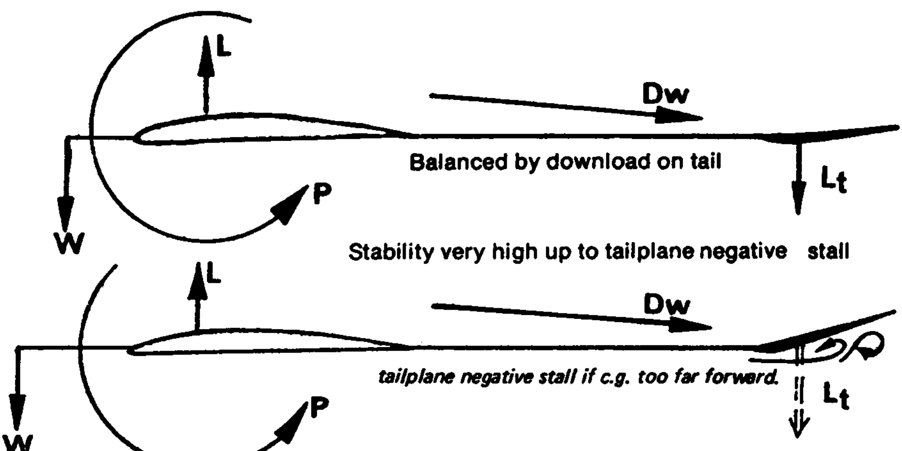

Fig. 12.9
The centre of gravity may be moved forward of the mainplane aerodynamic centre. The tail download is then increased. Stability is very high. For minimum profile drag the tail is cambered negatively. A vortex drag penalty is inevitable [$L - L_t = W$]

flight trim, the tailplane will pass through a zero load point.

12.10 BALANCE WITH NO TAIL

Figure 12.7 shows that a wing which has no pitching moment at any normal angle of attack may be balanced without a tail or forewing. Such a wing may be of symmetrical profile, since such aerofoils do not produce any pitching forces except when stalled, or a profile with a reflex or 'cubic' camber line may be employed (see Figure 7.3). Figure 12.8 shows a common tailless aircraft layout which helps to overcome stability problems.

12.11 BALANCE WITH FORWARD CENTRE OF GRAVITY

Figure 12.9 shows that balance is possible with the centre of gravity ahead of the mainplane's aerodynamic centre, on a model of orthodox layout. The tailplane and wing will generate additional vortex drag, so there is no advantage in such an arrangement except that it tends to be very stable, as will appear. Some scale model aircraft with stability problems have been flown successfully with this kind of trim.

12.12 TAILPLANE LOADS AND THE ELEVATOR POSITION

Modellers frequently are puzzled at the fact that tail loads are normally downwards in a dive or fast trim, when the elevator has to be held down to hold the attitude.

This is related closely to stability. In Figure 12.5 the tailplane is shown carrying zero load and its exact angular setting to achieve this depends on the downwash from the main wing. Suppose the pilot wishes to re-trim for a faster flight speed. The elevator (or all-moving tailplane) must first be moved down and this momentarily produces a lifting force on the tail which causes the nose to go down. But the change of wing angle of attack reduces the C_L and this in turn reduces the downwash at the tail. There is, therefore, an increase of angle of attack at the tail tending to produce a lifting force there. If the nose-down pitch brought about by the initial elevator movement is not quickly checked, the combined effect of down elevator and reduced downwash will cause the nose-down motion to continue and become exaggerated. Hence as soon as the new flight attitude is reached or earlier, the elevator must be re-set for a new set of conditions. If the model is stable, it will finally be trimmed to give a download where previously it was at zero, but this condition will be reached with a small amount of down elevator at the control end.

An unstable model will react differently. The initial down elevator movement will, as before, produce a nose-down pitch, increase of flight speed, and reduced downwash, but to prevent the motion going too far, the elevator will have to be checked more quickly and the eventual trimmed position will be elevator *up*. That is, an unstable aircraft will dive with elevator up, and fly slowly with elevator down, even thought the initial control movements needed to bring these attitudes into being will still be in the usual sense.

A neutrally stable model will respond normally to control movements, but every flight attitude will trim out with the elevators neutral.

To achieve zero tail loads at a number of flight speeds, for the sake of reducing parasitic drag, it is possible to use an adjustable centre of gravity. This is done in some full-sized sailplanes, by means of mercury reservoirs in nose and tail. At low flight speeds when zero tail load is required with high C_L and strong downwash, the mercury is all pumped into the forward tank to bring the c.g. as far forward as possible. When high speed trim is required, and tail drag becomes more significant, an aft c.g. is required and the mercury is pumped to the tail.

Unfortunately, this reduces stability and as any radio controlled model flier knows, as the stability is reduced the elevator control becomes increasingly sensitive and even 'twitchy'. To fly a sailplane, or any other aeroplane, at very high speeds with aft centre of gravity is very dangerous since a small twitch on the controls can precipitate a severe pitching nose up or down, and this can break the wing or tail. It is probably wiser to put up with some loss of high speed performance for the sake of safety. At low speed the gain is very slight in any case.

12.13 STICK-FREE AND STICK-FIXED STABILITY

In full-sized aviation, designers must consider what an aircraft will do if the pilot lets go of all the controls and allows them to float freely under the various air loads. Stick-free stability is the art of designing aircraft so that they will fly themselves, at least for some little time, without a pilot at all. In model aviation this is not of concern. The controls are normally fixed, as in free flight models, or they are held in whatever position they are placed by means of servo motors, control rods or wires. This is the case even if the pilot lets go of the radio transmitter sticks, because these are spring-loaded to centralise automatically (except for the throttle, as a rule). This is the condition known as 'stick fixed', although of course it does not imply that the controls do not move. On the contrary, they move, but only in response to command.

Another factor in full-sized stability calculations is 'stick force per G'. This refers to the force which has to be exerted by the pilot on the control column, in order to produce an acceleration force of one 'G' (either positive or negative) on the aircraft. In a loop or a turn there is always some 'G' force. If an aircraft has very light controls a small stick pull or push can produce a large 'G' force and with clumsy handling this can overstress the structure. For ordinary aeroplanes, not intended for aerobatics, stick force per 'G' is made large so that a pilot will have to pull very hard to produce a 'tight' loop, for instance, and the danger of overstressing is less. Aerobatic aircraft, flown by experts, are lighter on the controls.

With radio controlled models the stick forces felt by the pilot are those of the transmitter springs and do not relate directly to the forces felt by servos and pushrods in the model. There is, however, a similarity in that for a given stick force at the transmitter, a model with relatively small stability will respond more sharply. The same applies; clumsy handling may produce a disaster.

12.14 STATIC AND DYNAMIC STABILITY

Static stability refers to the stability in flight of an aircraft and has nothing to do with a model standing still. A model with positive static stability will always endeavour to hold its trimmed attitude. However, as mentioned above, some oscillation almost always occurs, the model will swing a little either way from its desired position, and will usually take a little time, and a few oscillations, to settle down. Occasionally, with a statically stable model the oscillations do not die away but continue or even become larger as time goes on. This is dynamic instability. Models with high drag, such as biplanes and most sport aircraft, have good dynamic damping and such problems rarely arise. With very 'clean', low drag models, especially sailplanes, gentle 'phugoid' oscillations are more common. The model follows a slightly wavy path; nose up, nose down, nose up, nose down, and this wave-like motion may not be damped of its own accord. In an extreme case the up and down flight may develop into a series of stalls followed by dives and the oscillation may tend to magnify rapidly. Fortunately, the cure is found by increasing the static stability, which tends to damp the motion down as a rule. It also helps to keep the extremities of the model light so that inertia forces at the tail and extreme nose are less likely to take over.

12.15 THE NEUTRAL POINT

As described previously, every wing or wing-like surface in an airstream at a moderate angle of attack has an aerodynamic centre close to the quarter chord point. This applies to fins, tailplanes, foreplanes and such streamlined shapes as struts, wheel spats, nacelles, faired undercarriage axles, etc, etc. Even long, slender forms such as arrow shafts or fuselages have an aerodynamic centre and this is normally close to the quarter length position for moderate angles of attack.

If the structure of a model is fairly stiff, it may be treated as a fully rigid body. Then it is possible to regard the entire aircraft as one object which produces lift and drag at some fixed point equivalent to the aerodynamic centre of the whole. The exact position of this point may be found by finding the a.c. of each separate component first, then, with an allowance for the efficiency of each part as a producer of aerodynamic force (area, angle of attack, body shape etc, and whether or not in the wake of another component), the total effect of all may be added and the aerodynamic centre of the entire aircraft found. As with a wing, providing the airflow is not generally separating the centre of forces so found remains in one place at all usable flight trims.

It has already been pointed out that, for a model to be in trim, the total of all pitching moments on it, at any place on the fore and aft centre line, must be zero. Hence, when the aerodynamic centre of the aeroplane is located, if it is in trim the pitching moments of all the various components will total zero at this point.

For *stability*, however, it is necessary that if there is a disturbance of equilibrium, causing a nose-down or a nose-up pitch, then a *corrective* pitching moment should appear. Then, a nose-up disturbance causing an increase of the total lift force at the aerodynamic centre of the model must automatically produce a nose-down moment, and vice versa, a nose-down upset must produce a nose-up moment.

An unstable aircraft will produce the reverse, a nose-up pitch will produce a nose-up moment, making the situation worse, and again, vice versa.

A neutrally stable aircraft, when pitched either way, will produce no pitching force either way, leaving the attitude to be determined by chance gusts and random disturbances of the air. In Figure 12.7 a symmetrical wing was shown, in trim, with zero pitching moment and the centre of gravity exactly at the aerodynamic centre of the wing. A disturbance of such a wing would produce no pitching moment either way, because symmetrical wings have no pitching moment (unless stalled). Evidently, the condition of neutral stability for an entire aircraft just described is exactly similar: no corrective force arises either way if the model pitches.

If the centre of gravity of any aeroplane or glider is at the aerodynamic centre of the entire aircraft, neutral static stability is the result. For this reason, the aerodynamic centre of an aeroplane is termed the neutral point. Figure 12.10 shows the results if the centre of gravity is at, behind or in front of the neutral point in a disturbance. In Fig. 12.10a the c.g. is at the neutral point. A gust throwing the model into a climbing attitude causes an increase of the total lift force on the whole model. The c.g. and lift are still acting at the neutral point and no pitching moment results. With a nose-down upset, again, there is no corrective force.

In Figure 12.10b, the c.g. is aft of the n.p. Now a nose-up disturbance produces an increase in lift and this produces a nose-up pitching moment. Vice versa for the nose-down disturbance; the lift is reduced and the nose-down pitch is worsened.

It follows that for static stability the situation of Figure 12.10c is essential. The centre

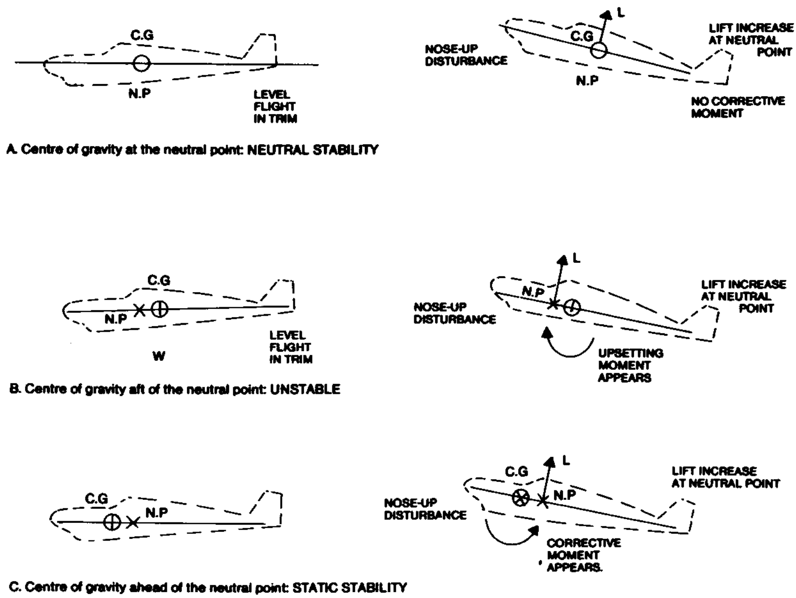

Fig. 12.10 Aerodynamic centre, neutral point, and the centre of gravity.

of gravity of the aircraft *must* be in front of the neutral point. Then a nose-up disturbance produces an increase of lift behind the c.g. and this tends to restore the normal trimmed and balanced flight attitude. A nose-down change produces a decrease of the lift aft of the c.g., and a nose-up moment arises. This applies to all model layouts, as in Figure 12.11.

12.16 THE STATIC MARGIN

The distance between the centre of gravity and the neutral point is termed the static margin of the aircraft. It gives a very useful standard of comparison of one aircraft with another, since if they have similar static margins they will have similar static stability. The larger the margin, the greater the stability. This concept also brings into emphasis that a shift of the centre of gravity of any model aircraft can change the stability margin. By this very simple means a dangerously unstable model can be made stable, or an over-stable one made more sensitive and responsive. Stability is thus almost entirely under the control of the model flier and can be varied, within limits, by the addition or subtraction of ballast at nose or tail. Any such change of ballast of course will require a new trim setting.

12.17 LOCATION OF THE NEUTRAL POINT

As just mentioned, the model flier does not actually need to know where the neutral point of his aircraft is, because stability can so easily be adjusted by careful use of ballast.

Fig 12.11 Stable layouts: C.G. ahead of N.P.

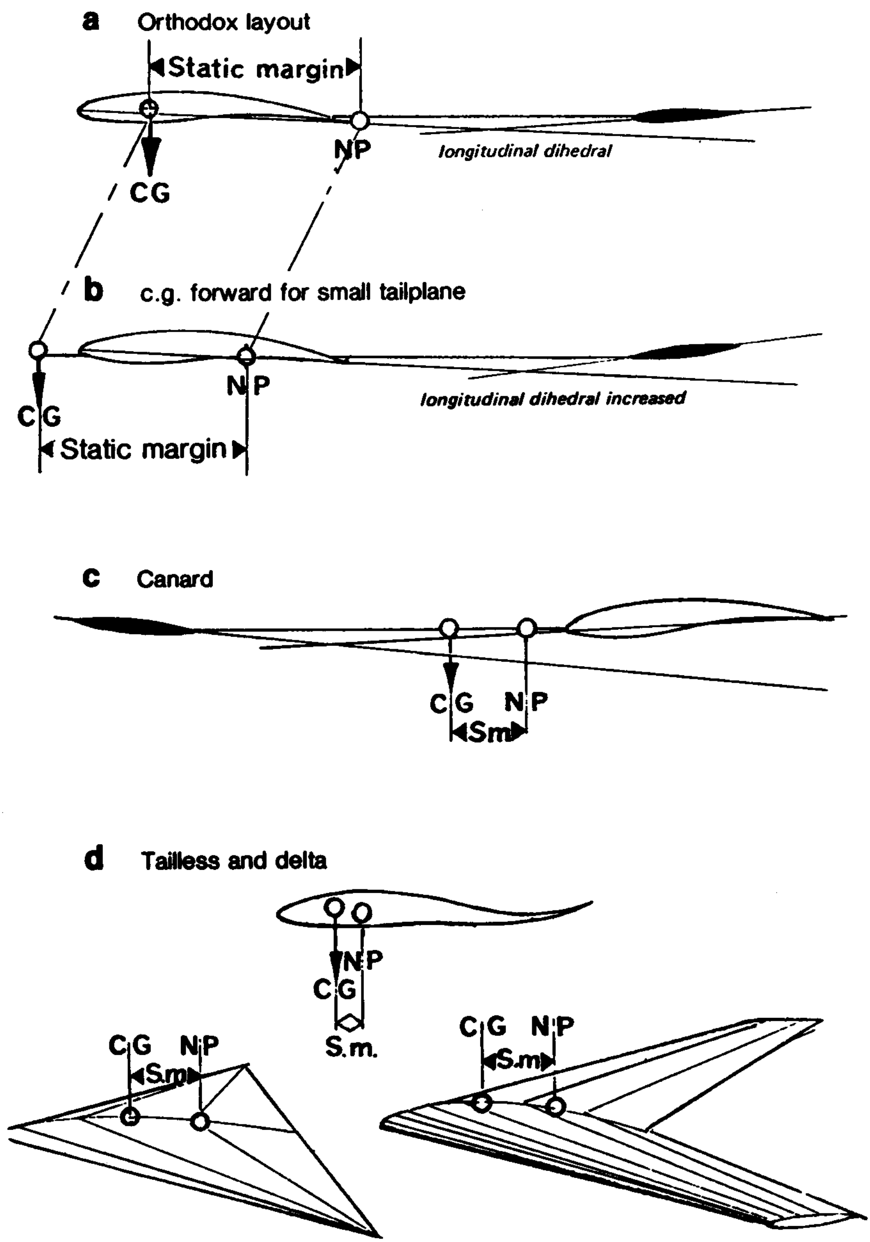

However, it is useful and interesting to know how the neutral point may be found if a new model is being designed or if two models are being compared.

The most important determinants of neutral point position are the mainplane and the tail or foreplane. Any lifting surface ahead of the centre of gravity will naturally tend to move the neutral point forward and so is destabilising. This applies to canards. The foreplane causes the neutral point to lie ahead of the mainplane's aerodynamic centre, so a centre of gravity position like that of Figure 12.4 is unstable. For stability, the canard must have the c.g. forward as shown in Figure 12.11c. Thus, the foreplane of a stable canard carries, for trim, not only the camber induced pitching load, but an additional load caused by the forward c.g. Any surface behind the centre of gravity, such as a tailplane, has a stabilising effect, since it brings the neutral point aft. Unfortunately, the efficiency of the tailplane is adversely affected by the wing, especially if it lies in the wing wake or comes into the wake at some angles of attack. Despite this, a useful measure of the tailplane's stabilising effect may be obtained by working out the stabiliser volume coefficient.

Fig. 12.12 Unstable layouts C.G. behind N.P.

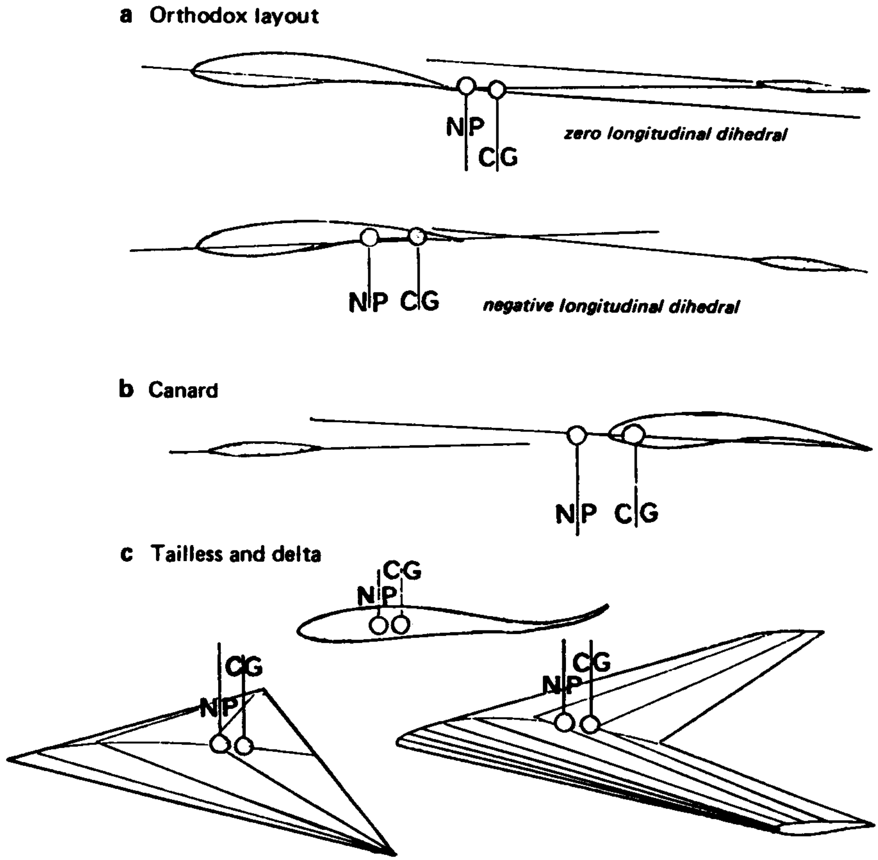

The formula relates the tail volume to the wing and fuselage length:

$$V_S = \frac{S_S \times L_S}{S_W \times c}$$

Here, V_S is the tail volume coefficient, S_S and S_W are tail and wing areas respectively, L_S is the distance of the tailplane's quarter chord point from the wing's aerodynamic centre (allowing for any sweep of either surface), and c is the mean wing chord (S_W/Span). Strictly, the coefficient so found should be reduced by some factor to allow for loss of tail efficiency. A high-mounted 'T' tail may be as much as 90% efficient, a low tailplane behind a fattish fuselage, in the wake from the wing, may be only 50% efficient. Some guesswork is involved in making such estimates. For a canard the same formula may be used to assess the de-stabilising effect of the forewing.

Various ways are used to calculate the position of the neutral point, using the wing and tail alone and ignoring any other effects. A way of doing this without calculation is suggested in Figure 12.13. Such crude methods are of course only approximate. A method of more exact calculation appears in Appendix 1.

12.18 FUSELAGE AND OTHER EFFECTS

The effect of the fuselage is destabilising. Any long, slender body moving through the air tends to turn broadside to the airflow. This can easily be confirmed by experiments with throwing sticks and arrows. Even the addition of a weight at one end does not change this much. As any archer will confirm, arrows which lose their fletching will yaw wildly sideways in flight. Rockets and bombs require fins for the same reason. The fuselage therefore must be regarded as moving the neutral point forward of the location determined by wing and stabiliser alone. In full-sized work, attempts are made to estimate this numerically, but the upshot is invariably that the static margin must be large enough to cope with the fuselage effect. That is, the centre of gravity must be far enough forward to achieve the desired stability, whatever may interfere. The propeller also has a destabilising effect which is considerably greater with power on than when the propeller is stationary or feathered. There is usually a difference in stability power on and power off, which is caused by this, among other factors.

Every other component of the aircraft which has air flowing over or through it will exert some influence on the neutral point position. For instance, a large horizontal undercarriage axle, faired, ahead of the centre of gravity, will tend to destabilise, but a broad strut, bracing a tailplane, will act in some respects like a second tailplane. Ultimately, the static margin has to be adjusted to cater for all these factors to produce a satisfactory result.

12.19 MULTIPLANES AND TANDEMS

The aerodynamic centre of a biplane, or other multiplane wing arrangement, may be roughly worked out by assuming that the two, or more, wings can be replaced by a single equivalent surface which will have its aerodynamic centre on a line joining the quarter chord points of the two (or more) wings. It will lie on this line at a point determined by the relative efficiencies of the wings and their areas. The lower wing of a biplane is usually somewhat less efficient than the upper wing, so if two wings are of equal area and span, the combined a.c. will be slightly nearer the upper wing. With a sesquiplane, the combined wing a.c. will of course be much nearer the larger top wing than the smaller bottom one, and so on.

With a tandem, the rear plane may be treated exactly as a tailplane, for determination

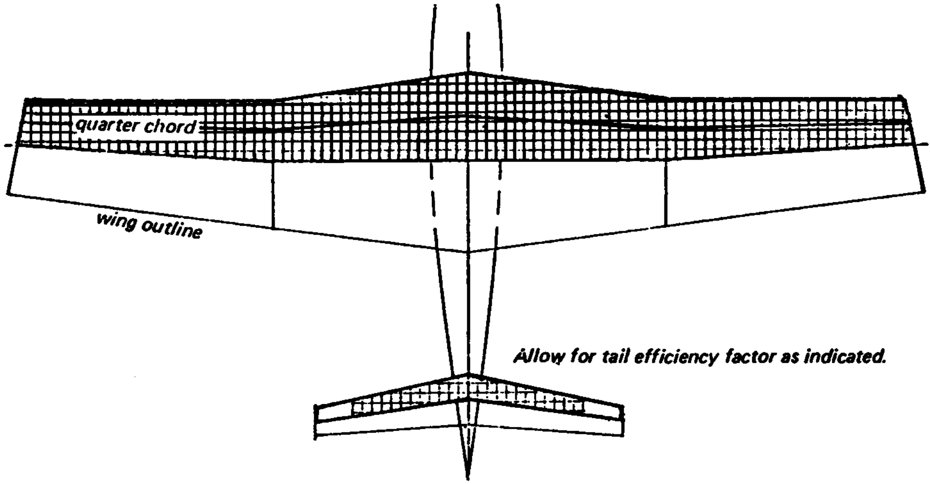

Fig. 12.13 Finding the neutral point

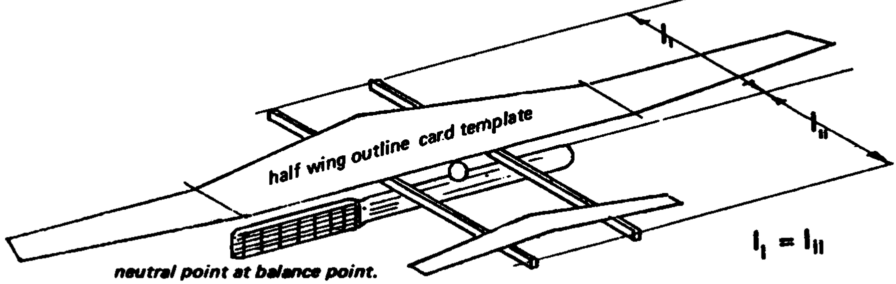

1. From an accurate scale drawing of the model in plan view, make stiff cardboard templates of the front half of wing and tailplane. Use identical weight card for both.
2. Mount templates on two stiff, light balsa strips and find balance point. Trim balsa strips by trial and error so that $1_1 = 1_2$ when balance point found.
3. Check over drawing. C.g. of model must be ahead of neutral point as found above.

of the neutral point position. The fact that it shares the lift load makes no difference in this respect: the centre of gravity must still be in front of the combined neutral point, for stability.

12.20 HOW LARGE A STATIC MARGIN?

Depending on the methods used to calculate the position of the neutral point and the various allowances made for tailplane efficiency, fuselage effects, etc, estimates of the size of the static margin required for adequate, but not excessive, stability vary a good deal. However, when the static margin is worked out, it is usually expressed as a decimal fraction of the mean wing chord. It is then usually found that a satisfactory s.m. comes out less than 0.2 mean chords, for radio controlled power models. Much greater figures than this suggest too much stability for satisfactory control response and much less begins to approach 'twitchiness' which may nevertheless suit an aerobatic model. For most free flight models, higher margins are required as a rule. If only wing and tail areas and moments are taken into account, the static margin should be on the generous side to allow for the other factors. As already noted, the degree of stability any particular pilot requires depends to a large extent on the kind of model and flying done, and the centre of gravity position can be adjusted to suit personal preference.

12.21 SPECIAL PROBLEMS: DEEP STALLING

The T-tail configuration has several aerodynamic advantages in normal flight attitudes, but it may in some circumstances lead to a trouble known as deep stalling. In jet airliners, an example is the BAC 111 prototype which crashed, killing all on board, in 1963. The aircraft lost most of its forward speed and descended in a flat attitude. Model aircraft with 'tip up tail' dethermalisers are placed in this deep stalled condition deliberately to bring them down, but some T-tailed models may do the same thing when the modeller does not intend it, and the controls may be incapable of returning the model to normal flight. The cause is quite complex. As the main wing approaches the stall, the wake becomes broader and at the same time the tailplane, because the nose of the model is rising, comes down into the wake and loses efficiency. If the centre of gravity is rather too far back, this also contributes to the undesirable nose-up pitch. When the main wing is stalled, the wake tends to strike the whole tailplane, whereas a low mounted tail will be out of the wake and will be more efficient than usual. Once in the deep stalled condition, the model may be unable to get out of it because the airflow over the fuselage, or engine nacelles mounted at the rear, causes the formation of strong rotating vortices similar to those at the tips of a lifting wing. Given a bad combination of circumstances, the downwash caused by these vortices may strike the high tail and keep it down in spite of the pilot's efforts to restore forward flying speed. The problem is baffling unless the modeller understands the cause, since an aircraft that flies perfectly well most of the time may without warning fall out of the sky and pancake, with fuselage more or less horizontal and hardly any forward velocity. After repairs, the same model may fly satisfactorily again for some time without 'deep stalling'. On the other hand, in gusty weather or in aerobatics, the trouble may strike at any moment (the BAC 111 prototype that crashed had completed many hours of successful test flying before the accident.) The cure may be simply to return to an orthodox low tailplane configuration, but the tailplane will then probably need to be enlarged to cope with normal flight stability requirements. Other possible modifications that might be effective include increasing tailplane span with or without an increase of area, or adding dihedral to the tailplane, both with the object of getting some of the tail area out of the downwash from the fuselage vortices. Carrying the tail still higher would have the same effect but might be impossible for structural reasons. Moving the centre of gravity forward and re-trimming may also help and will in any case improve stability in normal flight, so reducing the danger of stalling in the first place. The fuselage may be modified in an effort to reduce the strength of the downwash. A broad fuselage is more likely to give trouble than a slender one, and engine pods or nacelles have a bad effect in some positions, especially just ahead of the tail unit. Either lengthening or shortening of the fuselage may change the relationship of tailplane to vortices enough to solve the problem. Once the model is deep stalled, none of the controls except possibly wing flaps have much effect. The elevator tends to be useless and may even be forced upwards against the stops. The ailerons on a 'super stalled' wing are totally ineffective, and the rudder is not powerful enough to roll the model out of its horizontal position. It might be possible to yaw the model and the fuselage vortices might then clear one side of the tailplane. The application of engine power is usually not enough to restore the situation.

Wing flaps, however, may give a sufficiently powerful nose-down pitching moment to overcome the tail downwash effect. On the other hand, air brakes or spoilers may create more vortices or a more turbulent wing wake and make things worse. A model fitted with a tail parachute can be saved from the deep stall; the 'chute when deployed slows the model still more, the whole thing then hangs nose-down from the supporting parachute, and after a few seconds normal flight may be resumed with the parachute jettisoned.

12.22 SPECIAL PROBLEMS: SAILPLANE TUCK UNDER

Radio controlled sailplanes sometimes run away out of control in a dive, which steepens rapidly until, despite full up elevator the model is vertical and even beyond. Quick thinking by the pilot can sometimes save the situation by pushing the stick forward and so helping the model through the 'bunt', to emerge at high speed in level flight, but inverted. The strains of such a manoevre may cause structural failure, but if not the model may be saved.

The cause is almost certainly lack of static margin. That is to say, the centre of gravity should be moved *forward* and the tailplane re-trimmed to improve static stability. This seems difficult for some model fliers to grasp, since they tend to equate a nose-down pitch with too great a weight in the nose of the model. The foregoing discussion of balance should disabuse them. If the model is balanced in straight and level flight, by suitable tail trim angle, it will still be balanced in a dive, but if the c.g. is too far aft it may lack stability and tuck under with elevators up.

Another very likely cause is structural flexibility. The models which exhibit this tendency are often lightly built and have strongly cambered wings. The camber increases the negative pitching moment and if the tailplane and rear fuselage are somewhat flexible, or if the control rods and linkages are sloppy, there may be enough distortion to reduce the stability of the model to a dangerous extent when it is flying fast, as in a shallow dive. The wings twist also, as the pitching forces increase, and they may break or flutter. The discussion of stability above, it should be remembered, assumed a rigid structure (12.14).

A method of trimming a model sailplane which has been widely advocated is the so-called 'dive test'. This is not to be recommended although some pilots evidently like the feel of models which have been set up in this way. Following the dictates of the dive test generally increases tail drag and so tends to spoil the all round performance of the model slightly, though probably not enough for this to be apparent to the pilot. More importantly, it may reduce the inherent stability of the model to the point where a runaway 'tuck under' is more likely. Some models have in fact been written off in 'tuck under' accidents during attempts to follow the dive test procedure.

In brief, the dive test, as described in some publications, requires the model flier to put the sailplane into a steep dive of about 60 degrees and hold it there for several seconds to allow the airspeed to build up. Obviously this has to be done when the sailplane is at a considerable height. The controls are then returned to neutral and the model is observed to see how it responds. That is, the elevator is first set for diving and held for a count of five to ten seconds, then it is returned to the position for level flight.

The question is whether or not the sailplane will obey the controls. Advocates of the dive test evidently prefer a model which does not respond normally. What they seek is a model which continues in the steep dive even when the elevators are in the neutral position. To achieve this they progressively move the centre of gravity aft, reducing the stability of the model until this result is arrived at. A model which does in fact behave this way is on the verge of tucking under.

A stable model will respond to the elevator in the normal way. That is, when the elevator is moved from the diving position to the level flight trim, the model will obey and pull out of the dive. Because of the excess airspeed of course the model will not return instantly to level flight but will over-correct – the nose will rise beyond the horizontal, followed by the usual stable oscillating, nose up, nose down, response which the pilot should have no difficulty in smoothing out to restore level flight. Such a response is perfectly normal and safe.

The model which does not pull itself out of a steep dive with the controls central, is neutrally stable and in a very dangerous condition. Such a trim is not the trim for least drag (see section 12.8 above).

As explained above (sections 12.12 and 12.20), the stability of a model is entirely under the control of the operator and can be adjusted by moving the centre of gravity, i.e., by adding or removing ballast from the nose. Such changes have an immediate effect on the sensitivity of the elevator. Some pilots prefer a docile model which does not require constant attention, once trimmed for a particular airspeed. Others prefer more sensitivity and may move the c.g. aft slightly to achieve this. But to move the c.g. so far aft that the model no longer pulls itself out of a steep dive with neutral controls, is asking for trouble.

12.23 SPECIAL PROBLEMS: POWER MODELS 'GOING FLAT'

Free flight duration engine-powered models sometimes instead of climbing steeply and fast, 'go flat' and fly very fast, more or less horizontally or at a shallow angle of descent, to hit the ground.

It seems very likely that the cause is the same as that of the 'tucking-under' glider. These models frequently have the static margin reduced by aft centre of gravity location. Under power, a static margin that may be adequate for gliding or climbing may be reduced so that the model verges on neutral stability. Some flights then may succeed but on occasions a minor variation in launching technique may bring the model to a dangerous condition.

12.24 SPECIAL PROBLEMS: VERY SMALL MODELS

Very little is known about airflows at Reynolds numbers verging on, or below, the critical where the flow tends to separate completely from the wing. In some small models it seems the flow may change abruptly from one condition to the other more than once during a flight. This seems particularly likely with 'chuck' gliders which are launched fast and are at relatively safe Re number during the initial stages of a flight, but which slow down fairly rapidly and may then fall into a sub-critical state. Once in this condition they may not recover, in which case a very poor flight results. Associated with the flow break away there is a change of pitching moment which upsets the normal stability. The likely solution to such problems is to increase the wing chord and use an aerofoil which is not badly affected by low Re numbers. Probably the closer the profile comes to a flat plate section the more consistently it will behave, although performance in the absolute sense is likely to suffer.

Quite different stability problems appear with indoor, microfilm covered models. These are so flimsy in structure that distortion under flight loads is commonplace. The uneven unwinding of rubber motors also can cause serious shifts of centre of gravity position during a flight, which upsets both balance and stability. Humidity and air temperature also make differences which affect other models very much less. It becomes practically impossible to work out static margins or even trimming angles, since in flight these change. Even with all these effects, it still seems that a centre of gravity that is at least in the right place to start with will improve stability and hence consistency. There is no advantage, apparently, in using 'lifting' tailplanes of large area, when, by adding the excess area to the wing and moving the c.g. forward, stability would be improved without loss of aerodynamic efficiency.

12.25 WEATHERCOCK OR YAW STABILITY

The cardboard cut-out method described in Fig. 12.13 for finding the neutral point for longitudinal stability resembles a method which is still sometimes advocated for determining the size of fin required on a model. This was originally suggested in its simplest form in Frank Zaic's *1934 Yearbook*. A side view of the model is drawn to scale on card, cut out and balanced to ensure that the so-called centre of lateral area falls behind the centre of gravity. If not, the fin area is adjusted until it does so. Unfortunately this method, although attractively simple, is based on a misunderstanding of the behaviour of fuselages. As mentioned above, a long slender body like a fuselage tends to turn broadside on to the airflow. Without a fin the fuselage of an aircraft will tend to turn the whole aircraft in this sense also. However long the fuselage, it will not naturally align itself with the direction of flight. As Fig. 12.14 shows, if the theory in this form is applied it indicates that no fin at all is required on most models, which is easily disproved by trying to do without one. This still occurs in most cases if the projected dihedral area is included in the cutout. Dihedral does have an important influence on lateral stability but if the fuselage is of normal length the simple method still suggests that the fin may be dispensed with in many cases, which is not so. From these results it is hard to believe that any successful model has ever really been designed by this 1934 method.

An elaboration of the c.l.a. theory was due to Charles H. Grant and described in his book, *Model Airplane Design* published in 1941.[1] The concern at that time was with free flight engine powered models for which high reserves of spiral stability were essential. The cardboard cutout is prepared as before but the dihedral and any other parts of the model which are duplicated on right and left sides (such as the undercarriage and wheels, or twin fins) are doubled in card thickness. The balancing procedure is then gone through and the c.l.a. located. This point should, according to Grant, lie on a horizontal line through the centre of gravity with the model in a level flying attitude, and about 30 to 35% of the distance from the c.g. to the aerodynamic centre of the vertical tail surface. Further work was required to find the centre of lateral areas ahead of and behind the c.l.a. of the whole, and the line joining these was termed the displacement axis. A good deal was thought to depend on the precise relationship of this axis to the c.l.a. as a whole and to the centre of gravity.

If Grant's methods are adopted, and some designers do still use them, successful models result. They turn out as a rule to be very similar in general layout and appearance to many other satisfactory models of similar general proportions, including canard designs and models with large floats for operation from water. Applied to aircraft of different proportions, especially to advanced modern sailplanes, aerobatic and pylon racing power models, the results turn out rather differently, especially if long, slender fuselages are used and if there is no wing dihedral.

It is probably fair to conclude that while the c.l.a. method produces safe models resembling many others already known to be satisfactory, it is nevertheless based on a shaky theoretical foundation and should not be relied on if anything much out of the ordinary is proposed.

The correct size of fin for a model can be computed by methods sometimes used in full-sized studies, but the work is lengthy and the results still not always reliable. Previous experience and trial are better guides, with a background of general theory to direct

[1] The author is grateful to Andy Lennon for drawing his attention to this work and for subsequent discussions of it.

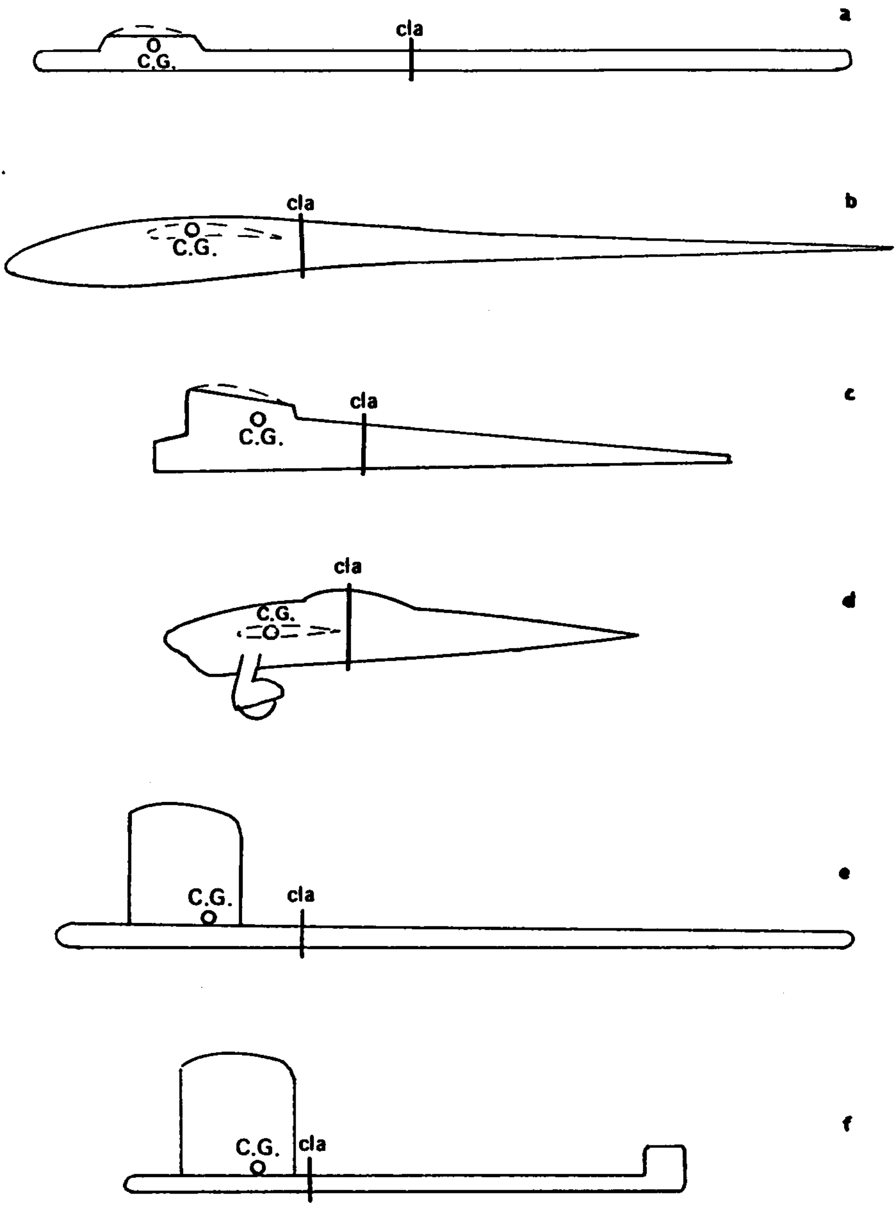

Fig. 12.14 The fallacy of the c.l.a. theory
Each of the models in this figure has the centre of lateral area aft of the centre of gravity even with c.g. well back in some cases. The theory suggests that fins are unnecessary, which is a fallacy.

experiments. The main principle is that fin and dihedral do need to be considered together. In practice, quite large variations in the size and disposition of the vertical tail areas are possible without greatly upsetting the control and handling of a radio controlled model.

12.26 DUTCH ROLL

If the fin area is too small and the dihedral large, a 'Dutch roll' or lateral oscillation results. The model, if disturbed by a side gust, tends to sideslip. The dihedral responds to this, as shown in Figure 12.15, by rolling the model against the sideslip, raising the 'into slip' wing. The fuselage, however, with too small a fin, tends to turn broadside to the flow. The initial small sideslip thus becomes a yaw increasing the slip combined with a roll away from it and the tendency increases until the wing may be rolled almost to the vertical

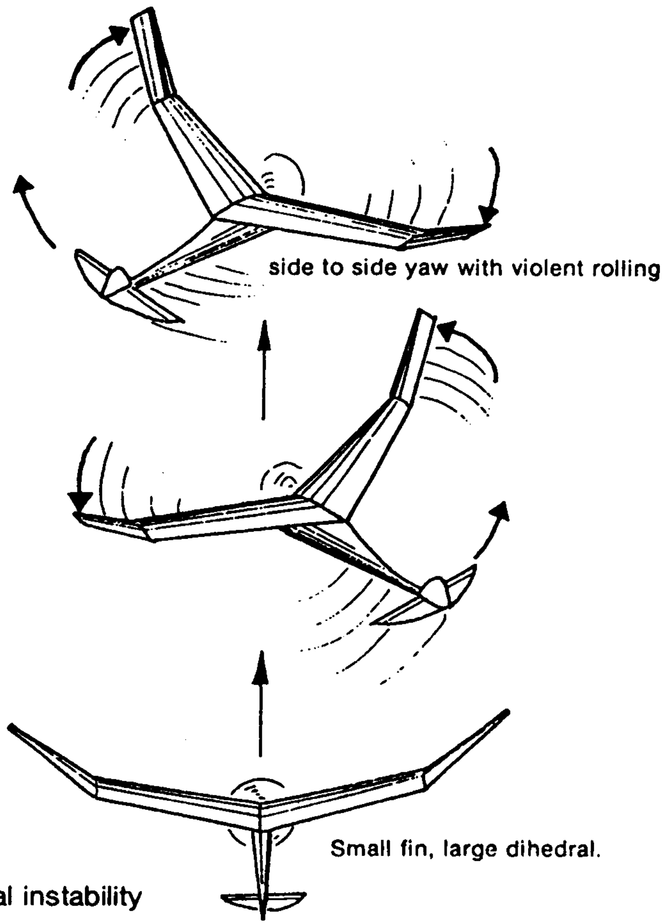

Fig. 12. 15
Dutch roll
or oscillatory lateral instability

while the fuselage is at a considerable angle to the original flight direction. In this state, the fuselage yawing force, having achieved a more broadside-on attitude weakens, but the model is steeply banked. The result is a return sideslip in the opposite direction. The dihedral responds to the change by rolling the wing back the other way, the fuselage attempts to turn broadside to the new slip direction and the model begins a wild oscillation from side to side rolling and yawing with the tail swinging wildly through an arc. The cure is to increase fin area or decrease dihedral, or both. The model with adequate fin power then yaws into sideslips, it has so-called weathercock stability. The dihedral, when the model is stable, is not so pronounced that it raises the into-slip wing very much. The model responds to a side gust with a mild yaw into the gust with only a very slight roll. The requirements for lateral oscillatory stability are thus large fin area with small dihedral.

12.27 SPIRAL INSTABILITY

Unfortunately, such a combination can lead to the converse of lateral instability, which is spiral instability. This arises if the fin area is too large relative to the dihedral. The initial small side-slip causes a strong weathercocking yaw. The dihedral, being slight, provides very small or no counter-rolling force, and the decrease of airspeed on the inner wing of the yaw causes that wing to drop. As mentioned in the next chapter, a similar effect arises when a model is yawed by means of the rudder control. With a spirally unstable model, the wing drop caused by the yaw is sufficiently sharp to increase the side-slip. The fin then attempts to weathercock the model further, and the wing drop again is too much and the sideslip continues, the bank angle increases and the model enters a turn which tends to tighten into a spiral. Since, as the angle of bank increases, the yaw relative to the ground becomes increasingly nose-down in direction, the spiral turn becomes a spiral dive at increasing airspeed, the bank angle approaches the vertical and the inertia loads on the wings rapidly multiply so that, if the model does not hit the ground first, the wings or tail are likely to break.

Fig. 12. 16 Spiral instability

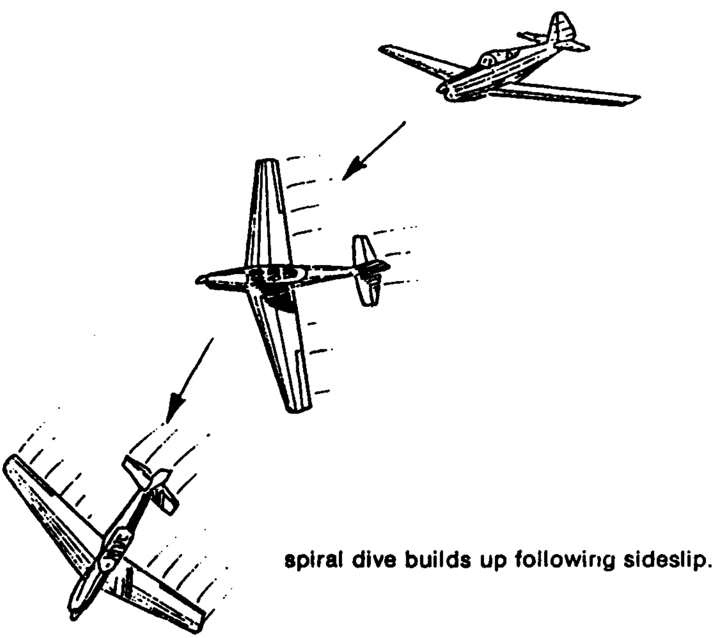

High powered duration models are particularly prone to spiral instability since they are usually trimmed for a spiral climb and it is very easy for such a climb to become a spiral dive. To prevent this, fins are small and dihedral large, even at the cost of some Dutch rolling tendency. Free flight gliders generally, while less critical in this respect, tend in the same direction since while the Dutch roll is unpleasant and inefficient, it is comparatively safe, whereas the spiral dive invariably leads to a broken model. Radio controlled models, however, are usually spirally unstable to some extent. As with full-sized aircraft, the early stages of a spiral dive are easily recognised and corrected, the dive does not build up immediately. As the nose begins to drop, a slight correction is given on the elevators, together with rudder and ailerons to check the yaw and roll. The Dutch roll, on the contrary, begins quite suddenly and, once started, is hard to stop because the pilot's reactions are likely to be slow. It is even possible for the correcting control movements to be in phase with the oscillations, tending to increase them rather than damp them out. The pilot recognises the yaw and roll a short time after they begin, and a moment later applies the controls to correct the condition. But by the time they take effect, the aircraft has already reached the limit of its swing in one direction, and the counter-movement in the other direction has begun. The pilot's effort then helps only to make the next swing more violent, and when, after a momentary delay he realises this and moves the controls the other way, the aeroplane has already passed through its maximum oscillation and again, the control movements make the condition worse. The pilot's best hope is to centralise the controls and wait in the hope that the model has enough natural stability (i.e. enough fin area) to damp down the oscillation of its own accord. Another technique which often succeeds is to move the elevator control forward for a faster flight speed. This changes the wing lift coefficient and hence the forces at work may be damped.

The designer's difficulties are increased by the fact that a model which is both spirally and laterally stable *at one airspeed* will not be so at all speeds. At high angles of attack spiral stability is very difficult to achieve. It requires generous dihedral on the wing, and quite small fin area, as on 'duration' models. At high speeds, however, the dihedral is too much and there is a tendency for such models to oscillate from side to side. The fin area needs to be larger to damp out oscillations. This tends to cause spiral instability. Fortunately, most models are designed mainly to fly at one speed, and a stable 'one speed' model is not impossible. For R.C. sailplanes, and powered duration models, which fly at varying speeds, there is no solution for all conditions. If the model is primarily a thermal soarer which will spend most of its flight time circling, effort should be concentrated on spiral stability – large dihedral with smallish fin. This will usually mean some tendency to wander and swing from side to side during 'penetration' glides or climb under power at high speeds. For the hill-soarer, long periods of circling flight are unusual, so spiral stability is less important. The fin area may be increased and dihedral reduced. Turns can be controlled carefully to check the tendency to develop a spiral dive. If control is by rudder only, however, dihedral must be quite large.

12.28 DIHEDRAL

A wing with no dihedral is neutrally stable in roll. Any roll which starts will be damped out, but there will be no tendency to correct the attitude of the model once the roll has been arrested. If one wing is down, it will stay down. Damping in roll has already been mentioned in Chapter 4 (see Fig. 5.9). As the wing rolls, the down-going wing meets the air at a greater angle of attack while the angle of attack of the up-going wing is reduced by the same amount. There arises an imbalance of lift on the two sides, which tends to bring the roll to a stop. Once the roll does cease, the angle of attack of each wing is the same, so no tendency to return to level flight is present. The model, canted over at an angle, sideslips.

It is sometimes suggested in the modelling press that dihedral operates to stabilise a model as indicated in Figure 12.17. In level flight the weight, acting vertically down, is supported by the vertical component of lift on the two wings. Since the wings are set at a dihedral angle, the actual lift force has to be resolved as shown, into a relatively large vertical force and a small horizontal component acting inwards. If the model is canted over by a gust, one wing tends more toward the horizontal position and the other is at a steeper angle. As the diagram shows, the vertical component of the lift on the down side is then larger and that on the higher side, smaller. A corrective restoring moment appears tending to roll the model back to level flight again.

Unfortunately, this explanation, although sufficing for small and momentary disturbances, is far from adequate. In a more complete explanation, not only the lift forces but the weight too must be resolved into one component acting at right angles to the axis of the aircraft, the other then slanting toward the down-wing side. This creates an unbalanced situation. As soon as any such banking occurs, the model will begin to sideslip towards the lower wing. The sideslip changes the angles of attack of the two wings differentially and it is this which provides the powerful, corrective rolling force of dihedral.

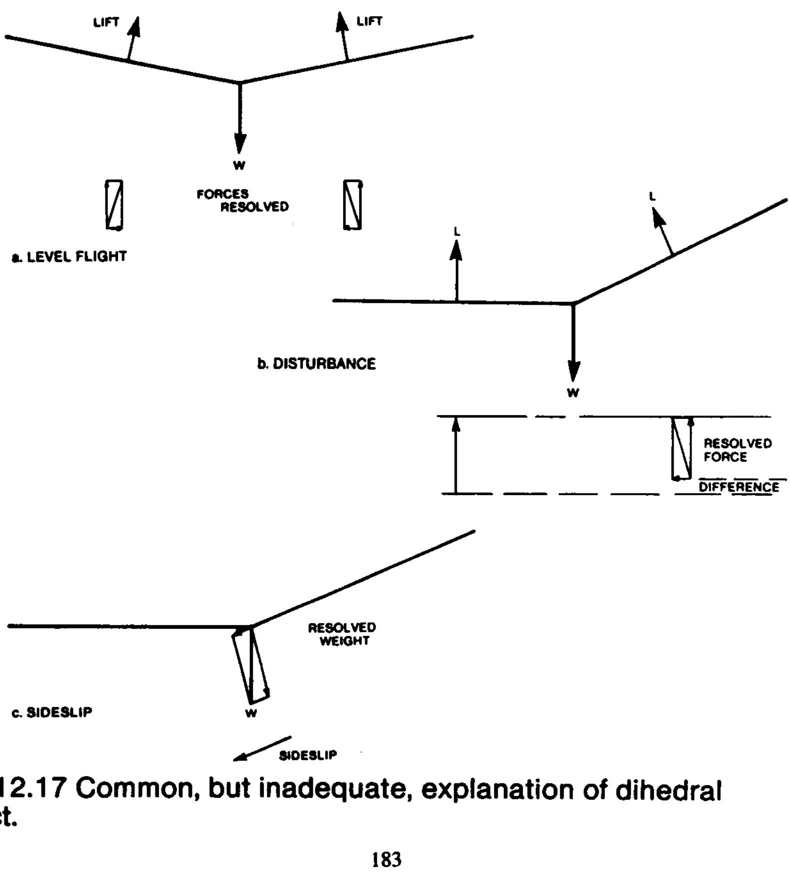

Fig. 12.17 Common, but inadequate, explanation of dihedral effect.

Figure 12.18 shows how, in a sideslip, the angle of attack of the into-slip wing is increased and that of the other decreased. The lift on the into-slip side increases and a rolling force appears. Any increase of lift coefficient on a wing also increases the strength of the vortex at the tip. Hence in a sideslip, the dihedral not only creates a strong rolling force to raise the into-slip wing, but a drag force also appears tending to yaw the aircraft towards the slip – a yaw one way, combined with a rolling force the other. Correction of the yaw depends mainly on the weathercock stability, which is why dihedral and fin areas are so closely coupled.

The yawing effect of dihedral in slipping or skidding is similar to the adverse yaw of ailerons, which will be discussed below (Chapter 13).

12.29 RUDDER-STEERED MODELS

Models which rely for directional control on the rudder only, without ailerons, rely on the dihedral to turn. Insufficient dihedral may cause lack of turning power even with a large rudder. The rudder yaws the aircraft, thus causing the wing on one side to present a larger angle of attack, and the dihedral rolls the aircraft into a banked position. The total lift force of the whole wing is then tilted and this force, not the rudder, turns the aircraft. With well matched vertical tail areas and dihedral angles, the model turns quite efficiently since the brief yaw at the start is promptly countered by the roll. Once the turn is established, there should be little of no slip or skid with a suitable angle of bank. Flat, skidding turns are very inefficient.

12.30 AILERONS AND DIHEDRAL

With ailerons, the amount of dihedral required for radio controlled models is quite small, and for aerobatics none at all.

Figure 12.18 shows that too large a dihedral angle reduces the efficiency of a wing. The drag force will be no less, but because of the inclination of the wing, a component of the lift is directed horizontally. The true wing area is represented by the vertical projection in plan, rather than by the length of the wing span as the model is built on the building board. Only the minimum dihedral needed for stability should be used. For free flight models and thermal soaring R.C. gliders, it is advantageous to employ polyhedral. The steeper dihedral of the outer wing panels is more effective, due to their greater leverage arm from the model centre line. Polyhedral is a means of reducing the total dihedral of the wing compared with a straight wing model. To achieve the same effect with a straight dihedral requires a greater average dihedral angle. As with planform, an elliptical dihedral form is theoretically best, but although models have been built in this style, the gain in efficiency is very slight and there is considerable difficulty in laying out such a form on the building board. Extreme forms of dihedral should always be avoided since they promote cross flows on the wing and create vortices, increasing drag. It is also possible to have so much dihedral that turning becomes impossible.

12.31 SPINNING

Spinning is caused by stalling of the main wing in an asymmetrical fashion as shown in Figure 12.19. In a fully developed spin, the whole wing is stalled but one side is further beyond the stalling angle than the other, which causes that wing to drop and 'auto-rotation' of the model follows with a high rate of descent. To recover, the rotation must be stopped and the wing unstalled, usually requiring both elevator and fin or rudder action. Models differ widely in their spin characteristics and some cannot be made to spin at all.

Fig. 12.18 Dihedral

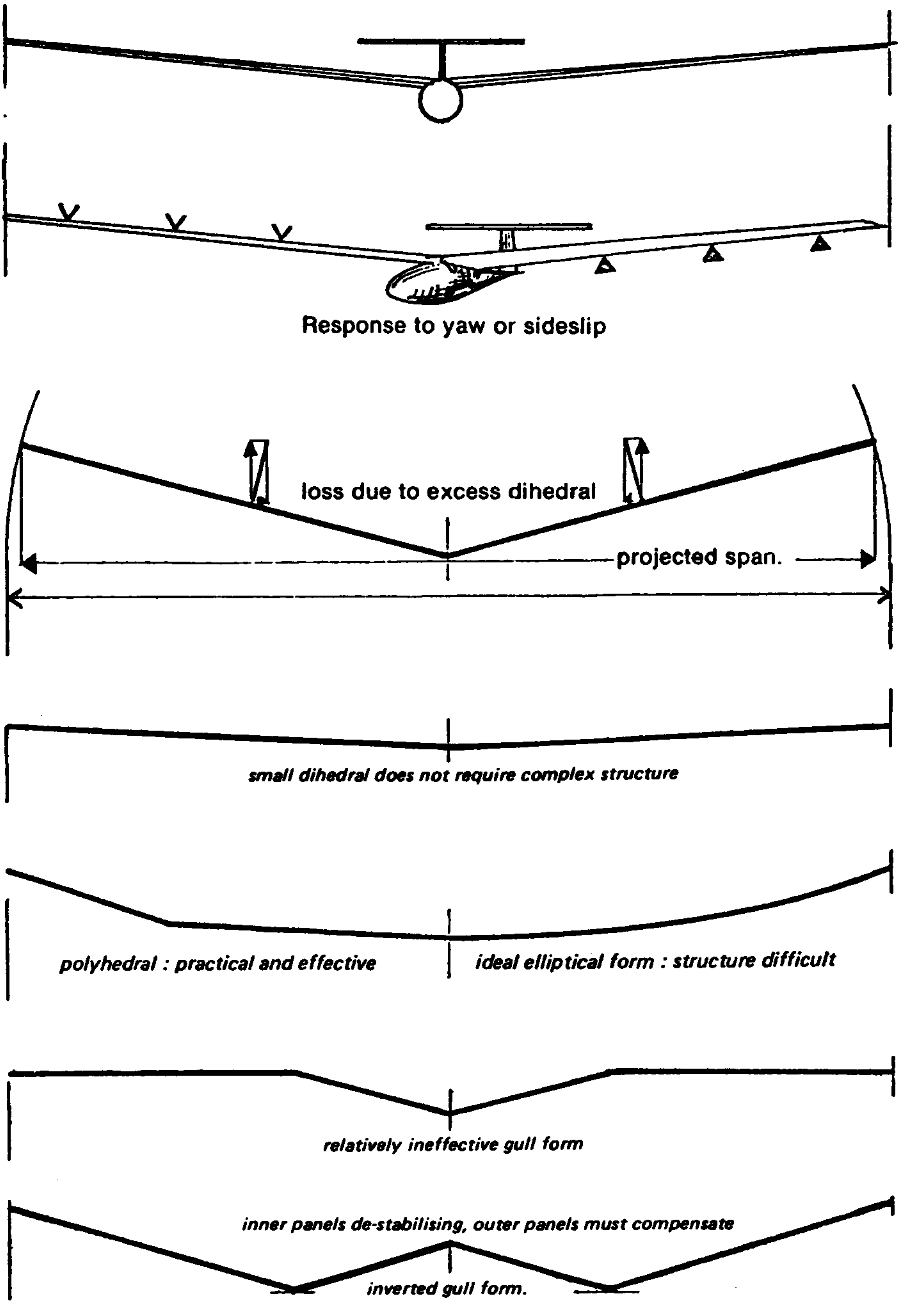

These are usually models with large fin areas and centre of gravity well forward. Wings with generous tip chords and washout are less likely to drop a wing when stalling, and so are less likely to enter a spin. For aerobatics, strongly tapered wings without washout and small fins promote entry to spins and a rearward c.g. will help to maintain the spin. Of course these features, if overdone, may also prevent recovery. If the c.g. is too far aft, a 'flat spin' may result, with no possibility of recovery.

If, during a spin, the rudder and fin are blanketed by the disturbed flow over the tailplane, recovery may be impossible. The rudder as far as possible should be mounted below the tailplane or in one of the positions suggested in Figure 12.19. A fully aerobatic model may be required to spin inverted. In this case the rudder might be disposed equally above and below the tailplane and if possible ahead of it or well behind. A low aspect ratio fin, as mentioned in Chapter 5, is desirable for spin recovery.

The position of ailerons in spinning, and in entry and recovery, will vary from model to model. In some cases entry to the spin is aided by ailerons applied against the intended direction of spin. This increases the aerodynamic angle of attack on the 'down' aileron side and since a cambered aerofoil reaches its stalling angle sooner (see Fig. 7.4 and 13.2) this wing may stall first and initiate the spin. In other cases, especially with broad chord wing tips, the ailerons continue to work in their normal sense even beyond the stall, in which case aileron opposed to the spin direction may prevent entry or even precipitate spinning the other way. The same applies during recovery. No general rule can be laid down, each model must be investigated and the best procedures found.

12.32 POWER-ON BALANCE

So far both stability and balance have been discussed without reference to the effects of power. In longitudinal balance, the position of the thrust line relative to the model's aerodynamic centre is of some importance. If the thrust line is relatively high or low a pitching moment arises which must, as a rule, be balanced by the tailplane. At the same time, the slipstream over the tail changes its lifting power for a given C_L, since the velocity of flow over it is greater. In a steep climb, the weight force still acts vertically down while the lift force of the wing is at right angles to the line of flight, which changes the balance to some extent if the c.g. is fairly low relative to the aerodynamic centre. The resulting, complex force system for a typical 'pylon' duration power model is sketched in Fig. 12.20. The trim of such a model is highly sensitive to small changes of power. A safer arrangement, if the model has variable camber and trim, and can be made to climb straight, is sketched in the lower part of Figure 12.20. Here it is supposed that the tail is symmetrical and at zero angle of attack relative to the downwash from the mainplane. The thrust line is directed through the model's aerodynamic centre and the c.g. also is close to the thrust line, though still ahead of the neutral point. The increased velocity of the slipstream over the tailplane, at zero angle of attack, creates no increase of pitching moment from that source. The tail becomes a stabiliser. The thrust line and drag create no pitching moment. The wing pitching moment is small because the camber is reduced (flaps up) during the climbing phase of flight. In practice no doubt this arrangement will not be attained exactly since some compromise with the requirements of glide trim and stability will still be needed, and the pitching moment coefficient will increase when the flaps go down at the end of the power run. In general, however, the climb of such a model should be less difficult to control, especially since no steep turning is required. Note that dihedral raises the centre of drag.

The speed of the slipstream over the tail of a radio controlled model changes the effectiveness of the controls so that rudder and elevator which are sensitive when power is full may become insufficient for control on the glide. There is little hope of real escape

Fig. 12.19 Spinning

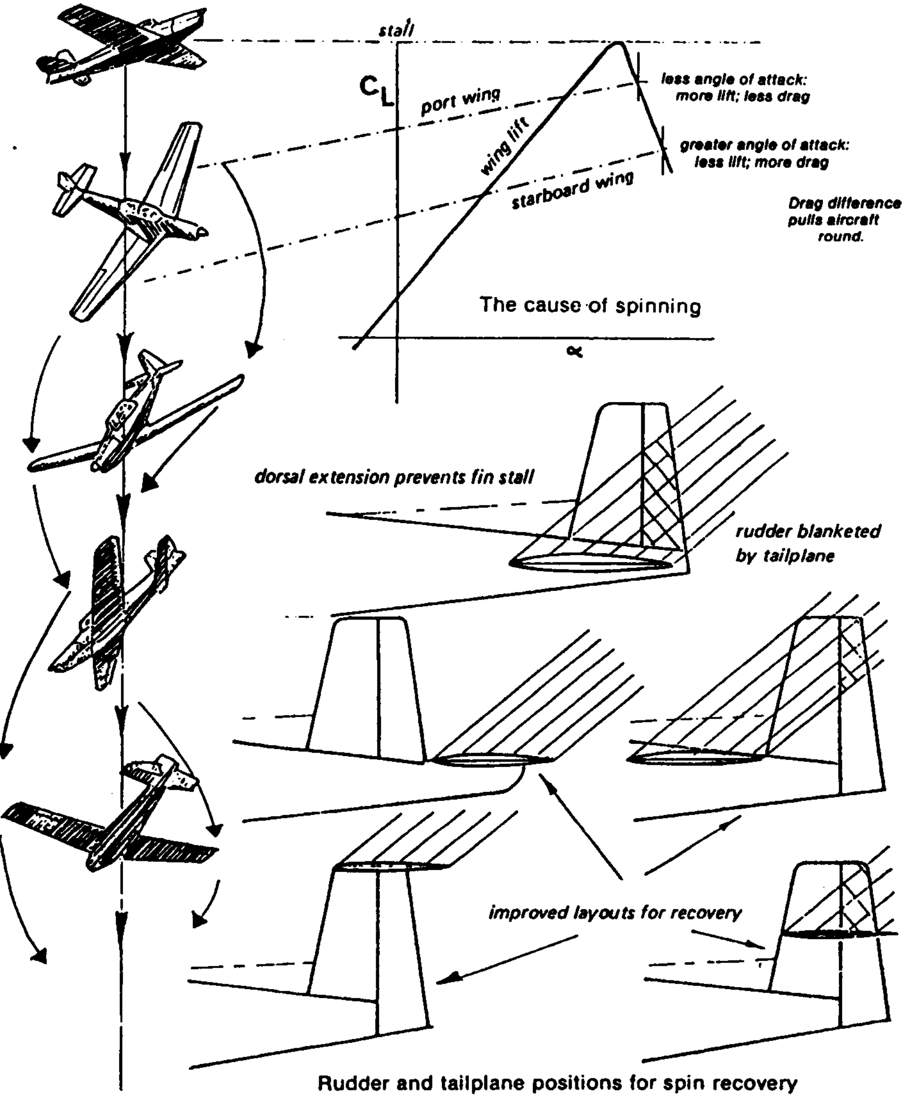

Rudder and tailplane positions for spin recovery

from this difficulty, but a satisfactory compromise is usually attainable.

The fact that the slipstream rotates may cause a model to swing on take off, since the flow over the fin and rudder is at an angle. This effect is more important than the torque of the propeller, which is a force tending, in the first instance to rotate the model in roll about the propeller shaft axis, rather than to turn or yaw it. A bank induced by torque, of course, will lead to a turn if uncorrected, in the air. Such a rolling tendency can, on the ground, cause a swing because unequal load is thrown onto the undercarriage, but in flight the natural way to control torque is by a counter rolling force from the wing, either a slight twist in the appropriate direction, or by means of a trim tab or aileron. In a power model climbing straight, this will probably be essential. The slipstream effect on the rudder may be controlled by 'side thrust' i.e. inclining the propeller shaft slightly to the fuselage datum line. This has the advantage that the correction operates only while the power is on, and does not affect the glide trim. In full-sized practice, the rudder is trimmed at various angles to give the same effect, or the whole fin is cambered slightly to give a constant anti-yaw effect. Downthrust, as already mentioned, is often valuable to adjust the thrust line for longitudinal balance, and as before, the effect disappears when the motor cuts, so the glide trim is unaffected. Radio controlled models may imitate full-sized methods by trimming the controls appropriately for various flight conditions.

12.33 'POWER-ON' STABILITY

As mentioned before, to achieve balance in flight does not imply stability. When power is on, the stability equations also vary, generally making the model less stable because the propeller acts as a small forewing in front of the fuselage. The more power the propeller is applying to the air, the more destabilising its effects. Fortunately, this can usually be catered for by a slight increase in the static margin, but variations of torque when power is applied suddenly or reduced are less easy to trim out. In particular, when opening the throttle in order to 'go round again' after an aborted landing, the ailerons and rudder of a model are operating in low speed airflows and lose some effectiveness, while the sharp increase in the torque rolling force can be quite large. This is a common cause of accidents.

It is less well known that a high thrust line is more favourable for pitch stability than a low one. Hence, although the trimming arrangements will differ for the power-on and power-off conditions, because the balance of forces is different, once trimmed the high thrust line aircraft will be slightly more stable under power than when gliding.

This effect is offset to some extent by the propeller destabilising forces, but the combination of high power and low thrust line is unfavourable for stability in both respects, whereas high thrust line and propeller effects tend to cancel each other out to some extent.

12.34 SAILPLANES ON THE TOWLINE

Somewhat analogous to the stability and balance problems of powered models are the conditions prevailing when a glider is on tow. The force of the towline creates a pitching moment which must be balanced by the tailplane, and the speed of flight on tow, especially in the early stages, is greater than normal, so the model is more sensitive. A rudder tab setting just sufficient to cause a gentle turn on the glide may cause a violent yaw on tow, which explains why 'auto-rudders' are needed for free flight sailplanes. If a model has stability problems on the glide, it will almost certainly behave worse under tow. As usual, a good deal of experiment and trial is needed for consistent results. A further effect to be guarded against is the distortion of wings and slender fuselages during the tow, due to the combination of extra load from the line and additional speed. A model which is perfectly satisfactory on the glide may become uncontrollable on tow if the wings twist differentially or if a slight warp is present. These effects too, are mainly matters for practical solution by means of stiffer structures and more accurate constructional methods.

Sometimes when being launched by towline or winch, a sailplane will begin to swing from side to side more or less violently and may go so far over to one side that it turns

Fig. 12.20 Balance of forces on a climbing power model

Moments about aerodynamic centre

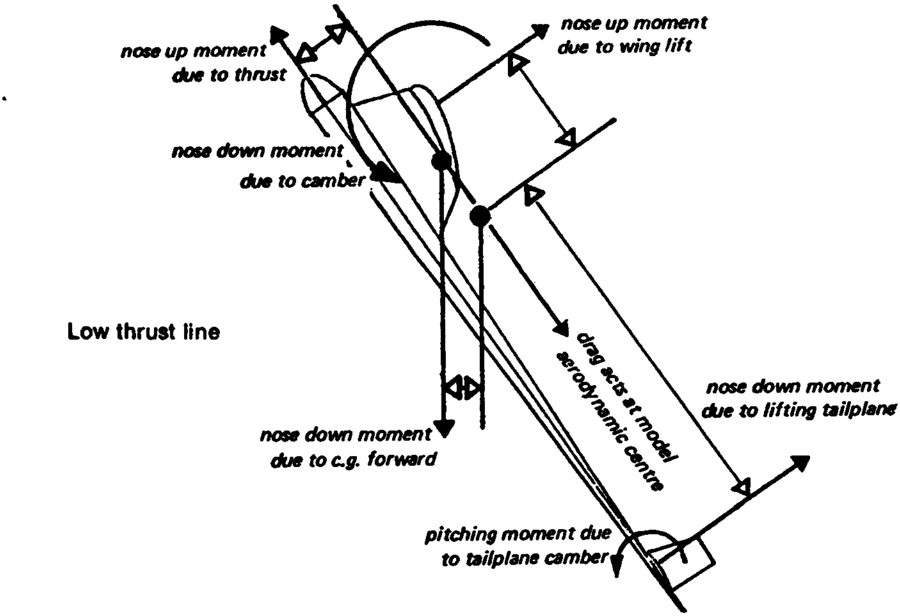

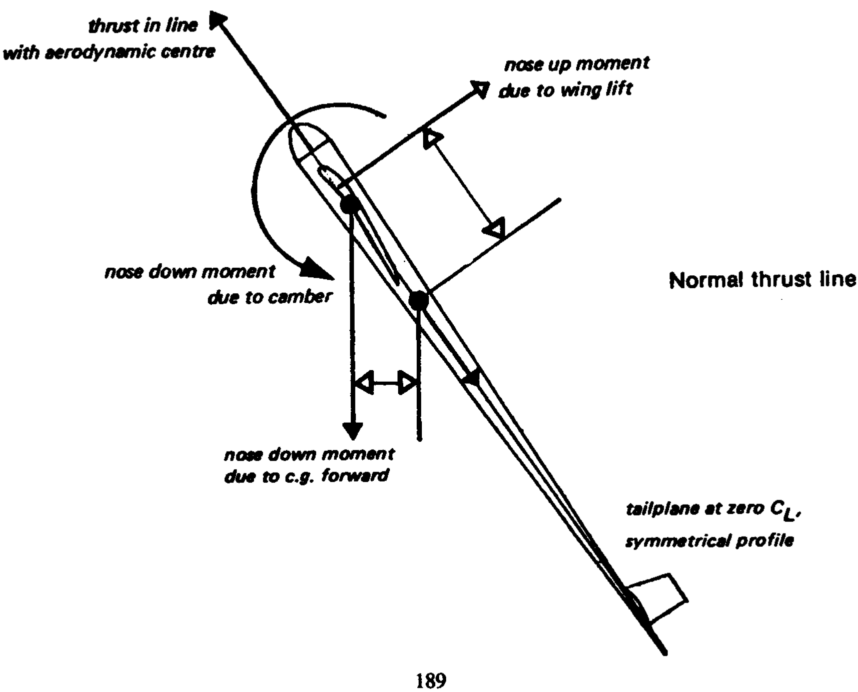

through 180 degrees and either comes off the line or crashes heavily. The immediate solution in practice is to trim the elevator slightly down reducing the angle of attack of the mainplane. This is not possible with a free flight model, of course, but the basic cause is a wing operating at high lift coefficient. The position of the towhook too far forward may be a contributory factor.

As mentioned above, it is very difficult to achieve both spiral and weathercock lateral stability for all airspeeds and loading conditions. This tends to show up when a model is being pulled hard and fast by towline. Reducing the angle of attack changes the relationships of the wing, fin and dihedral-induced yaw and at the same time reduces the tension in the line.

Free flight sailplanes are usually towed fast and, after some time in the commonly practised 'circular' tow configuration while searching for lift, are pulled hard to increase airspeed then released with the line under tension, to gain some additional height. This tends to send them into a stall, with loss of height, and if stability is not good, they may not recover at all. Much ingenuity has been put into designing towhooks for the circular tow. If some similar efforts were directed to elevator trim for adjusting to line tension, the problem might disappear.

Although wing tip stalling can happen on tow, it is very much less common than the side-to-side oscillation mentioned above which is not a tip-stall problem.

13
Control

13.1

Like full-sized aircraft, radio controlled models rely mainly on hinged or pivoted control surfaces which alter, at the pilot's command, the lift, drag and pitching forces to bring about a change of the aircraft's attitude and hence its speed, rate of turn or pitch rotation, etc. The power output is controlled by the motor throttle. As the general principles of Chapter 1 and 2 show, an increase or decrease of thrust without any control surface movement will change the model's attitude. For level flight, at different power settings, re-trimming is also required.

13.2 ELEVATORS

The simplest control surface is the elevator. Wind tunnel tests carried out at Stuttgart by D. Althaus on Wortmann tailplane profiles show the effect of various angular deflections of an elevator, on both the lift and drag curves, and for different sizes of hinged surface, 20% and 30% wide in terms of the chord of the whole tailplane (Fig. 13.1). The effect of a rudder on a vertical fin is of course identical. As indicated in Chapter 6, the deflection of such a surface over small angles does not change the slope of the lift curve, but moves it upwards and to the left (the elevator moving down). The c_l max. increases, but the stalling angle measured geometrically *decreases* exactly as with a cambered aerofoil. At elevator deflections of more than 15 degrees, however, the curves show irregularities indicative of flow separation, and at the same time the drag curves show a sharp rise. As with the ordinary aerofoil section, increasing camber shifts the drag curve to higher c_l positions. This is quite important since it indicates that an elevator which is trimmed to a small deflection to balance the model in flight will not necessarily generate more profile drag than when it is neutral. However, the tailplane as a whole will, in this position, probably be exerting a lifting force either upwards or downwards, and this will generate some induced drag. The wind tunnel tests also show the effect of increasing the chord of the control surface. The movement of an elevator from neutral to 10 degrees deflection with a 20% wide proportion raises c_l by approximately 0.46. Increasing the flap chord to 30% increases the effect only a very little more to about 0.47 (Fig. 13.1). The increase of control surface chord improves its effectiveness only very slightly, but the loads placed on the controlling servo motor in a model are considerably greater. The operator on the ground should be aware that any broad chord surfaces on his model are quite probably causing problems. Sometimes the control rods may bend or the model's structure distort slightly under such loads, with the result that the actual effectiveness of the broad surface

Fig. 13.1 The effect of hinged control surfaces

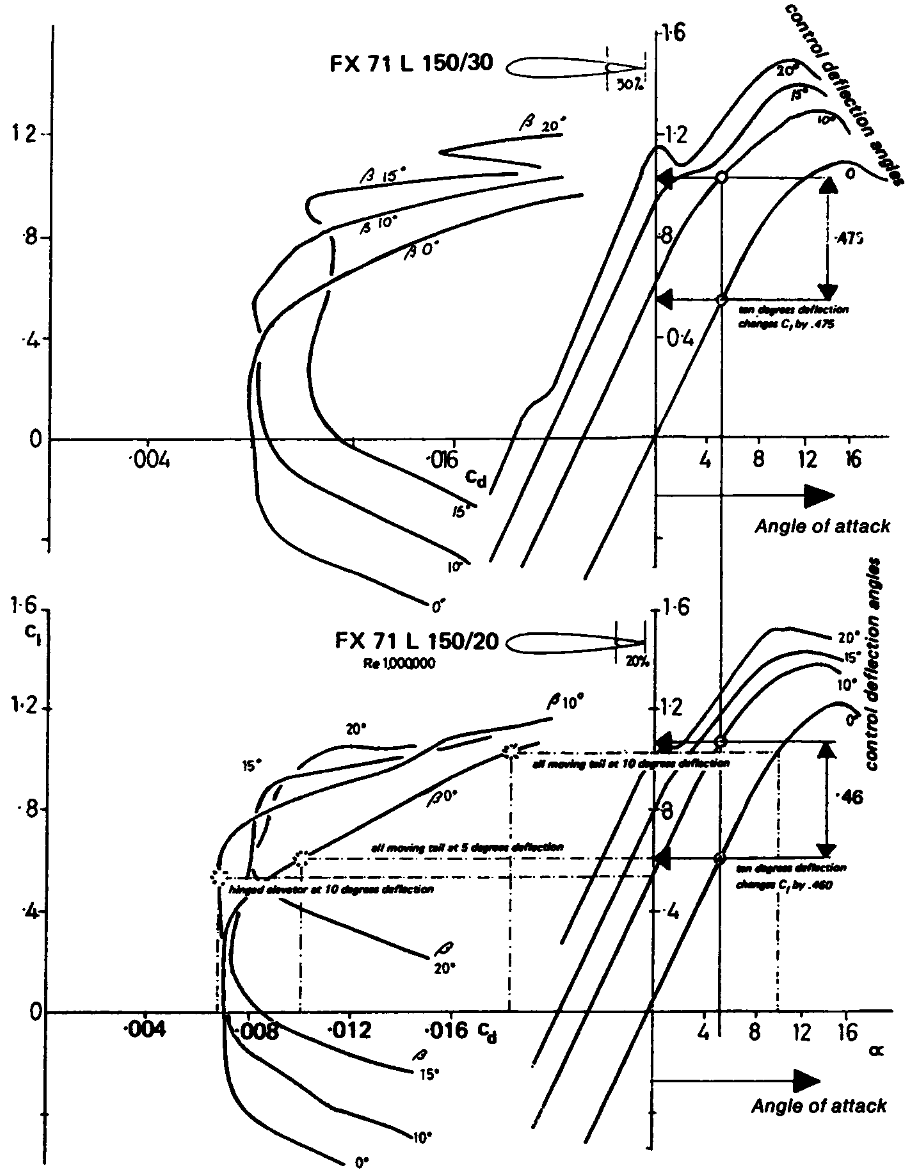

Note: angles of attack are measured relative to the chord line of the aerofoil with zero control deflection. Deflection of the hinged surface cambers it and the aerodynamic zero moves to the negative geometric side.

is reduced. The same principles are even more valid for ailerons on both symmetrical and cambered wings: the effectiveness of the surface is increased only slightly by broadening, but the loads on the servo are greatly magnified. If an increase of area is essential, it should if possible be achieved by increasing the spanwise extent of the hinged flap, rather than its chord. The camber of more wing surface will then be changed, with magnified effect at small cost in servo load.

The wind tunnel tests of Figure 13.1 are not, unfortunately, at low enough Re for most models. They illustrate correctly the general principles involved. They are fully valid for fast models which operate close to Re 700,000 with symmetrical or near symmetrical wing profiles. The Wortmann profiles in the 71-L-150 series (ordinates given in Appendix 3) are specifically designed for tailplanes and rudders, to give low drag when the control surface is deflected. They may be useful on aerobatic models with symmetrical wings and full-span ailerons. The aerofoils are carefully designed for use with a specific flap or elevator chord, 20, 25 or 30% as indicated by the last two figures of the aerofoil designation. This should not be changed.

13.3 THE ALL-MOVING TAILPLANE

The all-moving tailplane, or 'pendulum' elevator, is sometimes thought to have aerodynamic advantages over the orthodox hinged elevator and fixed tailplane. Its effectiveness or sensitivity is greater for each degree of deflection. This may be established by comparing the change in c_l of a symmetrical profile deflected ten degrees with that of an elevator deflected the same amount, i.e. in Figure 13.1, by comparing the lift curve of the basic profile with the curve for 10 degrees elevator. Changing the angle of attack of the symmetrical section ten degrees takes the curve up to c_l about 1.1, compared with a ten degree elevator effect of about 0.5 or 0.6. However, this same ten degree angle of deflection increases the profile drag of the 'pendulum' elevator by more than twice, since it moves out of the 'low drag bucket'. The hinged flap changes the camber and so shifts the drag curve favourably, for small angles of deflection. Since the pendulum elevator is more effective, it can achieve the same result by moving through a small angle. If, for example, the symmetrical profile is shifted to an angle of attack about 5 degrees, it will be as effective as a hinged flap at 10 degrees. Even this small movement takes the symmetrical profile out of the low drag range, which is quite narrow on the thin aerofoils normally used for tailplanes. However, this increase of drag lasts only while the control is effecting a change of attitude. Once settled down in a new flight trim, as discussed in Chapter 12, the tailplane load will depend on the centre of gravity position and the static margin. Usually the load will be downwards, on a stable model. Then the hinged elevator-tailplane combination, with elevator down, is cambered the wrong way. This may take the tail out of the low drag range, whereas an all-moving, symmetrical tailplane may remain within the 'bucket'. Better still, perhaps, an all moving tail with *negative* camber should produce less profile drag, on average. Such effects are small for normal aircraft since tail deflections required for trim are not large.

By careful siting of the pivot point, the symmetrical pendulum elevator may be made to throw no loads at all on the servo. Since symmetrical profiles have no pitching moment about their quarter chord point, the pivot may be sited there and the servo then has only the function of overcoming friction forces and holding the elevator in position. Full-sized sailplanes which have pendulum elevators usually have swept back tails combined with a very slight camber in order to give the pilot some aerodynamic feel in the control column. Alternatively, counter-balance tabs may be fitted. For models these are entirely superfluous and should not be imitated, except of course for exact scale types. 'Overbalancing' the all moving elevator, by pivoting it aft of the aerodynamic centre, is a somewhat risky matter, though it is sometimes done. The elevator may even be used to help drive coupled flaps, reducing the combined control loads. This requires special attention to pivot bearings and push rod stiffness.

A further consideration with the all-moving tail is the difficulty of preventing gaps and aerodynamic traps where the tailplane joins the fuselage or fin. If the elevator is pivoted on the side of the fuselage or fin a gap at the root is almost inevitable. This source of parasite drag is very diffictul to seal. If a 'T' tail is used, the all-moving tailplane may be built in one piece but then the problem of mounting it neatly on the top of the fin arises. Very few installations are as tidy, from the aerodynamic point of view, as fixed tailplane and simple hinged elevator may be. It should go without saying that the elevator hinge line on an orthodox layout should be well designed to conform with the aerofoil, and sealed against leakages from bottom surface to top or vice versa.

13.4 FLAPS AND AILERONS

The function of the elevator is to control the angle of attack of the wing. The wing itself may have flaps or variable camber, which can assist, oppose, or even supplant the elevator. In a well-designed model if the wing flaps are lowered, this increases the camber and simultaneously alters the geometric angle of incidence, measured from the flap trailing edge. The increase of camber causes an increase of the nose-down pitching force but, at the same time, the lift coefficient will rise, increasing downwash on the tail, tending to raise the nose. When the model settles down into a new equilibrium, it will be at a lower airspeed, but it may have only a slightly nose down or nose up attitude depending on the precise balance of flap angle, pitching moment and downwash. If, then, the elevator is

Fig. 13.2 The effect of hinged control surfaces

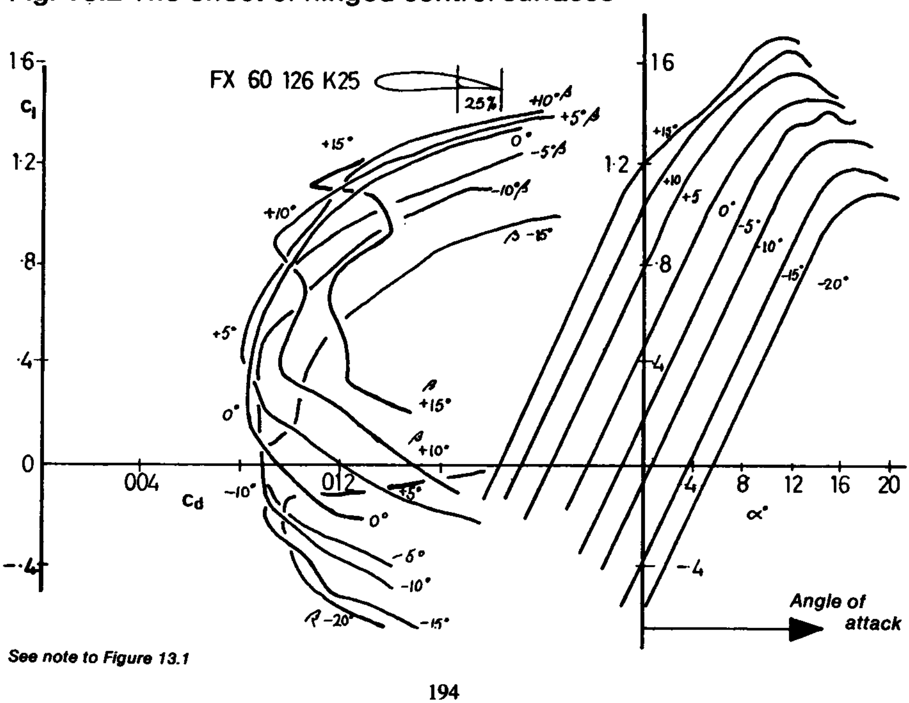

See note to Figure 13.1

moved up, the airspeed will fall still further in the normal manner, but because of the greater camber with flaps down, the stall will come at a lower geometric angle of attack. Flap movement in the opposite sense has the reverse effects – c_l falls, the pitching moment is reduced but so is downwash. Speed rises without much change of attitude. Depression of the elevator will lead to a further increase in airspeed. Some models, particularly control line aerobatic types, have been built with elevators and flaps coupled. The advantage of this system is mainly the quick response of such a model to control movements, allowing 'square cornered' looping manoeuvres to be performed. The elevator must be powerful enough to overcome the adverse increased pitching moment as the flaps go down. Then the wing C_L rises very sharply and momentarily the total lift force exceeds the weight of the model, the speed not having had time to fall off. The excess lift accelerates the model in the desired direction and the elevator simultaneously rotates it into the new position. Radio controlled models find similar coupling useful.

As Figure 13.2 shows, the general effects of hinged flaps or ailerons fitted to a cambered wing are almost the same as those of a symmetrical profile similarly fitted. The only important difference is that the cambered zero flap setting has a negative zero lift or 'absolute zero' angle of attack. Otherwise, as before, increasing camber raises the lift curve to the left, decreasing camber moves it down to the right. The drag curve shift is also as expected. The wind tunnel results given here are again at a Reynolds number too high for any models likely to employ such a cambered profile, but the general principles are not affected.

As shown in Figure 7.8 (Chapter 7) a model in a turn must bank in order that a sideways force can be produced by the wing lift, to balance the outward inertia force against the turn. Banking is accomplished normally by the action of the ailerons aided by the rudder of a model. The operation of ailerons can be understood from Fig. 7.6. As one aileron goes up, the other goes down, creating an imbalance of the lift forces on the wings, and the model rolls. The rolling movement is damped as described in Chapter 5, by the change in angle of attack on the up and down moving wings, so in a steady roll, the damping forces are exactly balanced and equalled by the imbalance caused by the ailerons. To achieve a fast rate of roll, powerful ailerons are required, together with small damping, which implies small wing span with ailerons occupying up to 80% of the trailing edge of the wing. As Figure 13.1 showed, increasing the chord of a control surface increases its effect only slightly, but extending it along the span allows it to change the camber over most of the wing, rather than only near the tips, and this is by far the best way of improving aileron control. Ailerons, however, should not be reduced in chord too far. They work in the area where the boundary layer is thick, and very narrow surfaces, or 'strip' ailerons suspended behind the trailing edge proper, may be blanketed and hence ineffective. It is probably best not to extend them all the way into the wing tip vortex, or completely to the wing root.

13.5 ADVERSE AILERON DRAG

It is apparent from Figure 13.1 also that an aerobatic model with a symmetrical wing profile will hardly suffer from any adverse drag effects of aileron applications. The profile drag curve moves with the aileron, so, contrary to many statements in articles hitherto, there is no increase of *profile* drag caused by the downgoing aileron, and no decrease on the other side. There is, however, an increase in c_l on one side and a decrease on the other. This does cause a variation of the *vortex-induced* drag, more lift on the rising wing creates an induced drag force tending to slow that wing down, while on the downgoing side, less lift creates less induced drag, tending to speed that wing up. A high speed model with a symmetrical profile will normally be operating at a low C_L in the first place, and induced

Fig. 13.3 Aileron drag

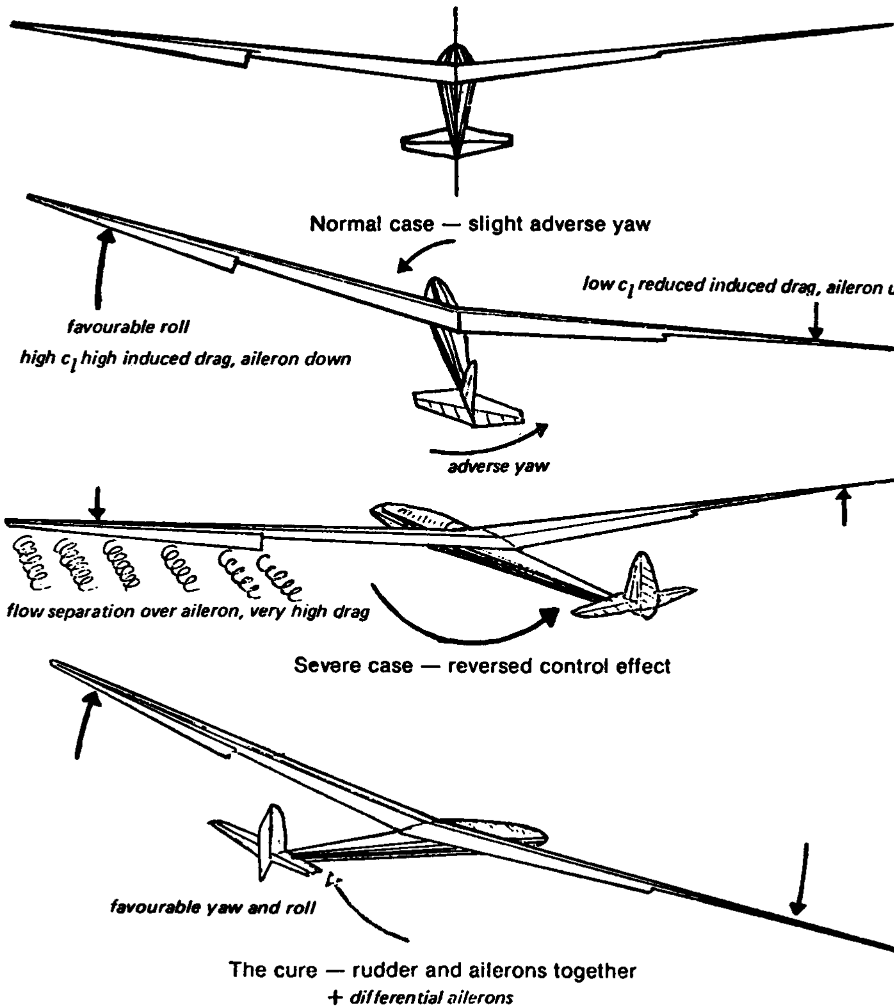

drag, as shown in Fig. 4.9, is small at high speeds and low angles of attack. It is possible to ignore the 'adverse yaw' effect of ailerons alone. If a slight adverse yaw is noticeable, when flying slowly, it can be corrected by use of the rudder, but for normal aerobatic flying, and on racing models, ailerons are the essential turning controls and rudder is employed mainly to counteract yaw due to slipstream effects. Exactly the same applies with full-sized, fast light aeroplanes.

At low speeds and especially on sailplanes with large span, induced drag is dominant and the adverse drag caused by ailerons is serious. As the aileron on one side moves down the local c_l, already high because the model is flying slowly, rises still more, and the induced drag increases sharply on that side, tending to yaw the model against the desired direction of turn. On the other side, the c_l drops, induced drag falls, which aids the adverse yaw (Fig. 13.3). If the model is operating close to the edge of the wing profile's low drag 'bucket', it is quite likely that this increase of induced drag on the upward moving wing (down-aileron side) will be supplemented by an increase of profile drag, caused by flow separation over the aileron. This will be particularly likely if the ailerons are badly designed with a clumsy hinge line, or gaps promoting flow breakaway. In extreme cases the adverse yaw caused by the ailerons may be so severe that it overcomes the rolling effect due to the lift imbalance. The model in such a case will yaw violently away from the turn, the slow moving wing with aileron down may actually develop less lift than the fast moving one with aileron up (lift force depends on airspeed), and the turn will be the opposite of that desired by the pilot. Some very early types of full-sized sailplane suffered from this effect at low speeds, while at high speeds the torsional flexibility of their wings also rendered ailerons ineffective. Only within a narrow speed range between did the ailerons work. Some model sailplanes suffer from similar troubles. On a sailplane at low speed, it is essential to use the rudder with ailerons to initiate a turn. There is an excellent case for coupling of ailerons and rudder, the adverse yaw of the ailerons being countered by simultaneous application of rudder. Modern radio control equipment makes such coupling very easy and it may be switched in or out as required, in flight.

As a rule, some elevator action to control flying speed is necessary. In any turn, some of the wing lift force is directed horizontally, but the model's weight must still be balanced by the *vertical* lift component (Fig. 7.8). This requires either an increase of speed or the wing must operate at a higher C_L, and hence a higher angle of attack, than in level flight. Since a soaring sailplane is likely to be operating already close to the stalling angle, it is necessary to increase the flight speed in a turn to avoid a 'wing drop' caused by the inner wing in the turn stalling. This implies a steeper glide angle in the turn, and a higher sinking speed. The steeper the turn, the greater the loss of efficiency. In thermal soaring, since the model must turn to remain in the thermal, some penalty in performance has to be accepted. In hill soaring, the loss is small and in good or moderate conditions is hardly noticeable. However, in weak lift, the height lost on turns may be just enough to make soaring impossible. In such conditions it is common to find small patches of better 'lift' here and there along the slope, with weak or even nil lift between. If the turns are made in the better spots, not only is the increased sinking speed in the turn more likely to be overcome, but the model remains in the rising air longer than if it were allowed to fly straight through it. The 'beat' worked on such a day, if possible, should thus begin and end in rising air, with straight flight between through weaker areas (Fig. 13.4). Note that all turns must be correctly banked. A flat, skidding turn creates excessive drag and increases sinking speed.

Once in the turn, a model with spiral stability will continue to turn with centralised controls until brought straight again by opposite aileron and rudder. This is a desirable

Fig. 13.4 Hill soaring in weak lift

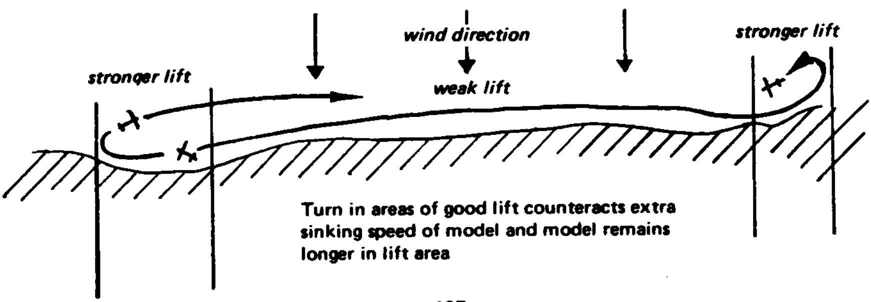

Fig. 13.5 Control linkage for differential ailerons

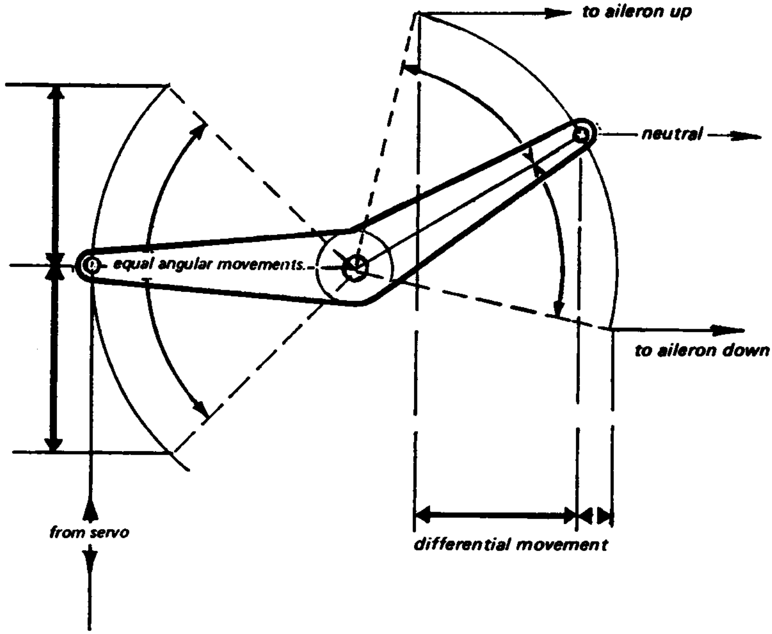

state of affairs but may require various adjustments of dihedral angle, fin area, and gearing of rudder and ailerons, before being achieved. 'Holding off' excess bank with ailerons is usually necessary to some extent with large span aircraft.

Some reduction of the adverse aileron yaw effect can be achieved by gearing the ailerons differentially. This is easily done by arranging bell cranks in the control circuit as shown in Figure 13.5 or by electronic means. The down-going movement will be less than the upward deflection, so the bulk of the rolling effect will come from the reduction of lift on the wing inside the turn. Differential ailerons cannot altogether overcome adverse yaw. The rudder is still essential for a clean turning action. Other devices, such as the Frise aileron (Fig. 13.9) or spoilers which open on one side as the aileron on that side goes up, are effective but cause increased drag and should be adopted only if all else fails.

The disadvantage of mechanical coupling of ailerons and rudder is that some special manoeuvres such as sideslips, in which the model is deliberately yawed away from the down-going wing to increase fuselage drag (so descending faster without increase of airspeed), cannot be performed. On rare occasions it may also be more difficult to enter and recover from spin, because the aileron deflection changes the stalling angle of the wing tips. In aerobatics, rolls are often accomplished by ailerons and rudder working independently.

13.6 THE PYLON RACER IN TURNS

Racing models need to turn efficiently at very high speeds. This is done by banking with ailerons and bringing the banked wing to a high angle of attack by applying up elevator. It is the wing lift, directed sideways, that turns the model. Too much up elevator can bring the wing to its stalling angle and precipitate a crash.

In a turn, since the wing is necessarily at a higher C_L than in level flight, wing vortex drag increases and the model loses speed. This loss is unavoidable. To attempt to turn with insufficient bank produces very high drag and even greater slowing down in a wide, skidding and yawing turn.

13.7 THE RUDDER-STEERED MODEL

Many model sailplanes, and some elementary powered models, are turned by the rudder alone with no ailerons. This, as mentioned in the previous chapter, requires the wings to be set at a dihedral angle. The yaw induced by the rudder increases the angle of attack of the wing on the side pointing into the resulting side-slip, and this wing rises. The resulting bank produces the turning force. Compared with the well executed aileron-plus-rudder turn, this control system is less efficient in that the initial yaw and slip creates some drag, but with a well trimmed model, once the turn is established little if any control deflection is needed to maintain it. When the span is large, the rudder action may be somewhat slow, but providing no rapid turns are required, as may usually be the case with thermal soarers, the 'rudder only' control may be quite acceptable. The dihedral angle must be rather large for adequate control.

13.8 AIRBRAKES, SPOILERS AND FLAPS

As landing aids, split flaps are excellent. Their advantage is that they create high drag with high lift coefficient, slowing the approach speed and steepening the glide angle, enabling better judgement of the point of touch down to be made. Operating loads on such surfaces are high at high airspeeds, and the modeller may well find the servo incapable of lowering the flaps fully if the model is not at the right speed (Fig. 13.6). As airbrakes, such flaps are usually beyond the servo's power to operate when most needed.

On sailplanes, various types of spoilers and airbrakes are used. The spoiler is a simple hinged surface which can be raised on the upper wing surface to disrupt the airflow and create more drag. It also reduces the maximum lift coefficient and raises the stalling speed, which is a disadvantage. The nose-down pitching moment may also be quite severe. Such spoilers are usually somewhat ineffective as drag producers, especially if mounted too far aft on the wing. They are also usually a source of extra drag in normal flight, since there is some air leakage from inside the wing to the upper surface around the spoiler. Unless they are very carefully fitted, when shut, they break the aerofoil profile's contours and may cause separation or, on a laminar flow wing, transition. Some of the same criticisms apply to air brakes, which are raised vertically by some form of 'parallel ruler' type of linkage (Fig. 13.6c), either on one surface of the wing, or both. These are usually much more effective than spoilers, especially at high speeds. They may be used to prevent the airspeed in prolonged dives from exceeding safe limits. This is useful in bringing sailplanes down out of strong thermals. There are two types of such parallel action brakes. In the first, the brakes are directly above one another, and extend equally above and below the wing. Between them there is a gap in the wing through which the air can flow from bottom to top surface. The effect on drag is very powerful, and the air leakage also reduces C_L markedly. On closing the brakes, the gap is sealed as far as possible by the brakes themselves, but there is still usually some leakage. To avoid this, the two leaves of the brakes may be separated, so that there is never any gap through the wing, each brake component retracting into its own sealed box inside. These brakes are slightly less effective, but interfere less with flight when retracted. It is very common to use brakes which extend from only one side of the wing, the upper or lower. These, like

Fig. 13.6 Landing and approach aids

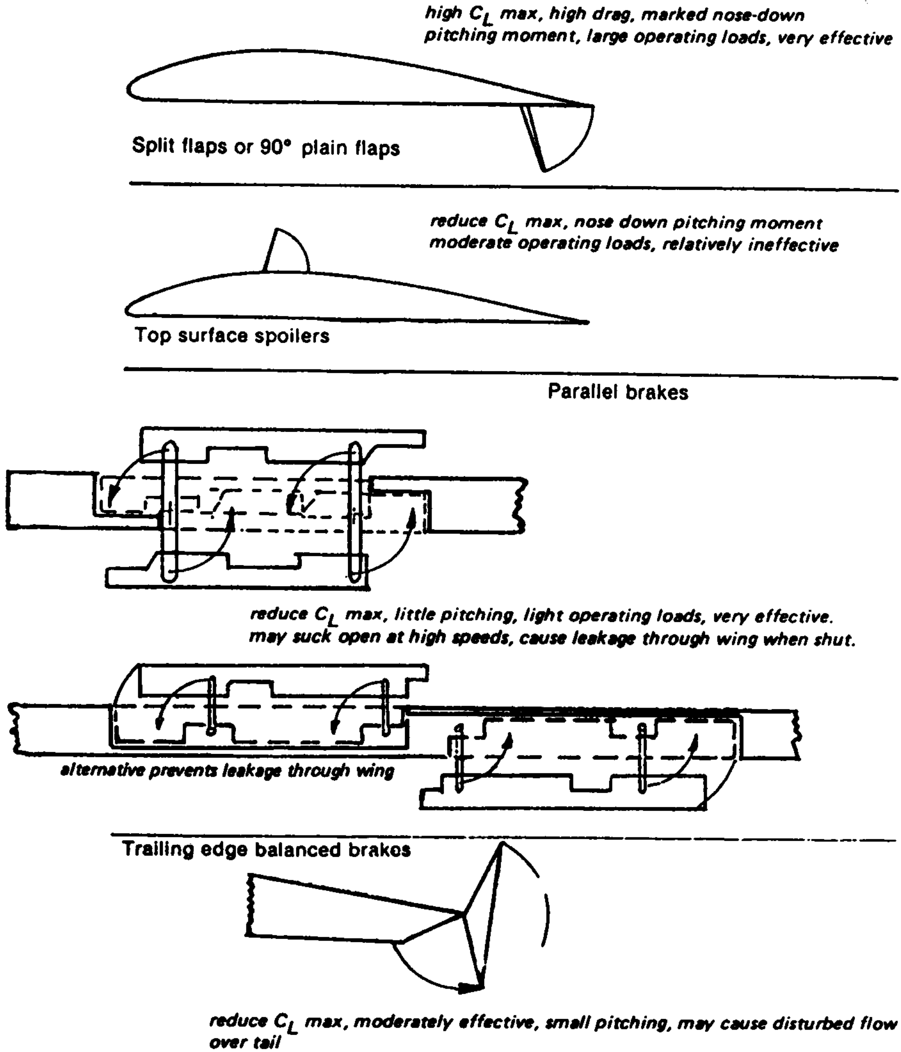

spoilers, may cause some pitching moments, requiring re-trimming.

To avoid the leakage and fitting problems of brakes which retract into the wing, several types of trailing edge air brakes are possible, the best being those which are self balancing and so require only small power from the servo. These may sometimes cause pitching oscillations of the model due to the formation of rotating vortices behind them, which also may strike the tailplane. The brakes should be placed outboard of the tailplane, or a 'T' or 'V' tail used to ensure that the surface is clear of the turbulent wake.

A very effective type of braking system which has become popular for sailplanes, is the so-called 'crow' or 'butterfly' mix. This normally requires sophisticated radio equipment which permits the mixing of the ailerons and the flaps, together with the elevator.

When the action is required, the flaps, extending over the whole inboard section of the wing trailing edge from aileron ends to wing root, are arranged to go down fully to 90 degrees or as close to this as possible. At the same time, both the ailerons move up together by 15 to 25 degrees. The flaps create very high drag in this position and also at their outer end, adjacent to the ailerons, a strong vortex forms which adds yet more drag. The lift over the flapped part of the wing remains high. The ailerons, because they are raised, remain effective as lateral controls. They effectively reverse the camber of the outer wing so the lift there is greatly reduced.

The braking effect is very powerful but there is usually a very strong nose-up pitch as the flaps go down. This requires the elevator to be coupled to the landing system to prevent the glider rearing up into a stall. Once the crow landing system is deployed, the model remains controllable for the final approach and touch down. A minor problem arises if the flaps, at their fully down position, make contact with the ground as the model lands. This can cause damage. Raising the flaps just before touchdown, or designing the model so that they cannot touch the ground in any position, will prevent trouble.

Parachute airbakes are excellent, providing they can be made reliable. The parachute itself may be housed in a special compartment in the fuselage, or following full-sized practice, in the bottom of the rudder. A light spring may be needed to ensure ejection of the brake 'chute. As a rule, such brakes are 'one shot' only, i.e. they cannot be retracted after deployment. Either the modeller must develop good judgement so that the parachute is never deployed at the wrong time, or some means of jettisoning it must be devised, so that an error can be retrieved. Full-sized sailplanes using such brakes usually possess other forms of air brakes as well, in case the parachute fails to deploy when needed, or in case the pilot inadvertently pulls the jettison handle instead of the deployment knob. The Polish 'Zefir' sailplane of 1958–62 possessed a brake parachute which could be retracted by means of a small hand winch, but the mechanical complications were considerable and the device was not used on later aircraft. Parachute brakes are a good choice for 'flying wing' models. Noel Falconer suggests a two point attachment for the brake 'chute, so that

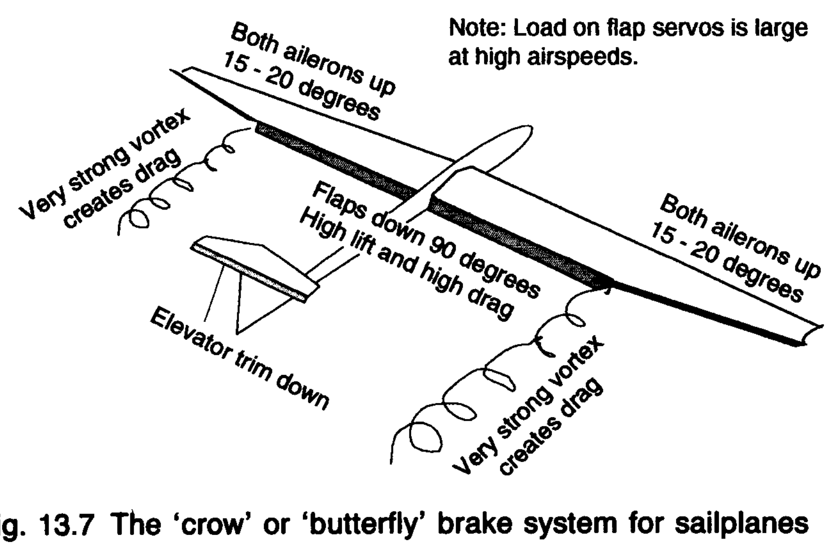

Fig. 13.7 The 'crow' or 'butterfly' brake system for sailplanes

deployment is more certain. One attachment may then be released to allow the parachute to trail, if an undershoot must be avoided.

Other forms of air brake are sometimes employed, including flaps sticking out of the side of the fuselage, split rudders which open like clam shells, and even broad wing struts which rotate through 90 degrees to give a braking effect. All these work to some extent but less effectively than the orthodox brakes described.

13.9 FLUTTER

Any hinged control surface on a model may flutter. Flutter is an oscillation or violent shaking to and fro of the control surface, and it may set off sympathetic flutter in the wings or tail, or in other hinged members. In some cases, such flutter may be mild and almost harmless. The control surface affected vibrates slightly at certain airspeeds, possibly emitting an audible buzzing, but the oscillation does not build up and ceases as soon as the air speed drops. In other cases the flutter builds up rapidly and the model becomes uncontrollable, sheds control surfaces, or breaks up, with very little warning. The operator may have no idea what happened. The incident may be blamed on radio interference, or lack of structural strength.

In a simple case of flutter, the first cause is the inertia of the control surface itself. The effect may be simulated in an elementary way if a model fuselage with a hinged rudder disconnected from its control rod, is shaken from side to side violently. As the rear end of the fuselage moves, then reaches the end of its 'shake' and starts in the other direction, the hinged surface tends to bang over against its stops. It then follows the fuselage through the next movement, and when the fuselage stops moving to begin its return swing, the control surface bangs against the stops again in the other direction. When the model is flying, it is evident that such a control movement may be in phase with the oscillation of the fuselage. A rudder movement by the pilot, or a gust, causes the rear end of the model to swing. The rudder goes with this swing but when the fuselage stops, the rudder's mass carries it further, which applies aerodynamic force tending to start the fuselage on its return swing. At the end of this second movement, the fuselage again stops and begins to swing back, but the rudder carries on, and again helps to push the fuselage on its way. At some critical airspeed the result will be a continuing oscillation, the rudder will bang violently from side to side and the fuselage with it. Something, usually the rudder itself, will break if this

Fig. 13.8 Aileron flutter

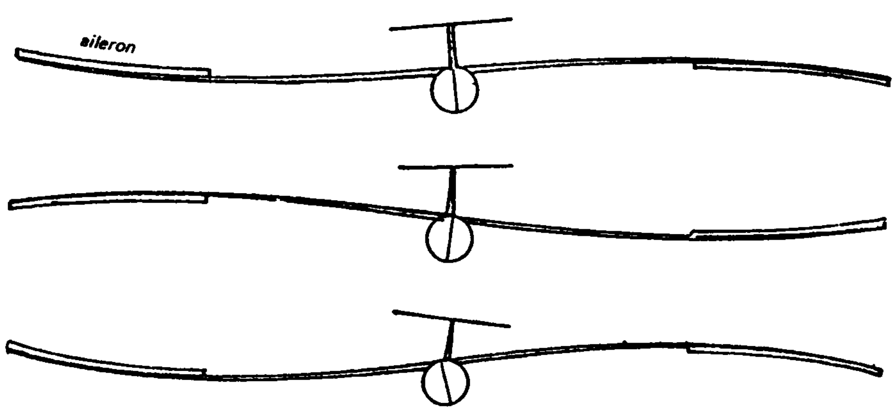

continues. Flutter of an elevator begins in the same fashion, and can be more dangerous since loss of the elevator control is usually disastrous for the model. Aileron flutter is even more common. Since wings are usually flexible, and ailerons large and relatively heavy, flutter is quite probable, especially at high speeds. Wings without ailerons, if too flexible in torsion, will also flutter at high speeds, the tip sections twisting to and fro almost as if they were hinged to the stiffer inboard panels. The twisting changes the angle of attack causing the wings to bend up and down rapidly.

Modellers who have never seen genuine wing flutter sometimes mistakenly refer to the normal up and down bending of wings under varying loads as flutter. Any wing will flex and must do so in flight. Flutter of a wing is a rapid, rhythmic oscillation with simultaneous twisting. It is unmistakable, and, once started, hard to stop.

The case of the lightweight wing which flutters often arises when a model is based on an earlier free flight design, which was successful when trimmed for slow flight. Fitted with radio and controlled by rudder and elevator, the model may develop wing flutter when flown at speeds for which its wing was never really intended. In such cases the solution is to stiffen the structure.

If the torsional axis of the wing, i.e. the line around which the outer panels twist, lies ahead of the wing's centre of gravity, flutter is sure to occur at some speed. The stiffening should be added to the leading edge, usually in the form of sheet balsa covering and vertical spar webbing, to produce a 'D' shaped torsion tube. The extra weight added near the leading edge also helps to bring the centre of gravity nearer to the torsional 'hinge' line. This is in effect a partial mass balance. Other forms of stiffening, such as diagonal ribs, or (as in some older types of wooden full-sized aircraft) by twin spars with diagonal strutting internally between the spars, is less effective because it does not move the centre of gravity of the structural members forward.

To prevent flutter it is essential for the hinged surfaces, especially on fast models, to be without slop, and for the wings and fuselage to be stiff. Stiffness is not the same thing as

Fig. 13.9 Wing flutter

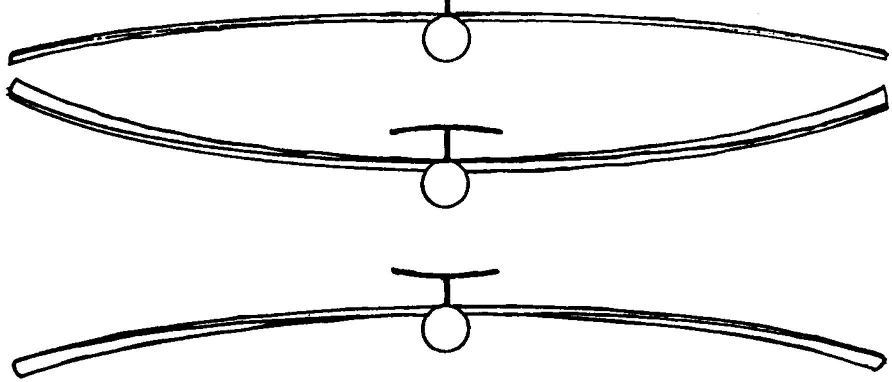

strength. A fibre glass rod or arrow shaft is very strong, but is not very stiff, indeed the flexibility of glass combined with strength is its main recommendation to archers who use it for bows as well as arrows. Some sailplane models, like their full-sized counterparts, with slender fibreglass fuselages, are inviting tail flutter at high speeds. Secondly, the control rods and cables, and all their linkages, should be free from 'play' and again, as stiff as possible. This does not necessarily mean the pivots should be hard to move (although this, too, will help to prevent flutter), but the control rods themselves should not be easily flexed or bent by end loads. In models this is far from easy to arrange, but in general wooden push rods of adequate strength are usually stiff enough, whereas stranded cables, nylon 'snake' tubes, etc. are less so. Tubular metal (light alloy) arrow shafts are probably best of all, but costly. Finally, the control surfaces themselves should be as lightly built and as stiff as possible, and, where possible, mass-balanced. It is the mass of the control surface itself that is primarily responsible for flutter and it follows that if the mass can be reduced, flutter is less likely. However, if the control can be balanced so that its centre of mass, or centre of gravity, is ahead of the hinge line, the inertia of the balanced surface will prevent flutter altogether. Repeating the experiment with a rudder on a model fuselage, if the mass balancing is correctly done, the rudder will always be opposed to the fuselage oscillation, however violent.

13.10 MASS BALANCING

Mass balancing is achieved in many different ways on full-sized aircraft. In some cases a lead weight is mounted on an arm projecting ahead of the hinge line. The arm and weight may be concealed within the wing, fin or fuselage, but sometimes this is not possible and the mass balance weight protrudes, as a source of parasite drag. In other cases, control surfaces are built with portions projecting ahead of the hinge line, with the balance weight inside. The projection may be concealed or used, for example on a Frise aileron, as a means of overcoming adverse yaw in turns, or, on elevators and rudders, as an aerodynamic balance to reduce loads for the pilot. In models, similar devices may be useful if flutter arises, though the need for aerodynamic balancing is rare. Complete mass balancing is not always necessary, since within the speed range of a particular aircraft, flutter may be a problem only for some of the controls at the highest speeds, and even these may require only partial balancing. Since mass balancing adds weight, it should not be used if not essential.

Even with the suggested precautions, most aircraft have a critical airspeed beyond which flutter of some member or other will begin. In full-sized sailplanes, for example, flutter may start sometimes even below the nominal 'red line' or structural 'never-exceed-airspeed'. This can occur if the control linkages are worn with use and hence have become sloppy. If no further mass balancing or structural stiffening is practicable (if, for example, the aircraft would become too heavy after such modifications) the only solution is to fly always below the critical flutter airspeed. The modeller often does not know what this speed is until his model begins to flutter, and unfortunately, this may result in rapid loss of control or the radio gear being damaged by severe vibrations, heavy oscillating loads, etc. Once started, flutter is very hard to stop. Only a reduction or airspeed will be effective in damping the oscillations down, and if it happens to be the elevator or flaps that are involved in the fluttering, speed control may be impossible. Quite apart from the more predictable effects of poor stability, radio or servo failure, and pilot error in exceeding the structural limits of the model, some apparently inexplicable mid air break ups of model aircraft are caused by flutter. In other cases, models can be seen or heard to flutter quite violently, yet survive unharmed. Quite small variations in structure will make a difference. For example, the stiffening effect of tissue paper or silk covering as opposed to

Fig. 13.10 Mass balancing

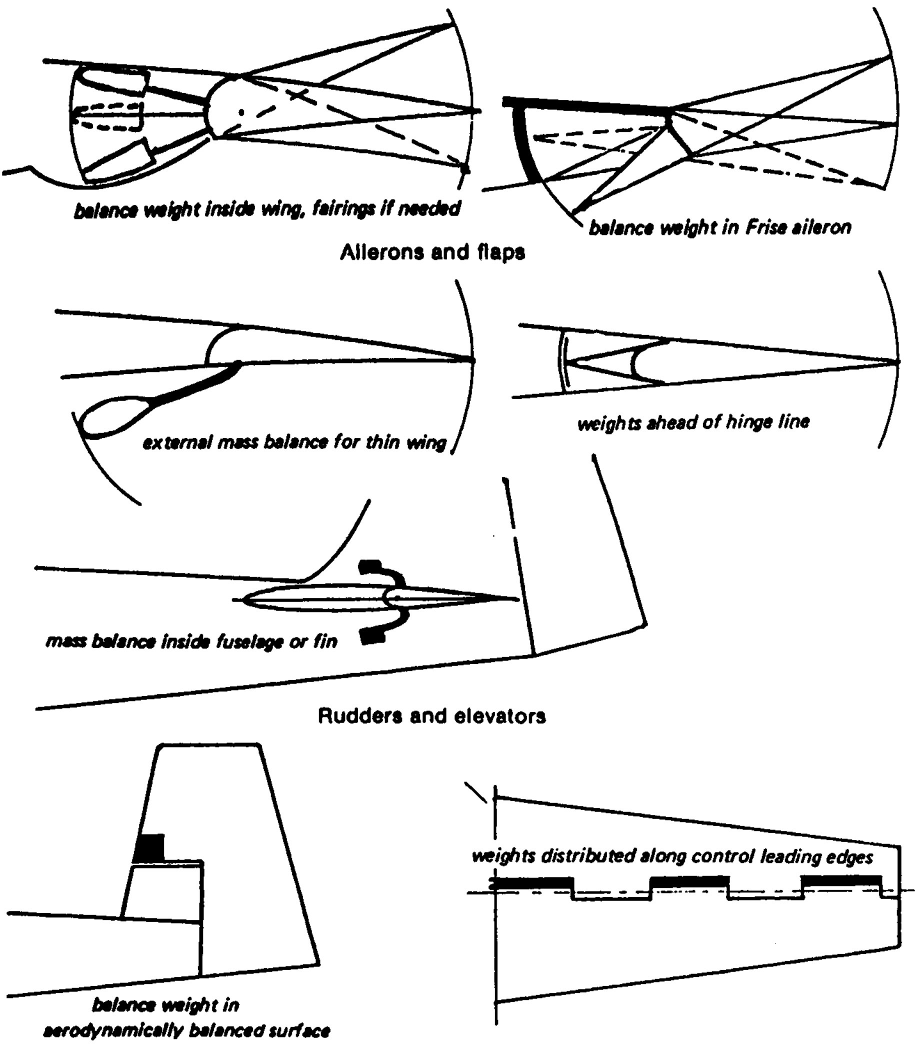

the flexibility of plastic film is well known. A heavy piece of balsa built into a trailing edge may encourage early onset of wing flutter, when an otherwise identical model may escape, and so on. As usual, theory is useful to help explain what went wrong, but unless the model designer is prepared to spend many hours in calculations, he will have to rely on practical experience combined with an intelligent appreciation of the forces involved, when a new model is under consideration.

14
Propellers

14.1 THE PROPELLER AS AN ACTUATOR DISC

Early research on propellers, by Rankine and Froude in the 19th century, was concerned with ships' water screws, but the basic equations of that time remain valid. The propeller was treated as an 'actuator disc' which transferred power from the drive shaft to the fluid medium. In the first instance, no attention was paid to the details of the propeller, number of blades and blade shape. The idea was to establish the main principles first, thus opening the way for systematic trials and tests of various propeller forms.

14.2 PROPELLER EFFICIENCY

In Figure 14.1 the propeller is represented by a disc of diameter D. It is assumed that the rotation of the blades causes a reduction of pressure over the entire front face of the disc, from P_0, the static air pressure at some distance in front of the aeroplane, to p at the disc. The energy transferred to the air by the propeller causes an increase of pressure by some relatively small amount labelled dp (where the small d stands for 'a relatively small

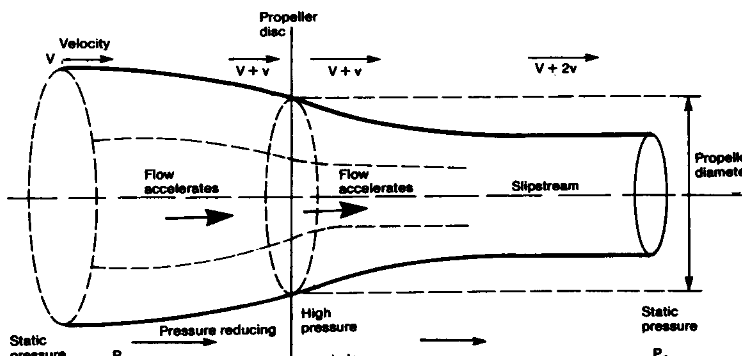

Fig. 14.1 The propeller as an actuator disc

difference of'). The air pressure just behind the disc is then p + dp. Far behind the disc the pressure returns to the static value, P_0. The assumption that the pressure change is evenly spread over the whole disc area is false, particularly near the hub of a real propeller, but this obvious simplification and others are taken care of by recognising that no real propeller will be as efficient as the theoretical actuator disc.

Propeller efficiency is defined as the ratio of power supplied to the propeller by the drive shaft, to the useful work or power output: i.e.

$$\text{Efficiency} = E_p = \frac{\text{useful power output}}{\text{shaft power input}} = \frac{\text{Thrust} \times \text{Velocity}}{\text{Power}}$$

The difference in pressure between the front and rear of the disc produces thrust. The total thrust can be found very simply by multiplying the difference, dp, by the disc area, which is found from the usual formula for area of a circle. Hence thrust $= 0.7854 \times D^2 \times dp$, where D is the diameter.

As the diagram shows and as Bernoulli's theorem leads us to expect (see 2.12), the reduced pressure in front of the disc causes the air to accelerate towards the propeller, V, which corresponds to the airspeed of the aeroplane, thus becoming V + v as the air passes through the disc. Behind the propeller, because of the increased pressure there, the flow accelerates away so the velocity increases further to V + 2v some distance behind. Half the increase of 'slipstream' velocity thus occurs ahead of a propeller and half behind it. (This is why loose objects such as grass clippings or the end of model flier's tie flapping loose, may be drawn into the propeller disc.) The slipstream diameter contracts both in front of and behind the propeller, as shown.

The ratio of v to V, the velocity of flight compared with the increment of flow speed through the disc, is of great importance and is termed the 'inflow factor', often represented in formulae by a tagged letter a, thus: Inflow Factor $= a' = v/V$.

The Froude or 'ideal' efficiency of a propeller is found by relating thrust to flight speed and the inflow factor. The figure resulting is always less than 1.0. The equation is:

$$\text{Froude efficiency} = E_i = \frac{\text{Thrust} \times \text{Velocity}}{\text{Thrust} \times (V + v)} = \frac{T \times V}{T \times (V + v)}$$

The thrust factor cancels out and since $v/V = a'$, the formula simplifies to:

$$E_i = \frac{1}{1 + a'}$$

It is now possible to measure the actual thrust, and inflow factor, of any real propeller and compare the figures with the Froude ideal, which determines an absolute limit at a particular airspeed and power input. Exceptionally well designed propellers may exceed 90% efficiency at best. A crude propeller, even though looking something like the right shape, may only achieve 50% or so efficiency. It is clear that no model flier can afford to neglect the propeller, since a bad choice may be equivalent to using a motor with forty percent less power output.

14.3 GENERAL POINTS ARISING FROM THE FROUDE EQUATION

The inflow factor is large if the increase of flow velocity produced by the propeller is large. If, for example, v, the flow speed increment added by the propeller to the slipstream, is equal to the flight speed, so that the speed of the slipstream behind the aeroplane becomes V + 2V = 3V, the ratio of v/V is 1.0 and the Froude efficiency equals 0.5. If the inflow factor is smaller, an increase in efficiency results: if v is only one tenth of V so that the

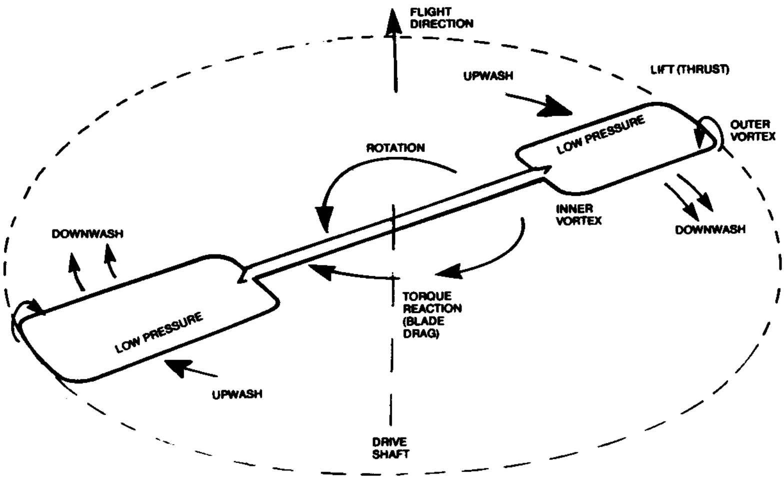

Fig. 14.2 A simple paddle-type propeller

slipstream velocity aft is V + (1/5 × V) or 1.2V, the ideal efficiency is 0.909. A given thrust can be obtained either by using a propeller of large diameter driven at a low rate, to produce a small pressure difference spread over a large disc area, or by a small propeller turning faster, creating a larger pressure difference spread over a smaller disc. The large diameter propeller, as the above examples show, would be much more efficient. This point applies quite generally for model aeroplanes.

With full-sized aircraft propellers and helicopter rotors, a limitation to propeller diameter is set by the tip speed of the blades. If this approaches the speed of sound, efficiency falls off, quite apart from the high stresses and noise produced. Model propellers rarely enter such regions although it is possible for them to do so. There are other obvious limits for models and all aeroplanes to the practical diameter of a propeller. Ground clearance and undercarriage length usually prevent the use of the most efficient propeller diameter when the engine power is great.

With model internal combustion engines, which are rarely geared down, rates of rotation at maximum power are high and it is important, in competition flying, that the engine should run at its maximum power r.p.m. when required. A large diameter propeller will not develop more thrust than a small one, if it overloads the engine and prevents it reaching its best r.p.m. But it follows that if two engines of equal maximum power output are available and one runs at a lower r.p.m. than the other, more thrust will be obtained from a larger propeller on the slower engine. A crucial point here is the diameter to pitch ratio, of which more appears below.

The inflow factor also depends on the flight velocity. It is large if V is small and vice versa. If V is zero, as when the aeroplane is standing on the ground with engine running, no matter how much velocity the slipstream has, the propeller efficiency is zero. As the aircraft speeds up, efficiency increases. A limit is set to the attainable (level flight) speed of a model aeroplane by the total drag which will increase as the model accelerates until it comes to equal the thrust. The rate of climb is subject to equivalent restrictions. If the drag is reduced by some aerodynamic improvement the potential will not be fully realised unless the propeller is changed to one which reaches its maximum efficiency at a higher speed. Every change to the aircraft requires a change to the propeller, if the best performance is to be attained.

Fig. 14.3 Pitch at a point on a propeller blade

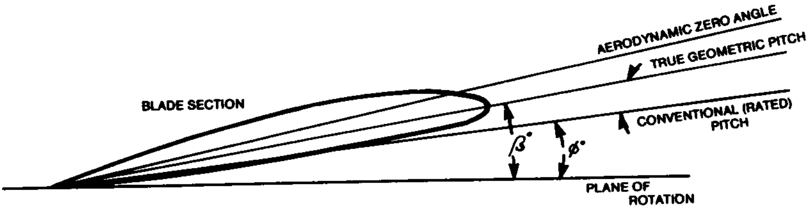

On the other hand, if a propeller is designed very exactly to reach its peak efficiency at a particular flight attitude, speed and power, it will, at all other times, be working 'off design' and will be less efficient. In particular, take-off performance, when propeller efficiency is bound to be low because V is small, will suffer if a high speed propeller is used. Racers need to take off smartly and accelerate to their best speed quickly. With simple propellers, some compromise has to be struck. With aerobatic models a propeller which has a narrow peak of efficiency will perform badly, because the airspeed varies constantly during the aerial pattern flying. In a vertical climb, V is low, yet the climb must be maintained. Yet rapid acceleration and high entry speed is needed for some manoeuvres. A propeller with a wide tolerance is required. The same applies, though with less urgency, to sport flying models generally.

14.4 THE PROPELLER AS A ROTATING WING SYSTEM

In more detail, each blade of a propeller is a wing which rotates. In some very simple forms the blades are paddle shaped as shown in Figure 14.2. The paddles are set at an angle now called the *pitch*, to the swept disc, so that they produce lift forces nearly at right angles to the plane of rotation. Drag forces resist the rotary motion, producing a torque reaction against the drive shaft. The aeroplane experiences this torque as a force tending to cause it to roll one way or the other, depending on the direction of propeller rotation. (Some aileron trim is required to counteract this.)

When the drag-torque reaction equals the shaft torque from the engine, the maximum rate of rotation is reached for the particular set of conditions. One way of increasing propeller efficiency is to reduce the drag of the blades, so allowing a higher rate of rotation for a given power input and hence, a larger difference in pressure behind the actuator disc and more thrust. As with wings, blade drag is of two kinds, vortex-induced and profile drag.

Since the paddles produce lift in the same way as a wing does, by generating a pressure difference between the surfaces, there are rotating vortices at both the outer, or tip, end and at the inner end of each blade. The vortices produce drag, the amount depending, as with a wing, on the propeller's equivalent of aspect ratio, blade planform and twist. Because the blade travels at different speeds relative to the air, depending on the radial distance of each part of it from the hub, the shape and twist cannot be simply laid out as if for a wing. There are, however, equivalent techniques.

Also like a wing, a blade, or part of it, may stall, producing very high drag with little lift. Or, if a blade meets the air at a negative angle of attack it may produce negative lift which, in the case of a propeller, becomes a braking force.

All such faults and losses, inevitable as they are to some extent, reduce the efficiency of a propeller so that it cannot achieve the Froude ideal. To minimise the losses is the aim

Fig. 14.4 Angle of attack at a point on a propeller blade

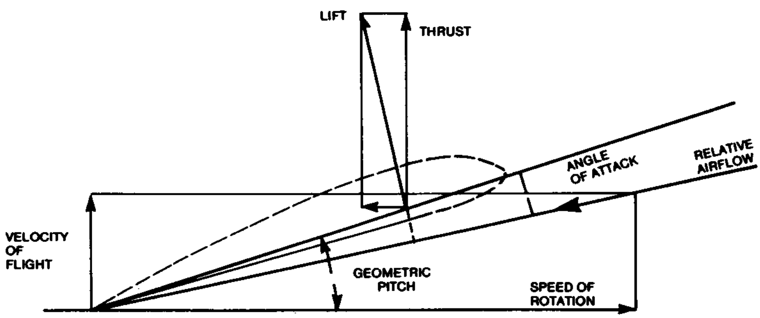

NOTE: IN OLD TEXTBOOKS, THE DIFFERENCE BETWEEN THE RELATIVE AIRFLOW AND THE ANGLE OF THE BLADE WAS REFERRED TO AS 'SLIP'. IT IS ACTUALLY THE ANGLE OF ATTACK

of the designer who must nonetheless produce a propeller which will not fly apart under the considerable stresses caused by high rotational speeds, and will distort as little as possible under the air loads.

14.5 PITCH

If a small segment of a propeller blade, at some distance from the hub, is viewed in cross section, as in Figure 14.3, the meaning of *pitch* may be clarified. Conventionally, when a model propeller is being measured, using a simple pitch gauge, the flat, or flattish, back face of the blade is used as a reference. A radial station of 75% of the distance from the hub to the tip is generally used as the point for such a measurement, which yields the 'rated' pitch. This is usually given as a length (cm. or ins.), the reason for which appears below.

If the blade section is undercambered, a line tangential to the back face of the blade is used. However, most aerofoils on real propellers are not truly flat on one side. There is a true chord line which runs from the trailing edge to the leading edge. If this is used as the reference line for pitch calculations or measurements, as the diagram shows, the true geometric pitch will be greater than that based on the rated pitch. This may be part of the explanation for the very noticeable variations in pitch measured with the model flier's gauge and the advertised rating of many commercially produced propellers. It should also be remembered that blade sections invariably change from root to tip, for structural reasons. The segments near the tip are usually thin and those nearer the hub considerably thicker. The geometric chord line may stand in a different relationship, at each place on the blade, to the underside tangential reference.

A further reference line on the drawing is also of importance. Every aerofoil section has an aerodynamic zero angle of attack. Only in the case of a symmetrical profile does this coincide with the geometric chord line. With cambered profiles, the aerodynamic zero line is at a greater angle to the propeller disc than either the conventional or the geometric reference. The aerodynamic zero line represents the angle of attack at which this part of a real propeller blade would produce zero lift and hence no thrust. Such a condition can be reached, for instance in a dive with the engine at low throttle. Beyond this negative angle the propeller becomes an air brake.

14.6 BLADE LIFT AND PROPELLER THRUST

Figure 14.4 shows how the thrust produced by a propeller blade depends upon the speed of rotation and the velocity of flight. The speed of the blade at any radial point, relative to the air, is a resultant of its speed around the circumference of the circle at its radial distance, and the forward velocity. The relative airflow is thus expressed in both speed and direction by the diagonal line appropriately labelled in the drawing. The angle of attack, measured from the geometric chord, relates to this relative flow line and is obviously less than the pitch.

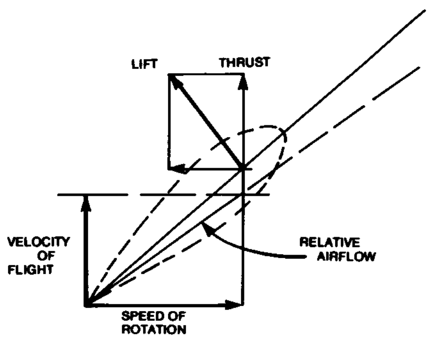

Fig. 14.5 Angle of attack and thrust near the propeller hub.

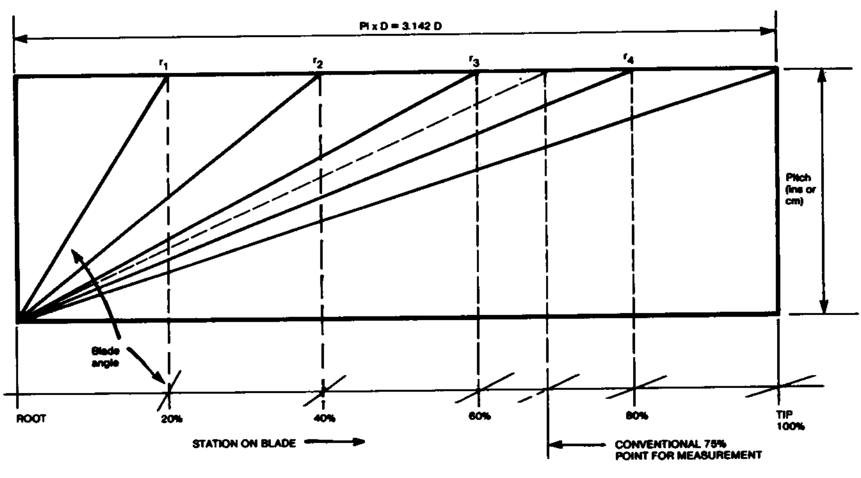

Fig. 14.6 Layout of a constant pitch propeller

So long as the angle of attack is greater than the aerodynamic zero of the section, lift will be produced but at right angles to the airflow, not to the propeller disc. The lift vector is thus inclined backwards relative to the plane of rotation. Resolution of the lift force demonstrates that the effective thrust is less than the lift and there is a component which must be added to the total blade drag.

At any radial station closer to the hub of the propeller than this, although the forward velocity must be the same, the speed of rotation is less. The relative speed and direction of the airflow at such a point is represented in Figure 14.5. To keep the blade here at the same angle of attack to the air, its angle to the disc plane must be increased. The effect of this is to tilt the lift vector considerably more against the rotation so that a large proportion of the force is available for thrust and more goes to resisting the rotation.

Since the relative flow speed is less than further out on the blade, the absolute magnitude of the lift force is less in any case, if the blade chord is similar.

For these reasons, the inner segments of a propeller are considerably less efficient as producers of thrust than the outer parts. Close to the hub the relative flow is almost directly along the axis of rotation and no thrust comes from this part of the blade at all. In practice, about 20% of each blade, measuring from the drive shaft outwards, may be neglected and, for the sake of all-round drag reduction, may be faired by a spinner with very little, if any, sacrifice of thrust.

14.7 CONSTANT PITCH

The idea of constant pitch has already been implied in the foregoing. For minimal profile drag, each small segment of a propeller blade should be set at the aerodynamic angle of attack which gives the best lift-drag ratio. What this angle is may be found from wind tunnel tests for the aerofoil section concerned. Since the profile changes from root to tip, ideally there should be a range of tunnel test results for a number of different points on the blade, and the eventual propeller layout should take account of these. On model propellers such precision is rarely found.

Whether or not the precise best angle for each aerofoil is known, the layout of a constant pitch propeller may be done by means of a diagram like that of Figure 14.6. Here, the desired pitch is represented on the vertical scale and expressed as a length (usually inches in English-speaking countries but centimetres or millimetres if SI units are used.) The basis of this figure is the notional distance the propeller would advance in one revolution if it were literally screwing itself through a solid medium like a screw or bolt. This is, indeed, the origin of the words 'airscrew' and 'pitch' in this connection, by analogy with the pitch of the thread on a bolt. (The idea of 'slip' of a propeller as indicated in Figure 14.4, also originates here. Slip of a propeller blade is the angle of attack of the blade to the relative airflow and has no other meaning.) The distance that each segment of blade travels as the propeller rotates is represented by the horizontal scale. The extreme tip follows the circumference of a circle whose length is found from the standard circle formula:

$$C = 3.142 \times D$$

On such a diagram the same scale proportion must be used for both horizontal and vertical scales. By ruling a number of straight lines radiating from the lower corner of diagram, the actual pitch angles required at each point are found and may be transferred directly from the drawing to the propeller block or master blade for production. If correctly done, this produces a propeller which will have, at one airspeed and one rate of rotation, every part of the blade at the most efficient angle of attack. This is why such a propeller is termed 'constant pitch'. At typical result is shown in Figure 14.7.

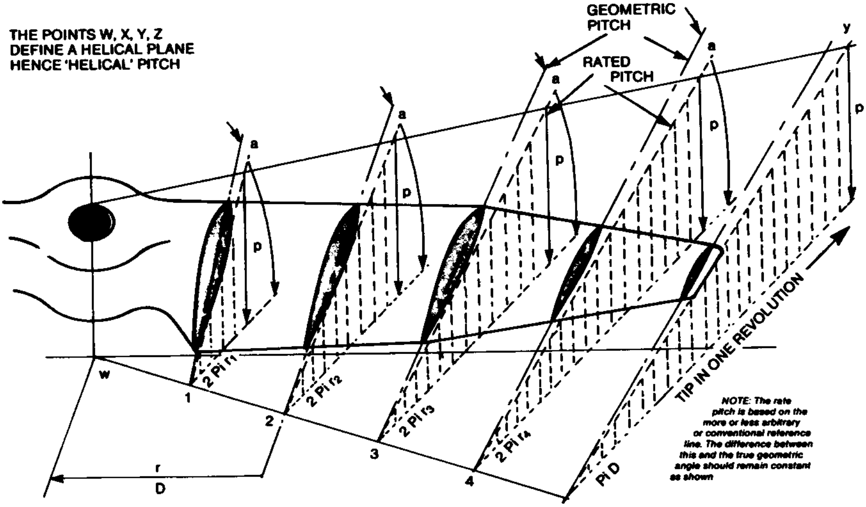

Fig. 14.7 Layout of a constant pitch propeller blade.

The pitch, as a length, is represented by the vertical arrows. The distance round the hub travelled in one revolution is Pi x D at the tip and 2 Pi r at each radial station. *Drawing courtesy J. Lnenicka.*

It is clear from the above that at other airspeeds than the one for which the propeller is designed, even if the the rate of rotation is the same, the angle of attack will nowhere be at its best. This emphasises again that the propeller should be matched to the engine. It may be that a particular engine can turn a propeller of a certain diameter and pitch, at a certain rate. A model may be designed to fly at a speed which corresponds to this pitch. If, however, the model has more drag than anticipated it will not achieve the designed speed and the propeller will not be at its most efficient either. There is a double penalty. On the other hand, if the model drag is less than expected although a faster flight will result, the propeller will again not be at its best efficiency. A better result would be attained with a greater (coarser) pitch.

The constant pitch propeller just described is evidently 'peaky', in that it is designed for best results at one speed and r.p.m. It is also efficient if the r.p.m. and flight speed vary 'in step' with one another, in a way that maintains the best angle of attack everywhere along the blade. This is indicated in Figure 14.8. There is at least a rough correspondence in reality since reduced engine power (low r.p.m.) results in lower flight speed. However, such a fortunate harmony is not likely to prevail at critical times. During take off, for instance, forward velocity is low and revolutions high. The coarse-pitch propeller blade is then at a higher angle of attack than optimum and may even stall (Fig. 14.9a). Racing aeroplanes have sometimes been incapable of taking off for this reason; the Schneider Trophy seaplane racers sometimes exemplifying this. Similarly, if, on a slow landing approach it becomes necessary to open the throttle to 'go round again' a stalled propeller could be disastrous. At the other end of the scale, a propeller designed for greatest efficiency in the take off mode, or climbing, will be working at lower angles of attack than optimum at high speed. Such a 'fine pitch' propeller will accelerate a model quickly from standstill but will lose efficiency rapidly as the airspeed increases (Fig. 14.9b).

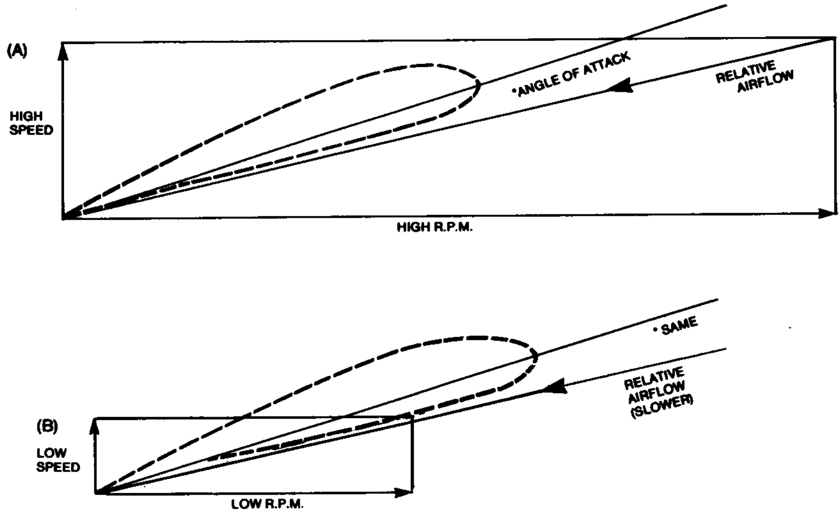

Fig. 14.8 Variation of R.P.M. & Speed may not change angle of attack

14.8 NON-CONSTANT PITCH PROPELLERS

It is possible, by modifying the diagram of Figure 14.6, to lay out a propeller which will not have constant pitch from root to tip of the blade. Instead, the angle of attack will vary in some consistent manner. The nominal or rated pitch, measured at the 75% point, would not necessarily reflect this variation, which is another reason why commercial propellers

Fig. 14.9 'Coarse' and 'fine' pitch

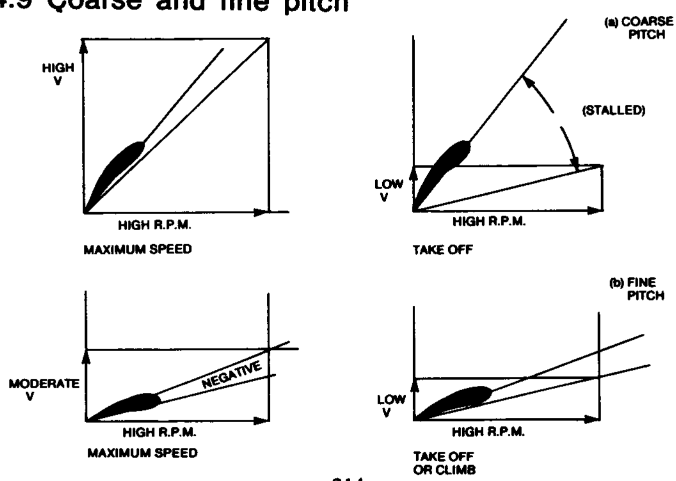

often differ from one another and perform differently even though rated the same. The advantages of such radial pitch changes are chiefly that although the propeller is never quite so efficient as the constant pitch variety at its designed operation point, there is a broader band of operating conditions under which the propeller will be reasonably effective. For sport flying models and for aerobatics, this is generally much preferred. To vary the pitch in the way suggested in Figure 14.10 is equivalent to 'washout' of a wing, reducing the angle of attack at both 'tips', i.e. the inner and outer ends of the blades. Various alternative approaches are possible, as illustrated in Figure 14.11. Since the hub end of the blade is least effective, modifications to pitch here are not likely to make much difference, but changes to the outer third of the blade can be very significant and competitive model fliers frequently do a great deal of work on their propellers to improve their performance in this area.

14.9 VARIABLE PITCH

To overcome the deficiencies of high speed, coarse pitch propellers at take off or in the climb, in full-sized aviation the variable pitch propeller is widely used. In this a fairly complex mechanism allows the pilot to select the blade pitch required to give efficient propeller performance, and hence good thrust, over the whole speed range. This is done by rotating the blades axially at the hub; it is not feasible to change the twist of the blades themselves. Hence such a propeller will still lose some efficiency at speeds other than the design point, but this detracts only slightly from the all-round improvement in efficiency and safety. Model aircraft have been flown with variable pitch propellers and experimentation continues. The cost is likely to be high if a propeller is broken and the danger of shedding blades requires a great deal of care in design of the hub and gearing. Rubber driven models offer scope for improvement here too, and variable pitch propellers have shown up very well in experiments although not, as yet, widely adopted.

A constant speed propeller is one in which the pitch is varied automatically to maintain a constant engine r.p.m. The engine has a most economical speed and fuel can be saved if the propeller pitch is matched to this under all or most flight conditions.

14.10 THE DIAMETER: PITCH RATIO

Propellers for models are 'fixed pitch' and are normally marketed with a stated diameter to pitch ratio. The ratio itself is independent of the units and dimensions used, since a 28×18 cm propeller, with D/P ratio of 1.56 is practically the same as an 11×7 inch propeller, with the exact ratio of 1.57. A propeller with a diameter of 40 cm and pitch of 26 cm would have a D/P ratio of almost the same value. Since the resistance of a propeller to the air depends greatly on the diameter as well as the pitch, if the diameter is increased, the pitch must be reduced if the engine is to drive the new propeller at the same r.p.m. That is, for a given power input, the diameter/pitch ratio must be increased.

14.11 THE ADVANCE RATIO

Much of the foregoing may be expressed in a single figure, the advance ratio, represented by the letter J. The formula is:

$$\text{Advance ratio} = J = \frac{V}{\text{RPM} \times D}$$

where D is the diameter and V the flight speed. As shown above, the angle of attack of the blade, for a constant pitch propeller, depends on the flight speed and rate of rotation. The

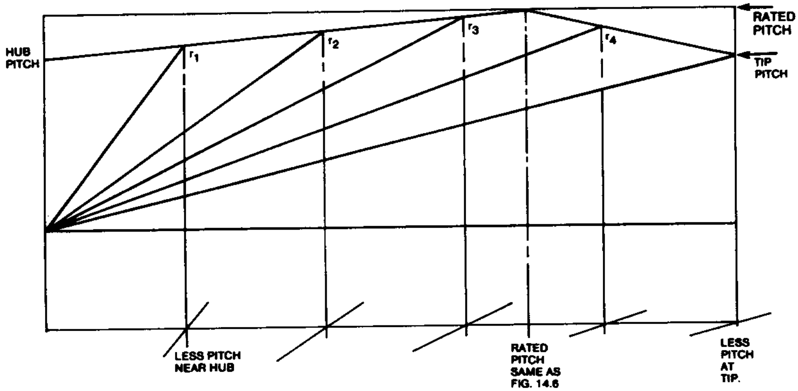

Fig. 14.10 Non-constant pitch layout

remaining variable is the diameter which, at a given RPM, determines the actual speed through the air of the propeller tips and, at a given pitch, has a dominant effect on the power required to drive the propeller at the stated RPM.

14.12 RELATION OF PITCH TO SPEED

Since the pitch is the distance advanced by a blade in one revolution, the relationship of pitch to RPM and speed is fixed, nominally. This does not mean that fitting a propeller of a certain pitch will mean a model must reach the appropriate speed, because this will depend on the engine's ability to drive the propeller at the required RPM and the thrust even then may not equal the aircraft drag at the nominal speed. It is nonetheless useful to know the nominal speed for a given pitch/RPM relationship since this can be related to the engine power curve published by the manufacturers or in model aircraft magazine engine review articles. Knowing the RPM attainable with a given propeller, the model flier then can assess the suitability of the propeller for a model which flies at a particular speed, or which is intended for that speed. The chart in Figure 14.12 expresses the pitch –

Fig. 14.11 Layout schemes for varieties of non-constant pitch [nominally rated equal at 75% radius]

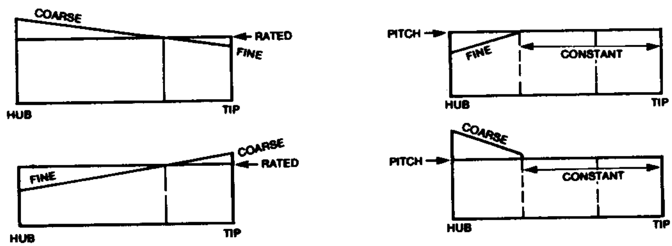

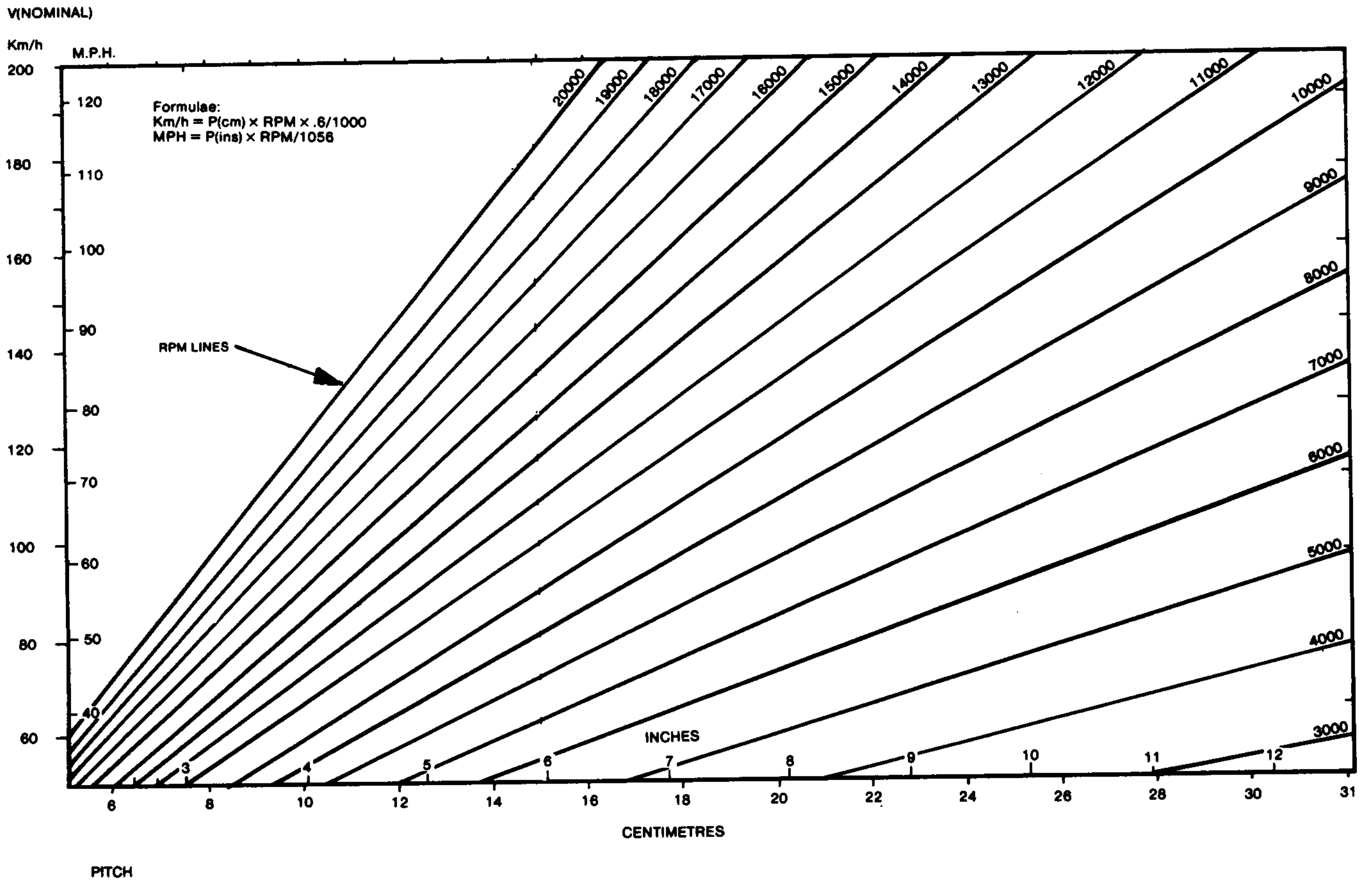

Fig. 14.12 Chart relating pitch and RPM to V

RPM – Speed relationship graphically and may be used in several ways. If the engine's RPM for maximum power is known, the appropriate RPM diagonal may be followed to read off nominal speeds and the pitches required for each. Or the design speed may be the starting point and then a series of RPM and pitch figures may be found. For points out of range of the chart, the formulae shown may be used.

The actual flight speed attained by a model depends on the thrust-drag relationship. The chart suggests not that any particular speed will be attained but only what propeller pitch is appropriate for a particular r.p.m. and speed.

14.13 MATCHING PROPELLER TO POWER

Matching propellers to the power of the engine and to a particular aeroplane is mainly a matter of experience and experiment. Engine tests carried out on behalf of model aircraft magazines and published therein usually state a range of propeller sizes and rotational speeds achieved, which form a very useful guide. The test reports also usually include a graph of power against r.p.m. (Power is rated in Watts and Kilowatts in SI units and Horsepower in Imperial measure).

An equation which is of some help in choosing a propeller diameter for a particular engine and application is the following:

$$D = \sqrt[4]{\frac{KW}{RPM^2 \times Km/h \times 24.8}} \times 24{,}500$$

where propeller diameter, D, is in centimetres and in Imperial units:

$$D = \sqrt[4]{\frac{BHP}{RPM^2 \times mph \times 53.5}} \times 10{,}000$$

Although based on work done for full-sized aircraft this gives results which seem to be applicable to model engines and propellers, although not necessarily quite accurate in every case. A scientific pocket calculator with a 'fourth root' function is required. With a rough idea of the speed of flight to be flown the pitch of the propeller follows approximately from Figure 14.12.

14.14 DOWNWASH

Like the wing, each blade of a propeller generates upwash and downwash and every blade works in the downwash created by the blade ahead of it and in the upwash of the one behind, as they follow one another round.

The distinction should be made here between blade wake and downwash. The wake of each blade, a greatly disturbed, but relatively thin, layer of air that trails behind the blade from the trailing edge, is carried away from the propeller disc by the slipstream. The profile drag of the blade is measurable as the wake thickness and loss of momentum.

The downwash is induced by the tip and root vortices and this is a general distortion of the airflow, just as with a wing. A tailplane on an aeroplane may lose efficiency by being immersed in the wing wake. But even if the tail is mounted well clear of the wake (as with a T tail), the general downwash effect is still present. With a propeller blade, the downwash of the preceding lifting surface is felt in very much the same way. Also, just as a canard foreplane works in the upwash *preceding* the mainplane, every propeller blade experiences a certain upwash effect from the blade following it. This is more pronounced in propellers with three, four or more blades and tends to reduce their efficiency compared

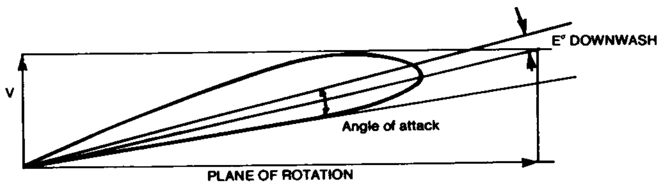

Fig. 14.13 Downwash effect on angle of attack

with a two-bladed propeller. But there are vortex-induced losses with two bladed propellers even so, because there is always a preceding and a following blade: the same one. Even a single bladed propeller, which does gain a little efficiency over the two bladed variety, works constantly in its own downwash and upwash. (Single bladed propellers must be balanced and this usually requires at least a stump, suitably weighted, opposed to the blade. This creates drag, so the full gain in efficiency is not realised in practice.)

Figure 14.13 shows how the aerodynamic angle of attack of a propeller blade is affected by downwash. As with a wing, the effect is a considerable increase in drag for a given lift coefficient. However, because the propeller is turning and the outer segments necessarily move through the air at a greater speed than the inner ones, and the blade itself is twisted, the pattern of the vortices is more complicated than for a wing.

In Figure 14.14, a single blade is shown with a vortex at the outer tip and one at the root. It is assumed for the moment that the blade is of the paddle type so that there is nothing to interfere very much with the formation of the inner vortex. The blade is physically twisted to accord with the constant pitch requirement. The vortex from the outer tip of the blade leaves the tip with the relative airflow there. Since the tip is moving forwards as well as rotating, the vortex forms in a helical fashion behind the propeller. The vortex at the hub end or root also leaves the blade aligned roughly with the relative flow, but here the airstream is almost aligned with the direction of flight and the inner vortex therefore streams more or less directly aft.

If the single blade is now supplemented by a second one in the usual way, a fuller pattern appears. Two outer vortices are produced which trail away helically with the

Fig. 14.14 Vortices from a single blade

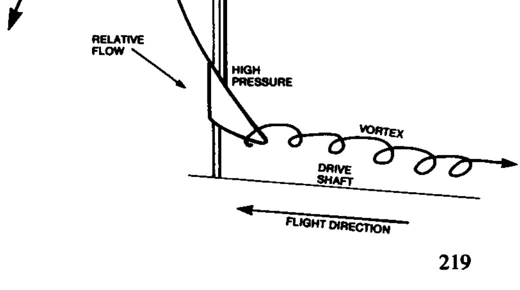

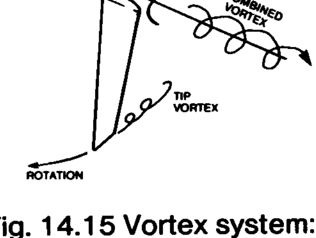

Fig. 14.15 Vortex system: two bladed propeller

general airstream. At the centre, the two inner vortices, which are rotating in the same direction, wind together to form one central vortex which streams directly aft.

The final vortex pattern is thus represented in Figures 14.15 and 14.16. Of course, immediately behind the hub of a real propeller there is usually an aeroplane fuselage or at least a nacelle containing an engine, with, probably, various cooling ducts and cowlings. The hub itself may be faired with a spinner. All these interfere with the central vortex and restrain it, just as an end wall in a wind tunnel restrains the tip vortex if the test wing entirely spans the gap between the walls. Nonetheless, the propeller produces, as far as it can, a strongly rotating vortex which flows immediately over the parts of the aircraft that lie in its path. The rotation lends its strength to the general slipstream rotation which is caused by the profile drag of the blades and their wakes.

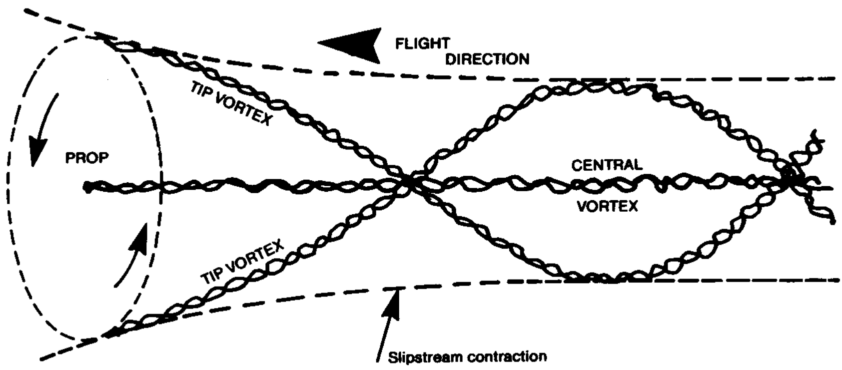

Fig. 14.16 The vortex system of a two-bladed propeller

14.15 REDUCING VORTEX DRAG ON PROPELLERS

The least vortex drag for a wing is found with a perfectly elliptical chord distribution. The equivalent shape for a propeller can be found by calculation but it is not an ellipse. This is because the tips of the blades move faster through the air than the roots, so that, in a given time, more air mass is affected by them. The effect of this and other factors is to require, for least vortex drag, a narrower blade profile near the tips than a purely elliptical form, and, near the blade roots, a somewhat broader than elliptical shape. (This refers to the developed planform, when the chord at each place along the blade is plotted in two dimensions as if the blade were straightened out.)

The importance of this discovery, largely due to Eugene Larrabee, may be gauged from the fact that the manpowered aircraft, Gossamer Albatross, which crossed the English Channel, was incapable of staying in the air for more than a few minutes, until Larrabee's design of propeller was adopted. Unfortunately, model aircraft propellers generally are constrained in design by factors other than aerodynamics, especially the need for strength and stiffness under very high loads, and ease of manufacture.

14.16 BLADE SECTIONS

The choice of aerofoil section for propellers is also conditioned by structural factors, especially near the hub, where strength is very necessary and the profile must be thickened considerably. Fortunately, this part of the blade is least important from a thrust point of view. Because of the high r.p.m. at which the model engines run, Reynolds number effects are less significant, on all but rubber-powered models, than for wings. The blade Re of a model propeller usually is comparable with that of a light aeroplane. Accordingly, aerofoils which are satisfactory on large propellers prove the same on models. Many of the boundary layer flow characteristics that plague model wings tend to disappear with propellers, again except for the rubber driven variety. In addition, the boundary layer flow on a propeller is very much more complex than on a simple wing. The lowest layers, which are dragged along almost at the same velocity as the blade itself, are accordingly subject to strong centrifugal forces, which extend upwards to the rest of the boundary layer in proportion as the air travels round with the blade rather than staying with the general airflow. Within the boundary layer there are strong cross flows. Small vortices form, which almost certainly turbulate the air and probably prevent laminar flow altogether. Partly for this reason, not much effort has been put into designing very refined, low drag profiles for propellers on model aircraft. With rubber driven and indoor types, although there has been much experiment and experience over the years, it cannot be claimed that any very startling improvements have appeared.

14.17 ENGINE VIBRATION EFFECTS

Model internal combustion engines, usually one or two cylinders, tend to transmit their power to the propeller in a series of rapid jolts which cause great stresses in the propeller blade. There is also an aerodynamic effect of almost unknown importance. It may be that the boundary layer is repeatedly stripped off and left behind as the blade accelerates after

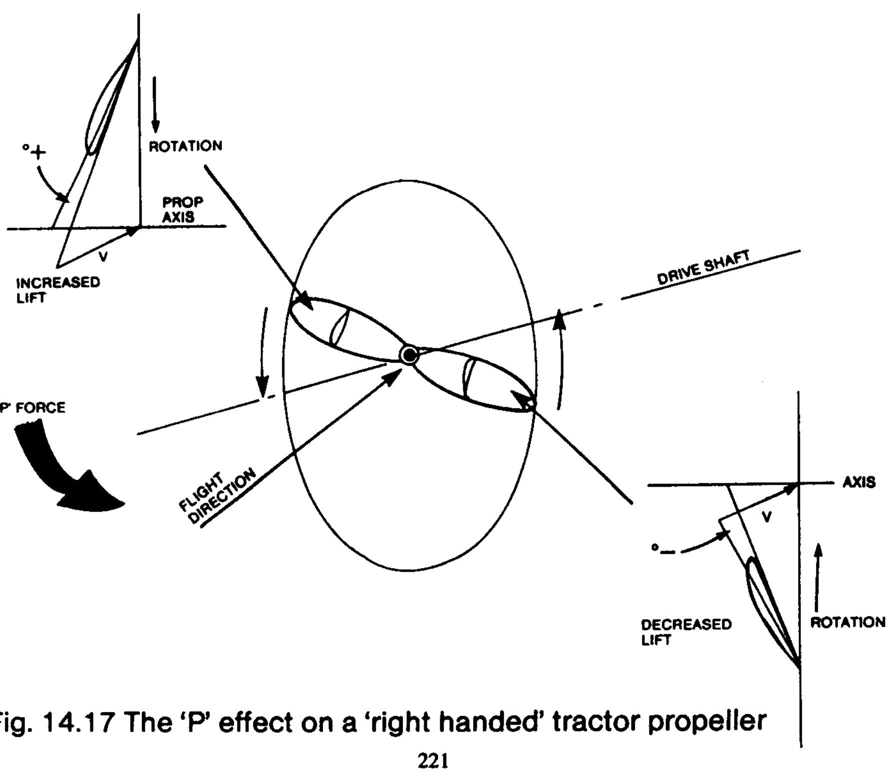

Fig. 14.17 The 'P' effect on a 'right handed' tractor propeller

the power stroke of the motor, to re-form briefly before the next stroke. Just what effects this has on the efficiency of the propeller is hard to say. So far as known, no serious research has been done on the matter. This effect is not important with electric motors.

14.18 THE 'P' EFFECT

Even if, by careful design and trimming, the drive shaft of the propeller is exactly aligned with the flight direction at some airspeed, in every other trim, such as 'nose-up' just prior to landing, the propeller will not meet the airflow exactly 'square' on. The disc of rotation will be inclined at some angle other than 90 degrees to the approaching flow.

This produces a force component acting at right angles to the drive shaft. The explanation is sketched in Figure 14.17. Here the aeroplane is in a 'nose-up' trim. The propeller blade on the port side experiences a reduction in angle of attack and the blade on the starboard side an increase. This produces more thrust on the starboard side and less on the other so the 'P' force tends to yaw the aeroplane to port (left, viewed from aft). Similarly, if the propeller disc is aligned nose-down, the 'P' force tends to yaw it to the right and side slipping trims have equivalent nose-up or nose-down force effects.

In normal flight, these forces are trimmed out without any difficulty. That is, part of the exercise of trimming a model for level flight involves use of rudder to counteract any yawing imbalances and elevators to balance the total pitching moments, whatever their cause. Model fliers are thus rarely conscious of the 'P' force since this is lost in the general balance equation. However, if there is a *change* during flight, in the alignment of the propeller axis, the 'P' force changes and the balance is upset. However, the reaction of the propeller to such an imbalance is not a simple yawing or pitching force. The 'P' force is at right angles to the drive shaft, and the propeller's reaction, due to gyroscopic precession, is at right angles again to the 'P' force, in such a manner as to de-stabilise the aircraft, i.e. to exaggerate the change.

14.19 GYROSCOPIC EFFECTS

Gyroscopic effects arise from the propeller and rotating parts of the engine. Fortunately on models these are small, but may sometimes be responsible for unexpected behaviour. The propeller on normal models rotates anti-clockwise when viewed from the front. A turn or yaw of the model to the left rotates the gyroscopic axis of propeller and motor. The response is a force tending to raise the nose of the model. This nose up pitch causes a gyroscopic reaction to the right. This yaw or turn to the right causes a nose down pitch and as the model pitches nose down gyroscopic reaction tends to yaw it left, and a nose up pitch follows again, causing a yaw to the right. This sequence is known as precession, and if the effect is noticeable at all, which it may be with a propeller which is heavy and rotating relatively fast, the model may 'precess' continuously under power, apparently 'weaving' slightly: up, to the side, down, to the other side, up, and so on. A spinning top exhibits a similar pattern, and on some early full-sized aircraft with 'rotary' engines, the effect was very pronounced and responsible for many accidents. In a model the 'weaving' caused by precession may react with torque or other more truly aerodynamic effects, to cause stability problems. The 'P' force of a propeller is a case in point. A change of trim to bring the model in for landing causes a yaw due to the 'P' effect. This produces a nose-up gyroscopic precession (see also 15.7). In a spiral climb gyroscopic forces are particularly important since the model is turning all the time in one direction, bringing about a nose up or nose down gyroscopic moment. Substitution of a lighter propeller may help the modeller in such a situation. Note, however, that in a straight climb at a constant angle, no gyroscopic reaction arises.

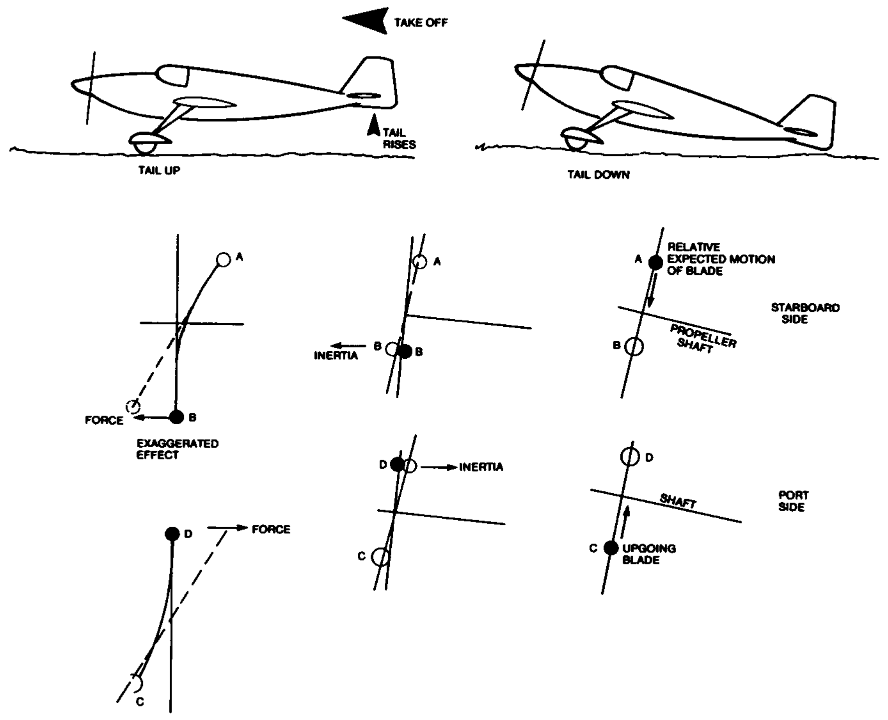

Fig. 14.18 Gyroscopic effects

Gyroscopic reactions at take off with 'tail dragging' models may cause problems. As the tail wheel or skid comes off the ground, the rotating mass at the nose of the model is forced to change the direction of its axis and responds with the usual leftward rotation, causing the model to swing. A 'ground loop' can result. Tricycle undercarriages do not suffer in the same way (although no less affected by slipstream on the fin).

A simple explanation of the cause of gyroscopic reactions is given in Figure 14.18. Here an aeroplane is shown in a rapidly changing pitch motion such as during a take-off. The plane of the propeller disc is thus rotated in such a way that each blade, instead of following its usual path, is forced to follow an arc such as A–B, relative to the original disc plane. The mass of the blade resists this change and produces a strong reaction: a force appears which tries to return the blades to their original plane. On one side of the aeroplane this force acts forwards and on the other aft, so the resultant couple yaws the aircraft to one side. With the standard right-handed propellers used on models, the yaw is to the port (left) side.

The take-off phase is particularly tricky for this situation since the rudder control which must be used to counteract the yaw while the wheels are still on the ground may be relatively ineffective due to the low forward airspeed. Full rudder may be needed sometimes, if the propeller is relatively massive and if the change of attitude when the tail comes off the ground is large. Some full-sized fighter aeroplanes have proved almost uncontrollable at this moment.

14.20 DUCTED FANS

Many models have flown very successfully with ducted fan propulsion instead of propellers. This kind of arrangement is particularly suitable for scale models of jet aircraft. Fan design is a highly specialised matter and cannot be dealt with in detail here. In theory the fan can achieve more thrust than a propeller of the same diameter, at low speeds of flight, for a variety of reasons. The duct constrains the air so that all the energy from the fan is expended in accelerating the flow. The constriction of the 'slipstream' diameter characteristic of propellers does not occur.

The walls of the duct act as endplates to the fan blades, restraining the tip vortices and increasing their efficiency. Because the fan is of small diameter, high rotation speeds are attainable and the number of blades may be increased to create high thrust.

The disadvantages, for models, are that the engine is mounted within the duct and relies on the flow through it for cooling. This increases the drag and reduces thrust. The duct walls, which, in scale models, are usually very long relative to the fan diameter, exert drag on the airstream both before and after it passes through the fan. The size of the duct opening and exit are of critical importance and it is often necessary to increase these, departing from scale outlines, in order to achieve adequate thrust. Resonance of the blades can also cause trouble (an odd number of blades is necessary).

As has been demonstrated frequently, with careful design and experiment, these problems can be overcome, but there is, as yet, no very precise method of designing a model fan which can be guaranteed to equal the thrust from an equivalent (though larger diameter) two bladed propeller and engine.

15
The helicopter rotor

15.1 GENERAL POINTS

A complete account of helicopter aerodynamics, even a very simple one, would require another book. A full analysis would fill, and does fill, many books, necessarily of a highly mathematical and specialised kind. An excellent non-technical introduction to the subject is to be found in John Fay's book, *The Helicopter, History and How it Flies*. There are several very good practical guides to radio control model helicopters, some of which are listed at the end of this chapter. All that will be attempted here is to give a very brief account of some aspects of the helicopter rotor of particular interest to the aerodynamicist.

15.2 THE ROTOR AS A PROPELLER

The basic idea of the helicopter is simple enough at first sight. A propeller rotating round a vertical axis with suitable blade pitch and power is able to carry an aeroplane straight up in a vertical climb. A helicopter rotor is a very large propeller adapted to give all the support needed for flight without any fixed wing surfaces.

Most of what has been said already about propellers may therefore be applied, with necessary changes, to rotors. Each rotor blade is of appropriate aerofoil cross section and generates lift because it meets the airflow at a positive angle of attack. Like a propeller blade, a rotor blade may stall if the angle of attack is too large. The forces upon it are resolved into lift and drag and there is a pitching moment, the last being zero if the profile is symmetrical (Figure 15.1). Because the blades are usually of very high aspect ratio and slender, they tend to flex in flight and severe stresses are set up. Strong centrifugal forces

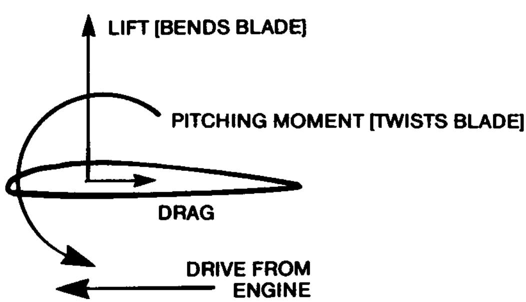

Fig. 15.1 Forces on a rotor blade

are caused by the rapid rate of rotation. As with a propeller, the tips achieve much greater airspeeds than the roots and on full-sized rotors, high Mach numbers are reached and compressibility and noise problems arise.

Like a propeller, the drag of the rotor, consisting of profile and vortex drag, sets up a strong torque reaction at the hub. In twin rotor helicopters, the two rotors turn in opposite directions and cancel each other's torque. The first truly successful helicopter, the Focke Achgelis of 1936, was of this kind. With the much more common single rotor arrangement, the torque is trimmed out by a small second rotor set on a boom with its plane of rotation at right angles to the main rotor disc. By changing the speed and pitch of the blades of the tail rotor, varying torques from the main rotor can be balanced in all flight conditions. Flow conditions around the torque-balancing rotor are extremely complex because it works in air greatly disturbed by the main rotor. It is known that considerable differences in control and handling of a helicopter arise when the tail rotor is arranged as a 'tractor' on one side of the supporting boom, instead of as a 'pusher' on the other.

15.3 HOVERING

In hovering flight, the vertical upward lift from the rotor equals the weight of the entire aircraft plus an additional quantity to account for the drag of the rotor wash, or slipstream, over the body (Fig. 15.2).

The Froude efficiency criterion used for propellers is of little meaning for helicopters since, when hovering, it is zero. The efficiency of a rotor in hover is sometimes expressed as a figure of merit, which relates the engine power delivered at the drive shaft to the minimum power required to support the aircraft. The more efficient the rotor and the higher the figure of merit, the less engine power is wasted.

15.4 GROUND EFFECT

When near the ground, the rotor wash spreads out and the high pressure region under the helicopter forms a cushion similar to that which supports a hovercraft, though without the restraining side curtains. Because of this ground effect, power needed near the ground is less than higher up. This may be of assistance when taking off but can cause difficulties if power is insufficient to climb away afterwards. On landing, the ground effect tends to check the rate of descent and may cause an aerial 'bounce' (Figure 15.3, p.220).

15.5 VERTICAL CLIMB

To climb vertically the total lift force required, once the ascent is established at a steady rate, is slightly greater than for hovering, the difference being only the difference in drag of

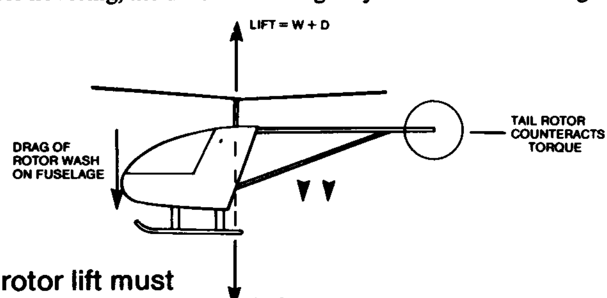

Fig. 15.2 In hovering, rotor lift must equal weight plus drag.

Fig. 15.3 Ground effect

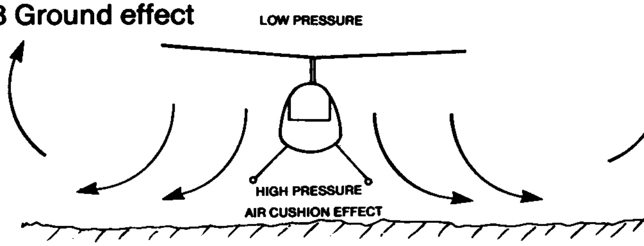

the fuselage in the rotor slipstream, which is faster than when hovering (Figure 15.4). However, the engine power required is considerably more. To initiate the climb, either the rotor speed must be increased, to produce more lift, or the angle of attack of all the blades must be increased. Many successful model helicopters have flown with the rotor speed as the only control for climbing or descending. The disadvantage is that the engine and rotor cannot respond instantly to commands so there is a delay with each change as the rotor accelerates or decelerates. More commonly now, and universally with full-sized helicopters, the lift is governed by collective pitch control (Figure 15.5, p.221).

The collective pitch control rotates all the blades simultaneously to a greater pitch so that they present a higher angle of attack to the air. Since they work at an increased lift coefficient, the strength of the vortices at the tip of the blades increases at once. The profile drag may also increase, depending on the aerofoils section and its drag bucket (see Chapter 9). In any case, there is a marked increase of drag and torque. To keep the rotor turning sufficiently fast to produce the required additional lift to start the ascent, more engine power must be used. In full-sized helicopters it is usual to couple the collective pitch control to the engine throttle to ensure that this extra power is provided automatically when required. Without this, it is easy for the pilot, by coarse use of collective pitch, to slow the rotor down and this can result in less, rather than more, lift force and a descent instead of a climb.

Once the vertical climb has been established, the motion causes further changes of the relationship of pitch angle to airflow, just as a propeller in forward flight has the relative angle of its blades changed by the forward flight velocity.

15.6 VERTICAL DESCENT: VORTEX RINGS

With reduced power and/or less collective pitch, the helicopter can descend vertically. In doing so, it tends to fly into its own slipstream and if the rate of sinking is rapid, it may come to equal, or nearly equal, the rotor downwash. In this rather dangerous condition not only is the air very turbulent, but a vortex ring may easily develop. The slipstream from the rotor is at high pressure while above the blades the pressure is low. The air flows up round the limits of the rotor disc and re-enters the low pressure zone, to be drawn down

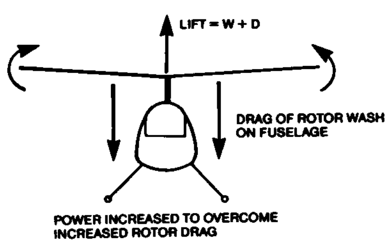

Fig. 15.4 Vertical climb

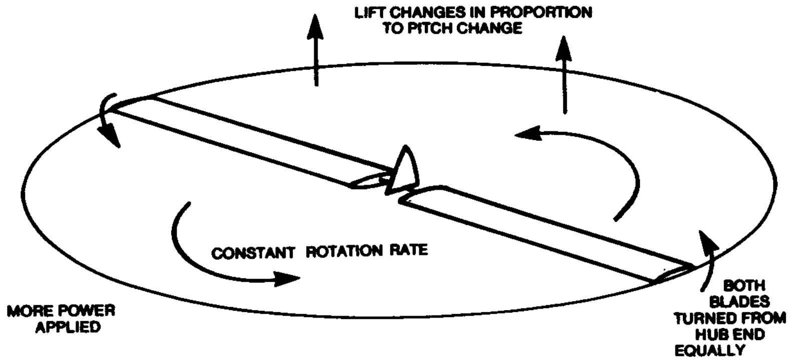

Fig. 15.5 Collective pitch change

again through the rotor. The helicopter then is effectively flying in the middle of a strong downdraught of its own making. The entire vortex ring tends to become a self-contained system and sinks through the surrounding air rapidly. (Figure 15.6. The situation is closely analogous to the ascent of a buoyant ring-vortex thermal.) Fortunately, the danger of a crash can be avoided by trimming for a forward (or any other direction) motion so that the rotor does not drop into its own slipstream but constantly enters new, relatively undisturbed air.

15.7 TRANSLATIONAL FLIGHT

A helicopter relies on its main rotor for thrust as well as lift. By tilting the plane of rotation (Figure 15.7) the lift vector is inclined forwards (or in another direction) and the resolved forces then move the aircraft horizontally. The direction of the motion is not dependent on the alignment of the fuselage, but only on the tilting of the rotor disc. Thus helicopters can move sideways or backwards with ease. To save fuselage drag in normal operations, the tail rotor is used to align the body with the flight direction.

Once moving, less engine power is needed, at a given altitude, than when hovering. The situation is roughly comparable to the efficiency of a propeller when not moving forward and when flying fast. In a given unit of time, a larger mass of air moves through the actuator disc, so the thrust, or lift, required can be obtained by giving a smaller

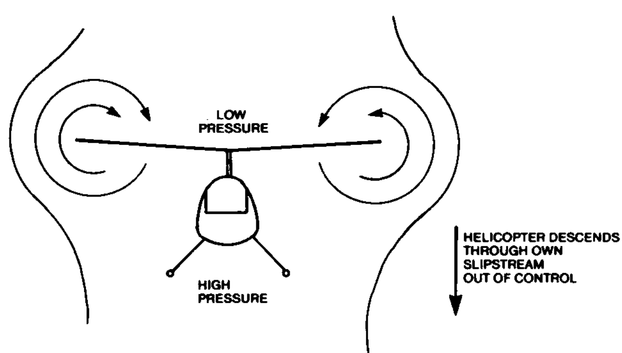

Fig. 15.6 The vortex ring

Fig. 15.7 Tilting the rotor disc to provide horizontal force

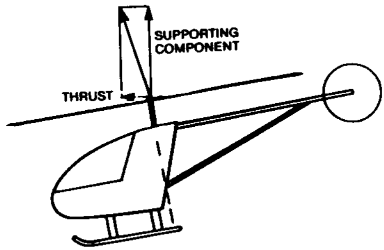

momentum to a large mass instead of a large momentum to the smaller quantity of air. Because of this, helicopters are capable of very much higher flight ceilings when in translational flight than hovering. In marginal take-off conditions it is possible to use the ground effect to get off the ground and immediately to move forward, taking advantage of the increased efficiency to gain height.

15.8 CYCLIC PITCH CONTROL

It is possible to tilt the rotor of a helicopter, relative to the body, by changing the alignment of the entire drive shaft and even the engine, which can be suspended on gimbals to permit this. The complications are considerable and there is a much better way of tilting the plane of rotation which involves cyclic pitch change of the rotor blade's angles. By means of a swash plate or some equivalent device, as each blade rotates it is turned progressively to a different pitch so that in relation to the air it reaches a maximum angle of attack, and so produces more lift, at one radial position, and a minimum angle at the diametrically opposite pole. In the case of a two bladed rotor, one blade is at the maximum when the other is at the minimum. The cyclic pitch changes are superimposed on the collective pitch so that each blade maintains the same average pitch and lift as it rotates and the total lift of the entire rotor system is maintained at that required to support the aircraft, while at any particular place round the circle, an individual blade may be at lower or higher angle of attack than the mean.

The individual blades are hinged near the hub, or are mounted on a supporting member which is flexible so that the cyclic pitch changes cause the blades to ride up when the pitch is large and descend when it is less.

Viewing the entire rotor disc as a whole, somewhat like a large wheel, the cyclic pitch change applies a force tending to change the rotational axis. There is a gyroscopic reaction which is 90 degrees out of phase with the tilting force. Hence the actual disc tilt is 90 degrees out of phase with the cyclic pitch control. This kind of effect appears on

Fig. 15.8a Cyclic pitch tilts rotor

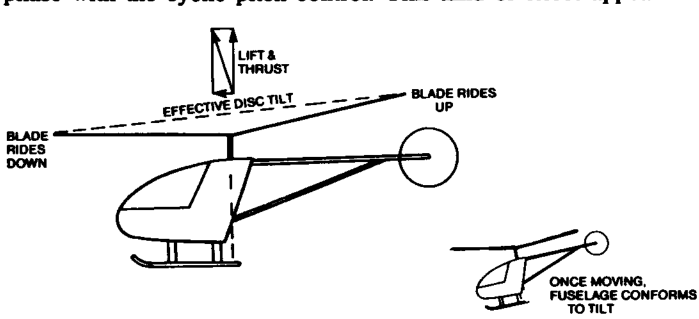

Fig. 15.8b Cyclic pitch control

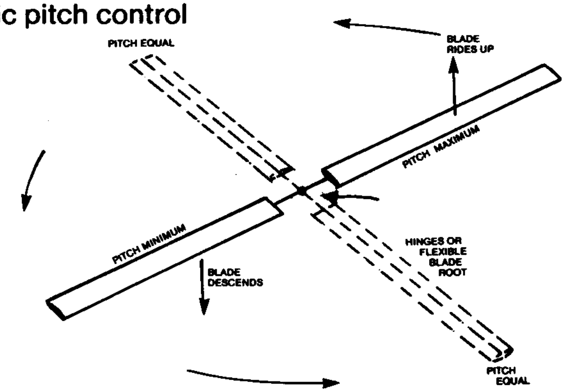

propellers too, as shown in Figure 14.18, where a 'tail up' change of the axis produces a yaw to the side. If the diagram or Fig. 14.18 is imagined as representing a helicopter rotor with the disc more or less horizontal, the effect of cyclic pitch may be more readily understood. (An even more impressive demonstration may be done with a bicycle wheel. If the wheel, detached from its supporting frame, is spun rapidly in a horizontal plane and an attempt is made to tilt it by applying a force in one direction, the actual response is a tilt 90 degrees out of phase – i.e. a sideways tilting effort producing a forward or backward tilt.)

Once the helicopter is moving in the desired direction, the drive axis aligns itself with the new angle of the disc, so the fuselage of the aircraft in forward flight takes up a nose-down attitude. Relative to the aircraft, the disc is then not tilted and the cyclic pitch control may be returned to neutral, being used thereafter only to trim for the desired speed. This is an important feature of controlling helicopter flight, since the normal 'down trim' required with a stable, fixed wing aircraft is not required or desirable with a helicopter. In this sense, helicopters tend to be neutrally stable. (Refer to Figure 12.1)

15.9 BLADE FLAP

In translational flight, the blade on one side of the line of movement, now called the advancing blade, meets the air at a higher velocity than the other retreating, blade. Since, at a given angle of attack, lift depends on flow speed, this would cause an effect on the helicopter rotor exactly analogous to the 'P' effect on propellers when these are not aligned with the flight direction (Fig. 15.10). To prevent this, it is essential to reduce the angle of attack of the advancing blade and increase that of the retreating blade, to

Fig. 15.9 Gyroscopic 90° out-of-phase reaction

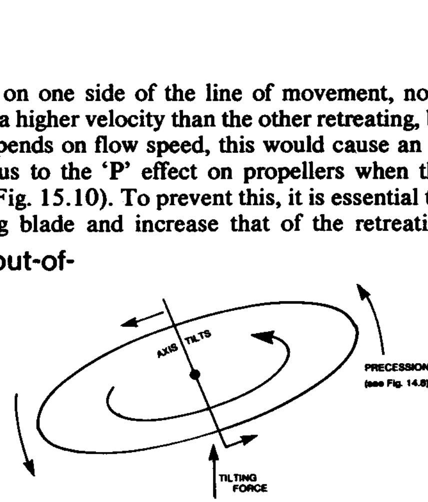

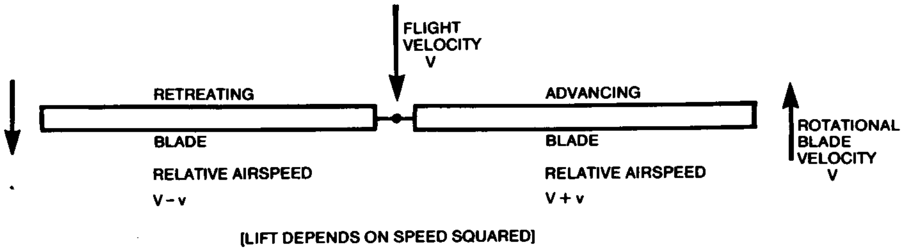

Fig. 15.10 Lateral imbalance

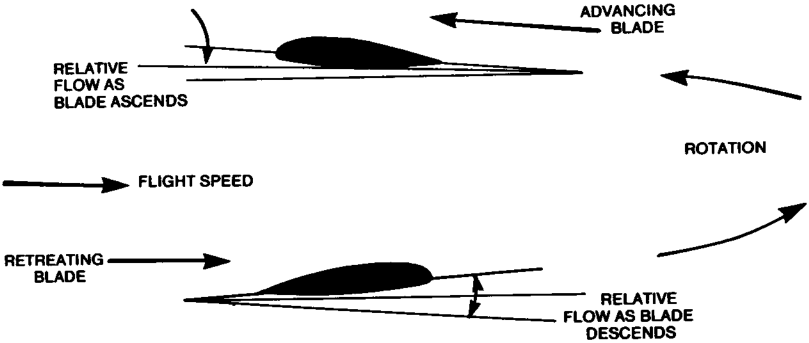

Fig. 15.11 Blade flapping to equalise lift in forward flight

maintain equal forces on both sides. This is achieved by allowing the blades to hinge, or flex, up and down freely under the air loads they meet. As the advancing blade rises, its angle to the airflow is reduced (Figure 15.11). Conversely, as it moves round to the retreating position, it flaps down, so increasing its angle of attack. The total lift force is thus equalised laterally. Blade flapping is automatic and self adjusting to a large extent, since any untoward rolling force causes the blades to hinge up and down rather than tilting the helicopter as a whole.

15.10 RETREATING BLADE FLOW REVERSAL

The forward speed of the helicopter at any time may be compared with the rearward speed of any segment of the retreating blade. The innermost part of the blade moves aft relatively slowly compared to the forward velocity of the entire rotor system. Even at slow flight speeds, some part of the rotor on the retreating side will therefore experience reversed flow. Since the first few percent of the blade is invariably occupied with hub mechanism, pitch control pushrods and hinges or flexible support, the effect is of little importance when the forward speed is slow.

As the helicopter accelerates towards its maximum flight speed, even though the rotor speed as a whole may increase, the area of blade which comes under reversed flow extends further outwards (Figure 15.12). When this begins to affect the aerofoil shaped part of the blade, not only does this segment produce no supporting lift but, because the blade is now meeting the air backwards at a negative angle of attack, a downforce results. Further out still there is a point on the blade where there is no relative movement of the air (other than some outward dragging because of centrifugal forces). Beyond this, the blade begins again to produce lift.

The outer parts of the retreating blade at high speed are required to produce as much lift, at their lower relative airspeed, as the entire advancing rotor on the other side, plus an additional quantity to compensate for the downforce in the reversed flow region. To do this, blade flap increases the angle of attack on the retreating side considerably.

15.11 RETREATING BLADE STALL

The limit to a helicopter's forward speed is reached when the retreating blade's outer parts reach their stalling angle.

15.12 AUTOROTATION

If a helicopter suffers engine failure it may be trimmed for autorotation, which is equivalent to gliding with a fixed wing aircraft. In this condition, instead of air being

Fig. 15.12 Reversed flow on retreating blade

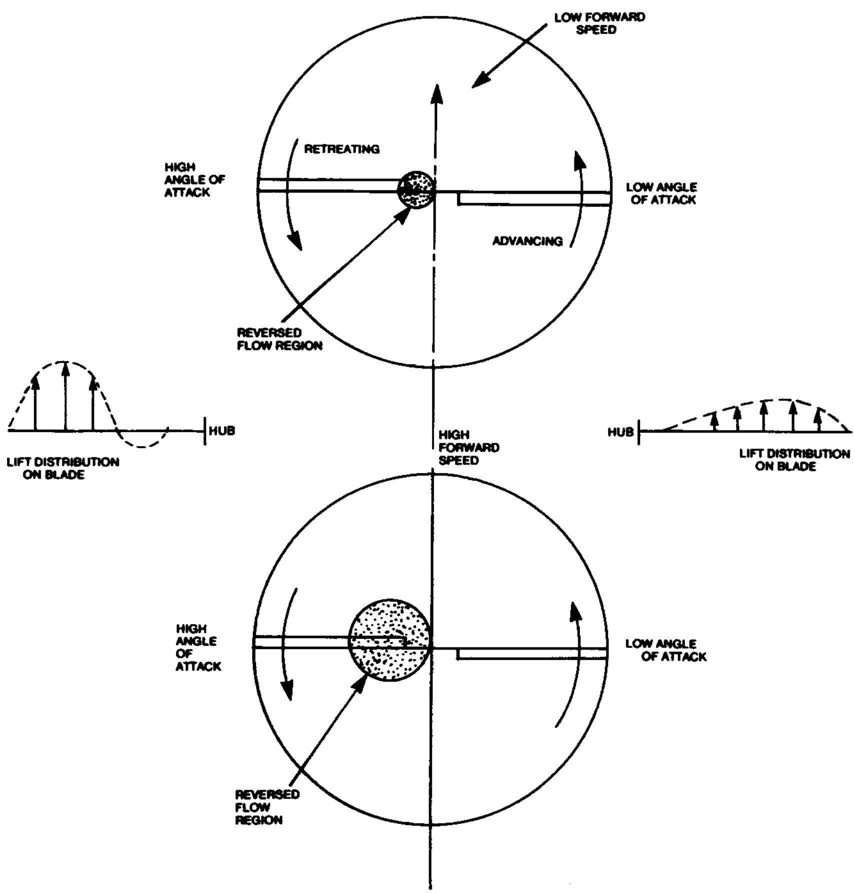

Fig. 15.13 Forces on autorotating blade

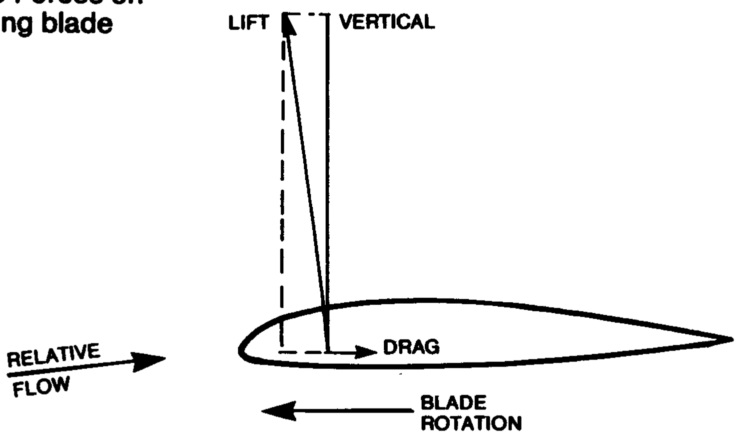

drawn down through the rotor disc the rotor as a whole is inclined at a slight positive angle to the airflow, which streams upwards through the disc. The conditions on an individual blade are such that they continue to turn rapidly enough to provide support. As shown in Figure 15.13, the forces on an autorotating blade are identical with those on the whole wing of a glider, a component of the lift being set off against the drag to keep the aerofoil moving through the air. The helicopter as a whole then may glide some distance before being compelled to touch down and it may be steered with the cyclic pitch control.

15.13 GYROCOPTERS AND AUTOGYROS

The autorotation capability of a rotor enabled gyrocopters (autogyros) to fly successfully long before helicopters were developed. Forward motive power is supplied by an ordinary propeller, rigged either as a 'tractor' or 'pusher', but the lift comes from a freely spinning rotor which may be tilted to provide control, and has the usual hinged and flapping blade system. Take-off may be accomplished by running along the ground until the rotor is turning sufficiently fast to give the required lift. The take-off distance can be shortened if the rotor is given a preliminary spin by hand before starting the ground run.

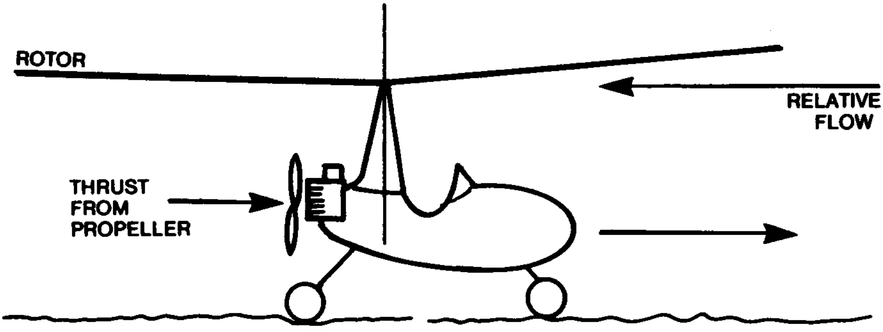

Fig. 15.14 The gyrocopter taking off

Juan de Cierva's autogyros of pre-1939 times were capable of near vertical take-off because a drive shaft was connected to the rotor with a clutch from the main engine. With blades set in zero collective pitch the rotor was spun up to high speed and allowed then to turn freely while the drive was declutched, all the engine power turning the propeller. The rotor was then set to positive pitch and the craft would leap into the air, quickly accelerating horizontally under the propeller thrust. Landings were by gliding descent and the ground run was very brief.

Model autogyros are occasionally seen and all the same principles apply to them as to the full-sized aircraft. Although there is no strong torque reaction, as there is with a helicopter, the autogyro rotor does tend to turn the fuselage because of the friction of the main bearings, which cannot be entirely removed. It is therefore necessary to provide some aerodynamic means of aligning the fuselage with the airflow and this requires at least a vertical fin to give a weathercocking action. A rudder is also useful. Other wing and tail-like surfaces may also be used to supplement the rotor lift and control the attitude in flight.

15.14 REFERENCES

JOHN FAY *The Helicopter, History and How it Flies.*

JOHN DRAKE *Radio Control Helicopter Models*, Argus Books, 1980.

DAVE DAY *Flying Model Helicopters*, Argus Books, 1986.

DIETER SCHLÜTER *Schlüter's Radio Controlled Helicopters*, Argus Books 1986

Appendix 1

In this appendix a few of the more interesting calculations that amplify the main text are given in more detail. No attempt has been made to include everything relevant. It is assumed that modellers wishing to go deeper into aerodynamic theory will seek out appropriate standard textbooks for themselves. The examples worked here, however, are in all cases mathematically very simple and are not beyond the powers of the average aeromodeller. Some important textbooks for further reading are listed below. These, in turn, will refer the student to more advanced works if required.

SYSTEMS OF UNITS

In measuring mass and forces in engineering, various systems of units are used. Which system is adopted is a matter of convention and convenience, but the Système Internationale or S.I. system is adopted officially in many parts of the world. In this system the unit of mass is the ***kilogramme***, the unit of acceleration is the ***metre-per-second-per-second***, or m/s^2. A force, as the second law of motion indicates, is measured in terms of the acceleration of a mass, or: Force = Mass × Acceleration. In S.I. units, the unit of force becomes the ***Newton***, one Newton being the force required to accelerate one kilogramme of mass at one m/s^2. The mass of a model, on or near the planet Earth, is constantly acted on by the acceleration due to gravity, which has for practical purposes the value of 9.81 m/s^2. Hence a model of 1 kg. ***mass*** exerts a downward force or ***weight*** of 1×9.81 Newtons. Metric kitchen scales in common use do not usually read in Newtons, but so long as they are used on Earth, they may be taken as reading kilogrammes directly as units of mass. In aerodynamic figuring, however, the forces must be expressed as Newtons to maintain consistency. Many modellers are accustomed to other systems, such as the British Imperial system, or some variety of it. In this, the unit of mass is the ***slug***, of acceleration the ***foot-per-second-per-second***, of force, the ***pound-force***. Scales reading in pounds measure the ***force*** exerted by one slug of mass under the influence of Earth's gravity. The acceleration due to gravity is 32.2 $ft./s^2$.

There are other systems of units. Which is used is a matter of individual preference, but whichever is employed it must be consistent, so that one unit of force always equals one unit of mass multiplied by one unit of acceleration. If this rule is not observed confusion results. A fuller explanation of the rival systems of units with conversion scales may be found in ***Metrication for the Modeller*** (M.A.P. Technical Publication, 1972).

WORKING OUT THE LIFT COEFFICIENT

To calculate the lift coefficient of a model in a given trim condition it is necessary to know the speed at which it is flying, its wing area, and flying weight. The speed is easy to determine if the model can be flown several times over a measured distance and timed with a stopwatch. Allow for any wind. For free flight models such timed flights can be done by making a series of straight glides from a high point, in calm air. Radio controlled models are, of course, easier to time accurately.

The standard lift formula may be re-arranged to give C_L in terms of model weight. If it scales 1 kg. this indicates a mass of 1 kg. It then needs a lift force of 1×9.81 Newtons to support it. The formula then may be applied as shown:

$$C_L \text{ (whole model)} = \frac{9.81}{\frac{1}{2}\rho V^2 S}$$

A numerical example: Suppose the model mass is 1 kg., area 0.2 m^2, speed 12 metres per second. Assume air at standard mass density of 1.225 kg./m^3.

$$\begin{aligned} C_L &= 9.81 \div (\tfrac{1}{2} \times 1.225 \times 12 \times 12 \times 0.2) \\ &= 9.81 \div 17.64 \\ &= 0.556 \end{aligned}$$

The same example worked in Imperial Units:
1 Newton force equals 2.205 lbs. force, 12m/sec equals 39.37 ft/sec., 0.2 sq. metres equals 2.1492 squ. ft. Assume standard density of .002378 slugs/cu. ft.

$$\begin{aligned} C_L &= 2.205 \div (\tfrac{1}{2} \times .002378 \times 39.37 \times 39.37 \times 2.1492) \\ &= 2.205 \div 3.9608 \\ &= 0.556 \end{aligned}$$

This establishes that the coefficient of lift is the same whatever units are employed in the calculation, providing a coherent system of units is adopted.

The value of performing such a calculation in practical modelling is that it enables a modeller to improve his choice of aerofoil, particularly its *camber*. It may also indicate possible improvements in wing rigging angles, tailplane size, and fuselage design.

Suppose an F3B sailplane of span 3 metres and wing area 0.75 sq.m weighs, with ballast, 4 kg. It is hoped to complete the 60 metre (4×150m) speed task in 17 secs. This represents $V = 600/17 = 35.3$m/sec. on average, which includes the turns. (The actual speed on the straight will be greater.)

The lift coefficient, on average, is found from the formula:

$$C_L \text{ (mean)} = \frac{9.81 \times 4}{\frac{1}{2} \times 1.225 \times 35.3^2 \times 0.75} = \frac{39.24}{572.4} = 0.07$$

(More in the turns, less on the straight)

Suppose now the same model, unballasted, weighs 1.5 kg. and when trimmed for minimum sink flies at about 5.5m/sec. on a timed glide. The C_L then becomes

$$C_L \text{ (min sink)} = \frac{9.81 \times 1.5}{\frac{1}{2} \times 1.225 \times 5.5^2 \times .75} = \frac{14.715}{13.896} = 1.06$$

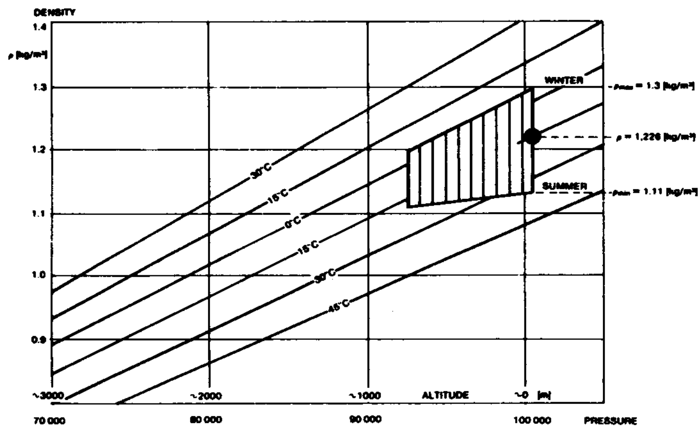

Fig. A1 Chart showing variation of air mass density with air temperature and pressure.
[Drawn by Lnenicka]

An aerofoil for such a model would require a low drag 'bucket' extending from $C_L < .05$ (nearly zero) to at least 1.06. This might be attained by using flaps.

Since the lift coefficient in the speed task is so low, very little camber is required here. A symmetrical profile would be satisfactory except in the turns. Much more camber is needed for soaring. C_L for the distance task can also be calculated.

Parasitic drag is very important at high speed, less so at soaring or distance task speeds. The fuselage should therefore be set, relative to the wing, at the angle for C_L .07 with corrections as explained below.

WHAT SHOULD THE CAMBER BE?

A mean camber line, such as those presented in Figs. 7.2 and 7.3, is designed to operate at one ideal design value of c_l. Once the camber is determined, any symmetrical thickness form or envelope may be fitted to it to give an aerofoil which will operate most efficiently at the design c_l.

For a racing model, it is first necessary to decide the speed at maximum power, straight and level. This may be measured from a real model in flight, or estimated for a new design, from previous experience. Then the model C_L may be worked out as described above. Knowing the C_L, the type of mean line required should be chosen from those in the tables (or from any similar source). Most of the NACA mean lines are worked out for a design c_l of unity. This allows the designer to arrive at the camber for his aerofoil by simple multiplication of the camber line ordinates in the NACA tables.

A worked example follows: the figures used are not intended to be representative of any modern racing model.

Model weight 1 kg. wing area 0.2 sq. metres, designed speed 20 metres per second.

$$\text{Model } C_L = \frac{1 \times 9.81}{\frac{1}{2} \times 1.225 \times 20^2 \times 0.2} = \frac{9.81}{49.00} = 0.2$$

Hence the ordinates for the NACA a = 1 mean line may be multiplied throughout by 0.200 to give the desired camber line.

For example, at 50% chord, the maximum camber point on this mean line, the camber should be:

.200 × 5.515 = 1.103, i.e. a 1.1% camber approx. for flight at this speed with this model.

If the model is in a steep turn, the required lift force, and hence the effective weight, increase perhaps to three or four times the above. The formula then must be modified:

C_L (in steep turn) = 4 × .200 = .8, requiring a camber of .8 × 5.515 = 4.120%.

A flight speed of 50 metres/sec yields: $\dfrac{9.81}{306.25} = .032 = C_L$

The required camber is then .032 × 5.515 = 0.177% and in the steep turn 0.708%. Cambers of less than 1% are thus required for pylon racing models with speeds over 180 k.p.h. or 100 m.p.h. Note also the width of the low drag range or 'bucket' on modern laminar flow symmetrical aerofoils (see Chapter 9).

THE POWER FACTOR DERIVATION

Lift in level flight may be taken as equal to weight. Then by re-arranging the lift formula:

$$V = \sqrt{\frac{W}{\frac{1}{2}\rho S C_L}}$$

For a glider the rate of sink is given by V × Sin α where α is the glide angle. As the ratio of drag to lift is also (very nearly) equal to Sin α the above expressions may be combined:

$$\text{Sinking speed} = \frac{W}{\frac{1}{2}\rho S C_L} \times \frac{C_D}{C_L} = V \sin\alpha$$

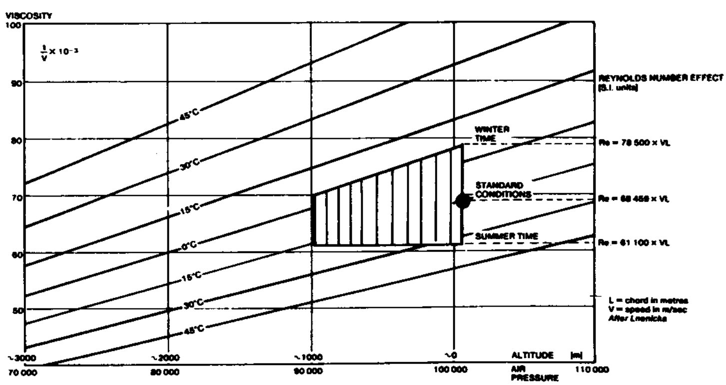

Fig. A2 Chart showing variation of Reynolds number with air temperature and pressure [altitude].
The formulae in the right hand margin give the equations for Re extremes of winter and summer at near sea level. The shaded area indicates variations with seasons and altitudes up to 1000m (3281ft).

This is simplified as shown:

$$\sqrt{\frac{W}{\frac{1}{2}\rho SC_L}} = \frac{\sqrt{W}}{\sqrt{\frac{1}{2}\rho S} \times \sqrt{C_L}} = \frac{\sqrt{W}}{\sqrt{\frac{1}{2}\rho S} \times C_L{}^{\frac{1}{2}}} = \sqrt{\frac{W}{\frac{1}{2}\rho S}} \times \frac{1}{C_L{}^{\frac{1}{2}}}$$

Hence:

$$\text{Sinking speed} = \sqrt{\frac{W}{\frac{1}{2}\rho S}} \times \frac{1}{C_L{}^{\frac{1}{2}}} \times \frac{C_D}{C_L} = \sqrt{\frac{W}{\frac{1}{2}\rho S}} \times \frac{C_D}{C_L{}^{3/2}}$$

From this it is seen that two factors affect the sinking speed, one of these contains the *wing loading*, W/S, the other is the factor $C_D/C_L{}^{3/2}$. To decrease the sinking speed, the wing loading W/S may be decreased, but this factor appears within a square root, so the effect of a large decrease of wing loading is relatively small. To obtain a larger improvement in sinking speed, $C_D/C_L{}^{1.5}$ must be reduced, or, what amounts to the same thing, $C_L{}^{1.5}/C_D$ must be increased. For steeper angles of glide, more than 10 degrees, the wing loading factor remains unchanged but the other factor is slightly modified to:

$$C_D\ (C_L{}^2 + C_D{}^2)^{3/4}$$

For a power model the lift formula is accurate for level flight, so the minimum *power* to sustain flight is arrived at thus: Power = force × distance in unit time
= Drag × Speed = DV

$$\text{Drag} = D = W\frac{D}{L} = W\frac{C_D}{C_L} \text{ (Formula for V is given above)}$$

$$\text{Hence Power} = \sqrt{W\frac{C_D}{C_L} \times \frac{W}{\frac{1}{2}\rho SC_L}} = \text{Drag} \times \text{speed.}$$

This simplifies along similar lines to the gliding equation to:

$$\text{Power} = W \times \sqrt{\frac{W}{\frac{1}{2}\rho S}} \times \frac{C_D}{C_L{}^{3/2}}$$

As with gliding, the wing loading, W/S, and the power factor must both be adjusted to achieve flight at minimum power. In addition, the *weight* alone plays a major part and the formula shows that a heavy model necessarily needs greater power for sustained flight.

THE POWER FACTOR AND L/D RATIO

For a soaring glider or duration model when gliding the total power factor, $C_L{}^{1.5}/C_D$ should be as high as possible. The most suitable wing profile is that with a high *section* power factor, $C_L{}^{1.5}/C_d$. This may be calculated from the wind tunnel results.

The table opposite indicates the method. A pocket calculator should be used to speed the work. The section l/d ratio is also worked out in the tables. This gives a general idea of the profile's efficiency, while the minimum drag coefficient indicates the potential of the aerofoil for high speed flight. A low c_d at low c_l is essential for a speed model wing.

THE BEST ANGLE OF CLIMB

It is assumed here that a duration power model has enough power available to achieve any desired angle of climb. The problem is to know which *angle* of climb, at maximum power, will give the best *rate* of ascent.

A COMPARISON OF TWO AEROFOILS AT Re 100.000

1	2	3	4	5	6	GÖTTINGEN 801 Re 100 000 (KRAEMER TEST)
c_l	c_d	c_l/c_d	c_l^3	$\sqrt{c_l^3}$	$\sqrt{c_l^3}/c_D$	
FROM TEST	FROM TEST	$\frac{\text{Column (1)}}{\text{Column (2)}}$	$(\text{Col (1)})^3$	$\sqrt{\text{Col (4)}}$	$\frac{\text{Col (5)}}{\text{Col (2)}}$	
0.4	0.0289	13.84	0.064	0.253	8.754	
0.5	0.0241	20.75	0.125	0.3535	14.668	
0.6	$\boxed{0.0218}$	27.75	0.216	0.4648	21.32	Min C_d at c_l 0.6
0.7	0.0220	31.82	0.343	0.5857	26.53	
0.8	0.0240	33.33	0.512	0.7156	29.82	
0.9	0.0260	34.62	0.729	0.854	32.85	
1.0	0.0300	33.33	1.000	1.000	33.33	
1.1	0.0317	34.70	1.331	1.154	36.40	
1.2	0.034	$\boxed{35.29}$	1.728	1.315	38.68	Max $l/_d$ at c_l 1.2
1.3	0.0378	34.39	2.197	1.482	$\boxed{39.21}$	Max power factor, c_l 1.3
1.4	0.0518	27.03	2.744	1.656	31.20	
						GÖTTINGEN 796, Re
0.4	0.0222	18.02	0.064	0.253	11.396	107,000 G. Muessman Test
0.5	$\boxed{0.0221}$	22.62	0.125	0.3535	15.995	Min. C_d at c_l 0.5
0.6	0.0222	27.03	0.216	0.4648	20.936	
0.7	0.0223	31.39	0.343	0.5857	26.26	
0.8	0.0224	35.71	0.512	0.7156	31.95	
0.9	0.0235	$\boxed{38.30}$	0.129	0.854	36.34	Max $1/_d$ at c_l 0.9
1.0	0.0265	37.74	1.000	1.000	$\boxed{37.77}$	Max
1.135	0.0400	28.37	1.462	1.209	30.23	

Starting from level flight trim, the power is increased step by step. In level flight, as already seen:

$$\text{Lift (Level flight)} = L_O = W = \tfrac{1}{2}\rho V^2 SC_L$$

This may be re-arranged to give an equation for speed:

$$V^2 \text{ (level flight)} = V_O^2 = W/\tfrac{1}{2}\rho SC_L$$

In the climb Lift (Climb) $= L_c = W \cos\theta$ Also, if V_c = speed *along the inclined flight path* then

$$L_c = \tfrac{1}{2}\rho V_c^2 SC_L = W \cos\theta$$

Re-arranging this in turn to obtain equation for V_c^2, $V_c^2 = W \cos\theta/\tfrac{1}{2}\rho SC_L$.
From the foregoing:

$$\frac{V_c^2}{V_O^2} = \left(\frac{W\cos\theta}{\tfrac{1}{2}\rho SC_L}\right) \div \left(\frac{W}{\tfrac{1}{2}\rho SC_L}\right) = \frac{W\cos\theta}{\tfrac{1}{2}\rho SC_L} \times \frac{\tfrac{1}{2}\rho SC_L}{W}$$

which cancels down to:

$$\frac{V_c^2}{V_O^2} = \cos\theta \text{ and so } \frac{V_c}{V_O} = \sqrt{\cos\theta}$$

(This is on the assumption that C_L remains unchanged, i.e. the model is not retrimmed.) In the small diagram Figure A3, V_c, the flight speed along the inclined path, is

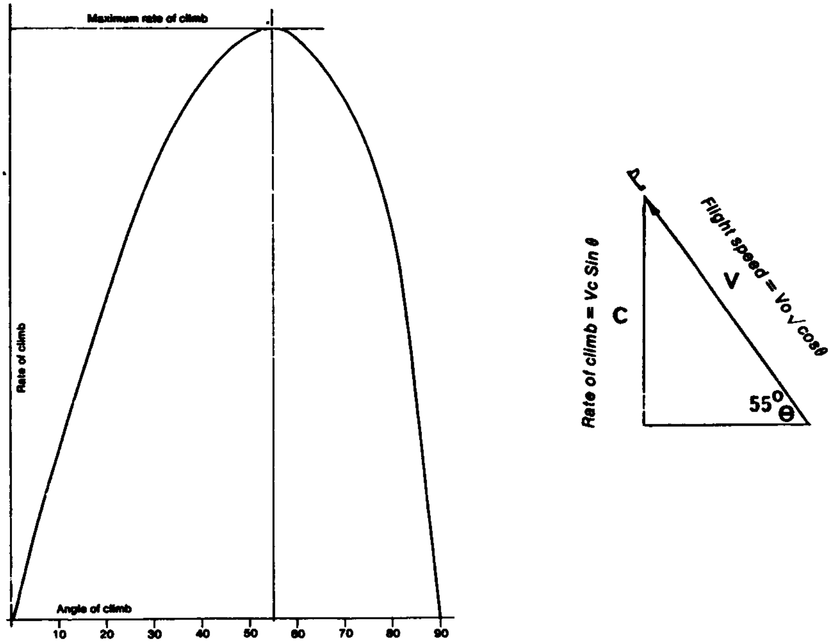

Fig. A3 The best angle of climb for a high-powered model

represented by a line at angle θ to the horizontal. The length of this line is proportional to $V_c = V_o \times \sqrt{\text{Cos } \theta}$

The *rate* of climb on this diagram is proportional to the length of the line marked C. From basic trigonometry,

$$\frac{C}{V_c} = \text{Sin } \theta \text{ or } C = V_c \text{ Sin } \theta$$

And therefore:

$$C = V_o \times \sqrt{\text{Cos } \theta} \times \text{Sin } \theta$$

For a particular model and trim condition, V_o is constant. The factor $\sqrt{\text{Cos } \theta} \times \text{Sin } \theta$ may easily be worked out, with the aid of standard tables of Sine and Cosine, for any value of climb angle, θ. The result may be plotted against θ, as has been done in Figure 4.6. The maximum rate of climb is then found to occur when the graphed curved reaches its maximum close to 55 degrees. The result is approximate. Departures of four or five degrees either way make little difference. The practical trimming procedure is thus to aim at achieving the desired climb angle by adjustments of trim, wing camber, flaps etc. then to ensure that the engine propeller combination yields maximum thrust at that angle.

ASPECT RATIO CORRECTIONS

The section power factor, and l/d ratio, as calculated above is directly taken from wind tunnel results at infinite aspect ratio. To discover the power factor for the wing on the model, the wind tunnel figures must be corrected. In the example worked below, based on the Stuttgart figures for the FX63-137 aerofoil at Re 280,000, correction for two aspect ratios has been applied to show the great effect of a.r. on soaring ability. This Re is of course high for a model, but the method is the same at any Re. Induced drag is found from the standard formula:

$$C_{Di} = \frac{C_L^2}{3.142 \times \text{Aspect ratio}} \times \text{ k.}$$

At the two example aspect ratios, 7.5 and 15, the C_{di}, the vortex-induced drag coefficient of the wing thus is found. The plan form correction, k, is assumed to be 1 for purposes of this calculation.

$$C_{Di} \text{ (a.r. 7.5)} = \frac{C_L^2}{3.142 \times 7.5} = \frac{C_L^2}{23.562}$$

$$C_{Di} \text{ (a.r. 15)} = \frac{C_L^2}{3.142 \times 15} = \frac{C_L^2}{47.124}$$

In the table, this allows the drag increment for each C_L and A.R. to be worked out in the first four columns, this is added to the profile drag coefficient read from the tunnel tests,

ASPECT RATIO EFFECTS CALCULATION

1	2	3	4	5	6	7
c_l	c_l^2	C_{di}(7.5)	C_{di}(15)	PROFILE Cd	$C_{di} + C_{dp}$	$C_{di} + C_{dp}$
from tests	$C_l \times C_l$	C_l^2/23.562	C_l^2/47.124	From tests	a.r. = 7.7	a.r. = 15
0.4	0.16	0.00679	0.00395	0.012	0.01879	0.01595
0.6	0.36	0.01528	0.00764	0.0098	0.02508	0.01744
0.8	0.64	0.02716	0.01358	0.0101	0.03726	0.02368
1.0	1.00	0.04244	0.02122	0.0107	0.05314	0.03192
1.2	1.44	0.06115	0.03056	0.0113	0.07245	0.04186
1.4	1.96	0.08318	0.04159	0.0125	0.09568	0.05409
1.5	2.25	0.09549	0.04775	0.0137	0.10919	0.06145
1.6	2.56	0.10864	0.05432	0.0149	0.12354	0.06922
1.675	2.81	0.11925	0.05963	0.0162	0.13545	0.0783

8	9	10	11	12	
C_L/C_D	C_L/C_D	$\sqrt{C_L^3}$	$\sqrt{C_L^3}/C_{di} + C_{dp}$	$\sqrt{C_L^3}/C_{di} + C_{dp}$	
a.r. 7.5	a.r. 15		a.r. 7.5	a.r. 15	
21.3	25.078	0.253	13.46	15.86	
$\boxed{23.92}$	$\boxed{34.40}$	0.465	18.54	26.66	Compare Max. L/D
21.47	33.78	0.716	$\boxed{19.22}$	30.24	
18.82	31.33	1.000	18.82	31.33	Compare Max.
16.56	28.66	1.315	18.15	$\boxed{31.41}$	Power factors
14.63	25.88	1.657	17.32	30.63	
13.31	24.41	1.837	16.82	29.21	
12.95	23.11	2.024	16.38	29.89	
12.36	22.09	2.168	16.01	28.59	

and the calculation of the L/D ratio and power factor for the wing proceeds exactly as in the table on p.163.
N.B. For an accurate result the 5th column should be modified to allow for different Re effects on profile drag, for the two different wing chords.

ALLOWANCE FOR PARASITE DRAG

After correcting wind tunnel results for aspect ratio effects, to arrive at an estimate of drag for the whole model, parasite drag must be taken into account. This may be estimated from tunnel tests on fuselages, undercarriages, etc. with an additional quantity for interference drag. As a rule such detailed estimates are not necessary for modelling. To illustrate the effect of parasite drag on performance, however, the above example is taken further. It is assumed (arbitrarily but not unreasonably) that the model with a.r. 7.5 of the previous example has a parasite drag coefficient of 0.01, this remaining constant throughout the flight attitudes considered. This assumption breaks down if the fuselage is not aligned with the average flow direction, but is sufficiently accurate for purposes of illustration.

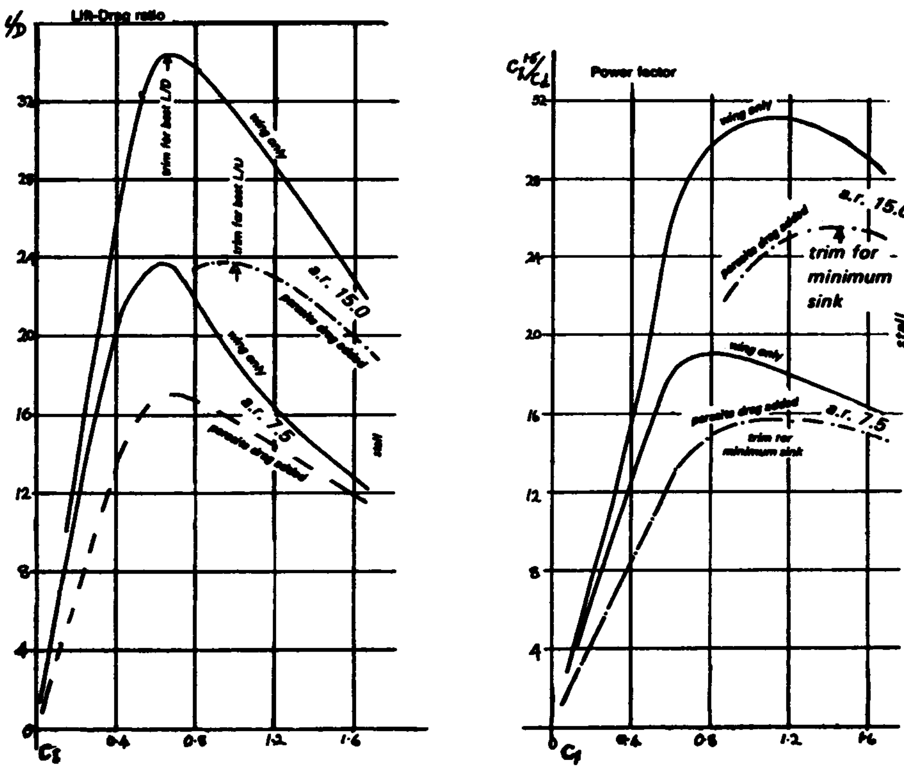

Fig. A4 Aspect ratio and parasite drag effects
Note: parasite drag has a considerable effect on the trim for best performance, shifting the peaks of the curves to the higher C_L (higher angle of attack) side.

The calculation proceeds as before: the parasitic increment of drag is added to the total of profile and induced drag, to give the total drag coefficient of the whole model. This new total is then used to work out the *model* power factor and L/D.

1	2	3	4	5	6	
cl	$C_{di} \times C_{d\rho}$ a.r. 7.5	Add parasite $C_d = .01$	$\sqrt{cl^3}$	$\sqrt{cl^3}/C_D$ Total	C_L/C_L	
.4	.01879	.02879	0.253	8.788	13.89	
.6	.02508	.03508	0.465	13.255	$\boxed{17.10}$	Max. L/D
.8	.03726	.04726	0.716	15.150	16.93	
1.0	.05314	.06314	1.000	15.837	15.84	
1.2	.07245	.08245	1.315	$\boxed{15.949}$	14.55	Max. Power Factor
1.4	.09568	.10568	1.657	15.679	13.25	
1.5	.10919	.11919	1.837	15.412	12.58	
1.6	.12354	13354	2.024	15.156	11.98	
1.675	.13545	.14545	2.168	14.905	11.52	

The power factor and L/D worked out in columns 5 and 6 are graphed and from this graph the desired C_L for trimming is found. The values for a.r. 15 are also plotted for comparison (Fig. A4).

Assuming the model weight and wing area are known, the sinking speed can be computed and plotted as shown to give the 'polar' curve of the model. This gives the minimum sinking speed by inspection. The sinking speed of a model glider (from page 232) is given by

$$\text{Sinking speed} = \sqrt{\frac{W}{S\frac{1}{2}\rho} \times \frac{C_D}{C_L^{1.5}}}$$

Assuming a model wing loading of W/S = 3 kg/sq.m. the first term becomes 6.932. Thus sinking speed at each C_L and V value is as shown for the a.r. 7.5 model:

1	2	3	4	
C_L	$V_{m/sec}$	$1/C_L^{1.5}/C_d$	Sinking Speed, M/Sec	
.4	10.96	0.11379	.7895	
.6	8.9	0.07544	.5229	
.8	7.75	0.06601	.4576	
1.0	6.93	0.06314	.4377	
1.2	6.33	0.06269	.4346*	*MINIMUM SINK
1.4	5.86	0.06378	.4421	
1.5	5.66	0.06488	.4498	
1.6	5.48	0.06598	.4574	
1.675	5.36	0.06709	.4651	

A more complete performance estimate may be attempted if full wind tunnel test results are available for the aerofoil to be used. Interesting studies are possible to illustrate the effect of increased wing loading and aspect ratio. If the wing loading is increased, the glider flies faster, which raises the Re and may improve the drag characteristics of the aerofoil. Given complete tunnel results this improvement may be estimated, and the profile drag figures in the calculation table will show the difference. Whether the improvement in profile drag is enough to offset the increased sinking speed due to the higher wing loading will depend entirely on the aerofoil and how much it is affected by the increased Re. Similarly, with a model of given wing area and wing loading, increasing the aspect ratio decreases induced drag but reduces Re, and so increases profile drag. Given adequate wind tunnel tests results, it is possible to compute the effects on model performance of such changes, and so determine the best aspect ratio.

Fig. A5 Glide polar

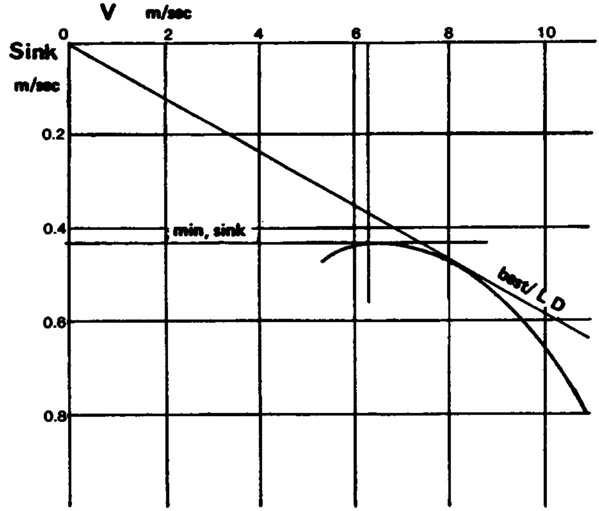

Some examples have been published by the author and are listed among the references at the end of Chapter 10.

As an illustration of the results possible, the following tables and polar curve are included, but a full explanation of the method would occupy too much space.

Velocity, M/sec: 8.30 Mean Reynolds number: 113043
Root angle of attack 15.721

Cl	Chord	Re number	Profile Cd
1.09	0.210	119345	0.02062
1.09	0.210	119345	0.02062
1.08	0.210	119345	0.02055
1.05	0.210	119345	0.01950
1.02	0.203	115634	0.03117
1.00	0.192	109108	0.03355
0.94	0.182	103534	0.03430
0.84	0.174	99050	0.03280
0.65	0.169	95766	0.03212
0.37	0.165	93763	0.02542

Mean Lift Coefficient = 1.00

Profile drag coefficient 0.0256
Induced drag coefficient 0.02256
Efficiency 0.961 K factor = 1.041

V =8.30 L/D = 20.7 Sink = 0.400

Result of calculation of glider performance at speed of 8.3m/sec. The mean Re is 113043 but the wing is tapered so Re varies across the span. Note the Profile drag and section C_L coefficient vary as the chord and vortex-induced downwash change toward the tips, and the Re falls.

THE DRAG BUDGET

Figure 4.9 was produced by applying the methods outlined above. The contribution of each type of drag to the model C_D at each C_L may easily be found in the foregoing tables;

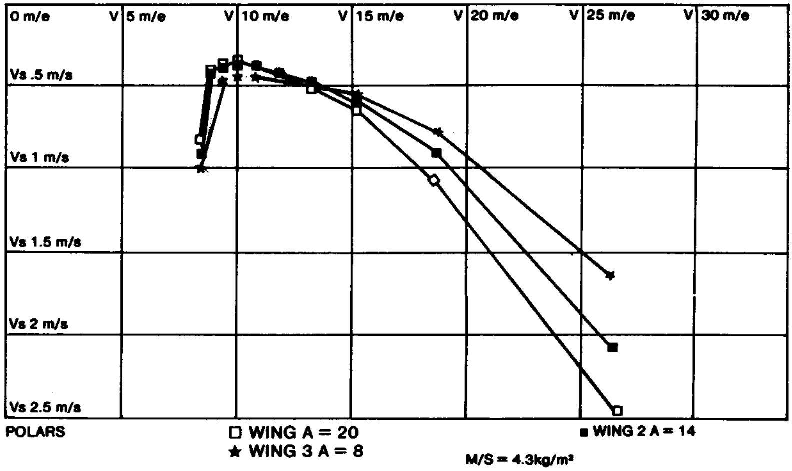

Fig. A6 Polar curves of three sailplane wings of different aspect ratios but all of the same aerofoil section.
[The low A models are ballasted to bring them to the same M/S as the A = 20 model.] Note the marked superiority of the [ballasted] A = 8 model at high speed. At low speed there is little to choose between A = 14 [ballasted] and A = 20. The low Re of the high A wing is responsible.

these are entered in the table below.

To find the drag *force* contributed at each flying speed, first the velocity of flight at each C_L is found by applying the standard formula:

$$V = \sqrt{\frac{W \times 9.81}{\frac{1}{2}S \times 1.225\ C_L}} = \sqrt{\frac{3 \times 9.81}{\frac{1}{2} \times 1.225 \times 1 \times C_L}} = \sqrt{\frac{48.048}{C_L}}$$

For the purpose of the example calculation, W/S (wing loading) was assumed 3 kg./sq. metre (approx. 9.8 ozs./sq.ft.), and a model weight of 3kg. assumed (6.615lbs.).

Next, each C_d is multiplied by $\frac{1}{2}\rho SV^2$ to produce drag force in kg. The results are of course only approximate since no proper allowance has been made for varying Re. The assumed model would achieve Re approx. 280,000 to match the wind tunnel results if its VL (velocity multiplied by chord) was about 4. This corresponds to a model with chord 0.3 metres flying at 13.3 metres per second (11.8 ins. at 29.8 m.p.h.). As the figures below show, the model would reach this speed at C_L between 0.2 and 0.4. The aspect ratio of 7.5 gives a span of 2.74 metres, wing area 1 sq. metre.

The drag budget is worked out in the table overleaf, and plotted as in Figure 4.9.

THE ANGLE OF INCIDENCE

The problem is to set the fuselage at such an angle to the flight path of the model that it creates the least possible drag. For a racer this will depend on the angle of attack of the wing when it is flying at maximum speed. For a soaring sailplane the angle of attack when flying at maximum $C_L^{1.5}/C_D$ is what counts, though the performance gain caused by

DRAG BUDGET

1 C_L	2 V^2	3 V_m/sec	4 Assumed Parasite C_d	5 Induced C_{di}	6 Profile C_D	7 Total C_L	8 (4) × V^2
0.4	120.12	10.96	0.010	.00679	.0120	.02879	1.2
0.6	80.08	8.95	0.010	.01528	.0098	.03508	.8
0.8	60.06	7.75	0.010	.02716	.0101	.04730	.6
1.0	48.05	6.93	0.010	.04244	.0107	.06314	.48
1.2	40.04	6.33	0.010	.06115	.0113	.08245	.40
1.4	34.32	5.86	0.010	.08318	.0125	.10568	.34
1.5	32.03	5.66	0.010	.09549	.0137	.11919	.32
1.6	30.03	5.48	0.010	.10864	.0149	.13354	.30
1.675	28.69	5.36	0.010	.11925	.0162	.14545	.29

FINAL DRAG BUDGET, Kg. FORCE

			PARASITE	INDUCED	PROFILE	TOTAL
9 (5) × V^2	10 (6) × V^2	11 (7) × V^2	12 (8) × ½ρS	13 (9) × ½ρS	14 (10) × ½ρS	15 (11) × ½ρS
0.82	1.44	3.46	0.735	0.502	0.882	2.119
1.22	0.79	2.83	0.490	0.747	0.484	1.721
1.63	0.61	2.84	0.368	0.998	0.374	1.740
2.04	0.51	3.03	0.294	1.250	0.314	1.858
2.45	0.45	3.30	0.245	1.501	0.276	2.022
2.86	0.43	3.63	0.208	1.752	0.263	2.223
3.06	0.44	3.82	0.196	1.874	0.270	2.340
3.26	0.45	4.01	0.184	1.997	0.276	2.457
3.42	0.47	4.17	0.178	2.095	0.288	2.561

saving parasite drag at this low speed will be very small. For a 'penetration' sailplane, correct fuselage alignment at high speed is important, less so at low speed.

For a racer, ensure that the wing camber is such that the wing profile minimum drag is at the average operational C_L for speeds at which the model will fly (see Chapter 6). From wind tunnel test results if available, or if not, by assuming a lift curve slope of 0.11 c_l per degree (from zero lift angle of attack) find the angle of attack of the wing profile at the operating c_l. This angle is for a wing of 'infinite' aspect ratio. It must be corrected for downwash effects as shown below.

For a penetrating sailplane the section angle of attack chosen will depend on the extent of the aerofoil's low drag range or 'bucket'. Flight at a lower angle of attack than this will bring a marked deterioration (steepening) of the glide due to increased profile drag. Wind tunnel results at the Re appropriate to flight at this C_L and airspeed allow this to be estimated, or, if NACA 6 series aerofoils are used, the extent of the low drag range can be judged roughly from the third digit – e.g. 64_3618 gives a low drag range of 0.3 c_l above and below the ideal c_l of 0.6, hence the low drag bucket ends at c_l 0.3. From this it is possible to estimate the angle of attack (infinite a.r.).

For a soarer, the operating C_L must be found by the methods given in this appendix and the angle of attack found from the wind tunnel results.

Knowing the angle of attack of the wing at infinite aspect ratio, the correction to the angle for the real model wing, affected by downwash, is found by the formula:

Angle of attack increment: $\dfrac{(18.25 \times C_L)}{A}$ (Assuming a nearly elliptical lift distribution)

Thus, for the model considered earlier the C_L for minimum sink with a.r. 7.5 was found to be 1.55. The induced angle of attack for this a.r. is:

$18.25 \times 1.55/7.5 = 3.77$ degrees

From the tunnel tests (unfortunately not at the correct Re, so this is useful only as an example of method) the aerofoil yields c_l 1.55 at 8.0 degrees. The rigging angle of wing to fuselage should be $8.0 + 3.77 = 11.77$ degrees.

For penetration the low drag range of the aerofoil ends at approx. $c_l = 0.5$, which develops at -2.3 degrees.
The induced angle of attack will be $18.25 \times 0.5/7.5 = 1.22$.
The rigging angle should thus be $- 2.3 + = -1.08$.
(The aerofoil is highly cambered and not very suitable for a fast flying model sailplane. Its performance is very good at high c_l, for which it was designed. The figures above illustrate the method only.)

A pylon racer with a symmetrical aerofoil, flying at a C_L of 0.05 with the same aspect ratio would require an angel of incidence as worked out below:

$18.25 \times 0.05 : 7.5 = 0.122$.

The symmetrical profile would reach c_l 0.05 at $0.11/0.05 = 0.45$ degrees. The rigging angle should thus be $0.122 + 0.45 = 0.57$ degrees.

FINDING THE AERODYNAMIC CENTRE OF A WING

For trimming a model it is often necessary to know the position of the wing aerodynamic centre. The model's centre of gravity should normally be at this point or very slightly behind it, as discussed in Chapter 12. If the c.g. is too far aft, parasite drag will increase since a larger tail will be required for stability and induced drag also will rise, due to load being transferred from wing to tail. If too far forward, a down load on the tailplane will be required for balance, which also leads to increased tail drag although the model's stability will be high.

If the wing is not swept back or forward, *with respect to its quarter-chord line*, the aerodynamic centre for all practical purposes may be taken as one quarter of the chord aft of the root leading edge, and for wings of normal plan, with only a *very slight* sweep, this point will as a rule be close enough, for trimming, to the true a.c.

With wings of complex form, or swept, locating the a.c. is both more important and more difficult, important because for preliminary trial flights the centre of gravity must be as close as possible to the right place before launching. For a straight-tapered wing, the graphical construction shown in the upper part of Figure A7 may be used. Where *t* is the tip chord and *r* the root chord, by drawing on an accurate plan of the wing half panel, extend the root chord by *t*, and the tip chord by *r* as shown, and join the extensions with a diagonal line. Where this line cuts the line joining mid-points of root and tip chords is the *geometric centre of area* of the wing panel. The chord through this point should be drawn parallel to the aircraft centre line. The wing aerodynamic centre lies a quarter of the way along this chord line, measured from the leading edge. This point should be projected onto the centre line to give the required balance point.

With more complex wing planforms, the following procedure may be used. Although fairly laborious, the exercise is worthwhile whenever a wing of unusual form is designed.

1. Calculate the mean chord, $c = S/b$, where S is the wing area and b the span.

2. Consider the wing on one side of the centre line and divide into a convenient number of panels (With a curved outline divide the wing into panels with nearly straight lines to arrive at a close approximation.) (See lower part of Fig. A7.)

3. Find the area, dS, of each panel.
4. Find the centre of area of each panel, using the construction method of Fig. A7.
5. Find the centre of area of the wing by taking moments about the centre line:

$$\bar{y} = \frac{(dS_1 \times \bar{y_1}) + (dS_2 \times \bar{y_2}) + (dS_3 \times \bar{y_3}) \text{ etc.}}{S/2}$$

(In this formula $DS_{1\ 2\ 3\ 4}$, etc. refer to the areas of the successive panels of the wing marked out in step 2, and $y_{1\ 2\ 3}$, etc. refer to the distances of each panel's centre of area from the centre line. The whole formula gives y which is the distance from the centre line of the centre of area of the half wing.)

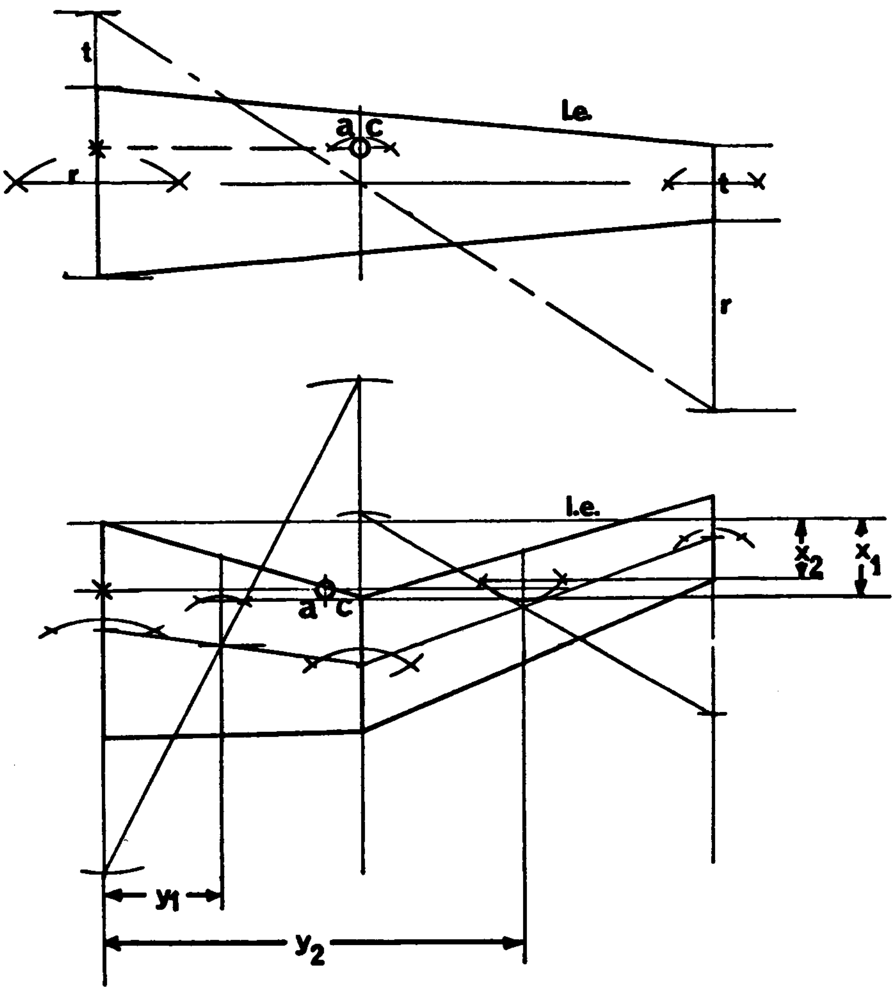

Fig. A7 Geometric method of finding the wing aerodynamic centre

6. Locate the quarter-chord points for the chord through the centre of area of each panel.

7. Find the chordwise distances, x_1 x_2 x_3 x_4 etc. of these quarter-chord points measured from some convenient transverse axis such as the line through the leading edge at the root of the wing.

8. Find the fore and aft location of the mean quarter-chord point, x by taking moments about a transverse axis (i.e. the line through the leading edge at the root, as before).

$$x = \frac{(dS_1 \times x_1) + (dS_2 \times x_2) + (dS_3 \times x_3) \text{ etc.}}{S/2}$$

9. Locate the mean chord c (calculated in step 1) in a plane through the centre of area (calculated in step 5) with its quarter chord point marked the distance x aft of the reference line.

CALCULATION OF THE NEUTRAL POINT AND STATIC MARGIN

A formula which gives satisfactory results for the position of the neutral point is

$$h_n = \left(h_o + \eta_s \times V_s \times [a_1/a] \times \left[1 - \frac{d\varepsilon}{d\alpha}\right]\right)$$

Here, the meanings of the symbols are:

h_n = position of the neutral point as a decimal fraction of the wing standard mean chord.

h_o = position of the aerodynamic centre of the wing with allowance for fuselage effects, on the standard mean chord. (Fuselage may be ignored for rough estimates, in which case use $h_o = 0.25$)

η_s = stabiliser efficiency. This must be estimated: $\simeq 0.9$ for a 'T' tail, $\simeq 0.6$ for a normal tail, $\simeq 0.4$ or 0.3 if tail is near wing wake or on a fat fuselage in disturbed flow. A canard foreplane may be assumed .95 to 1.0 efficient.

V_s = stabiliser volume coefficient calculated from the formula:

$$V_s = \frac{l_s \times S_{(stabiliser)}}{c \times S_{(wing)}}$$

See Chapter 12, 12.16.

a_1 = slope of the lift curve of the stabiliser. [From wind tunnel charts with aspect ratio correction.]

a = slope of the lift curve of the wing [Wind tunnel, corrected for A.]

$\frac{d\varepsilon}{d\alpha}$ = change of downwash angle at the stabiliser with change of wing angle of attack. The average is ½ to ⅓, i.e. downwash at tail changes about half to one third as much as the wing angle of attack, in disturbance.

Canard foreplanes are in the upwash ahead of the main wing, which also must be allowed for.

A worked example:
'BANTAM' sport power model.
Dimensions:

Span	=	b	=	1.25m
Wing area	=	S_w	=	$0.29m^2$
Aspect ratio	=	A	=	5.39
Mean chord	=	c	=	0.232m

$$\begin{aligned}
\text{Stabiliser span} &= b_s = 0.5\text{m} \\
\text{Stab. area} &= S_s = 0.07\text{m}^2 \\
\text{Stab. Asp. ratio} &= A_s = 3.57 \\
\text{Stab mean ch.} &= c_s = 0.14\text{m} \\
\text{Length of tail arm} &= l_s = 0.557\text{m}
\end{aligned}$$

$h_o = 0.25$ [Fuselage ignored]

$\eta_s = 0.65$ ['Normal' tail]

$$V_s = \frac{l_s \times S_s}{c \times S_w} = \frac{.557 \times .07}{.232 \times .29} = \frac{0.039}{0.067} = 0.58$$

Slope of wing lift curve: Wing is a 13.7% thick profile similar to the thickened Clark Y or Göttingen 796. Assume a lift curve slope of $a_\infty = 0.11$ (i.e., at 'infinite' aspect ratio, about 2π/Radian which is $\simeq 0.11\ C_l$ per degree $\alpha°$)

Slope of tail lift curve: Tail is a thick flate plate section with rounded leading edge and knife trailing edge. (9.5 mm thick balsa) Assume lift curve slope similar to flat plate, $a_\infty = .095$, which is a conservative (pessimistic) figure.

These must be corrected for wing and tail aspect ratios, using the formula below:

$$a_{(\text{corrected})} = \frac{a_\infty}{1 + \left(\dfrac{18.25}{A} \times a_\infty\right)}$$

$$\text{Hence } a_{(\text{wing})} = \frac{0.11}{1 + \left(\dfrac{18.25}{5.39} \times .11\right)} = \frac{0.11}{1 + .372} = .080$$

$$a_{(\text{stab})} = \frac{0.095}{1 + \left(\dfrac{18.25}{3.57} \times .095\right)} = \frac{0.095}{1 + 0.486} = .064$$

$$\text{Then } \frac{a_1}{a} = \frac{.064}{.080} = 0.8$$

[This means that if the wing C_L changes by 1.0, the stabiliser C_L would change by 1.0×0.8 for the same angle of attack change. But, because of downwash, the change of angle at the tail will be *less* than the wing which is allowed for in estimating $d\varepsilon/d\alpha$ below]

For estimation of $d\varepsilon/d\alpha$, various elaborate methods are available (see D. Stinton, book listed below). For a rough calculation, use the formula:

$$\frac{d\varepsilon}{d\alpha} = 35a/A \text{ for monoplane } (55a/A \text{ for biplane})$$

In this case:

$$\frac{35 \times 0.08}{5.39} = 0.519$$

Then the neutral point position is

$$h_n = 0.25 + (0.65 \times 0.58 \times 0.8 \times [1 - 0.519]) = 0.25 + 0.145 = 0.395$$

That is, the neutral point lies at about 0.4 or 40% of the wing mean chord aft of the wing's aerodynamic centre

The recommended position of the balance point on the plan is 33% of s.m.c., i.e. 0.33 × mean chord. The static margin is found by subtraction·

$$sm = h_n - 0.33 = 0.07$$

This is a stable position but perhaps would prove 'hot' especially since propeller and fuselage destabilising influences have been ignored. By moving the c.g. forward 0.5 cm the s.m. would be increased to about 0.1, and a full 1.0 cm movement would give s.m. = 0.12.

Note that for a canard layout, the foreplane is *destabilising*, i.e. it brings the neutral point *forward* and the appropriate sign change must be made in the formula:
Canard

$$h_n = h_o - \left(\eta_f \times V_f \times [a_f/a_w] \times \left[\frac{d\varepsilon_f}{d\alpha_w}\right]\right)$$

where the f subscript indicates a foreplane.

With a tandem layout, treat the rear wing as a tailplane.

USEFUL REFERENCES

I.H. ABBOTT & A.E. VON DOENHOFF *Theory of Wing Sections* Dover Publications 1959 (Gives ordinates and data on many NACA profiles.)

F.W. RIEGELS *Aerofoil Sections* Translated from German by D.G. Randall, Butterworths, 1961. (Gives ordinates and data on all Göttingen profiles, many NACA and others.)

S.F. HOERNER *Fluid Dynamic Drag* 2nd Edition 1958, Midland Park. (A valuable reference work.)

E.L. HOUGHTON & A.E. BROCK *Aerodynamics for Engineering Students* E. Arnold Ltd., 1970 (Second edition in S.I. units, earlier edition in Imperial units.)

R.J. CARROLL *The Aerodynamics of Powered Flight* J. Wiley & Sons, 1960 (A useful introduction to general principles.)

F.G. IRVING *An Introduction to the Longitudinal Stability of Low Speed Aircraft* Pergamon Press, 1966 (A valuable elementary treatment with a worked example for longitudinal stability of a sailplane.)

A. POPE & J.J. HARPER *Low Speed Wind Tunnel Testing* J. Wiley & Sons, 1966 (A detailed explanation of wind tunnel methods and techniques, including very brief discussion of model aircraft wings and a chapter on very small wind tunnels.)

A.H. SHAPIRO *Shape and Fluid Flow* Heinemann, 1970 (An excellent simple introduction to boundary layer theory, with simple experiments.)

D. STINTON *The Design of the Aeroplane* (A valuable, if costly book full of useful practical advice and examples.)

C.D. PERKINS & R.E. HAGE *Airplane performance stability and Control* J. Wiley & Sons, 1960 (A fairly advanced text.)

F.W. SCHMITZ *Aerodynamic des Flugmodells* Translated by M. Flint and published by the British Air Ministry as R.T.P. Translations 2460, 2204, 2442 and 2457, from the original German text published by Carle O Lange Verlag, 1942 and 1953 and 1976. See also the references at the end of Chapter 10.

Appendix 2

For explanation, see Chapter 10.12. Graphs of wind tunnel test results appear on the following pages:

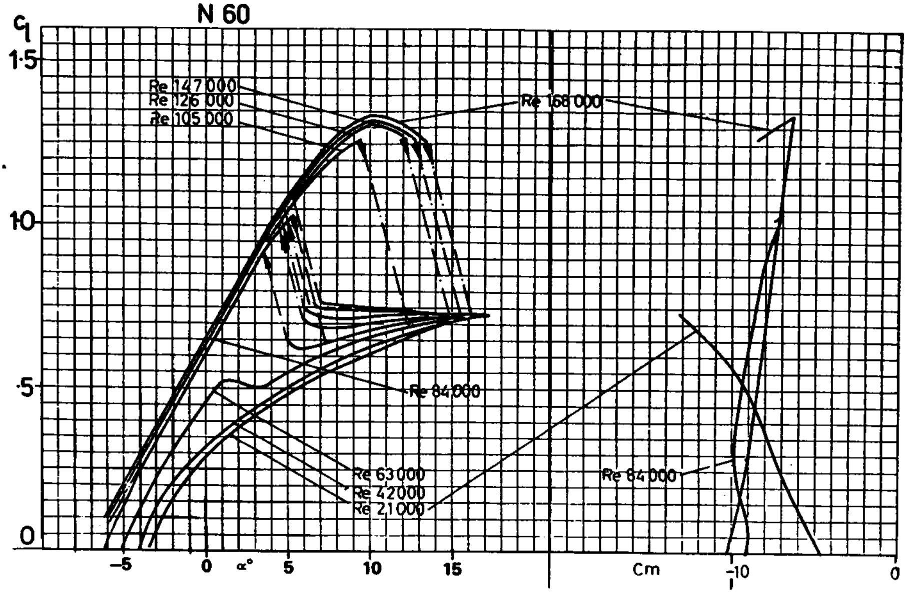

N 60
c_l
1·5
1·0
·5
0
Re 147 000
Re 126 000
Re 105 000
Re 168 000
Re 84 000
Re 63 000
Re 42 000
Re 21 000
Re 84 000
−5
0
α°
5
10
15
Cm
−10
0

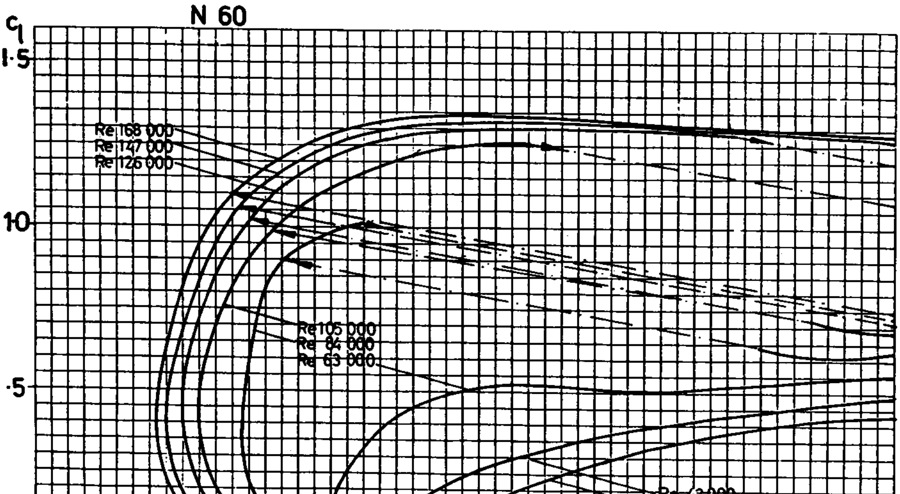

N 60
c_l
1·5
1·0
·5
0
Re 168 000
Re 147 000
Re 126 000
Re 105 000
Re 84 000
Re 63 000
Re 42 000
Re 21 000
0
c_d
·05
·10

N 60 R

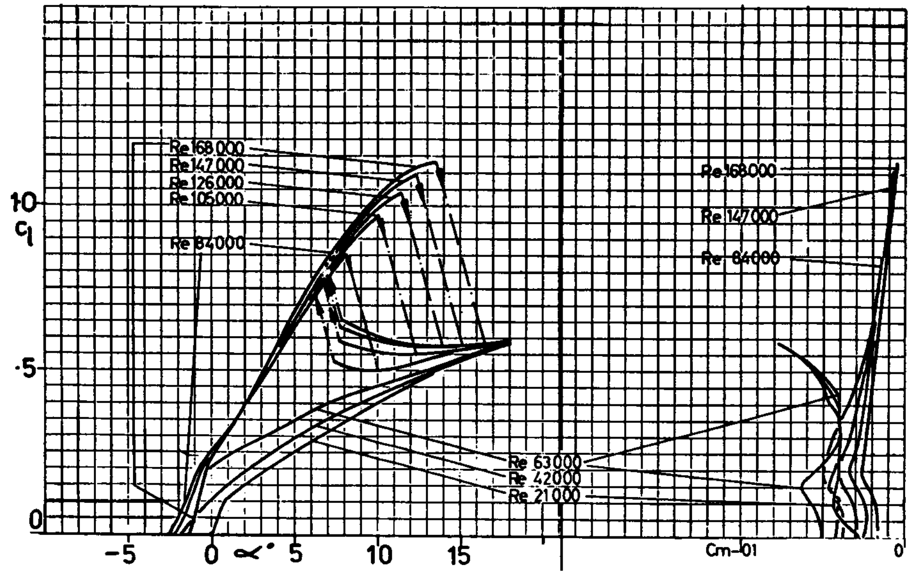
Re 168 000
Re 147 000
Re 126 000
Re 105 000
Re 84 000
Re 168000
Re 147000
Re 84000
Re 63000
Re 42000
Re 21000
1·0
c_l
·5
0
−5
0
α°
5
10
15
Cm−·01
0

N 60 R

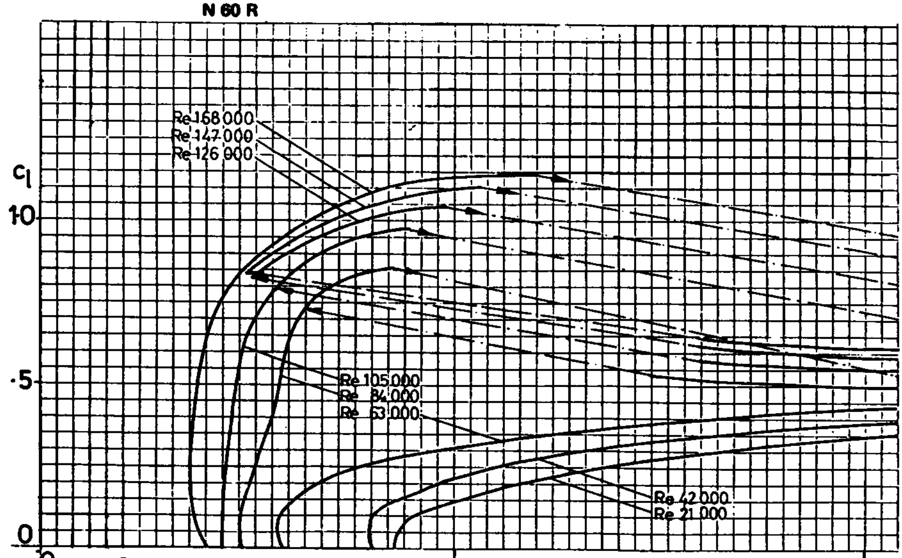
Re 168 000
Re 147 000
Re 126 000
Re 105 000
Re 84 000
Re 63 000
Re 42 000
Re 21 000
c_l
1·0
·5
0
0
c_d
·05
·10

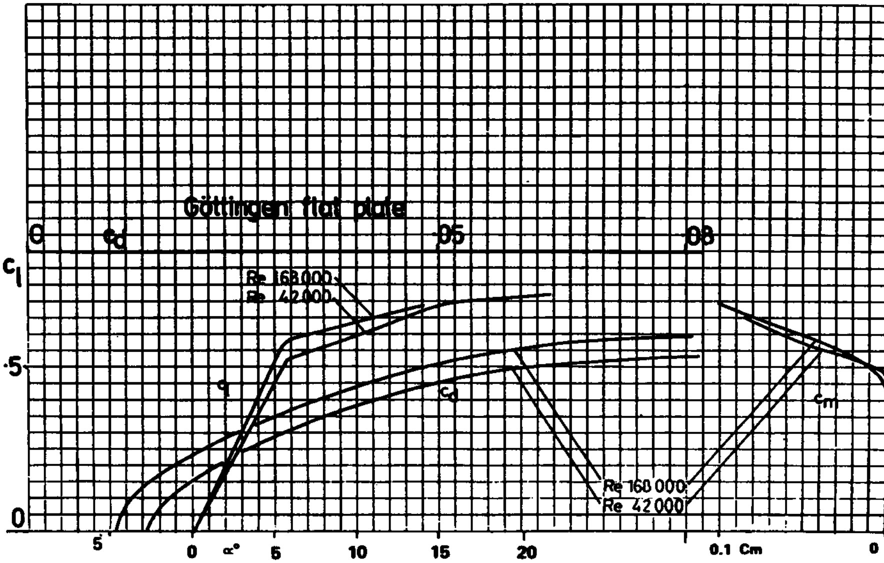

Göttingen flat plate
0
c_d
·05
·08
c_l
Re 168 000
Re 42 000
·5
c_l
c_d
c_m
Re 168 000
Re 42 000
0
5
0
α°
5
10
15
20
0.1 Cm
0

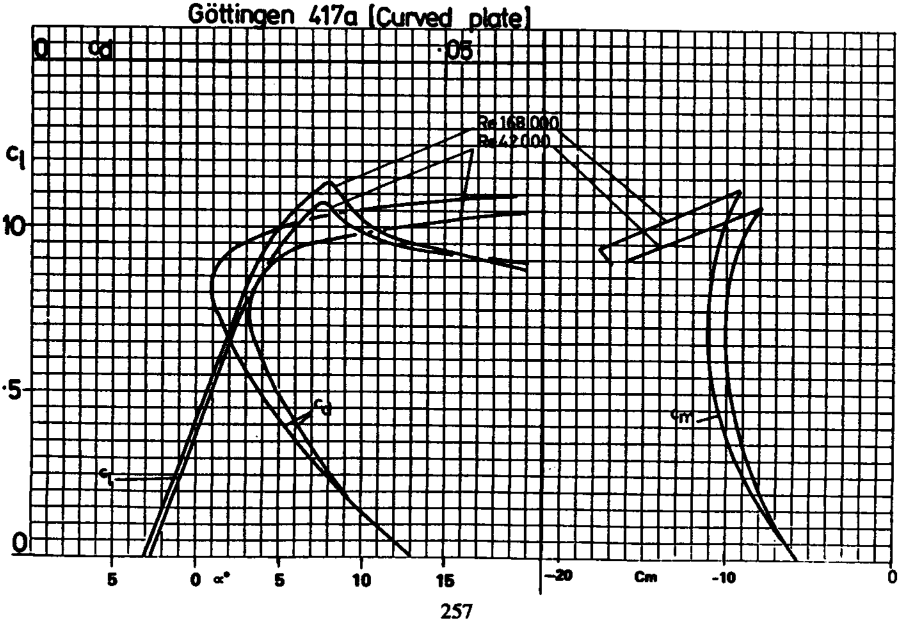

Göttingen 417a (Curved plate)
0
cd
·05
c_l
Re 168 000
Re 42 000
10
·5
c_d
c_m
c_l
0
5
0
α°
5
10
15
−20
Cm
−10
0

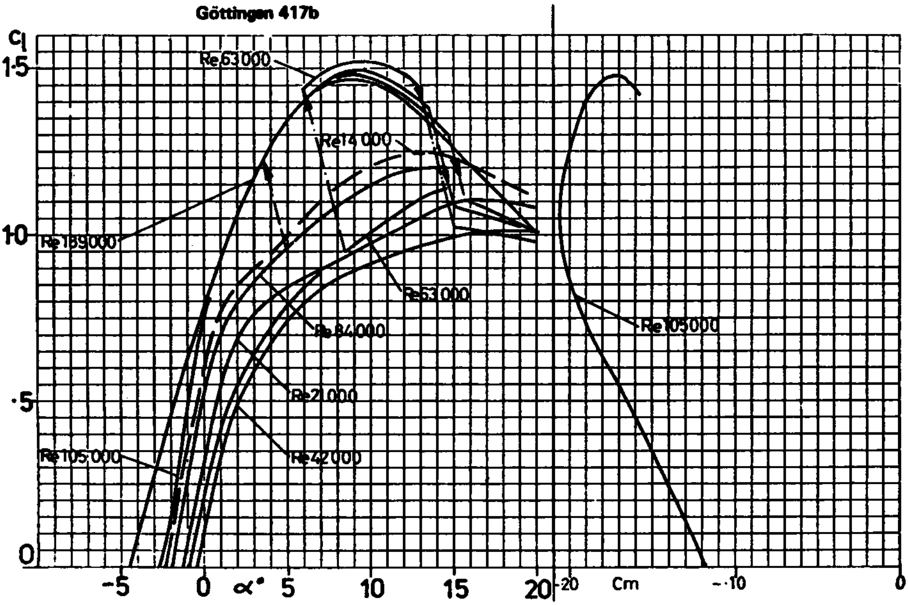
Göttingen 417b
c_l
1·5
1·0
·5
0
Re 63000
Re 14 000
Re 189000
Re 63 000
Re 84000
Re 105000
Re 21 000
Re 105 000
Re 42000
-5
0
$\alpha°$
5
10
15
20
·20
Cm
-·10
0

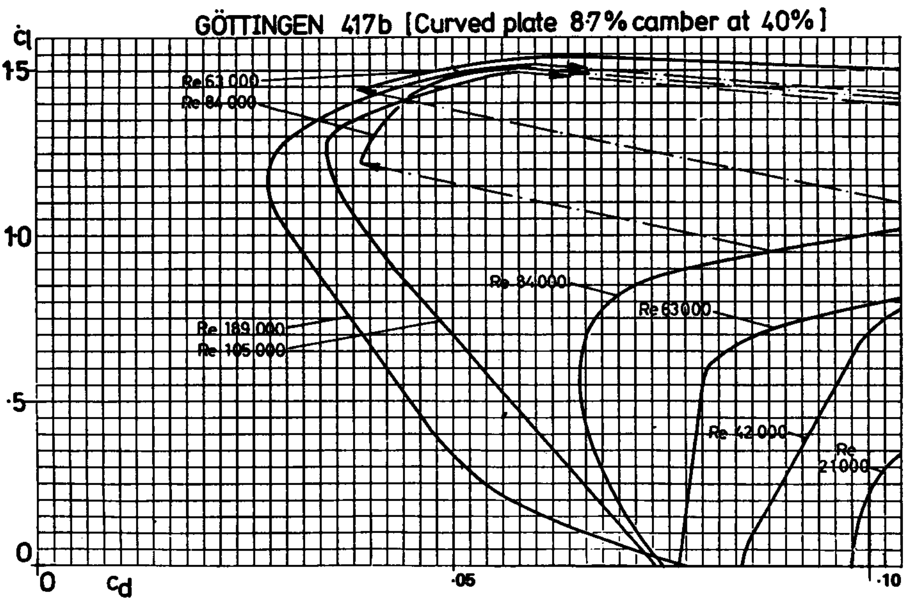
GÖTTINGEN 417b [Curved plate 8·7% camber at 40%]
c_l
1·5
1·0
·5
0
Re 63 000
Re 84 000
Re 84 000
Re 63 000
Re 189 000
Re 105 000
Re 42 000
Re 21 000
0
c_d
·05
·10

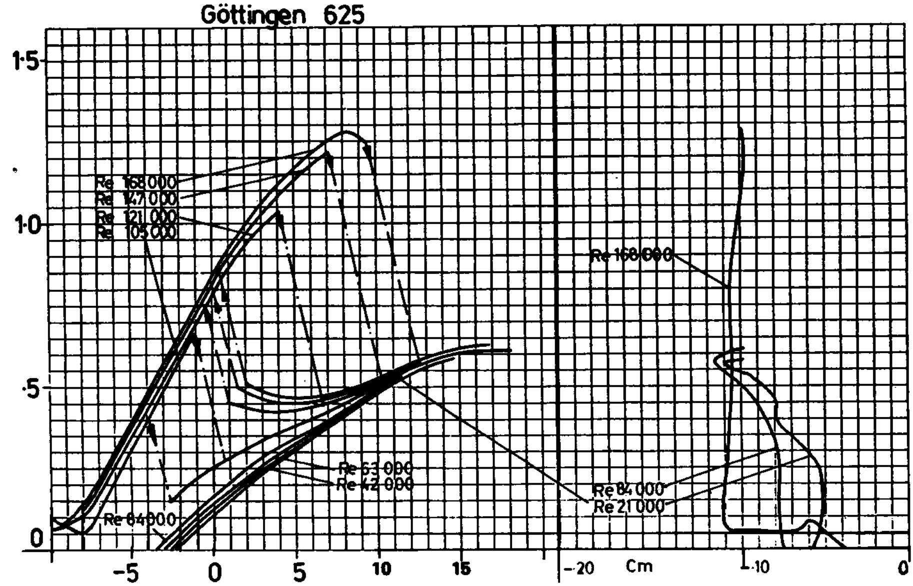

Göttingen 625
1·5
1·0
·5
0
Re 168 000
Re 147 000
Re 121 000
Re 105 000
Re 63 000
Re 42 000
Re 84000
Re 168 000
Re 84 000
Re 21 000
-5
0
5
10
15
-20
Cm
-10
0

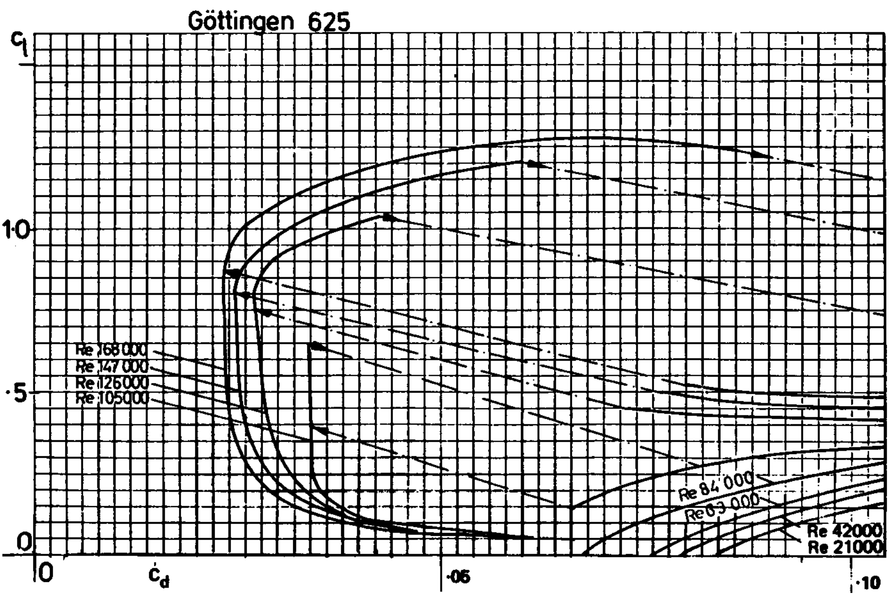

Göttingen 625
c_l
1·0
·5
0
Re 168 000
Re 147 000
Re 126000
Re 105000
Re 84 000
Re 63 000
Re 42000
Re 21000
0
c_d
·05
·10

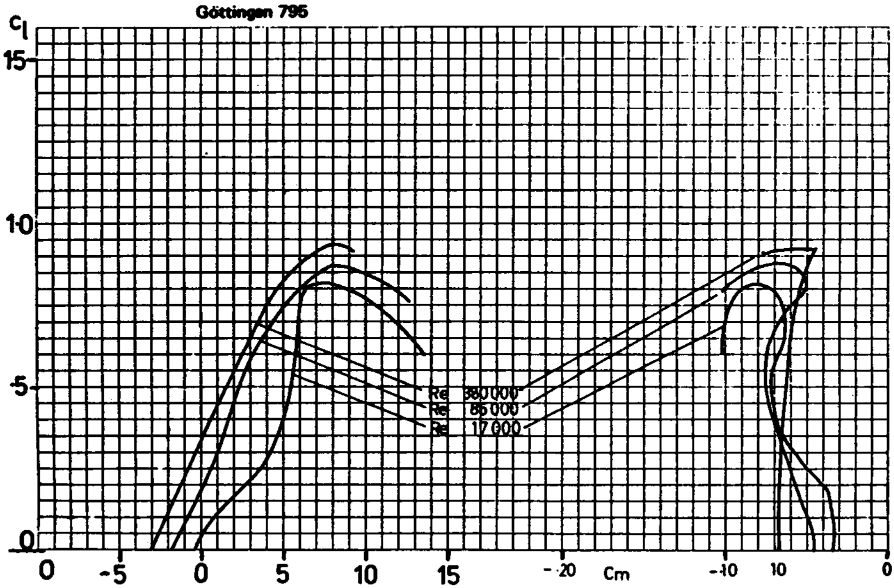
Göttingen 795
c_l
1·5
1·0
·5
0
-5
0
5
10
15
-·20
Cm
-·10
10
0
Re 380 000
Re 85 000
Re 17 000

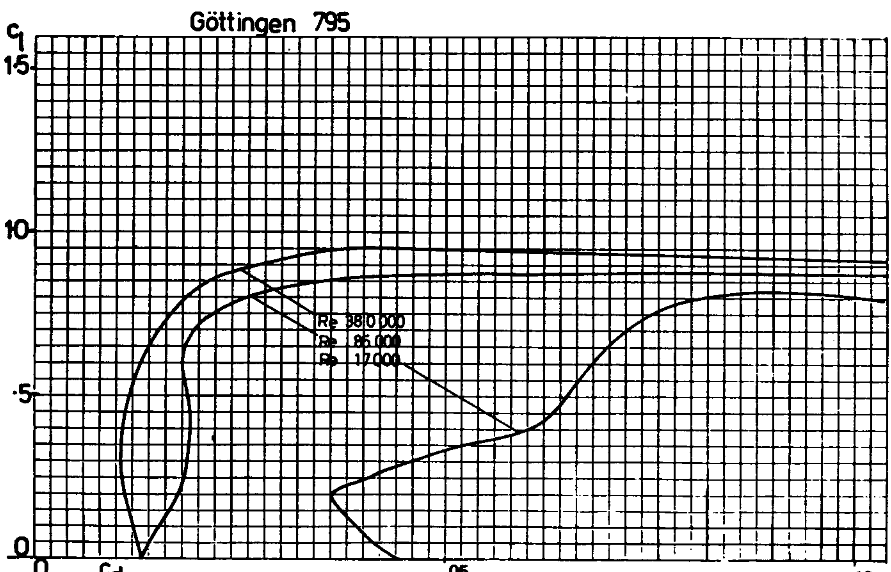
Göttingen 795
c_l
1·5
1·0
·5
0
c_d
.05
.10
Re 380 000
Re 85 000
Re 17 000

Göttingen 796

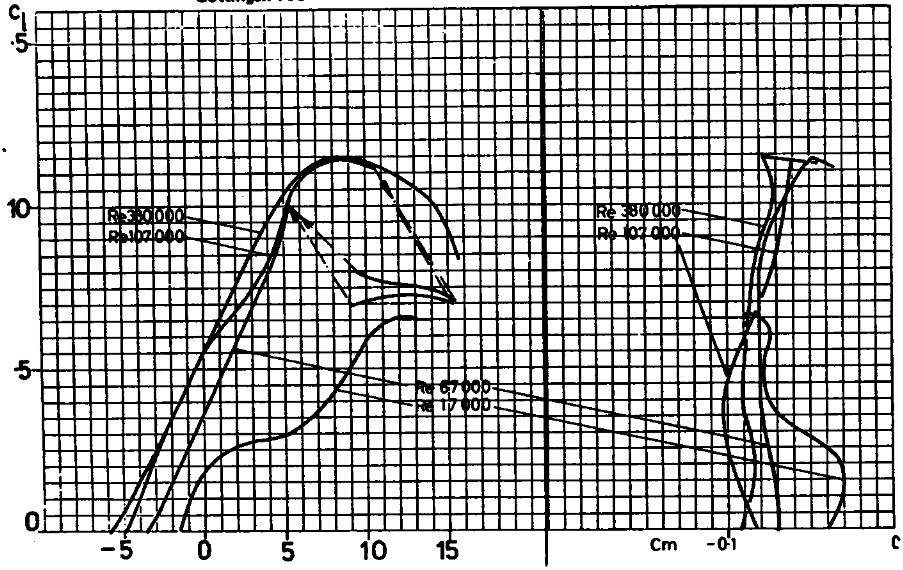

Göttingen 796

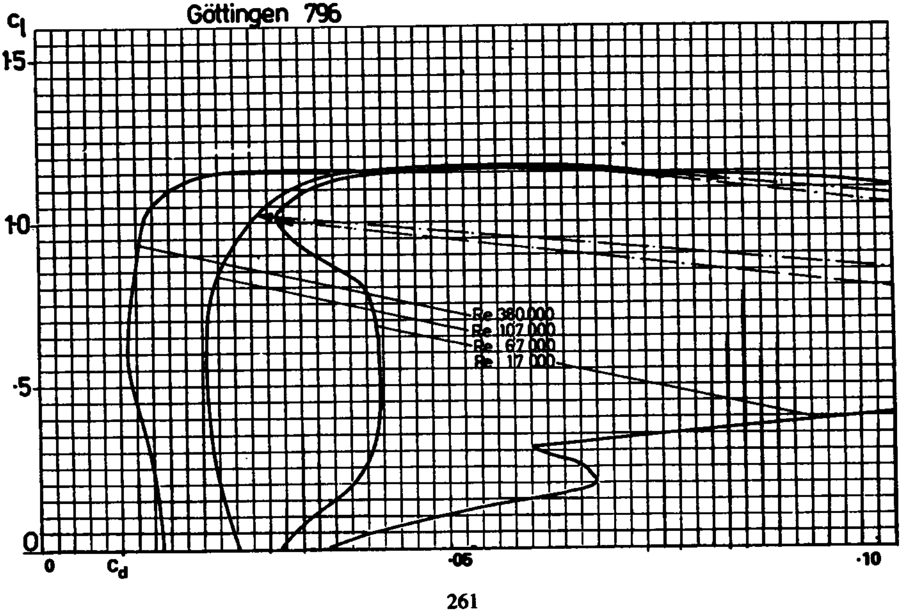

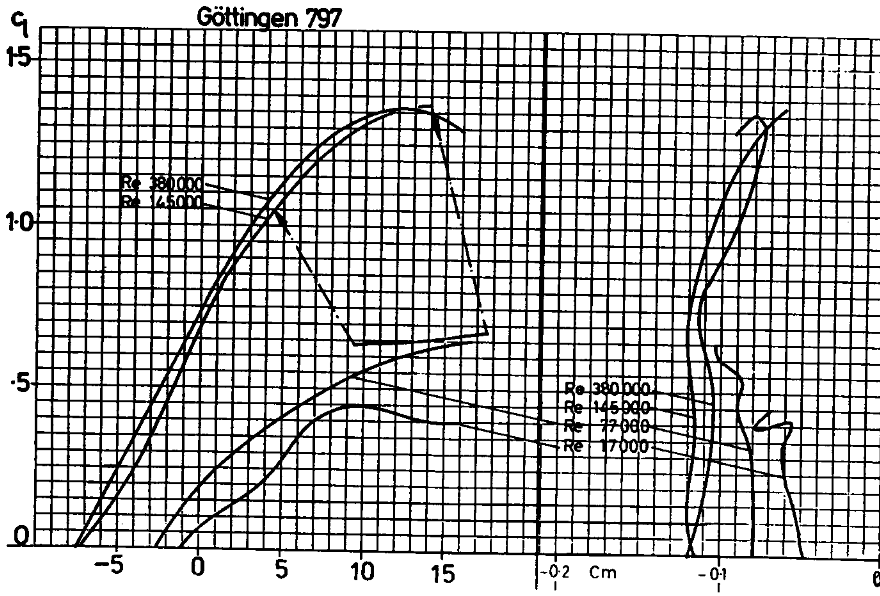
Göttingen 797
c_l
1·5
1·0
·5
0
Re 380000
Re 145000
Re 380 000
Re 145 000
Re 77 000
Re 17 000
−5
0
5
10
15
-0·2
Cm
-0·1
0

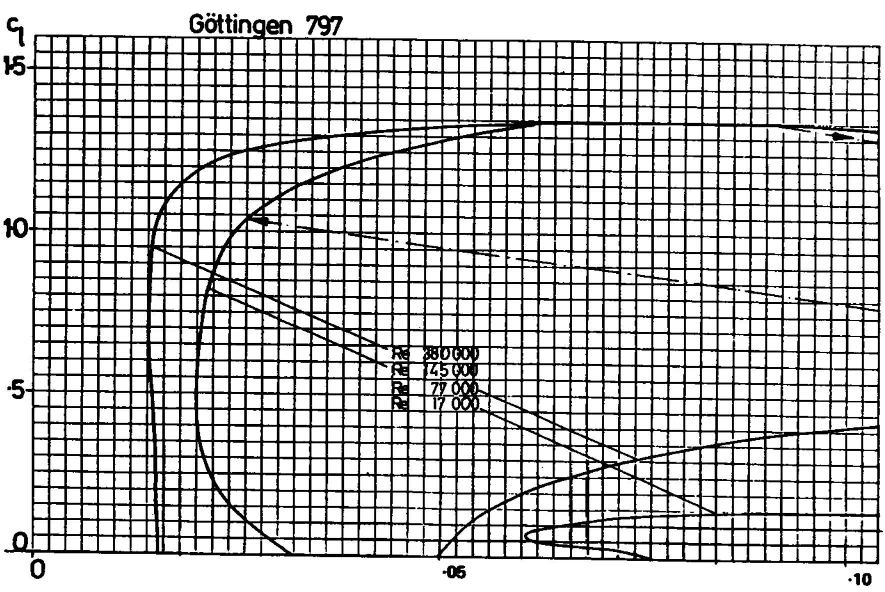
Göttingen 797
c_l
1·5
1·0
·5
0
Re 380 000
Re 145 000
Re 77 000
Re 17 000
0
·05
·10

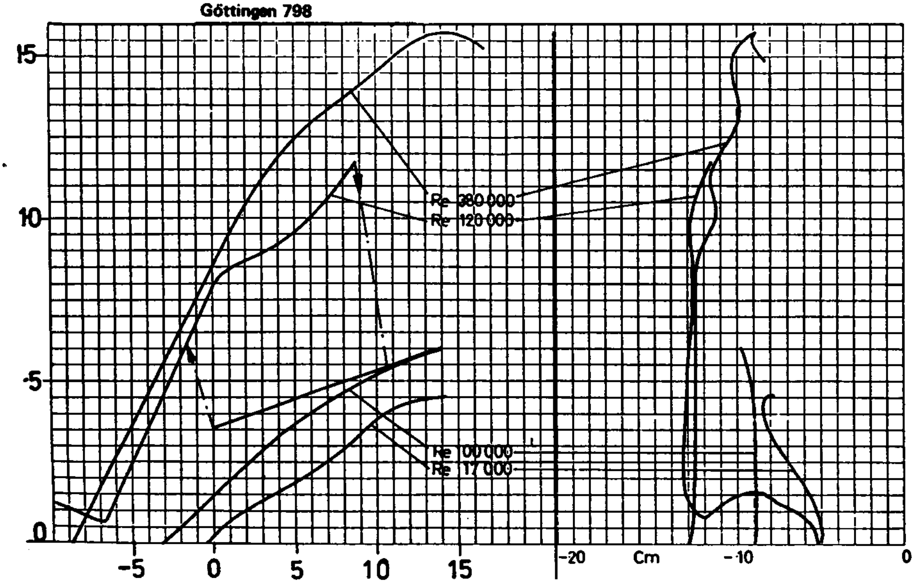
Göttingen 798
Re 380 000
Re 120 000
Re 100 000
Re 17 000
1·5
1·0
·5
0
-5
0
5
10
15
-20
Cm
-·10
0

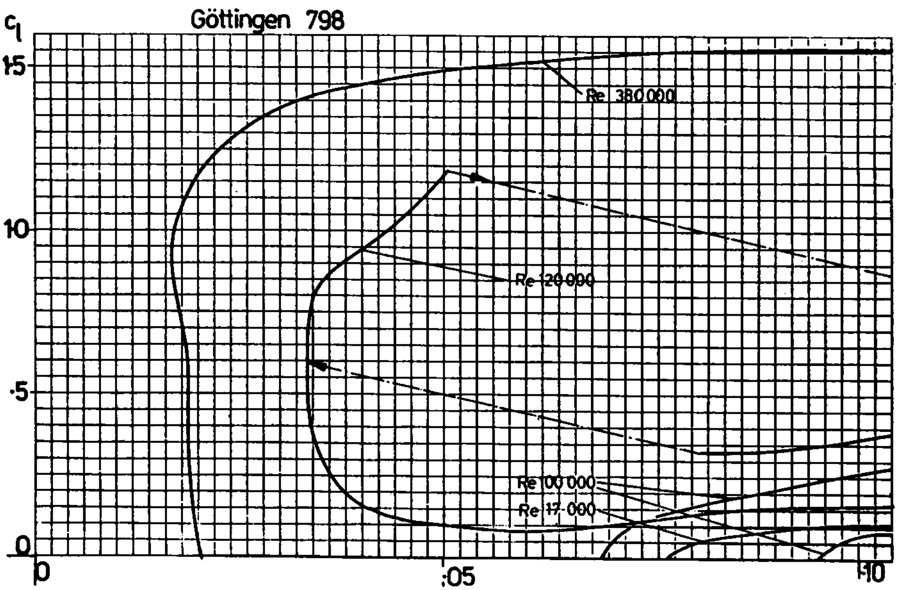
c_l
Göttingen 798
Re 380 000
Re 120 000
Re 100 000
Re 17 000
1·5
1·0
·5
0
0
·05
·10

Göttingen 801

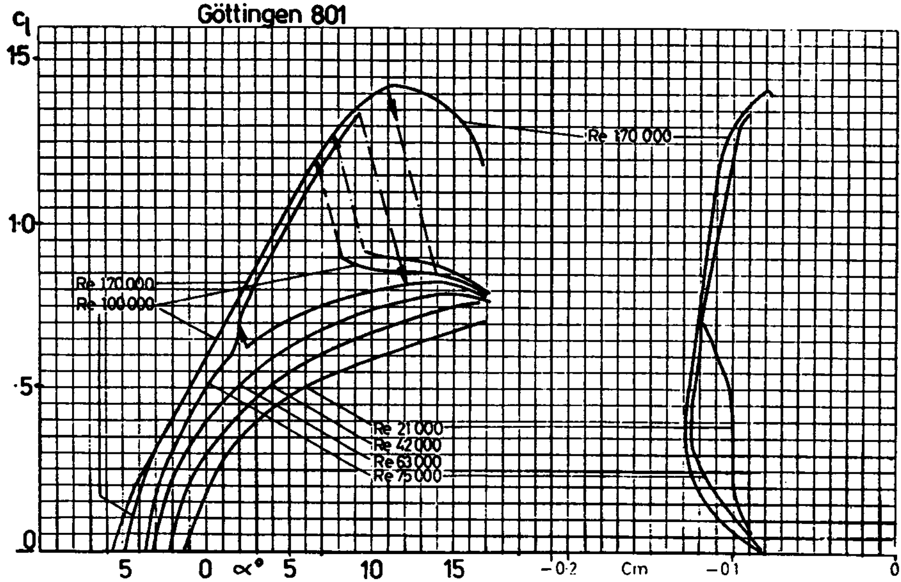

Göttingen 801

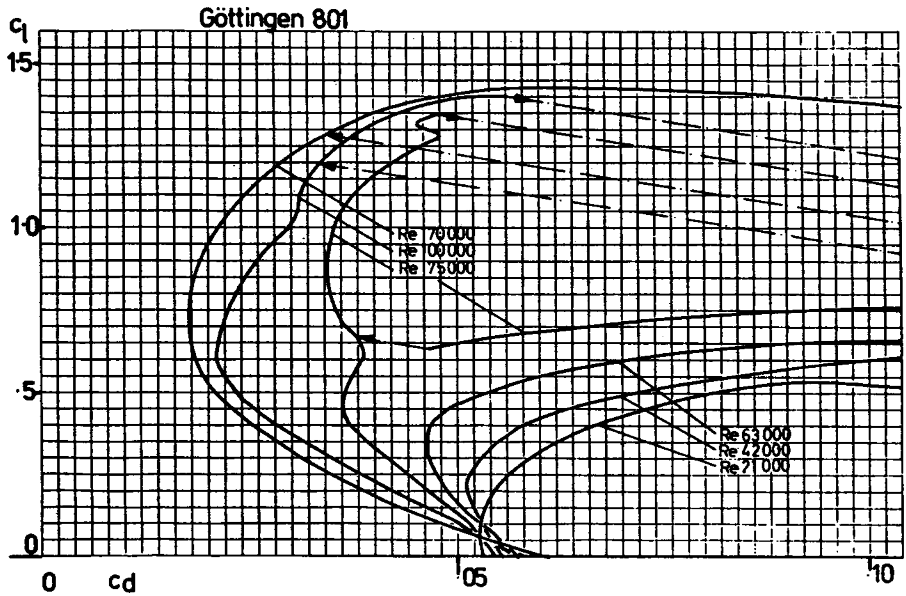

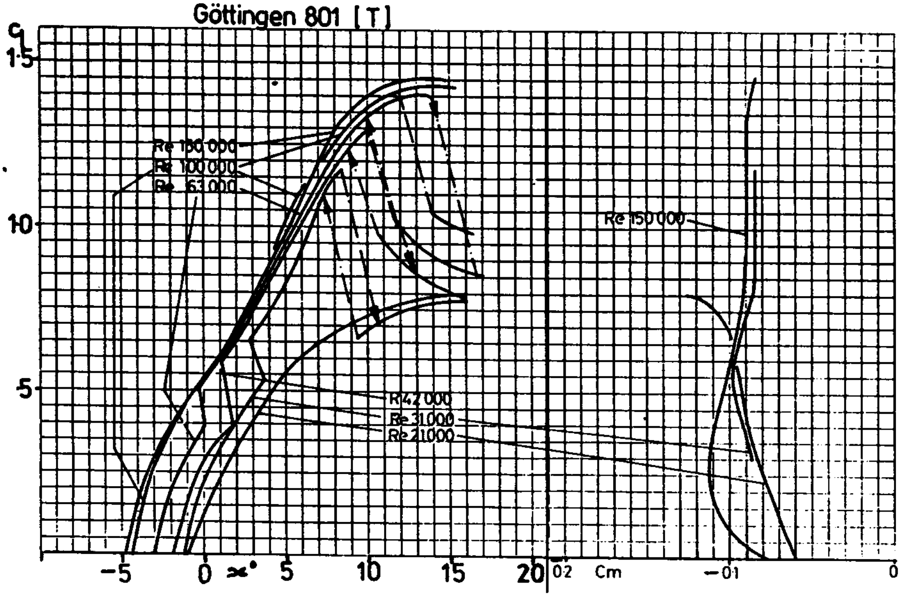

Göttingen 801 [T]
c_l
1·5
1·0
·5
Re 150 000
Re 100 000
Re 63 000
Re 150 000
R 42 000
Re 31 000
Re 21 000
−5
0
α°
5
10
15
20
0·2
Cm
−0·1
0

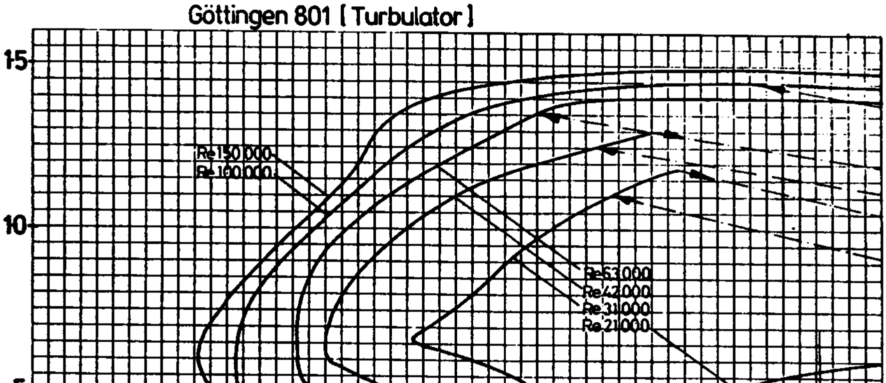

Göttingen 801 [Turbulator]
1·5
1·0
·5
Re 150 000
Re 100 000
Re 63 000
Re 42 000
Re 31 000
Re 21 000
0
c_d
·05
·10

Göttingen 801 [P]

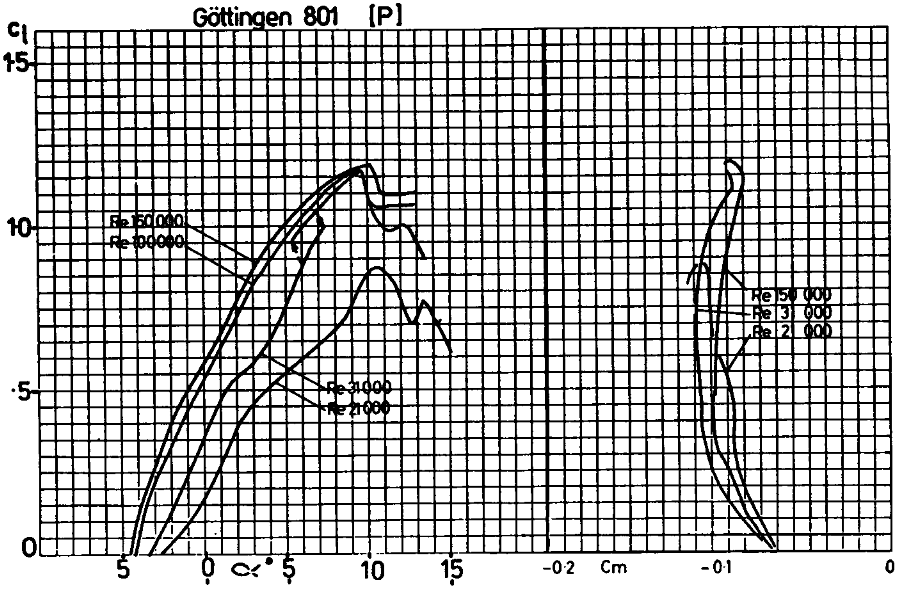

Göttingen 801 [Paper covered]

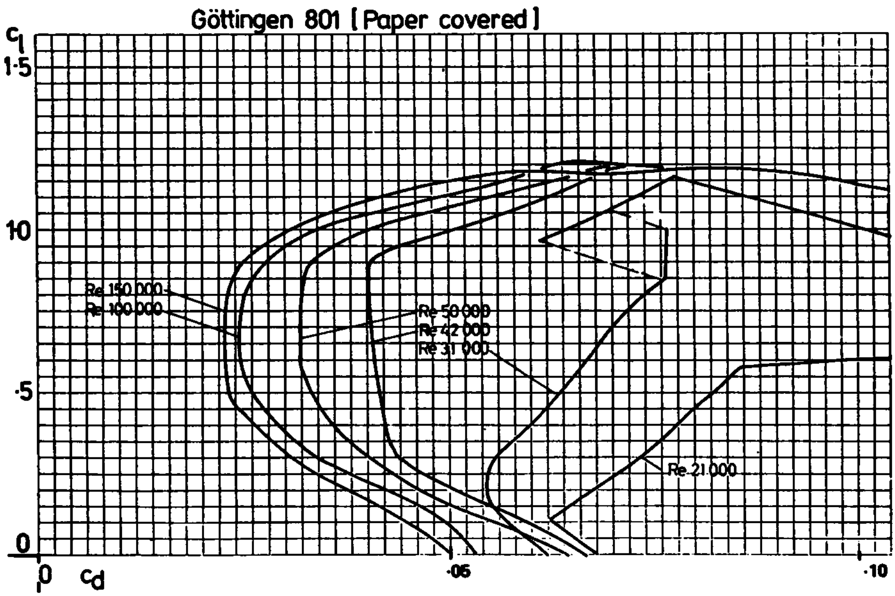

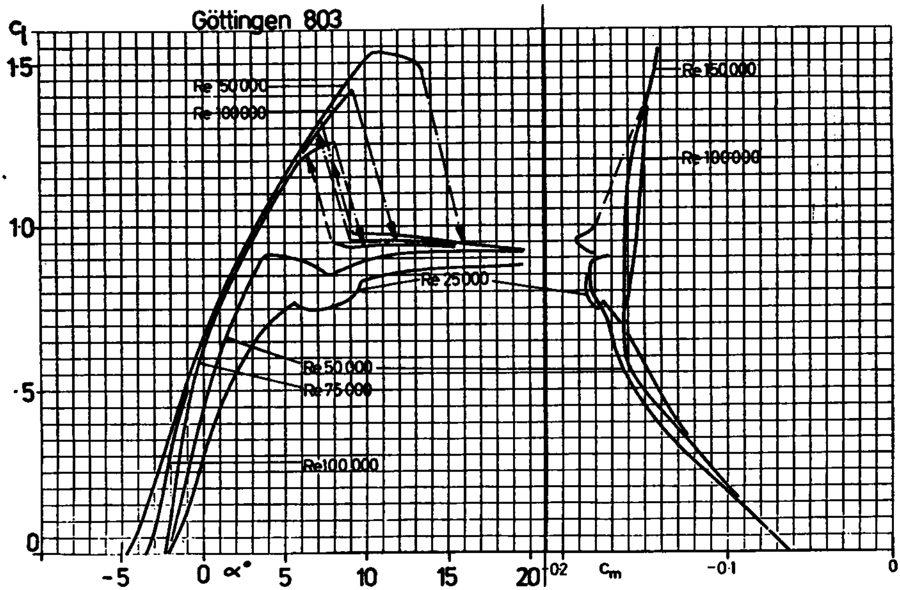
Göttingen 803
c_l
1·5
1·0
·5
0
Re 50 000
Re 100 000
Re 150 000
Re 100 000
Re 25 000
Re 50 000
Re 75 000
Re 100 000
-5
0
$\alpha°$
5
10
15
20
·02
c_m
-0·1
0

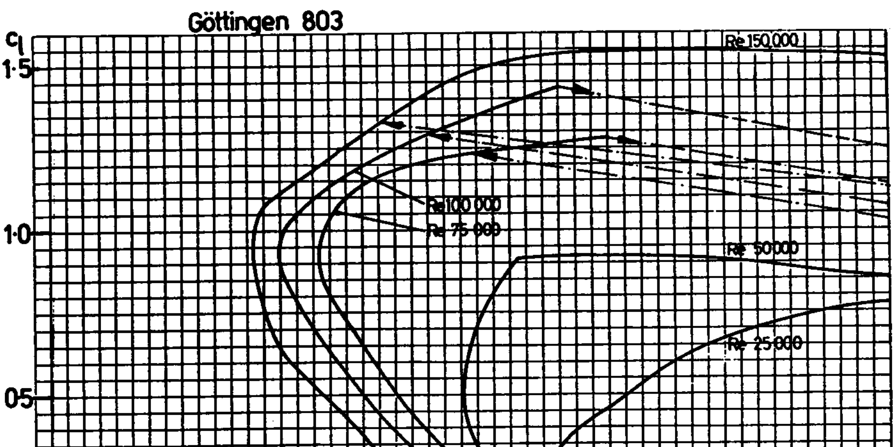
Göttingen 803
c_l
1·5
1·0
0·5
0
Re 150 000
Re 100 000
Re 75 000
Re 50 000
Re 25 000
0
c_d
·05
·10

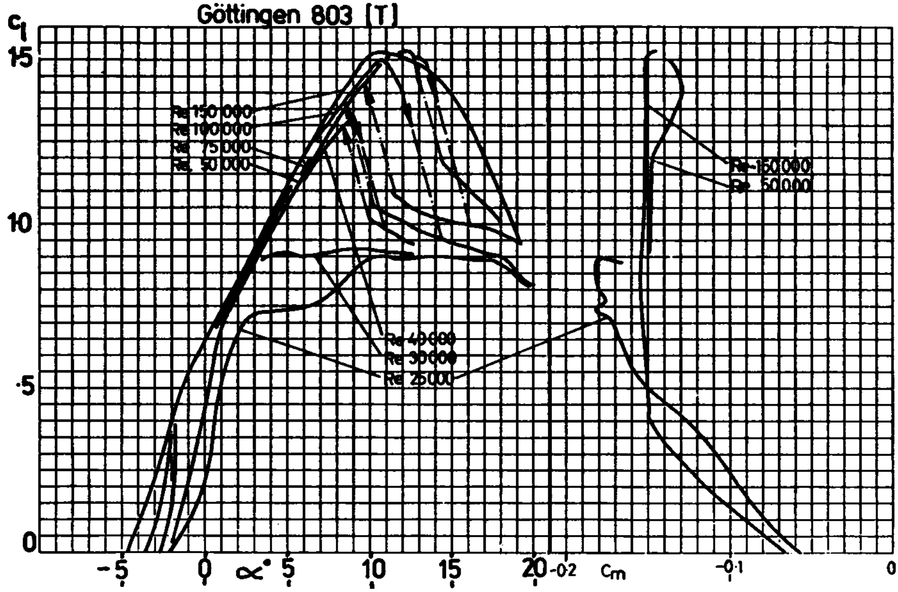
Göttingen 803 [T]
c_l
1·5
1·0
·5
0
Re 150 000
Re 100 000
Re 75 000
Re 50 000
Re 40 000
Re 30 000
Re 25 000
Re 150 000
Re 50 000
−5
0
α°
5
10
15
20
-0·2
c_m
-0·1
0

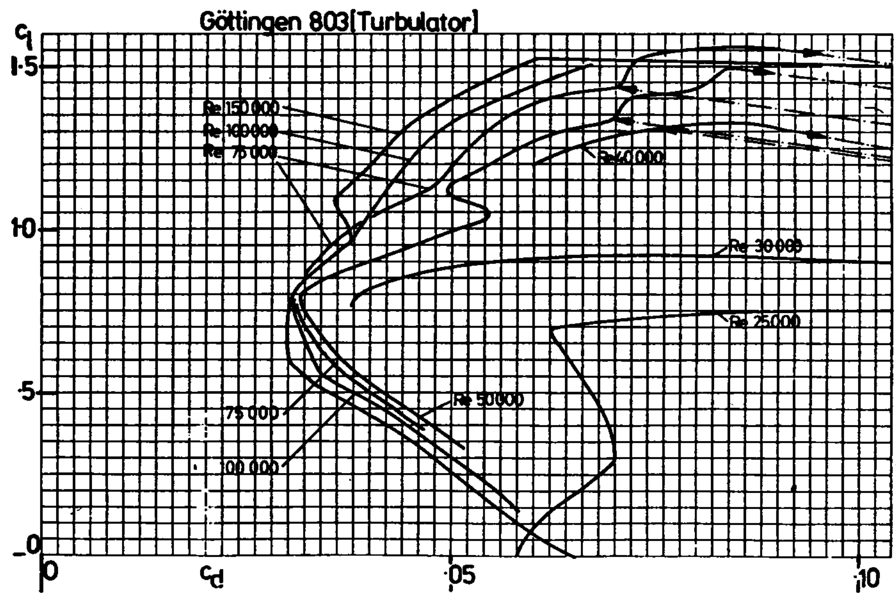
Göttingen 803 [Turbulator]
c_l
1·5
1·0
·5
0
Re 150 000
Re 100 000
Re 75 000
Re 40 000
Re 30 000
Re 25 000
Re 50 000
75 000
100 000
0
c_d
·05
·10

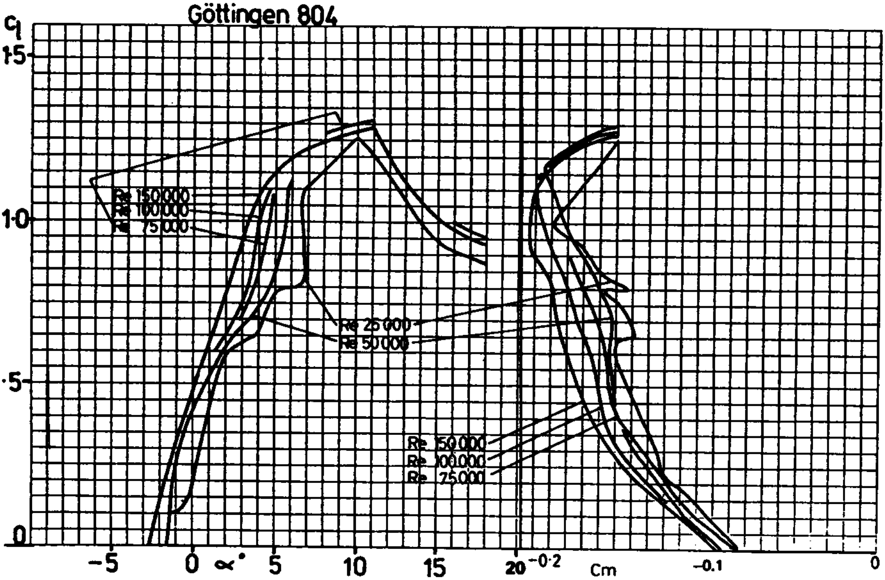
Göttingen 804
c_l
1·5
1·0
·5
0
Re 150 000
Re 100 000
Re 75 000
Re 25 000
Re 50 000
Re 150 000
Re 100 000
Re 75 000
−5
0
α°
5
10
15
20
−0·2
Cm
−0.1
0

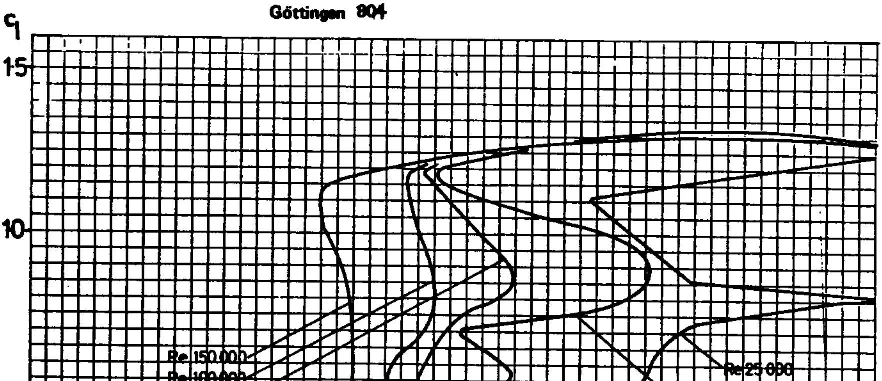
Göttingen 804
c_l
1·5
1·0
·5
0
Re 150 000
Re 100 000
Re 75 000
Re 25 000
Re 50 000
0
c_d
·05
·10

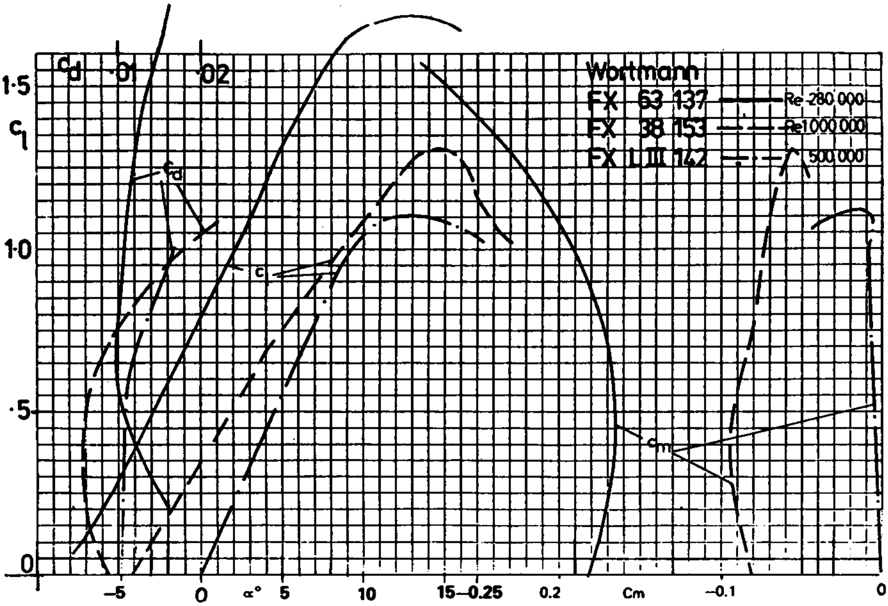
Wortmann
FX 63 137 Re 280 000
FX 38 153 Re 1000 000
FX L III 142 500 000
c_d ·01 ·02
c_l
1·5
1·0
·5
0
c_d
c_l
c_m
−5 0 α° 5 10 15 −0.25 0.2 Cm −0.1 0

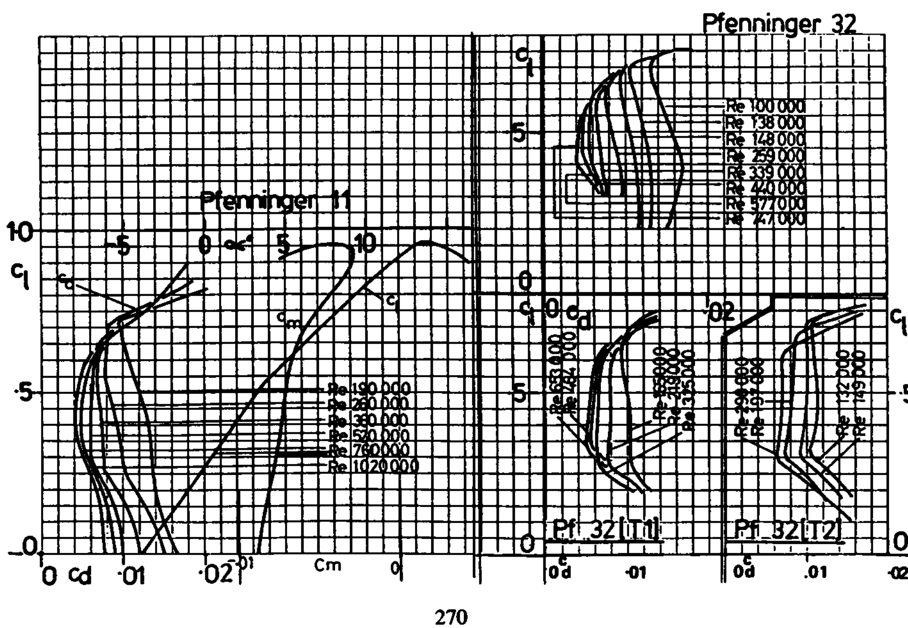
Pfenninger 11
Re 190 000
Re 260 000
Re 360 000
Re 520 000
Re 760 000
Re 1020 000
−5 0 α° 5 10
c_l
c_d
c_m
1·0
·5
0
0 cd ·01 ·02 ·01 Cm 0
Pfenninger 32
Re 100 000
Re 138 000
Re 148 000
Re 259 000
Re 339 000
Re 440 000
Re 577 000
Re 747 000
Pf 32 [T1]
Pf 32 [T2]
·02
·01
·5
0

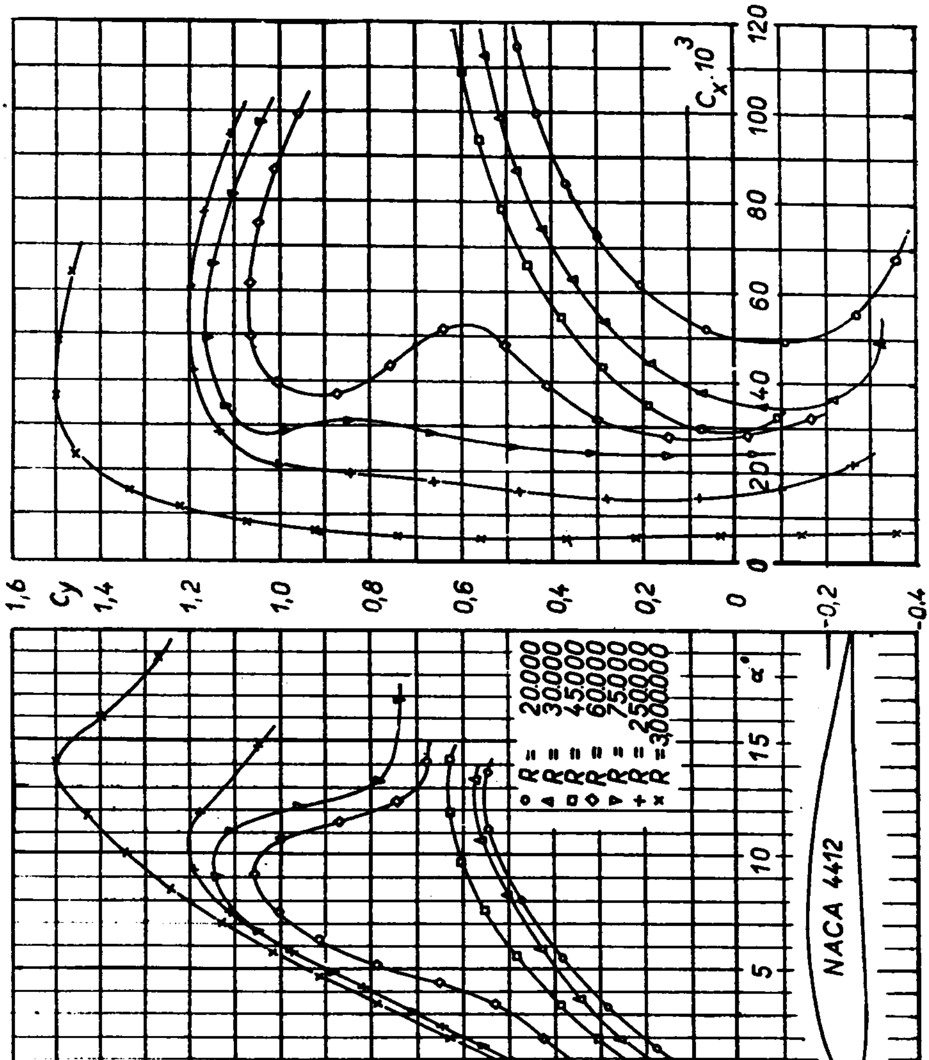
NACA 4412
R = 20.000
R = 30.000
R = 45.000
R = 60.000
R = 75.000
R = 250.000
R = 3.000.000
C_y
$C_x \cdot 10^3$
$\alpha°$

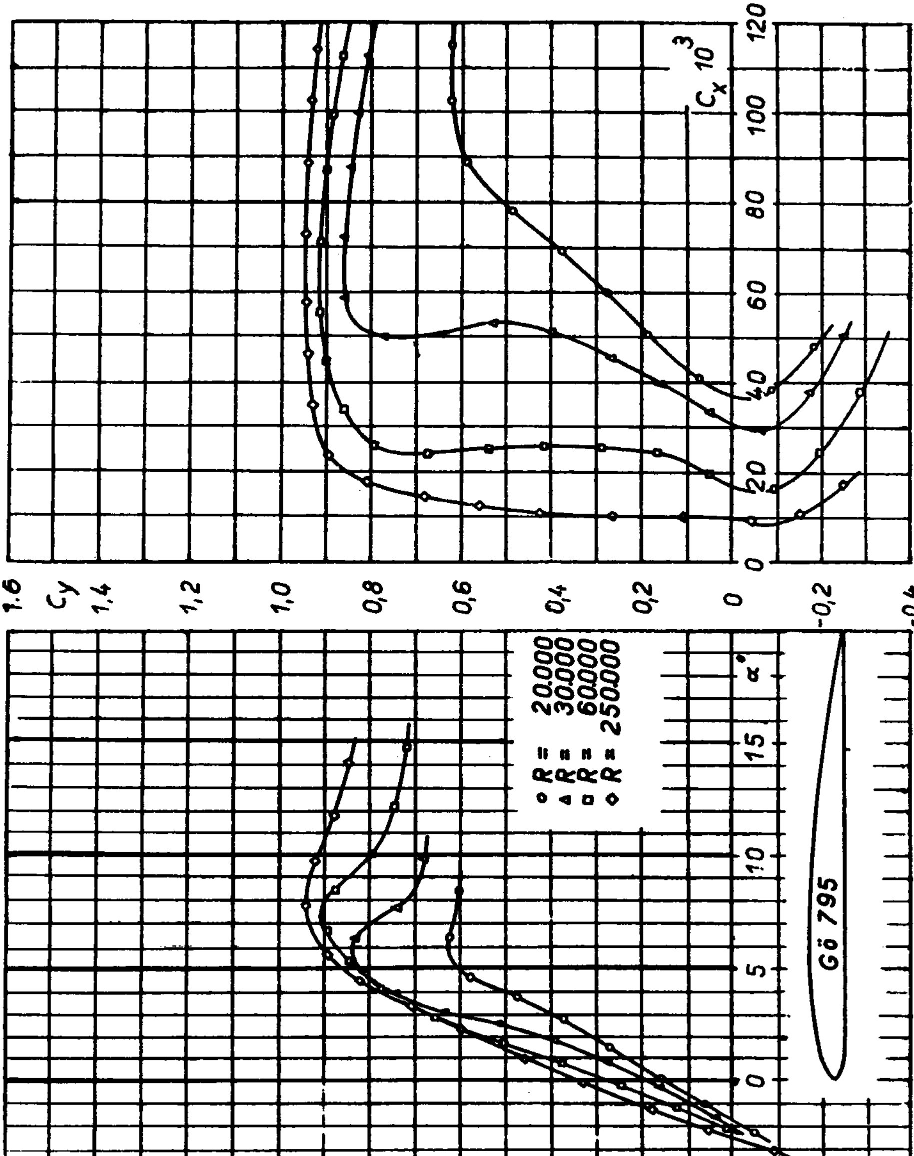
Gö 795
R = 20.000
R = 30.000
R = 60.000
R = 250.000
c_y
$c_x\ 10^3$
α°
1,6
1,4
1,2
1,0
0,8
0,6
0,4
0,2
0
-0,2
-0,4
-5
0
5
10
15
20
40
60
80
100
120

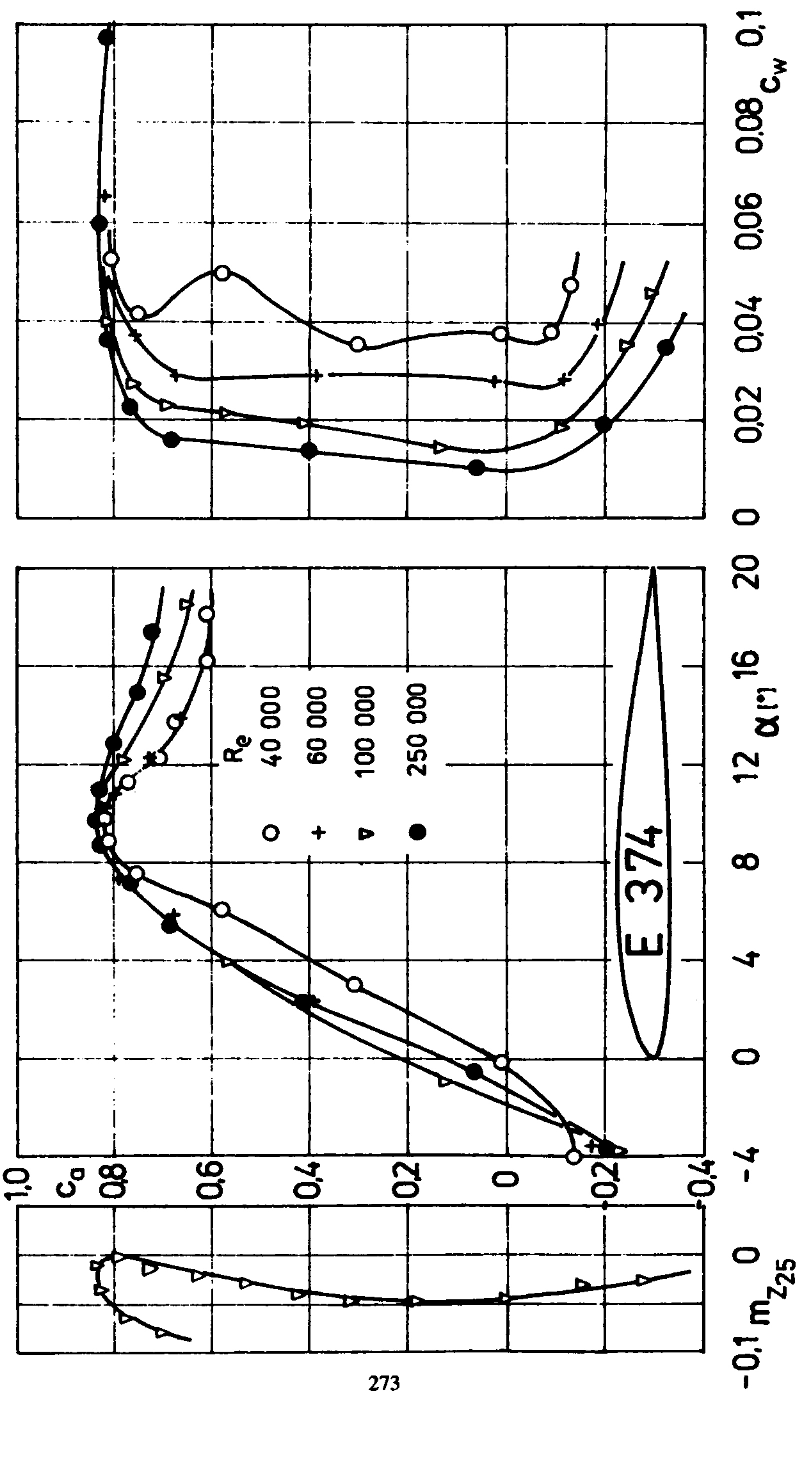

E 374
R_e
40 000
60 000
100 000
250 000
c_a
1,0
0,8
0,6
0,4
0,2
0
-0,2
-0,4
-4
0
4
8
12
α [°]
16
20
0
0,02
0,04
0,06
0,08
c_w
0,1
-0,1
m_z25
0

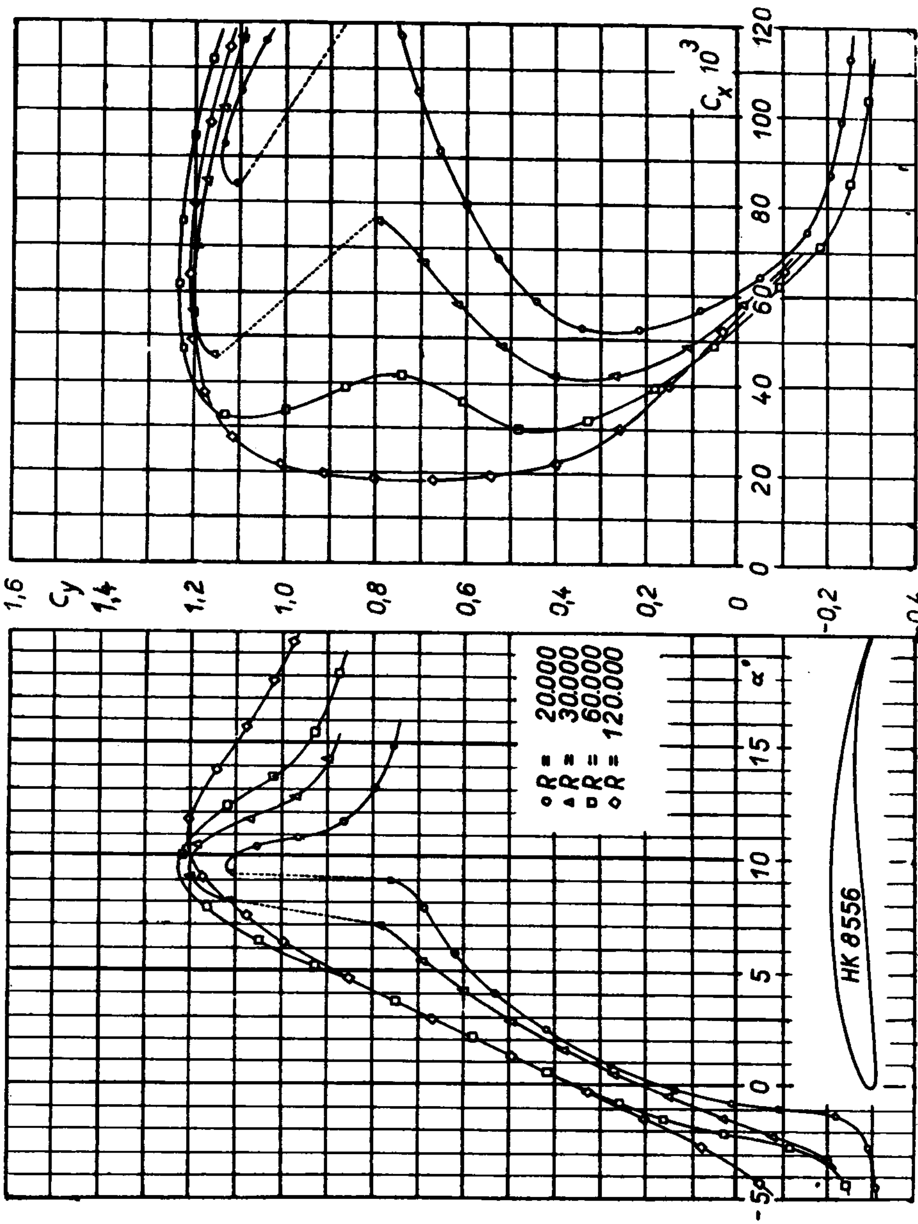

C_y
1,6
1,4
1,2
1,0
0,8
0,6
0,4
0,2
0
-0,2
-0,4
0
20
40
60
80
100
120
$C_x \; 10^3$
-5
0
5
10
15
α°
∘ R = 20.000
▵ R = 30.000
□ R = 60.000
◇ R = 120.000
HK 8556

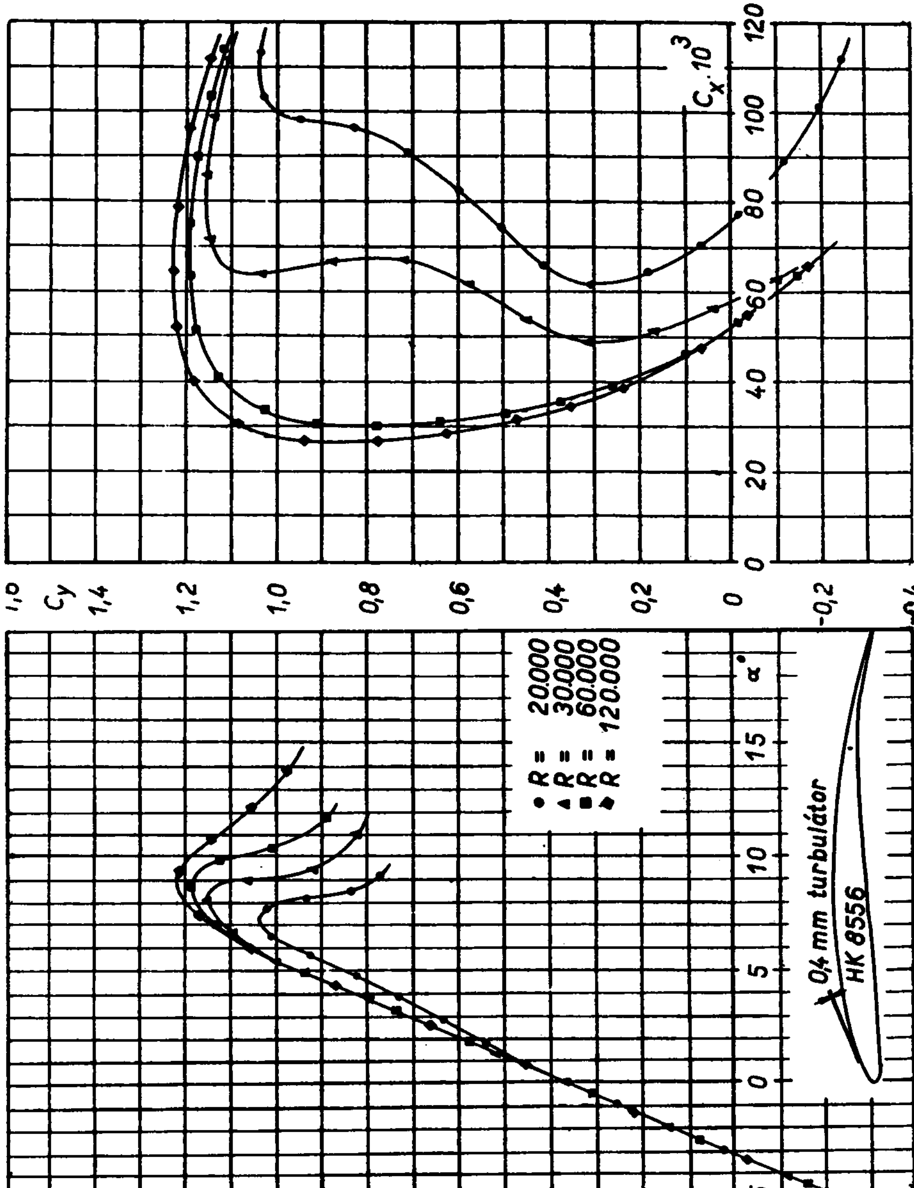
C_y
1,4
1,2
1,0
0,8
0,6
0,4
0,2
0
-0,2
-0,4
$C_x \cdot 10^3$
0
20
40
60
80
100
120
R = 20.000
R = 30.000
R = 60.000
R = 120.000
α°
-5
0
5
10
15
0,4 mm turbulátor
HK 8556

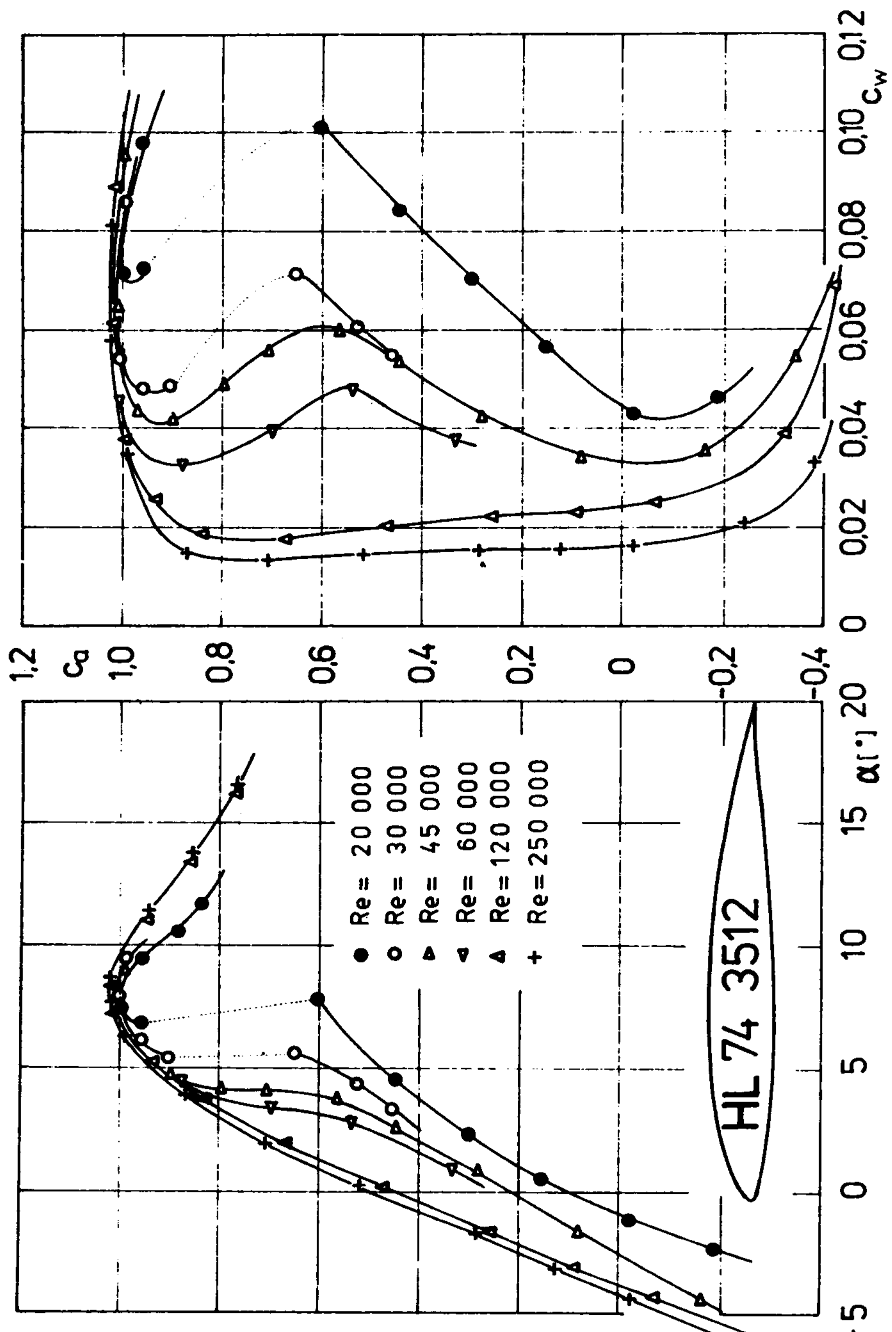
HL 74 3512
Re = 20 000
Re = 30 000
Re = 45 000
Re = 60 000
Re = 120 000
Re = 250 000
c_a
c_w
α[°]
1,2
1,0
0,8
0,6
0,4
0,2
0
-0,2
-0,4
0
0,02
0,04
0,06
0,08
0,10
0,12
-5
0
5
10
15
20

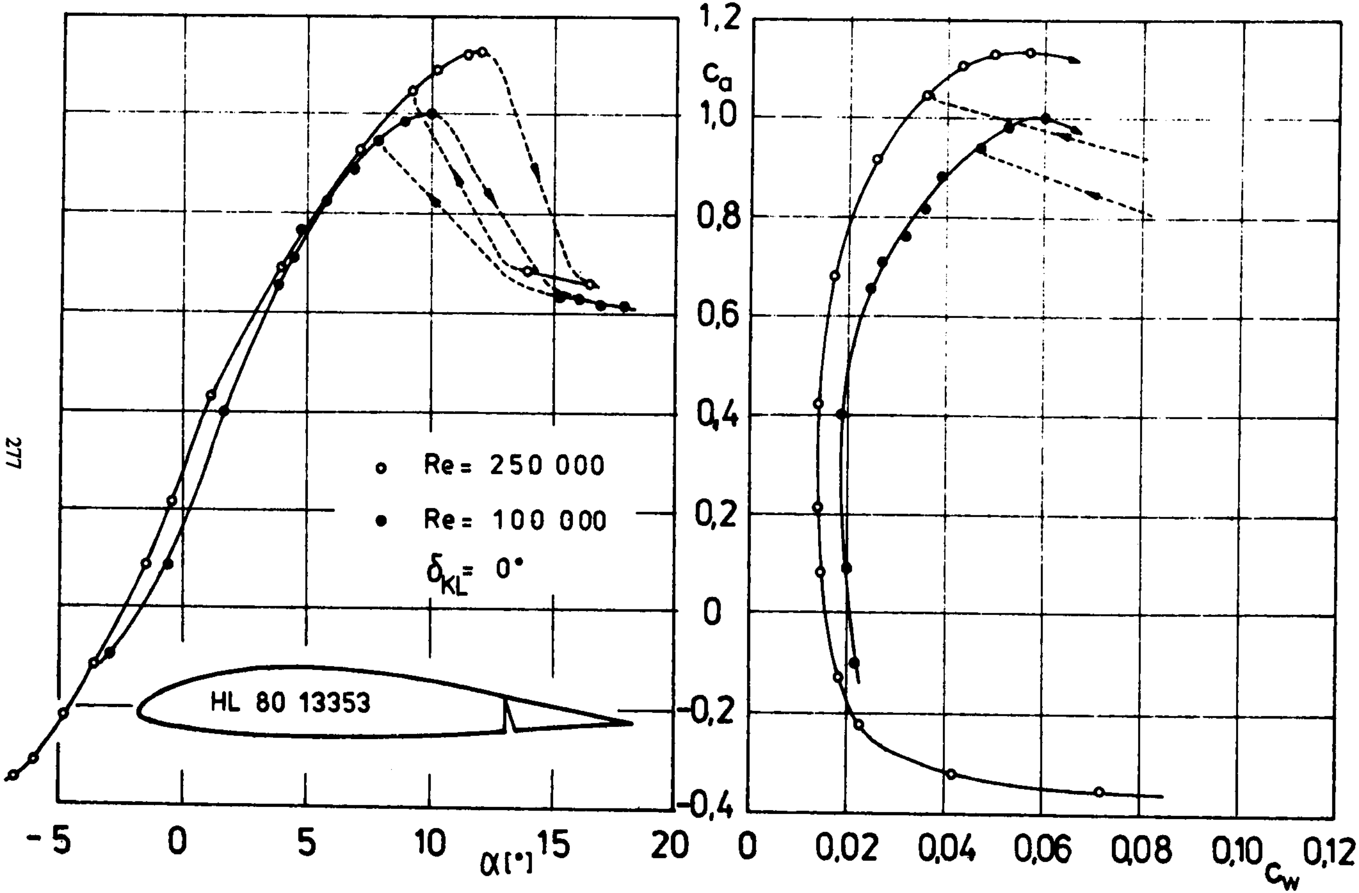

Re = 250 000
Re = 100 000
$\delta_{KL} = 0°$
HL 80 13353
c_a
1,2
1,0
0,8
0,6
0,4
0,2
0
-0,2
-0,4
-5
0
5
10
15
20
α [°]
0,02
0,04
0,06
0,08
0,10
0,12
c_w

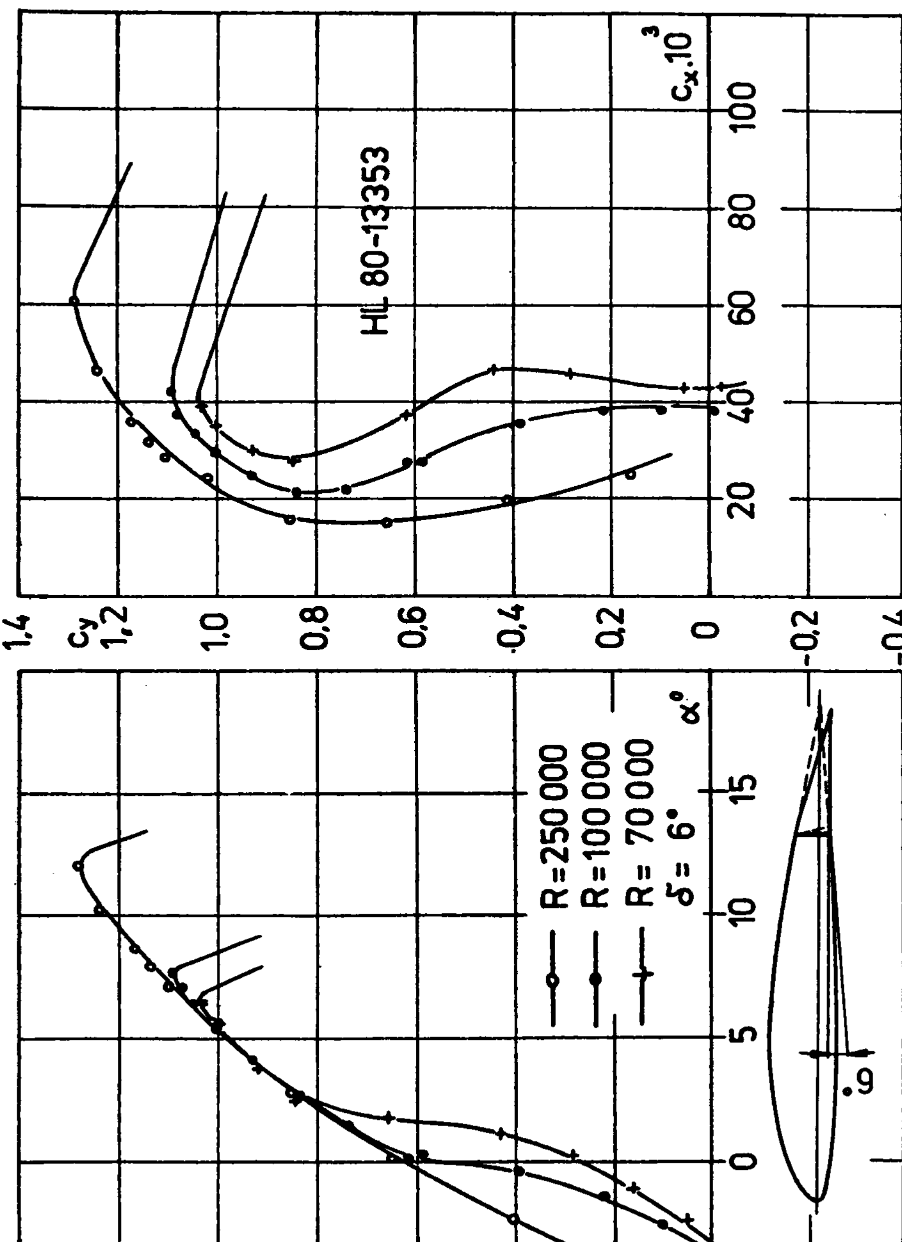
HL 80-13353
c_y
$c_x.10^3$
$\alpha°$
R = 250 000
R = 100 000
R = 70 000
δ = 6°
1,4
1,2
1,0
0,8
0,6
0,4
0,2
0
-0,2
-0,4
20
40
60
80
100
-5
0
5
10
15
6

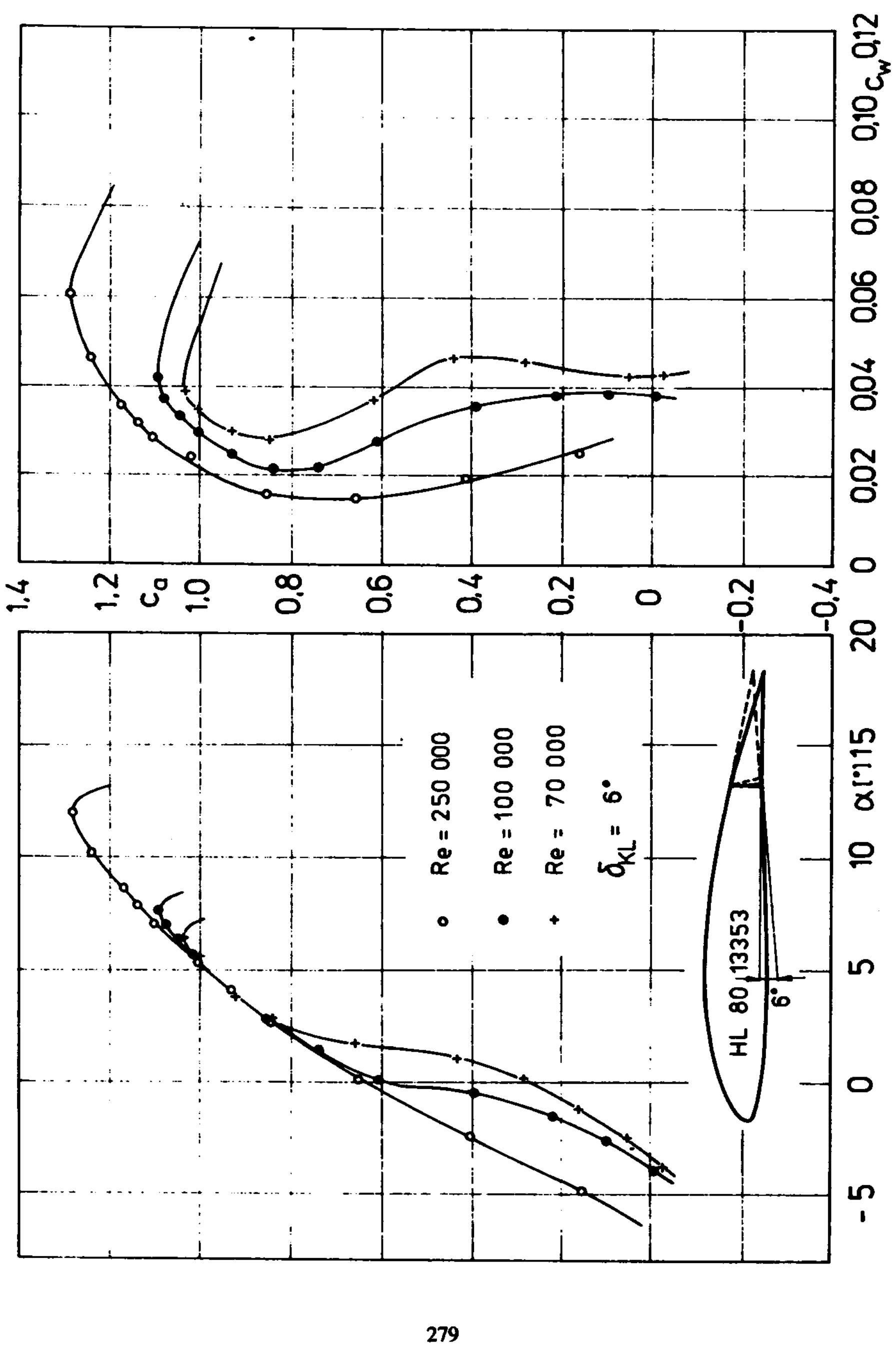

Re = 250 000
Re = 100 000
Re = 70 000
δ_{KL} = 6°
HL 80 13353
6°
c_a
1.4
1,2
1.0
0,8
0,6
0,4
0,2
0
-0,2
-0,4
α [°] 15
-5
0
5
10
20
0
0,02
0,04
0,06
0,08
0,10 c_w 0,12

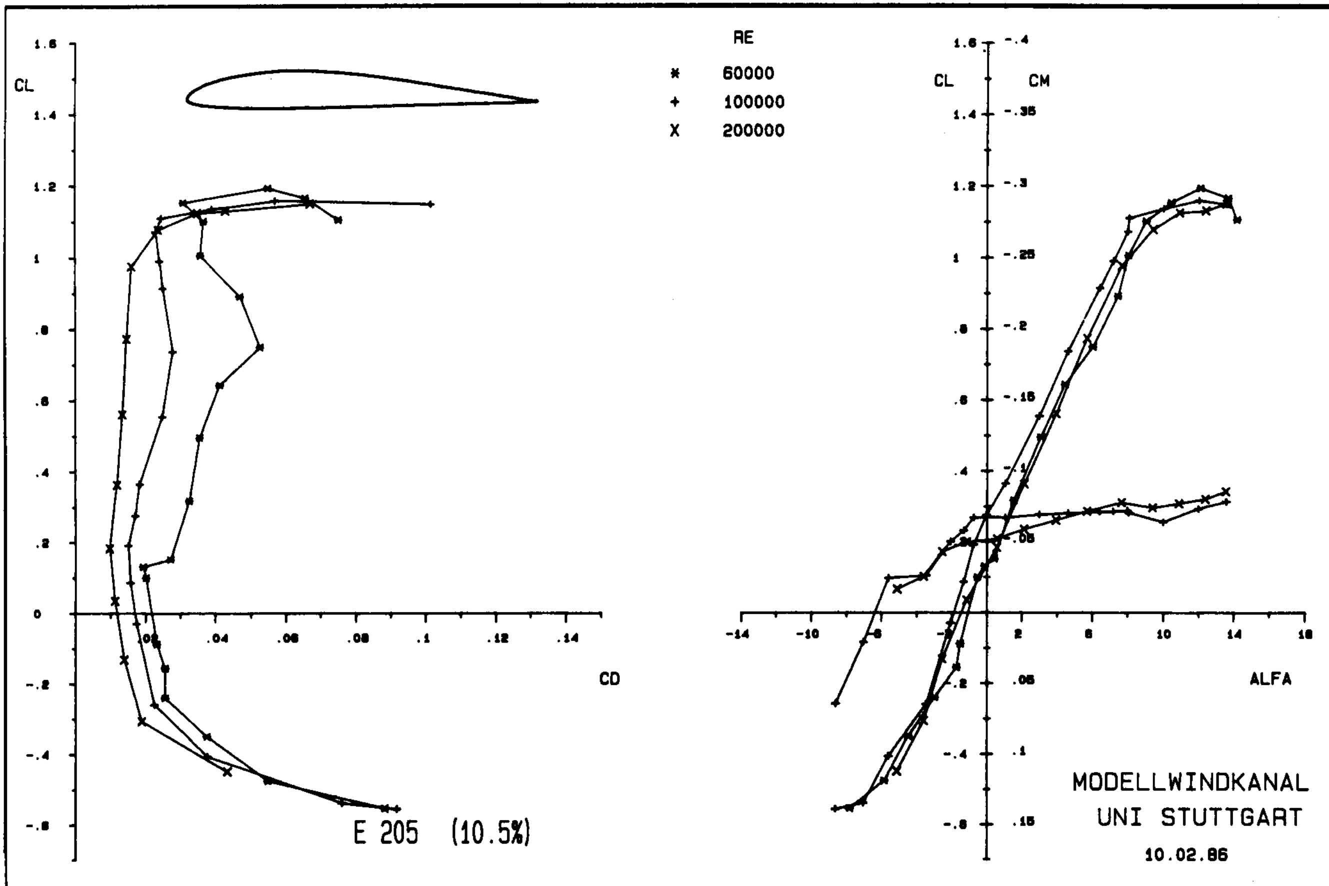

CL
1.6
1.4
1.2
1
.8
.6
.4
.2
0
-.2
-.4
-.6
.02
.04
.06
.08
.1
.12
.14
CD
RE
* 60000
+ 100000
X 200000
CM
-.4
-.35
-.3
-.25
-.2
-.15
-.1
-.05
.05
.1
.15
-14
-10
-6
2
6
10
14
18
ALFA
E 205 (10.5%)
MODELLWINDKANAL
UNI STUTTGART
10.02.86

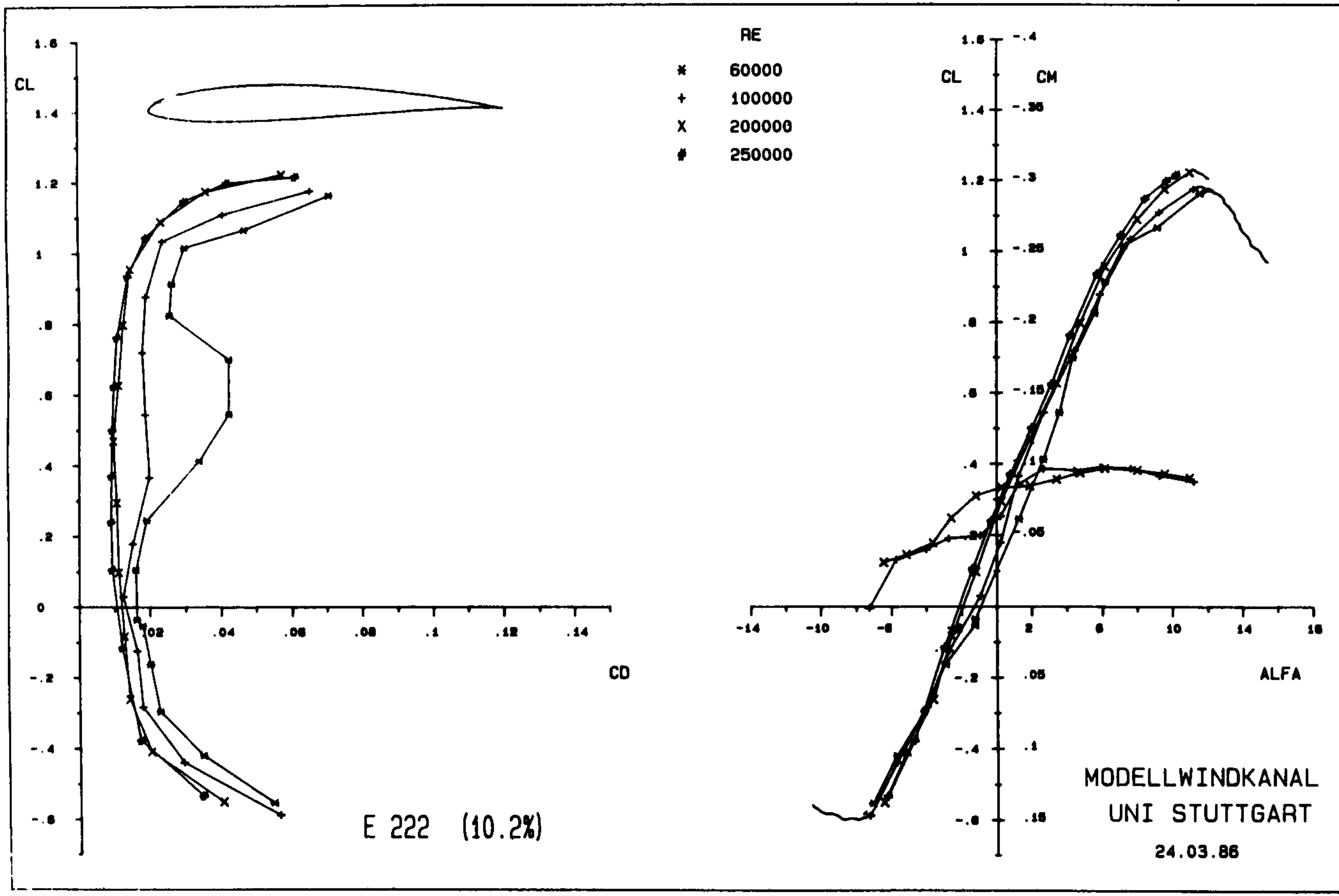

E 222 (10.2%)
RE
* 60000
+ 100000
X 200000
250000
CL
CD
CM
ALFA
MODELLWINDKANAL
UNI STUTTGART
24.03.86

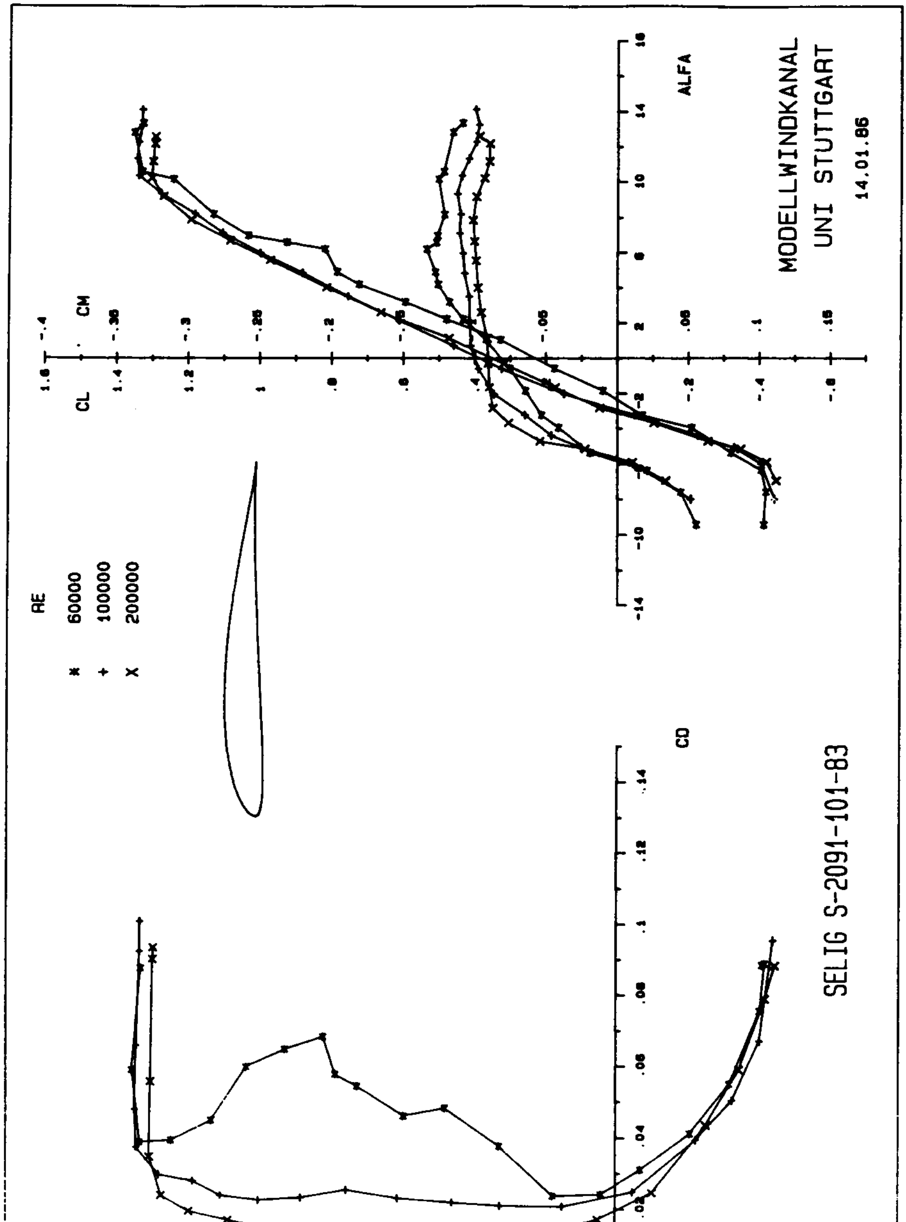
SELIG S-2091-101-83
MODELLWINDKANAL
UNI STUTTGART
14.01.86
RE
60000
100000
200000
CL
CD
CM
ALFA

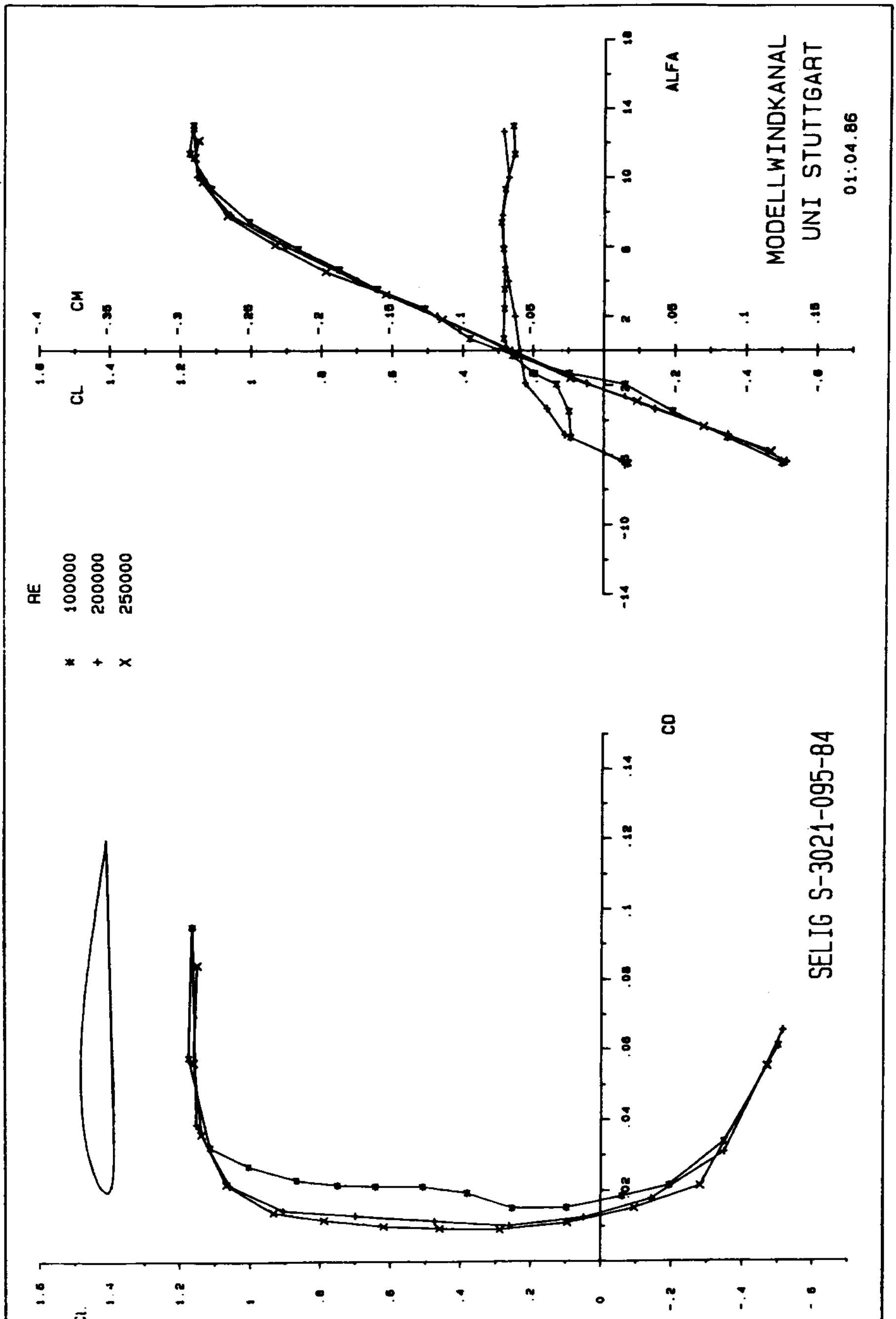
MODELLWINDKANAL
UNI STUTTGART
01:04.86
SELIG S-3021-095-84
RE
100000
200000
250000
CL
CM
ALFA
CD
CL

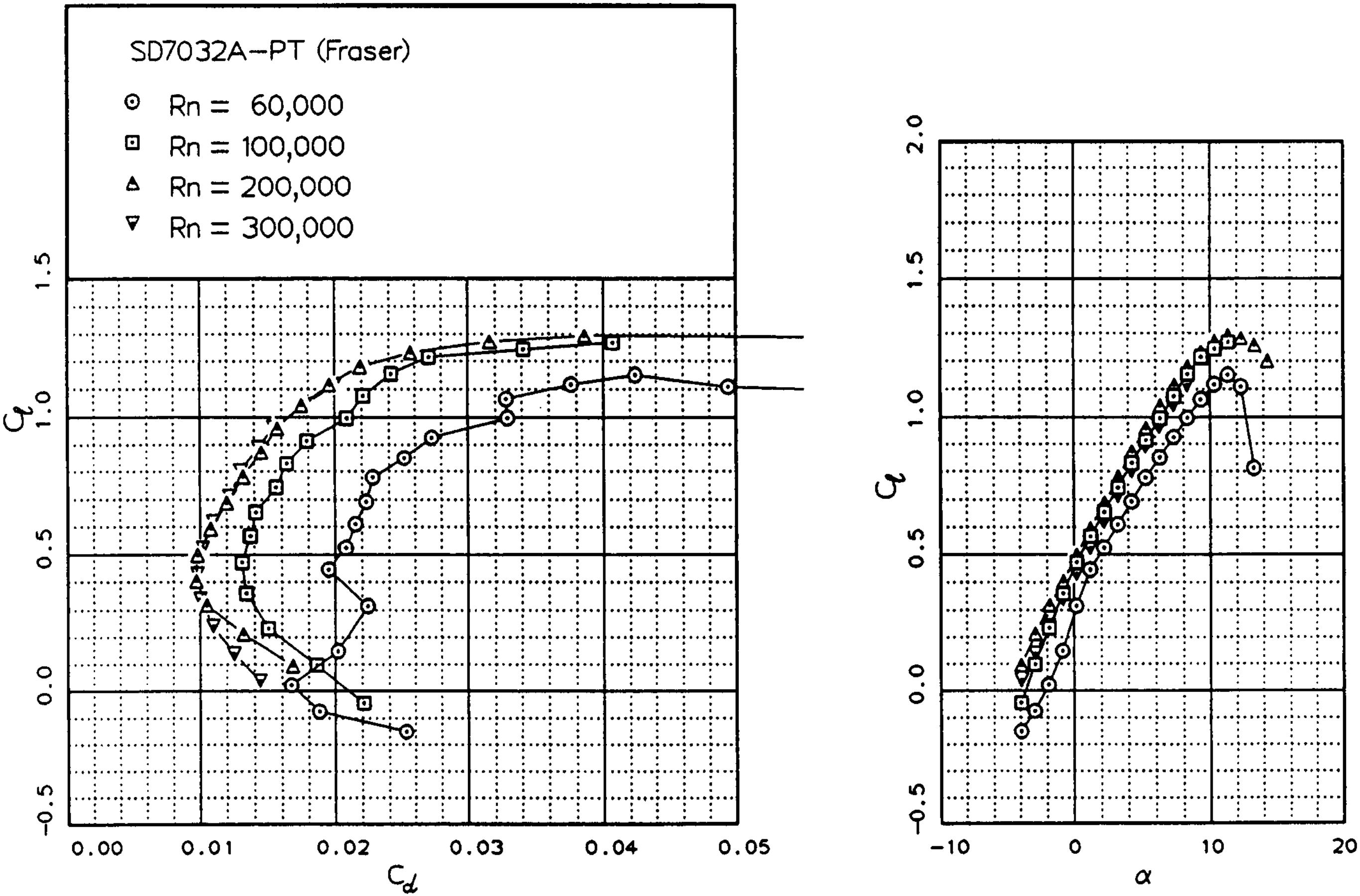
SD7032A—PT (Fraser)
Rn = 60,000
Rn = 100,000
Rn = 200,000
Rn = 300,000
C_l
C_d
α
0.00
0.01
0.02
0.03
0.04
0.05
−0.5
0.0
0.5
1.0
1.5
2.0
−10
0
10
20

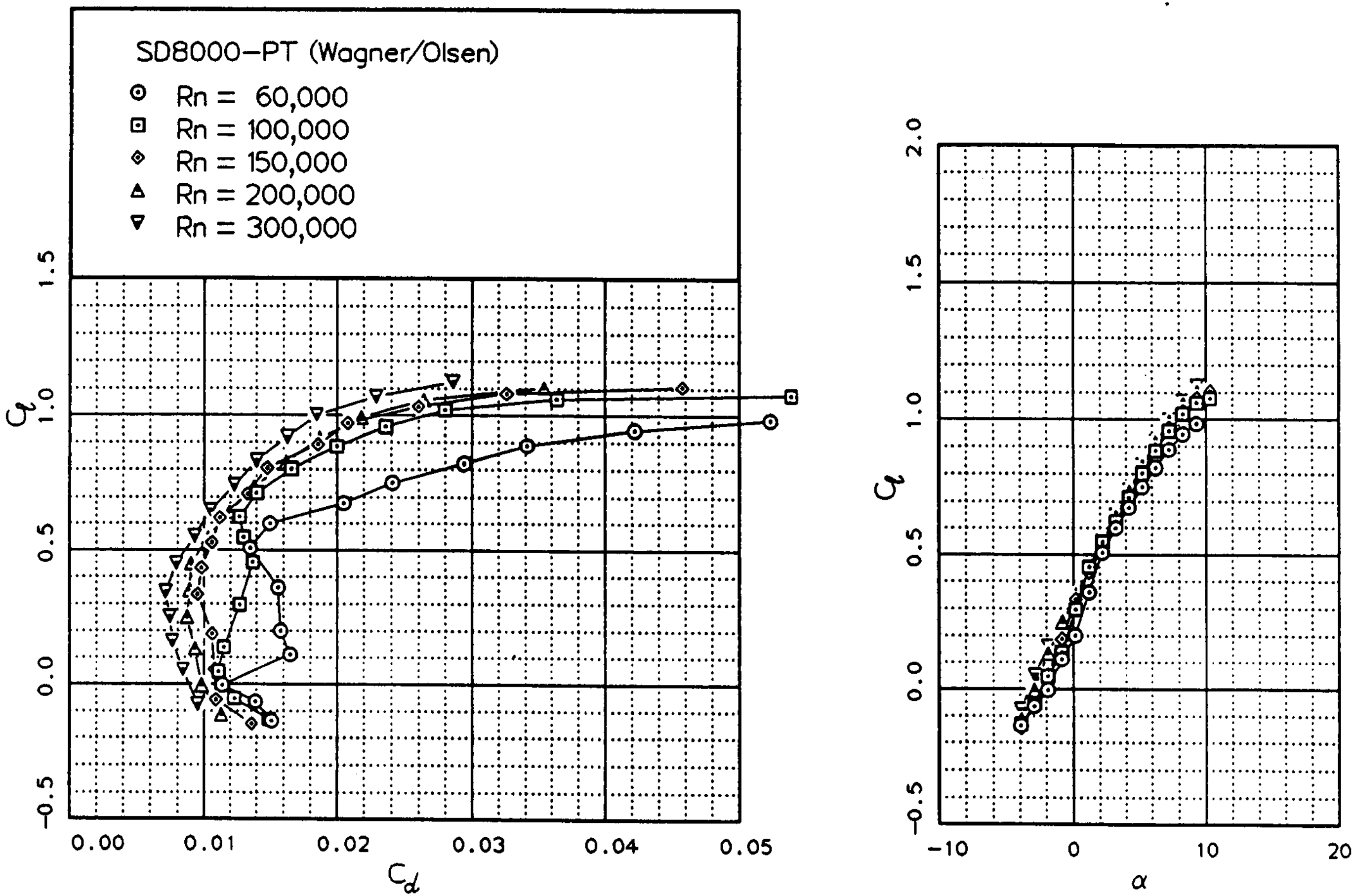
SD8000–PT (Wagner/Olsen)
Rn = 60,000
Rn = 100,000
Rn = 150,000
Rn = 200,000
Rn = 300,000
C_l
C_d
α
-0.5
0.0
0.5
1.0
1.5
2.0
0.00
0.01
0.02
0.03
0.04
0.05
-10
0
10
20

Appendix 3

Ordinates for nearly 200 different aerofoils are given in this appendix, together with four low drag bodies (Young bodies) for fuselages, fairings, wheel spats etc. Not all profiles will be satisfactory for models, some have been included only to amplify comments in the text. The modeller should choose his aerofoils with discretion, bearing in mind the general principles discussed in the relevant chapters.

The profile drawings given here have been plotted by a computer. In many cases, the results are accurate enough for the drawing to be enlarged or reduced photographically to produce a perfect template outline for modelling. In other cases, where the ordinates give a coarser outline, the mechanical plotter produces an angular drawing with segments of straight lines and other small irregularities. In these cases the modeller should smooth the outline with a 'zip' or 'French' curve before cutting the template. The ordinates for the Wortmann M 2 aerofoil in particular produce an irregular, corrugated leading edge. This should be smoothed in practice. The corrugations are a result of the approximate methods of calculations used by Wortmann for this very early, low speed aerofoil.

Hand plotting is laborious but can produce accurate results if carefully done. The method is described in most elementary books on aeromodelling. The more advanced aerofoils given in this appendix have been produced by computer and the old, standard plotting points are not used. Instead there may be different chord stations for upper and lower surfaces.

DESIGNING NEW AEROFOILS

A mathematical method of working out new ordinates, starting from a chosen camber line and a symmetrical thickness form, is given in the standard text, *Theory of Wing Sections* by Abbott and Von Doenhoff. Although not a quick procedure, the calculations required are not difficult. Failing this method, a modeller may devise his own wing sections by the graphical method outlined in Fig. A 8. The camber line is plotted first, then at each station a circle is drawn, the radius being taken from the ordinates for the thickness form, and the centre being on the camber line at the appropriate point. Finally a smooth curve is drawn *tangentially* to all the circles and the nose radius to produce the aerofoil.

WORKING OUT THE CAMBER

Many aerofoil designations contain information about camber and thickness. The NACA systems are described in Chapter 7, with further information in Abbott and Von

Doenhoff as above. The Benedek Aerofoils give the camber, in percent of chord in the last digit, thus B 10355 is cambered 5 percent, 8356, 6 percent and so on. The first figure gives the profile thickness, the central figure or figures the position of the maximum thickness point, hence Benedek B 12355 is 12% thick at 35%, and cambered 5%.

In other cases it is sometimes possible to work out the maximum camber arithmetically. This is applicable only where the aerofoil ordinates are based on a chord line running through the leading edge and trailing edge. In these cases, by finding the thickness of the profile at a number of stations and subtracting half this figure, at each place, from the *upper* surface ordinate, the approximate ordinate for the camber line is found and the maximum value then easily discovered. Note that in finding the profile thickness in this way, minus signs below the chord line must be allowed for. This method of halving the thickness will *not* produce accurate ordinates for the aerofoil camber line, especially near the nose and trailing edge, but it will produce a correct figure for the maximum camber and its location.

The camber of other aerofoils, plotted on tangential chord lines or on other arbitrary reference lines, may be estimated by measuring from the plotted profile. The true chord line, nose to trailing edge, must first be drawn in, then the half thickness plotted as accurately as possible, and the camber measured.

More accurate estimates of camber from the ordinates may be carried out by somewhat more complex arithmetic, but this is seldom necessary.

Fig. A8 Fig. A8

i take ordinates of desired camber line, and plot.
ii take radii of circles from desired thickness and draw on arc as shown.
iii draw smooth curved lines tangential to circles.

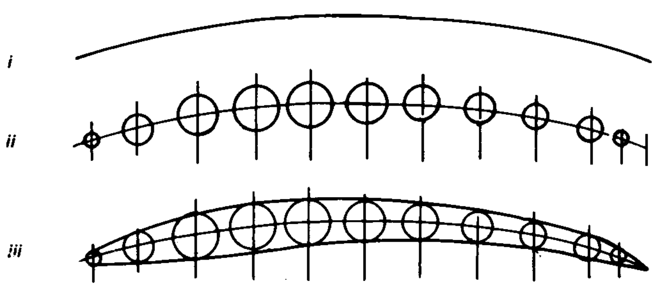

INDEX OF AEROFOILS

Mean lines, low drag bodies and symmetrical profiles are grouped at the beginning of this section. The N.A.C.A. '6' thickness forms are arranged in order of increasing laminar flow (min. pressure point at 30, 40, 50% chord etc), and in increasing thickness (6, 9, 10, 12, 15, 18% etc.) In the section devoted to cambered profiles, the N.A.C.A. 6 series aerofoils are arranged in order of increasing thickness (9 to 18%), then by increasing camber (shown by the third figure from the right which indicates the 'ideal' c_l in tenths – .2, .3, .4, .6 etc), and then by increasing proportion of laminar flow (given by the second digit from the left, 30%, 40%, 50% etc.) The various letters and other additions indicate minor modifications to the profiles (e.g., $A = 0.5$ indicates the use of $A = 0.5$ mean line instead of the usual $A = 1$).

The Benedek aerofoils are arranged first by increasing camber, usually given in percent by the last figure (2, 3, 4, 5% etc). They are then arranged by order of increasing thickness, given by the first figure (8, 9, 10, 12% etc.) and finally, in order of increasingly-rearward position of the maximum thickness point, given by the two central digits (30, 35, 40, 45, 50, 55% etc.) Additional figures such as B, F, B/3, etc., indicate minor modifications. The other profiles are not arranged in any special order. No attempt has been made to include all the new aerofoil sections produced during the past decade. However, some less well known profiles designed by Girsberger and Selig as well as some of the HQ profiles of Helmut Quast, have been included in this edition, along with a few additional Eppler profiles.

Publisher's note
In order to include all these aerofoils it has been necessary to reduce the size of ordinates and illustrations. Work may be simplified by increasing the size of a page containing a selected aerofoil by 130–150% using an enlarging photocopier.

MEAN LINES

Reflex for zero pitching moment, scale to reqd camber		NACA 210, CL Ideal 0.3		NACA A = 0.0		NACA A = 0.5		NACA A = 0.9		NACA A = 1.0	
Chord Station	Upper Surface	Chord Station	Upper Surface	Chord Station	Upper Surface	Chord Station	Upper Surface	Chord Station	Upper Surface	Chord Station	Upper Surface
XU	YU	XU	YU	XU	YU	XU	YU	XU	YU	XU	YU
.000	.000	.000	.000	.000	.000	.000	.000	.000	.000	.000	.000
5.000	3.240	1.250	.596	.500	.460	.500	.345	.500	.269	.500	.250
10.000	5.770	2.500	.928	.750	.641	.750	.485	.750	.379	.750	.350
15.000	7.650	5.000	1.114	1.250	.964	1.250	.735	1.250	.577	1.250	.535
20.000	8.940	7.500	1.087	2.500	1.641	2.500	1.295	2.500	1.008	2.500	.930
25.000	9.700	10.000	1.058	5.000	2.693	5.000	2.205	5.000	1.720	5.000	1.580
30.000	9.990	15.000	.999	7.500	3.507	7.500	2.970	7.500	2.316	7.500	2.120
35.000	9.880	20.000	.940	10.000	4.161	10.000	3.630	10.000	2.835	10.000	2.585
40.000	9.430	25.000	.881	15.000	5.124	15.000	4.740	15.000	3.707	15.000	3.365
45.000	8.700	30.000	.823	20.000	5.747	20.000	5.620	20.000	4.410	20.000	3.980
50.000	7.760	40.000	.705	25.000	6.114	25.000	6.310	25.000	4.980	25.000	4.475
55.000	6.660	50.000	.588	30.000	6.277	30.000	6.840	30.000	5.435	30.000	4.860
60.000	5.460	60.000	.470	35.000	6.273	35.000	7.215	35.000	5.787	35.000	5.150
65.000	4.240	70.000	.353	40.000	6.130	40.000	7.430	40.000	6.045	40.000	5.355
70.000	3.040	80.000	.235	45.000	5.871	45.000	7.490	45.000	6.212	45.000	5.475
75.000	1.940	90.000	.118	50.000	5.516	50.000	7.350	50.000	6.290	50.000	5.515
80.000	.990	95.000	.059	55.000	5.081	55.000	6.965	55.000	6.279	55.000	5.475
85.000	.260	100.000	.000	60.000	4.581	60.000	6.405	60.000	6.178	60.000	5.355
90.000	-.190			65.000	4.032	65.000	5.725	65.000	5.981	65.000	5.150
95.000	-.300			70.000	3.455	70.000	4.955	70.000	5.681	70.000	4.860
100.000	.000			75.000	2.836	75.000	4.130	75.000	5.265	75.000	4.475
				80.000	2.217	80.000	3.265	80.000	4.714	80.000	3.980
				85.000	1.604	85.000	2.395	85.000	3.987	85.000	3.365
				90.000	1.013	90.000	1.535	90.000	2.984	90.000	2.585
				95.000	.467	95.000	.720	95.000	1.503	95.000	1.580
				100.000	.000	100.000	.000	100.000	.000	100.000	.000

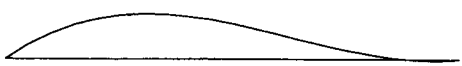

REFLEX MEAN LINE FOR ZERO PITCHING MOMENT SCALE TO REQUIRED CAMBER

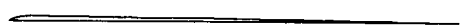

NACA 210 MEAN LINE CL IDEAL 0.3

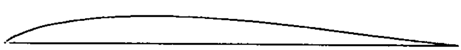

NACA A = 0.0 MEAN LINE

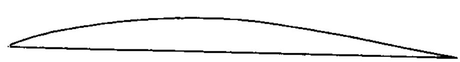

NACA A = 0.5 MEAN LINE

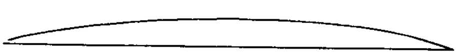

NACA A = 0.9 MEAN LINE

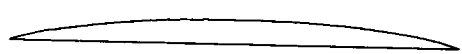

NACA A = 1.0 MEAN LINE

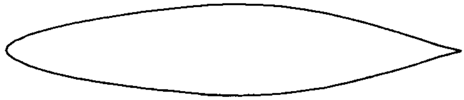

LOW DRAG BODY LAMINAR FLOW TO 60 PERCENT NOSE RADIUS 0.986 PERCENT

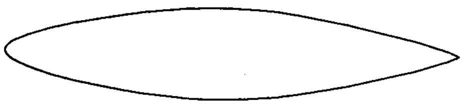

LOW DRAG BODY LAMINAR FLOW TO 50 PERCENT NOSE RADIUS 1.026 PERCENT

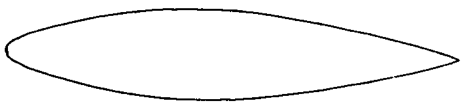

LOW DRAG BODY LAMINAR FLOW TO 40 PERCENT NOSE RADIUS 1.465 PERCENT

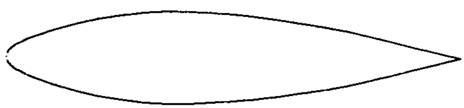

LOW DRAG BODY LAMINAR FLOW TO 30 PERCENT NOSE RADIUS 1.562 PERCENT

Low Drag Body. Laminar Flow to 60 Percent. Nose radius 0.986 Percent.

Chord Station XU	Upper Surface YU	Chord Station XL	Lower Surface YL
.000	.000	.000	.000
.100	.335	.100	-.335
.200	.620	.200	-.620
.300	.770	.300	-.770
.400	.899	.400	-.899
.500	1.000	.500	-1.000
1.000	1.460	1.000	-1.460
1.500	1.800	1.500	-1.800
2.000	2.100	2.000	-2.100
2.500	2.336	2.500	-2.336
5.000	3.405	5.000	-3.405
10.000	4.938	10.000	-4.938
15.000	6.085	15.000	-6.085
20.000	7.002	20.000	-7.002
25.000	7.781	25.000	-7.781
30.000	8.462	30.000	-8.462
35.000	9.048	35.000	-9.048
40.000	9.520	40.000	-9.520
45.000	9.845	45.000	-9.845
50.000	9.991	50.000	-9.991
55.000	9.921	55.000	-9.921
60.000	9.612	60.000	-9.612
65.000	9.047	65.000	-9.047
70.000	8.223	70.000	-8.223
75.000	7.150	75.000	-7.150
80.000	5.860	80.000	-5.860
85.000	4.399	85.000	-4.339
90.000	2.860	90.000	-2.860
95.000	1.314	95.000	-1.314
97.500	.613	97.500	-.613
100.000	.000	100.000	.000

Low Drag Body. Laminar Flow to 50 Percent. Nose radius 1.026 Percent.

Chord Station XU	Upper Surface YU	Chord Station XL	Lower Surface YL
.000	.000	.000	.000
.100	.340	.100	-.340
.200	.625	.200	-.625
.300	.775	.300	-.775
.400	.920	.400	-.920
.500	1.030	.500	-1.030
1.000	1.500	1.000	-1.500
1.500	1.850	1.500	-1.850
2.000	2.150	2.000	-2.150
2.388	2.500	-2.388	2.500
5.000	3.480	5.000	-3.480
10.000	5.039	10.000	-5.039
15.000	6.197	15.000	-6.197
20.000	7.154	20.000	-7.154
25.000	7.987	25.000	-7.987
30.000	8.715	30.000	-8.715
35.000	9.313	35.000	-9.313
40.000	9.743	40.000	-9.743
45.000	9.967	45.000	-9.967
50.000	9.959	50.000	-9.959
55.000	9.709	55.000	-9.709
60.000	9.224	60.000	-9.224
65.000	8.528	65.000	-8.528
70.000	7.662	70.000	-7.662
75.000	6.676	75.000	-6.676
80.000	5.610	80.000	-5.610
85.000	4.483	85.000	-4.483
90.000	3.258	90.000	-3.258
95.000	1.827	95.000	-1.827
97.500	.978	97.500	-.978
100.000	.000	100.000	.000

Low Drag Body. Laminar Flow to 40 Percent. Nose radius 1.465 Percent.

Chord Station XU	Upper Surface YU	Chord Station XL	Lower Surface YL
.000	.000	.000	.000
.100	.570	.100	-.570
.200	.780	.200	-.780
.300	.970	.300	.970
.400	1.120	.400	-1.120
.500	1.240	.500	-1.240
1.000	1.770	1.000	-1.770
1.500	2.140	1.500	-2.140
2.000	2.440	2.000	-2.440
2.500	2.679	2.500	-2.679
5.000	3.776	5.000	-3.776
10.000	5.373	10.000	-5.373
15.000	6.640	15.000	-6.640
20.000	7.716	20.000	-7.716
25.000	8.601	25.000	-8.601
30.000	9.280	30.000	-9.280
35.000	9.738	35.000	-9.738
40.000	9.988	40.000	-9.988
45.000	9.988	45.000	-9.988
50.000	9.753	50.000	-9.753
55.000	9.339	55.000	-9.339
60.000	8.753	60.000	-8.753
65.000	8.028	65.000	-8.028
70.000	7.190	70.000	-7.190
75.000	6.269	75.000	-6.269
80.000	5.278	80.000	-5.278
85.000	4.209	85.000	-4.209
90.000	3.017	90.000	-3.017
95.000	1.659	95.000	-1.659
97.500	.874	97.500	-.874
100.000	.000	100.000	.000

Low Drag Body. Laminar Flow to 30 Percent. Nose radius 1.562 Percent

Chord Station XU	Upper Surface YU	Chord Station XL	Lower Surface YL
.000	.000	.000	.000
.100	.600	.100	-.600
.200	.860	.200	-.860
.300	1.050	.300	-1.050
.400	1.210	.400	-1.210
.500	1.340	.500	-1.340
1.000	1.880	1.000	-1.880
1.500	2.270	1.500	-2.270
2.000	2.690	2.000	-2.690
2.500	2.882	2.500	-2.882
5.000	4.075	5.000	-4.075
10.000	5.847	10.000	-5.847
15.000	7.243	15.000	-7.243
20.000	8.363	20.000	-8.363
25.000	9.194	25.000	-9.194
30.000	9.732	30.000	-9.732
35.000	9.992	35.000	-9.992
40.000	10.000	40.000	-10.000
45.000	9.795	45.000	-9.795
50.000	9.413	50.000	-9.413
55.000	8.891	55.000	-8.891
60.000	8.258	60.000	-8.258
65.000	7.528	65.000	-7.528
70.000	6.706	70.000	-6.706
75.000	5.783	75.000	-5.783
80.000	4.749	80.000	-4.749
85.000	3.603	85.000	-3.603
90.000	2.343	90.000	-2.343
95.000	1.104	95.000	-1.104
97.500	.513	97.500	-.513
100.000	.000	100.000	.000

NACA 63 009

Chord Station XU	Upper Surface YU	Chord Station XL	Lower Surface YL
.000	.000	.000	.000
.500	.749	.500	-.749
.750	.906	.750	-.906
1.250	1.151	1.250	-1.151
2.500	1.582	2.500	-1.582
5.000	2.196	5.000	-2.196
7.500	2.655	7.500	-2.655
10.000	3.024	10.000	-3.024
15.000	3.591	15.000	-3.591
20.000	3.997	20.000	-3.997
30.000	4.442	30.000	-4.442
40.000	4.447	40.000	-4.447
50.000	4.056	50.000	-4.056
60.000	3.358	60.000	-3.358
70.000	2.458	70.000	-2.458
80.000	1.471	80.000	-1.471
90.000	.550	90.000	-.550
95.000	.196	95.000	-.196
100.000	.000	100.000	.000

NACA 63 006

Chord Station XU	Upper Surface YU	Chord Station XL	Lower Surface YL
.000	.000	.000	.000
.050	.160	.050	-.160
.100	.240	.100	-.240
.200	.350	.200	-.350
.400	.500	.400	-.500
.500	.503	.500	-.503
.750	.609	.750	-.609
1.250	.771	1.250	-.771
2.500	1.057	2.500	-1.057
5.000	1.462	5.000	-1.462
7.500	1.766	7.500	-1.766
10.000	2.010	10.000	-2.010
15.000	2.386	15.000	-2.386
20.000	2.656	20.000	-2.656
30.000	2.954	30.000	-2.954
40.000	2.971	40.000	-2.971
50.000	2.723	50.000	-2.723
60.000	2.267	60.000	-2.267
70.000	1.670	70.000	-1.670
80.000	1.008	80.000	-1.008
90.000	.383	90.000	-.383
95.000	.138	95.000	-.138
100.000	.000	100.000	.000

NACA 0010 L.E. radius 1.10 Percent

Chord Station XU	Upper Surface YU	Chord Station XL	Lower Surface YL
.000	.000	.000	.000
.200	.620	.200	-.620
.400	.910	.400	-.910
.600	1.120	.600	-1.120
.800	1.250	.800	-1.250
1.250	1.578	1.250	-1.578
2.500	2.178	2.500	-2.178
5.000	2.962	5.000	-2.962
7.500	3.500	7.500	-3.500
10.000	3.902	10.000	-3.902
15.000	4.455	15.000	-4.455
20.000	4.782	20.000	-4.782
25.000	4.952	25.000	-4.952
30.000	5.002	30.000	-5.002
40.000	4.837	40.000	-4.837
50.000	4.412	50.000	-4.412
60.000	3.803	60.000	-3.803
70.000	3.053	70.000	-3.053
80.000	2.187	80.000	-2.187
90.000	1.207	90.000	-1.207
95.000	.672	95.000	-.672
100.000	.105	100.000	-.105

NACA 0009 L.E. radius 0.89 Percent

Chord Station XU	Upper Surface YU	Chord Station XL	Lower Surface YL
.000	.000	000	000
.200	.490	.200	-.490
.400	.820	.400	-.820
.600	1.010	.600	-1.010
.800	1.170	.800	-1.170
1.250	1.420	1.250	-1.420
2.500	1.961	2.500	-1.961
5.000	2.666	5.000	-2.666
7.500	3.150	7.500	-3.150
10.000	3.512	10.000	-3.512
15.000	4.009	15.000	-4.009
20.000	4.303	20.000	-4.303
25.000	4.456	25.000	-4.456
30.000	4.501	30.000	-4.501
40.000	4.352	40.000	-4.352
50.000	3.971	50.000	-3.971
60.000	3.423	60.000	-3.423
70.000	2.748	70.000	-2.748
80.000	1.967	80.000	-1.967
90.000	1.086	90.000	-1.086
95.000	.605	95.000	-.605
100.000	.095	100.000	-.095

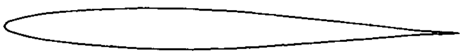

NACA 63 009

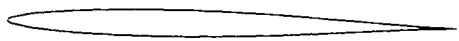

NACA 63 006

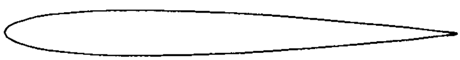

NACA 0010 LE RADIUS 1.10 PERCENT

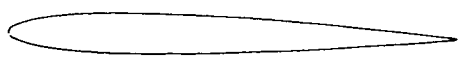

NACA 0009 LE RADIUS 0.89 PERCENT

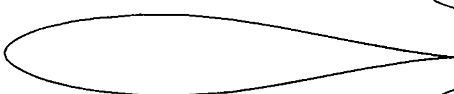

NACA 63 3 018

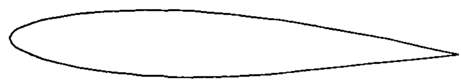

NACA 63 2 A 015

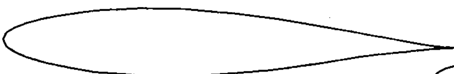

NACA 63 2 015

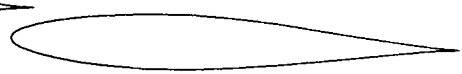

NACA 63 1 012

NACA 63 3 018

Chord Station XU	Upper Surface YU	Chord Station XL	Lower Surface YL
.000	.000	.000	.000
.500	1.404	.500	-1.404
.750	1.713	.750	-1.713
1.250	2.217	1.250	-2.217
2.500	3.104	2.500	-3.104
5.000	4.362	5.000	-4.362
7.500	5.308	7.500	-5.308
10.000	6.068	10.000	-6.068
15.000	7.225	15.000	-7.225
20.000	8.048	20.000	-8.048
30.000	8.913	30.000	-8.913
40.000	8.845	40.000	-8.845
50.000	7.942	50.000	-7.942
60.000	6.455	60.000	-6.455
70.000	4.622	70.000	-4.622
80.000	2.691	80.000	-2.691
90.000	.985	90.000	-.985
95.000	.348	95.000	-.348
100.000	.000	100.000	.000

NACA 63 2 A 015

Chord Station XU	Upper Surface YU	Chord Station XL	Lower Surface YL
.000	.000	.000	.000
.500	1.203	.500	-1.203
.750	1.448	.750	-1.448
1.250	1.844	1.250	-1.844
2.500	2.579	2.500	-2.579
5.000	3.618	5.000	-3.618
7.500	4.382	7.500	-4.382
10.000	4.997	10.000	-4.997
15.000	5.942	15.000	-5.942
20.000	6.619	20.000	-6.619
30.000	7.384	30.000	-7.384
40.000	7.435	40.000	-7.435
50.000	6.858	50.000	-6.858
60.000	5.820	60.000	-5.820
70.000	4.468	70.000	-4.468
80.000	2.991	80.000	-2.991
90.000	1.512	90.000	-1.512
95.000	.772	95.000	-.772
100.000	.000	100.000	.000

NACA 63 2 015

Chord Station XU	Upper Surface YU	Chord Station XL	Lower Surface YL
.000	.000	.000	.000
.500	1.204	.500	-1.204
.750	1.462	.750	-1.462
1.250	1.878	1.250	-1.878
2.500	2.610	2.500	-2.610
5.000	3.648	5.000	-3.648
7.500	4.427	7.500	-4.427
10.000	5.055	10.000	-5.055
15.000	6.011	15.000	-6.011
20.000	6.693	20.000	-6.693
30.000	7.421	30.000	-7.421
40.000	7.386	40.000	-7.386
50.000	6.665	50.000	-6.665
60.000	5.453	60.000	-5.453
70.000	3.934	70.000	-3.934
80.000	2.310	80.000	-2.310
90.000	.852	90.000	-.852
95.000	.300	95.000	-.300
100.000	.000	100.000	.000

NACA 63 1 012

Chord Station XU	Upper Surface YU	Chord Station XL	Lower Surface YL
.000	.000	.000	.000
.500	.985	.500	-.985
.750	1.194	.750	-1.194
1.250	1.519	1.250	-1.519
2.500	2.102	2.500	-2.102
5.000	2.925	5.000	-2.925
7.500	3.542	7.500	-3.542
10.000	4.039	10.000	-4.039
15.000	4.799	15.000	-4.799
20.000	5.342	20.000	-5.342
30.000	5.930	30.000	-5.930
40.000	5.920	40.000	-5.920
50.000	5.370	50.000	-5.370
60.000	4.420	60.000	-4.420
70.000	3.210	70.000	-3.210
80.000	1.902	80.000	-1.902
90.000	.707	90.000	-.707
95.000	.250	95.000	-.250
100.000	.000	100.000	.000

NACA 64 010 L.E. radius 0.720 Percent

Chord Station XU	Upper Surface YU	Chord Station XL	Lower Surface YL
.000	.000	.000	.000
.500	.820	.500	-.820
.750	.989	.750	-.989
1.250	1.250	1.250	-1.250
2.500	1.701	2.500	-1.701
5.000	2.343	5.000	-2.343
7.500	2.826	7.500	-2.826
10.000	3.221	10.000	-3.221
15.000	3.842	15.000	-3.842
20.000	4.302	20.000	-4.302
30.000	4.864	30.000	-4.864
40.000	4.988	40.000	-4.988
50.000	4.586	50.000	-4.586
60.000	3.820	60.000	-3.820
70.000	2.827	70.000	-2.827
80.000	1.722	80.000	-1.722
90.000	.671	90.000	-.671
95.000	.248	95.000	-.248
100.000	.000	100.000	.000

NACA 64 009 L.E. radius 0.579 Percent

Chord Station XU	Upper Surface YU	Chord Station XL	Lower Surface YL
.000	.000	.000	.000
.500	.739	.500	-.739
.750	.892	.750	-.892
1.250	1.128	1.250	-1.128
2.500	1.533	2.500	-1.533
5.000	2.109	5.000	-2.109
7.500	2.543	7.500	-2.543
10.000	2.898	10.000	-2.898
15.000	3.455	15.000	-3.455
20.000	3.868	20.000	-3.868
30.000	4.373	30.000	-4.373
40.000	4.490	40.000	-4.490
50.000	4.136	50.000	-4.1[illegible]
60.000	3.452	60.000	-3.452
70.000	2.561	70.000	-2.561
80.000	1.564	80.000	-1.564
90.000	.611	90.000	-.611
95.000	.227	95.000	-.227
100.000	.000	100.000	.000

NACA 64 006

Chord Station XU	Upper Surface YU	Chord Station XL	Lower Surface YL
.000	.000	.000	.000
.500	.494	.500	-.494
.750	.596	.750	-.596
1.250	.754	1.250	-.754
2.500	1.024	2.500	-1.024
5.000	1.405	5.000	-1.405
7.500	1.692	7.500	-1.692
10.000	1.928	10.000	-1.928
15.000	2.298	15.000	-2.298
20.000	2.572	20.000	-2.572
30.000	2.907	30.000	-2.907
40.000	2.995	40.000	-2.995
50.000	2.775	50.000	-2.775
60.000	2.331	60.000	-2.331
70.000	1.740	70.000	-1.740
80.000	1.072	80.000	-1.072
90.000	.423	90.000	-.423
95.000	.157	95.000	-.157
100.000	.000	100.000	.000

NACA 63 4 021

Chord Station XU	Upper Surface YU	Chord Station XL	Lower Surface YL
.000	.000	.000	.000
.500	1.583	.500	-1.583
.750	1.937	.750	-1.937
1.250	2.527	1.250	-2.527
2.500	3.577	2.500	-3.577
5.000	5.065	5.000	-5.065
7.500	6.182	7.500	-6.182
10.000	7.080	10.000	-7.080
15.000	8.441	15.000	-8.441
20.000	9.410	20.000	-9.410
30.000	10.412	30.000	-10.412
40.000	10.298	40.000	-10.298
50.000	9.206	50.000	-9.206
60.000	7.441	60.000	-7.441
70.000	5.290	70.000	-5.290
80.000	3.054	80.000	-3.054
90.000	1.113	90.000	-1.113
95.000	.392	95.000	-.392
100.000	.000	100.000	.000

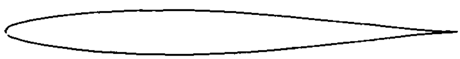

NACA 64 010 LE RADIUS 0.720 PERCENT

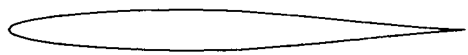

NACA 64 009 LE RADIUS 0.579 PERCENT

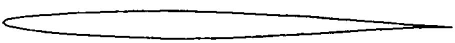

NACA 64 006

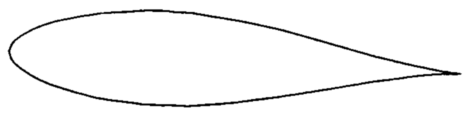

NACA 63 4 021

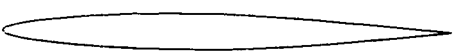

NACA 65 A 006

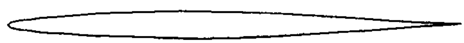

NACA 65 006

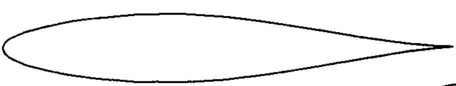

NACA 64 2 015 LE RADIUS 1.590 PERCENT

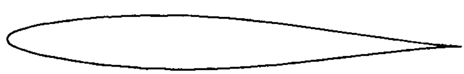

NACA 64 1 012

NACA 65 A 006

Chord Station XU	Upper Surface YU	Chord Station XL	Lower Surface YL
.000	.000	.000	.000
.500	.615	.500	-.615
.750	.746	.750	-.746
1.250	.951	1.250	-.951
2.500	1.303	2.500	-1.303
5.000	1.749	5.000	-1.749
7.500	2.120	7.500	-2.120
10.000	2.432	10.000	-2.432
15.000	2.926	15.000	-2.926
20.000	3.301	20.000	-3.301
30.000	3.791	30.000	-3.791
40.000	3.995	40.000	-3.995
50.000	3.895	50.000	-3.895
60.000	3.456	60.000	-3.456
70.000	2.763	70.000	-2.763
80.000	1.898	80.000	-1.898
90.000	.960	90.000	-.960
95.000	.489	95.000	-.489
100.000	.018	100.000	-.018

NACA 65 006

Chord Station XU	Upper Surface YU	Chord Station XL	Lower Surface YL
.000	.000	.000	.000
.500	.476	.500	-.476
.750	.574	.750	-.574
1.250	.717	1.250	-.717
2.500	.956	2.500	-.956
5.000	1.310	5.000	-1.310
7.500	1.589	7.500	-1.589
10.000	1.824	10.000	-1.824
15.000	2.197	15.000	-2.197
20.000	2.482	20.000	-2.482
30.000	2.852	30.000	-2.852
40.000	2.988	40.000	-2.988
50.000	2.900	50.000	-2.900
60.000	2.518	60.000	-2.518
70.000	1.935	70.000	-1.935
80.000	1.233	80.000	-1.233
90.000	.510	90.000	-.510
95.000	.195	95.000	-.195
100.000	.000	100.000	.000

NACA 64 2 015 L.E. radius 1.590 Percent

Chord Station XU	Upper Surface YU	Chord Station XL	Lower Surface YL
.000	.000	.000	.000
.500	1.208	.500	-1.208
.750	1.456	.750	-1.456
1.250	1.842	1.250	-1.842
2.500	2.528	2.500	-2.528
5.000	3.504	5.000	-3.504
7.500	4.240	7.500	-4.240
10.000	4.842	10.000	-4.842
15.000	5.785	15.000	-5.785
20.000	6.480	20.000	-6.480
30.000	7.319	30.000	-7.319
40.000	7.473	40.000	-7.473
50.000	6.810	50.000	-6.810
60.000	5.620	60.000	-5.620
70.000	4.113	70.000	-4.113
80.000	2.472	80.000	-2.472
90.000	.950	90.000	-.950
95.000	.346	95.000	-.346
100.000	.000	100.000	.000

NACA 64 1 012

Chord Station XU	Upper Surface YU	Chord Station XL	Lower Surface YL
.000	.000	.000	.000
.500	.978	.500	-.978
750	1.179	.750	-1.179
1.250	1.490	1.250	-1.490
2.500	2.035	2.500	-2.035
5.000	2.810	5.000	-2.810
7.500	3.394	7.500	-3.394
10.000	3.871	10.000	-3.871
15.000	4.620	15.000	-4.620
20.000	5.173	20.000	-5.173
30.000	5.844	30.000	-5.844
40.000	5.981	40.000	-5.981
50.000	5.480	50.000	-5.480
60.000	4.548	60.000	-4.548
70.000	3.350	70.000	-3.350
80.000	2.029	80.000	-2.009
90.000	.786	90.000	-.786
95.000	.288	95.000	-.288
100.000	.000	100.000	.000

NACA 65 3 018 L.E. radius 1.96 Percent

Chord Station XU	Upper Surface YU	Chord Station XL	Lower Surface YL
.000	.000	.000	.000
.500	1.337	.500	-1.337
.750	1.608	.750	-1.608
1.250	2.014	1.250	-2.014
2.500	2.751	2.500	-2.751
5.000	3.866	5.000	-3.866
7.500	4.733	7.500	-4.733
10.000	5.457	10.000	-5.457
15.000	6.606	15.000	-6.606
20.000	7.476	20.000	-7.476
30.000	8.595	30.000	-8.595
40.000	8.999	40.000	-8.999
50.000	8.568	50.000	-8.568
60.000	7.267	60.000	-7.267
70.000	5.426	70.000	-5.426
80.000	3.338	80.000	-3.338
90.000	1.319	90.000	-1.319
95.000	.490	95.000	-.490
100.000	.000	100.000	.000

NACA 65 2 015 L.E. radius 1.505 Percent

Chord Station XU	Upper Surface YU	Chord Station XL	Lower Surface YL
.000	.000	.000	.000
.500	1.124	.500	-1.124
.750	1.356	.750	-1.356
1.250	1.702	1.250	-1.702
2.500	2.324	2.500	-2.324
5.000	3.245	5.000	-3.245
7.500	3.959	7.500	-3.959
10.000	4.555	10.000	-4.555
15.000	5.504	15.000	-5.504
20.000	6.223	20.000	-6.223
30.000	7.152	30.000	-7.152
40.000	7.498	40.000	-7.498
50.000	7.168	50.000	-7.168
60.000	6.118	60.000	-6.118
70.000	4.600	70.000	-4.600
80.000	2.858	80.000	-2.858
90.000	1.144	90.000	-1.144
95.000	.428	95.000	-.428
100.000	.000	100.000	.000

NACA 65 1 012

Chord Station XU	Upper Surface YU	Chord Station XL	Lower Surface YL
.000	.000	.000	.000
.500	.923	.500	-.923
.750	1.109	.750	-1.109
1.250	1.387	1.250	-1.387
2.500	1.875	2.500	-1.875
5.000	2.606	5.000	-2.606
7.500	3.172	7.500	-3.172
10.000	3.647	10.000	-3.647
15.000	4.402	15.000	-4.402
20.000	4.975	20.000	-4.975
30.000	5.716	30.000	-5.716
40.000	5.997	40.000	-5.997
50.000	5.757	50.000	-5.757
60.000	4.943	60.000	-4.943
70.000	3.743	70.000	-3.743
80.000	2.345	80.000	-2.345
90.000	.947	90.000	-.947
95.000	.356	95.000	-.356
100.000	.000	100.000	.000

NACA 65 A 010

Chord Station XU	Upper Surface YU	Chord Station XL	Lower Surface YL
.000	.000	.000	.000
.500	.765	.500	-.765
.750	.928	.750	-.928
1.250	1.183	1.250	-1.183
2.500	1.623	2.500	-1.623
5.000	2.182	5.000	-2.182
7.500	2.650	7.500	-2.650
10.000	3.040	10.000	-3.040
15.000	3.658	15.000	-3.658
20.000	4.127	20.000	-4.127
30.000	4.742	30.000	-4.742
40.000	4.995	40.000	-4.995
50.000	4.863	50.000	-4.863
60.000	4.304	60.000	-4.304
70.000	3.432	70.000	-3.432
80.000	2.352	80.000	-2.332
90.000	1.188	90.000	-1.188
95.000	.604	95.000	-.604
100.000	.021	100.000	-.021

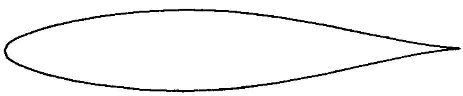

NACA 65 3 U18 LE RADIUS 1.95 PERCENT

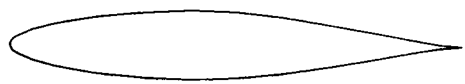

NACA 65 2 U15 LE RADIUS 1.505 PERCENT

Wortmann FX-71-L-150/K 20 For 20 Percent flap

Chord Station XU	Upper Surface YU	Chord Station XL	Lower Surface YL
.000	.000	.000	.000
.107	.829	.107	-.829
.428	1.474	.428	-1.474
.961	1.917	.961	-1.917
1.704	2.463	1.704	-2.463
2.653	2.952	2.653	-2.952
3.896	3.471	3.896	-3.471
5.158	3.953	5.158	-3.953
6.899	4.442	6.899	-4.442
8.427	4.887	8.427	-4.887
10.332	5.337	10.332	-5.337
12.408	5.731	12.408	-5.731
14.645	6.114	14.645	-6.114
17.033	6.445	17.033	-6.445
19.562	6.753	19.562	-6.753
22.221	6.997	22.221	-6.997
25.000	7.314	25.000	-7.314
27.886	7.360	27.886	-7.360
30.866	7.470	30.866	-7.470
33.928	7.501	33.928	-7.501
37.059	7.482	37.059	-7.482
40.245	7.369	40.245	-7.369
43.474	7.304	43.474	-7.304
46.730	6.950	46.730	-6.950
50.000	6.630	50.000	-6.630
53.270	6.225	53.270	-6.225
56.526	5.771	56.526	-5.771
59.755	5.244	59.755	-5.244
62.941	4.696	62.941	-4.696
66.072	4.137	66.072	-4.137
69.134	3.582	69.134	-3.582
72.114	3.034	72.114	-3.034
75.000	2.527	75.000	-2.527
77.779	2.050	77.779	-2.050
80.438	1.643	80.438	-1.643
82.967	1.346	82.967	-1.346
85.356	1.116	85.355	-1.116
87.592	.931	87.592	-.931
91.573	.626	87.592	-.626
94.844	.384	94.844	-.324
97.347	.210	97.347	-.210
99.039	.083	99.039	-.083
99.893	.009	99.893	-.009
100.000	.000	100.000	.000

Wortmann FX-71-L-150/K 25 For 25 percent flap

Chord Station XU	Upper Surface YU	Chord Station XL	Lower Surface YL
.000	.000	.000	.000
.107	.821	.107	-.821
.428	1.455	.428	-1.455
.961	1.903	.961	-1.903
1.704	2.446	1.704	-2.446
2.653	2.941	2.653	-2.941
3.896	3.457	3.896	-3.457
5.158	3.944	5.158	-3.944
6.699	4.431	6.699	-4.431
8.427	4.880	8.427	-4.880
10.332	5.326	10.332	-5.326
12.408	5.724	12.408	-5.724
14.645	6.105	14.645	-6.105
17.033	6.438	17.033	-6.438
19.562	6.742	19.562	-6.742
22.221	6.991	22.221	-6.991
25.000	7.204	25.000	-7.204
27.886	7.355	27.886	-7.355
30.866	7.462	30.866	-7.462
33.928	7.501	33.928	-7.501
37.059	7.463	37.059	-7.463
40.245	7.396	40.245	-7.396
43.474	7.327	43.474	-7.327
46.730	6.998	46.730	-6.998
50.000	6.689	50.000	-6.689
53.270	6.320	53.270	-6.320
56.526	5.891	56.526	-5.891
59.755	5.457	59.755	-5.457
62.941	4.949	62.941	-4.949
66.072	4.413	66.072	-4.413
69.134	3.854	69.134	-3.854
72.114	3.299	72.114	-3.299
75.000	2.771	75.000	-2.771
77.779	2.265	77.779	-2.265
80.438	1.921	80.438	-1.921
82.967	1.628	82.967	-1.628
85.356	1.377	85.355	-1.377
87.592	1.140	87.592	-1.140
91.573	.731	91.573	-.731
94.844	.425	94.844	-.425
97.347	.223	97.347	-.223
99.039	.087	99.039	-.087
99.893	.010	99.893	-.010
100.000	.000	100.000	.000

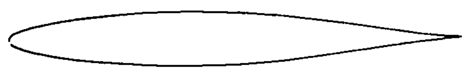

NACA 66 1 012

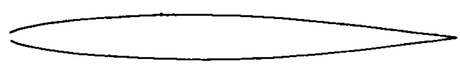

NACA 66 A 010

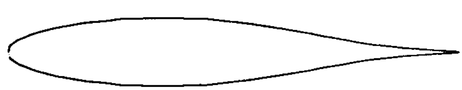

WORTMAN FX-71-L-150/K 20 FOR 20 PERCENT FLAP

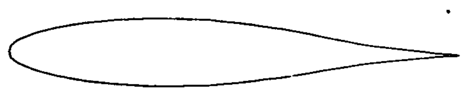

WORTMAN FX-71-L-150/K 25 FOR 25 PERCENT FLAP

Wortmann FX LIII-142/K 25
For 25 percent flap

Chord Station XU	Upper Surface YU	Chord Station XL	Lower Surface YL
.000	.000	.000	.000
.102	.420	.102	-.420
.422	.980	.422	-.980
.960	1.620	.960	-1.620
1.702	2.240	1.702	-2.240
2.650	2.820	2.650	-2.820
3.802	3.340	3.802	-3.340
5.158	3.880	5.158	-3.880
6.694	4.360	6.694	-4.360
8.422	4.840	8.422	-4.840
10.330	5.240	10.330	-5.240
12.403	5.620	12.403	-5.620
14.643	5.960	14.643	-5.960
17.037	6.280	17.037	-6.280
19.558	6.560	19.558	-6.560
22.221	6.780	22.221	-6.780
24.998	6.940	24.998	-6.940
27.891	7.060	27.891	-7.060
30.861	7.100	30.861	-7.100
33.933	7.080	33.933	-7.080
37.056	6.980	37.056	-6.980
40.243	6.820	40.243	-6.820
43.469	6.600	43.469	-6.600
46.733	6.300	46.733	-6.300
49.997	5.900	49.997	-5.900
53.274	5.520	53.274	-5.520
56.525	5.060	56.525	-5.060
59.750	4.630	59.750	-4.630
62.938	4.160	62.938	-4.160
66.074	3.780	66.074	-3.780
69.133	3.340	69.133	-3.340
72.115	2.920	72.115	-2.920
74.995	2.600	74.995	-2.600
77.773	2.340	77.773	-2.340
80.435	1.920	80.435	-1.920
82.970	1.620	82.970	-1.620
85.350	1.380	85.350	-1.380
87.590	1.140	87.590	-1.140
89.644	.960	89.644	-.960
91.571	.760	91.571	-.760
93.299	.580	93.299	-.580
94.848	.480	94.848	-.480
96.192	.340	96.192	-.340
97.344	.260	97.344	-.260
98.291	.200	98.291	-.200
99.034	.140	99.034	-.140
99.671	.080	99.671	-.080
99.891	.060	99.891	-.060
100.000	.000	100.000	.000

Wortmann FX-71-L-150/K 30

Chord Station XU	Upper Surface YU	Chord Station XL	Lower Surface YL
.000	.000	.000	.000
.107	.813	.107	-.813
.428	1.437	.428	-1.437
.961	1.896	.961	-1.896
1.704	2.442	1.704	-2.442
2.653	2.945	2.653	-2.945
3.896	3.465	3.896	-3.465
5.158	3.958	5.158	-3.958
6.699	4.450	6.699	-4.450
8.427	4.902	8.427	-4.902
10.332	5.354	10.332	-5.354
12.408	5.753	12.408	-5.753
14.645	6.136	14.645	-6.136
17.033	6.467	17.033	-6.467
19.562	6.774	19.562	-6.774
22.221	7.014	22.221	-7.014
25.000	7.229	25.000	-7.229
27.886	7.369	27.886	-7.369
30.866	7.477	30.866	-7.477
33.928	7.500	33.928	-7.500
37.059	7.486	37.059	-7.486
40.245	7.372	40.245	-7.372
43.474	7.219	43.474	-7.219
46.730	6.969	46.730	-6.969
50.000	6.667	50.000	-6.667
53.270	6.271	53.270	-6.271
56.526	5.845	56.526	-5.845
59.755	5.363	59.755	-5.363
62.941	4.850	62.941	-4.850
66.072	4.264	66.072	-4.264
69.941	3.729	69.134	-3.729
72.114	3.140	72.114	-3.140
75.000	2.742	75.000	-2.742
77.779	2.347	77.779	-2.347
80.438	2.040	80.438	-2.040
82.967	1.709	82.967	-1.709
85.355	1.448	85.355	-1.448
87.592	1.177	87.592	-1.177
91.573	.756	91.573	- .756
94.844	.435	94.844	-.435
97.347	.227	97.347	-.227
99.039	.089	99.039	-.089
99.893	.010	99.893	-.010
100.000	.000	100.000	.000

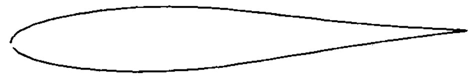

WORTMAN FX-L111-142/K 25 FOR 25 PERCENT FLAP

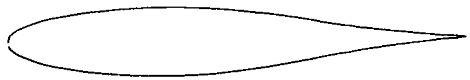

WORTMAN FX-71-L-150/K 30 FOR 30 PERCENT FLAP

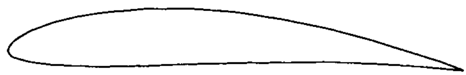

R.A.F. 32

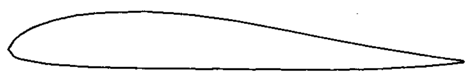

N 60 R

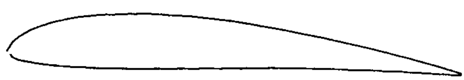

N 60

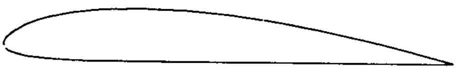

CLARK Y

R.A.F. 32

Chord Station XU	Upper Surface YU	Chord Station XL	Lower Surface YL
.000	3.420	.000	3.420
.200	4.200	.200	2.800
.400	4.550	.400	2.560
.600	4.870	.600	2.400
.800	5.140	.800	2.200
1.250	5.560	1.250	1.980
2.500	6.520	2.500	1.500
5.000	7.840	5.000	.880
10.000	9.720	10.000	.300
15.000	11.020	15.000	.080
20.000	11.920	20.000	.000
30.000	12.980	30.000	.300
40.000	13.100	40.000	.700
50.000	12.460	50.000	1.100
60.000	11.080	60.000	1.460
70.000	9.100	70.000	1.600
80.000	6.650	80.000	1.460
90.000	3.600	90.000	.920
95.000	1.980	95.000	.520
100.000	.120	100.000	.120

N 60 R

Chord Station XU	Upper Surface YU	Chord Station XL	Lower Surface YL
.000	3.400	.000	3.400
1.250	5.800	1.250	1.910
2.500	6.760	2.500	1.460
5.000	8.240	5.000	.980
7.500	9.330	7.500	.620
10.000	10.140	10.000	.400
15.000	11.320	15.000	.150
20.000	11.980	20.000	.040
30.000	12.410	30.000	.040
40.000	11.950	40.000	.140
50.000	10.790	50.000	.210
60.000	9.180	60.000	.340
70.000	7.420	70.000	.540
80.000	5.750	80.000	.890
90.000	4.280	90.000	1.610
95.000	3.660	95.000	2.130
100.000	3.200	100.000	2.800

N 60

Chord Station XU	Upper Surface YU	Chord Station XL	Lower Surface YL
.000	3.400	.000	3.400
1.250	5.600	1.250	1.910
2.500	6.760	2.500	1.460
5.000	8.240	5.000	.960
7.500	9.330	7.500	.620
10.000	10.140	10.000	.400
15.000	11.320	15.000	.150
20.000	11.980	20.000	.040
30.000	12.410	30.000	.040
40.000	12.030	40.000	.220
50.000	11.080	50.000	.480
60.000	9.550	60.000	.710
70.000	7.660	70.000	.780
80.000	5.500	80.000	.640
90.000	3.040	90.000	.370
95.000	1.720	95.000	.190
100.000	.400	100.000	.000

Clark Y
For 30 percent flap

Chord Station XU	Upper Surface YU	Chord Station XL	Lower Surface YL
.000	3.500	.000	3.500
.200	4.260	.200	2.920
.400	4.610	.400	2.620
.800	5.090	.800	2.250
1.250	5.550	1.250	1.960
2.500	6.500	2.500	1.470
5.000	7.900	5.000	.930
7.500	8.850	7.500	.630
10.000	9.600	10.000	.420
15.000	10.680	15.000	.150
20.000	11.360	20.000	.030
25.000	11.600	25.000	.000
30.000	11.700	30.000	.000
40.000	11.400	40.000	.000
50.000	10.520	50.000	.000
60.000	9.150	60.000	.000
70.000	7.350	70.000	.000
80.000	5.220	80.000	.000
90.000	2.800	90.000	.000
100.000	.120	100.000	.000

Göttingen 535 (1930 Vintage)

Chord Station XU	Upper Surface YU	Chord Station XL	Lower Surface YL
.000	4.300	.000	4.300
.250	6.450	.250	3.450
.500	7.050	.500	2.988
.750	7.600	.750	2.720
1.000	8.050	1.000	2.500
1.250	8.350	1.250	2.300
2.500	9.750	2.500	1.550
5.000	11.550	5.000	.800
7.500	12.900	7.500	.500
10.000	13.950	10.000	.300
15.000	15.300	15.000	.050
20.000	16.050	20.000	.000
30.000	16.300	30.000	.250
40.000	15.350	40.000	1.150
50.000	13.750	50.000	2.200
60.000	11.650	60.000	3.000
70.000	9.220	70.000	3.000
80.000	6.550	80.000	2.500
90.000	3.550	90.000	1.450
95.000	1.900	95.000	.650
100.000	.150	100.000	.150

Göttingen Flat Plate

Chord Station XU	Upper Surface YU	Chord Station XL	Lower Surface YL
.000	.000	.000	.000
1.250	.800	1.250	-.800
2.500	1.000	2.500	-1.000
5.000	1.300	5.000	-1.300
7.500	1.400	7.500	-1.400
10.000	1.450	10.000	-1.450
70.000	1.450	70.000	-1.450
80.000	1.400	80.000	-1.400
90.000	.800	90.000	-.800
95.000	.400	95.000	-.400
100.000	.000	100.000	.000

Göttingen 801 le radius 1.2 percent camber 7 percent at 35 percent

Chord Station XU	Upper Surface YU	Chord Station XL	Lower Surface YL
.000	1.200	.000	1.200
.500	2.810	.500	.510
1.000	3.470	1.000	.260
1.500	4.070	1.500	.130
2.000	4.560	2.000	.050
2.500	5.100	2.500	.000
5.000	6.800	5.000	.200
7.500	8.000	7.500	.400
10.000	8.900	10.000	.600
15.000	10.200	15.000	1.000
20.000	11.100	20.000	1.400
30.000	11.800	30.000	2.000
40.000	11.600	40.000	2.200
50.000	10.700	50.000	2.100
60.000	9.400	60.000	1.900
70.000	7.700	70.000	1.600
80.000	5.500	80.000	1.100
90.000	3.000	90.000	.500
95.000	1.700	95.000	.200
100.000	.400	100.000	.000

NACA M 6

Chord Station XU	Upper Surface YU	Chord Station XL	Lower Surface YL
.000	.000	.000	.000
.200	.750	.250	-.950
.400	1.130	.500	-1.225
.600	1.370	.750	-1.475
1.000	1.760	1.000	-1.620
1.250	1.970	1.250	-1.760
2.500	2.810	2.500	-2.200
5.000	4.030	5.000	-2.730
7.500	4.940	7.500	-3.030
10.000	5.710	10.000	-3.240
15.000	6.820	15.000	-3.470
20.000	7.550	20.000	-3.620
25.000	8.010	25.000	-3.710
30.000	8.220	30.000	-3.790
40.000	8.050	40.000	-3.900
50.000	7.260	50.000	-3.940
60.000	6.030	60.000	-3.820
70.000	4.580	70.000	-3.480
80.000	3.060	80.000	-2.830
90.000	1.550	90.000	-1.770
95.000	.880	95.000	-1.080
100.000	.000	100.000	.000

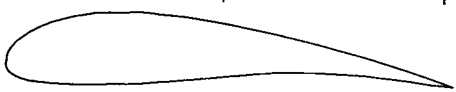

GOTTINGEN 535 (1930 VINTAGE)

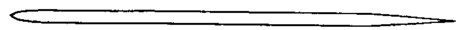

GOTTINGEN FLAT PLATE

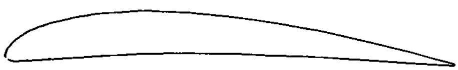

GOTTINGEN 801 LE RADIUS 1.2 PERCENT CAMBER 7 PERCENT AT 35 PERCENT

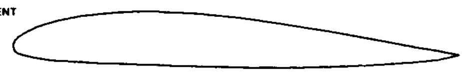

NACA M6

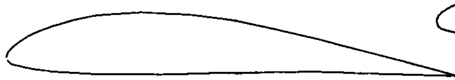

GOTTINGEN 549 (1930 TO 1950 PERIOD)

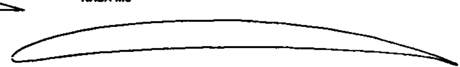

GOTTINGEN 804 (EPPLER EA 8 (-1) -12.06) LE RADIUS .5 CAMBER 0.67 AT 50

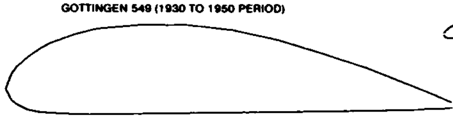

GOTTINGEN 798 LE RADIUS 3.6 PERCENT CAMBER 6.5 PERCENT

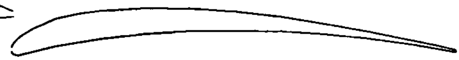

GOTTINGEN 803 (HACKLINGER) LE RADIUS 1.2 PERCENT CAMBER 7 PERCENT AT 40

Gottingen 549 (1930 to 1950 period)

Chord Station XU	Upper Surface YU	Chord Station XL	Lower Surface YL
.000	3.450	.000	3.450
.200	4.300	.200	2.860
.400	4.680	.400	2.560
.600	4.940	.600	2.370
.800	5.220	.800	2.220
1.250	5.700	1.250	1.950
2.500	6.800	2.500	1.600
5.000	8.450	5.000	1.100
7.500	9.650	7.500	.750
10.000	10.700	10.000	.550
15.000	12.250	15.000	.250
20.000	13.200	20.000	.050
30.000	13.850	30.000	.000
40.000	13.400	40.000	.100
50.000	12.050	50.000	.300
60.000	10.050	60.000	.550
70.000	7.900	70.000	.650
80.000	5.350	80.000	.550
90.000	2.700	90.000	.300
95.000	1.400	95.000	.150
100.000	.000	100.000	.000

Gottingen 804 (Eppler EA 8 (-1) -12 06) L.E. radius .5 camber 0.67 at 50

Chord Station XU	Upper Surface YU	Chord Station XL	Lower Surface YL
.000	.700	.000	.700
.500	1.500	.500	.130
1.000	1.980	1.000	.040
1.500	2.380	1.500	.000
2.000	2.700	2.000	.040
2.500	3.000	2.500	.100
5.000	4.100	5.000	.300
7.500	5.000	7.500	.600
10.000	5.700	10.000	1.000
15.000	6.900	15.000	1.600
20.000	7.700	20.000	2.200
30.000	8.900	30.000	2.900
40.000	9.400	40.000	3.400
50.000	9.500	50.000	3.700
60.000	9.000	60.000	3.700
70.000	8.000	70.000	3.400
80.000	6.300	80.000	3.000
90.000	3.700	90.000	2.300
95.000	2.100	95.000	1.500
100.000	.300	100.000	.000

Gottingen 803 (Hacklinger) L.E. radius 1.2 percent camber 7 percent at 40

Chord Station XU	Upper Surface YU	Chord Station XL	Lower Surface YL
.000	1.300	.000	1.300
.500	2.580	.500	.360
1.000	3.230	1.000	.100
1.500	3.710	1.500	.030
2.000	4.120	10.000	1.900
2.500	4.500	15.000	2.700
5.000	5.900	20.000	3.400
7.500	6.900	30.000	4.400
10.000	8.000	40.000	4.900
15.000	9.000	50.000	5.000
20.000	9.600	60.000	4.800
30.000	10.100	70.000	4.200
40.000	10.000	80.000	3.200
50.000	9.300	90.000	1.800
60.000	8.100	95.000	.900
70.000	6.500	100.000	.000
80.000	4.700		
90.000	2.700		
95.000	1.700		
100.000	.500		

Gottingen 798 L.E. radius 3.6 percent camber 6.5 percent

Chord Station XU	Upper Surface YU	Chord Station XL	Lower Surface YL
.000	6.000	.000	6.000
1.250	9.380	1.250	3.250
2.500	11.000	2.500	2.250
5.000	13.250	5.000	1.200
7.500	14.880	7.500	.600
10.000	16.120	10.000	.380
15.000	17.880	15.000	.100
20.000	19.120	20.000	.000
30.000	20.000	30.000	.000
40.000	19.750	40.000	.000
50.000	18.500	50.000	.000
60.000	16.200	60.000	.000
70.000	13.120	70.000	.000
80.000	9.620	80.000	.000
90.000	5.500	90.000	.000
95.000	3.250	95.000	.100
100.000	1.000	100.000	.250

Göttingen 417A (curved plate)

Chord Station XU	Upper Surface YU	Chord Station XL	Lower Surface YL
.000	1.450	.000	1.450
.200	2.150	.200	.700
.400	2.450	.400	.340
.600	2.660	.600	.295
.800	2.770	.800	.160
1.000	2.870	1.000	.060
1.250	3.000	1.250	.050
1.450	3.080	.1450	.000
1.500	3.125	1.500	.005
2.000	3.380	2.000	.120
2.500	3.650	2.500	.450
5.000	4.700	5.000	1.550
7.500	5.600	7.500	2.500
10.000	6.300	10.000	3.300
15.000	7.150	15.000	4.200
20.000	7.750	20.000	4.820
30.000	8.600	30.000	5.700
40.000	8.800	40.000	5.900
50.000	8.450	50.000	5.550
60.000	7.850	60.000	4.950
70.000	6.900	70.000	4.000
80.000	5.700	80.000	2.800
90.000	4.250	90.000	1.300
95.000	3.550	95.000	.600
100.000	1.450	100.000	1.450

Göttingen 625 L.E. radius 3.4 percent

Chord Station XU	Upper Surface YU	Chord Station XL	Lower Surface YL
.000	5.500	.000	5.500
1.250	9.000	1.250	3.300
2.500	10.800	2.500	2.350
5.000	13.300	5.000	1.250
7.500	14.950	7.500	.750
10.000	16.350	10.000	.400
15.000	18.250	15.000	.150
20.000	19.300	20.000	.100
30.000	20.000	30.000	.000
40.000	19.060	40.000	.000
50.000	17.350	50.000	.000
60.000	15.060	60.000	.000
70.000	12.100	70.000	.000
80.000	8.600	80.000	.000
90.000	4.750	90.000	.000
95.000	2.750	95.000	.000
100.000	.650	100.000	.000

Göttingen 797 L.E. radius 2.3 Percent camber 5.1 percent

Chord Station XU	Upper Surface YU	Chord Station XL	Lower Surface YL
.000	4.800	.000	4.800
.200	5.800	.200	3.860
.400	6.160	.400	3.480
.600	6.520	.600	3.230
.800	6.900	.800	3.040
1.250	7.500	1.250	2.600
2.500	8.800	2.500	1.800
5.000	10.600	5.000	.960
7.500	11.900	7.500	.480
10.000	12.900	10.000	.300
15.000	14.300	15.000	.080
20.000	15.300	20.000	.000
30.000	16.000	30.000	.000
40.000	15.800	40.000	.000
50.000	14.800	50.000	.000
60.000	12.960	60.000	.000
70.000	10.500	70.000	.000
80.000	7.700	80.000	.000
90.000	4.400	90.000	.000
95.000	2.600	95.000	.080
100.000	.800	100.000	.200

Göttingen 796 L.E. radius 1.3 Percent Camber 3.7 percent

Chord Station XU	Upper Surface YU	Chord Station XL	Lower Surface YL
.000	3.600	.000	3.600
.200	4.350	.200	3.000
.400	4.680	.400	2.650
.600	4.930	.600	2.400
.800	5.180	.800	2.220
1.250	5.620	1.250	1.950
2.500	6.600	2.500	1.350
5.000	7.950	5.000	.720
7.500	8.920	7.500	.360
10.000	9.680	10.000	.220
15.000	10.720	15.000	.060
20.000	11.480	20.000	.000
30.000	12.000	30.000	.000
40.000	11.850	40.000	.000
50.000	11.100	50.000	.000
60.000	9.720	60.000	.000
70.000	7.880	70.000	.000
80.000	5.780	80.000	.000
90.000	3.300	90.000	.000
95.000	1.950	95.000	.060
100.000	.600	100.000	.150

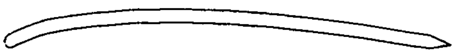

GOTTINGEN 417a (CURVED PLATE)

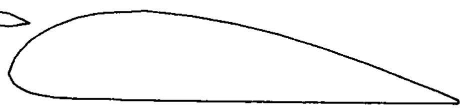

GOTTINGEN 625 LE RADIUS 3.4 PERCENT

GOTTINGEN 797 LE RADIUS 2.3 PERCENT CAMBER 5.1 PERCENT

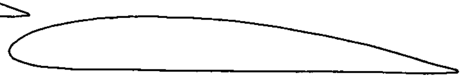

GOTTINGEN 796 LE RADIUS 1.3 PERCENT CAMBER 3.7 PERCENT

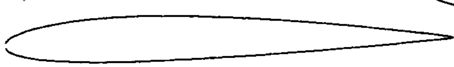

NACA 1410 LE RADIUS 1.10 PERCENT

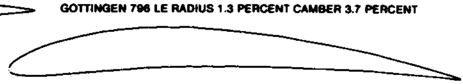

NACA 6409

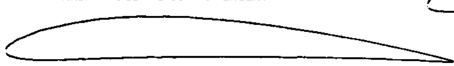

NACA 4409 LE RADIUS 0.89 PERCENT

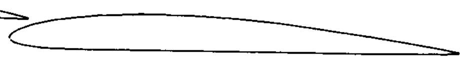

GOTTINGEN 795 LE RADIUS 0.58 PERCENT CAMBER 2.4 PERCENT

NACA 1410 L.E. radius 1.10 percent

Chord Station XU	Upper Surface YU	Chord Station XL	Lower Surface YL
.000	.000	.000	.000
.200	.560	.200	-.570
.400	.975	.400	-.810
.600	1.170	.600	-.990
.800	1.375	.800	-1.130
1.174	1.639	1.326	-1.515
2.398	2.297	2.602	-2.065
4.870	3.194	5.130	-2.726
7.358	3.837	7.642	-3.157
9.854	4.338	10.146	-3.462
14.861	5.062	15.139	-3.844
19.880	5.531	20.120	-4.031
24.907	5.809	25.093	-4.091
29.937	5.940	30.063	-4.064
40.000	5.836	40.000	-3.836
50.025	5.385	49.975	-3.439
60.042	4.692	59.958	-2.914
70.051	3.804	69.949	-2.304
80.049	2.741	79.951	-1.629
90.034	1.513	89.966	-.901
95.021	.832	94.979	-.512
100.000	.105	100.000	-.105

NACA 6409

Chord Station XU	Upper Surface YU	Chord Station XL	Lower Surface YL
.000	.000	.000	.000
.200	.720	.200	-.380
.400	1.120	.400	-.560
.600	1.370	.600	-.670
.800	1.620	.800	-.750
1.250	2.060	1.250	-.880
2.500	2.960	2.500	-1.110
5.000	4.300	5.000	-1.180
7.500	5.420	7.500	-1.080
10.000	6.310	10.000	-.880
15.000	7.780	15.000	-.360
20.000	8.880	20.000	.170
25.000	9.650	25.000	.690
30.000	10.130	30.000	1.120
40.000	10.350	40.000	1.650
50.000	9.810	50.000	1.860
60.000	8.780	60.000	1.920
70.000	7.280	70.000	1.760
80.000	5.340	80.000	1.360
90.000	2.950	90.000	.740
95.000	1.570	95.000	.350
100.000	.090	100.000	-.090

NACA 4409 L.E. radius 0.89 percent

Chord Station XU	Upper Surface YU	Chord Station XL	Lower Surface YL
.000	.000	.000	.000
.200	.800	.200	-.390
.400	1.100	.400	-.600
.600	1.300	.600	-.730
.800	1.500	.800	-.850
1.250	1.810	1.250	-1.050
2.500	2.610	2.500	-1.370
5.000	3.740	5.000	-1.650
7.500	4.640	7.500	-1.740
10.000	5.370	10.000	-1.730
15.000	6.520	15.000	-1.550
20.000	7.330	20.000	-1.300
25.000	7.900	25.000	-1.020
30.000	8.250	30.000	-.760
40.000	8.350	40.000	-.350
50.000	7.870	50.000	-.070
60.000	7.000	60.000	.140
70.000	5.760	70.000	.260
80.000	4.210	80.000	.260
90.000	2.330	90.000	.140
95.000	1.260	95.000	.030
100.000	.090	100.000	-.090

Gottingen 795 L.E. radius 0.58 percent camber 2.4 percent

Chord Station XU	Upper Surface YU	Chord Station XL	Lower Surface YL
.000	2.400	.000	2.400
.200	2.880	.200	2.030
.400	3.130	.400	1.800
.600	3.310	.600	1.670
.800	3.470	.800	1.540
1.250	3.750	1.250	1.300
2.500	4.400	2.500	.900
5.000	5.300	5.000	.480
7.500	5.950	7.500	.240
10.000	6.450	10.000	.150
15.000	7.150	15.000	.040
20.000	7.850	20.000	.000
30.000	8.000	30.000	.000
40.000	7.900	40.000	.000
50.000	7.400	50.000	.000
60.000	7.400	50.000	.000
70.000	5.250	70.000	.000
80.000	3.850	80.000	.000
90.000	2.200	90.000	.000
95.000	1.300	95.000	.040
100.000	.400	100.000	.100

NACA 6412 L.E. radius 1.58

Chord Station	Upper Surface	Chord Station	Lower Surface
XU	YU	XL	YL
.000	.000	.000	.000
.000	.850	.200	-.430
.200	1.350	.400	-.690
.600	2.000	.600	-.840
.800	2.270	.800	-.960
1.250	2.730	1.250	-1.230
2.500	3.800	2.500	-1.640
5.000	5.360	5.000	-1.990
7.500	6.570	7.500	-2.050
10.000	7.580	10.000	-1.990
15.000	9.180	15.000	-1.670
20.000	10.340	20.000	-1.260
25.000	11.140	25.000	-.780
30.000	11.650	30.000	-.380
40.000	11.800	40.000	.200
50.000	11.160	50.000	.550
60.000	9.950	60.000	.780
70.000	8.230	70.000	.850
80.000	6.030	80.000	.730
90.000	3.330	90.000	.390
95.000	1.790	95.000	.160
100.000	.120	100.000	-.120

NACA 4412 L.E. radius 1.58 percent

Chord Station	Upper Surface	Chord Station	Lower Surface
XU	YU	XL	YL
.000	.000	.000	.000
.200	1.200	.200	-.500
.400	1.560	.400	-.770
.600	.1800	.600	-.950
.800	.2060	.800	-1.120
1.250	2.440	1.250	-1.430
2.500	3.390	2.500	-1.950
5.000	4.730	5.000	-2.490
7.500	5.760	7.500	-2.740
10.000	6.590	10.000	-2.860
15.000	7.890	15.000	-2.880
20.000	8.800	20.000	-2.740
25.000	9.410	25.000	-2.500
30.000	9.760	30.000	-2.260
40.000	9.800	40.000	-1.800
50.000	9.190	50.000	-1.400
60.000	8.140	60.000	-1.000
70.000	6.690	70.000	-.650
80.000	4.890	80.000	-.390
90.000	2.710	90.000	-.220
95.000	1.470	95.000	-.130
100.000	.130	100.000	-.160

NACA 2412 L.E. radius 1.58 percent

Chord Station	Upper Surface	Chord Station	Lower Surface
XU	YU	XL	YL
.000	.000	.000	.000
.200	.920	.200	-.610
.400	1.280	.400	-.900
.600	1.510	.600	-1.100
.800	1.730	.800	-1.291
1.250	2.150	1.250	-1.660
2.500	2.990	2.500	-2.270
5.000	4.130	5.000	-3.010
7.500	4.960	7.500	-3.460
10.000	5.630	10.000	-3.750
15.000	6.610	15.000	-4.100
20.000	7.260	20.000	-4.230
25.000	7.670	25.000	-4.220
30.000	7.880	30.000	-4.120
40.000	7.800	40.000	-3.800
50.000	7.240	50.000	-3.340
60.000	6.360	60.000	-2.760
70.000	5.180	70.000	-2.140
80.000	3.750	80.000	-1.500
90.000	2.080	90.000	-.820
95.000	1.140	95.000	-.480
100.000	.130	100.000	-.130

NACA 2410 L.E. radius 1.10 percent

Chord Station	Upper Surface	Chord Station	Lower Surface
XU	YU	XL	YL
.000	.000	.000	.000
1.098	1.694	1.402	-1.448
2.297	2.411	2.703	-1.927
4.742	3.420	5.258	-2.482
7.217	4.169	7.783	-2.809
9.710	4.766	10.290	-3.016
14.722	5.665	15.278	-3.227
19.761	6.276	20.239	-3.276
24.814	6.668	25.186	-3.230
29.875	6.875	30.125	-3.125
40.000	6.837	40.000	-2.837
50.049	6.356	49.951	-2.468
60.085	5.580	59.915	-2.024
70.102	4.551	69.898	-1.551
80.097	3.296	79.903	-1.074
90.067	1.816	89.933	-.594
95.041	.990	94.959	-.352
100.000	.105	100.000	-.105

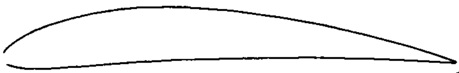

NACA 6412 LE RADIUS 1.58

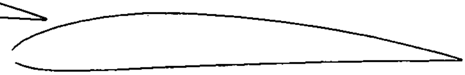

NACA 4412 LE RADIUS 1.58 PERCENT

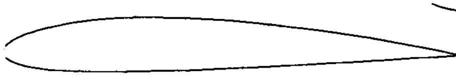

NACA 2412 LE RADIUS 1.58 PERCENT

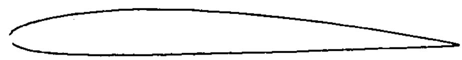

NACA 2410 LE RADIUS 1.10 PERCENT

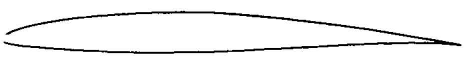

NACA 64-409

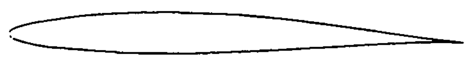

NACA 63-209

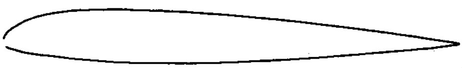

NACA 23012 LE RADIUS 1.58 PERCENT

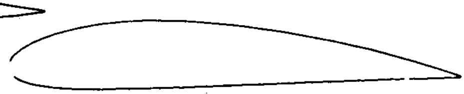

NACA 4415 LE RADIUS 2.48 PERCENT

NACA 64-409

Chord Station	Upper Surface	Chord Station	Lower Surface
XU	YU	XL	YL
.000	.000	.000	.000
.377	.829	.623	-.629
.613	1.021	.887	-.741
1.095	1.331	1.405	-.903
2.322	1.895	2.678	-1.151
4.803	2.732	5.197	-1.468
7.297	3.383	7.703	-1.687
9.798	3.925	10.202	-1.857
14.810	4.796	15.190	-2.104
19.830	5.456	20.170	-2.272
24.854	5.967	25.146	-2.377
29.882	6.315	30.118	-2.427
34.912	6.538	35.088	-2.418
39.942	6.632	40.058	-2.348
44.972	6.564	45.028	-2.174
50.000	6.342	50.000	-1.930
60.045	5.594	59.955	-1.310
70.069	4.504	69.931	-.616
80.069	3.154	79.931	-.030
90.043	1.644	89.979	.424
95.021	.858	94.979	.406
100.000	.000	100.000	.000

NACA 63-209

Chord Station	Upper Surface	Chord Station	Lower Surface
XU	YU	XL	YL
.000	.000	.000	.000
.437	.796	.563	-.696
.680	.973	.820	-.833
1.170	1.255	1.330	-1.041
2.408	1.765	2.592	-1.393
4.897	2.510	5.103	-1.878
7.394	3.077	7.606	-2.229
9.894	3.539	10.106	-2.506
14.901	4.263	15.099	-2.917
19.912	4.792	20.088	-3.200
24.925	5.169	25.075	-3.379
29.940	5.414	30.060	-3.470
34.956	5.530	35.044	-3.470
39.971	5.518	40.029	-3.376
44.986	5.391	45.014	-3.201
50.000	5.159	50.000	-2.953
60.022	4.429	59.978	-2.287
70.033	3.430	69.967	-1.486
80.032	2.267	79.968	-.676
90.019	1.087	89.981	-.033
95.009	.512	94.991	.120
100.000	.000	100.000	.000

NACA 23012 L.E. radius 1.58 percent

Chord Station	Upper Surface	Chord Station	Lower Surface
XU	YU	XL	YL
.000	.000	.000	.000
.200	1.300	.200	-.488
.400	1.680	.400	-.730
.600	1.920	.600	-.910
.800	2.200	.800	-1.030
1.250	2.670	1.250	-1.230
2.500	3.610	2.500	-1.710
5.000	4.910	5.000	-2.260
7.500	5.800	7.500	-2.610
10.000	6.430	10.000	-2.920
15.000	7.190	15.000	-3.500
20.000	7.500	20.000	-3.970
25.000	7.600	25.000	-4.280
30.000	7.550	30.000	-4.460
40.000	7.140	40.000	-4.480
50.000	6.410	50.000	-4.170
60.000	5.470	60.000	-3.670
70.000	4.360	70.000	-3.000
80.000	3.080	80.000	-2.160
90.000	1.680	90.000	-1.230
95.000	.920	95.000	-.700
100.000	.130	100.000	-.130

NACA 4415 L.E. radius 2.48 percent

Chord Station	Upper Surface	Chord Station	Lower Surface
XU	YU	XL	YL
.000	.000	.000	.000
.000	.840	.200	-.550
.200	1.560	.400	-.920
.600	2.250	.600	-1.180
.800	2.550	.800	-1.400
1.250	3.070	1.250	-1.790
2.500	4.170	2.500	-2.480
5.000	5.740	5.000	-3.270
7.500	6.910	7.500	-3.710
10.000	7.840	10.000	-3.980
15.000	9.270	15.000	-4.180
20.000	10.250	20.000	-4.150
25.000	10.920	25.000	-3.980
30.000	11.250	30.000	-3.750
40.000	11.250	40.000	-3.250
50.000	10.530	50.000	-2.720
60.000	9.300	60.000	-2.140
70.000	7.630	70.000	-1.550
80.000	5.550	80.000	-1.030
90.000	3.080	90.000	-.570
95.000	1.670	95.000	-.360
100.000	.160	100.000	-.160

NACA 64-A-410

Chord Station XU	Upper Surface YU	Chord Station XL	Lower Surface YL
.000	.000	.000	.000
.350	.902	.650	-.678
.582	1.112	.918	-.796
1.059	1.451	1.441	-.969
2.276	2.095	2.724	-1.251
4.749	3.034	5.251	-1.592
7.230	3.865	7.770	-1.919
9.737	4.380	10.263	-1.996
14.748	5.366	15.252	-2.244
19.770	6.126	20.330	-2.406
24.800	6.705	25.200	-2.499
29.834	7.131	30.166	-2.537
34.871	7.414	35.129	-2.518
39.910	7.552	40.090	-2.436
44.950	7.522	45.050	-2.266
49.989	7.344	50.011	-2.024
60.057	6.624	59.943	-1.418
70.108	5.490	69.892	-.760
80.151	3.967	79.849	-.229
90.104	2.038	89.896	-.076
95.053	1.028	94.947	-.048
100.000	.021	100.000	-.021

NACA 64-A-310

Chord Station XU	Upper Surface YU	Chord Station XL	Lower Surface YL
.000	.000	.000	.000
.399	.873	.601	-.723
.638	1.068	.862	-.858
1.123	1.379	1.377	-1.057
2.353	1.961	2.647	-1.403
4.837	2.759	5.163	-1.847
7.332	3.436	7.668	-2.164
9.832	3.970	10.168	-2.420
14.842	4.819	15.158	-2.809
19.859	5.464	20.141	-3.076
24.879	5.946	25.121	-3.262
29.902	6.294	30.098	-3.378
34.927	6.513	35.073	-3.423
39.952	6.601	40.048	-3.389
44.977	6.536	45.023	-3.252
50.000	6.334	50.000	-3.030
60.039	5.627	59.961	-2.415
70.063	4.584	69.937	-1.668
80.070	3.296	79.930	-.908
90.066	1.836	89.944	-.286
95.038	1.014	94.962	-.065
100.000	.021	100.000	-.021

NACA 64-A-210

Chord Station XU	Upper Surface YU	Chord Station XL	Lower Surface YL
.000	.000	.000	.000
.424	.856	.576	-.744
.665	1.044	.835	-.886
1.153	1.342	1.347	-1.100
2.387	1.895	2.613	-1.473
4.874	2.685	5.126	-1.963
7.369	3.288	7.631	-2.316
9.868	3.792	10.132	-2.600
14.874	4.592	20.115	-3.030
19.885	5.200	10.115	-3.340
24.900	5.656	25.100	-3.564
29.917	5.984	30.083	-3.688
34.935	6.192	35.065	-3.744
39.955	6.274	40.045	-3.716
44.975	6.208	45.025	-3.580
49.975	6.014	50.006	-3.354
60.028	5.323	59.972	-2.719
70.054	4.310	69.946	-1.944
80.076	3.307	79.924	-1.167
90.052	1.551	89.948	-.571
95.027	.785	94.974	-.206
100.000	.021	100.000	-.021

NACA 63-A-210

Chord Station XU	Upper Surface YU	Chord Station XL	Lower Surface YL
.000	.000	.000	.000
.423	.868	.577	-.756
.664	1.058	.836	-.900
1.151	1.367	1.349	-1.125
2.384	1.944	2.616	-1.522
4.869	2.769	5.131	-2.047
7.364	3.400	7.363	-2.428
9.863	3.917	10.137	-2.725
14.869	4.729	15.131	-3.167
19.882	5.328	20.118	-3.468
24.898	5.764	25.102	-3.662
29.916	6.060	30.084	-3.764
34.935	6.219	35.065	-3.771
39.955	6.247	40.045	-3.689
44.975	6.151	45.025	-3.523
49.994	5.943	50.006	-3.283
60.028	5.245	59.972	-2.641
70.052	4.227	69.948	-1.861
80.074	2.974	79.926	-1.104
90.050	1.519	89.950	-.539
95.026	.769	94.974	-.279
100.000	.021	100.000	-.021

NACA 63-1-212

Chord Station XU	Upper Surface YU	Chord Station XL	Lower Surface YL
.000	.000	.000	.000
.417	1.032	.583	-.932
.657	1.260	.843	-1.120
1.145	1.622	1.356	-1.408
2.378	2.284	2.622	-1.912
4.863	3.238	5.137	-2.606
7.358	3.963	7.642	-3.115
9.859	4.554	10.141	-3.520
14.868	5.470	15.132	-4.124
19.882	6.137	20.118	-4.545
24.900	6.606	25.100	-4.816
29.920	6.901	30.080	-4.957
34.941	7.030	35.059	-4.970
39.962	6.991	40.038	-4.849
44.982	6.799	45.018	-4.609
50.000	6.473	50.000	-4.267
60.029	5.491	59.971	-3.349
70.043	4.182	69.957	-2.238
80.042	2.698	79.958	-1.108
90.025	1.224	89.975	-.190
95.012	.566	94.988	.086
100.000	.000	100.000	.000

NACA 65-210

Chord Station XU	Upper Surface YU	Chord Station XL	Lower Surface YL
.000	.000	.000	.000
.436	.819	.565	-.712
.678	.999	.822	-.859
1.169	1.273	1.331	-1.059
2.408	1.757	2.592	-1.385
4.898	2.491	5.102	-1.859
7.394	3.069	7.606	-2.221
9.894	3.565	10.106	-2.521
14.899	4.338	15.101	-2.992
19.909	4.938	20.091	-3.346
24.921	5.397	25.079	-3.607
29.936	5.732	30.064	-3.788
34.951	5.954	35.049	-3.894
39.968	6.067	40.032	-3.925
44.984	6.068	45.016	-3.868
50.000	5.915	50.000	-3.709
60.027	5.217	59.973	-3.076
70.043	4.128	69.957	-2.184
80.044	2.783	79.956	-1.191
90.028	1.327	89.972	-.293
95.014	.622	94.986	.010
100.000	.000	100.000	.000

NACA 64-A-910

Chord Station XU	Upper Surface YU	Chord Station XL	Lower Surface YL
.000	.000	.000	.000
.215	.977	.785	-.527
.884	1.651	1.616	-.688
2.072	2.470	2.928	-.796
4.520	3.699	5.480	-.855
7.003	4.699	7.997	-.853
9.503	5.487	10.497	-.834
14.530	6.814	15.470	-.756
19.578	7.833	20.422	-.699
24.639	8.620	25.361	-.585
29.707	9.202	30.293	-.454
34.780	9.598	35.220	-.328
39.855	9.813	40.145	-.174
44.930	9.822	45.070	.034
50.000	9.648	50.000	.280
60.117	8.839	59.883	.801
70.189	7.495	69.811	1.253
80.208	5.675	79.792	1.489
90.165	3.376	89.835	1.277
95.112	1.951	94.888	.893
100.000	.000	100.000	.000

NACA 64-A-810 (A=0.8MOD)

Chord Station XU	Upper Surface YU	Chord Station XL	Lower Surface YL
.000	.000	.000	.000
.214	.976	.785	-.526
.881	1.650	1.619	-.686
2.064	2.475	2.936	-.787
4.506	3.716	5.494	-.832
6.984	4.703	8.016	-.811
9.479	5.541	10.521	-.771
14.500	6.902	15.500	-.658
19.543	7.968	20.457	-.526
24.601	8.795	25.399	-.383
29.668	9.420	30.332	-.232
34.742	9.857	35.258	-.065
39.820	10.107	40.180	.123
44.900	10.150	45.100	.364
49.977	10.006	50.023	.637
60.114	9.225	59.886	1.187
70.215	7.850	69.785	1.610
80.300	5.819	79.700	1.657
90.204	3.004	89.796	.920
95.104	1.512	94.896	.450
100.000	.021	100.000	-.021

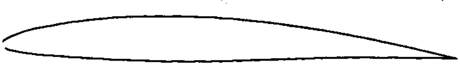

NACA 64-A-410

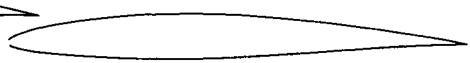

NACA 64-A-310

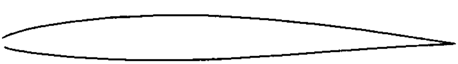

NACA 64-A210

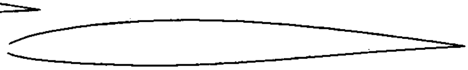

NACA 63-A-210

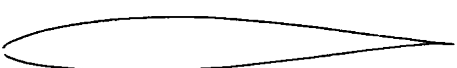

NACA 63-1-212

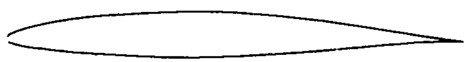

NACA 65-210

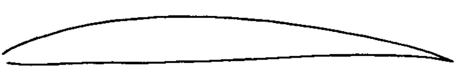

NACA 64-A-910

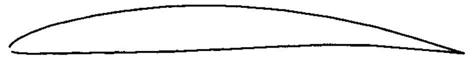

NACA 64-A-810 (A=0.8 MOD)

NACA 63-2-415

Chord Station XU	Upper Surface YU	Chord Station XL	Lower Surface YL
.000	.000	.000	.000
.300	1.287	.700	-1.087
.525	1.585	.975	-1.306
.991	2.074	1.509	-1.646
2.198	2.964	2.802	-2.220
4.660	4.264	5.340	-3.000
7.147	5.261	7.853	-3.565
9.647	6.077	10.353	-4.009
14.669	7.348	15.331	-4.656
19.705	8.279	20.295	-5.095
24.750	8.941	25.250	-5.361
29.800	9.362	30.200	-5.474
34.852	9.559	35.148	-5.439
39.905	9.527	40.095	-5.243
44.956	9.289	45.045	-4.909
50.000	8.871	50.000	-4.459
60.070	7.595	59.930	-3.311
70.106	5.877	69.894	-1.989
80.102	3.900	79.898	-.716
90.059	1.884	89.941	-.184
95.028	.931	94.972	.333
100.000	.000	100.000	.000

NACA 64-1-612

Chord Station XU	Upper Surface YU	Chord Station XL	Lower Surface YL
.000	.000	.000	.000
.260	1.098	.740	-.798
.482	1.358	1.018	-.938
.946	1.780	1.554	-1.138
2.149	2.563	2.851	-1.447
4.609	3.731	5.391	-1.835
7.096	4.642	7.904	-2.098
9.596	5.401	10.404	-2.299
14.619	6.623	15.381	-2.585
19.658	7.560	20.341	-2.774
24.708	8.253	25.292	-2.883
29.764	8.755	30.236	-2.923
34.823	9.065	35.177	-2.885
39.884	9.193	40.116	-2.767
44.945	9.083	45.055	-2.513
50.000	8.789	50.000	-2.171
60.088	7.760	59.912	-1.834
70.135	6.263	69.865	-.431
80.134	4.413	79.866	.363
90.082	2.333	89.918	.769
95.040	1.233	94.960	.663
100.000	.000	100.000	.000

NACA 64-1-412

Chord Station XU	Upper Surface YU	Chord Station XL	Lower Surface YL
.000	.000	.000	.000
.338	1.064	.662	-.864
.569	1.305	.931	-1.025
1.045	1.690	1.455	-1.262
2.264	2.393	2.736	-1.649
4.738	3.430	5.262	-2.166
7.229	4.231	7.771	-2.535
9.730	4.896	10.270	-2.828
14.745	5.959	15.255	-3.267
19.722	6.760	20.228	-3.576
24.805	7.363	25.195	-3.783
29.842	7.786	30.158	-3.898
34.882	8.037	35.118	-3.917
39.923	8.123	40.077	-3.839
44.963	7.988	45.037	-3.608
50.000	7.686	50.000	-3.274
60.059	6.690	59.941	-2.406
70.090	5.293	69.910	-1.405
80.089	3.619	79.911	-.435
90.055	1.818	89.945	-.250
95.027	.919	94.973	.345
100.000	.000	100.000	.000

NACA 64-1-A-212

Chord Station XU	Upper Surface YU	Chord Station XL	Lower Surface YL
.000	.000	.000	.000
.409	1.013	.591	-.901
.648	1.233	.852	-1.075
1.135	1.580	1.365	-1.338
2.365	2.225	2.635	-1.803
4.849	3.145	5.151	-2.423
7.343	3.846	7.567	-2.874
9.842	4.432	10.158	-3.240
14.849	5.358	15.151	-3.796
19.862	6.060	20.138	-4.200
24.880	6.584	25.120	-4.482
29.900	6.956	30.100	-4.660
34.922	7.189	35.078	-4.741
39.946	7.272	40.054	-4.714
44.970	7.177	45.030	-4.549
49.993	6.935	50.007	-4.275
60.034	6.103	59.966	-3.499
70.064	4.903	69.936	-2.537
80.090	3.433	79.910	-1.563
90.062	1.751	89.938	-.771
95.032	.888	94.968	-.398
100.000	.025	100.000	-.025

NACA 65-2-415 (A=0.5)

Chord Station XU	Upper Surface YU	Chord Station XL	Lower Surface YL
.000	.000	.000	.000
.245	1.233	.755	-.957
.464	1.520	1.036	-1.132
.927	1.965	1.573	-1.377
2.126	2.812	2.874	-1.776
4.574	4.099	5.426	-2.335
7.054	5.122	7.946	-2.746
9.549	5.985	10.451	-3.081
14.568	7.383	15.432	-3.591
19.611	8.459	20.389	-3.963
24.671	9.280	25.329	-4.232
29.743	9.883	30.257	-4.411
34.825	10.280	35.175	-4.508
39.916	10.470	40.084	-4.526
45.019	10.423	44.981	-4.431
50.152	10.106	49.848	-4.226
60.307	8.672	59.693	-3.548
70.294	6.573	69.706	-2.609
80.199	4.157	79.801	-1.545
90.077	1.755	89.923	-.527
95.027	.715	94.973	-.139
100.000	.000	100.000	.000

NACA 65-2-215 (A=0.5)

Chord Station XU	Upper Surface YU	Chord Station XL	Lower Surface YL
.000	.000	.000	.000
.370	1.185	.630	-1.047
.605	1.445	.895	-1.251
1.086	1.841	1.414	-1.547
2.311	2.575	2.689	-2.057
4.786	3.679	5.214	-2.797
7.276	4.547	7.724	-3.359
9.774	5.274	10.226	-3.822
14.783	6.448	15.217	-4.552
19.806	7.344	20.194	-5.096
24.835	8.024	25.165	-5.500
29.871	8.519	30.129	-5.783
34.912	8.838	35.088	-5.952
39.958	8.984	40.042	-6.012
45.009	8.925	44.991	-5.929
50.076	8.638	49.924	-5.698
60.154	7.396	59.846	-4.834
70.147	5.589	69.853	-3.607
80.100	3.509	79.900	-2.203
90.039	1.450	89.961	-.836
95.013	.572	94.987	-.284
100.000	.000	100.000	.000

NACA 64-2-415

Chord Station XU	Upper Surface YU	Chord Station XL	Lower Surface YL
.000	.000	.000	.000
.299	1.291	.000	.000
.526	1.579	.000	.000
.996	2.038	.000	.000
2.207	2.833	.701	-1.091
4.673	4.121	.974	-1.299
7.162	5.075	1.504	-1.610
9.662	5.864	2.793	-2.139
14.681	7.122	5.327	-2.857
19.714	8.066	7.838	-3.379
24.756	8.771	10.338	-3.796
29.803	9.260	15.319	-4.430
34.853	9.541	20.286	-4.882
39.904	9.614	25.244	-5.191
44.954	9.414	30.197	-5.372
50.000	9.016	35.147	-5.421
60.072	7.762	40.096	-5.330
70.111	6.055	45.046	-5.034
80.109	4.062	50.000	-4.604
90.066	1.982	59.928	-3.478
95.032	.976	69.889	-2.167
100.000	.000	79.891	-.878
		89.934	-.086
		94.968	.288
		100.000	.000

NACA 63-2-615

Chord Station XU	Upper Surface YU	Chord Station XL	Lower Surface YL
.000	.000	.000	.000
.205	1.317	.759	-1.017
.418	1.634	1.082	-1.214
.866	2.159	1.634	-1.517
2.050	3.129	2.950	-2.013
4.492	4.560	5.508	-2.664
6.973	5.667	8.027	-3.123
9.473	6.578	10.527	-3.476
14.504	8.010	15.496	-3.972
19.558	9.066	20.442	-4.290
24.625	9.830	25.375	-4.460
29.700	10.331	30.300	-4.499
39.857	10.598	40.143	-4.172
50.000	9.974	50.000	-3.356
60.105	8.665	59.895	-2.239
70.159	6.847	69.841	-1.015
80.153	4.693	79.847	-.083
90.089	2.398	89.911	.704
95.042	1.245	94.958	.651
100.000	.000	100.000	.000

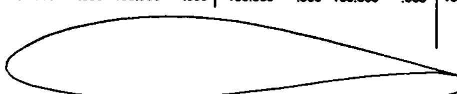

NACA 63-2-415

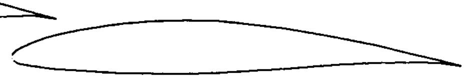

NACA 64-1-612

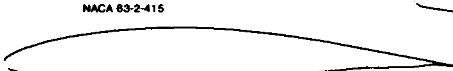

NACA 64-1-412

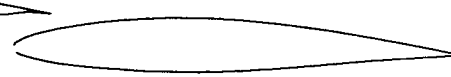

NACA 64-A-212

NACA 65-2-415 (A=0.5)

NACA 65-2-215 (A=0.5)

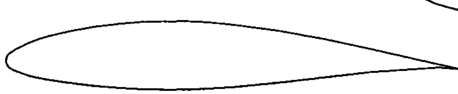

NACA 64-2-415

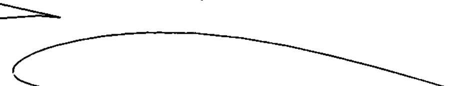

NACA 63-2-615

NACA 63-2-618

Chord Station XU	Upper Surface YU	Chord Station XL	Lower Surface YL
.000	.000	.000	.000
.156	1.511	.844	-1.211
.361	1.878	1.139	-1.458
.797	2.491	1.703	-1.849
1.965	3.616	3.035	-2.500
4.393	5.268	5.607	-3.372
6.868	6.542	8.132	-3.998
9.367	7.586	10.633	-4.484
14.404	9.219	15.596	-5.181
19.469	10.418	20.531	-5.642
24.549	11.273	25.451	-5.903
29.640	11.822	30.360	-5.990
34.734	12.086	35.266	-5.906
39.829	12.056	40.171	-5.630
44.919	11.767	45.081	-5.197
50.000	11.251	50.000	-4.633
60.125	9.667	59.875	-3.241
70.187	7.534	69.813	-1.702
80.178	5.073	79.897	-.297
90.103	2.531	89.897	.571
95.048	1.293	94.952	.603
100.000	.000	100.000	.000

NACA 65-2-415

Chord Station XU	Upper Surface YU	Chord Station XL	Lower Surface YL
.000	.000	.000	.000
.313	1.208	.687	-1.008
.542	1.480	.958	-1.200
1.016	1.900	1.484	-1.472
2.231	2.680	2.769	-1.936
4.697	3.863	5.303	-2.599
7.184	4.794	7.816	-3.098
9.682	5.578	10.318	-3.510
14.697	6.842	15.303	-4.150
19.726	7.809	20.274	-4.625
24.764	8.550	25.236	-4.970
29.807	9.093	30.193	-5.205
34.854	9.455	35.146	-5.335
39.903	9.639	40.097	-5.355
44.953	9.617	45.047	-5.237
50.000	9.374	50.000	-4.962
60.079	8.260	59.921	-3.976
70.124	6.542	69.876	-2.654
80.126	4.447	79.874	-1.263
90.080	2.175	89.920	-.107
95.040	1.058	94.960	-.206
100.000	.000	100.000	.000

Sigurd Isaacson 33006
Le radius 0.0 percent

Chord Station XU	Upper Surface YU	Chord Station XL	Lower Surface YL
.000	.000	.000	.000
.200	.280	100.000	.000
.400	.530		
.800	.950		
1.250	1.350		
2.500	2.300		
5.000	3.500		
10.000	4.900		
20.000	5.800		
30.000	6.000		
40.000	5.700		
50.000	5.300		
60.000	4.700		
70.000	3.800		
80.000	2.900		
90.000	1.600		
100.000	.000		

Sigurd Isaacson 03010

Chord Station XU	Upper Surface YU	Chord Station XL	Lower Surface YL
.000	.000	.000	.000
.200	.250	.200	-.250
.400	.410	.400	-.410
.600	.550	.600	-.550
1.250	.900	1.250	-.900
2.500	1.500	2.500	-1.500
5.000	2.500	5.000	-2.500
10.000	3.600	10.000	-3.600
20.000	4.800	20.000	-4.800
30.000	5.0000	30.000	-5.000
40.000	4.900	40.000	-4.900
50.000	4.500	50.000	-4.500
60.000	4.000	60.000	-4.000
70.000	3.500	70.000	-3.500
80.000	2.800	80.000	-2.800
90.000	1.500	90.000	-1.500
100.000	.000	100.000	.000

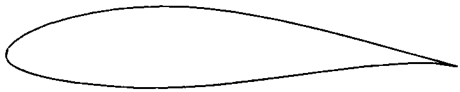

NACA 63-2-618

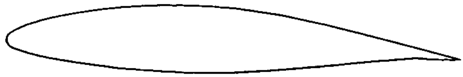

NACA 65-2-415

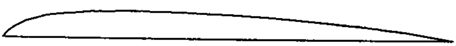

SIGURD ISAACSON 33006 LE RADIUS 0.0 PERCENT

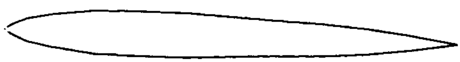

SIGURD ISAACSON 03010

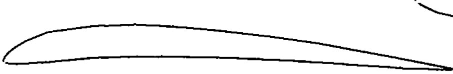

SIGURD ISAACSON 53507 LE RADIUS 0.5 PERCENT

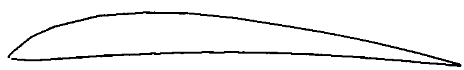

SIGURD ISAACSON 64009 LE RADIUS 0.3 PERCENT

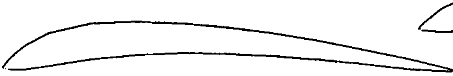

SIGURD ISAACSON 73508 LE RADIUS 0.4 PERCENT

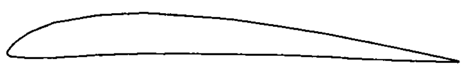

SIGURD ISAACSON 53009 LE RADIUS 0.8 PERCENT

Sigurd Isaacson 53507
L.E. radius 0.5 percent

Chord Station XU	Upper Surface YU	Chord Station XL	Lower Surface YL
.000	.000	.000	.000
.000	.200	.200	-.230
.200	.700	.400	-.330
.400	1.025	.800	-.405
1.250	1.970	1.250	-.475
2.500	3.000	2.500	-.500
5.000	4.600	5.000	-.400
10.000	6.700	10.000	.000
20.000	8.300	20.000	1.200
30.000	8.700	30.000	1.600
40.000	8.400	40.000	1.800
50.000	7.600	50.000	1.800
60.000	6.600	60.000	1.500
70.000	5.300	70.000	1.200
80.000	3.700	80.000	.600
90.000	2.000	90.000	.100
100.000	.300	100.000	.000

Sigurd Isaacson 64009
L.E. radius 0.3 percent

Chord Station XU	Upper Surface YU	Chord Station XL	Lower Surface YL
.000	.000	.000	.000
.000	.150	.200	-.170
.200	.480	.400	-.240
.600	.900	.800	-.350
1.250	1.520	1.250	-.420
2.500	2.600	2.500	-.500
5.000	4.600	5.000	-.600
10.000	7.000	10.000	-.300
20.000	9.600	20.000	.600
30.000	10.500	30.000	1.300
40.000	10.500	40.000	1.800
50.000	9.700	50.000	2.000
60.000	8.300	60.000	2.000
70.000	6.700	70.000	1.800
80.000	4.800	80.000	1.300
90.000	2.700	90.000	.600
100.000	.200	100.000	.000

Sigurd Isaacson 73508
L.E. radius 0.4 percent

Chord Station XU	Upper Surface YU	Chord Station XL	Lower Surface YL
.000	.000	.000	.000
.000	.200	.200	-.210
.200	.550	.400	-.290
.400	.810	.600	-.310
1.250	1.780	1.250	-.350
2.500	3.000	2.500	-.400
5.000	5.000	5.000	-.400
10.000	7.600	10.000	.400
20.000	9.900	20.000	2.000
30.000	10.300	30.000	3.000
40.000	10.000	40.000	3.500
50.000	9.200	50.000	3.400
60.000	8.000	60.000	3.000
70.000	6.500	70.000	2.300
80.000	4.600	80.000	1.400
90.000	2.700	90.000	.400
100.000	.400	100.000	.000

Sigurd Isaacson 53009
L.E. radius 0.8 percent

Chord Station XU	Upper Surface YU	Chord Station XL	Lower Surface YL
.000	.000	.000	.000
.000	.600	.200	-.250
.200	1.000	.400	-.400
.600	1.550	.600	-.450
1.250	2.260	1;250	-.530
2.500	3.400	2.500	-.600
5.000	5.100	5.000	-.800
10.000	7.300	10.000	-.600
20.000	9.000	20.000	.100
30.000	9.600	30.000	.600
40.000	9.200	40.000	.700
50.000	8.500	50.000	.700
60.000	7.200	60.000	.700
70.000	5.800	70.000	.600
80.000	4.100	80.000	.200
90.000	2.200	90.000	.100
100.000	.200	100.000	.000

Benedek B9403B
L.E. radius 1.0 percent

Chord Station XU	Upper Surface YU	Chord Station XL	Lower Surface YL
.000	3.000	.000	3.000
.200	3.620	.200	2.410
.400	3.980	.400	2.210
.600	4.250	.600	2.070
.800	4.510	.800	1.930
1.250	4.900	1.250	.1700
2.500	5.750	2.500	1.300
5.000	6.750	5.000	.700
7.500	7.500	7.500	.460
10.000	8.000	10.000	.300
15.000	8.600	15.000	.060
20.000	8.950	20.000	.000
25.000	9.000	25.000	.100
30.000	9.000	30.000	.250
40.000	8.650	40.000	.500
50.000	7.850	50.000	.600
60.000	6.750	60.000	.650
70.000	5.500	70.000	.560
80.000	4.050	80.000	.450
90.000	2.350	90.000	.250
95.000	1.450	95.000	.150
100.000	.450	100.000	.000

Benedek B8403B
L.E. radius 0.9 percent

Chord Station XU	Upper Surface YU	Chord Station XL	Lower Surface YL
.000	2.100	.000	2.100
.200	2.780	.200	1.480
.400	3.050	.400	1.380
.600	3.310	.600	1.280
.800	3.545	.800	1.170
1.250	3.950	1.250	1.000
2.500	4.750	2.500	.600
5.000	5.900	5.000	.200
7.500	6.600	7.500	.050
10.000	7.200	10.000	.000
15.000	7.950	15.000	.250
20.000	8.350	20.000	.450
25.000	8.500	25.000	.550
30.000	8.500	30.000	.660
40.000	8.200	40.000	.760
50.000	7.500	50.000	.830
60.000	6.500	60.000	.900
70.000	5.250	70.000	.800
80.000	4.000	80.000	.650
90.000	2.300	90.000	.400
95.000	1.350	95.000	.200
100.000	.350	100.000	.000

Benedek B8353B/2
L.E. radius 0.6 percent

Chord Station XU	Upper Surface YU	Chord Station XL	Lower Surface YL
.000	2.000	.000	2.000
.200	2.460	.200	1.550
.400	2.700	.400	1.400
.600	2.900	.600	1.280
.800	3.110	.800	1.180
1.250	3.500	1.250	1.000
2.500	4.400	2.500	600
5.000	5.500	5.000	.200
7.500	6.250	7.500	.050
10.000	6.900	10.000	.000
15.000	7.600	15.000	.200
20.000	8.000	20.000	.350
25.000	8.200	25.000	.500
30.000	8.200	30.000	.650
40.000	7.800	40.000	.800
50.000	7.000	50.000	.900
60.000	6.000	60.000	.900
70.000	4.700	70.000	.800
80.000	3.300	80.000	.600
90.000	1.900	90.000	.300
95.000	1.150	95.000	.180
100.000	.400	100.000	.000

Benedek B8452B
L.E. radius 0.6 percent

Chord Station XU	Upper Surface YU	Chord Station XL	Lower Surface YL
.000	2.300	.000	2.300
.200	2.820	.200	1.890
.400	3.020	.400	1.750
.600	3.220	.600	1.625
.800	3.440	.800	1.510
1.250	3.800	1.250	1.300
2.500	4.700	2.500	1.000
5.000	5.700	5.000	.550
7.500	6.400	7.500	.350
10.000	6.850	10.000	.200
15.000	7.450	15.000	.050
20.000	7.800	20.000	.000
25.000	8.000	25.000	.050
30.000	8.000	30.000	.100
40.000	7.600	40.000	.300
50.000	6.850	50.000	.500
60.000	5.800	60.000	.550
70.000	4.650	70.000	.550
80.000	3.250	80.000	.450
90.000	1.850	90.000	.250
95.000	1.150	95.000	.150
100.000	.400	100.000	.000

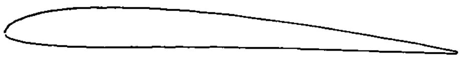

BENEDEK B9403B LE RADIUS 1.0 PERCENT

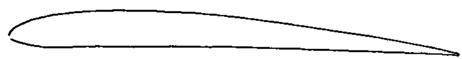

BENEDEK B8403B LE RADIUS 0.9 PERCENT

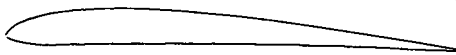

BENEDEK B8353B/2 LE RADIUS 0.6 PERCENT

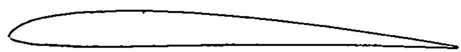

BENEDEK B8452B LE RADIUS 0.6 PERCENT

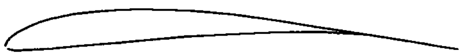

BENEDEK B7455E/2

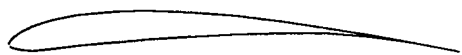

BENEDEK B7455E

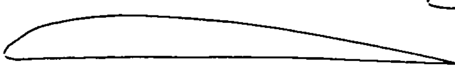

BENEDEK B9404B LE RADIUS 1.0 PERCENT

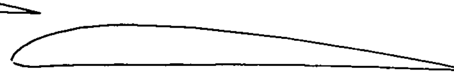

BENEDEK B9304B

Benedek B7455E/2

Chord Station XU	Upper Surface YU	Chord Station XL	Lower Surface YL
.000	1.150	.000	1.150
.200	1.700	.200	.700
.400	2.000	.400	.550
.600	2.300	.600	.430
.800	2.590	.800	.320
1.250	3.000	1.250	.150
2.500	3.960	2.500	.000
5.000	5.200	5.000	.100
7.500	6.260	7.500	.300
10.000	7.000	10.000	.400
15.000	8.000	15.000	.850
20.000	8.550	20.000	1.250
25.000	8.900	25.000	1.700
30.000	9.000	30.000	2.100
40.000	8.750	40.000	3.000
50.000	7.900	50.000	3.600
60.000	6.450	60.000	3.950
70.000	4.800	70.000	4.000
80.000	3.300	80.000	3.300
90.000	1.650	90.000	1.650
95.000	.820	95.000	.820
100.000	.000	100.000	.000

Benedek B7455E

Chord Station XU	Upper Surface YU	Chord Station XL	Lower Surface YL
.000	1.500	.000	1.500
.200	1.990	.200	1.060
.400	2.290	.400	.910
.600	2.520	.600	.790
.800	2.800	.800	.680
1.250	3.200	1.250	.500
2.500	4.100	2.500	.250
5.000	5.300	5.000	.000
7.500	6.200	7.500	.200
10.000	7.000	10.000	.450
15.000	7.950	15.000	1.100
20.000	8.500	20.000	1.600
25.000	8.900	25.000	2.050
30.000	9.000	30.000	2.500
40.000	8.650	40.000	3.150
50.000	7.850	50.000	3.700
60.000	6.550	60.000	4.000
70.000	5.100	70.000	3.900
80.000	3.500	80.000	3.200
90.000	1.750	90.000	1.750
95.000	.900	95.000	.900
100.000	.000	100.000	.000

Benedek B9404B L.E. radius
1.0 Percent

Chord Station XU	Upper Surface YU	Chord Station XL	Lower Surface YL
.000	1.400	.000	1.400
.200	2.010	.200	.800
.400	2.330	.400	.600
.600	2.580	.600	.480
.800	2.870	.800	.370
1.250	3.300	1.250	.200
2.500	4.250	2.500	.000
5.000	5.950	5.000	.150
7.500	7.200	7.500	.250
10.000	8.050	10.000	.350
15.000	9.000	15.000	.450
20.000	9.800	20.000	.600
25.000	10.000	25.000	.750
30.000	10.050	30.000	.850
40.000	9.550	40.000	.960
50.000	8.700	50.000	1.000
60.000	7.450	60.000	1.000
70.000	5.900	70.000	.850
80.000	4.050	80.000	.550
90.000	2.200	90.000	.300
95.000	1.100	95.000	.150
100.000	.000	100.000	.000

Benedek B9304B

Chord Station XU	Upper Surface YU	Chord Station XL	Lower Surface YL
.000	1.500	.000	1.500
.200	2.075	.200	.990
.400	2.400	.400	.810
.600	2.675	.600	.720
.800	2.950	.800	.650
1.250	3.400	1.250	.500
2.500	4.500	2.500	.150
5.000	5.800	5.000	.000
7.500	6.800	7.500	.100
10.000	7.600	10.000	.250
15.000	8.750	15.000	.450
20.000	9.300	20.000	.550
25.000	9.500	25.000	.600
30.000	9.450	30.000	.650
40.000	9.000	40.000	.750
50.000	8.000	50.000	.850
60.000	6.950	60.000	.850
70.000	5.500	70.000	.800
80.000	4.000	80.000	.600
90.000	2.200	90.000	.300
95.000	1.250	95.000	.150
100.000	.250	100.000	.000

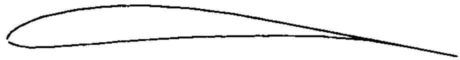

BENEDEK B8505E

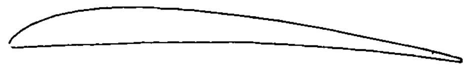

BENEDEK B8405B

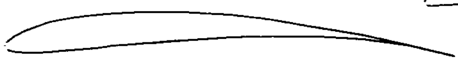

BENEDEK B7505E

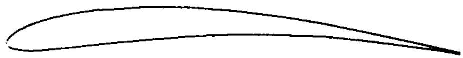

BENEDEK B7505D

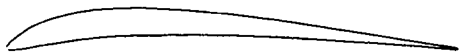

BENEDEK B6306B

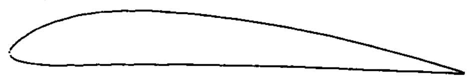

BENEDEK B12355B

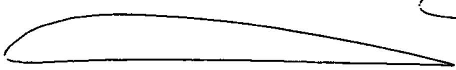

BENEDEK B10355B

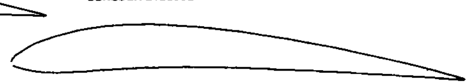

BENEDEK B10305B LE RADIUS 1.0 PERCENT

Benedek B8505E

Chord Station	Upper Surface	Chord Station	Lower Surface
XU	YU	XL	YL
.000	1.700	.000	1.700
.200	2.330	.200	1.230
.400	2.660	.400	1.050
.600	2.930	.600	.900
.800	3.200	.800	.770
1.250	3.800	1.250	.600
2.500	4.500	2.500	.250
5.000	5.700	5.000	.000
7.500	6.700	7.500	.100
10.000	7.400	10.000	.300
15.000	8.550	15.000	.800
20.000	9.200	20.000	1.200
25.000	9.800	25.000	1.750
30.000	9.750	30.000	2.150
40.000	9.350	40.000	3.000
50.000	8.350	50.000	3.500
60.000	6.800	60.000	3.900
70.000	5.150	70.000	3.950
80.000	3.500	80.000	3.300
90.000	1.750	90.000	1.750
95.000	.900	95.000	.900
100.000	.000	100.000	.000

Benedek B8405B

Chord Station	Upper Surface	Chord Station	Lower Surface
XU	YU	XL	YL
.000	1.000	.000	1.000
.200	1.560	.200	.420
.400	1.860	.400	.220
.600	2.120	.600	.100
.800	2.400	.800	.030
1.250	2.850	1.250	.000
2.500	3.900	2.500	.100
5.000	5.400	5.000	.350
7.500	6.500	7.500	.550
10.000	7.450	10.000	.750
15.000	8.600	15.000	1.100
20.000	9.350	20.000	1.400
25.000	9.750	25.000	1.800
30.000	9.950	30.000	2.100
40.000	9.700	40.000	2.560
50.000	8.950	50.000	2.900
60.000	7.900	60.000	2.800
70.000	6.450	70.000	2.400
80.000	4.650	80.000	1.850
90.000	2.900	90.000	1.000
95.000	1.960	95.000	.500
100.000	.700	100.000	.000

Benedek B7505E

Chord Station	Upper Surface	Chord Station	Lower Surface
XU	YU	XL	YL
.000	1.500	.000	1.500
.200	2.000	.200	1.050
.400	2.260	.400	.900
.600	2.500	.600	.785
.800	2.720	.800	.680
1.250	3.100	1.250	.500
2.500	4.000	2.500	.200
5.000	5.060	5.000	.100
7.500	6.000	7.500	.100
10.000	6.850	10.000	.300
15.000	7.800	15.000	.800
20.000	8.400	20.000	1.200
25.000	8.950	25.000	1.950
30.000	9.100	30.000	2.250
40.000	9.100	40.000	3.100
50.000	8.600	50.000	3.700
60.000	7.600	60.000	4.000
70.000	6.000	70.000	4.050
80.000	4.400	80.000	3.600
90.000	2.300	90.000	2.300
95.000	1.150	95.000	1.150
100.000	.000	100.000	.000

Benedek B7505D

Chord Station	Upper Surface	Chord Station	Lower Surface
XU	YU	XL	YL
.000	1.700	.000	1.700
.200	2.300	.200	1.250
.400	2.600	.400	1.020
.600	2.850	.600	.880
.800	3.100	.800	.750
1.250	3.500	1.250	.550
2.500	4.500	2.500	.250
5.000	5.750	5.000	.000
7.500	6.650	7.500	.100
10.000	7.400	10.000	.350
15.000	8.400	15.000	.900
20.000	9.100	20.000	1.500
25.000	9.450	25.000	2.050
30.000	9.750	30.000	2.550
40.000	9.750	40.000	3.400
50.000	9.150	50.000	3.950
60.000	8.000	60.000	3.950
70.000	6.450	70.000	3.650
80.000	4.600	80.000	2.750
90.000	2.550	90.000	1.550
95.000	1.450	95.000	.950
100.000	.200	100.000	.000

Benedek B6306B

Chord Station	Upper Surface	Chord Station	Lower Surface
XU	YU	XL	YL
.000	.700	.000	.700
.200	1.200	.200	.200
.400	1.400	.400	.075
.600	1.600	.800	.020
.800	1.780	.700	.000
1.250	2.180	1.250	.030
2.500	3.170	2.500	.150
5.000	4.770	5.000	.550
7.500	6.000	7.500	1.000
10.000	6.870	10.000	1.430
15.000	8.130	15.000	2.220
20.000	8.830	20.000	2.760
25.000	9.200	25.000	3.140
30.000	9.240	30.000	3.350
40.000	8.770	40.000	3.460
50.000	7.850	50.000	3.270
60.000	6.570	60.000	2.930
70.000	5.100	70.000	2.340
80.000	3.550	80.000	1.700
90.000	1.930	90.000	.930
100.000	.320	100.000	.000

Benedek B12355B

Chord Station	Upper Surface	Chord Station	Lower Surface
XU	YU	XL	YL
.000	2.680	.000	2.680
.200	3.350	.200	2.100
.400	3.680	.400	1.840
.600	3.900	.800	1.650
.800	4.160	.800	1.490
1.250	4.670	1.250	1.200
2.500	5.800	2.500	.770
5.000	7.460	5.000	.330
7.500	8.700	7.500	.100
10.000	9.730	10.000	.000
15.000	11.250	15.000	.130
20.000	12.090	20.000	.370
25.000	12.500	25.000	.550
30.000	12.550	30.000	.670
40.000	12.070	40.000	.770
50.000	11.100	50.000	.820
60.000	9.650	60.000	.800
70.000	7.820	70.000	.670
80.000	5.650	80.000	.430
90.000	3.000	90.000	.200
100.000	.250	100.000	.000

Benedek B10355B

Chord Station	Upper Surface	Chord Station	Lower Surface
XU	YU	XL	YL
.000	1.530	.000	1.530
.200	2.250	.200	1.090
.400	2.580	.400	.870
.600	2.820	.600	.710
.800	3.060	.800	.575
1.250	3.530	1.250	.400
2.500	4.630	2.500	.170
5.000	6.320	5.000	.000
7.500	7.560	7.500	.060
10.000	8.420	10.000	.120
15.000	9.750	15.000	.390
20.000	10.430	20.000	.650
25.000	10.700	25.000	.820
30.000	10.700	30.000	.900
40.000	10.180	40.000	.930
50.000	9.280	50.000	.900
60.000	7.960	60.000	.750
70.000	6.400	70.000	.550
80.000	4.650	80.000	.380
90.000	2.500	90.000	.200
100.000	.250	100.000	.000

Benedek B10305B L.E. radius 1.0 Percent

Chord Station	Upper Surface	Chord Station	Lower Surface
XU	YU	XL	YL
.000	2.320	.000	2.320
.200	3.000	.200	1.800
.400	3.220	.400	1.560
.600	3.410	.600	1.430
.800	3.620	.800	1.300
1.250	4.050	1.250	1.080
2.500	5.000	2.500	.720
5.000	6.420	5.000	.280
7.500	7.530	7.500	.060
10.000	8.420	10.000	.000
15.000	9.760	15.000	.270
20.000	10.670	20.000	.730
25.000	11.180	25.000	1.170
30.000	11.380	30.000	1.500
40.000	11.000	40.000	1.750
50.000	10.000	50.000	1.720
60.000	8.670	60.000	1.530
70.000	6.950	70.000	1.220
80.000	4.930	80.000	.920
90.000	2.790	90.000	.500
100.000	.250	100.000	.000

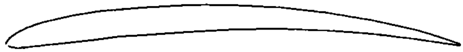

BENEDEK B6556C LE RADIUS 0.6 PERCENT

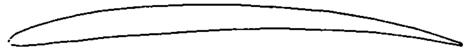

BENEDEK B6556B LE RADIUS 0.7 PERCENT

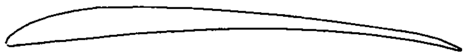

BENEDEK B6456F

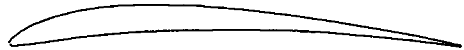

BENEDEK B63556B LE RADIUS 0.7 PERCENT

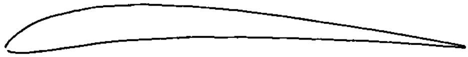

BENEDEK B8356B LE RADIUS 0.9 PERCENT

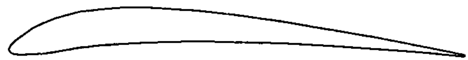

BENEDEK B8306B LE RADIUS 0.9 PERCENT

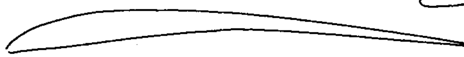

BENEDEK B7456D

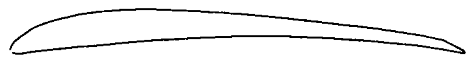

BENEDEK B7406F

Benedek B6556C L.E. radius 0.6 Percent

Chord Station	Upper Surface	Chord Station	Lower Surface
XU	YU	XL	YL
.000	1.000	.000	1.000
.200	1.450	.200	.560
.400	1.700	.400	.440
.600	1.900	.600	.480
.800	2.100	.800	.330
1.250	2.500	1.250	.250
2.500	3.400	2.500	.000
5.000	4.600	5.000	.200
7.500	5.400	7.500	.450
10.000	6.150	10.000	.750
15.000	7.250	15.000	1.300
20.000	8.000	20.000	1.800
25.000	8.550	25.000	2.350
30.000	8.950	30.000	2.700
40.000	9.400	40.000	3.350
50.000	9.300	50.000	3.800
60.000	8.750	60.000	4.000
70.000	7.650	70.000	3.600
80.000	5.900	80.000	2.850
90.000	3.550	90.000	1.500
96.000	2.000	95.000	.800
100.000	.400	100.000	.000

Benedek B6556B L.E. radius 0.7 Percent

Chord Station	Upper Surface	Chord Station	Lower Surface
XU	YU	XL	YL
.000	1.000	.000	1.000
.200	1.500	.200	.500
.400	1.770	.400	.360
.600	1.950	.600	.300
.800	2.150	.800	.280
1.250	2.500	1.250	.200
2.500	3.200	2.500	.000
5.000	4.250	5.000	.250
7.500	5.000	7.500	.400
10.000	5.750	10.000	.700
15.000	6.900	15.000	1.200
20.000	7.700	20.000	1.750
25.000	8.300	25.000	2.250
30.000	8.750	30.000	2.600
40.000	9.150	40.000	3.300
50.000	9.100	50.000	3.750
60.000	8.550	60.000	3.950
70.000	7.600	70.000	3.600
80.000	6.000	80.000	3.000
90.000	3.700	90.000	1.750
95.000	2.100	95.000	.850
100.000	.450	100.000	.000

Benedek B6456F

Chord Station	Upper Surface	Chord Station	Lower Surface
XU	YU	XL	YL
.000	.750	.000	.750
.200	1.310	.200	.320
.400	1.600	.400	.160
.600	1.830	.600	.090
.800	2.100	.800	.030
1.250	2.600	1.250	.000
2.500	3.600	2.500	.200
5.000	4.950	5.000	.500
7.500	6.000	7.500	.800
10.000	6.900	10.000	1.100
15.000	8.000	15.000	1.600
20.000	8.700	20.000	2.200
25.000	8.950	25.000	2.800
30.000	9.000	30.000	3.250
40.000	8.900	40.000	4.000
50.000	8.300	50.000	4.500
60.000	7.500	60.000	4.500
70.000	6.400	70.000	4.050
80.000	5.050	80.000	3.300
90.000	3.700	90.000	2.000
95.000	2.600	95.000	1.100
100.000	.500	100.000	.000

Benedek B63556B L.E. radius 0.7 Percent

Chord Station	Upper Surface	Chord Station	Lower Surface
XU	YU	XL	YL
.000	.700	.000	.700
.200	1.200	.200	.220
.400	1.400	.400	.060
.600	1.600	.700	.000
.800	1.800	.800	.010
1.250	2.180	1.250	.030
2.500	3.140	2.500	.150
5.000	4.550	5.000	.420
7.500	5.650	7.500	.780
10.000	6.530	10.000	1.120
15.000	7.780	15.000	1.850
20.000	8.550	20.000	2.450
25.000	9.000	25.000	2.920
30.000	9.150	30.000	3.250
40.000	8.960	40.000	3.570
50.000	8.230	50.000	3.650
60.000	7.100	60.000	3.500
70.000	5.750	70.000	3.000
80.000	4.080	80.000	2.220
90.000	2.230	90.000	1.190
100.000	.220	100.000	.000

Benedek B8356B L.E. radius 0.9 Percent

Chord Station	Upper Surface	Chord Station	Lower Surface
XU	YU	XL	YL
.000	1.110	.000	1.110
.000	1.400	.200	.680
.200	1.810	.400	.490
.400	2.070	.600	.380
.800	2.530	.800	.300
1.250	3.000	1.250	.170
2.500	4.150	2.500	.030
5.000	5.830	5.000	.050
7.500	7.080	7.500	.250
10.000	8.000	10.000	.500
15.000	9.150	15.000	1.190
20.000	9.970	20.000	1.870
25.000	10.280	25.000	2.350
30.000	10.370	30.000	2.700
40.000	9.910	40.000	3.050
50.000	8.880	50.000	2.980
60.000	7.500	60.000	2.670
70.000	5.900	70.000	2.220
80.000	4.200	80.000	1.620
90.000	2.320	90.000	.890
100.000	.330	100.000	.000

Benedek B8306B L.E. radius 0.9 Percent

Chord Station	Upper Surface	Chord Station	Lower Surface
XU	YU	XL	YL
.000	1.180	.000	1.180
.200	1.740	.200	.600
.400	2.050	.400	.420
.600	2.310	.600	.320
.800	2.550	.800	.270
1.250	3.020	1.250	.170
2.500	4.110	2.500	.000
5.000	5.830	5.000	.070
7.500	7.130	7.500	.280
10.000	8.180	10.000	.650
15.000	9.500	15.000	1.470
20.000	10.220	20.000	2.130
25.000	10.510	25.000	2.560
30.000	10.500	30.000	2.830
40.000	9.900	40.000	3.000
50.000	8.830	50.000	2.900
60.000	7.470	60.000	2.620
70.000	5.850	70.000	2.170
80.000	4.150	80.000	1.530
90.000	2.330	90.000	.830
100.000	.350	100.000	.000

Benedek B7456D

Chord Station	Upper Surface	Chord Station	Lower Surface
XU	YU	XL	YL
.000	.850	.000	.850
.200	1.350	.200	.350
.400	1.620	.400	.250
.600	1.830	.600	.150
.800	2.080	.800	.030
1.250	2.500	1.250	.000
2.500	3.460	2.500	.200
5.000	4.900	5.000	.450
7.500	5.950	7.500	.700
10.000	6.700	10.000	.950
15.000	8.000	15.000	1.450
20.000	8.700	20.000	1.950
25.000	9.000	25.000	2.500
30.000	9.050	30.000	3.000
40.000	8.800	40.000	4.000
50.000	8.000	50.000	4.500
60.000	6.900	60.000	4.000
70.000	5.500	70.000	3.000
80.000	3.950	80.000	2.000
90.000	2.250	90.000	1.000
95.000	1.400	95.000	.500
100.000	.500	100.000	.000

Benedek B7406F

Chord Station	Upper Surface	Chord Station	Lower Surface
XU	YU	XL	YL
.000	.900	.000	.900
.200	1.500	.200	.420
.400	1.900	.400	.300
.600	2.200	.600	.220
.800	2.490	.800	.170
1.250	2.950	1.250	.100
2.500	3.950	2.500	.100
5.000	5.600	5.000	.450
7.500	6.600	7.500	.800
10.000	7.400	10.000	1.000
15.000	8.550	15.000	1.500
20.000	9.200	20.000	1.950
25.000	9.550	25.000	2.400
30.000	9.650	30.000	2.800
40.000	9.300	40.000	3.400
50.000	8.600	50.000	3.800
60.000	7.700	60.000	3.750
70.000	6.650	70.000	3.400
80.000	5.400	80.000	2.650
90.000	3.950	90.000	1.600
95.000	2.900	95.000	.900
100.000	.500	100.000	.000

Benedek B8406B L.E. radius 1.4 Percent

Chord Station XU	Upper Surface YU	Chord Station XL	Lower Surface YL
.000	2.220	.000	2.220
.200	3.000	.200	1.500
.400	3.310	.400	1.180
.600	3.580	.600	1.000
.800	3.780	.800	.790
1.250	4.140	1.250	.500
2.500	4.970	2.500	.180
5.000	6.160	5.000	.000
7.500	7.090	7.500	.110
10.000	7.820	10.000	.360
15.000	9.000	15.000	1.100
20.000	9.850	20.000	1.790
25.000	10.460	25.000	2.400
30.000	10.900	30.000	2.890
40.000	10.950	40.000	3.310
50.000	10.300	50.000	3.470
60.000	9.210	60.000	3.380
70.000	7.640	70.000	3.000
80.000	5.630	80.000	2.360
90.000	3.180	90.000	1.330
95.000	1.810	95.000	.700
100.000	.330	100.000	.000

Benedek B8406A L.E. radius 1.4 Percent

Chord Station XU	Upper Surface YU	Chord Station XL	Lower Surface YL
.000	1.850	.000	1.850
.200	2.550	.200	1.160
.400	2.890	.400	.880
.600	3.100	.600	.660
.800	3.310	.800	.500
1.250	3.720	1.250	.290
2.500	4.580	2.500	.060
5.000	5.860	5.000	.020
7.500	6.860	7.500	.170
10.000	7.640	10.000	.430
15.000	8.880	15.000	1.110
20.000	9.780	20.000	1.760
25.000	10.350	25.000	2.320
30.000	10.600	30.000	2.810
40.000	10.460	40.000	3.310
50.000	9.830	50.000	3.460
60.000	8.780	60.000	3.390
70.000	7.280	70.000	3.030
80.000	5.370	80.000	2.360
90.000	3.040	90.000	1.340
95.000	1.710	95.000	.680
100.000	.280	100.000	.000

Benedek B8365B/3 L.E. radius 0.8 Percent

Chord Station XU	Upper Surface YU	Chord Station XL	Lower Surface YL
.000	1.100	.000	1.100
.200	1.660	.200	.560
.400	1.970	.400	.400
.600	.2220	.600	.300
.800	2.460	.800	.260
1.250	2.960	1.250	.250
2.500	3.950	2.500	.050
5.000	5.450	5.000	.050
7.500	6.550	7.500	.450
10.000	7.450	10.000	.800
15.000	8.700	15.000	1.450
20.000	9.400	20.000	1.950
25.000	9.850	25.000	2.400
30.000	10.000	30.000	2.650
40.000	9.900	40.000	2.900
50.000	9.300	50.000	2.900
60.000	8.250	60.000	2.600
70.000	6.900	70.000	2.100
80.000	5.050	80.000	1.550
90.000	3.150	90.000	.900
95.000	2.000	95.000	.450
100.000	.550	100.000	.000

Benedek B8356B/2 L.E. radius 1.1 Percent

Chord Station XU	Upper Surface YU	Chord Station XL	Lower Surface YL
.000	1.800	.000	1.800
.200	2.450	.200	1.190
.400	2.790	.400	.880
.600	3.020	.600	.690
.800	3.240	.800	.500
1.250	3.700	1.250	.230
2.500	4.600	2.500	.030
5.000	6.000	5.000	.060
7.500	7.050	7.500	.300
10.000	7.900	10.000	.630
15.000	9.180	15.000	1.400
20.000	10.060	20.000	2.040
25.000	10.580	25.000	2.560
30.000	10.710	30.000	2.900
40.000	10.350	40.000	3.240
50.000	9.400	50.000	3.100
60.000	8.190	60.000	2.800
70.000	6.620	70.000	2.380
80.000	4.740	80.000	1.750
90.000	2.650	90.000	.830
95.000	1.510	95.000	.490
100.000	.330	100.000	.000

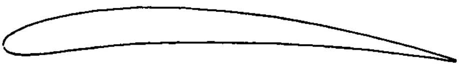

BENEDEK B8406B LE RADIUS 1.4 PERCENT

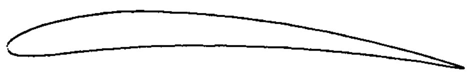

BENEDEK B8406A LE RADIUS 1.4 PERCENT

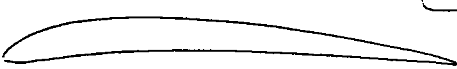

BENEDEK B8365B/3 LE RADIUS 0.8 PERCENT

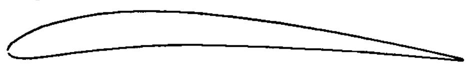

BENEDEK B8356B/2 LE RADIUS 1.1 PERCENT

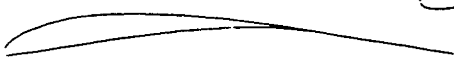

BENEDEK B6407E

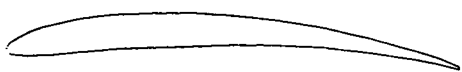

BENEDEK B8556B LE RADIUS 0.6 PERCENT

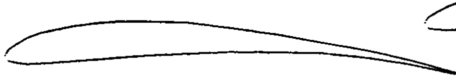

BENEDEK B8456D

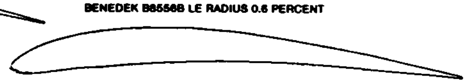

BENEDEK B8406C LE RADIUS 0.8 PERCENT

Benedek B6407E

Chord Station XU	Upper Surface YU	Chord Station XL	Lower Surface YL
.000	.800	.000	.800
.200	1.290	.200	.330
.400	1.575	.400	.200
.600	1.800	.600	.120
.800	2.050	.800	.060
1.250	2.500	1.250	.000
2.500	3.500	2.500	.200
5.000	4.900	5.000	.450
7.500	5.900	7.500	.800
10.000	6.700	10.000	1.100
15.000	7.950	15.000	1.900
20.000	8.600	20.000	2.700
25.000	8.950	25.000	3.450
30.000	9.000	30.000	4.100
40.000	8.650	40.000	5.200
50.000	7.700	50.000	5.900
60.000	6.300	60.000	5.900
70.000	4.800	70.000	4.800
80.000	3.200	80.000	3.200
90.000	1.600	90.000	1.600
95.000	.800	95.000	.800
100.000	.000	100.000	.000

Benedek B8556B Le radius 0.6 Percent

Chord Station XU	Upper Surface YU	Chord Station XL	Lower Surface YL
.000	1.400	.000	1.400
.200	1.910	.200	.950
.400	2.180	.400	.750
.600	2.390	.600	.630
.800	2.770	.800	.420
1.250	3.000	1.250	.300
2.500	4.000	2.500	.100
5.000	5.300	5.000	.000
7.500	6.300	7.500	.200
10.000	7.000	10.000	.400
15.000	8.250	15.000	1.000
20.000	9.150	20.000	1.500
25.000	9.750	25.000	2.100
30.000	10.200	30.000	2.500
40.000	10.500	40.000	3.200
50.000	10.200	50.000	3.750
60.000	9.350	60.000	4.000
70.000	8.200	70.000	3.200
80.000	6.400	80.000	3.200
90.000	4.000	90.000	2.000
95.000	2.500	95.000	1.100
100.000	.600	100.000	.000

Benedek B8456D

Chord Station XU	Upper Surface YU	Chord Station XL	Lower Surface YL
.000	1.750	.000	1.750
.200	2.305	.200	1.160
.400	2.600	.400	.975
.600	2.860	.600	.820
.800	3.130	.800	.690
1.250	3.550	1.250	.500
2.500	4.500	2.500	.250
5.000	5.950	5.000	.000
7.500	6.950	7.500	.200
10.000	7.600	10.000	.450
15.000	8.800	15.000	1.050
20.000	9.500	20.000	1.500
25.000	10.050	25.000	2.000
30.000	10.200	30.000	2.500
40.000	10.150	40.000	3.200
50.000	9.200	50.000	3.750
60.000	8.000	60.000	4.000
70.000	6.400	70.000	3.900
80.000	4.700	80.000	3.100
90.000	2.700	90.000	1.800
95.000	1.500	95.000	.900
100.000	.300	100.000	.000

Benedek B8406C Le radius 0.8 Percent

Chord Station XU	Upper Surface YU	Chord Station XL	Lower Surface YL
.000	1.200	.000	1.200
.200	1.900	.200	.870
.400	2.230	.400	.690
.600	2.510	.600	.590
.800	2.750	.800	.500
1.250	3.200	1.250	.400
2.500	4.170	2.500	.100
5.000	5.600	5.000	.100
7.500	6.720	7.500	.400
10.000	7.600	10.000	.760
15.000	8.900	15.000	1.380
20.000	9.600	20.000	1.600
25.000	10.150	25.000	2.150
30.000	10.400	30.000	2.650
40.000	10.400	40.000	3.050
50.000	9.600	50.000	3.200
60.000	8.200	60.000	2.950
70.000	6.650	70.000	2.400
80.000	4.800	80.000	1.700
90.000	2.550	90.000	.900
95.000	1.520	95.000	.450
100.000	.400	100.000	.000

Benedek B7457D

Chord Station	Upper Surface	Chord Station	Lower Surface
XU	YU	XL	YL
.000	.900	.000	.900
.200	1.400	.200	.400
.400	1.670	.400	.250
.600	1.900	.600	.170
.800	2.120	.800	.090
1.250	2.550	1.250	.000
2.500	3.550	2.500	.100
5.000	5.200	5.000	.300
7.500	6.300	7.500	.500
10.000	7.200	10.000	.900
15.000	8.450	15.000	1.500
20.000	9.250	20.000	2.100
25.000	9.800	25.000	2.750
30.000	10.000	30.000	3.250
40.000	9.850	40.000	4.250
50.000	9.250	50.000	4.900
60.000	8.100	60.000	4.550
70.000	6.550	70.000	3.900
80.000	4.900	80.000	2.800
90.000	2.800	90.000	1.500
95.000	1.700	95.000	.800
100.000	.500	100.000	.000

Benedek B7407D

Chord Station	Upper Surface	Chord Station	Lower Surface
XU	YU	XL	YL
.000	1.000	.000	1.000
.200	1.700	.200	.550
.400	2.075	.400	.475
.600	2.350	.600	.380
.800	2.610	.800	.270
1.250	3.050	1.250	.150
2.500	4.000	2.500	.100
5.000	5.500	5.000	.400
7.500	6.600	7.500	.700
10.000	7.500	10.000	1.000
15.000	8.800	15.000	1.600
20.000	9.550	20.000	2.200
25.000	9.900	25.000	2.800
30.000	10.000	30.000	3.450
40.000	9.500	40.000	4.600
50.000	8.500	50.000	5.450
60.000	7.200	60.000	4.600
70.000	5.650	70.000	3.450
80.000	4.050	80.000	2.250
90.000	2.400	90.000	1.100
95.000	1.500	95.000	.550
100.000	.600	100.000	.000

Benedek B6557B L.E. radius 0.6 Percent

Chord Station	Upper Surface	Chord Station	Lower Surface
XU	YU	XL	YL
.000	1.000	.000	1.000
.200	1.510	.200	.560
.400	1.780	.400	.420
.600	2.000	.600	.360
.800	2.210	.800	.290
1.250	2.600	1.250	.200
2.500	3.500	2.500	.000
5.000	4.600	5.000	.350
7.500	5.500	7.500	.750
10.000	6.350	10.000	1.100
15.000	7.500	15.000	1.700
20.000	8.400	20.000	2.400
25.000	9.150	25.000	3.000
30.000	9.650	30.000	3.600
40.000	10.000	40.000	4.500
50.000	9.900	50.000	5.100
60.000	9.200	60.000	5.150
70.000	8.000	70.000	4.800
80.000	6.000	80.000	3.900
90.000	3.550	90.000	2.200
95.000	2.000	95.000	1.100
100.000	.500	100.000	.000

Benedek B6457E

Chord Station	Upper Surface	Chord Station	Lower Surface
XU	YU	XL	YL
.000	.800	.000	.800
.200	1.300	.200	.390
.400	1.580	.400	.300
.600	1.810	.600	.260
.800	2.070	.800	.220
1.250	2.500	1.250	.150
2.500	3.450	2.500	.000
5.000	4.850	5.000	.300
7.500	5.900	7.500	.700
10.000	6.700	10.000	1.000
15.000	7.900	15.000	1.750
20.000	8.600	20.000	2.500
25.000	9.000	25.000	3.150
30.000	9.150	30.000	3.750
40.000	9.000	40.000	4.800
50.000	8.250	50.000	5.500
60.000	7.100	60.000	6.000
70.000	5.500	70.000	5.300
80.000	3.750	80.000	3.750
90.000	1.900	90.000	1.900
95.000	.850	95.000	.850
100.000	.000	100.000	.000

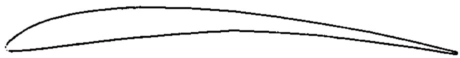

BENEDEK B7457D

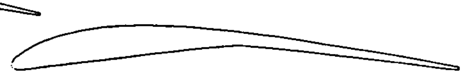

BENEDEK B7407D

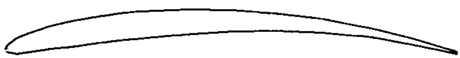

BENEDEK B6557B LE RADIUS 0.6 PERCENT

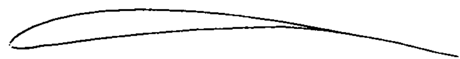

BENEDEK B6457E

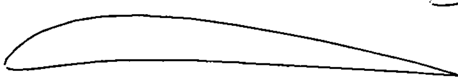

BENEDEK B10307B

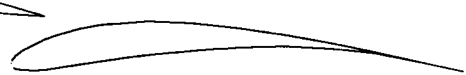

BENEDEK B8457E

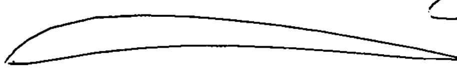

BENEDEK B8257B

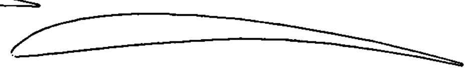

BENEDEK B7457D/2

Benedek B10307B

Chord Station	Upper Surface	Chord Station	Lower Surface
XU	YU	XL	YL
.000	1.150	.000	1.150
.200	2.010	.200	.760
.400	2.390	.400	.550
.600	2.650	.600	.385
.800	2.940	.800	.280
1.250	3.480	1.250	.100
2.500	4.850	2.500	.000
5.000	6.800	5.000	.120
7.500	8.330	7.500	.400
10.000	9.450	10.000	.750
15.000	11.000	15.000	1.430
20.000	11.920	20.000	2.000
25.000	12.350	25.000	2.400
30.000	12.400	30.000	2.570
40.000	11.900	40.000	2.670
50.000	10.780	50.000	2.420
60.000	9.220	60.000	2.000
70.000	7.330	70.000	1.550
80.000	5.120	80.000	1.000
90.000	2.780	90.000	.530
100.000	.000	100.000	.000

Benedek B8457E

Chord Station	Upper Surface	Chord Station	Lower Surface
XU	YU	XL	YL
.000	1.500	.000	1.500
.200	2.200	.200	.900
.400	2.480	.400	.700
.600	2.750	.600	.520
.800	3.000	.800	.400
1.250	3.400	1.250	.250
2.500	4.400	2.500	.100
5.000	5.600	5.000	.000
7.500	6.900	7.500	.150
10.000	7.750	10.000	.500
15.000	9.100	15.000	1.250
20.000	10.000	20.000	2.000
25.000	10.450	25.000	2.800
30.000	10.800	30.000	3.400
40.000	10.400	40.000	4.500
50.000	9.400	50.000	5.200
60.000	8.000	60.000	5.500
70.000	6.200	70.000	5.000
80.000	4.200	80.000	4.000
90.000	2.000	90.000	2.000
95.000	1.000	95.000	1.000
100.000	.000	100.000	.000

Benedek B 8257 B

Chord Station	Upper Surface	Chord Station	Lower Surface
XU	YU	XL	YL
.000	.000	.000	.000
.200	.380	.200	-.180
.400	.690	.400	-.220
1.000	1.380	1.000	-.310
1.250	1.690	1.250	-.350
2.500	3.000	2.500	-.400
5.000	5.000	5.000	-.400
10.000	7.600	10.000	.400
20.000	9.900	20.000	2.000
30.000	10.300	30.000	3.000
40.000	10.000	40.000	3.500
50.000	9.200	50.000	3.400
60.000	8.000	60.000	3.000
70.000	6.500	70.000	2.300
80.000	4.600	80.000	1.400
90.000	2.700	90.000	.400
100.000	.400	100.000	.000

Benedek B7457D/2

Chord Station	Upper Surface	Chord Station	Lower Surface
XU	YU	XL	YL
.000	.900	.000	.900
.200	1.400	.200	.400
.400	1.670	.400	.250
.600	1.900	.600	.170
.800	2.120	.800	.090
1.250	2.550	1.250	.000
2.500	3.550	2.500	.100
5.000	5.200	5.000	.300
7.500	6.300	7.500	.600
10.000	7.200	10.000	.900
15.000	8.450	15.000	1.500
20.000	9.250	20.000	2.100
25.000	9.800	25.000	2.750
30.000	10.000	30.000	3.250
40.000	9.850	40.000	4.250
50.000	9.250	50.000	4.900
60.000	8.100	60.000	4.900
70.000	6.550	70.000	4.300
80.000	4.900	80.000	3.150
90.000	2.800	90.000	1.750
95.000	1.700	95.000	.950
100.000	.500	100.000	.000

Benedek B8306B

Chord Station XU	Upper Surface YU	Chord Station XL	Lower Surface YL
.000	.900	.000	.900
.200	1.580	.200	.330
.400	1.980	.400	.150
.600	2.270	.600	.060
.800	2.570	.900	.000
1.250	3.250	1.250	.000
2.500	4.600	2.500	.100
5.000	6.630	5.000	.470
7.500	8.130	7.500	1.000
10.000	9.230	10.000	1.530
15.000	10.680	15.000	2.750
20.000	11.830	20.000	3.720
25.000	12.170	25.000	4.280
30.000	12.200	30.000	4.580
40.000	11.500	40.000	4.670
50.000	10.200	50.000	4.330
60.000	8.550	60.000	3.770
70.000	6.670	70.000	3.000
80.000	4.630	80.000	2.050
90.000	2.540	90.000	1.030
100.000	.300	100.000	.000

Benedek B8256B L.E. radius 0.9 Percent

Chord Station XU	Upper Surface YU	Chord Station XL	Lower Surface YL
.000	.900	.000	.900
.200	1.600	.200	.350
.400	2.050	.400	.155
.600	2.400	.600	.060
.800	2.750	.900	.000
1.250	3.500	1.250	.000
2.500	5.030	2.500	.250
5.000	7.120	5.000	.770
7.500	8.720	7.500	1.390
10.000	9.930	10.000	2.060
15.000	11.350	15.000	3.430
20.000	12.120	20.000	4.030
25.000	12.280	25.000	4.400
30.000	12.150	30.000	4.520
40.000	11.290	40.000	4.370
50.000	9.870	50.000	4.030
60.000	8.220	60.000	3.480
70.000	6.400	70.000	2.720
80.000	4.450	80.000	1.880
90.000	2.430	90.000	1.000
100.000	.250	100.000	.000

Benedek B6356B

Chord Station XU	Upper Surface YU	Chord Station XL	Lower Surface YL
.000	.700	.000	.700
.200	1.200	.200	.200
.400	1.480	.400	.075
.600	1.700	.600	.020
.800	1.920	.700	.000
1.250	2.330	1.250	.070
2.500	3.400	2.500	.250
5.000	5.190	5.000	.830
7.500	6.530	7.500	1.440
10.000	7.640	10.000	2.100
15.000	9.250	15.000	3.200
20.000	10.200	20.000	4.100
25.000	10.820	25.000	4.800
30.000	11.090	30.000	5.220
40.000	10.850	40.000	5.510
50.000	9.920	50.000	5.290
60.000	8.450	60.000	4.730
70.000	6.670	70.000	3.840
80.000	4.650	80.000	2.750
90.000	2.510	90.000	1.430
100.000	.250	100.000	.000

Benedek B6306B L.E. radius 0.7 Percent

Chord Station XU	Upper Surface YU	Chord Station XL	Lower Surface YL
.000	.700	.000	.700
.200	1.200	.200	.220
.400	1.500	.400	.060
.600	1.730	.700	.000
.800	2.140	.800	.030
1.250	2.420	1.250	.060
2.500	3.620	2.500	.320
5.000	5.380	5.000	.970
7.500	6.850	7.500	1.700
10.000	8.120	10.000	2.430
15.000	9.830	15.000	3.730
20.000	10.800	20.000	4.680
25.000	11.220	25.000	5.190
30.000	11.250	30.000	5.350
40.000	10.730	40.000	5.420
50.000	9.630	50.000	5.120
60.000	8.140	60.000	4.500
70.000	6.380	70.000	3.700
80.000	4.440	80.000	2.620
90.000	2.390	90.000	1.230
100.000	.280	100.000	.000

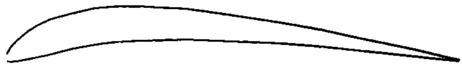

BENEDEK B8306B

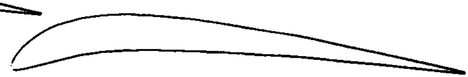

BENEDEK B8256B LE RADIUS 0.9 PERCENT

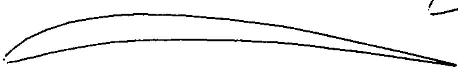

BENEDEK B6356B

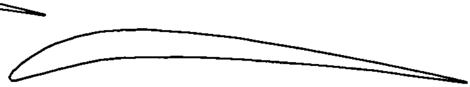

BENEDEK B6306B LE RADIUS 0.7 PERCENT

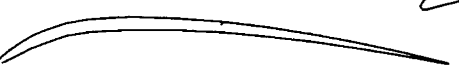

BENEDEK B3309B LE RADIUS 0.4 PERCENT

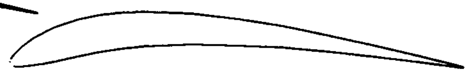

BENEDEK B8356B

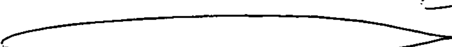

PFENNINGER LAMINAR 4910 LE RADIUS 0.9 PERCENT

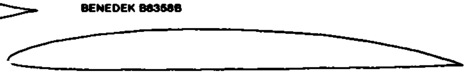

PFENNINGER LAMINAR 11 LE RADIUS 0.8 PERCENT

Benedek B3309B L.E. radius 0.4 Percent

Chord Station XU	Upper Surface YU	Chord Station XL	Lower Surface YL
.000	.400	.000	.400
.000	.750	.200	.220
.200	1.000	.400	.180
.400	1.220	.600	.200
.800	1.600	.800	.225
1.250	1.970	1.250	.380
2.500	3.000	2.500	.960
5.000	4.730	5.000	2.200
7.500	6.170	7.500	3.400
10.000	7.330	10.000	4.480
15.000	9.120	15.000	6.170
20.000	10.090	20.000	7.100
25.000	10.470	25.000	7.500
30.000	10.630	30.000	7.670
40.000	10.330	40.000	7.600
50.000	9.470	50.000	7.090
60.000	8.200	60.000	6.130
70.000	6.600	70.000	4.890
80.000	4.670	80.000	3.400
90.000	2.500	90.000	1.780
100.000	.100	100.000	.000

Benedek B8356B

Chord Station XU	Upper Surface YU	Chord Station XL	Lower Surface YL
.000	1.000	.000	1.000
.200	1.650	.200	.550
.400	2.000	.400	.380
.600	2.300	.600	.280
.800	2.540	.800	.180
1.250	3.000	1.250	.050
2.500	4.300	2.500	.000
5.000	6.220	5.000	.230
7.500	7.680	7.500	.600
10.000	8.870	10.000	1.150
15.000	10.490	15.000	2.340
20.000	11.500	20.000	3.330
25.000	12.040	25.000	4.100
30.000	12.180	30.000	4.580
40.000	11.780	40.000	4.900
50.000	10.670	50.000	4.760
60.000	9.080	60.000	4.260
70.000	7.140	70.000	3.470
80.000	4.980	80.000	2.410
90.000	2.720	90.000	1.250
100.000	.310	100.000	.000

Pfenninger Laminar 4910 L.E. radius 0.9 Percent

Chord Station XU	Upper Surface YU	Chord Station XL	Lower Surface YL
.000	.107	.000	.107
.200	.750	.200	-.397
.400	.930	.400	-.580
.600	1.060	.600	-.700
1.250	1.390	1.250	-.900
2.500	1.900	2.500	-1.400
5.000	2.567	5.000	-1.954
10.000	3.435	10.000	-2.720
15.000	4.040	15.000	-3.235
20.000	4.460	20.000	-3.840
30.000	5.110	30.000	-4.110
40.000	5.470	40.000	-4.310
50.000	5.560	50.000	-4.430
60.000	5.500	60.000	-4.275
70.000	5.020	70.000	-3.940
80.000	3.930	80.000	-3.290
85.000	3.090	85.000	-2.670
90.000	1.940	90.000	-1.926
92.500	1.334	95.000	1.440
95.000	.780	95.000	-.880
97.500	.406	97.500	-.310
100.000	.000	100.000	.000

Pfenninger Laminar 11 L.E. radius 0.8 Percent

Chord Station XU	Upper Surface YU	Chord Station XL	Lower Surface YL
.000	.000	.000	.000
.100	.530	.100	-.250
.200	.680	.200	-.400
.500	.890	.500	-.620
1.250	1.330	1.250	-.880
2.500	1.900	2.500	-1.150
5.000	2.850	5.000	-1.420
10.000	4.190	10.000	-1.740
20.000	5.810	20.000	-1.900
30.000	6.800	30.000	-1.820
40.000	7.230	40.000	-1.660
50.000	7.230	50.000	-1.420
60.000	6.920	60.000	-1.260
70.000	6.170	70.000	-.950
80.000	4.860	80.000	-.710
90.000	2.880	90.000	-.320
95.000	1.540	95.000	-.120
97.500	.870	97.500	.000
100.000	.000	100.000	.000

Pfenninger Laminar 4414
Le radius 1.9 Percent

Chord Station	Upper Surface	Chord Station	Lower Surface
XU	YU	XL	YL
.000	.300	.000	.300
.200	1.000	.200	-.600
.400	1.400	.400	-.930
.800	1.900	.800	-1.320
1.250	2.330	1.250	-1.560
2.500	3.240	2.500	-1.800
5.000	4.430	5.000	-2.240
10.000	6.000	10.000	-2.840
20.000	7.880	20.000	-3.800
30.000	8.920	30.000	-4.200
40.000	9.400	40.000	-4.360
50.000	9.360	50.000	-4.360
60.000	8.680	60.000	-4.160
70.000	7.360	70.000	-3.600
80.000	4.920	80.000	-2.840
90.000	1.400	90.000	-1.480
95.000	.400	95.000	-.680
100.000	.000	100.000	.000

Lindner Spinne

Chord Station	Upper Surface	Chord Station	Lower Surface
XU	YU	XL	YL
.000	1.090	.000	1.090
.200	1.660	.200	.600
.400	1.940	.400	.410
.600	2.140	.600	.290
.800	2.340	.800	.200
1.250	2.730	1.250	.090
2.500	3.520	2.500	.000
5.000	4.780	5.000	.200
7.500	5.620	7.500	.560
10.000	6.370	10.000	.850
15.000	7.360	15.000	1.520
20.000	8.050	20.000	2.130
30.000	8.650	30.000	2.970
40.000	8.680	40.000	3.640
50.000	8.200	50.000	3.880
60.000	7.320	60.000	3.820
70.000	6.080	70.000	3.400
80.000	4.580	80.000	2.810
90.000	2.670	90.000	1.520
100.000	.250	100.000	.000

Sawyer Cascade L.E. radius 0.666

Chord Station	Upper Surface	Chord Station	Lower Surface
XU	YU	XL	YL
.000	.414	.000	.000
1.000	1.642	1.000	-.580
2.000	2.429	2.000	-.718
3.000	3.078	3.000	-.738
4.000	3.671	4.000	-.718
5.000	4.224	5.000	-.676
7.500	5.480	7.500	-.400
10.000	6.625	10.000	-.110
15.000	8.585	15.000	.538
20.000	10.186	20.000	1.242
25.000	11.456	25.000	1.960
30.000	12.436	30.000	2.540
35.000	13.085	35.000	3.036
40.000	13.499	40.000	3.464
45.000	13.747	45.000	3.823
50.000	13.651	50.000	4.182
55.000	13.223	55.000	4.431
60.000	12.450	60.000	4.624
65.000	11.470	65.000	4.693
70.000	10.297	70.000	4.610
75.000	8.916	75.000	4.375
80.000	7.315	80.000	3.906
85.000	5.576	85.000	3.340
90.000	3.782	90.000	2.457
95.000	1.918	95.000	1.284
97.500	1.063	97.500	.594
100.000	.166	100.000	-.166

Hacklinger HA 12

Chord Station	Upper Surface	Chord Station	Lower Surface
XU	YU	XL	YL
.000	1.300	.000	1.300
.200	2.350	.200	.760
.400	2.740	.400	.500
.600	3.000	.600	.380
.800	3.240	.800	.280
1.250	3.700	1.250	.200
2.500	4.800	2.500	.150
5.000	5.750	5.000	.500
7.500	6.700	7.500	.950
10.000	7.500	10.000	1.450
15.000	8.500	15.000	2.350
20.000	9.150	20.000	3.100
30.000	9.550	30.000	4.200
40.000	9.450	40.000	4.950
50.000	8.750	50.000	5.350
60.000	7.650	60.000	5.150
70.000	6.350	70.000	4.400
80.000	4.550	80.000	3.250
90.000	2.700	90.000	1.750
100.000	.400	100.000	.000

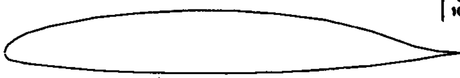

PFENNINGER LAMINAR 4414 LE RADIUS 1.9 PERCENT

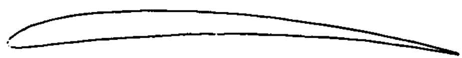

LINDNER SPINNE

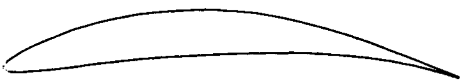

SAWYER CASCADE LE RADIUS 0.666

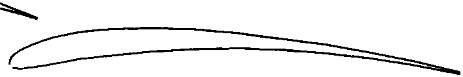

HACKLINGER HA 12

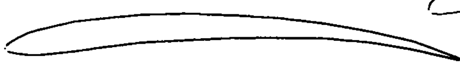

HACKLINGER HA 13

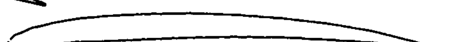

EPPLER 59

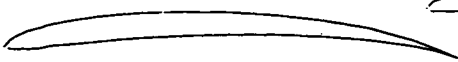

EPPLER 58

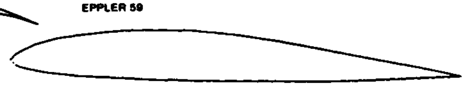

EPPLER 374

Hacklinger HA 13

Chord Station	Upper Surface	Chord Station	Lower Surface
XU	YU	XL	YL
.000	1.300	.000	1.300
.200	1.800	.200	.950
.400	2.050	.400	.800
.600	2.250	.600	.720
.800	2.430	.800	.630
1.250	2.800	1.250	.500
2.500	3.500	2.500	.250
5.000	4.800	5.000	.000
7.500	5.650	7.500	.000
10.000	6.200	10.000	.200
15.000	7.450	15.000	.950
20.000	8.100	20.000	1.600
30.000	9.300	30.000	3.100
40.000	9.700	40.000	3.700
50.000	9.450	50.000	4.300
60.000	8.850	60.000	4.500
70.000	7.750	70.000	4.400
80.000	6.100	80.000	3.700
90.000	3.900	90.000	2.200
100.000	.400	100.000	.000

Eppler 59

Chord Station	Upper Surface	Chord Station	Lower Surface
XU	YU	XL	YL
.000	2.000	.000	2.000
1.250	3.600	1.250	1.400
2.500	4.100	2.500	1.500
5.000	5.200	5.000	1.500
7.500	5.800	7.500	1.600
10.000	6.600	10.000	1.900
15.000	7.600	15.000	2.500
20.000	8.300	20.000	2.800
25.000	8.800	25.000	3.200
30.000	9.200	30.000	3.600
40.000	9.700	40.000	4.300
50.000	9.600	50.000	4.800
60.000	9.300	60.000	5.100
70.000	8.500	70.000	5.000
80.000	7.200	80.000	4.700
90.000	5.200	90.000	3.900
95.000	3.800	95.000	3.200
100.000	2.000	100.000	2.000

Eppler 58

Chord Station	Upper Surface	Chord Station	Lower Surface
XU	YU	XL	YL
.000	2.000	.000	2.000
1.250	3.500	1.250	1.500
2.500	4.400	2.500	1.500
5.000	5.600	5.000	1.600
7.500	6.300	7.500	1.800
10.000	7.200	10.000	2.400
15.000	8.300	15.000	2.900
20.000	9.200	20.000	3.600
25.000	9.800	25.000	4.200
30.000	10.300	30.000	4.700
40.000	10.800	40.000	5.500
50.000	10.900	50.000	6.000
60.000	10.500	60.000	6.200
70.000	9.700	70.000	6.100
80.000	8.200	80.000	5.600
90.000	5.700	90.000	4.500
95.000	4.000	95.000	3.500
100.000	2.000	100.000	2.000

Eppler 374

Chord Station	Upper Surface	Chord Station	Lower Surface
XU	YU	XL	YL
.000	.000	.000	.000
1.250	1.400	1.250	-1.100
2.500	2.200	2.500	-1.500
5.000	3.400	5.000	-2.000
7.500	4.200	7.500	-2.400
10.000	4.900	10.000	-2.700
15.000	5.900	15.000	-3.000
20.000	6.600	20.000	-3.100
25.000	7.200	25.000	-3.200
30.000	7.500	30.000	-3.300
40.000	7.700	40.000	-3.200
50.000	7.100	50.000	-2.900
60.000	6.000	60.000	-2.600
70.000	4.800	70.000	-2.200
80.000	3.100	80.000	-1.500
90.000	1.600	90.000	-.800
95.000	.900	95.000	-.400
100.000	.000	100.000	.000

Eppler 195 Aerodynamic Zero -3.05 Degrees

Chord Station XU	Upper Surface YU	Chord Station XL	Lower Surface YL
.000	.000	.000	.000
.008	.112	.196	-.498
.393	.860	.986	-1.043
1.228	1.719	2.295	-1.553
2.500	2.627	4.112	-1.998
4.198	3.549	6.422	-2.370
6.310	4.458	9.206	-2.663
8.817	5.332	12.441	-2.875
11.697	6.152	16.098	-3.008
14.922	6.901	20.140	-3.066
18.460	7.562	24.526	-3.053
22.276	8.121	29.209	-2.975
26.330	8.562	34.136	-2.832
30.580	8.864	39.260	-2.624
34.994	9.002	44.545	-2.361
39.550	8.966	49.935	-2.071
44.222	8.754	55.362	-1.775
48.985	8.373	60.754	-1.485
53.813	7.834	66.043	-1.210
58.686	7.169	71.158	-.960
63.559	6.427	76.043	-.738
68.368	5.647	80.605	-.548
73.046	4.858	84.809	-.391
77.529	4.083	88.590	-.267
81.763	3.340	91.895	-.167
85.658	2.646	94.685	-.083
89.185	2.014	96.935	-.017
92.280	1.448	98.607	.014
94.904	.948	99.646	.009
97.037	.527	100.000	.000
98.640	.220		
99.652	.050		
100.000	.000		

Eppler EC 86(-3) -914 Camber 4.5 percent at 70 Percent Chord

Chord Station XU	Upper Surface YU	Chord Station XL	Lower Surface YL
.000	.000	.000	.000
.170	1.060	.090	-.060
1.090	2.300	1.020	-.780
4.840	5.050	2.820	-1.680
10.890	7.570	5.300	-2.540
14.780	8.510	8.450	-3.290
19.290	9.280	12.160	-3.830
29.720	10.320	21.550	-4.090
35.470	10.590	33.140	-3.790
47.570	10.610	45.940	-3.090
59.770	9.940	58.850	-1.920
71.230	8.630	71.660	.230
81.340	6.730	84.210	1.860
93.030	2.890	94.510	1.520
98.030	.790	97,720	.750
100.000	.000	100.000	.000

122 Eppler 387

Chord Station XU	Upper Surface YU	Chord Station XL	Lower Surface YL
.000	2.000	.000	2.000
1.250	3.500	1.250	1.200
2.500	4.500	2.500	.800
5.000	5.600	5.000	.800
7.500	6.500	7.500	.500
10.000	7.200	10.000	.500
15.000	8.300	15.000	.500
20.000	9.200	20.000	.700
25.000	9.700	25.000	.800
30.000	10.100	30.000	1.000
40.000	10.200	40.000	1.400
50.000	9.500	50.000	1.700
60.000	8.200	60.000	2.000
70.000	6.800	70.000	2.200
80.000	5.200	80.000	2.300
90.000	3.600	90.000	2.300
95.000	2.800	95.000	2.200
100.000	2.000	100.000	2.000

Eppler 385

Chord Station XU	Upper Surface YU	Chord Station XL	Lower Surface YL
.000	2.000	.000	2.000
1.250	3.400	1.250	1.200
2.500	4.600	2.500	1.200
5.000	6.000	5.000	1.200
7.500	7.100	7.500	1.300
10.000	8.000	10.000	1.400
15.000	9.200	15.000	1.800
20.000	10.200	20.000	2.300
25.000	10.900	25.000	2.800
30.000	11.400	30.000	3.100
40.000	11.800	40.000	3.600
50.000	11.200	50.000	4.100
60.000	10.100	60.000	4.400
70.000	8.500	70.000	4.400
80.000	6.600	80.000	4.100
90.000	4.600	90.000	3.500
95.000	3.300	95.000	2.800
100.000	2.000	100.000	2.000

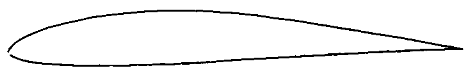

EPPLER 195 AERODYNAMIC ZERO -3.05 DEGREES

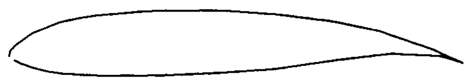

EPPLER EC 86(-3) -914 CAMBER 4.5 PERCENT AT 70 PERCENT CHORD

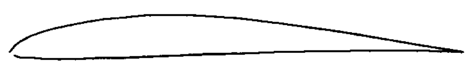

122 EPPLER 387

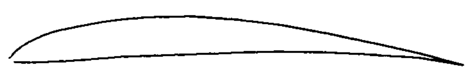

EPPLER 385

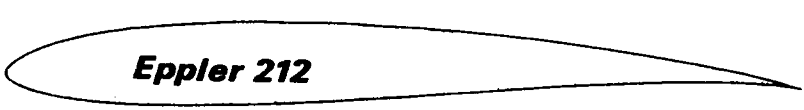

No.	1	2	3	4	5	6	7	8	9	10	11	12	13	14	15	16	17	18	19	20
X	99.68	98.76	97.35	95.47	93.12	90.32	87.09	83.47	79.53	75.28	70.80	66.11	61.28	56.36	51.38	46.42	41.50	36.69	32.02	27.55
Y	0.092	0.372	0.803	1.307	1.844	2.418	3.023	3.645	4.269	4.881	5.465	6.008	6.496	6.915	7.256	7.507	7.660	7.708	7.647	7.473

No.	21	22	23	24	25	26	27	28	29	30	31	32	33	34	35	36	37	38	39	40
X	23.30	19.33	15.65	12.31	9.327	6.729	4.534	2.758	1.410	0.499	0.032	0.122	0.800	1.984	3.648	5.780	8.363	11.38	14.81	18.62
Y	7.188	6.794	6.295	5.701	5.023	4.275	3.473	2.636	1.790	0.987	0.224	-0.398	-0.970	-1.532	-2.045	-2.486	-2.840	-3.087	-3.252	-3.301

No.	41	42	43	44	45	46	47	48	49	50	51	52	53	54	56	56	57	58	59	60
X	22.79	27.28	32.05	37.06	42.26	47.59	53.00	58.43	63.82	69.09	74.18	79.02	83.53	87.64	91.28	94.38	96.85	98.62	99.66	100.0
Y	-3.248	-3.099	-2.861	-2.548	-2.175	-1.759	-1.320	-0.878	-0.452	-0.063	0.271	0.535	0.713	0.794	0.776	0.659	0.458	0.231	0.061	00.00

Eppler 64

AIRFOIL 64 8.45% 2.00 8.00

V-DISTR. FOR THE ABOVE ALPHA REL. ZERO-LIFT LINE

N	X	Y	2.00	8.00
0	1.00000	0.00000	0.862	0.854
1	0.99679	0.00076	0.891	0.888
2	0.98761	0.00311	0.947	0.948
3	0.97324	0.00686	1.006	1.013
4	0.95409	0.01145	1.042	1.055
5	0.93022	0.01659	1.057	1.077
6	0.90185	0.02223	1.073	1.099
7	0.86942	0.02829	1.090	1.123
8	0.83336	0.03455	1.105	1.146
9	0.79408	0.04081	1.119	1.167
10	0.75200	0.04691	1.132	1.188
11	0.70756	0.05267	1.143	1.208
12	0.66122	0.05793	1.153	1.228
13	0.61344	0.06257	1.161	1.246
14	0.56469	0.06646	1.168	1.264
15	0.51543	0.06950	1.173	1.281
16	0.46615	0.07162	1.177	1.298
17	0.41731	0.07275	1.179	1.315
18	0.36938	0.07288	1.180	1.331
19	0.32280	0.07197	1.178	1.348
20	0.27803	0.07004	1.175	1.365
21	0.23547	0.06710	1.168	1.382
22	0.19553	0.06322	1.159	1.401
23	0.15858	0.05844	1.145	1.420
24	0.12494	0.05285	1.124	1.441
25	0.09490	0.04653	1.095	1.464
26	0.06872	0.03960	1.052	1.487
27	0.04658	0.03221	0.986	1.511
28	0.02863	0.02453	0.881	1.531
29	0.01496	0.01680	0.705	1.543
30	0.00560	0.00931	0.382	1.525
31	0.00056	0.00258	0.286	1.429
32	0.00075	-0.00255	1.503	0.752
33	0.00675	-0.00664	1.390	0.199
34	0.01818	-0.01038	1.318	0.529
35	0.03477	-0.01348	1.260	0.683
36	0.05640	-0.01582	1.215	0.766
37	0.08293	-0.01735	1.178	0.814
38	0.11415	-0.01810	1.146	0.843
39	0.14979	-0.01809	1.118	0.861
40	0.18954	-0.01740	1.093	0.872
41	0.23300	-0.01610	1.071	0.879
42	0.27973	-0.01431	1.051	0.882
43	0.32924	-0.01212	1.032	0.884
44	0.38098	-0.00965	1.015	0.883
45	0.43439	-0.00701	0.999	0.882
46	0.48884	-0.00434	0.984	0.879
47	0.54370	-0.00173	0.970	0.876
48	0.59831	0.00069	0.956	0.873
49	0.65199	0.00284	0.943	0.869
50	0.70409	0.00461	0.930	0.864
51	0.75392	0.00595	0.918	0.859
52	0.80082	0.00678	0.906	0.855
53	0.84416	0.00709	0.894	0.849
54	0.88331	0.00686	0.883	0.844
55	0.91770	0.00612	0.871	0.839
56	0.94675	0.00491	0.861	0.833
57	0.96990	0.00333	0.857	0.835
58	0.98661	0.00169	0.861	0.843
59	0.99665	0.00046	0.865	0.853
60	1.00000	0.00000	0.862	0.854

ALPHAO = 4.55 DEGREES CMO =-0.1222
ETA = 1.071

WARNING - SUBROUTINE SMOOTH HAS SLOPES
-0.380 AND-0.482 BETWEEN POINTS 32 AND 3

Eppler 65

AIRFOIL 65 8.86% 2.00 8.00

N	X	Y	2.00	8.00
0	1.00000	0.00000	0.879	0.871
1	0.99680	0.00070	0.899	0.895
2	0.98762	0.00289	0.949	0.951
3	0.97319	0.00639	1.005	1.012
4	0.95387	0.01066	1.035	1.048
5	0.92963	0.01543	1.042	1.061
6	0.90067	0.02079	1.051	1.077
7	0.86743	0.02675	1.063	1.095
8	0.83042	0.03321	1.076	1.116
9	0.79018	0.04006	1.092	1.139
10	0.74727	0.04713	1.110	1.166
11	0.70230	0.05421	1.130	1.195
12	0.65586	0.06106	1.152	1.227
13	0.60854	0.06739	1.176	1.262
14	0.56091	0.07288	1.201	1.300
15	0.51352	0.07697	1.229	1.342
16	0.46624	0.07915	1.222	1.348
17	0.41897	0.07974	1.215	1.354
18	0.37224	0.07905	1.206	1.361
19	0.32654	0.07718	1.197	1.369
20	0.28233	0.07422	1.185	1.377
21	0.24007	0.07024	1.171	1.385
22	0.20017	0.06536	1.154	1.395
23	0.16305	0.05966	1.133	1.405
24	0.12905	0.05326	1.106	1.417
25	0.09851	0.04627	1.070	1.430
26	0.07170	0.03886	1.022	1.444
27	0.04888	0.03119	0.954	1.461
28	0.03022	0.02343	0.852	1.480
29	0.01589	0.01583	0.686	1.502
30	0.00600	0.00865	0.381	1.519
31	0.00061	0.00241	0.304	1.519
32	0.00079	-0.00234	1.504	0.752
33	0.00693	-0.00629	1.390	0.199
34	0.01838	-0.00993	1.318	0.530
35	0.03500	-0.01295	1.260	0.683
36	0.05664	-0.01522	1.216	0.766
37	0.08317	-0.01670	1.178	0.814
38	0.11439	-0.01741	1.146	0.843
39	0.15004	-0.01736	1.118	0.861
40	0.18979	-0.01664	1.094	0.873
41	0.23325	-0.01533	1.071	0.879
42	0.27999	-0.01352	1.051	0.883
43	0.32950	-0.01131	1.033	0.884
44	0.38126	-0.00884	1.016	0.884
45	0.43467	-0.00621	0.999	0.882
46	0.48912	-0.00354	0.984	0.880
47	0.54399	-0.00095	0.970	0.876
48	0.59861	0.00145	0.956	0.873
49	0.65230	0.00357	0.943	0.869
50	0.70440	0.00531	0.930	0.864
51	0.75424	0.00661	0.918	0.860
52	0.80115	0.00740	0.906	0.855
53	0.84450	0.00765	0.894	0.850
54	0.88365	0.00736	0.883	0.844
55	0.91803	0.00654	0.872	0.839
56	0.94709	0.00522	0.861	0.834
57	0.97019	0.00350	0.860	0.837
58	0.98680	0.00175	0.870	0.852
59	0.99671	0.00046	0.880	0.867
60	1.00000	0.00000	0.879	0.871

ALPHAO = 4.56 DEGREES CMO =-0.1205
ETA = 1.072

WARNING - SUBROUTINE SMOOTH HAS SLOPES
-0.406 AND-0.491 BETWEEN POINTS 32 AND

	EPPLER 205 PROFIL E 205 10.48%		EPPLER 207 PROFIL E 207 12.04%		EPPLER 209 PROFIL E209 13.78%	
N	X	Y	X	Y	X	Y
0	100.000	0.000	100.000	0.000	100.000	0.000
1	99.655	.039	99.647	.045	99.639	.052
2	98.649	.174	98.625	.202	98.600	.232
3	97.049	.427	97.011	.489	96.969	.557
4	94.916	.778	94.870	.881	94.821	.992
5	92.285	1.196	92.238	1.337	92.187	1.488
6	89.175	1.668	89.128	1.841	89.077	2.027
7	85.624	2.199	85.576	2.400	85.523	2.615
8	81.684	2.786	81.633	3.011	81.577	3.253
9	77.412	3.419	77.357	3.666	77.295	3.930
10	72.866	4.088	72.806	4.352	72.738	4.634
11	68.108	4.777	68.043	5.055	67.968	5.352
12	63.204	5.470	63.132	5.759	63.049	6.065
13	58.218	6.147	58.139	6.441	58.047	6.753
14	53.217	6.782	53.129	7.079	53.028	7.393
15	48.265	7.342	48.169	7.638	48.058	7.949
16	43.410	7.785	43.306	8.075	43.185	8.380
17	38.680	8.081	38.567	8.362	38.436	8.657
18	34.101	8.214	33.981	8.483	33.841	8.764
19	29.699	8.177	29.573	8.430	29.424	8.694
20	25.496	7.970	25.363	8.205	25.208	8.448
21	21.508	7.606	21.371	7.819	21.211	8.037
22	17.764	7.111	17.626	7.300	17.461	7.490
23	14.302	6.507	14.162	6.669	13.997	6.830
24	11.157	5.811	11.018	5.944	10.854	6.073
25	8.360	5.040	8.225	5.143	8.065	5.237
26	5.937	4.211	5.808	4.282	5.656	4.341
27	3.909	3.344	3.791	3.383	3.651	3.406
28	2.292	2.461	2.189	2.468	2.066	2.454
29	1.097	1.589	1.015	1.565	.916	1.517
30	.331	.766	.279	.714	.216	.635
31	.002	.055	.000	−.015	.007	−.106
32	.233	−.506	.304	−.626	.398	−.775
33	1.065	−.988	1.212	−1.204	1.379	−1.467
34	2.419	−1.420	2.628	−1.750	2.852	−2.140
35	4.291	−1.776	4.543	−2.234	4.804	−2.765
36	6.669	−2.053	6.943	−2.649	7.219	−3.329
37	9.534	−2.252	9.807	−2.991	10.073	−3.821
38	12.864	−2.378	13.109	−3.257	13.340	−4.233
39	16.627	−2.436	16.817	−3.448	16.986	−4.561
40	20.783	−2.435	20.893	−565	20.974	−4.799
41	25.290	−2.384	25.292	−3.611	25.258	−4.943
42	30.097	−2.292	29.966	−3.586	29.793	−4.985
43	35.149	−2.168	34.861	−3.487	34.524	−4.909
44	40.388	−2.021	39.937	−3.302	39.430	−4.683
45	45.751	−1.859	45.165	−3.044	44.516	−4.322
46	51.174	−1.689	50.495	−2.744	49.749	−3.884
47	56.591	−1.516	55.860	−2.425	55.057	−3.409
48	61.938	−1.345	61.189	−2.102	60.368	−2.923
49	67.149	−1.180	66.414	−1.787	65.609	−2.446
50	72.160	−1.023	71.467	−1.488	70.708	−1.993
51	76.911	−.876	76.283	−1.212	75.594	−1.576
52	81.343	−.740	80.796	−.963	80.197	−1.205
53	85.400	−.614	84.948	−.744	84.451	−.884
54	89.034	−.380	91.942	−.390	91.665	−.400
55	92.195	−.380	91.942	−.390	91.665	−.400
56	94.860	−.252	94.699	−.239	94.522	−.222
57	97.017	−.125	96.930	−.108	96.834	−.089
58	98.635	−.036	98.598	−.026	98.558	−.014
59	99.651	−.003	99.643	−.000	99.633	.003
60	100.000	.000	100.000	.000	100.000	−.000

EPPLER 205: CM = −.0460 β = 2.37°

EPPLER 207: CM = −.0499 β = 2.33°

EPPLER 209: CM = −.0547 β = 2.28°

Eppler 203 Aerodynamic Zero -3.31 Degrees

Chord Station XU	Upper Surface YU	Chord Station XL	Lower Surface YL
.000	.000	.000	.000
.002	.054	.258	-.623
.344	.825	1.115	-1.293
1.162	1.713	2.471	-1.951
2.427	2.650	4.311	-2.562
4.128	3.600	6.616	-3.111
6.250	4.534	9.366	-3.586
8.772	5.432	12.534	-3.977
11.671	6.273	16.091	-4.279
14.920	7.041	19.999	-4.487
18.486	7.718	24.218	-4.596
22.332	8.291	28.702	-4.600
26.419	8.744	33.398	-4.482
30.704	9.056	38.286	-4.206
35.154	9.204	43.378	-3.797
39.748	9.176	48.643	-3.312
44.460	8.974	54.007	-2.800
49.264	8.605	59.395	-2.288
54.130	8.088	64.730	-1.799
59.028	7.453	69.937	-1.350
63.910	6.742	74.940	-.953
68.712	5.989	79.665	-.620
73.369	5.218	84.043	-.353
77.819	4.451	88.005	-.156
82.000	3.705	91.489	-.024
85.854	2.995	94.441	.051
89.325	2.333	96.813	.076
92.361	1.723	98.561	.060
94.932	1.158	99.636	.021
97.030	.660	100.000	.000
98.625	.282		
99.645	.066		
100.000	.000		

Eppler 201 Aerodynamic Zero -3.34 Degrees

Chord Station XU	Upper Surface YU	Chord Station XL	Lower Surface YL
.000	.000	.000	.000
.011	.128	.187	-.488
.407	.875	.964	-1.046
1.258	1.730	2.258	-1.575
2.547	2.632	4.055	-2.041
4.264	3.544	6.341	-2.438
6.396	4.443	9.097	-2.756
8.925	5.305	12.298	-2.993
11.828	6.112	15.916	-3.149
15.078	6.847	19.915	-3.227
18.642	7.496	24.253	-3.229
22.484	8.042	28.883	-3.157
26.565	8.471	33.753	-3.010
30.843	8.763	38.823	-2.777
35.285	8.895	44.069	-2.471
39.870	8.856	49.439	-2.131
44.572	8.644	54.864	-1.783
49.365	8.271	60.272	-1.444
54.222	7.753	65.591	-1.126
59.110	7.122,	70.749	-.839
63.984	6.418	75.676	-.591
68.777	5.677	80.305	-.386
73.427	4.923	84.572	-.225
77.871	4.176	88.416	-.107
82.048	3.464	91.782	-.027
85.899	2.771	94.625	.025
89.369	2.141	96.912	.051
92.406	1.565	98.602	.046
94.977	1.042	99.646	.017
97.069	.589	100.000	.000
98.650	.250		
99.652	.058		
100.000	.000		

Eppler 197 Aerodynamic Zero -2.7 Degrees

Chord Station XU	Upper Surface YU	Chord Station XL	Lower Surface YL
.000	.000	.000	-.200
.318	.789	.279	-.640
1.104	1.683	1.164	-1.278
2.335	2.633	2.556	-1.893
3.996	3.600	4.438	-2.454
6.075	4.556	6.797	-2.945
8.551	5.478	9.610	-3.365
11.402	6.345	12.852	-3.706
14.599	7.139	16.493	-3.955
18.112	7.844	20.495	-4.125
21.902	8.442	24.818	-4.195
25.933	8.918	29.414	-4.185
30.159	9.250	34.231	-4.085
34.551	9.413	39.236	-3.855
39.085	9.394	44.415	-3.535
43.736	9.191	49.723	-3.166
48.474	8.806	55.091	-2.765
53.282	8.246	60.447	-2.366
58.146	7.542	65.718	-1.965
63.028	6.752	70.834	-1.595
67.860	5.920	75.725	-1.266
72.576	5.079	80.323	-.965
77.105	4.254	84.564	-.715
81.384	3.466	88.388	-.506
85.349	2.733	91.738	-.325
88.939	2.068	94.572	-.185
92.096	1.478	96.864	-.075
94.778	.960	98.572	-.009
96.960	.530	99.637	-.006
98.604	.219	100.000	.000
99.642	.050		
100.000	.000		

Eppler 193 Aerodynamic Zero -3.39 degrees

Chord Station XU	Upper Surface YU	Chord Station XL	Lower Surface YL
.000	.000	.000	.000
.026	.190	.129	-.375
.465	.915	.819	-.838
1.344	1.740	2.044	-1.252
2.652	2.608	3.791	-1.588
4.383	3.487	6.049	-1.841
6.525	4.352	8.801	-2.010
9.061	5.181	12.026	-2.098
11.967	5.957	15.697	-2.112
15.218	6.663	19.778	-2.061
18.780	7.284	24.227	-1.955
22.620	7.805	28.998	-1.807
26.696	8.213	34.035	-1.628
30.967	8.487	39.280	-1.430
35.402	8.603	44.672	-1.244
39.979	8.551	50.145	-1.019
44.673	8.332	55.630	-.824
49.458	7.954	61.059	-.645
54.306	7.436	66.384	-.486
59.186	6.808	71.479	-.350
64.052	6.112	76.339	-.239
68.839	5.381	80.882	-.153
73.484	4.642	85.050	-.091
77.923	3.914	88.788	-.048
82.096	3.214	92.048	-.018
85.945	2.558	94.794	.010
89.414	1.957	97.003	.032
92.452	1.415	98.640	.034
95.023	.932	99.655	.014
97.108	.522	100.000	.000
98.674	.220		
99.661	.051		
100.000	.000		

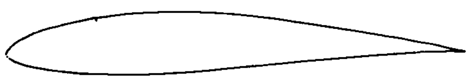

EPPLER 203 AERODYNAMIC ZERO -3.31 DEGREES

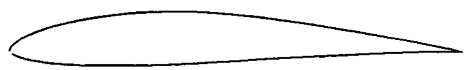

EPPLER 201 AERODYNAMIC ZERO -3.34 DEGREES

Wortmann FX 60-1261

Chord Station XU	Upper Surface YU	Chord Station XL	Lower Surface YL
.000	.000	.000	.000
.102	.359	.102	-.472
.422	1.279	.422	-.675
.960	2.086	.960	-.983
1.702	2.856	1.702	-1.308
2.650	3.545	2.650	-1.710
3.802	4.307	3.802	-2.017
5.158	4.962	5.158	-2.342
6.694	5.636	6.694	-2.594
8.422	6.224	8.422	-2.852
10.330	6.815	10.330	-3.042
12.403	7.331	12.403	-3.220
14.643	7.835	14.643	-3.327
17.037	8.260	17.037	-3.412
19.558	8.663	19.558	-3.426
22.221	8.962	22.221	-3.409
24.998	9.227	24.998	-3.319
27.891	9.405	27.891	-3.191
30.861	9.533	30.861	-2.992
33.933	9.577	33.933	-2.752
37.056	9.567	37.056	-2.449
40.243	9.478	40.243	-2.117
43.469	9.337	43.469	-1.746
46.733	9.122	46.733	-1.371
49.997	8.862	49.997	-.985
53.274	8.542	53.274	-.614
56.525	8.183	56.525	-.253
59.750	7.774	59.750	.072
62.938	7.334	62.938	.365
66.074	6.854	66.074	.609
69.133	6.354	69.133	.815
72.115	5.829	72.115	.978
74.995	5.295	74.995	1.106
77.773	4.759	77.773	1.190
80.435	4.237	80.435	1.236
82.970	3.739	82.970	1.239
87.590	2.830	87.590	1.146
89.644	2.427	89.644	1.060
91.571	2.064	91.571	.955
93.299	1.707	93.299	.836
94.848	.1381	94.848	.706
96.192	1.072	96.192	.568
97.344	.784	97.344	.427
98.291	.528	98.291	.292
99.034	.323	99.034	.182
99.571	.161	99.571	.089
99.891	.052	99.891	.021
100.000	.000	100.000	.000

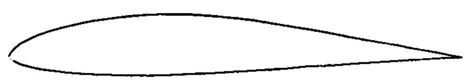

EPPLER 197 AERODYNAMIC ZERO -2.7 DEGREES

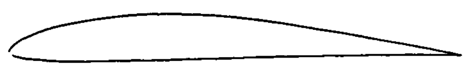

EPPLER 193 AERODYNAMIC ZERO -3.39 DEGREES

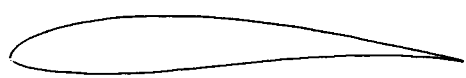

WORTMANN FX 60-1261

Wortmann FX 60-126
Camber 3.6 Percent

Chord Station XU	Upper Surface YU	Chord Station XL	Lower Surface YL
.000	.000	.000	.000
.102	.675	.102	-.301
.422	1.349	.422	-.641
.960	2.096	.960	-1.012
1.702	2.802	1.702	-1.404
2.650	3.493	2.650	-1.792
3.802	4.174	3.802	-2.132
5.158	4.808	5.158	-2.482
6.694	5.457	6.694	-2.761
8.422	6.021	8.422	-3.045
10.330	6.585	10.330	-3.262
12.403	7.077	12.403	-3.465
14.643	7.555	14.643	-3.598
17.037	7.958	17.037	-3.707
19.558	8.327	19.558	-3.746
22.221	8.615	22.221	-3.751
24.998	8.859	24.998	-3.683
27.891	9.019	27.891	-3.574
30.861	9.130	30.861	-3.392
33.933	9.160	33.933	-3.167
37.056	9.138	37.056	-2.877
40.243	9.041	40.243	-2.553
43.469	8.893	43.469	-2.188
46.733	8.679	46.733	-1.814
49.997	8.425	49.997	-1.421
53.274	8..118	53.274	-1.036
56.525	7..781	56.525	-.653
59.750	7.402	59.750	-.298
62.938	6.994	62.938	.029
66.074	6.549	66.074	.307
69.133	6.082	69.133	.547
72.115	5.589	72.115	.741
74.995	5.084	74.995	.897
77.773	4.567	77.773	1.006
80.435	4.055	80.435	1.073
82.970	3.552	82.970	1.093
87.590	2.611	87.590	1.022
89.644	2.181	89.644	.944
91.571	1.777	91.571	.845
93.299	1.412	93.299	.732
94.848	1.084	94.848	.610
96.192	.798	96.192	.483
97.344	.554	97.344	.357
98.291	.353	98.291	.239
99.034	.198	99.034	.146
99.571	.088	99.571	.068
99.891	.024	99.891	.014
100.000	.000	100.000	.000

Wortmann FX 61-163
Camber 2.6 Percent

Chord Station XU	Upper Surface YU	Chord Station XL	Lower Surface YL
.000	.000	.000	.000
.102	.566	.102	-.248
.422	1.234	.422	-.560
.960	1.925	.960	-.907
1.702	2.641	1.702	-1.272
2.650	3.402	2.650	-1.656
3.802	4.175	3.802	-2.027
5.158	4.929	5.158	-2.412
6.694	5.687	6.694	-2.786
8.422	6.412	8.422	-3.160
10.330	7.109	10.330	-3.518
12.403	7.760	12.403	-3.870
14.643	8.371	14.643	-4.199
17.037	8.924	17.037	-4.511
19.558	9.422	19.558	-4.792
22.221	9.844	22.221	-5.044
24.998	10.194	24.998	-5.252
27.891	10.455	27.891	-5.421
30.861	10.635	30.861	-5.537
33.933	10.723	33.933	-5.609
37.056	10.728	37.056	-5.625
40.243	10.639	40.243	-5.585
43.469	10.457	43.469	-5.474
46.733	10.168	46.733	-5.293
49.997	9.780	49.997	-5.039
53.274	9.303	53.274	-4.719
56.525	8.772	56.525	-4.324
59.750	8.208	59.750	-3.845
62.938	7.637	62.938	-3.288
66.074	7.064	66.074	-2.635
69.133	6.497	69.133	-2.079
72.115	5.935	72.115	-1.517
74.995	5.388	74.996	-1.014
77.773	4.856	77.773	-.576
80.435	4.347	80.435	-.201
82.970	3.861	82.970	.110
85.350	3.403	85.350	.358
87.590	2.968	87.590	.542
89.644	2.560	89.644	.667
91.571	2.176	91.571	.734
93.299	1.817	93.299	.749
94.848	1.481	94.848	.715
96.192	1.167	96.192	.637
97.344	.875	97.344	.526
98.291	.610	98.291	.392
99.034	.390	99.034	.273
99.571	.206	99.571	.150
99.891	.069	99.891	.044
100.000	.000	100.000	.000

Wortmann FX 67-K-150 For
17.0 Percent flap

Chord Station XU	Upper Surface YU	Chord Station XL	Lower Surface YL
.000	.000	.000	.000
.107	.462	.107	-.145
.428	.989	.428	-.375
.961	1.566	.961	-.607
1.704	2.284	1.704	-.804
2.653	2.992	2.653	-1.015
3.806	3.752	3.806	-1.224
5.156	4.536	5.156	-1.422
6.699	5.327	6.699	-1.661
8.427	6.110	8.427	-1.788
10.332	6.882	10.332	-1.955
12.408	7.629	12.408	-2.107
14.645	8.348	14.645	-2.246
17.003	9.027	17.003	-2.368
19.562	9.663	19.562	-2.474
22.221	10.246	22.221	-2.562
25.000	10.771	25.000	-2.632
27.886	11.230	27.886	-2.684
30.866	11.619	30.866	-2.717
33.928	11.928	33.928	-2.730
37.059	12.152	37.059	-2.724
40.245	12.285	40.245	-2.698
43.474	12.318	43.474	-2.653
46.730	12.239	46.730	-2.588
50.000	12.041	50.000	-2.504
53.270	11.716	53.270	-2.399
56.526	11.269	56.526	-2.274
59.755	10.702	59.755	-2.130
62.941	10.025	62.941	-1.967
66.072	9.249	66.072	-1.784
69.134	8.395	69.134	-1.575
72.114	7.490	72.114	-1.339
75.000	6.570	75.000	-1.080
77.779	5.670	77.779	-.813
80.438	4.827	80.438	-.559
82.967	4.065	82.967	-.334
85.355	3.394	85.355	-.148
87.592	2.809	87.592	-.006
91.573	1.856	91.573	.157
94.844	1.130	94.844	.193
97.347	.599	97.347	.142
99.039	.233	99.039	.060
99.893	.026	99.893	.007
100.000	.000	100.000	.000

Wortmann FX 63-137 MPA
Camber 5.9 Percent

Chord Station XU	Upper Surface YU	Chord Station XL	Lower Surface YL
.000	.000	.000	.000
.102	1.012	.102	-.232
.422	2.077	.422	-.566
.960	2.740	.960	-.996
1.702	3.625	1.702	-1.254
2.650	4.471	2.650	-1.537
3.802	5.248	3.802	-1.698
5.158	6.005	5.158	-1.887
6.694	6.836	6.694	-1.992
8.422	7.566	8.422	-2.122
10.330	8.313	10.330	-2.180
12.403	8.961	12.403	-2.256
14.643	9.622	14.643	-2.263
17.037	10.165	17.037	-2.277
19.558	10.704	19.558	-2.220
22.221	11.122	22.221	-2.161
24.998	11.522	24.998	-2.034
27.891	11.792	27.891	-1.895
30.861	12.024	30.861	-1.688
33.933	12.128	33.933	-1.460
37.056	12.191	37.056	-1.167
40.243	12.137	40.243	-.848
43.469	12.042	43.469	-.486
46.733	11.833	46.733	-.103
49.997	11.578	49.997	.307
53.274	11.221	53.274	.716
56.525	10.823	56.525	1.112
59.750	10.331	59.750	1.475
62.938	9.804	62.938	1.813
66.074	9.204	66.074	2.098
69.133	8.590	69.133	2.343
72.115	7.927	72.115	2.530
74.995	7.273	74.995	2.668
77.773	6.606	77.773	2.745
80.435	5.962	80.435	2.768
82.970	5.323	82.970	2.729
87.590	4.114	87.590	2.479
89.644	3.553	89.644	2.284
91.571	3.018	91.571	2.052
93.299	2.516	93.299	1.794
94.848	2.043	94.848	1.514
96.192	1.601	96.192	1.219
97.344	1.189	97.344	.921
98.291	.818	98.291	.630
99.034	.501	99.034	.373
99.571	.249	99.571	.169
99.891	.082	99.891	.040
100.000	.000	100.000	.000

Wortmann M2

Chord Station XU	Upper Surface YU	Chord Station XL	Lower Surface YL
.000	.000	.000	.000
.102	.968	.102	-.960
.422	1.774	.422	-.454
.960	2.073	.960	-.907
1.702	3.519	1.702	-.727
2.650	4.009	2.650	-.932
3.802	5.202	3.802	-.662
5.158	5.706	5.158	-.749
6.694	6.656	6.694	-.443
8.422	7.061	8.422	-.453
10.330	7.739	10.330	-.145
12.430	7.977	12.430	-.117
14.643	8.421	14.643	.170
17.037	8.506	17.037	.204
19.558	8.750	19.558	.442
22.221	8.719	22.221	.473
24.998	8.809	24.998	.694
27.891	8.680	27.891	.731
30.861	8.660	30.861	.919
33.933	8.437	33.933	.960
37.056	8.306	37.056	1.110
40.243	8.026	40.243	1.131
43.469	7.822	43.469	1.260
46.733	7.493	46.733	1.272
49.997	7.228	49.997	1.370
53.274	6.865	53.274	1.371
56.525	6.561	56.526	1.444
59.750	6.182	59.750	1.434
62.938	5.858	62.938	1.478
66.074	5.471	66.074	1.456
69.133	5.128	69.133	1.473
72.115	4.737	72.115	1.438
74.995	4.381	74.995	1.424
77.773	3.993	77.773	1.356
80.435	3.625	80.435	1.302
82.970	3.239	82.970	1.217
85.350	2.872	85.350	1.144
87.590	2.499	87.590	1.048
89.664	2.146	89.664	.959
91.571	1.802	91.571	.851
93.299	1.482	93.299	.746
94.848	1.176	94.848	.631
96.192	.894	96.192	.516
97.344	.632	97.344	.391
98.291	.406	98.291	.268
99.034	.227	99.034	.160
99.571	.097	99.571	.073
99.891	.024	99.891	.020
100.000	.000	100.000	.000

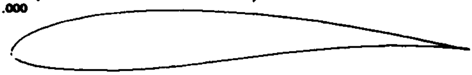

WORTMANN FX 60-126 CAMBER 3.6 PERCENT

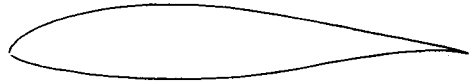

WORTMANN FX 61-163 CAMBER 2.6 PERCENT

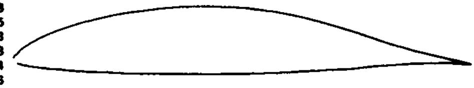

WORTMANN FX 67-K-150 FOR 17.0 PERCENT FLAP

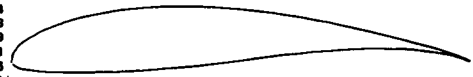

WORTMANN FX 63-137 MPA CAMBER 5.9 PERCENT

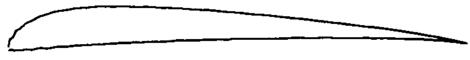

WORTMANN M2

Wortmann FX 38-153
Camber 2.1 Percent

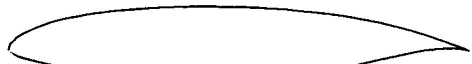

WORTMANN FX 38-153 CAMBER 2.1 PERCENT

Chord Station XU	Upper Surface YU	Chord Station XL	Lower Surface YL
.000	.000	.000	.000
.102	.645	.102	-.245
.422	1.349	.422	-.519
.960	1.914	.960	-.910
1.702	2.630	1.702	-1.228
2.650	3.270	2.650	-1.629
3.802	3.975	3.802	-1.962
5.158	4.611	5.158	-2.348
6.694	5.266	6.694	-2.687
8.422	5.846	8.422	-3.063
10.330	6.424	10.330	-3.386
12.403	6.929	12.403	-3.735
14.643	7.426	14.643	-4.034
17.037	7.853	17.037	-4.345
19.558	8.266	19.558	-4.610
22.221	8.611	22.221	-4.871
24.998	8.932	24.998	-5.088
27.891	9.182	27.891	-5.303
30.861	9.402	30.861	-5.466
33.933	9.551	33.933	-5.618
37.056	9.670	37.056	-5.712
40.243	9.718	40.243	-5.785
43.469	9.739	43.469	-5.803
46.733	9.695	46.733	-5.796
49.997	9.618	49.997	-5.727
53.274	9.482	53.274	-5.622
56.525	9.311	56.525	-5.458
59.750	9.083	59.750	-5.254
62.938	8.821	62.938	-4.979
66.074	8.503	66.074	-4.640
69.133	8.148	69.133	-4.214
72.115	7.732	72.115	-3.716
74.995	7.272	74.995	-3.141
77.773	6.759	77.773	-2.535
80.435	6.203	80.435	-1.926
82.970	5.596	82.970	-1.354
85.350	4.958	85.350	-.836
87.590	4.291	87.590	-.406
89.644	3.628	89.644	-.059
91.571	2.988	91.571	.203
93.299	2.395	93.299	.381
94.848	1.856	94.848	.479
96.192	1.383	96.192	.503
97.344	.970	97.344	.461
98.291	.624	98.291	.371
99.034	.354	99.034	.259
99.571	.159	99.571	.142
99.891	.042	99.891	.051
100.000	.000	100.000	.000

WORTMANN FX 62-K-131 FOR 171 PERCENT FLAP

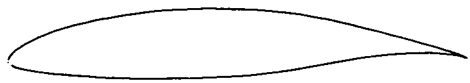

WORTMANN FX 62-K-153 FOR 20.0 PERCENT FLAP

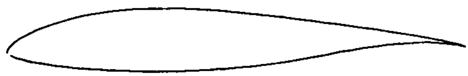

WORTMANN FX 61-140

WORTMANN FX 61-147

Wortmann FX 62-K-131
For 17 Percent Flap

Chord Station XU	Upper Surface YU	Chord Station XL	Lower Surface YL
.000	.000	.000	.000
.102	.516	.102	-.159
.422	1.037	.422	-.386
.960	1.606	.960	-.613
1.702	2.207	1.702	-.837
2.650	2.855	2.650	-1.061
3.802	3.511	3.802	-1.282
5.158	4.175	5.158	-1.486
6.694	4.830	6.694	-1.682
8.422	5.477	8.422	-1.862
10.330	6.108	10.330	-2.037
12.403	6.721	12.403	-2.195
14.643	7.306	14.643	-2.345
17.037	7.859	17.037	-2.476
19.558	8.369	19.558	-2.596
22.221	8.829	22.221	-2.696
24.998	9.232	24.998	-2.776
27.891	9.577	27.891	-2.828
30.861	9.860	30.861	-2.853
33.933	10.084	33.933	-2.846
37.056	10.245	37.056	-2.814
40.243	10.337	40.243	-2.752
43.469	10.355	43.469	-2.686
46.733	10.300	46.733	-2.548
49.997	10.173	49.997	-2.395
53.274	9.983	53.274	-2.199
56.525	9.728	56.525	-1.962
59.750	9.402	59.750	-1.683
62.938	9.000	62.938	-1.370
66.074	8.523	66.074	-1.025
69.133	7.976	69.133	-.646
72.115	7.374	72.115	-.239
74.995	6.732	74.995	.177
77.773	6.076	77.773	.573
80.435	5.425	80.435	.919
82.970	4.797	82.970	1.191
85.350	4.203	85.350	1.386
87.590	3.645	87.590	1.503
89.644	3.123	89.644	1.548
91.571	2.637	91.571	1.523
93.299	2.183	93.299	1.437
94.848	1.759	94.848	1.293
96.192	1.363	96.192	1.102
97.344	.994	97.344	.876
98.291	.661	98.291	.636
99.034	.394	99.034	.427
99.571	.180	99.571	.228
99.891	.034	99.891	.062
100.000	.000	100.000	.000

Wortmann FX 62-K-153
For 20.0 Percent Flap

Chord Station XU	Upper Surface YU	Chord Station XL	Lower Surface YL
.000	.000	.000	.000
.102	.711	.102	-.166
.422	1.325	.422	-.478
.960	1.974	.960	-.785
1.702	2.643	1.702	-1.082
2.650	3.344	2.650	-1.371
3.802	4.049	3.802	-1.645
5.158	4.755	5.158	-1.903
6.694	5.453	6.694	-2.149
8.422	6.142	8.422	-2.385
10.330	6.815	10.300	-2.611
12.403	7.467	12.403	-2.826
14.643	8.090	14.643	-3.026
17.037	8.688	17.037	-3.212
19.558	9.220	19.558	-3.382
22.221	9.712	22.221	-3.533
24.998	10.156	24.998	-3.660
27.891	10.546	27.891	-3.763
30.861	10.879	30.861	-3.833
33.933	11.151	33.933	-3.870
37.056	11.331	37.056	-3.868
40.243	11.448	40.243	-3.825
43.469	11.494	43.469	-3.734
46.733	11.463	46.733	-3.592
49.997	11.356	49.997	-3.390
53.274	11.167	53.274	-3.126
56.525	10.899	56.525	-2.797
59.750	10.548	59.750	-2.404
62.938	10.111	62.938	-1.947
66.074	9.584	66.074	-1.443
69.133	8.968	69.133	-.914
72.115	8.278	72.115	-.399
74.995	7.541	74.995	.068
77.773	6.790	77.773	.460
80.435	6.053	80.435	.772
82.970	5.343	82.970	1.004
85.350	4.669	85.350	1.164
87.590	4.034	87.590	1.256
89.644	3.442	89.644	1.284
91.571	2.890	91.571	1.257
93.299	2.382	93.299	1.181
94.848	1.915	94.848	1.060
96.192	1.488	96.192	.903
97.344	1.100	97.344	.719
98.291	.755	98.291	.522
99.034	.471	99.034	.350
99.571	.240	99.571	.186
99.891	.073	99.891	.061
100.000	.000	100.000	.000

Wortmann FX 61-140

Chord Station XU	Upper Surface YU	Chord Station XL	Lower Surface YL
.000	.000	.000	.000
.102	.504	.102	-.198
.422	1.072	.422	-.491
.960	1.678	.960	-.804
1.702	2.314	1.702	-1.122
2.650	2.988	2.650	-1.454
3.802	3.684	3.802	-1.778
5.158	4.378	5.158	-2.098
6.694	5.070	6.694	-2.413
8.422	5.742	8.422	-2.721
10.330	6.393	10.330	-3.016
12.403	7.006	12.403	-3.294
14.643	7.575	14.643	-3.553
17.037	8.081	17.037	-3.788
19.558	8.521	19.558	-3.996
22.221	8.877	22.221	-4.176
24.998	9.152	24.998	-4.324
27.891	9.336	27.891	-4.435
30.861	9.435	30.861	-4.509
33.933	9.444	33.933	-4.539
37.056	9.368	37.066	-4.524
40.243	9.211	40.243	-4.459
43.469	8.986	43.469	-4.344
46.733	8.704	46.733	-4.167
49.997	8.376	49.997	-3.935
53.274	8.014	53.274	-3.643
56.525	7.622	56.525	-3.297
59.750	7.207	59.750	-2.887
62.938	6.778	62.938	-2.415
66.074	6.338	66.074	-1.890
69.133	5.893	69.133	-1.344
72.115	5.446	72.115	-.810
74.995	5.000	74.995	-.326
77.773	4.561	77.773	.094
80.435	4.130	80.435	.438
82.970	3.709	82.970	.710
85.350	3.302	85.350	.905
87.590	2.909	87.590	1.031
89.644	2.532	89.644	1.090
91.571	2.173	91.571	1.091
93.299	1.881	93.299	1.038
94.848	1.505	94.848	.939
96.192	1.194	96.192	.798
97.344	.897	97.344	.628
98.291	.622	98.291	.445
99.034	.394	99.034	.291
99.571	.201	99.571	.146
99.891	.068	99.891	.030
100.000	.000	100.000	.000

Wortmann FX 61-147

Chord Station XU	Upper Surface YU	Chord Station XL	Lower Surface YL
.000	.000	.000	.000
.102	.688	.102	-.166
.422	1.322	.422	-.475
.960	1.996	.960	-.789
1.702	2.698	1.702	-1.099
2.650	3.440	2.650	-1.409
3.802	4.204	3.802	-1.708
5.158	4.965	5.158	-2.001
6.694	5.721	6.694	-2.288
8.422	6.455	8.422	-2.570
10.330	7.165	10.330	-2.839
12.403	7.831	12.403	-3.093
14.643	8.453	14.643	-3.327
17.037	9.006	17.037	-3.542
19.558	9.489	19.558	-3.730
22.221	9.883	22.221	-3.892
24.998	10.194	24.998	-4.023
27.891	10.410	27.891	-4.120
30.861	10.537	30.861	-4.180
33.933	10.567	33.933	-4.199
37.066	10.511	37.056	-4.174
40.243	10.366	40.243	-4.103
43.469	10.151	43.469	-3.980
46.733	9.870	46.733	-3.805
49.997	9.539	49.997	-3.574
53.274	9.164	53.274	-3.288
56.525	8.754	56.525	-2.950
59.750	8.315	59.750	-2.552
62.938	7.855	62.938	-2.096
66.074	7.378	66.074	-1.592
69.133	6.888	69.133	-1.070
72.115	6.388	72.115	-.565
74.995	5.882	74.995	-.115
77.773	5.375	77.773	.265
80.435	4.871	80.435	.568
82.970	4.370	82.970	.793
85.350	3.880	85.350	.939
87.590	3.405	87.590	1.012
89.644	2.953	89.664	1.025
91.571	2.525	91.571	.990
93.299	2.121	93.299	.917
94.848	1.741	94.848	.819
96.192	1.382	96.192	.698
97.344	1.047	97.344	.559
98.291	.741	98.291	.409
99.034	.484	99.034	.276
99.571	.266	95.571	.148
99.891	.099	99.891	.040
100.000	.000	100.000	.000

Girsberger RG-8

AIRFOIL 0008 10.80%

N	X	Y
0	100.000	0.0
1	99.664	0.082
2	98.714	0.338
3	97.253	0.740
4	95.321	1.211
5	92.908	1.712
6	90.028	2.250
7	86.722	2.819
8	83.033	3.407
9	79.007	4.001
10	74.689	4.586
11	70.131	5.147
12	65.381	5.672
13	60.492	6.147
14	55.516	6.558
15	50.504	6.895
16	45.508	7.146
17	40.577	7.303
18	35.760	7.359
19	31.103	7.309
20	26.649	7.149
21	22.440	6.878
22	18.512	6.498
23	14.898	6.013
24	11.627	5.431
25	8.724	4.763
26	6.211	4.023
27	4.105	3.230
28	2.421	2.405
29	1.169	1.577
30	0.360	0.779
31	0.004	0.079
32	0.219	-0.521
33	1.024	-1.097
34	2.328	-1.645
35	4.124	-2.137
36	6.398	-2.559
37	9.136	-2.903
38	12.318	-3.170
39	15.914	-3.363
40	19.884	-3.484
41	24.185	-3.538
42	28.769	-3.525
43	33.580	-3.446
44	38.562	-3.299
45	43.655	-3.069
46	48.825	-2.728
47	54.071	-2.287
48	59.361	-1.802
49	64.626	-1.317
50	69.792	-0.862
51	74.784	-0.463
52	79.524	-0.138
53	83.934	0.102
54	87.940	0.252
55	91.469	0.315
56	94.456	0.302
57	96.845	0.233
58	98.586	0.133
59	99.645	0.040
60	100.000	0.000

ALPHA0 = 3.74 DEGREES
CM0 =-0.1028

Girsberger RG-12

AIRFOIL 12 9.27%

N	X	Y
0	100.000	0.0
1	99.665	0.052
2	98.701	0.219
3	97.190	0.497
4	95.174	0.837
5	92.660	1.213
6	89.671	1.629
7	86.251	2.080
8	82.447	2.557
9	78.304	3.047
10	73.875	3.538
11	69.209	4.018
12	64.361	4.472
13	59.384	4.889
14	54.331	5.256
15	49.257	5.562
16	44.213	5.795
17	39.251	5.948
18	34.419	6.013
19	29.765	5.984
20	25.331	5.857
21	21.158	5.631
22	17.282	5.308
23	13.736	4.892
24	10.551	4.391
25	7.750	3.815
26	5.357	3.176
27	3.389	2.492
28	1.859	1.779
29	0.772	1.067
30	0.140	0.393
31	0.026	-0.161
32	0.486	-0.652
33	1.483	-1.155
34	2.985	-1.618
35	4.983	-2.030
36	7.462	-2.382
37	10.404	-2.673
38	13.781	-2.903
39	17.558	-3.074
40	21.697	-3.190
41	26.153	-3.252
42	30.876	-3.266
43	35.813	-3.235
44	40.907	-3.161
45	46.098	-3.046
46	51.327	-2.891
47	56.530	-2.694
48	61.646	-2.448
49	66.629	-2.128
50	71.476	-1.732
51	76.164	-1.318
52	80.621	-0.934
53	84.773	-0.604
54	88.550	-0.342
55	91.881	-0.155
56	94.705	-0.039
57	96.969	0.020
58	98.632	0.032
59	99.654	0.014
60	100.000	0.0

ALPHA0 = 2.07 DEGREES
CM0 =-0.0527

Girsberger RG-14

AIRFOIL 14 8.47%

N	X	Y
0	100.000	0.0
1	99.667	0.045
2	98.707	0.195
3	97.194	0.446
4	95.169	0.760
5	92.645	1.112
6	89.647	1.506
7	86.218	1.937
8	82.405	2.394
9	78.255	2.867
10	73.817	3.344
11	69.145	3.811
12	64.292	4.256
13	59.310	4.666
14	54.254	5.029
15	49.178	5.334
16	44.133	5.570
17	39.172	5.727
18	34.343	5.800
19	29.692	5.780
20	25.262	5.666
21	21.895	5.456
22	17.226	5.151
23	13.689	4.755
24	10.513	4.275
25	7.725	3.721
26	5.344	3.104
27	3.388	2.439
28	1.867	1.744
29	0.786	1.048
30	0.150	0.390
31	0.022	-0.139
32	0.465	-0.595
33	1.447	-1.055
34	2.938	-1.468
35	4.931	-1.824
36	7.412	-2.116
37	10.363	-2.346
38	13.756	-2.515
39	17.559	-2.629
40	21.730	-2.690
41	26.227	-2.705
42	30.998	-2.680
43	35.989	-2.619
44	41.144	-2.527
45	46.401	-2.409
46	51.701	-2.267
47	56.979	-2.105
48	62.175	-1.921
49	67.227	-1.718
50	72.073	-1.480
51	76.689	-1.194
52	81.057	-0.890
53	85.121	-0.612
54	88.811	-0.382
55	92.063	-0.209
56	94.817	-0.091
57	97.026	-0.019
58	98.654	0.012
59	99.659	0.008
60	100.000	0.0

ALPHA0 = 1.95 DEGREES
CM0 =-0.0471

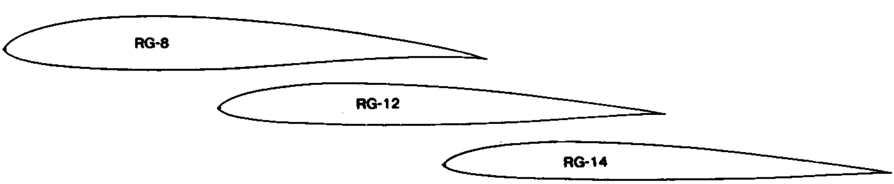

GIRSBERGER RG-15

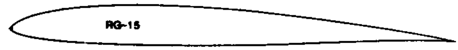

AIRFOIL	15	8.93%
N	X	Y
0	100.000	0.0
1	99.671	0.054
2	98.726	0.229
3	97.237	0.514
4	95.248	0.865
5	92.764	1.254
6	89.810	1.685
7	86.427	2.152
8	82.660	2.644
9	78.557	3.149
10	74.165	3.654
11	69.537	4.146
12	64.723	4.612
13	59.778	5.039
14	54.753	5.414
15	49.702	5.727
16	44.676	5.966
17	39.727	6.123
18	34.902	6.190
19	30.248	6.162
20	25.809	6.036
21	21.624	5.810
22	17.730	5.486
23	14.161	5.068
24	10.945	4.564
25	8.108	3.985
26	5.673	3.343
27	3.658	2.654
28	2.076	1.935
29	0.932	1.214
30	0.235	0.526
31	0.002	-0.048
32	0.336	-0.534
33	1.247	-1.006
34	2.670	-1.436
35	4.596	-1.811
36	7.010	-2.123
37	9.896	-2.372
38	13.224	-2.559
39	16.963	-2.688
40	21.073	-2.762
41	25.509	-2.785
42	30.221	-2.762
43	35.156	-2.696
44	40.257	-2.590
45	45.463	-2.446
46	50.713	-2.262
47	55.944	-2.025
48	61.128	-1.717
49	66.244	-1.366
50	71.237	-1.015
51	76.037	-0.691
52	80.575	-0.413
53	84.779	-0.192
54	88.583	-0.034
55	91.925	0.062
56	94.748	0.101
57	97.003	0.097
58	98.652	0.064
59	99.660	0.021
60	100.000	0.0

ALPHA0 = 2.61 DEGREES
CM0 =-0.0673

	JANOVEC 3-12		HL 74-3512		HL 80-133363	
X	Y1	Y2	Y1	Y2	Y1	Y2
0	0	0	0	0	0	0
0.5	1.00	—	—	—	—	—
1.25	1.80	−1.10	1.50	−1.00	2.02	−1.38
2.5	2.70	−1.60	2.35	−1.30	3.18	−1.80
5	4.00	−2.20	3.45	−1.80	4.76	−2.30
10	5.80	−2.80	5.10	−2.30	6.86	−2.97
15	6.90	—	6.20	−2.70	8.28	−3.30
20	7.80	−3.40	7.10	−3.00	9.10	−3.43
25	8.20	—	7.70	−3.25	9.63	−3.54
30	8.60	−3.50	8.10	−3.40	9.85	−3.55
40	8.50	−3.30	8.60	−3.30	9.66	−3.52
50	8.10	−2.80	8.40	−3.00	8.84	−3.45
60	7.00	−2.00	7.60	−2.40	7.37	−3.01
70	5.70	−1.00	6.30	−1.60	5.54	−2.29
80	3.90	−0.30	4.60	−0.80	3.71	−1.53
90	2.00	−0.20	2.80	0.00	1.88	−0.76
95	1.00	−0.01	1.50	−0.30	—	—
100	0.00	0.00	−0.40	−0.80	0.05	−0.05

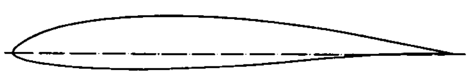

JANOVEC 3-12

SELIG S3002-099-83

1.00000	0.00000
.99676	.00048
.98723	.00205
.97191	.00463
.95131	.00867
.92576	.01330
.89553	.01862
.86104	.02463
.82286	.03124
.78161	.03825
.73787	.04538
.69214	.05226
.64481	.05868
.59634	.06441
.54711	.06930
.49758	.07328
.44820	.07627
.39944	.07823
.35178	.07915
.30572	.07900
.26173	.07776
.22026	.07537
.18165	.07181
.14619	.06711
.11417	.06135
.08583	.05460
.06135	.04701
.04087	.03873
.02450	.03000
.01234	.02105
.00440	.01211
.00048	.00360
.00051	-.00333
.00602	-.00831
.01778	-.01223
.03507	-.01544
.05763	-.01796
.08522	-.01976
.11761	-.02087
.15449	-.02145
.19537	-.02159
.23976	-.02136
.28711	-.02078
.33684	-.01986
.38835	-.01869
.44102	-.01717
.49424	-.01527
.54730	-.01294
.60027	-.01020
.65199	-.00697
.70250	-.00311
.75186	.00061
.79932	.00382
.84366	.00550
.88373	.00590
.91863	.00527
.94770	.00402
.97052	.00257
.98686	.00125
.99672	.00033
1.00000	-.00000

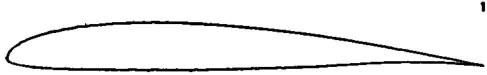

SELIG S3002-099-83

Selig

S2091-101-83 x	S2091-101-83 y	S2027-145-83 x	S2027-145-83 y	S3010-103-84 x	S3010-103-84 y	S3021-095-84 x	S3021-095-84 y
1.00000	0.00000	1.00000	0.00000	1.00000	0.00000	1.00000	0.00000
.99674	.00035	.99647	.00037	.99674	.00027	.99663	.00039
.98707	.00150	.98604	.00164	.98706	.00118	.98679	.00172
.97126	.00367	.96916	.00413	.97122	.00293	.97104	.00419
.94970	.00699	.94635	.00798	.94959	.00564	.94996	.00769
.92292	.01150	.91825	.01321	.92264	.00936	.92398	.01193
.89147	.01713	.88548	.01970	.89090	.01405	.89336	.01670
.85594	.02373	.84870	.02725	.85493	.01960	.85840	.02199
.81693	.03107	.80852	.03560	.81531	.02585	.81959	.02776
.77501	.03888	.76553	.04444	.77261	.03259	.77748	.03394
.73070	.04689	.72028	.05346	.72739	.03958	.73266	.04039
.68454	.05479	.67332	.06236	.68021	.04658	.68572	.04695
.63700	.06231	.62516	.07084	.63158	.05337	.63730	.05342
.58856	.06920	.57628	.07865	.58203	.05971	.58801	.05955
.53965	.07526	.52717	.08554	.53204	.06541	.53839	.06505
.49073	.08029	.47831	.09130	.48213	.07029	.48891	.06964
.44220	.08416	.43016	.09571	.43275	.07422	.43996	.07312
.39450	.08677	.38310	.09857	.38438	.07706	.39191	.07537
.34805	.08805	.33747	.09978	.33750	.07870	.34513	.07632
.30323	.08794	.29361	.09929	.29250	.07902	.29999	.07596
.26043	.08644	.25186	.09709	.24970	.07796	.25685	.07433
.22002	.08356	.21254	.09321	.20944	.07556	.21611	.07151
.18232	.07934	.17589	.08769	.17206	.07184	.17816	.06753
.14765	.07382	.14216	.08064	.13785	.06689	.14331	.06243
.11622	.06708	.11153	.07224	.10706	.06076	.11182	.05631
.08823	.05927	.08419	.06274	.07990	.05360	.08393	.04930
.06384	.05060	.06033	.05240	.05655	.04556	.05983	.04157
.04320	.04130	.04012	.04159	.03713	.03683	.03968	.03329
.02645	.03168	.02380	.03064	.02173	.02766	.02358	.02472
.01374	.02205	.01156	.01992	.01042	.01835	.01160	.01615
.00517	.01269	.00357	.00980	.00319	.00927	.00374	.00799
.00077	.00401	.00004	.00090	.00005	.00100	.00008	.00099
.00058	-.00312	.00226	-.00627	.00181	-.00543	.00191	-.00427
.00575	-.00864	.01078	-.01262	.00932	-.01048	.00984	-.00852
.01662	-.01315	.02476	-.01894	.02239	-.01506	.02320	-.01232
.03263	-.01645	.04376	-.02488	.04061	-.01894	.04178	-.01547
.05397	-.01844	.06752	-.03027	.06381	-.02203	.06542	-.01789
.08063	-.01936	.09581	-.03497	.09180	-.02427	.09394	-.01957
.11236	-.01939	.12833	-.03890	.12435	-.02567	.12712	-.02053
.14883	-.01873	.16474	-.04200	.16119	-.02625	.16464	-.02085
.18960	-.01750	.20467	-.04420	.20200	-.02610	.20613	-.02059
.23417	-.01581	.24773	-.04546	.24635	-.02531	.25118	-.01986
.28205	-.01374	.29350	-.04574	.29376	-.02399	.29928	-.01876
.33271	-.01142	.34154	-.04504	.34371	-.02221	.34988	-.01742
.38555	-.00894	.39139	-.04338	.39565	-.02009	.40237	-.01592
.43995	-.00643	.44256	-.04076	.44899	-.01769	.45611	-.01433
.49526	-.00398	.49465	-.03721	.50312	-.01514	.51046	-.01273
.55088	-.00171	.54723	-.03285	.55743	-.01252	.56475	-.01115
.60605	.00025	.59994	-.02792	.61127	-.00994	.61833	-.00963
.66005	.00182	.65225	-.02282	.66399	-.00749	.67055	-.00821
.71216	.00296	.70342	-.01790	.71495	-.00526	.72078	-.00690
.76168	.00367	.75270	-.01340	.76350	-.00332	.76839	-.00571
.80795	.00397	.79932	-.00946	.80901	-.00172	.81282	-.00462
.85036	.00391	.84257	-.00617	.85087	-.00051	.85354	-.00365
.88834	.00354	.88176	-.00360	.88851	.00031	.89004	-.00278
.92140	.00295	.91625	-.00174	.92140	.00075	.92186	-.00193
.94911	.00222	.94545	-.00055	.94905	.00086	.94875	-.00107
.97109	.00144	.96884	.00005	.97104	.00072	.97046	-.00035
.98705	.00073	.98597	.00020	.98703	.00042	.98659	.00003
.99674	.00020	.99646	.00009	.99674	.00013	.99660	.00008
1.00000	-.00000	1.00000	-.00000	1.00000	-.00000	1.00000	-.00000

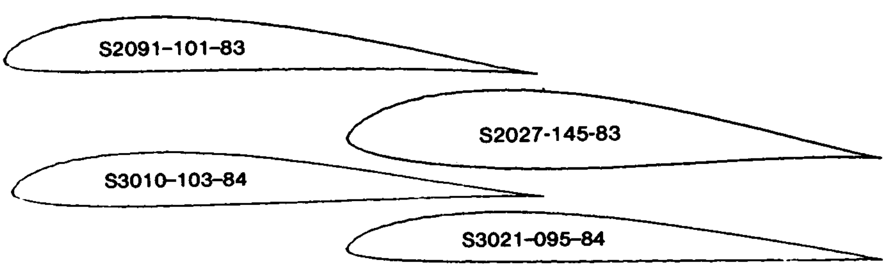

Selig

S4022-113-84 x	S4022-113-84 y	S4053-089-84 x	S4053-089-84 y	S4061-096-84 x	S4061-096-84 y	S4110-084-84 x	S4110-084-84 y
1.00000	0.00000	1.00000	0.00000	1.00000	0.00000	1.00000	0.00000
.99679	.00128	.99662	.00053	.99675	.00034	.99677	.00055
.98795	.00501	.98686	.00231	.98709	.00147	.98738	.00228
.97456	.01036	.97153	.00538	.97129	.00363	.97242	.00521
.95658	.01638	.95119	.00935	.94976	.00698	.95237	.00908
.93381	.02295	.92601	.01381	.92304	.01155	.92746	.01359
.90652	.03009	.89611	.01877	.89170	.01729	.89794	.01868
.87510	.03768	.86192	.02422	.85637	.02403	.86424	.02430
.83996	.04557	.82393	.03011	.81764	.03151	.82685	.03033
.80158	.05358	.78266	.03632	.77610	.03945	.78630	.03657
.76043	.06152	.73869	.04271	.73227	.04752	.74310	.04282
.71703	.06914	.69260	.04911	.68665	.05541	.69771	.04883
.67185	.07619	.64500	.05531	.63971	.06283	.65062	.05439
.62532	.08241	.59647	.06102	.59189	.06950	.60225	.05934
.57782	.08760	.54753	.06592	.54359	.07520	.55306	.06352
.52975	.09167	.49853	.06973	.49522	.07974	.50349	.06683
.48158	.09453	.44977	.07232	.44716	.08302	.45401	.06922
.43371	.09608	.40160	.07366	.39979	.08492	.40507	.07062
.38660	.09628	.35444	.07383	.35348	.08543	.35714	.07102
.34064	.09512	.30868	.07280	.30862	.08454	.31066	.07042
.29623	.09258	.26476	.07066	.26555	.08228	.26612	.06885
.25373	.08871	.22310	.06749	.22460	.07876	.22394	.06631
.21350	.08361	.18409	.06333	.18620	.07414	.18453	.06285
.17587	.07741	.14813	.05828	.15074	.06849	.14830	.05849
.14120	.07023	.11551	.05243	.11855	.06186	.11555	.05328
.10980	.06225	.08655	.04588	.08988	.05438	.08659	.04729
.08196	.05361	.06147	.03879	.06493	.04617	.06167	.04060
.05792	.04451	.04053	.03131	.04386	.03741	.04093	.03323
.03789	.03515	.02388	.02360	.02677	.02839	.02437	.02536
.02206	.02575	.01163	.01584	.01380	.01938	.01204	.01730
.01050	.01649	.00377	.00823	.00503	.01069	.00400	.00935
.00313	.00776	.00013	.00131	.00046	.00283	.00021	.00191
.00001	.00038	.00152	-.00392	.00079	-.00320	.00119	-.00408
.00246	-.00502	.00876	-.00781	.00681	-.00787	.00755	-.00892
.01117	-.00919	.02165	-.01116	.01835	-.01209	.01905	-.01317
.02553	-.01287	.03990	-.01388	.03499	-.01546	.03554	-.01630
.04522	-.01594	.06334	-.01592	.05668	-.01780	.05723	-.01820
.07000	-.01834	.09177	-.01729	.08328	-.01908	.08413	-.01911
.09959	-.02006	.12494	-.01808	.11474	-.01932	.11599	-.01920
.13368	-.02111	.16249	-.01840	.15085	-.01865	.15247	-.01865
.17189	-.02152	.20391	-.01829	.19129	-.01724	.19313	-.01757
.21378	-.02129	.24875	-.01771	.23565	-.01528	.23751	-.01605
.25888	-.02044	.29661	-.01671	.28345	-.01292	.28509	-.01417
.30669	-.01897	.34698	-.01541	.33413	-.01034	.33537	-.01202
.35670	-.01685	.39927	-.01392	.38706	-.00772	.38774	-.00970
.40838	-.01409	.45286	-.01231	.44159	-.00516	.44162	-.00728
.46124	-.01061	.50711	-.01064	.49702	-.00279	.49640	-.00487
.51493	-.00635	.56138	-.00896	.55265	-.00069	.55145	-.00258
.56931	-.00152	.61507	-.00731	.60776	.00107	.60606	-.00053
.62394	.00324	.66752	-.00579	.66163	.00245	.65957	.00121
.67803	.00747	.71809	-.00443	.71356	.00342	.71127	.00260
.73071	.01084	.76614	-.00328	.76287	.00400	.76051	.00360
.78110	.01311	.81105	-.00236	.80893	.00420	.80865	.00418
.82829	.01415	.85226	-.00165	.85114	.00406	.84906	.00436
.87139	.01390	.88923	-.00113	.88893	.00364	.88717	.00416
.90955	.01242	.92145	-.00075	.92183	.00301	.92046	.00363
.94190	.00982	.94854	-.00041	.94939	.00225	.94843	.00285
.96749	.00648	.97028	-.00003	.97126	.00146	.97068	.00193
.98569	.00321	.98646	.00018	.98713	.00074	.98686	.00102
.99645	.00085	.99655	.00010	.99677	.00020	.99670	.00029
1.00000	.00000	1.00000	.00000	1.00000	.00000	1.00000	.00000

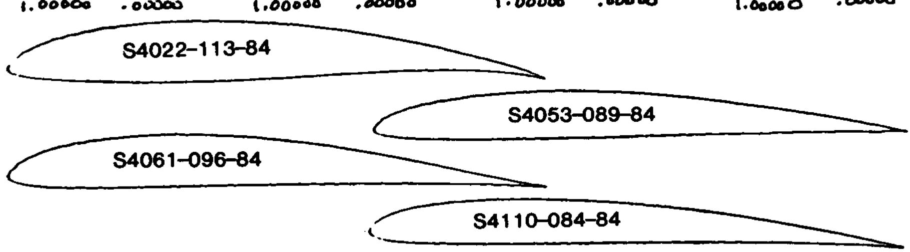

Selig

S4158-109-84		S4180-098-84		S4233-136-84		S4310-109-84	
x	y	x	y	x	y	x	y
1.00000	0.00000	1.00000	0.00000	1.00000	0.00000	1.00000	0.00000
.99654	.00023	.99684	.00036	.99650	.00042	.99665	.00043
.98621	.00111	.98746	.00156	.98618	.00186	.98675	.00184
.96923	.00307	.97208	.00376	.96949	.00461	.97069	.00444
.94604	.00654	.95106	.00702	.94697	.00881	.94893	.00834
.91742	.01182	.92483	.01132	.91927	.01444	.92202	.01351
.88428	.01890	.89384	.01661	.88703	.02138	.89054	.01984
.84751	.02757	.85861	.02279	.85088	.02939	.85507	.02714
.80801	.03745	.81971	.02971	.81146	.03817	.81616	.03516
.76666	.04799	.77768	.03718	.76933	.04740	.77439	.04365
.72424	.05830	.73313	.04497	.72503	.05674	.73029	.05230
.68083	.06722	.68661	.05280	.67907	.06586	.68439	.06084
.63593	.07442	.63859	.06042	.63196	.07443	.63721	.06896
.58958	.08025	.58961	.06762	.58414	.08218	.58923	.07640
.54234	.08482	.54019	.07420	.53609	.08881	.54091	.08285
.49464	.08805	.49083	.07997	.48820	.09406	.49265	.08806
.44690	.08996	.44204	.08472	.44078	.09770	.44477	.09187
.39957	.09057	.39427	.08829	.39411	.09969	.39761	.09421
.35312	.08992	.34798	.09050	.34857	.10001	.35154	.09504
.30808	.08804	.30355	.09118	.30450	.09867	.30694	.09439
.26485	.08486	.26126	.09018	.26227	.09571	.26416	.09231
.22375	.08044	.22127	.08751	.22219	.09119	.22361	.08889
.18512	.07496	.18383	.08329	.18457	.08523	.18569	.08418
.14938	.06857	.14916	.07770	.14971	.07798	.15073	.07822
.11693	.06137	.11757	.07095	.11788	.06963	.11898	.07113
.08808	.05342	.08935	.06323	.08935	.06040	.09072	.06303
.06297	.04484	.06476	.05468	.06437	.05056	.06611	.05406
.04177	.03594	.04398	.04553	.04320	.04033	.04530	.04443
.02474	.02697	.02726	.03596	.02602	.03000	.02840	.03437
.01209	.01814	.01467	.02606	.01301	.01987	.01546	.02416
.00392	.00965	.00607	.01606	.00433	.01032	.00643	.01419
.00018	.00185	.00129	.00643	.00017	.00183	.00130	.00509
.00127	-.00429	.00016	-.00200	.00156	-.00488	.00030	-.00210
.00801	-.00894	.00377	-.00814	.00916	-.01058	.00498	-.00721
.02053	-.01294	.01306	-.01234	.02237	-.01621	.01603	-.01117
.03845	-.01613	.02779	-.01523	.04069	-.02144	.03260	-.01434
.06167	-.01849	.04791	-.01670	.06388	-.02609	.05451	-.01664
.09001	-.02012	.07351	-.01680	.09171	-.03004	.08156	-.01807
.12317	-.02113	.10453	-.01584	.12392	-.03322	.11352	-.01869
.16075	-.02160	.14065	-.01417	.16018	-.03559	.15011	-.01857
.20228	-.02159	.18140	-.01202	.20012	-.03714	.19095	-.01784
.24730	-.02109	.22624	-.00957	.24337	-.03782	.23562	-.01661
.29534	-.02018	.27459	-.00696	.28950	-.03768	.28362	-.01503
.34590	-.01888	.32585	-.00433	.33802	-.03672	.33437	-.01323
.39838	-.01735	.37936	-.00178	.38846	-.03497	.38726	-.01133
.45218	-.01565	.43445	.00060	.44031	-.03249	.44162	-.00942
.50667	-.01385	.49043	.00273	.49308	-.02934	.49677	-.00758
.56120	-.01202	.54658	.00455	.54625	-.02558	.55203	-.00585
.61511	-.01022	.60221	.00601	.59939	-.02139	.60671	-.00428
.66775	-.00852	.65660	.00708	.65199	-.01703	.66013	-.00291
.71848	-.00696	.70908	.00774	.70341	-.01286	.71162	-.00175
.76666	-.00556	.75897	.00800	.75289	-.00910	.76053	-.00079
.81168	-.00437	.80564	.00786	.79966	-.00591	.80627	.00001
.85297	-.00337	.84847	.00735	.84299	-.00337	.84833	.00067
.88999	-.00257	.88692	.00652	.88219	-.00149	.88622	.00114
.92225	-.00193	.92046	.00548	.91664	-.00026	.91946	.00139
.94931	-.00140	.94862	.00407	.94576	.00043	.94757	.00137
.97083	-.00087	.97093	.00262	.96905	.00058	.97008	.00110
.98668	-.00035	.98703	.00131	.98608	.00043	.98655	.00065
.99659	-.00005	.99674	.00035	.99649	.00014	.99661	.00020
1.00000	.00000	1.00000	.00000	1.00000	.00000	.00000	.00000

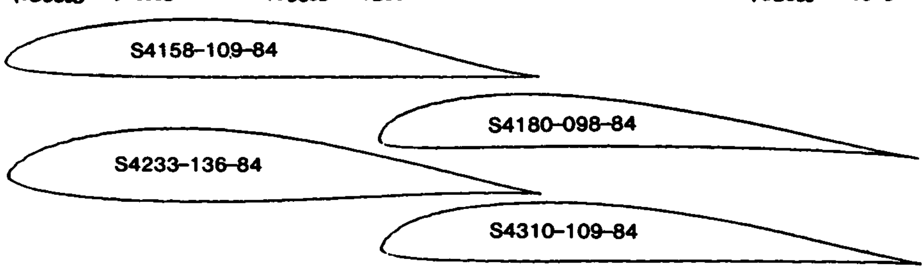

Selig

S4320-094-84

x	y
1.00000	0.00000
.99682	.00044
.98739	.00182
.97202	.00426
.95108	.00780
.92500	.01242
.89426	.01804
.85937	.02454
.82088	.03175
.77933	.03946
.73529	.04746
.68931	.05550
.64196	.06333
.59384	.07063
.54538	.07709
.49698	.08242
.44898	.08642
.40169	.08902
.35549	.09018
.31075	.08991
.26783	.08826
.22712	.08530
.18903	.08108
.15387	.07563
.12192	.06906
.09342	.06147
.06855	.05300
.04745	.04385
.03022	.03425
.01690	.02445
.00744	.01483
.00179	.00598
.00009	-.00116
.00380	-.00601
.01372	-.00931
.02926	-.01168
.05023	-.01305
.07648	-.01348
.10780	-.01304
.14390	-.01186
.18445	-.01009
.22900	-.00788
.27707	-.00540
.32807	-.00283
.38137	-.00031
.43629	.00206
.49213	.00417
.54818	.00596
.60374	.00738
.65811	.00838
.71057	.00894
.76047	.00905
.80716	.00871
.85000	.00791
.88833	.00671
.92161	.00526
.94939	.00373
.97133	.00229
.98719	.00110
.99678	.00029
.00000	.00000

S4063-094-86

AIRFOIL 4063 9.44%

N	X	Y	
0	1.00000	0.0	0.896
1	0.99673	0.00038	0.899
2	0.98704	0.00166	0.908
3	0.97122	0.00410	0.924
4	0.94972	0.00784	0.945
5	0.92314	0.01290	0.970
6	0.89207	0.01918	1.000
7	0.85714	0.02646	1.031
8	0.81896	0.03444	1.064
9	0.77806	0.04279	1.097
10	0.73496	0.05114	1.130
11	0.69010	0.05917	1.161
12	0.64391	0.06655	1.189
13	0.59679	0.07303	1.214
14	0.54909	0.07839	1.235
15	0.50118	0.08247	1.252
16	0.45341	0.08517	1.264
17	0.40613	0.08643	1.272
18	0.35967	0.08628	1.274
19	0.31439	0.08483	1.274
20	0.27074	0.08222	1.273
21	0.22921	0.07854	1.273
22	0.19024	0.07387	1.272
23	0.15425	0.06823	1.270
24	0.12156	0.06167	1.261
25	0.09241	0.05428	1.244
26	0.06702	0.04619	1.214
27	0.04554	0.03756	1.162
28	0.02807	0.02865	1.082
29	0.01475	0.01974	0.949
30	0.00565	0.01113	0.704
31	0.00077	0.00329	0.227
32	0.00065	-0.00269	0.779
33	0.00619	-0.00728	1.020
34	0.01736	-0.01141	1.091
35	0.03365	-0.01469	1.102
36	0.05500	-0.01693	1.093
37	0.08134	-0.01810	1.075
38	0.11256	-0.01823	1.054
39	0.14847	-0.01744	1.032
40	0.18877	-0.01593	1.013
41	0.23304	-0.01386	0.997
42	0.28079	-0.01142	0.981
43	0.33148	-0.00878	0.969
44	0.38447	-0.00611	0.958
45	0.43909	-0.00353	0.948
46	0.49465	-0.00117	0.940
47	0.55044	0.00090	0.933
48	0.60573	0.00260	0.927
49	0.65981	0.00390	0.922
50	0.71197	0.00476	0.918
51	0.76151	0.00521	0.915
52	0.80780	0.00526	0.912
53	0.85023	0.00496	0.909
54	0.88824	0.00437	0.907
55	0.92133	0.00357	0.905
56	0.94907	0.00265	0.904
57	0.97108	0.00171	0.902
58	0.98705	0.00086	0.900
59	0.99675	0.00024	0.898
60	1.00001	0.00000	0.896

ALPHAO = 3.90 DEGREES CMO =-0.0948

S5020-084-86

AIRFOIL S5020-

N	X	Y
0	1.00000	0.00000
1	0.99683	-0.00001
2	0.98736	0.00000
3	0.97160	0.00015
4	0.94964	0.00066
5	0.92171	0.00186
6	0.88833	0.00413
7	0.85028	0.00766
8	0.80846	0.01234
9	0.76339	0.01795
10	0.71594	0.02430
11	0.66672	0.03116
12	0.61644	0.03827
13	0.56576	0.04524
14	0.51519	0.05170
15	0.46516	0.05736
16	0.41608	0.06198
17	0.36830	0.06539
18	0.32218	0.06748
19	0.27803	0.06821
20	0.23620	0.06759
21	0.19702	0.06565
22	0.16081	0.06244
23	0.12785	0.05802
24	0.09837	0.05249
25	0.07257	0.04596
26	0.05059	0.03862
27	0.03252	0.03065
28	0.01843	0.02234
29	0.00833	0.01401
30	0.00219	0.00613
31	0.00002	-0.00049
32	0.00308	-0.00507
33	0.01226	-0.00815
34	0.02727	-0.01037
35	0.04807	-0.01192
36	0.07434	-0.01310
37	0.10563	-0.01404
38	0.14146	-0.01478
39	0.18141	-0.01534
40	0.22491	-0.01569
41	0.27150	-0.01583
42	0.32064	-0.01576
43	0.37179	-0.01550
44	0.42436	-0.01507
45	0.47776	-0.01449
46	0.53139	-0.01379
47	0.58462	-0.01297
48	0.63687	-0.01206
49	0.68752	-0.01108
50	0.73601	-0.01004
51	0.78178	-0.00896
52	0.82430	-0.00785
53	0.86308	-0.00672
54	0.89767	-0.00557
55	0.92767	-0.00440
56	0.95276	-0.00317
57	0.97279	-0.00188
58	0.98763	-0.00079
59	0.99686	-0.00016
60	1.00001	-0.00000

ALPHAO = 0.82 DEGREES

CMO = 0.0084

S5010-098-86

AIRFOIL S5010-86

N	X	Y
0	1.00000	0.0
1	0.99676	0.00001
2	0.98707	0.00007
3	0.97101	0.00036
4	0.94870	0.00106
5	0.92041	0.00256
6	0.88667	0.00516
7	0.84828	0.00903
8	0.80608	0.01406
9	0.76076	0.02008
10	0.71307	0.02688
11	0.66377	0.03420
12	0.61355	0.04163
13	0.56296	0.04877
14	0.51247	0.05529
15	0.46251	0.06093
16	0.41348	0.06546
17	0.36576	0.06873
18	0.31969	0.07063
19	0.27560	0.07113
20	0.23383	0.07023
21	0.19473	0.06799
22	0.15860	0.06445
23	0.12573	0.05968
24	0.09637	0.05377
25	0.07071	0.04686
26	0.04889	0.03915
27	0.03102	0.03081
28	0.01718	0.02214
29	0.00739	0.01348
30	0.00167	0.00533
31	0.00015	-0.00140
32	0.00424	-0.00650
33	0.01456	-0.01084
34	0.03028	-0.01471
35	0.05123	-0.01804
36	0.07718	-0.02082
37	0.10785	-0.02306
38	0.14291	-0.02481
39	0.18194	-0.02609
40	0.22448	-0.02688
41	0.27008	-0.02715
42	0.31829	-0.02691
43	0.36864	-0.02623
44	0.42055	-0.02517
45	0.47345	-0.02381
46	0.52675	-0.02219
47	0.57983	-0.02039
48	0.63209	-0.01846
49	0.68292	-0.01645
50	0.73173	-0.01443
51	0.77792	-0.01243
52	0.82095	-0.01049
53	0.86030	-0.00865
54	0.89547	-0.00691
55	0.92603	-0.00527
56	0.95163	-0.00367
57	0.97211	-0.00212
58	0.98730	-0.00088
59	0.99676	-0.00019
60	1.00001	-0.00000

ALPHAO = 0.64 DEGREES

CMO = 0.0086

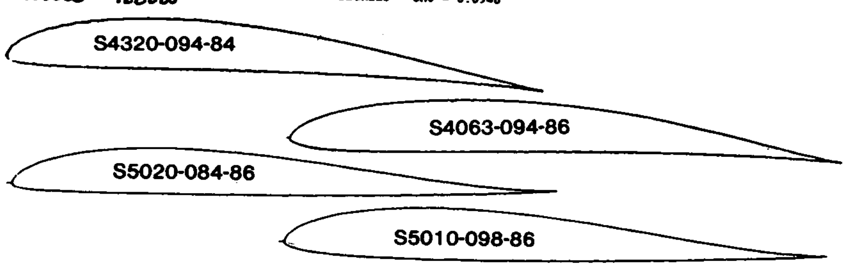

HQ - 1,0/8

	X(i)	Yo	Yu
1	0.0000	0.0000	0.0000
2	.0050	.0076	-.0054
3	.0125	.0115	-.0088
4	.0250	.0177	-.0128
5	.0500	.0253	-.0175
6	.1000	.0349	-.0229
7	.1500	.0414	-.0266
8	.2000	.0448	-.0284
9	.2500	.0473	-.0297
10	.3000	.0488	-.0302
11	.3500	.0496	-.0304
12	.4000	.0490	-.0295
13	.5000	.0463	-.0263
14	.6000	.0402	-.0208
15	.7000	.0312	-.0136
16	.8000	.0208	-.0069
17	.8500	.0153	-.0042
18	.9000	.0101	-.0021
19	.9500	.0047	-.0006
20	1.0000	0.0000	0.0000

HQ-1,0/9

	X(i)	Yo	Yu
1	0.0000	0.0000	0.0000
2	.0050	.0084	-.0062
3	.0125	.0128	-.0101
4	.0250	.0195	-.0147
5	.0500	.0280	-.0202
6	.1000	.0385	-.0265
7	.1500	.0456	-.0309
8	.2000	.0494	-.0325
9	.2500	.0521	-.0345
10	.3000	.0537	-.0351
11	.3500	.0546	-.0354
12	.4000	.0540	-.0344
13	.5000	.0508	-.0308
14	.6000	.0440	-.0246
15	.7000	.0340	-.0164
16	.8000	.0225	-.0087
17	.8500	.0165	-.0054
18	.9000	.0109	-.0029
19	.9500	.0050	-.0009
20	1.0000	0.0000	0.0000

HQ-1,0/10

	X(i)	Yo	Yu
1	0.0000	0.0000	0.0000
2	.0050	.0092	-.0070
3	.0125	.0141	-.0114
4	.0250	.0214	-.0166
5	.0500	.0307	-.0228
6	.1000	.0421	-.0301
7	.1500	.0499	-.0351
8	.2000	.0540	-.0375
9	.2500	.0569	-.0393
10	.3000	.0586	-.0400
11	.3500	.0596	-.0404
12	.4000	.0589	-.0393
13	.5000	.0554	-.0354
14	.6000	.0478	-.0284
15	.7000	.0368	-.0192
16	.8000	.0243	-.0104
17	.8500	.0177	-.0066
18	.9000	.0117	-.0037
19	.9500	.0054	-.0013
20	1.0000	0.0000	0.0000

HQ-1,5/8

	X(i)	Yo	Yu
1	0.0000	0.0000	0.0000
2	.0050	.0082	-.0048
3	.0125	.0128	-.0082
4	.0250	.0189	-.0115
5	.0500	.0273	-.0156
6	.1000	.0379	-.0199
7	.1500	.0451	-.0229
8	.2000	.0489	-.0243
9	.2500	.0517	-.0253
10	.3000	.0534	-.0255
11	.3500	.0544	-.0256
12	.4000	.0534	-.0246
13	.5000	.0513	-.0213
14	.6000	.0450	-.0159
15	.7000	.0356	-.0092
16	.8000	.0243	-.0035
17	.8500	.0181	-.0014
18	.9000	.0121	-.0002
19	.9500	.0057	-.0004
20	1.0000	0.0000	0.0000

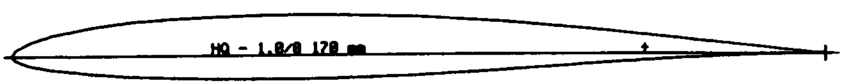

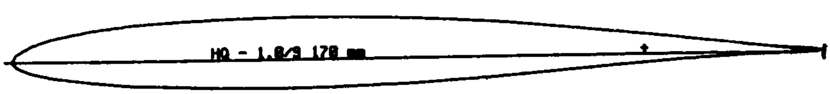

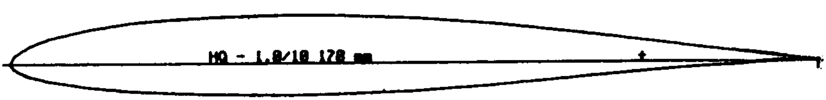

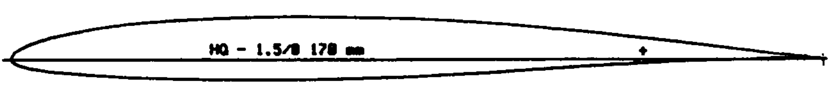

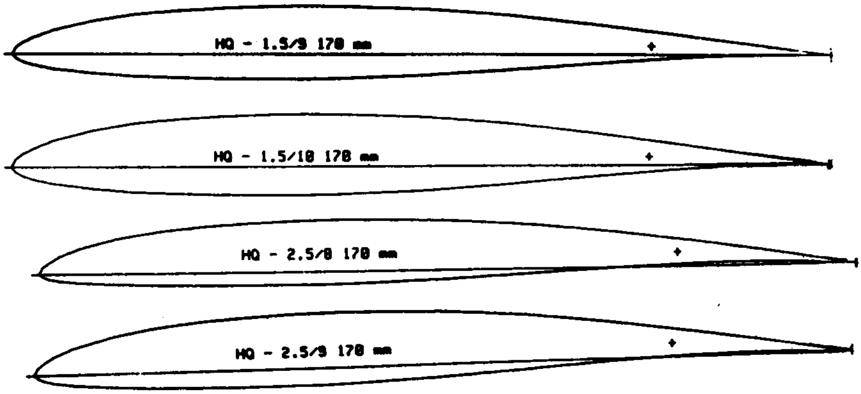

HQ-1,5/9

	X(i)	Yo	Yu
1	0.0000	0.0000	0.0000
2	.0050	.0090	-.0056
3	.0125	.0144	-.0094
4	.0250	.0208	-.0134
5	.0500	.0300	-.0182
6	.1000	.0415	-.0235
7	.1500	.0493	-.0272
8	.2000	.0535	-.0288
9	.2500	.0565	-.0301
10	.3000	.0583	-.0305
11	.3500	.0594	-.0306
12	.4000	.0588	-.0295
13	.5000	.0558	-.0258
14	.6000	.0488	-.0197
15	.7000	.0384	-.0120
16	.8000	.0260	-.0052
17	.8500	.0193	-.0026
18	.9000	.0129	-.0009
19	.9500	.0061	-.0001
20	1.0000	0.0000	0.0000

HQ-1,5/10

	X(i)	Yo	Yu
1	0.0000	0.0000	0.0000
2	.0050	.0098	-.0064
3	.0125	.0160	-.0107
4	.0250	.0227	-.0154
5	.0500	.0326	-.0209
6	.1000	.0451	-.0271
7	.1500	.0536	-.0314
8	.2000	.0581	-.0334
9	.2500	.0613	-.0349
10	.3000	.0633	-.0354
11	.3500	.0644	-.0356
12	.4000	.0637	-.0344
13	.5000	.0604	-.0304
14	.6000	.0526	-.0235
15	.7000	.0412	-.0148
16	.8000	.0277	-.0069
17	.8500	.0205	-.0038
18	.9000	.0137	-.0017
19	.9500	.0064	-.0002
20	1.0000	0.0000	0.0000

HQ-2,5/8

	X(i)	Yo	Yu
1	0.0000	0.0000	0.0000
2	.0050	.0084	-.0037
3	.0125	.0136	-.0068
4	.0250	.0213	-.0091
5	.0500	.0312	-.0116
6	.1000	.0439	-.0139
7	.1500	.0518	-.0156
8	.2000	.0571	-.0160
9	.2500	.0605	-.0165
10	.3000	.0627	-.0162
11	.3500	.0640	-.0160
12	.4000	.0637	-.0148
13	.5000	.0613	-.0113
14	.6000	.0547	-.0062
15	.7000	.0444	-.0004
16	.8000	.0312	.0035
17	.8500	.0236	.0042
18	.9000	.0161	.0038
19	.9500	.0078	.0025
20	1.0000	0.0000	0.0000

HQ-2,5/9

	X(i)	Yo	Yu
1	0.0000	0.0000	0.0000
2	.0050	.0091	-.0045
3	.0125	.0148	-.0080
4	.0250	.0232	-.0110
5	.0500	.0339	-.0143
6	.1000	.0475	-.0175
7	.1500	.0560	-.0198
8	.2000	.0617	-.0206
9	.2500	.0653	-.0213
10	.3000	.0676	-.0212
11	.3500	.0690	-.0210
12	.4000	.0686	-.0197
13	.5000	.0658	-.0158
14	.6000	.0585	-.0100
15	.7000	.0472	-.0032
16	.8000	.0329	.0017
17	.8500	.0249	.0030
18	.9000	.0169	.0031
19	.9500	.0081	.0022
20	1.0000	0.0000	0.0000

HQ-2,5/10

	X(1)	Yo	Yu
1	0.0000	0.0000	0.0000
2	.0050	.0093	-.0053
3	.0125	.0161	-.0093
4	.0250	.0251	-.0129
5	.0500	.0366	-.0170
6	.1000	.0511	-.0211
7	.1500	.0602	-.0241
8	.2000	.0663	-.0252
9	.2500	.0701	-.0261
10	.3000	.0725	-.0261
11	.3500	.0740	-.0260
12	.4000	.0735	-.0247
13	.5000	.0704	-.0204
14	.6000	.0623	-.0138
15	.7000	.0479	-.0060
16	.8000	.0347	0.0000
17	.8500	.0261	.0017
18	.9000	.0177	.0023
19	.9500	.0085	.0018
20	1.0000	0.0000	0.0000

HQ-3,5/8

	X(1)	Yo	Yu
1	0.0000	0.0000	0.0000
2	.0050	.0104	-.0026
3	.0125	.0149	-.0054
4	.0250	.0238	-.0067
5	.0500	.0351	-.0077
6	.1000	.0498	-.0078
7	.1500	.0598	-.0082
8	.2000	.0654	-.0078
9	.2500	.0693	-.0077
10	.3000	.0720	-.0069
11	.3500	.0736	-.0064
12	.4000	.0735	-.0050
13	.5000	.0713	-.0013
14	.6000	.0644	.0035
15	.7000	.0531	.0083
16	.8000	.0381	.0104
17	.8500	.0292	.0097
18	.9000	.0201	.0078
19	.9500	.0099	.0045
20	1.0000	0.0000	0.0000

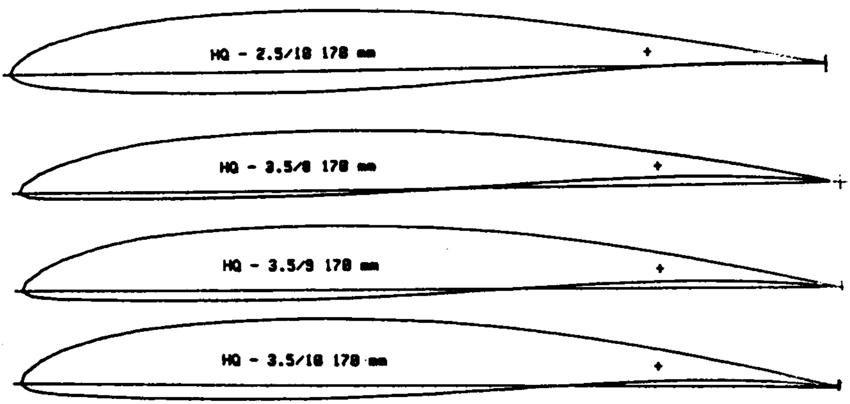

HQ-3,5/9

	X(1)	Yo	Yu
1	0.0000	0.0000	0.0000
2	.0050	.0112	-.0034
3	.0125	.0162	-.0067
4	.0250	.0257	-.0086
5	.0500	.0378	-.0104
6	.1000	.0535	-.0114
7	.1500	.0641	-.0124
8	.2000	.0699	-.0124
9	.2500	.0741	-.0124
10	.3000	.0769	-.0119
11	.3500	.0786	-.0114
12	.4000	.0784	-.0100
13	.5000	.0758	-.0058
14	.6000	.0682	-.0003
15	.7000	.0559	.0056
16	.8000	.0399	.0087
17	.8500	.0304	.0085
18	.9000	.0209	.0071
19	.9500	.0102	.0042
20	1.0000	0.0000	0.0000

HQ-3,5/10

	X(1)	Yo	Yu
1	0.0000	0.0000	0.0000
2	.0050	.0120	-.0042
3	.0125	.0175	-.0080
4	.0250	.0276	-.0105
5	.0500	.0405	-.0131
6	.1000	.0571	-.0151
7	.1500	.0683	-.0167
8	.2000	.0745	-.0170
9	.2500	.0789	-.0173
10	.3000	.0818	-.0166
11	.3500	.0836	-.0164
12	.4000	.0833	-.0149
13	.5000	.0804	-.0104
14	.6000	.0720	-.0041
15	.7000	.0587	.0027
16	.8000	.0416	.0069
17	.8500	.0316	.0073
18	.9000	.0217	.0063
19	.9500	.0105	.0039
20	1.0000	0.0000	0.0000

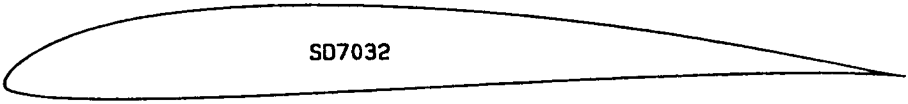

SD7032

1	1.00000	0.00000	17	0.45058	0.08154	33	0.00038	-.00223	49	0.60112	-.00190
2	0.99674	0.00048	18	0.40222	0.08385	34	0.00532	-.00701	50	0.65469	0.00030
3	0.98712	0.00204	19	0.35506	0.08500	35	0.01649	-.01088	51	0.70664	0.00224
4	0.97155	0.00485	20	0.30953	0.08493	36	0.03308	-.01403	52	0.75634	0.00379
5	0.95054	0.00894	21	0.26604	0.08359	37	0.05491	-.01635	53	0.80313	0.00485
6	0.92464	0.01420	22	0.22499	0.08096	38	0.08180	-.01787	54	0.84635	0.00535
7	0.89436	0.02041	23	0.18671	0.07703	39	0.11351	-.01862	55	0.88534	0.00526
8	0.86021	0.02731	24	0.15146	0.07182	40	0.14974	-.01867	56	0.91942	0.00458
9	0.82264	0.03460	25	0.11948	0.06548	41	0.19010	-.01810	57	0.94797	0.00350
10	0.78208	0.04199	26	0.09105	0.05809	42	0.23420	-.01699	58	0.97054	0.00226
11	0.73892	0.04925	27	0.06627	0.04976	43	0.28153	-.01547	59	0.98684	0.00113
12	0.69356	0.05620	28	0.04524	0.04078	44	0.33154	-.01363	60	0.99670	0.00030
13	0.64646	0.06270	29	0.02812	0.03145	45	0.38364	-.01152	61	1.00001	0.00000
14	0.59812	0.06861	30	0.01502	0.02206	46	0.43724	-.00922			
15	0.54902	0.07381	31	0.00606	0.01293	47	0.49176	-.00678			
16	0.49967	0.07816	32	0.00115	0.00448	48	0.54659	-.00430			

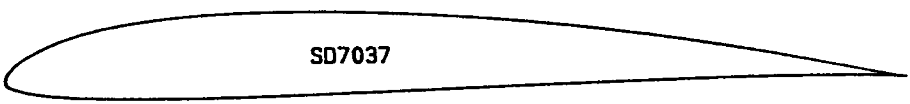

SD7037

1	1.00000	0.00000	17	0.44745	0.07211	33	0.00127	-.00393	49	0.60914	-.00549
2	0.99672	0.00042	18	0.39862	0.07410	34	0.00806	-.00839	50	0.66197	-.00349
3	0.98707	0.00180	19	0.35101	0.07504	35	0.02038	-.01227	51	0.71305	-.00168
4	0.97146	0.00436	20	0.30508	0.07488	36	0.03800	-.01541	52	0.76178	-.00014
5	0.95041	0.00811	21	0.26125	0.07358	37	0.06074	-.01777	53	0.80752	0.00104
6	0.92450	0.01295	22	0.21989	0.07113	38	0.08844	-.01934	54	0.84964	0.00182
7	0.89425	0.01865	23	0.18137	0.06754	39	0.12084	-.02017	55	0.88756	0.00220
8	0.86015	0.02490	24	0.14601	0.06286	40	0.15765	-.02032	56	0.92071	0.00218
9	0.82261	0.03141	25	0.11410	0.05715	41	0.19850	-.01987	57	0.94859	0.00185
10	0.78201	0.03788	26	0.08586	0.05049	42	0.24296	-.01891	58	0.97077	0.00132
11	0.73865	0.04413	27	0.06146	0.04300	43	0.29055	-.01754	59	0.98690	0.00071
12	0.69294	0.05011	28	0.04102	0.03486	44	0.34071	-.01586	60	0.99671	0.00021
13	0.64539	0.05572	29	0.02462	0.02632	45	0.39288	-.01396	61	1.00001	0.00000
14	0.59655	0.06085	30	0.01232	0.01770	46	0.44643	-.01190			
15	0.54693	0.06538	31	0.00418	0.00936	47	0.50074	-.00976			
16	0.49706	0.06917	32	0.00021	0.00185	48	0.55519	-.00760			

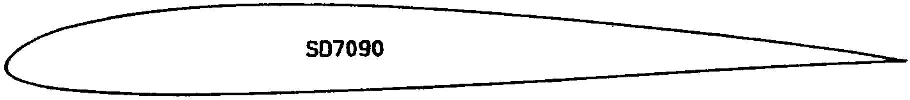

SD7090

1	1.00000	0.00000	17	0.43649	0.06457	33	0.00345	-.00734	49	0.61442	-.01948
2	0.99655	0.00050	18	0.38699	0.06674	34	0.01238	-.01318	50	0.66605	-.01658
3	0.98664	0.00219	19	0.33890	0.06795	35	0.02624	-.01834	51	0.71605	-.01363
4	0.97113	0.00512	20	0.29269	0.06814	36	0.04514	-.02262	52	0.76381	-.01083
5	0.95062	0.00882	21	0.24878	0.06724	37	0.06903	-.02605	53	0.80869	-.00829
6	0.92522	0.01284	22	0.20759	0.06522	38	0.09771	-.02873	54	0.85007	-.00609
7	0.89500	0.01718	23	0.16945	0.06206	39	0.13087	-.03067	55	0.88735	-.00426
8	0.86036	0.02188	24	0.13467	0.05780	40	0.16817	-.03188	56	0.92001	-.00279
9	0.82176	0.02691	25	0.10352	0.05249	41	0.20926	-.03240	57	0.94757	-.00160
10	0.77972	0.03218	26	0.07624	0.04621	42	0.25371	-.03229	58	0.96974	-.00066
11	0.73479	0.03760	27	0.05297	0.03907	43	0.30106	-.03161	59	0.98622	-.00009
12	0.68754	0.04304	28	0.03384	0.03125	44	0.35077	-.03046	60	0.99650	0.00004
13	0.63860	0.04834	29	0.01891	0.02298	45	0.40227	-.02889	61	1.00001	0.00000
14	0.58850	0.05329	30	0.00827	0.01458	46	0.45499	-.02696			
15	0.53777	0.05773	31	0.00196	0.00637	47	0.50832	-.02472			
16	0.48692	0.06153	32	0.00005	-.00097	48	0.56166	-.02221			

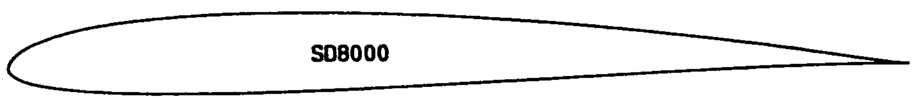

SD8000

1	1.00000	0.00000	17	0.43875	0.05780	33	0.00440	-.00749	49	0.61566	-.01459
2	0.99674	0.00030	18	0.38905	0.05929	34	0.01370	-.01315	50	0.66757	-.01179
3	0.98711	0.00130	19	0.34062	0.05996	35	0.02780	-.01814	51	0.71773	-.00910
4	0.97148	0.00321	20	0.29395	0.05978	36	0.04677	-.02225	52	0.76556	-.00662
5	0.95032	0.00607	21	0.24951	0.05872	37	0.07058	-.02544	53	0.81047	-.00445
6	0.92413	0.00984	22	0.20775	0.05675	38	0.09914	-.02776	54	0.85185	-.00268
7	0.89343	0.01434	23	0.16906	0.05389	39	0.13219	-.02929	55	0.88910	-.00132
8	0.85871	0.01936	24	0.13380	0.05012	40	0.16941	-.03008	56	0.92170	-.00040
9	0.82042	0.02466	25	0.10229	0.04548	41	0.21041	-.03020	57	0.94916	0.00013
10	0.77899	0.03000	26	0.07476	0.04000	42	0.25477	-.02969	58	0.97105	0.00032
11	0.73481	0.03521	27	0.05142	0.03377	43	0.30202	-.02864	59	0.98700	0.00026
12	0.68831	0.04017	28	0.03238	0.02686	44	0.35163	-.02710	60	0.99673	0.00009
13	0.63998	0.04478	29	0.01766	0.01948	45	0.40307	-.02514	61	1.00001	0.00000
14	0.59034	0.04894	30	0.00729	0.01194	46	0.45576	-.02284			
15	0.53991	0.05256	31	0.00136	0.00460	47	0.50913	-.02024			
16	0.48921	0.05553	32	0.00022	-.00175	48	0.56263	-.01744			

Index

The numbers in the index refer to paragraph numbers in the text.

No glossary has been included. Where a definition or explanation of a term is required it will normally be found in the index which will refer the reader to the paragraphs where the definition and explanation appears.